DMIC Report 210
October 26-28, 1964

PROBLEMS IN THE LOAD-CARRYING APPLICATION OF HIGH-STRENGTH STEELS

A Symposium Sponsored by the
Tripartite Technical Cooperation Program (TTCP)
Sub-Group P on Materials
Working Panel on Metals

DEFENSE METALS INFORMATION CENTER
Battelle Memorial Institute
Columbus, Ohio 43201

The Defense Metals Information Center was established at Battelle Memorial Institute at the request of the Office of the Director of Defense Research and Engineering to provide Government contractors and their suppliers technical assistance and information on titanium, beryllium, magnesium, aluminum, refractory metals, high-strength alloys for high-temperature service, corrosion- and oxidation-resistant coatings, and thermal-protection systems. Its functions, under the direction of the Office of the Director of Defense Research and Engineering, are as follows:

1. To collect, store, and disseminate technical information on the current status of research and development of the above materials.

2. To supplement established Service activities in providing technical advisory services to producers, melters, and fabricators of the above materials, and to designers and fabricators of military equipment containing these materials.

3. To assist the Government agencies and their contractors in developing technical data required for preparation of specifications for the above materials.

4. On assignment, to conduct surveys, or laboratory research investigations, mainly of a short-range nature, as required, to ascertain causes of troubles encountered by fabricators, or to fill minor gaps in established research programs.

Contract No. AF 33(615)-1121
Project No. 8975

Roger J. Runck

Roger J. Runck
Director

DMIC Report 210
October 26-28, 1964

PROBLEMS IN THE LOAD-CARRYING APPLICATION OF HIGH-STRENGTH STEELS

A Symposium Sponsored by the
Tripartite Technical Cooperation Program (TTCP)
Sub-Group P on Materials
Working Panel on Metals

to

OFFICE OF THE DIRECTOR OF DEFENSE
RESEARCH AND ENGINEERING

DEFENSE METALS INFORMATION CENTER
Battelle Memorial Institute
Columbus, Ohio 43201

TABLE OF CONTENTS

TABLE OF CONTENTS (Continued)

AUTHOR INDEX

PREFACE

S. L. Gertsman and N. E. Promisel*

In 1957, the President of the United States and the Prime Minister of Great Britain made a "Declaration of Common Purpose". Subsequently, the Canadian government also subscribed to this document, which has recently been reaffirmed by the three governments. The Declaration pointed out a principle of interdependence, based on the concept that the resources of the three countries, and in particular their skilled scientific and technical manpower, could be used to much greater advantage if closer collaboration could be achieved. Accordingly, provisions were made under this Declaration to exchange non-atomic information, independent of any atomic information exchange considerations.

From this Declaration of Common Purpose there has emerged the Tripartite Technical Cooperation Program, the primary objective of which is to eliminate wasteful duplication of Defense research and development and to transfer this effort to fields which are inadequately covered, thus enabling Defense funds to be applied more effectively. A sub-committee reviews the objectives, the resources employed, and the progress achieved in the three countries. It formulates proposals designed to obtain the maximum cooperation and optimum employment of the resources at hand. It also tries to insure complete and continuous interchange of information among the three countries in the specified fields of research and development. This should lead to improved equipment for the armed forces and also should increase the opportunities for the standardization of weapons.

As part of the organization of the TTCP, a Sub-Group on Materials was established which has within it the Working Panel on Metals, the sponsor of the symposium described in these proceedings. The establishment of the Sub-Group on Materials derived from full recognition that advances in performance of weapons and supporting equipment were increasingly dependent upon the improvement in the knowledge of the properties and applications of materials and on the improvement of the materials themselves. Ultrahigh-strength steels comprise one important segment in the spectrum of materials which, in the opinion of the Working Panel, required intensive exploration.

The Panel came to the conclusion that the expanded usage of these steels to many applications in which weight is a major design consideration was being delayed by inadequate knowledge connected with deficiencies in these materials, such as fracture behavior, and the lack of agreement concerning the design significance of the available test data. The applications that could be expected to benefit from these steels are exemplified in pressure vessels, hydrofoil plates, aircraft and missile structures, fittings and landing gear, gun components (tubes, mounts, breech rings, etc.), shell and war head components, combat vehicles, high-strength fasteners, portable military bridges, and many others. Discussion of these items led, naturally, to considering a symposium on ultrahigh-strength steels for these purposes.

In examining the desirability of such a symposium, the Working Panel was fully aware of the significant number of symposia which have been and are being held on this general subject, but were forced to conclude that, in spite of the excellence of the meetings held, the programs were not primarily oriented toward a definition of the problems and the obstacles which militated against the very beneficial expanded application of these steels. The decision was made, therefore, to hold a conference with the emphasis directed toward these problems. However, because the meaning of the words "high strength" depends on the field of application, and in order to limit the conference to a practical scope, the term "high-strength steels" for the purposes of this symposium was defined as wrought steels having a 0.2% proof strength of approximately 225,000 psi as a target minimum.

The objectives of this symposium, therefore, are to provide an effective means for reviewing the existing technical situation, examining the applications that would benefit from the use of the steels, defining the major problem areas that are retarding their use, describing what is being done in these areas, and indicating promising avenues for prospective improvement.

Pursuant to the above objectives and because of a practical necessity for limiting the symposium to two and one half days, five major topic areas and sessions were planned, with coverage as described under each session in the detailed program included later in this report of the symposium proceedings. The last session also included a summarization of the highlights of the papers and of the discussions as compiled by a special group that had been assigned, a priori, the responsibility for being particularly attentive to the presentations and discussions, for this very purpose. This approach made it possible for the Working Panel, in an executive session immediately following the symposium, to discuss specifically the highlights of the symposium while they were fresh in the minds of the Panel, and to proceed with planning appropriate subsequent activities. These highlights appear at the beginning of this report as a Summary, for ready reference and to permit the reader to select topics of particular interest to him for more detailed reading in the complete papers which follow.

The Working Panel on Metals desires to take this opportunity to state that, in its agonizing reappraisal of the symposium after its completion, it has concluded that the participants indeed represented and demonstrated an outstanding cross-section of capability in this field and that the information presented in this symposium provides a significant basis for establishing future cooperative efforts among the three countries. The Working Panel also desires to express its appreciation to all the participants for their important contributions.

* S. L. Gertsman, Chairman, Working Panel on Metals and N. E. Promisel, Chairman, Symposium Committee

CONCLUSIONS AND SUMMARY OF THE TTCP SYMPOSIUM ON HIGH-STRENGTH STEELS

N. H. Mason*

CONCLUSIONS

Despite several successful applications of hardened-and-tempered steels with 0.2% yield strengths of 225,000 psi and above, designers are cautious in adopting such steels on a wider scale. The reasons for this reluctance can be summarised under a number of headings.

Lack of Advantage

Certain applications of steel call for rigidity of the component and in such cases, replacement of a part by a lighter one in stronger steel is impractical because of loss of stiffness. What is needed in such cases is an increase in Young's modulus as well as an increase in ultimate tensile strength.

Cost

Vacuum melting of expensive materials to obtain a high degree of cleanness, special heat treatments for forging and to develop properties, special corrosion-protection treatments, and rigorous inspection lead to high cost. Although, when service equipment is concerned, cost alone is not a deterrent, there are limits to expenditure. High cost may be offset by weight saving and space saving, features not restricted to aircraft. Every pound saved in service equipment of all types results in a much greater saving by the time the equipment has reached its theatre of operation.

Manufacturing Difficulties

Most manufacturing difficulties have been overcome, at a cost, but extreme vigilance has to be maintained at every stage of design and manufacture of a part. Examples of special requirements are:

Avoidance of Stress Raisers

Obvious stress raisers are sharp corners and abrupt changes in section. Less obvious ones are superficial damage marks, residual stress as a result of inappropriate machining or grinding, or straining during assembly.

Fabrication

High-temperature heat treatment after welding is a complicating requirement for steels other than the maraging steels. This rules out steels for many applications. Cold forming of sheet by the conventional processes is either difficult or impossible (it is not possible to roll-form sheet thicker than 0.02 inch).

Machining

Most machining difficulties have been overcome and satisfactory techniques that sometimes depart widely from established practice have been evolved. It is necessary though to ensure adherence to them. Major hazards are the formation of untempered martensite, particularly in holes, and residual tensile stresses.

Corrosion Protection

Although some users have obtained years of satisfactory service from parts protected by conventional cadmium plating and parts treated with organic protectives, the risk of hydrogen embrittlement continues to be a deterrent. Plating baths that do not cause hydrogen embrittlement have been developed, but they lack the simplicity in operation that is essential to inspire confidence in their use in a plating shop. Another time-consuming activity is a need to protect the parts against corrosion during manufacture.

Unsatisfactory Mechanical Properties

The two shortcomings that occasion most unease are undoubtedly low resistance to crack initiation and low resistance to crack propagation. Low level and scatter of transverse properties and fatigue endurance are other drawbacks, but these are easier to combat than the first two.

Risk of Service Failure

The main risks of service failure are those resulting from corrosion either alone or accompanied by static or cyclic stress. The unavoidable interaction of these modes of failure with hydrogen embrittlement confuses the position even more, and tests to simulate behaviour under such complicated service conditions are impossible. The risk of failure under corroding conditions is heightened by the low tolerance of the steel to crack initiation and propagation.

Recommendations

The identifying of a shortcoming leads naturally to a recommendation that further work should be done on it. There is, therefore, little point in enumerating obvious fields of work that should be further explored. There is, though, one important inadequacy, i.e., the inadequacy of techniques for locating and identifying internal or physically obscured defects. The minimum size of defect detectable, the ability to find nonlaminar defects and defects not parallel to the surface, and the identification of the type of defect discovered all need to be improved.

*Chairman, Listening Panel; assisted by H. Tardif, I. Berman, P. Hendricks, J. Fielding, and R. Runck.

SUMMARY

Opening Session

The first session of the symposium deals with the broad subject of high-strength steels, including the state of the art, applications, and design-material relations. There were 5 papers in the session.

The first paper is a survey of the field of ultrahigh-strength steels.[1]* Eight types of steel are recognized, i.e., low alloy, 5% Cr-Mo-V, martensitic stainless, age-hardening martensitic stainless, cold-rolled austenitic, precipitation-hardening austenitic, 18% nickel maraging, and 9Ni-4Co. Usage patterns for the various types of steel with the exception of the last type have developed, but the strengths being employed in actual parts are appreciably lower than those obtainable by current treatments and considerably lower than those obtainable by treatments regarded today as being exotic. Ten reasons are given why figures obtainable by current treatments are not being used. Substantial increases in smooth-bar strength are possible through thermomechanical treatments, a subject dealt with more fully in another paper.[16] It is not unlikely that steels with a yield strength well in excess of 400,000 psi will be in use in a very few years, but this use is contingent on avoidance or elimination of the drawbacks referred to.

This paper is followed by three papers setting out service applications and property requirements. The papers were supplied by the U. S. Air Force, the U. S. Army, and the U. S. Navy.

The Air Force paper[2a] draws attention to the increased severity of conditions of service today as compared with those obtained a few years ago, and summarizes the problems involved in the successful use of very strong steels. It lists the requirements for the use of such steels as follows:

(1) Cleanness and suitable metallurgical structure (including optimum grain flow in forgings)

(2) Avoidance of stress raisers and sharp corners

(3) Avoidance of surface damage in processing

(4) Prevention of corrosion effects and hydrogen embrittlement

(5) Resistance to crack initiation and propagation

(6) Resistance to fatigue failure

(7) Development of adequate inspection techniques.

Examples are given of the serious consequences of not recognising the importance of, nor guarding against, the influence of some of these factors. Examples are the presence of untempered martensite in drilled holes, incorrect servicing procedures, penetration of plated cadmium into parts periodically heated, inappropriate plating procedure and incorrect grain flow. Of the physical properties needed, fracture toughness is cited as one of the most important. It is stressed that successful applications of the very strong steels call for a constant monitoring of processing techniques from the melting process to the servicing of the part. Current nondestructive-testing techniques are thought to be inadequate.

The Army contribution[2b] describes components which, when made in very strong steel, failed in service and had to be replaced by others in more ductile steel. Work in hand directed towards the solution of problems encountered in the use of the very strong steels is referred to. A straightforward replacement of a part by a lighter one in stronger steel is not always possible because a thinner part may fail due to instability, or the part could suffer from excessive deflections and natural frequency shifts that would affect its dynamic behaviour. Much effort is being devoted to the study of brittle behaviour and lines that are being followed are described. The need for refined stress analysis is indicated.

The Navy paper[2c] stresses the importance of structural reliability and notch sensitivity and draws attention to deficiencies in design and to surface deterioration. A service failure concerned a part that failed at only 12 percent of the expected breaking stress of 280,000 psi, as a result of a crack less than 0.2-inch deep. If the part had been heat treated to a lower strength level, it would most probably have withstood a much higher load. In another paper,[11] it is stated that the smallest flaw known to cause a failure (in a rocket-motor case) was 1/32-inch long and 1/32-inch deep. The severe conditions of service encountered by submarine hulls are quoted with the difficulties of satisfying these when employing a steel of the required 200,000-psi yield strength. The dangers of stress corrosion, the difficulty in detecting it, and the need for more effective means of preventing it, are emphasised, as also is the need to devise production methods that can take advantage of the fruits of research.

The final paper[3] in the session deals with design parameters in materials selection. The author utilizes a "design sciences" approach. This approach uses idealised structural configurations such as stiffened-box beams and stiffened cylinders as representative structures, to establish optimum designs to enable the efficiencies of various materials to be evaluated. Ultrahigh-strength steels do not appear to have any application for surface ship hulls nor for a specified range of hydrofoils. For subsonic and supersonic wings and tails, steels above the 300,000-psi yield strength level can be competitive with titanium at the higher end of the design-index range. For rocket-engine cases and ordnance, i.e., material that is subjected to short-time tension loading, steels at the 300,000-psi level

*Numbers refer to the papers listed in the Table of Contents.

have structural potential, although from the standpoint of minimum weight, titanium alloys and glass-filament-wound structures can be competitive. Deep submergence hulls, where the loading is in compression for a long time, are a likely use for 300,000-psi steel, although the insistence on welding would be a retarding factor. The low ductility of the steels also will militate against their use as pressure vessels. Possible design solutions for these two cases are suggested, and some approximate guide lines for the use of very strong steels in tension structures are laid down. Design requirements are related to stress-concentration factors ranging from 1 to more than 8. They vary from "meticulous" through "careful" to "routine". Approaches to ease the current limitations to the use of very strong steels are suggested.

The remainder of the papers related to specific properties and have been abstracted under these properties:

Effects of Primary Processing
Welding
Sheet Forming
Machining
Corrosion
Hydrogen Embrittlement
Notch Sensitivity
Factors Affecting Fracture
Fatigue
Maraging Steel
Quenched-and-Tempered Steels
Thermomechanical Treatment
Strengthening Mechanisms.

Effects of Primary Processing

The paper on primary processing[4] embraces melting, forging, and rolling processes. The melting and product characteristics of air-melted and vacuum-melted steels are described, the term "vacuum melting", including vacuum degassing plus carbon deoxidation as well as induction-vacuum melting (IVM), and consumable-electrode vacuum melting (CEVM), and combinations thereof. A combination of IVM and single or double CEVM, using vacuum-melted electrodes, gave a product superior in every way. Spectacular increases in the direction transverse to the principal direction of working were obtained. Examples of improved qualities developed in actual forgings are quoted, and reference is made to a new steel with useable ductility at 325,000-psi yield strength. The advantages of electron-beam melting, remelting through a flux blanket and carbon deoxidation are referred to, and in the field of hot working, the improvement in properties and performance resulting from special thermal cycles after hot working is described.

Welding

There are two papers devoted to welding. One is limited to joining problems of a metallurgical nature and the other deals with the factors that affect crack initiation and slow propagation.

In the first paper,[5] it is stated that the tungsten-inert-gas process, using a cold wire of matching composition is the usual method employed and is always followed by heat treatment. Four types of high-strength steel are considered, i.e., quenched and tempered, cold-worked stainless, precipitation-hardening stainless, and maraging. The defects and difficulties liable to be encountered in their welding are described and suggestions are made on how these may be overcome. The maraging steels offer the greatest promise as weldable high-strength steels, but more research is needed to establish an adequate welding technology. A testing technique designed to provide a quantitative evaluation of hot-cracking tendency is described.

The second paper[12] deals with the factors that affect crack initiation and propagation in thin-walled rocket-motor cases of welded construction. The paper differentiates between cracks initiated in the weld zone and in the parent metal outside the weld zone, and stresses the importance of using steel with a high resistance to hot cracking. The factors that influence crack initiation in the parent metal are discussed below under "Factors Affecting Fracture". Fatigue tests on welded 18Ni maraging steel[13] suggest that the material with the most inclusions gave the best performance. The author considers though that the conclusion is spurious and that further work is needed.

Sheet Forming

The paper on sheet forming[6] brings out the manufacturing problems encountered and the limitations that result from high tensile strength. High-strength steel sheet thicker than 0.020 inch cannot be rubber formed. The high creep resistance of most of the high-strength steels eliminates them from hot-finish forming, while resistance to deformation at temperatures below the recrystallization temperature eliminates them from hot forming in general. High-velocity forming tests of H-11 at room temperature were, however, successful and encouraging properties were obtained on 18%Ni maraging steel back-extrusion shear formed at room temperature. Sketches of typical forming failures are given and helpful data on forming of high-strength steel by various methods relative to other high-strength alloys are quoted. The paper has a strong practical flavour.

Machining

The paper on machining[7] draws attention to the advantages of low-stress machining and grinding conditions to control surface effects, such as plastic deformation, temperature gradient, residual stress, metallurgical transformation, over tempering, surface cracking, and surface texture. The ways in which these effects can affect properties and performance of a part are shown. One of the more important defects resulting from incorrect machining, including electrical-discharge machining, is untempered martensite, a danger referred to in another paper.[2] This constituent

is inherently brittle and often cracks almost immediately, and the cracks are very liable to propagate by stress corrosion, corrosion fatigue, or brittle fracture. A technique designed to measure the residual stress resulting from machining and grinding is described as are processes that minimise the depth of the stress layer by paying attention to wheel speed, type of wheel, depth of pass, and nature of grinding fluid. The magnitude of the residual stresses produced in high-strength steels by milling and grinding can be extremely high. Very bad practice has produced a residual tensile stress of 200,000 psi but 100,000 psi is frequently observed. Residual stresses may be considerably reduced by stress relieving at an appropriate temperature and by abrasive tumbling and shot peening. They can be detected by acid etching, which in severe cases will result in cracking and by X-ray diffraction techniques. The use of ultrasonics for the same purpose is being explored. Considerably more work is needed to help designers and manufacturing engineers to make parts more accurately by control of distortion and to make parts more reliable through control of their fatigue and stress-corrosion characteristics.

Corrosion

There is one paper on "Corrosion Protection" and one on "Stress-Corrosion Cracking and Corrosion Fracture".

The paper on "Corrosion Protection",[8] is confined to aerospace components requiring complete protection. A number of examples of failure in service are given. When dealing with the protection of very strong steels, the author stresses the unavoidable interaction that occurs with hydrogen embrittlement and lays down 12 characteristics of the ideal coating and coating process. Factors that affect the hydrogen-embrittlement characteristics of plating baths are stated and the Lawrence hydrogen-detector gauge is described. Although residual tensile stresses can be so reduced that they do not affect the behaviour of a part before it goes into service, they can induce failure by hydrogen embrittlement when they are supplemented by other stresses developed by mismatching or minor deformations resulting from incorrect stressing. Other undesirable effects of residual stresses that have been ostensibly nullified by a pretreatment are quoted. The Bureau of Naval Weapons procedure for the protection of parts in very strong steel is given, and there is sound advice on spray metallising and the use of vacuum-deposited cadmium. Protection techniques currently being examined are plasma spraying and aluminum deposition by methods other than spraying, such as decomposition of metallo-organic compounds and in pigments in inorganic and organic type binders. Protection where dissimilar metals are involved and the use of electrodeposited coatings to resist wear are discussed. The author believes that the study of solid surfaces by physicists using field-ion and field-electron microscopy and low-energy electron diffraction will eventually provide the knowledge needed for the understanding of corrosion processes and quotes some hitherto unpublished and highly informative work done in this field.

In the paper on stress-corrosion cracking and corrosion fatigue,[9] it is stated that present test methods indicate that many heat-treated steels are susceptible to stress-corrosion cracking at strength levels as low as 150,000 to 175,000-psi yield strength in reasonable environments; and as the susceptibility to hydrogen embrittlement also develops in this strength range, cathodic protection in seawater cannot be used. The disastrous effects which sometimes result from the extension of small flaws caused by stress corrosion are described. The need for impermeability of coatings to humid air is stressed and it is pointed out that organic coatings which are normally adequate for preventing general corrosion, may not prevent stress corrosion. When testing for stress-corrosion cracking and corrosion fatigue, it is preferable to start with a specimen containing a pre-existing crack that will result in high stress intensity, rather than a specimen containing a stress raiser such as a pit. Data obtained from the behaviour of such a specimen should, in principle, be related to the stress and crack size needed to cause a stress-corrosion crack to grow in a structure. Such a test would be in the "K" stress-intensity concept, and the author demonstrates the effects of stress-intensity and notch-toughness ratios on the time to fracture of precracked specimens. Interesting possibilities are demonstrated where the relationship between flaw size and susceptibility could be examined. The maximum flaw size that can be permitted without crack growth by stress corrosion can also be calculated.

As regards corrosion fatigue, there is a meagre amount of information available about the behaviour of very strong steels. One cannot consider it in isolation. To all the complexities of stress-corrosion cracking, one must add an infinite number of forms of load/time profile with variations in maximum load, average load, and frequency. There is little to be gained by making corrosion fatigue tests in seawater on a material that would fail rapidly in those conditions under static stress alone; and tests in the atmosphere or tests under extremely low-cycle high-stress conditions--similar to those employed in pressure-vessel testing--are likely to be most informative. Although impressed cathodic current can restore the air-fatigue life of mild steel under conventional conditions, it should not be assumed that cathodic protection can prevent corrosion fatigue of the steels under discussion.

The results of corrosion fatigue tests on maraging steel are summarised in the paragraph on "Maraging Steel".

Hydrogen Embrittlement

This subject is referred to in several papers, but one paper[10] is devoted solely to it. The author

sums up the current theories of hydrogen embrittlement and points out that there are only two facts that are known with certainty, i.e., that hydrogen moves through steel in the ionised atomic form and that the atoms move to regions under triaxial tensile stress. The nature and location of the hydrogen, the forms of hydrogen responsible for embrittlement, and the mechanism by which hydrogen reduces the cohesive strength of steel still await positive answers. In industrial applications it appears that cleanness of steel, surface compression stress, and the use of dry-cleaning processes as opposed to wet or acid-cleaning ones, are practices that will prevent the absorption of hydrogen. The production of satisfactory cadmium coatings still present difficulties. With adequate control of procedure satisfactory service lives can be obtained from plated parts. Many firms, however, prefer to use a phosphate treatment instead of electrodeposited coatings. Work designed to correlate hydrogen content with degree of embrittlement as shown by a sustained load-notched test has established a fair degree of correlation between embrittlement and hydrogen extractable at 200 to 300 C and a cooperative exercise between a number of U. K. laboratories established that 0.03 to 0.05 ppm of hydrogen extractable in the temperature range stated is the threshold quantity that causes embrittlement in steels of normal purity. For high-purity steels the threshold may be 0.3 to 0.5 ppm. The relation between hydrogen content and fatigue strength is discussed and between hydrogen embrittlement and stress corrosion. The theory that stress corrosion failure results from hydrogen embrittlement is not supported by the fact that 5%Cr steel and 18%Ni maraging steel are more susceptible to stress corrosion than to hydrogen embrittlement. In another paper[11], reference is made to the service failures of three aircraft parts in AISI 4340 with a yield strength of 235,000 psi. All the failures were attributed basically to this cause.

Notch Sensitivity

There is a most comprehensive paper on this subject.[11] Over a hundred publications were reviewed and 77 references are given. Notch toughness is defined as the reaction to stress concentrations, whether design discontinuities, surface cracks, or internal flaws. K is recognised as the stress intensity factor and G the crack extension force or energy release rate. Notch-toughness data are reviewed using four categories of steel, i.e., low alloy structural, hot die and tool, nickel alloy, and precipitation hardening. Two values are used, i.e., notch strength ratio and critical strength-intensity factor K_c or K_{Ic}. No data are included from Charpy impact tests as in the author's view the test is insufficiently discriminatory. The 18%Ni maraging steel was found to be definitely superior to the earlier steels used and the 9%Ni-4%Co steel is thought to have desirable characteristics. The poorest of the well known steels was H.11. The effects of processing variables on toughness, i.e., melting practice, chemical composition, thermomechanical treatments, environment, and loading rate are discussed. Contrary to general belief, it seems that vacuum melting does not necessarily produce a material with superior notch toughness. The effects of vacuum melting vary with the alloy but it has a general effect of reducing directionality. The effect of alloying elements in detail is not examined but there is strong evidence of the deleterious effects of sulphur and phosphorus. Decarburisation should be advantageous for such items as rocket-motor cases, but more information is needed on its effect on fatigue. Water or water-vapour environment can have an accelerating effect on slow crack growth and some alloys have been found to be more susceptible than others. There is little information on the effects of loading rate but where high strain rates are a service condition or a potential hazard, evaluation under comparable loading rates is advocated. The tests on actual parts are largely confined to those on pressure vessels but some have been made on recoilless rifles and aircraft landing gear. The rifles, which were made from steel with 220,000 psi yield strength were satisfactory. In dealing with design requirements the scatter in notch-toughness values on a particular alloy demands a notch-toughness test in a specification. The test should cater to any extremes of temperature that will be encountered in service as in general the notch toughness decreases with temperature. With the aid of fracture mechanics and a knowledge of the fracture toughness the critical flaw size for the operating conditions can be derived but to obtain the limiting initial flaw size, and hence the level of inspection required, data must be obtained on the rate of flaw growth. Examples are given of data of different types calculated using this approach. It is recommended that certain approaches be explored in connection with prediction of behaviour under cyclic loading. Numerous other design procedures and criteria, not all based directly on fracture mechanics are described. Referring in particular to steel with a yield strength above 200,000 psi, attention is drawn to work that has shown that at this level the Charpy V upper shelf or plateau energy may drop to 15-20 ft-lb, which means that the ductile energy absorption is comparable with the energy absorption for brittle fracture of lower strength steels. The consequence of this is that "no cleavage" fractures may start from small flaws at elastic stress levels close to the yield strength. In conclusion, the author points out that a number of criteria are now available to the designer of parts in ultrahigh-strength steel and that for "one-shot" loading the β_c criterion has been found to correlate well with service performance. For conditions involving cyclic loading allowance must be made for possible slow crack growth and the environment should be considered. Shock loading applications call for more severe tests. Simpler tests, e.g., the instrumented bend test, might profitably be explored for some applications.

Factors Affecting Fracture

In the paper devoted to this subject[12], the author maintains that to evaluate truly the suscep-

tibility of a material toward cracking in the absence of a mechanical notch, a bend test on a wide specimen is most suitable. The results of tests over formers of different radii show that the limiting radius is related to the impurity level of the steel. Using an instrumented bend test a "crack-initiation susceptibility" figure is derived. Other uses of the instrumented bend test are described, i.e., to study the effects of tempering temperature, decarburization, surface treatment, and corrosion on crack-initiation susceptibility in 3%Cr-Mo-V steel and 18%Ni maraging steel. There is evidence that the test may be made to record the deformation that occurs before crack initiation and also slow crack propagation. Satisfactory correlation was obtained between crack-initiation susceptibility values and values for structural efficiency of rocket-motor cases and tubes. There was also good correlation with plane-stress fracture toughness K_C values although it was found that a high K_C value did not always give a high structural efficiency, the higher efficiencies being obtained with the lower K_C values. One important finding is that the steel having the higher resistance to crack propagation had the greater susceptibility to crack initiation. This suggests that the evaluation of high-strength steel in terms of K_C only may not be adequate and highlights the need for more work on factors affecting crack initiation.

Fatigue

There is one paper[13] on this subject. A survey of the fatigue properties of 17 steels with a 0.2 per cent yield strength greater than 200,000 psi showed that regardless of the static strength the endurance limit for 10^8 cycles was limited to about 120,000 psi. High scatter of test results at low stress levels was found and evidence derived from statistical and metallurgical studies showed that more than one mechanism of fatigue is involved in causing failure in the region of the endurance limit. The statistical grouping might profitably be examined with the object of isolating the fatigue properties responsible for the different groups. Factors identified as influencing fatigue behaviour are environment (humidity) and hard inclusions. The replacement of the endurance limit by a new criterion called the "Rayleigh fatigue strength" is advocated. This criterion, which is described, is referred to as a unique repeatable test configuration which can be of great value in assessing fatigue strength under service loadings. The criterion has been employed to assess the effect of the manufacturing process, some effects of welding, and the effect of surface condition. Results of an intensive study of the fatigue properties of 18%Ni maraging steel are given. These are summarised in the paragraph below. The author considers that although the traditional constant amplitude type of fatigue test is discredited on statistical and economic grounds in its use to determine an endurance limit it may nevertheless be useful to isolate the different fatigue processes that seem to exist in metal fatigue. He advocates the use of a stationary random process type of fatigue test evaluation.

Maraging Steel

Maraging steels are referred to in several papers, but one paper[14] is devoted to their physical metallurgy and properties. The paper is restricted to the 18%Ni variety. Information is given on the following properties: recommended chemical composition, tensile properties (including K_{Ic}), transformation characteristics, microstructure, strengthening mechanisms, roles of alloying elements, effects of overaging, segregation, banding, retained austenite, thermal embrittlement, thermal stress and weld cracking, and effects of minor and residual elements. Fatigue properties are discussed in another paper.[13] In this investigation, the author uses three batches of steel made by consumable-electrode vacuum remelting with vacuum casting, air melting with vacuum-stream degassing, and air melting-air casting. The work was done to assess the fatigue life of a hydrofoil main foil. Preliminary rotating beam tests revealed that the scatter of test results at low stress levels could be consistently greater than 100 to 1. Using the Rayleigh criterion referred to earlier, it was found that vacuum techniques not only resulted in a greater mean endurance, but reduced the variability or scatter in the test results appreciably. Fatigue tests on welded joints established that the quality of the weld resulted in greater variability than the melting process and that the direction of the weld did not have much effect on the fatigue life. The effect of not machining away the scale formed on the surface of unwelded specimens when aged at 900 F was investigated and it was found that the notch effect resulting from the scale was of a similar magnitude to that obtained using weld specimens. Size effect was investigated and found to be appreciable. Corrosion fatigue was investigated both in the usual manner and by examining the effect of coolant used in grinding entrapped in welded joints. The endurance of smooth specimens tested as rotating beams in salt water gave an alternating stress value for an endurance of 10^7 cycles of only ± 14,000 psi compared with a published value of 84,000 psi in air. Corrosion-fatigue condition overrode the greater mean endurance and lower scatter encountered in the vacuum-melted steel.

Quenched and Tempered Steels

There is one paper devoted solely to this topic.[15] The paper is very comprehensive. The history of the development of the steels is given and their properties are summarised under the headings low alloy, modified die, and high alloy (9%Ni, 4%Co). Some reference is also made to the 18%Ni maraging steel. The effect of tempering temperature on ultimate tensile strength, 0.2% yield strength, elongation, reduction of area, and Charpy impact values of 4 quenched and tempered steels with some comparative values for 18%Ni maraging steels are given and it is shown that for the higher tempering temperatures the yield/ultimate ratio is about 0.9, which affects design concepts and manufacturing techniques. This value also occurs in the maraging steel. Although the Charpy V notch

test is criticised it is useful when considering parts subjected to high strain rates because high strain rates raise the ductile-to-brittle transition temperature and impact tests at low temperatures can be informative. The impact properties of HP 9-4-45 in the bainitic condition are outstanding. This superiority does not apply to fatigue properties according to the few results available. The main problems affecting the use of the steels are low level and scatter of transverse properties and fatigue endurance, poor impact properties (particularly low temperature transverse), poor fracture toughness, machining difficulties, hydrogen embrittlement, and stress corrosion. The deleterious effect on impurities is illustrated and the improvements derived from vacuum melting. For sheet at yield strengths of about 200,000 psi, there is little to choose between the steels on the score of notch tensile strength. Estimates of the flaw size that can be tolerated at various operating stress levels are given. It is suggested that isothermal transformation to a lower bainite structure as used for the HP 9-4-X alloys or limiting tempering to the end of the first stage of martensite breakdown might produce improved notch toughness. About hydrogen embrittlement, there is still insufficient information about the relative merits of various steels, but it is suggested that a steel with low diffusion rates would have a lower susceptibility to embrittlement. In the machining field more work is needed on tapping and perhaps milling. The quenched and tempered steels available permit the use of design based on 0.2% yield strength values up to 300,000 psi, but allowance would have to be made for the ductility to be expected. To improve the position, research is needed into the metallurgical factors that influence fracture toughness. Three main lines of alloy development are recommended, i.e., development of alloys suitable for ausforming, strengthening by precipitation of compounds other than carbides, and study of isothermal transformation to lower bainite and its effect on toughness.

Thermomechanical Treatment

In the main paper[16] on this subject, the author recognises three types of ausforming involving deformation either before, during, or after transformation of austenite, but the only one discussed is the first. The response of metastable austenite to deformation and the mechanism by which the condition of the strain-hardened austenite influences the strength of the final product are examined and support is found for the theory that alloy carbide precipitation during the austenite deformation phase is a major factor in the achieving of ultrahigh strength. The most effective carbide formers have been found to be molybdenum, chromium, and vanadium, and the higher strengths result only if the carbides are in solid solution in the austenite. The characteristics of ausformed martensitic structures are finely dispersed deformation-produced precipitate and high-dislocation density, the dislocations having been inherited from the austenite and also produced from the lattice shear and dilation associated with the austenite-martensite transformation. The controlling factors are carbon content, alloy composition, and conditions of deformation, and the optimum combination of strength, ductility, and fracture toughness is the result of the maximum amount of deformation compatible with the minimum amount of carbon to produce a desired strength level. A significant increase in strength is achieved by deformation exceeding about 50 per cent. In another paper[17], the high strength of ausformed steels is attributed to the additive effects of four hardening mechanisms, i.e., a fine grain size from the martensite, a dispersion of alloy carbides, a high dislocation density, and a component from solute elements in substitutional solid solution. Comparing the mechanical properties of ausformed steels with those of conventional quenched and tempered steels at the same strength level, the ausformed steels have superior fracture toughness and tend to retain the 50 per cent ratio of endurance limit to tensile strength at higher strength levels. Examples of the use of the steels are leaf springs, torsion bars and punches. A certain cold heading punch in ausformed steel had three times the life of the normal punch and had been made from steel containing about a quarter of the alloy content of the normal one. The reader is warned that the ausforming process is not simple. It requires close control of both temperature and deformation and is not the solution to all high-strength steel problems.

Strengthening Mechanisms

The author points out[17] that high strength in steels is the result of not a single hardening mechanism, but of combinations of mechanisms. Four basic hardening mechanisms are described, i.e., dislocation-dislocation, dislocation-solute, dislocation-dispersed phase, and dislocation-grain boundary interactions. These four can be combined in six different ways--taking two at a time--and in four different ways taking three at a time. There is also the possibility of making all four mechanisms operate simultaneously. There are, therefore, eleven cases of additive hardening possible. A brief discussion of the various cases in relation to iron and steel is given. The most effective combination of three hardening mechanisms is probably solid-solution plus dispersed phase plus work hardening. An example of additive hardening is hard drawn steel wire. In this case contributions from work hardening, precipitation hardening, solid-solution strengthening, and a dispersed phase are distinct possibilities. The high strengths of fine internally twinned high-carbon martensites probably result from three causes, i.e., solid-solution hardening from interstitial carbon, the substructure of martensite, and work hardening, usually from the high-dislocation density generated during the shear transformation. A better understanding of the reasons for the hardness of martensite is likely to come from a study of the mechanical properties and microstructure of iron-nitrogen alloys. Work on secondary hardening of vanadium steels shows that factors that tend to increase still further the dislocation density after the quench would enhance the hardening response.

HIGH-STRENGTH STEEL PERSPECTIVES

A. M. Hall*

INTRODUCTION

Man received his introduction to iron some 4,000 years ago, and on the basis of the tenuous acquaintanceship which developed, this element took its place among the seven metals of antiquity. However, to the ancients iron remained an enigma. Sometimes, it could be whetted to an edge of amazing keenness, and the metal was notably stronger than the best bronzes; at other times, it was as soft as copper, and occasionally as brittle as glass. As a consequence, no sustained use was made of iron in the early days of metallurgy.

It was not until the 19th century, nearly four millenia later, that significant strides were made toward understanding this intractable metal. It was not until then that the turbulent liaison between iron and carbon was recognized. Unknowingly, the ancient as well as the medieval iron worker had been struggling at one time with one offspring, and at another time with a different offspring of that alliance. Occasionally, the early metal worker dealt with alloys of iron and nickel obtained in the form of meteorites.

It took the development of analytical chemistry, the metallurgical microscope, and the dilatometer to get the job of comprehending the metal, iron, underway. Once an understanding dawned, ferrous metallurgy surged forward and rapidly evolved from art to science. In the brief period since the days of Réaumur, Sorby, and Osmond, and the birth of metallography, iron and its alloys have become thoroughly established among mankind's essential materials.

At the beginning of this period, the principal ferrous materials obtainable were cast iron, wrought iron, cement steel, and crucible steel. Today, scarcely 100 years later, several thousand steels and other alloys are available to fill a myriad of diverse applications. Iron has proved itself to be an extremely versatile metal, and its alloys display innumerable combinations of properties. Perhaps it is the very intractability of this metal that accounts for its versatility. In any event, it comes as no surprise that iron has responded and continues to respond, with outstanding effectiveness, to the ever-increasing demand for materials of higher and higher strength.

The manner in which ferrous materials have answered the call for high strength in structural applications is indicated in Figure 1. An incautious extrapolation of the upper curve in the figure would suggest a truly remarkable future for iron-base alloys as structural materials! Nonetheless, the facts are that by 1850 wrought iron, with a yield point in the range of 30,000 psi, had established itself as an important structural material for rugged service. A few decades later, with the advent of the Bessemer and open-hearth processes, mild steel emerged as a structural material and usable yield strengths increased. After World War I, quenched-and-tempered steels made a timid debut into structural applications at some 80,000-psi yield strength. By the mid 1950's, massive structures were being assembled from steels heat treated to yield strengths as high as 115,000 psi.

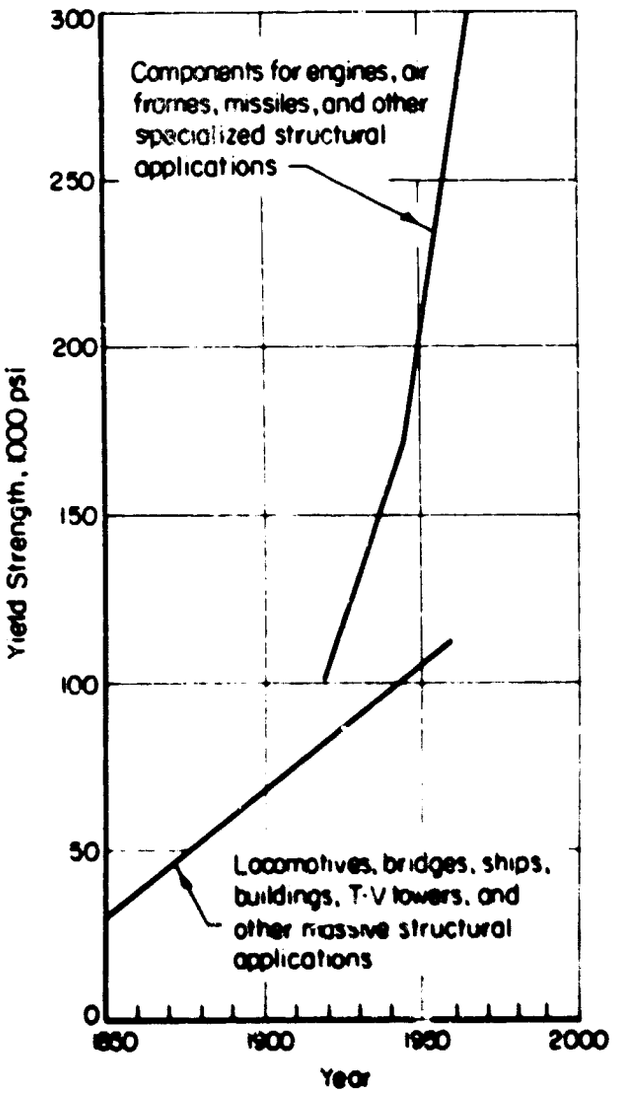

FIGURE 1. INCREASE IN THE YIELD STRENGTH OF STEELS USED IN STRUCTURAL APPLICATIONS DURING THE YEARS SINCE 1850

In the meantime, toward the close of World War I, quenched-and-tempered steels began to be used in a different type of structural application calling for the ultimate in performance and reliability. An early application of this type was components for airplane engines, the steels being heat treated to yield strengths of some 100,000 psi. By 1945 steels were being used in critical airframe applications at yield strengths in the order of 170,000 psi. Today, a number of low-alloy and other types of steel find specialized structural applications at yield strengths of 260,000 to as high as 300,000 psi.

*Chief, Ferrous and High Alloy Metallurgy Division, Battelle Memorial Institute, Columbus, Ohio.

Thus, in the 115-year span since 1850, the usable yield strength of steels in all kinds of structural applications has increased approximately tenfold.

Ultrastrong Steels Currently in Use

If the steels of interest to the present discussion are defined as those which are useful in structural applications at yield strengths of 225,000 psi and above, then several families encompassing some 100 individual steels fill the bill. The first family to have members meeting this definition are the medium-carbon low-alloy quenched-and-tempered steels. In the U. S., the progenitor of this family was the chromium-molybdenum steel, AISI 4130. This alloy was soon followed by the chromium-nickel-molybdenum steel, AISI 4340, which came into use where greater strength in thicker sections than could be handled by AISI 4130 was required. Numerous modifications of both of these types of steel have been developed. The purpose usually has been to increase toughness at very high strength levels and to improve weldability. The modifications have generally taken such forms as increasing the silicon content to avoid 500 F embrittlement on tempering at low temperatures to achieve ultrahigh strength; adding vanadium to promote toughness; consumable-electrode vacuum-arc remelting to reduce gas content, disperse nonmetallic inclusions, and increase homogeneity, thereby improving toughness and transverse ductility; reducing the sulfur and phosphorus contents for the same reasons; and lowering the carbon content slightly to improve welding characteristics as well as toughness.

In addition, as shown in Table 1, nickel-molybdenum and nickel-silicon-molybdenum steels, together with vanadium modifications thereof, have been developed for use at ultrahigh strength levels. At the same time, a strong multi-faceted program on quenched-and-tempered ultrahigh-strength steels has been in progress for many years in the U. K. Both wrought and cast steels are encompassed. Of particular interest has been the emergence from this effort of the copper-silicon-molybdenum-vanadium type of steel.

Another family of steels which have found application in the ultrahigh-strength structural field are the 5 per cent chromium-molybdenum-vanadium steels. These medium-alloy air-hardening steels are, in essence, aircraft-quality versions of the familiar chromium hot-work die steels adapted to structural applications and now available in sheet, strip, and other forms quite foreign to tool and die usage. The individual members of this family are, for the most part, proprietary and display considerable diversity of composition. However, most of them approximate to the composition of AISI Types H-11 or H-13. Variants of these steels are under study in Canada.

TABLE 1. TYPES OF ULTRAHIGH-STRENGTH LOW-ALLOY QUENCHED-AND-TEMPERED STEELS

Chromium-Molybdenum
Chromium-Nickel-Molybdenum
Increased Silicon
Plus Vanadium
Nickel-Molybdenum
Plus Vanadium
Nickel-Silicon-Molybdenum
Plus Vanadium
Copper-Silicon-Molybdenum-Vanadium

Several families of stainless steel, as enumerated in Table 2, have members capable of being used at ultrahigh strength levels. Included are martensitic chromium steels of the AISI 410 and 420 types, martensitic low-nickel chromium steels of the AISI 431 type, as well as age-hardenable martensitic stainless steels. The last-named are characterized by relatively low carbon contents which improve their weldability and the addition of such elements as copper, columbium, titanium, aluminum, and molybdenum which render them age hardenable. One martensitic stainless steel, known as AFC 77 and now becoming commercially available, contains considerable cobalt along with molybdenum and vanadium. This steel has outstanding strength at temperatures as high as 1200 F. Included also are cold-rolled austenitic stainless steels. The earliest of these in the U. S. was the 17 per cent chromium-7 per cent nickel type carrying the designation, AISI 301. Some of the newer types contain as much as 15 per cent manganese together with other elements such as nitrogen, molybdenum, and vanadium. Finally, there are the semiaustenitic stainless steels. The compositions of these steels are so balanced as to render them austenitic as annealed and martensitic through refrigeration or through alteration of the matrix composition by the precipitation of some compound (such as a chromium carbide) on heating at intermediate temperatures. A number of these steels contain such elements as aluminum and molybdenum which promote age hardening.

TABLE 2. HIGH-STRENGTH STAINLESS STEELS

Martensitic
Chromium
Chromium, Low Nickel
Age Hardenable
Cold-Rolled Austenitic
Chromium-Nickel
Chromium-Nickel-Manganese
High Manganese
Semiaustenitic

Among the various types of high-alloy steels in existence, two families have emerged which include members developed expressly for structural applications at yield strength levels above 225,000 psi. One family comprises the high-nickel "maraging" steels introduced a few years ago by The International Nickel Company, Inc. Several 18 per cent nickel variants within this family, which also contain substantial additions of cobalt, molybdenum, and titanium, have recently achieved the status of full commercial availability. Because of their extra low carbon content and their high nickel content, these steels are martensitic as annealed, but the martensite is quite tough and ductile and, hence, is amenable to forming, welding, and machining operations. In spite of its low carbon content, the martensitic structure of these steels is quite strong, having a yield strength in the order of 100,000 psi. A simple aging treatment at moderate temperatures brings about a tremendous increase in strength. Depending on the steel's composition, an increment in yield strength of as much as 200,000 psi can be obtained on aging.

The other family of high-alloy steels designed for ultrahigh-strength service was developed by Republic Steel Corporation. Known as 9Ni-4Co steels, they are hardened by quenching and tempering. One grade, containing nominally 0.25 per cent carbon, is designed for use at yield strengths up to about 200,000 psi. Another grade, with a nominal carbon content of 0.45 per cent, was developed for use at yield strength levels in the order of 250,000 psi.

In Table 3, an attempt is made to highlight the farthest advances, from the standpoint of smooth-bar strength, that have been made to date in the actual application of ultrahigh-strength steels to structural uses. In the table, the steels are treated by family, and the data presented are necessarily rather approximate, as the intent is to be indicative rather than definitive. The forms in which the low-alloy and 5Cr-Mo-V steels are usually used are sheet, strip, bar stock, and forgings. The martensitic stainless and the age-hardenable varieties of this type of steel are frequently used in the form of sheet, strip, small forgings, bar stock, and small castings. Usage of the cold-rolled stainless steels is confined to sheet, strip, and foil. The semiaustenitic stainless steels are generally employed in the form of sheet and bar stock. The high-nickel maraging steels find application usually in the form of forgings, bar stock, sheet, and plate.

The plain high-carbon steels were not included in the table. However, for years these steels, in the form of heavily cold-worked razor-blade strip and music wire, have achieved the highest strengths of any commercially available material. Tensile strengths up to 600,000 psi are obtainable in these materials. In earlier years, steels in such forms would not have been thought of for ultrahigh-strength structural applications. However, with the development of wrapping techniques for the manufacture of rocket-motor cases and the reinforcement of cylinders and other pressure vessels, such materials come in for serious consideration.

TABLE 3. APPROXIMATE UPPER LIMIT OF STRENGTH AT WHICH STEELS ARE USED TODAY

Type of Steel	Yield Strength, psi	Ultimate Tensile Strength, psi	Application
Low alloy	250,000	300,000	Landing-gear components
5Cr-Mo-V	240,000	290,000	Airframe structural and landing-gear components
Martensitic stainless	160,000	180,000	Bolts and high-shear rivets
Age-hardenable martensitic stainless	170,000	190,000	Clamps and brackets
Cold-rolled austenitic stainless steel	180,000	200,000	Liquid-propellant missile tankage
Semiaustenitic stainless steel	220,000	235,000	Honeycomb structures
18Ni maraging steel	295,000	300,000	Fasteners and shafts

Current Applications

Thus, some eight or nine families of steels have become available for ultrahigh-strength applications. At the same time, during the past few years the number of applications calling for ultrahigh strength has mounted. Several hundred can probably be catalogued. It is axiomatic that these applications feature extremely high strength-to-density ratios as a requirement. In many instances, such as airframe and rocket-motor-case applications, vitally important weight savings are brought about by using ultrahigh-strength steels. In other cases, ultrahigh-strength steels are used to reduce the bulk of the component to meet space requirements. This is always a consideration when equipment must fit inside an envelope of fixed size. Another extremely important reason for selecting steel is cost. Steels have lively competition in mechanical and other properties from numerous other materials. However, where the disparity is not vital, steel often wins the day on the basis of costs. The mill products may be less expensive and the cost of fabrication and construction may be less. As an example, costs have figured strongly in the choice of steels for large-sized rocket boosters.

Another advantage in using ultrahigh-strength steels in movable structures is the reduced inertia which accompanies the resulting decrease in weight. This is an important factor in rotating or reciprocating mechanisms such as pumps, engines, actuators, and valves. Finally, in such applications as

components of servomechanisms, the high hardness which accompanies high strength promotes essential wear resistance. The advantages of ultrahigh-strength steels are listed in Table 4.

TABLE 4. ADVANTAGES OF ULT. AHIGH-STRENGTH STEELS

Weight Savings
Reduction of Bulk
Cost Savings
Decreased Inertia
Improved Wear Resistance

The low-alloy quenched-and-tempered steels are particularly attractive because they are well known, are moderate in cost, and have high hardenability making them suited to use in thick sections. A few of their ultrahigh-strength applications are solid-propellant rocket-motor cases; gun tubes and breach blocks; bolts, pins, fittings, and structural components for aircraft; arresting hooks for naval aircraft; and axles, gears, and shafts of many kinds. The use of this type of steel for aircraft landing-gear components is illustrated in Figure 2, which shows the main landing gear for the B-58 supersonic bomber. The strut is a modified AISI 4340 chromium-nickel-molybdenum type steel heat treated to about 200,000-psi yield strength (about 220,000-psi ultimate tensile strength); the links, axles, and piston are the same steel heat treated to the level of about 235,000-psi yield strength (about 280,000-psi ultimate tensile strength). The components depicted are machined forgings. Figure 3 shows a naval aircraft equipped with an ultrahigh-strength low-alloy steel arresting hook.

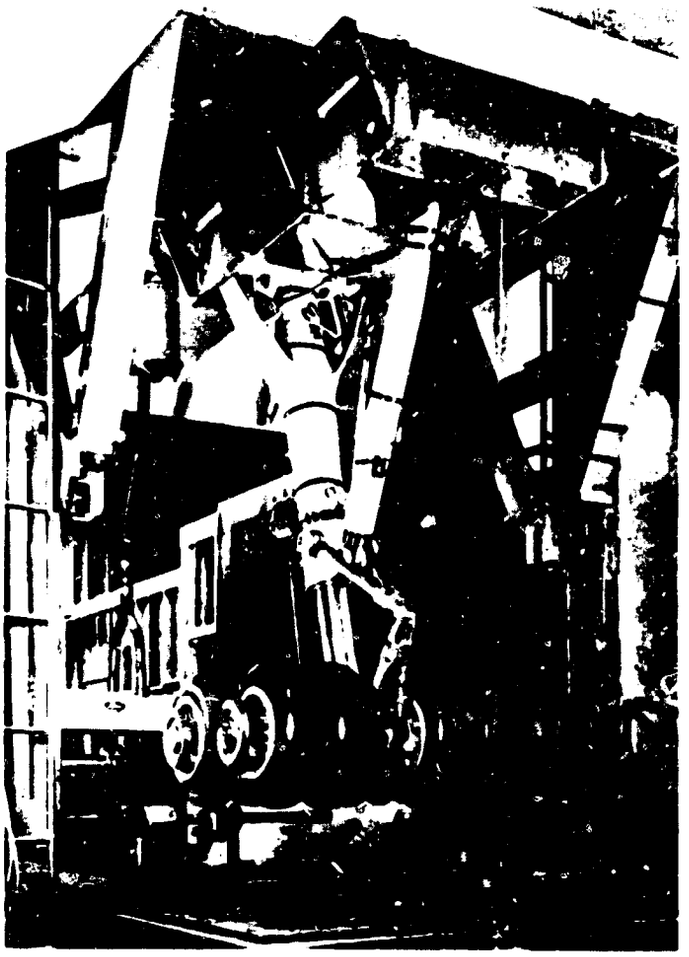

FIGURE 2. MAIN LANDING GEAR FOR THE B-58 BOMBER

Strut, piston, links, and axles are ultrahigh-strength low-alloy steel.

The usage of the 5Cr-Mo-V type of steel as an ultrahigh-strength structural material is somewhat similar to that of the low-alloy steels. A feature of this type of steel is its capability to be air hardened which minimizes the buildup of residual stresses in heat treatment. An example of the use of this kind of steel for airframe structural components is the fuselage frame for the A3J attack bomber shown in Figure 4. This component is built up from 0.080-inch-thick sheet heat treated to about 235,000-psi yield strength (about 280,000-psi ultimate tensile strength). Another example is the main landing-gear beam and brake housing for the XB-70 supersonic research bomber illustrated in Figure 5. As a rough forging this component weighed 18,000 lbs; its finish-machined weight is 9,316 lbs. The component is heat treated to a level of about 240,000-psi yield strength (i.e., 290,000-psi ultimate tensile strength).

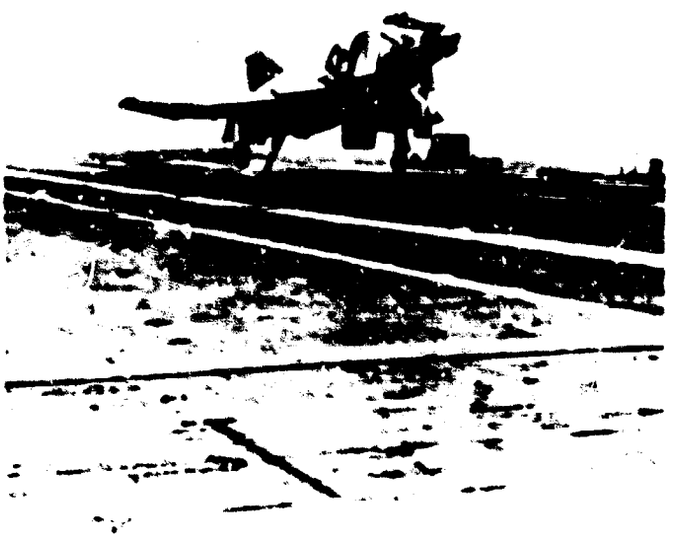

FIGURE 3. NAVAL AIRCRAFT EQUIPPED WITH AN ULTRAHIGH-STRENGTH LOW-ALLOY STEEL ARRESTING HOOK

The martensitic stainless steels are used in many small aircraft parts such as brackets, clamps, high-shear rivets, and bolts, as well as in large forgings and sheet-metal components where a measure of corrosion resistance is desired.

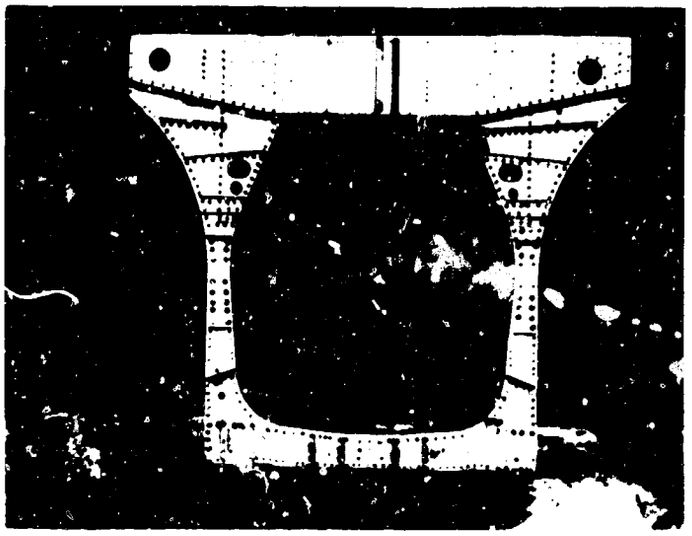

FIGURE 4. FUSELAGE FRAME FOR THE A3J ATTACK BOMBER

Constructed of 5Cr-Mo-V steel.

FIGURE 5. MAIN LANDING-GEAR BEAM AND BRAKE HOUSING FOR THE XB-70

A 9,316-lb forging of 5Cr-Mo-V steel heat treated to 290,000-psi tensile strength.

Figure 6 shows the use of an age-hardening martensitic stainless steel for the engine mounts of the B-58. The cold-rolled austenitic stainless steels find such ultrahigh-strength usage as skin for liquid fueled missiles and tanks for fuel and oxidizers. Examples of applications for the semiaustenitic stainless steels are stiffeners, interior frames, bulkheads, and longerons for aircraft; sandwich and honeycomb structure, skin, tanks, and ducts for aircraft, boat shafts and nuclear-reactor components. In the form of honeycomb structure, an example of which is shown in Figure 7, outstanding applications include skin for the XB-70 and the command module of Apollo.

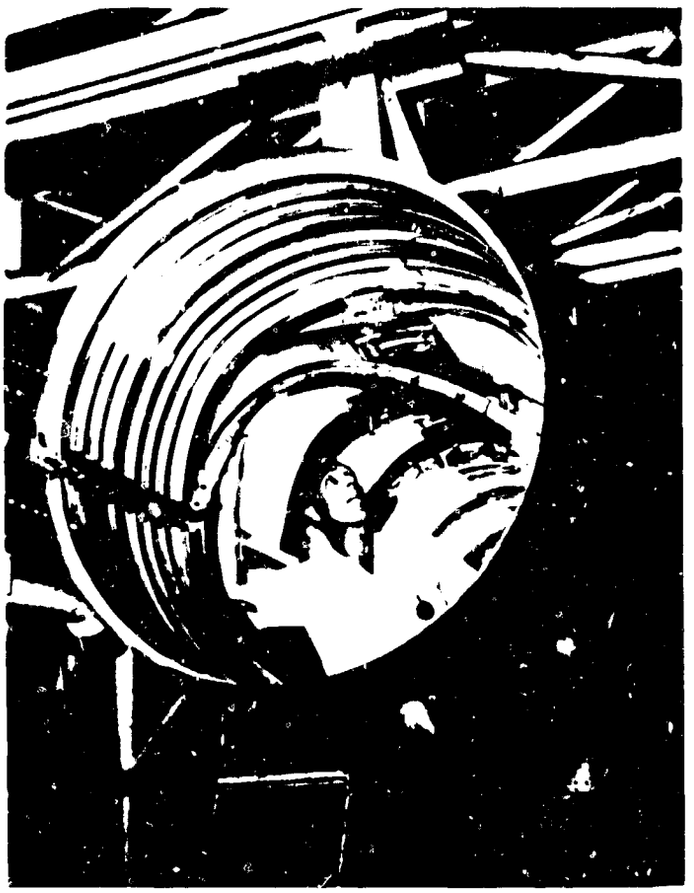

FIGURE 6. B-58 ENGINE MOUNT MADE OF AGE-HARDENABLE MARTENSITIC STAINLESS STEEL

FIGURE 7. AGE-HARDENABLE SEMIAUSTENITIC STAINLESS STEEL HONEYCOMB ASSEMBLY

In the short time since their introduction, the 18 per cent nickel maraging steels have developed a considerable spectrum of applications. One of the principal advantages of these steels is that the simple heat treatment, following forming and machining, causes virtually no distortion nor dimensional changes. This means that they can be finish machined in the soft condition. Thus, these steels

are ideal for ultrastrong high-precision parts. And it is in this type of usage that they will probably find their most sustaining applications. An example of such an application is the spline shaft shown in Figure 8. In addition, these steels have been selected for large-diameter solid-propellant rocket-motor cases of 156-inch and 260-inch diameter because of their weldability and the fact that, by simple local heat treatment, the welded joint can be made about as strong as the parent metal. The successful static firing of a 156-inch-diameter rocket motor, constructed from the grade which develops 250,000-psi yield strength, is shown in Figure 9. The motor was assembled from segments which had been made by rolling and welding 3/8-inch-thick plate.

A usage pattern has not yet been established for the 9Ni-4Co type of steel. However, these steels are currently being evaluated for such applications as components of special automotive equipment, gun tubes, hydrofoil components, aircraft landing-gear parts, and large-sized rocket-motor cases.

Potentialities and Limitations

The intent of the foregoing discussion has been to indicate the advances which have been made to date in the actual utilization of ultrahigh-strength steels. However, it should be noted that each family of steels discussed has members which can be, and have been, so treated as to display yield and ultimate tensile strengths considerably in excess of the levels used today in practice and shown in Table 3.

An indication of currently obtainable smooth-bar strength levels is given in Table 5. For most of the families of steels, two sets of strength values are shown in the table. One set corresponds to treating practices which are commercially feasible at the present time (principally featuring quenching and tempering), while the other set is indicative of the strength obtainable through the use of procedures most of which are presently considered exotic; namely, various thermal-mechanical treatments. The strength levels resulting from the latter type of treatments are significantly higher than those produced by the former.

In Table 5, tensile strengths over 500,000 psi are recorded for steels treated by unconventional procedures. Not shown in the table is the figure of 600,000-psi ultimate tensile strength obtainable in plain high-carbon steel wire. Add to this the figure of 1.9 million psi reported to have been obtained as the tensile strength of an iron whisker. Taken together, these sets of figures suggest a potential for ferrous materials, in terms of smooth-bar strength, far beyond the levels being realized in practic today.

On the other hand, when Table 5 is compared with Table 3, it is clear that most of the ultrahigh-strength steels are being employed at strength levels noticeably lower than those achievable even by ordinary methods of processing and treating. The low-alloy semiaustenitic and maraging steels should probably be considered as an exception to this observation. In some applications, they are now being used at, or near, the limit of strength obtainable by standard procedures.

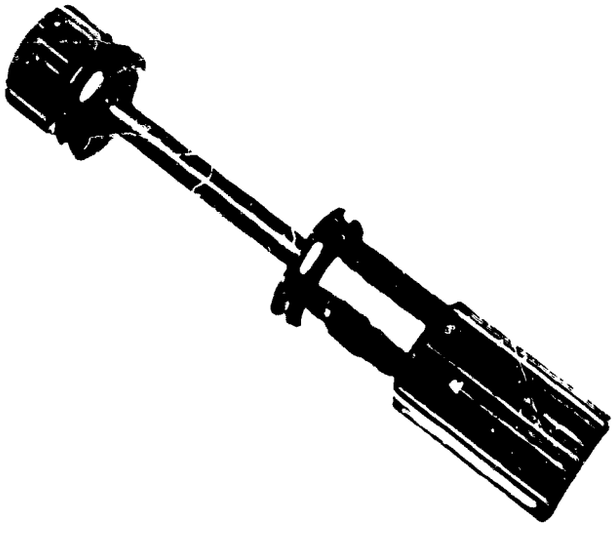

FIGURE 8. FLEXIBLE DRIVE SHAFT FOR THE B-47 JET BOMBER MADE OF 18Ni (250) MARAGING STEEL

FIGURE 9. STATIC FIRING OF 156-INCH-DIAMETER SOLID-FUELED ROCKET MOTOR

The segments are 18Ni (250) maraging steel.

TABLE 5. APPROXIMATE UPPER LIMIT OF STRENGTH CURRENTLY OBTAINED IN STEELS BY STANDARD AND BY UNUSUAL PROCEDURES

Type of Steel	Yield Strength, psi	Ultimate Tensile Strength, psi	Comments[a]
Low alloy	265,000	330,000	Q + T_1
	405,000	415,000	Cu-Si-Mo-V Steel - DMA + Q + T_1 High Si AISI 4340 - DMA + Q + T_1 + S + T_2
5Cr-Mo-V	250,000	325,000	Q + T_1
	395,000	410,000	S + T_2
Martensitic stainless	225,000	300,000	Subzero Q + T_1 + T_2
	256,000	271,000	AISI 410 - DMA + Q + Deformation on Tempering
Age-hardenable martensitic stainless	230,000	290,000	AFC 77 Subzero Q + double T at 1100 F + double T at 1000 F
	275,000	345,000	AFC 77 cold rolled 50% + T_1
Cold-rolled austenitic stainless steel	268,000	288,000	17-5 MNV cold rolled 60%
	295,000	300,000	AISI 301 stretch formed at cryogenic temperatures
Semiaustenitic stainless steel	220,000	235,000	PH15-7Mo subzero cooled and aged
	350,000	372,000	AM-355 strip rolled at cryogenic temperatures and aged
18Ni maraging steel	295,000	300,000	Annealed and aged
	340,000	345,000	Cold-rolled and aged
9Ni-4Co[b]	265,000	315,000	Q + T
	400,000	420,000	DMA + Q + T_1 + S + T_2
0.66C-5Ni[c]	520,000	526,000	DMA + Q + T_1 + S + T_2

(a) Q = Quenched; T_1 = Tempered; DMA = Deformed in the temperature range in which austenite is metastable; S = Strained; T_2 = Retempered.

(b) Has just become commercially available.

(c) An experimental steel.

The discrepancy between the strength levels now possible with current commercial procedures and those actually used in practice may usually be attributed to one or more of the factors shown in Table 6. One universally prevalent factor is the fact that the mechanical properties of a steel cannot be defined by a series of single values but must be described in terms of scatter bands. Practicality calls for use of the lower portions of these bands in establishing performance specifications. In this way, strength values may be adopted which are considerably lower than the obtainable maxima.

Another limiting factor is fracture toughness or notch strength, i.e., the ability of a material to sustain a load successfully in the presence of a sharp stress-raising notch or defect. The relationship between smooth-bar strength and notch strength for iron alloys can be expressed schematically by the curve in Figure 10. While notch strengthening tends to occur at the lower strength levels, it is clear that at higher strengths the tendency is for notch toughness to decrease with increasing smooth-bar strength. Of course, because steels differ with respect to notch sensitivity, no two steels could be represented by exactly the same curve.

TABLE 6. LIMITATIONS OF ULTRASTRONG STEELS

Reproducibility of Mechanical Properties
Fracture Toughness
Flaws in Mill Products
Nondestructive Inspection Techniques
Fatigue Resistance
Corrosion Fatigue
General Corrosion
Stress-Corrosion Cracking
Hydrogen-Stress Cracking
Joining

Notch toughness tends to converge along with two other factors to limit the strength level at which the material can be used with confidence. One of these factors is the fact that materials and structures as yet fall short of perfection, and hence, they tend to contain stress-raising defects. The other factor is that current nondestructive-inspection techniques have limitations with respect to their ability to detect and identify small defects. Thus, it happens that a structure may contain

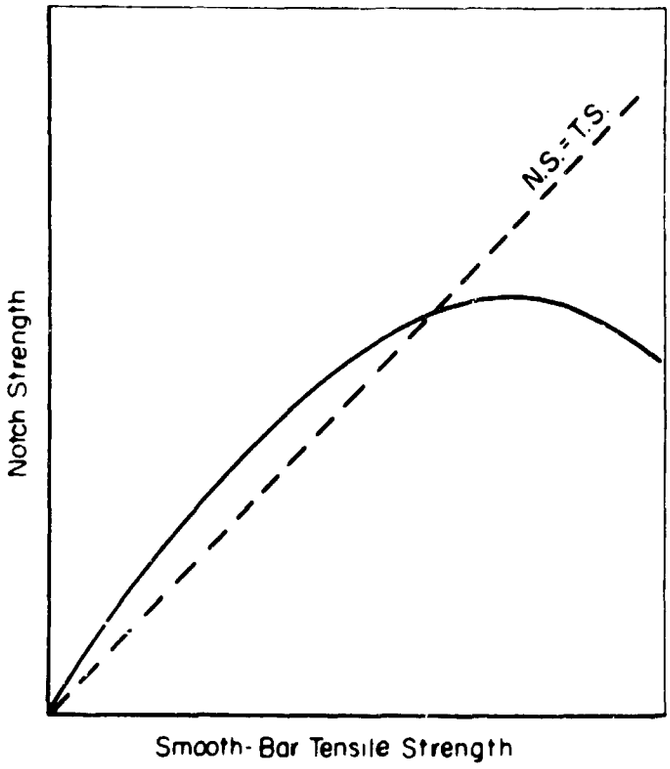

FIGURE 10. SCHEMATIC REPRESENTATION OF THE RELATIONSHIP BETWEEN NOTCH STRENGTH AND SMOOTH-BAR TENSILE STRENGTH

defects too large to be tolerated but too small to be detected, so they can be removed. The only way out of this dilemma, which is available at the moment, is to reduce the strength level at which the steel is used, and in this way, increase the allowable defect size to the point of detectability.

Resistance to fatigue is another factor which may limit the usefulness of steels at ultrahigh strength levels. Endurance limits are seldom more than half the ultimate tensile strength at best. Moreover, the ratio of endurance limit to tensile strength decreases markedly as ultimate tensile strength rises above some 200,000 psi. When the factor of corrosion is added to that of cyclic stressing, endurance limits disappear altogether.

Susceptibility to corrosive attack can certainly be considered as a limiting factor. High-strength steels, including the stainless varieties, are subject to attack in numerous commonly encountered media. The stainless steels, of course, are corroded in fewer environments, but on the other hand, they are quite susceptible to stress-corrosion cracking. The nonstainless steels also are subject to stress-corrosion cracking in a variety of environments.

Another factor to be taken into consideration is hydrogen-stress cracking. Hydrogen may be introduced into steel during melting, mill processing, electroplating operations, corrosion, or in connection with galvanic protection. Hydrogen-stress cracking is a problem to be reckoned with when yield strengths exceed approximately 70,000 psi.

Finally, attention must be called to the fact that joining tends to be a problem with ultrahigh-strength steels. Methods frequently used to join such steels are brazing and welding. Both invite dimensional changes, distortion, embrittlement, and the accumulation of unwanted internal stresses. In addition, there is the ever-present problem of making a joint which realizes the strength and fracture toughness of the parent metal.

The list of limitations and problems involved in using steels at ultrahigh strength levels is formidable, to say the least. And it might be argued that the ferrous metallurgist should be satisfied with the very creditable record already posted by steel, and that the better part of valor is to leave well enough alone. Were it not for three factors, the assumption of such a posture might be quite commendable. The first factor which militates against this position is the steady and insistent demand for constructional materials of ever-increased capabilities.

Another factor is that when other materials are employed in high-performance applications, a host of problems also arises. Frequently, the problems plaguing other materials are more severe than those encountered with the various steels. All the above-mentioned problems which limit the applicability of steels, together with some additional ones ones, are operative to a greater or lesser degree with other materials. Some materials, such as glass-fiber-reinforced plastics, may have higher strength-to-density ratios and better corrosion resistance but have low moduli of elasticity or poor compressive strength. Some materials may have desirably high strength, high fracture toughness, low density, and good corrosion resistance, but also may be expensive, difficult to fabricate, and troublesome to join. Titanium alloys tend to be in this category. Other materials, such as glass, may have excellent compressive strength, low density, and exceptional corrosion resistance, but are extraordinarily sensitive to the presence of stress-raising defects and discontinuities and are almost completely devoid of plasticity. Still other materials, such as aluminum and magnesium alloys, may lack elevated-temperature strength, or like the refractory metals, they may be extremely susceptible to oxidation.

The third factor is that, as the data in Table 5 suggest, approaches already have been discovered and are under extensive investigation, for adding another sizeable increment to the performance capabilities of steels.

Approaches Toward Higher Performance

An extremely promising avenue toward substantial increases in smooth-bar strength is

through thermal-mechanical treatments. These treatments are characterized by the introduction of strain into the structure at some point, or points, in a cycle which also includes heat treating A number of treatments of this type, as shown in Table 7, are currently being explored.

TABLE 7. SOME THERMAL-MECHANICAL TREATMENTS

Deformation During Transformation to Martensite
Deformation at Room Temperature
Deformation at Cryogenic Temperatures
Aging or Tempering After Deformation
Deformation of Martensite Followed By Tempering
Deformation at Room Temperature
Deformation at Tempering Temperature
Deformation of Tempered Martensite Followed by Retempering
Deformation of Metastable Austenite Before Transformation
Transformation to Martensite
Transformation to Bainite
Combination Treatments

One of the first thermal-mechanical treatments was simultaneous deformation and transformation from austenite to martensite. The rolling of the 17 per cent chromium, 7 per cent nickel type of stainless steel at room temperature can be considered as an illustration of this type of treatment. The strength of this and other austenitic stainless steels is greatly increased by this type of procedure especially when carried out at cryogenic temperatures. The strength levels obtainable in semiaustenitic stainless steels have been increased dramatically by such a procedure followed by an aging treatment. In fact, 4-inch-wide AM-355 strip, processed in this manner to 0.011-inch thickness, is currently being evaluated for rocket-motor cases constructed by the lap wrapping technique. A case made of AM-355 by this method is shown in Figure 11. The tensile strength of the steel was 372,000 psi.

A variant of this treatment is to deform previously formed martensite at room temperature and then age at a moderately elevated temperature. An effective alternate to this procedure may well be to carry out the deformation step at elevated temperatures such as those normally used for tempering. Another alternative procedure is to deform tempered martensite and then age or retemper. Very high strengths have been developed in age-hardenable martensitic stainless steels, medium-carbon low-alloy steels, and 5Cr-Mo-V steels by such procedures as these.

Another type of thermal-mechanical treatment, which has been under study for several years, is to deform austenite at comparatively low temperatures where it is metastable, before transformation to martensite or to bainite, and follow this by tempering. This procedure does not seem to result in as large strength increments as do most of the thermal-mechanical treatments just described.

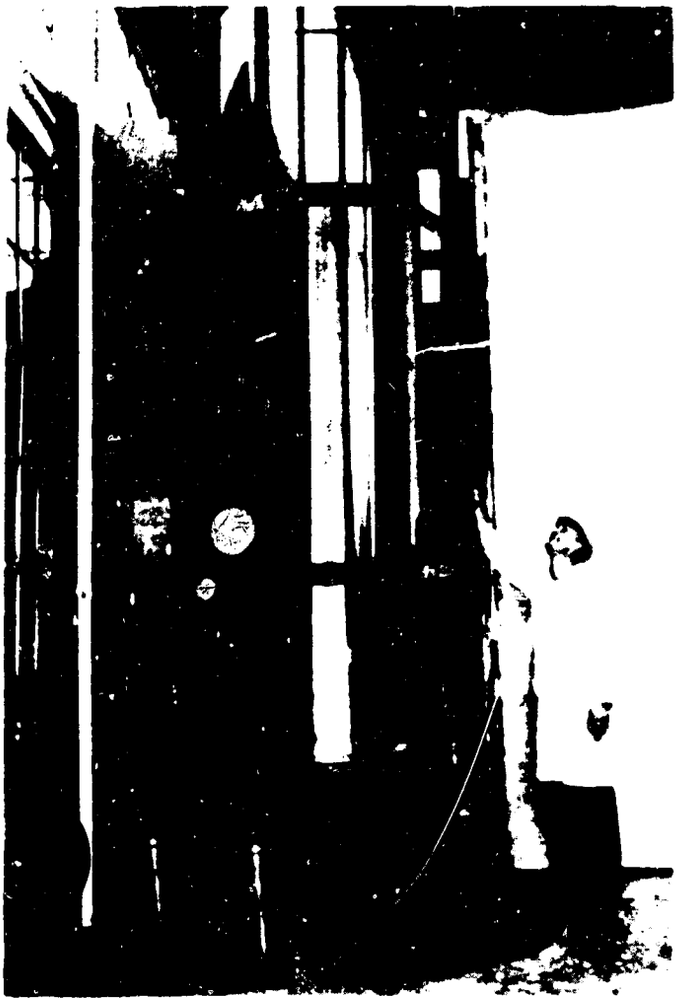

FIGURE 11. ROCKET-MOTOR CASE PRODUCED BY LAP WRAPPING AM-355 STRIP WHICH HAD BEEN THERMAL MECHANICALLY TREATED TO 372,000-PSI TENSILE STRENGTH

The greatest strength increments are currently being obtained by using combinations of thermal-mechanical treatments. For example, by deforming a 0.66 per cent carbon, 5 per cent nickel steel in the temperature range of metastable austenite, quenching to form martensite, tempering, straining the tempered martensite, and retempering, a yield strength of 520,000 psi and an ultimate tensile strength of 526,000 psi were obtained.

The principal reason for the great interest which has developed in thermal-mechanical processing is the very high smooth-bar strength levels which can be achieved by their use. However, there are indications that several of the different kinds of thermal-mechanical treatment also are capable of improving the fracture toughness vs yield strength relationship. They may be able either to increase toughness at constant strength or to maintain toughness while increasing strength.

For example, the ratio of fracture toughness to yield strength in the longitudinal direction of sheet material, for martensitic stainless steels and the 9Ni-4Co-0.40C steel, can be improved considerably by deforming them in the metastable austenitic condition followed by quenching and tempering.

Thermal-mechanical treatments are still in the developmental stage and are as yet being applied commercially to only a limited extent. In the application of these processes, a number of serious problems arise. To achieve reproducibility of properties requires close control of the degree of straining and the time and temperature range through which the straining is carried out. To achieve the desired amount of deformation throughout a part of odd or complex shape is something of a problem in itself. Another problem is anisotropy of mechanical properties and low toughness in the transverse direction. In addition, power requirements tend to be high because the steel usually exhibits great strength at the deformation temperature. Again, welding such materials is difficult without suffering considerable loss of strength in the area of the joint. At present, only relatively simple shapes and parts which need little final finishing are being fabricated by procedures encompassing thermal-mechanical treatments. However, the problems are under attack, and progress is being made.

Before leaving the subject of thermal-mechanical treatments, another possibility should be mentioned. The enormous work-hardening capability of the austenitic manganese steels suggests that very high strength is attainable in these steels by stretch forming or otherwise working them. Yield strengths of 180,000 psi have been developed in such steels by reducing them 50 per cent at room temperature. The corresponding Charpy V-notch values are quite high, being 51 ft-lbs at room temperature and 46 ft-lbs at -100 F. Thus, it is possible that, through somewhat greater amounts of deformation with or without subsequent aging, a combination of strength and toughness can be obtained in these steels by working them at ambient temperatures, which is at least as good, if not better than, that obtained in austenitic stainless steels deformed at cryogenic temperatures.

As shown in Table 8, there are many other avenues toward improved performance. One of them is to pay increased attention to steel composition. The principal uses to which alloying elements have been put in the past have been to improve corrosion resistance or increase hardenability. It is now recognized that alloying elements can have other roles. For example, the realization is growing that alloying elements influence fracture toughness. In quenched-and-tempered steels, there is evidence to suggest that additions of such elements as vanadium and nickel improve toughness. Manganese and silicon seem to be an effective combination promoting toughness. On the other hand, there are indications that chromium reduces the toughness of quenched-and-tempered steels. In addition, it is clear that the toughness of this type of steel tends to decrease as the carbon content is increased.

The development of the maraging steels and the 9Ni-4Co steels is a dramatic illustration of the pontentialities residing in the realm of alloying. These examples should serve as incentives to stimulate further efforts to make even greater gains through the use of alloying elements.

Another important aspect of steel composition relates to the unintended elements present in the steel. It is clear that this group, comprising such elements as sulfur, phosphorus, oxygen, nitrogen, and hydrogen, detract from ductility and toughness. Means of making steels containing only small amounts of these elements have come about through the development of advanced melting methods, such as the vacuum-induction and the consumable-electrode vacuum-arc remelting processes, in conjunction with increased availability of high-quality charge materials.

TABLE 8. AREAS WITH POTENTIALITIES FOR ACHIEVING INCREASED PERFORMANCE

Thermal-Mechanical Treatments
Composition
Effect of Alloying Elements
Influence of Unintended Elements
Composition-Influenced Approaches
Bainites
Self-Tempering Steels
Nitrogen Martensites
Nonmetallic Inclusions
Steels Tailored for Thermal-Mechanical Treatment
Flaws in Mill Products
Defects Introduced in Construction and Design
Nondestructive Inspection Methods
Design Philosophy
Coatings
Fundamental Research

Further steps along these lines, especially in the direction of charge materials of still higher purity, should be rewarding.

Several avenues which may lead to materials of improved performance combine considerations of composition with other factors. For example, evidence is available which indicates that, by proper alloying and adjustment of carbon content, tough high-strength bainites can be formed on continuous cooling from the austenite temperature region. In the same manner, the M_f temperature may be raised so as to render the steel self-

tempering and correspondingly tough on cooling from the austenitizing temperature. Developments of these kinds offer the additional opportunity of welding without preheat or postheat. Another composition-influenced area which has been explored but little, and might prove quite worthwhile to investigate, are iron alloy systems based on nitrogen martensites rather than carbon martensites. Another item which might come under the cloak of a composition-influenced matter is the taking of steps toward the production of steels with ever fewer and ever smaller nonmetallic inclusions. Here, the production of comparatively pure charge materials and the development of melting procedures using a vacuum or an artifical atmosphere have paved the way. An additional long step has been taken recently with the advent of vacuum carbon deoxidation. With this process, the products of deoxidation are gaseous and leave the melt rather than being liquids, or, occasionally, solids which remain with the molten metal to form nonmetallic inclusions. Finally, a worthwhile effort would seem to lie in the direction of developing steels, through alloying, which are designed for particular thermal-mechanical treatments. The convergence of an optimized thermal-mechanical treatment and a steel tailored specifically to that treatment should yield a product having an exceptional combination of strength and fracture toughness.

Steps already taken to decrease the number and size of defects in mill products have been very encouraging and point to this as another avenue toward improved performance. These steps start with charge materials and go on through melting operations, ingot practices, break-down procedures, hot and cold rolling, annealing, and, indeed, almost all aspects of mill processing. Improved charge materials and melting methods have already been mentioned. Other examples include the use of glassy slags to coat and protect ingot surfaces, the development of exothermic hot-top practices, removal of surface defects at intermediate stages in processing, and grinding and polishing the finished product. The importance of efforts along these lines can be stated this way: the smaller the defect which is present, the less fracture toughness is required in the material to insure reliable performance at a given strength level, or the higher the reliably usable strength for a given level of toughness.

Discussions of measures to improve the quality of mill products leads to a consideration of the contribution made by construction and design factors to the number and severity of defects present in the finished structure. Great strides have been made here also. In numerous quarters, particularly among missile and aircraft manufacturers, it is appreciated that such discontinuities as scratches, nicks, gouges, punch marks, undercut welds, mismatched joints, and grinding marks may initiate a failure as readily, if not more readily, than a mill defect in the material of construction. Likewise, the designer has learned of the dangers lurking in sharp fillets, slots, small holes, and other abrupt changes in section.

It appears, at this point, that the most severe problems impeding further efforts to reduce the number and severity of stress-raising defects in materials and structures resides in the shortcomings of currently available nondestructive inspection methods. The techniques for locating and identifying internal defects seem to have more limitations than those available to inspect surfaces. Opportunities for further advances appear to be in the directions of increasing the positiveness with which the equipment indicates the presence of a defect, decreasing the minimum size of identifiable defects, improving the capability to find nonlaminar internal defects and defects not parallel to the surface, and developing means of identifying the type of internal defect located.

The factor of design demands further discussion because the subject has another vitally important aspect. The use of steels in high-performance applications at ever-higher strength levels is due at least as much to changes in design philosophy as to increases in the capability of the material. Through the years, designers have been learning to adjust their thinking to the fact that, in order to use materials at higher and higher strength levels, they must accept less and less ductility and toughness. And experience has been teaching that reliable structures can be built with materials which not many years ago were considered to be rather brittle. A continuation of this trend in design philosopy will open the door to the application of ferrous materials at ever-higher strengths.

Most of the foregoing discussion has been concerned with means for securing higher performance in terms of strength and toughness. Other areas requiring improvement are general corrosion, stress-corrosion cracking, corrosion fatigue, and hydrogen-stress cracking. The extent of the advances in these areas which can be expected from such approaches as composition modifications, alloy additions, or special heat treating or mill processing procedures would seem to be somewhat limited. On the other hand, progress is being made toward an improved understanding of stress-corrosion cracking in stainless steels and the insights gained should lead to the development of stainless steels more resistant to this phenomenon. Likewise, hydrogen-stress cracking is becoming better understood.

Substantial opportunities are judged to lie in the field of coatings capable of shielding the metal from hostile environments. A great deal of progress has been made in the technology of coatings through the years. The area of organic coatings has been particularly active in recent years. Such an abundance of compounds has become available that the tailoring of the coating

formulation specifically to the particular application is standard practice. Great advances have been made also in coating methods. Recently developed processes make use of such techniques as the fluidized bed, electrostatics, electrophoresis, and glow discharge. Much remains to be done, and the current research effort in this field is quite considerable. The requirements to be met by coatings are rigorous; they include freedom from holidays and breakthroughs, ductility, adherence, reliability over wide temperature ranges, inertness, impermeability, inspectability, and ease of application. However, gains in this field are rewarding. And the very idea of avoiding corrosion and other environmentally influenced deterioration processes by creating an impenetrable barrier between the environment and the metal is a powerful incentive to further efforts and advances because of its inherent simplicity and practicality.

Finally, it must be emphasized that undergirding every approach to higher performance is the steady acquisition of new knowledge and new insights to the fundamental features of the behavior of metallic materials in general and steels in particular. This endeavor, which is really the basis of all approaches, is often left unidentified, if not overlooked entirely, in the mad scramble to build hardware to meet today's immediate needs and desires. To insure future gains, attention and support must be given in full measure to activities and efforts which are directed at comprehension of materials behavior.

Testing and Evaluation

An extensive subject about which much could be said is testing and evaluation. The vital role of these activities in materials development and usage needs no amplification here. Unfortunately, the uncertainties of theory and the paucity of fundamental knowledge of the behavior of materials, place these matters in the realm of question and controversy. So commonplace a measurement as yield strength, let alone Young's modulus, is still fraught with argument. Efforts to evaluate materials for their resistance to stress-corrosion cracking or corrosion fatigue are almost equivalent to voyages in uncharted seas. On top of these dilemmas is now added the extremely controversial problem of assessing the toughness of ultrastrong steels, that is, the capability of steels at ultrahigh strength levels to sustain loads in the presence of stress-raising notches and defects.

The problem of evaluating fracture toughness presses in from a number of directions. In the first place, the phenomenon of a ductile-to-brittle transition washes out at yield strengths of some 180,000 psi and above. Thus, the guide lines established for the behavior of steels of lower strength cannot be extrapolated to ultrastrong steels. Still, it is not difficult to evaluate the fracture toughness of ultrahigh strength steels in thin sections. Their load-carrying capability in the presence of the worst defect likely to be encountered, namely, a natural crack, can be estimated from direct measurement of fracture strength in the presence of that defect. This can be done by introducing the defect artificially into a sheet tensile specimen of the appropriate shape and size.

Trouble arises when the thickness of the structure or component reaches the point that the cross-sectional dimensions of the specimen make it too strong to be tested in the largest available equipment. This situation calls for subsized specimens and immediately poses the problem of extrapolating the data obtained from such specimens to full-scale conditions. Either a sound theory of crack propagation in ultrahigh-strength steels or a sufficiency of empirical experience with failures in thick sections of ultrastrong steels is needed to bridge this gap. Progress is being made along both lines. Currently, a number of different types of subsized specimens are in use, and there is considerable uncertainty regarding the meaning of the data obtained. However, it is not too much to expect that theory and test methods will so evolve, in the near future, as to yield quantitative values for fracture toughness which are of a type that can be used directly in design calculations.

Summary

In sum, 8 or 9 families of steels are available today for high-performance structural applications at ultrahigh-strength levels. While currently used maximum yield strengths are in the range of 260,000 to 300,000 psi, it has already been demonstrated that steels possess considerably greater capabilities. It is therefore reasonable to expect that, in the next few years, another long step forward will be taken in the usage of steels. It is not unlikely that these materials will be found in applications at yield strengths well over 400,000 psi in a very few years.

For components and structures made of steels at extreme strengths to be reliable will require the avoidance or elimination of some of the problem areas that place limitations on these materials today. A most important area is fracture toughness. Here, it seems certain that progress can be made by a convergence of several approaches: the development of steels with greater inherent toughness, the production of mill products containing fewer and smaller flaws, improvement in fabrication and construction methods, improvement in inspection procedures, and the continued evolution of design philosophy to encompass ever more brittle structural materials.

Hydrogen-stress cracking and the various destructive phenomena involving corrosion comprise another important area limiting the usefulness of steel where advances are urgently needed. More progress toward overcoming the problems residing in this area should be possible, especially in the coating field.

SELECTED BIBLIOGRAPHY

(1) Aitchison, L., A History of Metals, Interscience Publishers, Inc., New York (1960), 2 volumes, 647 pages.

(2) Manning, G. K., "How Should You Evaluate High-Strength Materials?", Met. Prog., 80, 65-67 (1961).

(3) Brenner, S. S., "Tensile Strength of Whiskers", J. App. Phys., 27, 1484-1491 (1956).

(4) Proceedings of Conference on Metallurgical Developments in High-Alloy Steels, held at Scarborough on June 2-4, 1964 jointly by British Iron and Steel Research Association and the Iron and Steel Institute, 15 papers, 171 pages.

(5) Kula, E. B., Radcliffe, S. V., "Thermomechanical Treatment of Steel", J. Met., 15, 755-762 (1963).

(6) Marschall, C. W., "Hot-Cold Working of Steel to Improve Strength", Defense Metals Information Center Report 192, BMI, Columbus, Ohio (October 11, 1963).

(7) Mechanical Working of Steel I, Philip H. Smith, Editor, Gordon and Breach, New York (1964), 417 pages.

(8) Campbell, J. E., "Steels for Large Solid-Propellant Rocket Motor Cases", Defense Metals Information Center Report 178, BMI, Columbus, Ohio (November 20, 1962).

(9) Matas, S. J., Hill, M., and Munger, H. P., "Current and Future Trends for Steels With High Strength and Toughness", Metals Engineering Quarterly, 3, 7-17 (1963).

(10) Hall, A. M., "A Discussion of the Physical Metallurgy of the 18 Per Cent Nickel Maraging Steels", Defense Metals Information Center Report 194, BMI, Columbus, Ohio (November 15, 1963).

(11) Alper, R. H., "Cryogenically Stretch-Formed Type 301 Stainless Steel for Cryogenic Service", Materials Research and Standards, 4, 525-532 (October 1964).

(12) Campbell, J. E., "Current Methods of Fracture-Toughness Testing of High-Strength Alloys with Emphasis on Plane Strain", Defense Metals Information Center Report 207, BMI, Columbus, Ohio (August 31, 1964).

MILITARY APPLICATIONS AND PROPERTY REQUIREMENTS

U. S. Air Force

(P. L. Hendricks, H. W. Zoeller, and I. Perlmutter, U. S. Air Force, AF Materials Laboratory, Wright-Patterson Air Force Base, Ohio)

Advances in new concepts for Air Force weapons systems have produced corresponding requirements for steels with much improved performance and service characteristics. Steels with high strength-to-weight ratios are, therefore, important Air Force structural requirements. The technology of high-strength steels has not been static, and many advances have been made toward fulfillment of the basic requirements for steels with higher strength-to-weight ratios.

Prior to the last decade, steels were commonly used with yield strengths in the 125-ksi range. Modest increases in strength were obtained during the war years, but since that time, increased emphasis has been placed upon increased strength-to-weight ratios with the result that really significant increases in strength levels have been obtained. The trend of increased yield strengths in high-strength steels since World War II has been steadily upward. It should be pointed out that, although the trend for yield strength levels has been increasing, limitations in the successful utilization of high-strength steels have resulted in a leveling off, and in many cases, an actual decrease in yield strength design levels in some current applications. The ability to use steels with high yield strengths would, of course, result in increases in performance and payloads in current and future air weapons systems. The high-strength steels are, in general, less ductile and more susceptible to brittle fracture than steels of lower strength levels. It is also important to note that many present applications require the utilization and performance of steels under conditions of stress and environments which are more severe than those encountered only a few years ago. The higher strengths and severe environments necessitate an increased attention to manufacturing processes, design details, and operating conditions. Many of the basic factors pertinent to the use of high-strength steels which will be considered in this paper are fairly well understood from a theoretical point of view. The difficulties lie in reducing these factors to consistent engineering practice. The utilization of currently available high-strength steels requires a knowledge and application of certain basic information, if reliable performance is to be obtained under service conditions. The problems involved in the successful application of present high-strength steels are twofold and can be summarized as follows: (1) recognition and application of the factors involved in securing a high degree of reliability in performance to insure freedom from failure of systems or components due to involvement of limiting factors in the use of high-strength steels, and (2) the development and application of new information which will lead to the production of superior high-strength steels which overcome many of the limiting factors associated presently with their use. Since this second category implies the overcoming of limitations of high-strength steel performance through the application of knowledge not yet generated, attention must, of necessity, be directed in the present discussion primarily to the limitations presently involved in the use of high-strength steels.

Most steels have been investigated to the point that their physical and mechanical properties are well known. It is, therefore, possible to design structures which should give reliable performance when available design information has been properly utilized. This has generally been true when steels were used at comparatively low strength levels (120 ksi). Attempts to use steels at high strength levels (250-300 ksi), however, have been very difficult and can be successfully accomplished only when many other factors are considered and are protected against when necessary. These factors place limitations upon the successful use of high-strength steels and some of the more important ones are listed as follows: (1) cleanliness and uniformity of metallurgical structure, (2) influence of sharp corners and stress risers, (3) necessity for proper grain flow in forgings, (4) damage through processing after heat treatment, (5) stress corrosion, hydrogen embrittlement, and other corrosion effects, (6) resistance to crack initiation and propagation, (7) fatigue-type failures, and (8) adequate inspection techniques. Failure to recognize the importance or guard against the influence of some of these factors listed has resulted in loss, by the Air Force on occasion, of complete weapons systems. On other occasions, subsystems or component parts made of high-strength steels have been involved in failures. In all cases, these failures exacted a high price in terms of money and/or manpower.

To show the influence of some of these factors, a few examples will be presented. Grinding and drilling operations after heat treatment should be accomplished with extreme precautions. However, the fabrication of aircraft parts frequently requires that fastener holes be drilled after heat treatment. When the hardness exceeds Rockwell "C" 44, the problem of drilling becomes critical. Overheating can occur, resulting in untempered martensite in the holes which can readily crack under the proper stress conditions. The formation

of cracks could bring about problems in one of two ways. In the first place, cracking could be so extensive as to reduce the load-carrying area sufficiently to cause failure of the part at stresses far below design loads. In the other instance, the formation of cracks could expose unprotected sites to the atmosphere and under proper conditions provide for the initiation of corrosion at these sites. The corrosion combined with stress could cause stress-corrosion cracking and subsequent failure of the part.

Figure 1 shows a trunion support rib fitting which holds the landing gear to the airframe or fuselage. The material was 4340M heat treated to 220 to 240-ksi tensile strength. The holes are drilled after heat treatment to meet required tolerances, and if overheating occurs, untempered martensite can occur in the holes (Figure 2). Untempered martensite is quite brittle and will crack quite readily under load, thus paving the way to failure by one of the two routes mentioned earlier. The importance of surface condition is illustrated in the failure of a landing gear made of 4340 steels heat treated to 260- to 280-ksi strength level. Investigation in this case revealed the fact that the aircraft involved had previously experienced a hard landing, causing three tires to blow out. The forward outboard wheel was replaced, using forward jacking point to raise the aircraft. However, the aft jacking point was too low to use the standard jack. A small hand hydraulic jack was placed under the truck beam assembly. Inspection revealed that the truck beam failure initiated on the under side at the point where the hand jack had contacted it. Other examinations showed that the surface marks (Figure 3) made by the hand jack served as points of initiation of the failure. This incident points up the necessity of constantly monitoring procedures used in the handling of high-strength steels. The problem of applying information intended to guard against adverse affects of certain limiting factors is often complicated because of the introduction of other factors. The following cases are typical examples.

A few years back, an investigation was conducted to determine the cause of failure of a wheel and axle assembly from an F-105B aircraft. The assembly was cadmium plated to protect it from atmospheric conditions. Information supplied indicated that the failure occurred after the aircraft had taxied for a considerable distance following an unusually fast landing. An examination of the fractured surface showed a brittle-type fracture with little evidence of ductility. In addition to the primary fracture, there were numerous other cracks. Several of these cracks were opened, and all that were examined showed indications that cadmium used as a plating had penetrated into the base metal. In some cases, the surface was smooth and shiny; in others, there was a layer of yellow or brown oxide. Spectrographic analysis indicated major amounts of cadmium on both fracture surfaces. Base metal was also analysed and

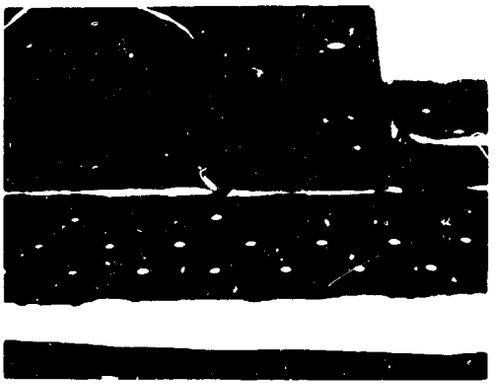

FIGURE 1. TRUNION SUPPORT FITTING

FIGURE 2. UNTEMPERED MARTENSITE

FIGURE 3. MARKS FROM HAND JACK

and found to be the proper chemistry for 4330 modified steel which was specified for the part. It was concluded that the part had failed from an unknown mechanism resulting from the penetration of the steel by the cadmium. During normal service, this part is periodically subjected to moderately high temperatures (600 to 700 F), while under stress. The unusually fast landing had also contributed to excessive heat in the part. This resulted in the penetration of the cadmium into the steel which reduced the load-carrying

ability of the material, thus causing it to fail. It was concluded that use of cadmium-plated steel in stressed parts above the melting point of cadmium should be avoided in all cases since premature failure can result.

Another example deals with the embrittlement of steel due to hydrogen. One of the principal sources of hydrogen in steel comes from electroplating. A high concentration of hydrogen collects at the surface under the plate. Baking after plating will effectively remove the hydrogen provided the plate is porous enough to permit the hydrogen to pass through. At strength levels above 200,000 psi, baking periods of the order of 23 hours at 375 F are required. The case in point involves a trunion support fitting which had been plated using a porous cadmium plate. After a period in service, cracks were observed in the fillet area of the fitting (Figure 4). There was a large generous radius in the area, and for a while, everyone was puzzled as to what had caused the failures. Mechanical properties were excellent for that strength level, particularly in the short transverse direction. During the investigation, four of the trunion fittings were loaded to about 3/4 of their yield strengths. This was done to determine if hydrogen embrittlement was a problem. No failures occurred after about 3 months under this sustained load, after which time the test articles were removed from the hanger and placed outside in the scrap yard. About 3 days later, it was noticed that three of the four test articles had failed in the fillet area. It had snowed during this period, and the fourth article failed shortly afterward. Later tests using sustained loads and moisture confirmed these observations. The parts had been cadmium plated using a less dense plate, and while in service under stress, moisture had collected on the surface of the plate, causing a stress corrosion, hydrogen embrittlement failure. These examples indicate that hydrogen embrittlement, stress corrosion, and failure through cadmium penetration can all be associated with attempts to protect the high-strength steels through the use of cadmium plating.

FIGURE 4. CRACK IN TRUNION SUPPORT FITTING

Another factor of importance in forgings is assurance that grain flow pattern is in the proper direction with respect to the manner in which the part is loaded. This is of particular significance as the strength level required of the steel is increased. A failure of a landing-gear truck beam is a typical example. Several failures had occurred and in each case the initiation point was on the bottom side of the front axle (Figure 5). The fractures are typical of stress corrosion in low-alloy steel (Figure 6). Investigation of these failures showed that the part was fabricated in such a way that the exposed surface was transverse to the direction of the grain flow. High-strength steel is more susceptible to stress-corrosion cracking in the short transverse direction than in the longitudinal direction. In this instance, it was concluded that the direction of the grain flow pattern at the point of fracture initiation was such that resistance to stress corrosion may have been materially reduced. There is a possibility that this failure may have been avoided if more consideration had been given to providing the proper grain flow orientation.

FIGURE 5. FAILED SECTION LANDING-GEAR TRUCK BEAM

FIGURE 6. STRESS-CORROSION CRACKING

One of the most important factors limiting service application of high-strength steels is fracture toughness. This parameter has been, and still is, receiving considerable attention. In many applications, this aspect is of such importance that it is the controlling factor in determining

whether a specific steel will be used in a given application. Extremely high yield strengths are of little importance if the steel has low resistance to the steady growth of cracks that may be present as a result of fabrication processes. In these steels, crack growth proceeds readily to the point of instability followed by failure in a brittle manner at stresses far below the yield strength of the material. The lack of this property has resulted in costly failures of Air Force weapons systems and components. The importance of this factor is recognized when one thinks of the necessity for obtaining 100 per cent reliability of material performance in many systems currently under consideration. It is not possible to adequately cover so important a topic in the time available. However, I am sure that more complete coverage will be given later in the symposium. These few illustrations point up the importance of limiting factors in obtaining reliability of performance in high-strength steels. These examples also point up the need for detailed attention to manufacturing processes, design details, and operating environments and conditions. All of these factors become increasingly important as the strength levels at which high-strength steels are used are increased. Many of the factors pertinent to the use of high-strength steels are somewhat understood from a theoretical point of view. The difficulty lies in incorporating these factors into practice so that systems and components can be built that operate with reliability approaching 100 per cent.

Steels in the 260-280-ksi category are currently being used in some applications by the Air Force. This is being accomplished through an awareness of the limiting factors involved in their use. Successful application requires a constant monitoring of processing techniques beginning with the melting process and continuing through completion of the component or system. A critical factor throughout the fabrication process is the availability and use of satisfactory inspection techniques. To insure reliability in performance, continual inspection following various fabrication procedures is mandatory. Present high-strength steels are so sensitive to processing, surface, and metallurgical defects, and other imperfections that this type of inspection is necessary. Although the need for rigid inspection is recognized, present inspection techniques and procedures are far from adequate to accomplish the requirements. The inadequacy of these techniques constitutes another limiting factor and decreases the likelihood of obtaining the degree of reliability of performance felt to be necessary for many applications. The development of new and much improved inspection techniques is required, if the full potential of currently available high-strength steel compositions is to be achieved.

As was suggested earlier, another approach to satisfactory utilization of high-strength steels is to develop new or improved compositions that are not subject to many of the limiting factors previously discussed. Efforts in this direction are continuing. Some progress has been made in various areas. One such instance is the development of a high-strength, corrosion-resistant martensitic steel by the Air Force under contract with Crucible Steel Company. This steel is currently designated as AFC-77 and offers higher strength at elevated temperatures (1000-1200 F) than any other corrosion-resistant steel presently available commercially. The nominal composition is 0.15C-14.5Cr-13.5Co-5Mo-0.5V. Its strength ranges from 300 ksi at room temperature to 164 ksi at 1100 F. The development of the maraging steels is another example of a noteworthy contribution to high-strength steel technology. These steels develop high strengths and are readily fabricable. In addition to the high strengths developed, the outstanding feature of these steels is their ability to withstand the presence of larger flaws or cracks than other steels of comparable strength level. This property has stimulated widespread interest in these steels and they are being considered for many present and future applications.

These steels, of course, do not overcome all of the limiting factors affecting performance. The AFC-77 provides corrosion resistance coupled with high strengths at room and elevated temperatures, but suffers the drawbacks of other limiting factors. The maraging steels suffer from banding and low fracture toughness of weld metal as well as other limiting factors. Both of these steels are important structural materials, and the above examples are used only to indicate that the probability of a steel that overcomes all of the limiting factors does not exist. It, therefore, should not be expected that new developments will lead to compositions that overcome the influence of all limiting factors. The developments that have occurred, however, do seem to indicate that it may be possible to produce steels that either overcome specific limiting factors or become much more tolerant to their influence in applications where these factors are critical.

In order to obtain steels with both high strength and reliability, several approaches have been used. Quenched and tempered steels constitute by far the great majority. The maraging steels constitute a very small group, and as previously pointed out, show great potential. Carbon-strengthened low-alloy steels processed to 100 per cent lower bainite constitute another promising approach. These steels combine high strengths with good fracture toughness and high weld-joint efficiencies. These compositions indicate that 100 per cent bainite properly formed has toughness superior to that obtained from tempered martensite at comparable strength levels. The use of thermo-mechanical treatments may also offer some advantages. The potential of this processing technique has not been fully explored; hence, a full assessment of the potential of steels so processed cannot adequately be made.

It should be noted that although steels have been used for many years, alloys with improved

properties and performance characteristics are continually being developed. Steels provide high strength-to-weight ratios and are economical. Steels are important Air Force structural metals and will likely play dominant roles in many future systems, but will probably never be completely free from all limiting factors. With the necessary attention to the processing, design details, and operating conditions, steels can and will be used to their best advantage. By continuing to advance in the physical metallurgy of steels and by applying the necessary engineering controls, it will be possible to continue the advancements in steel technology.

U. S. Army

(J. I. Bluhm, Army Materials Research Agency, Watertown, Massachusetts.)

Introduction

It seems unrealistic and somewhat arbitrary to try and break out differences in the nature of the problems of the use of high-strength steels in Air Force versus Navy versus Army applications. The behavior of a component is not influenced by the name of the using service, but rather by the specific environment in which it finds itself. Certainly, at today's technological level, it is difficult to visualize an environment which lies solely within the domain of any one service.

Therefore, rather than attempting to identify applications and problems unique to the Army, we shall initially describe briefly several specific Army components in which high-strength steels either have an important potential or where their use has led to catastrophic failures. Finally, we shall attempt to indicate the directions that studies are being directed in order to resolve some of the problems associated with their use.

By the term "failure", we shall restrict our attention, except when specifically stated to the contrary, to "fracture" and even more specifically to "brittle fracture". By "brittle fracture", in turn, we imply a rapid catastrophic fracturing process which takes place at stress levels considerably below the yield strength and which, therefore, provides no warning (by deformation or necking) of impending failure.

Applications and Associated Problems

Historically, the Army's first significant encounter with the then ill-defined "brittle behavior problem" developed during the Korean episode when considerable numbers of guns shattered in the field. The failures were generally characterized by: (a) the formation of many fragments during the fracturing process, (b) low ambient temperatures, (c) little or no readily detectable plastic flow, and (d) an unexpectedly short life.

Now, although these guns did not qualify as "high strength" in terms of the ground rules of the present symposium, their behavior did indicate the increased tendency toward brittle behavior as strength levels increased, and hence, highlighted the potential hazards of using high-strength steel.

Continuing and pressing requirements for lighter weight, higher performance components have, nevertheless, forced consideration of the use of higher and higher strength steels, brittle fracture risk notwithstanding. Entirely new families of weapons have been developed incorporating these steels.

The 155-mm recoilless rifle of the Davy Crockett vintage calls for ambient yield strength levels of 180,000-190,000-psi level with a 400 F requirement of 155,000 psi, and of course, adequate toughness. These strength levels are not optimum but represent compromise between strength and toughness. Steels were available with higher ambient yield strengths and equivalent toughness levels, but they showed greater strength degradation at the 400 F level. More recently, high-strength 4330V (Mod + Si) has been commercially produced with a 0.10 per cent offset yield strength of 200,000 psi and a -40 F "V"-notch Charpy value of 10-20 ft-lb. Current effort is being directed toward utilization of even higher yield-strength levels such as 250,000-300,000 psi in various missile and/or rocket applications.

Generalizing somewhat, we shall consider several experiences with other applications of the pressure-vessel type.

a. On or about 9 September, 1960, a small pressure vessel in a stored "Hawk" missile shattered completely destroying the missile. The pressure vessel is part of a hydraulic accumulator system used to actuate the hydraulic servo system and normally contains nitrogen gas at a nominal pressure of 4000 psi. Because of launch time considerations, this pressure vessel is charged with the 4000-psi nitrogen at the manufacturer's plant and remains charged until the missile is fired. Here failure--delayed failure--was attributed principally to: (1) the use of an inherently too brittle steel (H-11 Aero Material Spec AMS 6437 at a yield strength level of 200-220,000 psi), and (2) presence of moisture and/or other corrosive media leading to hydrogen embrittlement and impregnation. Combinations of these factors led to slow development of critical size defects in the 0.180-inch wall and subsequent rapid or catastrophic failure. Controlled laboratory tests repeatedly resulted in fragmentation of these pressure vessels into many small pieces--in some instances as high as 33--in the temperature range -65 F to +80 F and exhibited considerable scatter in the

burst pressures. The fracture surfaces showed no significant deformation or shear-lip formation; this is consistent with the brittleness expected from multiple fracture observations. The H-11 accumulators were eventually replaced with AISI 4340 steel at 160,000 to 180,000 yield strength with slightly increased wall thicknesses; burst tests demonstrated the marked superiority of this material; burst pressures were quite consistent relative to the H-11 tests. Furthermore, the fracture surfaces showed 100 per cent shear lip and the accumulators, at worst, burst into only two pieces in the extended temperature range -200 F to +80 F.

b. The "Redeye" and "Shillelagh" solid-propellant rocket-motor cases are indicative of another application area. These are particularly interesting in that they vividly demonstrate the applicability of a critical shear-lip thickness concept[1]* on the acceptability of a particular steel. Here, the Redeye, a 2.75-inch-diameter, 0.020-inch-thick H-11 vessel, burst tested at -65 F, repeatedly failed at stress levels consistent with the tensile strength, and the fractures were 100% shear. Furthermore, this 100% shear is consistent with the observed critical shear-lip thickness in H-11 of approximately 0.020 inch. The Shillelagh, on the other hand, is a 6-inch-diameter, 0.047-inch-thick case. Use of the same material, i.e., H-11, would have resulted in less than optimum shear-lip formation, and the toughness of the H-11 in the 0.047-inch thickness would have been severely degraded from that obtained in the 0.020-inch thickness range. An actual test of an H-11 0.047-inch-thick specimen showed that the fracture was approximately 50 per cent flat even at only -40 F, confirming the undesirability of using the H-11 in this greater thickness. Ultimately, D6AC was used on the thicker Shillelagh cases, since it was known from earlier work on D6AC that the critical shear-lip thickness at -65 F was in excess of 0.047 inch. Tests of D6AC Shillelagh cases were carried out at temperatures down to -85 F and resulted in no premature or brittle failures.

Other applications than pressure vessels obviously are also important. In the area of conventional monolithic armor, it has been established that the prime property requisite for defeat of projectiles is the armor hardness. This hardness leads to defeat of the projectile by causing shatter. By any of the customary means of evaluating armor, the effectiveness increases with hardness up to a given point and then falls with continued increase in hardness. This limit corresponds to the point at which the armor itself is so brittle that it shatters upon impact. Obviously, the problem then is to provide greater toughness at the desired high strength levels. This is, of course, a problem common to other applications and is the primary drawback to the trend toward use of higher and higher strength materials. Inadequate toughness usually associated with the higher strength materials frequently forces a backing down on strength level to achieve adequate toughness. This optimization of toughness and hardness is the function of the team composing the designer, metallurgist, and materials engineer.

Major inroads are being made currently in the development of lightweight composite armor consisting typically of a brittle ceramic facing tile and a tough back-up material. Although detailed data are classified, we can state that marked weight reductions have been achieved using such facings as boron carbide or alumina with various metallic and/or plastic and/or composite back-up plates. Although a detailed understanding of the mechanism of projectile defeat is still unclear, it does seem clear that the acoustic impedance mismatch is an important parameter. Here then, it is obvious that the material properties E, and ρ play a significant role as might be expected. High-toughness steels may find applications as a back-up material.

Having discussed the armor properties requirements, we now play the war game tactic of changing hats and wear the hat of projectile designer. How do we prolong the usefulness of the projectile? As indicated above, at certain armor hardnesses (and at critical speeds), the projectile is defective by shattering. What are the characteristics pertinent to the shattering process? Again, with some degree of vagueness, we associate shatter with inadequate damping of reflected stress waves, multiple forking of the crack fronts, and inadequate toughness.

Finally, we have a whole gamut of applications ranging from light vehicles, tractors, and tanks, to aircraft, launchers, missiles, and anchorage devices for mooring water-borne and/or submerged structures. Each may have its unique requirements on strength, toughness, stiffness, and susceptibility to corrosion.

We have, then, identified various specific as well as classes of applications of high-strength steels (occasionally identifying other properties which come into prominence in special cases) but have emphasized only one primary problem, namely, "brittle behavior". There are, of course, other problems associated with the use of high-strength steels per se, and very briefly we indicate a few of these problem areas that relate to design considerations.

First, we appreciate that as the strength level of steels increases, the thickness is naturally decreased if one is to take advantage of the weight decrease potentially derivable therefrom. But as thicknesses go down, there is a transition in the failure mode from flow or fracture to an instability or buckling failure. Buckling, at least of the elastic variety, is governed predominantly by elastic

*References are given on page 23.

modulus and geometry--particularly the thickness--for curved sheet, such as in motor cases, the R/t (radius to thickness) ratio; decreasing the thickness would naturally lead then to a greater susceptibility to this mode of failure.

Even outside of the buckling problem as the strength level of usable materials increases and thicknesses become less, one runs into the difficulty of excessive deflections, associated "softness", and natural frequency shifts which may have significant effects on the dynamic behavior of a system.

So much, however, for this slight diversion to other problem areas; we now return to the main thread of our discourse and ask in effect, "What has been and what is being done to provide solutions for the principal problem of brittle behavior?"

Solutions

Most studies of the brittle behavior problem are directed either at providing an interim design and/or specification solution or at the more basic approach aimed at providing a better fundamental understanding of the fracture process.

It has been reasonably well established that the more important factors affecting brittle behavior include the stress state and history, the geometry (though the influence of geometry is felt principally through its effect on the stress state), the material, the temperature, and inspection procedures and limitations.

Conventional design procedures which were based upon proportioning section sizes to the loads such that stress levels were constrained to not exceed the yield strength were unsatisfactory. Brittle failures occurred at nominal stress levels significantly below the yield strength and, in fact, low temperatures which led to higher yield strength aggravated the tendency to brittle behavior and increased the discrepancy between the yield strength and the live nominal stresses in the component at failure.

Recognition of the transitional behavior of steel from tough to brittle, with temperature provided great impetus to a series of interim preventative design procedures. Principal early effort in the Army was aimed at the development of the "V"-notch Charpy bar and its incorporation into military specifications for high-strength-steel components. The Charpy test combined smallness of specimen size, with ease of testing--even over a wide range of temperatures and strain rates; two principal observations derived from such tests: (a) the energy absorption, and (b) the fracture appearance. For specification purposes a table of Charpy values (at -40 F) versus strength level provided numerical acceptance levels. These values were, however, selected principally upon basis of experience with "well heat-treated steels" of the contemporary vintage and had no sound quantitative relation with design criteria. Nevertheless, the "V"-notch Charpy specimen did provide a most useful tool for the evaluation and relative rating of different materials. In fact, it correlated extremely well with the service performance of some components, e.g., armor plate.

More recently, in the light of studies which have led to a better understanding of the fracture process, the Charpy specimen is again being studied in greater detail. It has been suggested that the Charpy bar be used in a more sharply notched fashion than normally employed in the classical "V"-notch specimen. Some current studies employing fatigue-cracked Charpy bars are being considered more representative of the "worst" possible notch condition. Such fatigue cracks tend also to simplify the possibility of measuring plane-strain fracture toughness accurately. One principal disadvantage of the current use of Charpy specimen lies in its limitation with respect to thickness variation; very thin-sheet specimens buckle prematurely and are not easily tested as individual specimens. Further, the specimen is so shallow that only exceptionally does a steady state fracture mechanism come into play; rather, it seems the Charpy bar leads to a complex closely spaced sequence of failure, each of which is governed by locally different boundary conditions. This is evidenced, for example, by the frequently observed variation of shear lip along the fracture path. It would seem desirable, in order to make any use, say, of the constant shear-lip concept, that a steady state situation prevail at least for a recognizeable length along the fracture path. In the conventional Charpy, one measures the accumulated effect of (a) the initiation energy, (b) the varying propagation energy, if the speed is varying and the material is rate sensitive, (c) the termination energy, and (d) residual losses such as residual kinetic energy and load indentation energy.

Typically, the toughness of sheet steel increases with thickness up to a definite thickness level (the critical thickness, which is related to the critical shear-lip thickness), and then decreases approaching assymptotically the plane-strain fracture toughness usually designated G_{Ic}.

It has been suggested[1] that the shear-lip width, as obtained in a Charpy specimen, may be used as a quantitative basis for deriving the thickness influence on fracture toughness. Such an approach stems from the critical shear-lip concept and leads to calculated thickness effects which follow closely the observed trends. This critical shear-lip concept is not restricted to the Charpy-type specimen but rather may be applied to any of the common notched flat-sheet specimens. The precise conditions under which this concept is valid are not completely understood, however; and until a considerably greater understanding of the lip formation process is on hand, this scheme can, at most, be utilized only as another interim procedure or guide for material selection.

It is significant to note that if one takes into account the shear-lip thickness dependence upon temperature, then one can derive this characteristic shape of the toughness-temperature curve.[2] Of course, in such an approach, it is assumed that the transition is associated solely with the geometric proportions of shear lip and flat fracture, and in this sense, represents only the geometry sensitive aspect of the transitional behavior. If, however, the crystallographic mode of fracture changes with temperature, or if a phase change occurs in the temperature range in question, then these effects would have to be independently considered.

One interesting conclusion which the critical shear-lip concept does lead to is that, though high toughness levels are not readily achievable in bulk (thick) material, if this bulk can be achieved by means of laminating thin sheets, each of which is of the critical shear-lip thickness, then maximum toughness levels corresponding to plane stress can be achieved.

The Charpy approach and the critical shear-lip approach are but two efforts to provide an interim design tool and/or specification level to minimize risk of brittle fracture.

Major recent contributions to the understanding and prevention of brittle fracture stem from two initially divergent paths which now appear to be more intimately meshing. One, the "fracture mechanics" concept is based upon the Griffith "crack" and has been promulgated principally by Irwin. The other is the "continuum mechanics" approach.

The fracture mechanics approach stems from the point of view that all materials have idealized cracks (flaws) and that by means of the Griffith-type instability criterion, one can calculate the "critical" condition under which this "crack" will propagate. Considerable controversy is evident in the literature as to the validity of such a criterion as applied to materials which exhibit some, though slight, ductility at the crack tip. Principal opposition stems from the basic thought that the Griffith-Irwin criterion is a necessary but not sufficient condition for propagation and that energy barriers, e.g., initiation energy, may thwart the satisfaction of the Griffith-Irwin criterion. Principal additional deficiency of the Griffith-Irwin concept was the inadequacy of the treatment of the elastic-plastic zone. Early thrusts of the Griffith-Irwin approach were aimed at essentially by passing this problem by (a) considering the plastic zone small relative to the specimen dimension so that the zone was "contained" in an elastic field, and thus, that the stresses were essentially elastic; and (b) assuming the size of the plastic zone was determined by the elastic analysis. The early development of the ASTM suggestion for fracture testing which, for the great part, reflected the Griffith-Irwin approach, recognized these limitations but by-passed them. Obviously, the inconsistencies followed and interpretation of the significance of various empirical approaches quickly changed day by day as new inconsistent observations were noted and new empirical approaches were tried. Review of a single page, for example, of the "Fifth" special ASTM Committee Report on Fracture Testing reveals no less than four reversals of procedure previously proposed. Three of these can be attributed to complete arbitrariness in assumptions used.

It would seem desirable to build a solid foundation for our study of the mechanics of fracture. A realistic study of the elastic-plastic zone and its effect on "real cracks" is necessary. Perhaps we need to re-examine our concept of the necessity of an "ideal crack". Are not many of our applications such that a finite radius notch or filleted corner the governing geometric factors rather than the extreme "crack"? It is true that the "crack" provides a conservative approach, but by the same token, it is overly severe and leads to excessive weight or superfluous safety factors exacted at the expense of flexibility in choosing from a broader selection of materials.

From the long-range point of view, it would seem necessary to determine the point fracture criterion; for after all, fracture is a point-by-point process. We ought to strive for the ability to evaluate the point fracture toughness and see if there are characteristic toughness levels associated with various macroscopic and microscopic modes of fracture. Is fracture a necking process--even brittle fracture (on a much finer scale)? Is fracture associated with the "exhaustion of ductility" concept? Hopefully, answers to these questions will lead us closer to a rational design concept to minimize brittle behavior by sage selection of material and a knowledge of fracture criteria.

But aside from the material selection approach, there are other approaches one might adopt. More immediate solutions to the brittle behavior problem lie in the utilization of tools already available but all too frequently left unused. Stress analysis must be conducted on a much more subtle level than is customary. Detailed actual stress distribution must be experimentally determined in regions of discontinuities. For very high-strength or low-toughness materials, the effects of surface finish, i.e., scratches, must be watched with care. Scratches ordinarily considered acceptable or ignored may drastically degrade the structural integrity of the part. Design innovation is desirable to transform critically stressed tensile regions to compression, or ideally to reduce or eliminate local geometric stress concentration. Finally, one might attempt to design the component such that crack propagation is arrested by structural reinforcement prior to the functional failure of the component. Studies of plastic pressure vessels have demonstrated the arrest capability, for example, of circumferential ring stiffeners in a pressurized cylinder.

Thus, we observe that complete design against brittle fracture involves not only consideration of the material, the temperature, and inspection techniques, but also to a major degree requires a detailed, precise determination of the stress state as influenced by load history, load distribution, and the geometry of the component.

Summary

Summing up, we have described a number of applications of high-strength steels and have emphasized the primary problems associated with its use--brittle behavior. We have outlined briefly several interim techniques which are used to minimize the risk of brittle behavior and have suggested several directions which are being, or should be, followed in our further research to provide a firm foundation for the understanding and subsequent prevention of brittle fracture.

U. S. Navy

(G. M. Yoder, Bureau of Naval Weapons, Materials Branch, Washington, D. C.)

The prospective usage of steels at very high strength levels in Navy equipment depends largely on the resolution of problem areas, many of which have been indicated by prior speakers.

The problems with high-strength steels can be summarized in a very few words--the threat of unpredictable and unexpected failure. Such failures stem from a number of causes, including operator judgment and unavoidable over loads, materials and processing deficiencies, and deterioration with time of exposure to operating environments. Our immediate concern is limited to materials and design deficiencies and deterioration in service, which singly or in combination may cause failure at stresses below design stresses.

The classical approach was to design on the basis of the yield or tensile strength of the material. These properties are readily determined from simple tests on specially prepared specimens and were successfully employed to predict the load-carrying capacity of structures as long as the other properties were in balance; specifically, if the toughness level was high enough to render the steel relatively immune to the effects of stress concentrations at materials discontinuities. In response to the demand for ever-higher performance, design strengths have been raised in specific areas to the highest strength levels attainable within the commercial processing state of the art. Little consideration was given by designers to the attendant reduction in toughness because experience had not warned us that this deficiency would become a major problem area.

The inadequacy of the classical design approach was dramatically illustrated by the catastrophic failures of ship structures during World War II. Analyses of these fractures and the experimental investigations which ensued focused attention on the importance of a materials ability to arrest the development of a crack-like defect at the minimum operating temperature of the particular structure.

The increased usage of ultrahigh-strength steel has made the problems of structural reliability and notch sensitivity acute in many applications. One well documented failure at stresses far below design strength concerned a 0.080-inch sheet part in a new airframe undergoing structural static load tests. Strain gages located near the fracture indicated a general stress at fracture of approximately 34,000 psi, roughly 12 per cent of the anticipated breaking stress of 280,000 psi specified by the designer and confirmed by the usual Rockwell hardness test. The fracture revealed the pre-existance of a partial crack approximately 0.017 inch in depth by 0.080 inch in length, so oriented that only the 0.017 dimension opened to a surface exposed for inspection by conventional techniques. The flaw was not detected.

This fracture may be attributed to disregard of the notch sensitivity of the steel to manufacturing methods and workmanship which caused the pre-existing crack, and to failure of inspection to disclose the presence of a crack of unstable size. There is every reason to believe that this identical part--including the pre-existing crack--would have withstood much higher loads if heat treated to an intermediate yield strength level.

Another area in which strength levels were advanced beyond the point of diminishing returns concerns wires used in the construction of aircraft shipboard arresting cable. Knowing that multi-axial stress patterns place heavier demands on toughness than uniaxial stresses, one might expect that uniaxial tensile elements might be less susceptible to brittle failure. However, on two occasions wire rope laid up in the conventional manner using special processed very high-strength (380,000) wires of two distinctly different types, failed to pass the qualification test requirements applicable to conventional aircraft shipboard arresting cable. The toughness of the high-strength wire, as measured by torsional twist tests, had been reduced only 20 per cent.

Notch sensitivity is a threat to the service life of a part only when stress concentrations are present in localized areas. Factors which may cause such localized concentrations include metallurgical features such as segregation, inclusions, misorientation of slip systems between micro areas (grains), disturbance of the microstructure at welds, etc. Geometric stress concentrators include surface roughness, discontinuities, sharp corners, corrosion pits, mismatch of machined surfaces or joints. Design stress concentrators include abrupt changes of geometric section in load-carrying members, inappropriate selection of manufacturing methods--such as the drilling of

holes in fully hardened parts--and methods of applying protective coatings, avoidance of contact between electrochemically dissimilar metals, and avoidance of residual stresses. Residual stresses near a surface may reduce fatigue life and promote stress-corrosion cracking. Cleaning and plating techniques can embrittle because of the introduction of hydrogen.

The designer must be familiar with the above factors and with the limitations and capabilities of inspection techniques. It should be assumed that partial cracks of such size as will escape detection are, in fact, present on surfaces of parts; these cracks will grow during the life of a long-life structure, and if permitted to reach critical size, will cause failure. The critical or unstable crack size is an important consideration in the selection of steels.

The demands on structural steels for submerged hulls for equipment such as mines, torpedoes, and submarines to operate at depths of present interest, 6000 feet and more, are beyond the capability of HY 80, which has been the conventional hull steel since World War II. Both the propulsion systems and hull structures must be made stronger. This could be accomplished at the expense of buoyancy except that the demand for operating range and payload is also magnified because prospective targets will be stronger than today's structures. Ratios of collapse depth to structural weight, or hull weight to displacement, indicate that yield strength levels of not less than 200,000 psi are essential. Submerged hulls are subjected to multi-axial compressive loads with super-imposed pulsating stresses from the propulsion system, plus shock loads of uncertain magnitude. We must live with localized stress concentrations for a number of reasons, including the disturbance of the microstructures during welding, and because of surface irregularities as well as design configuration. The steel must be clean, tough, weldable, and resistant to stress corrosion. Fracture may occur without warning and is frequently catastrophic.

Deterioration and damage by corrosion and by the interraction of stress and corrosion are major factors with respect to reliability and maintenance cost. Corrosion per se is the lesser of the two problems provided appropriate precautions are observed in design and manufacture. However, methods of precleaning, applying, and even of removing protective coatings which have been successfully employed at lower strength levels embrittle steels to a degree which cannot be tolerated at high strength levels.

Stress corrosion is a particularly insidious cause of cracking because penetration rates can reach higher levels, and there is no readily detectable evidence of the location or extent of damage prior to fracture. It can be a serious problem in unused equipment, in parts under sustained loads such as aircraft landing gears, supporting structures, and around press-fitted inserts in dissimilar metals. It is much more serious, however, as a contributing factor toward failure of equipment during service. There is some indication that the tougher steels now being developed will be less susceptible. Various investigators have reported a correlation between plane-strain fracture toughness and resistance to attack by stress corrosion. However, more effective means of prevention and tests for detection of damage are needed.

Although our pursuit of higher strength levels has led to an intensification of a broad spectrum of problems, the objective--with some clarification--remains unchanged. Higher useable strength is essential; in other words, higher strength with toughness and weldability plus an acceptable level of stress corrosion behavior. Some advances have been attained through alloying, improved melting practices and hardening processing. Our research laboratories point to still higher levels of strength and toughness attainable by methods not yet adaptable to production. To devise production methods which will take full advantage of this knowledge may well prove one of the most difficult problems facing today's metallurgists.

References

(1) Bluhm, Joseph I., "A Model for the Effect of Thickness on Fracture Toughness", Proceedings ASTM, Vol 61, 1324 (1961).

(2) Bluhm, Joseph I., "Geometry Effect on Shear Lip and Fracture Toughness Transition Temperature for Bimodal Fracture", Proceedings ASTM, Vol 62, 1 (1962).

DESIGN PARAMETERS IN MATERIALS SELECTION

by

George Gerard*

SUMMARY

The potential use of ultrahigh-strength steels in various structural applications is assessed from the standpoint of minimum weight structural design. From the data presented, the aerospace, naval, and other military applications where ultrahigh-strength steels have an attractive potential for weight savings as compared to other competitive materials are identified and discussed in terms of design parameters. In addition, the areas where ultrahigh-strength steels are not competitive become evident from the data presented.

As a broad generalization, attractive ultrahigh-strength steels applications are related to tension-load applications. Under tension loading, the limited ductility and consequent notch sensitivity of high-strength materials require meticulous attention in design details, specialized materials testing and selection, and fabrication and inspection procedures. The various design aspects of this problem area are discussed in terms of the useable strength level of limited ductility materials in the presence of notches and cracks.

LIST OF SYMBOLS

d	diameter
D	structural design index
$\bar{e}$	ductility ratio
E	elastic modulus
h	height
k_e	elastic stress concentration factor
m	exponent
M	bending moment or material efficiency factor
N	axial compressive loading
p	pressure
S	structural strength or structural efficiency factor
w	width
W	weight efficiency factor
ρ	density
σ_{cy}	compressive yield strength
σ_{tu}	ultimate tensile strength
Σ_o	optimum solidity
β	buoyancy coefficient

STRUCTURAL POTENTIAL OF ULTRAHIGH-STRENGTH STEELS

The basic objective here is to assess the structural applications that could potentially benefit from the use of ultrahigh-strength steels. In doing so, a "design sciences" approach is utilized to identify the efficient use of structural materials. This approach, which has been developed during the past two decades, permits one to establish the significant design parameters by which the efficiency of various structural configurations and materials may be evaluated using minimum weight as the criterion of optimum design. It is an analytical approach which provides optimum design results directly; it does not involve multiple trial and error solutions on a computer.

Aircraft, spacecraft, surface ships, submarines and other vehicle types are generally characterized by the fact that the configuration, overall loads, and leading dimensions of the structure are specified within rather narrow limits by performance requirements; aerodynamics and hydrodynamics, launch loads and payloads. Consequently, the structural designer has some degree of freedom within the confines of the leading dimensions to subdivide the structure by use of suitable stiffening systems to achieve a minimum weight design. He also faces the problem of efficient material selection for the particular structure.

The design sciences approach synthesizes this statement of the design problem through the use of certain design indices which appropriately combine the external loads and leading dimensions. It then utilizes idealized structural configurations such as stiffened box beams and stiffened cylinders as representative structures to establish optimum designs from which the comparative efficiencies of various materials can be evaluated.

For our purposes, here, we shall not be concerned with the analytical developments in this area (see, for example, References 1-5*) but with the results that can be obtained from this approach. As a broad generalization, the results of various types of minimum weight analyses on representative structures can all be expressed in the following form:

$$W = S \cdot M \cdot D^m \qquad (1)$$

where: W = weight efficiency factor
S = structural efficiency factor
M = material efficiency factor
D = structural design index
m = exponent $(0 < m \leq 1)$.

The weight efficiency factor, W, can be interpreted in several different ways and for our purposes here is expressed in the form of a weight/strength ratio. The structural efficiency factor, S, is generally a nondimensional quantity, whereas M is generally a density/strength or density/modulus ratio representative of the material efficiency. The design conditions involving the external loads and leading dimensions are characterized by the structural design index, D. Thus, Equation (1) represents

* President, ARA Division Allied Research Associates, Inc., Concord, Massachusetts

* References are given on page 31.

the interrelationship among structures, materials, and design.

Box-Beam Structures

Surface ship hulls, aircraft wings and tails, and hydrofoil foils can be characterized in an idealized form as stiffened box beams under bending. The longitudinal stiffeners can be I, Z, or hat sections supported by transverse ribs at the optimum spacings. From Reference 2, the following relation can be obtained ($D_c/D_t = 1$, $\sigma_c = 1$) for stiffened box beams subject to buckling of the compression cover.

$$\frac{\text{Weight}}{\text{Strength}} = \frac{\rho \Sigma_o}{M/h^2 w} = 2.38 \frac{\rho}{E^{0.6}} \left(\frac{M}{h^2 w} \right)^{-0.4} \quad (2)$$

It is to be noted that Equation (2) is in the same form as Equation (1) when we identify the various terms as follows: $S = 2.38$, $M = \rho/E^{0.6}$, $D = M/h^2 w$.

While Equation (2) represents the stability limitation due to buckling, there is also a strength limitation that governs when the buckling strength equals or exceeds the compressive yield strength of the material. In this case, we have the simple relationship

$$\frac{\text{Weight}}{\text{Strength}} = \frac{\rho}{\sigma_{cy}} \quad (3)$$

Thus the material efficiency factors are $M = \rho/\sigma_{cy}$ when strength limitations govern and $M = \rho/E^{0.6}$ when stability limitations govern.

Results obtained by use of Equations (2) and (3) were determined for various high-strength sheet materials based on the properties given in Table 1. These results are shown in Figure 1 in terms of the design index, $M/h^2 w$. In the stability region, the lower density materials are more efficient whereas their inherent strength limitations cause a reversal of roles in the strength region. It can be observed that in the stability region, steel is the least efficient material of those considered by virtue of the highest value of $\rho/E^{0.6}$. In the strength region, steel is competitive with aluminum alloys at 225 ksi yield levels and with titanium alloys at 300 ksi.

The preceding results are obtained from the design science analysis. Now it is pertinent to relate these results to the state-of-the-art design index values representative of various types of vehicles. Such data have been gathered from a broad range of actual designs, and for box-beam types of structures characterize the maximum values of the design index at the midship section for surface ships and the root section of aircraft wings and tails. These data are shown in the lower portion of Figure 1.

TABLE 1. PROPERTIES OF HIGH-STRENGTH SHEET MATERIALS USED IN ANALYSIS

Alloy	Density (ρ), pci	Modulus (E), psi	Comp. Yield Strength (σ_{cy}), ksi
Magnesium	0.065	6.5×10^6	30
Aluminum	0.105	10.5	80
Titanium	0.165	16.5	180
Steel	0.285	28.5	225-300

By relating the design sciences results and the state-of-the-art index values shown in Figure 1, it is possible to arrive at some definitive conclusions concerning the efficient selection of materials:

(a) For surface ship hulls, stability considerations govern because of their relatively low index values and the lower density alloys are more efficient from a minimum weight standpoint. Ultrahigh-strength steels do not appear to have any application here.

(b) For both subsonic and supersonic wings and tails, magnesium, aluminum, and titanium alloys are efficient as the design index value is increased. Ultrahigh-strength steels above the 300-ksi yield strength level become competitive with titanium alloys only at the highest end the design index range.

(c) For the estimated hydrofoil foil range shown in Figure 1, aluminum and titanium alloys appear to be the most efficient materials for this application.

It is to be noted that various forms of Army combat vehicles and military bridges can be represented by the box-beam category of structures However, in the absence of data on such structures, no conclusions can be drawn here although it is suspected that the design index range probably corresponds to the surface ship hull region.

Stiffened Cylinder Structures

Aircraft fuselages, and missiles and launch vehicles can be idealized as stiffened cylinders under bending and axial compression, respectively. The longitudinal stiffeners can be I, Z, or hat sections supported by similarly shaped frames at the optimum spacing. From References 1 and 4, the following stability relation can be obtained for stiffened cylinders under axial compression:

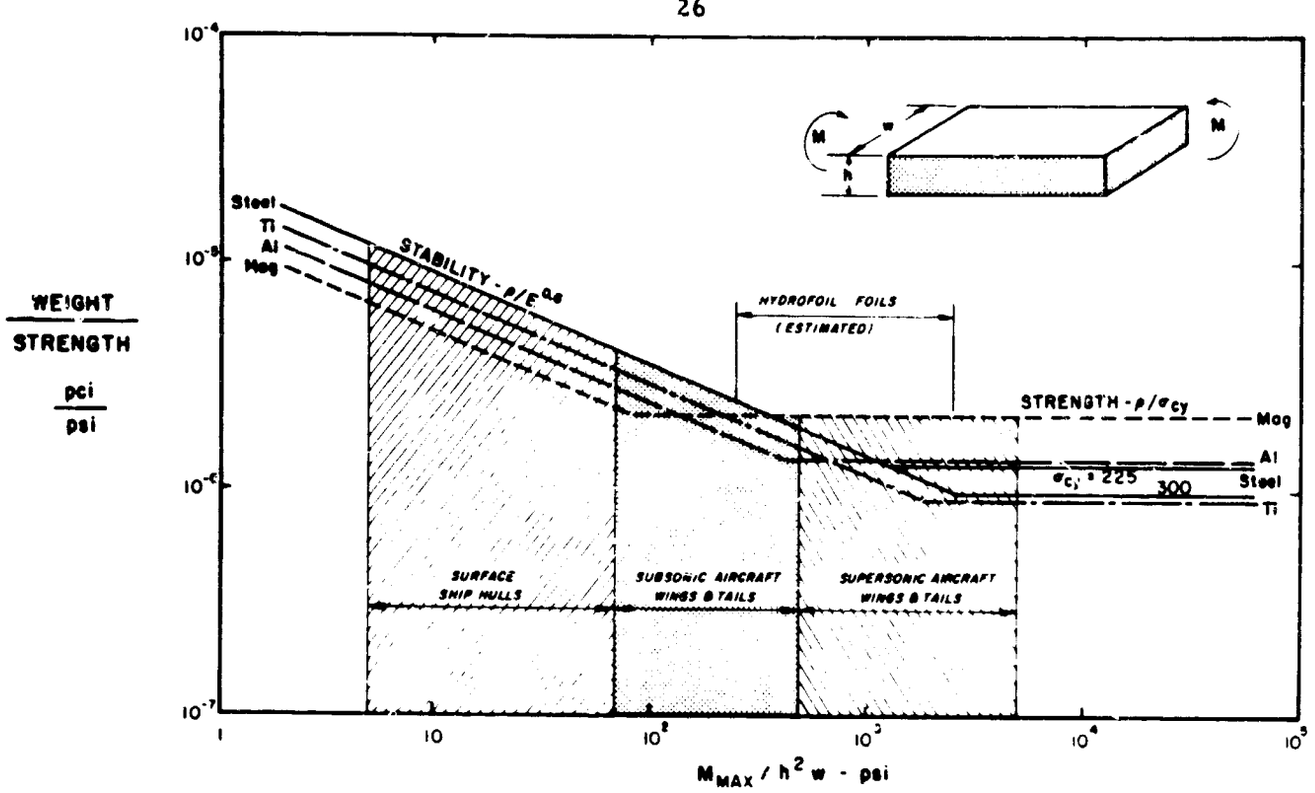

FIGURE 1. COMPARATIVE EFFICIENCIES OF MATERIALS IN STIFFENED BOX-BEAM APPLICATIONS

$$\frac{\text{Weight}}{\text{Strength}} = \frac{\rho \Sigma_o}{4N/d} = 1.25 \frac{\rho}{E^{0.6}} \left(\frac{N}{d}\right)^{-0.4} \quad (4)$$

By comparing Equations (4) and (1), S = 1.25, $M = \rho/E^{0.6}$, and D = N/d. While S and D are different as compared to stiffened box beams, note that M is the same for both cases. In addition, the strength limitation is the same as given by Equation (3).

Numerical results based on the use of Equations (3) and (4) in conjunction with the material properties listed in Table 1 are displayed in Figure 2. Also shown in the lower portion of Figure 2 is the design index range corresponding to the state-of-the-art for aircraft fuselages under bending and missiles and launch vehicles under axial compression. It is quite apparent that stability considerations govern the design of such vehicles and consequently the lower density alloys such as magnesium and aluminum are efficient. Ultrahigh-strength steels clearly are not efficient materials for these applications.

Pressure Vessels

Submarine pressure hulls, and solid-propellant rocket engines and various ordnance materiel items can be treated as pressure vessels under external or internal pressure, respectively. In the strength-limitation region, Equation (3) is valid for both loading cases. However, under external pressure, stability limitations can occur. For an I, Z, or hat frame stiffened cylinder (L/d = 1), the following is obtained from Reference 5:

$$\frac{\text{Weight}}{\text{Strength}} = \frac{\rho \Sigma_o}{2p} = 1.5 \frac{\rho}{E^{7/13}} (p)^{-6/13} \quad (5)$$

Numerical results based on the use of Equations (3) and (5) and Table 1 are given in Figure 3 together with the current design index range for solid-propellant rocket engines, deep-submergence pressure hulls, and ordnance materiel. Here we see that strength considerations play a governing role for all applications. Ultrahigh-strength steels and titanium alloys are competitive here and constitute the most efficient metallic materials in this area.

Although we have identified an application of potential for ultrahigh-strength steels, we must also recognize that this is also an area of potential for nonmetallic materials such as filament wound structures. Typical weight/strength ratios for glass filament wound composites are indicated in Figure 3 and it can be observed that these values are indeed attractive.

Potential Applications For Ultrahigh-Strength Steels

From the foregoing analysis, it appears that ultrahigh-strength steels at the 300-ksi yield strength level have a structural potential in the following applications:

Structural	Loading
deep-submergence hulls	compression - long time
rocket-engine cases	tension - short time
ordnance materiel	tension - short time

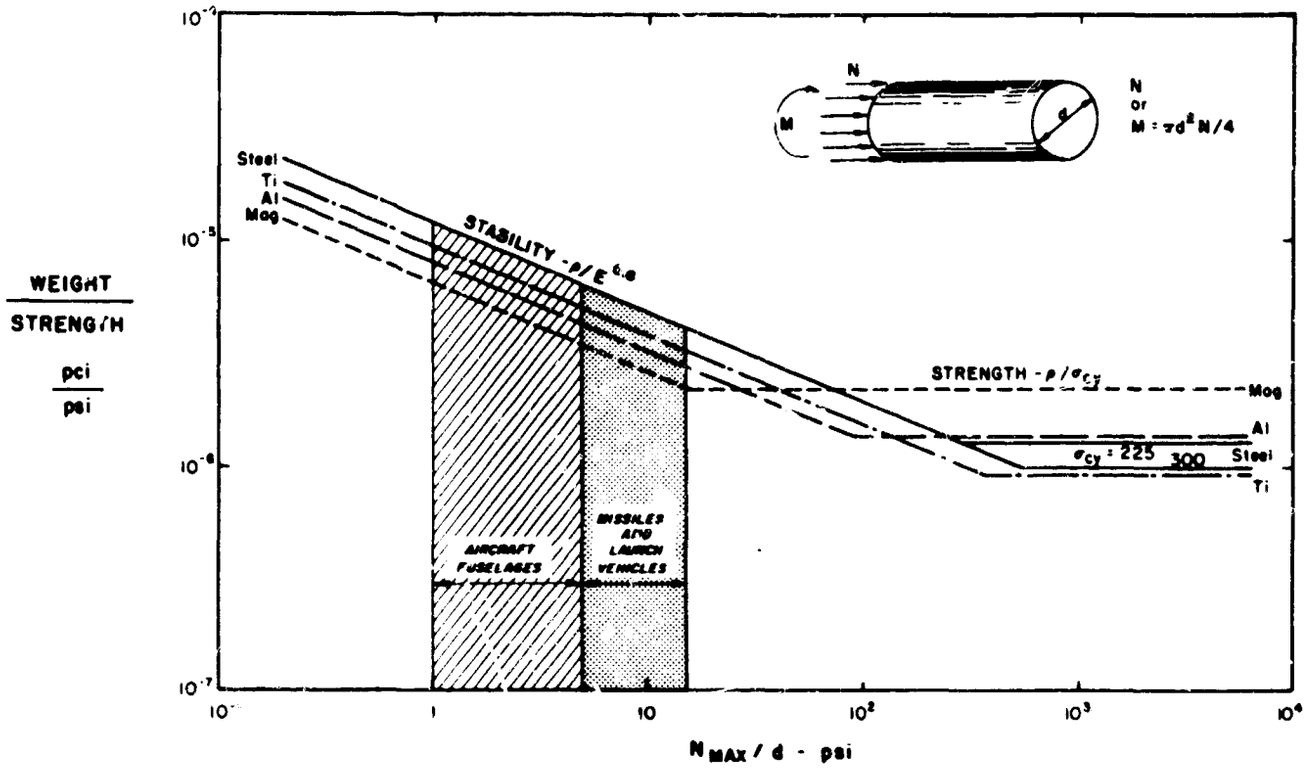

FIGURE 2. COMPARATIVE EFFICIENCIES OF MATERIALS IN STIFFENED CYLINDER APPLICATIONS

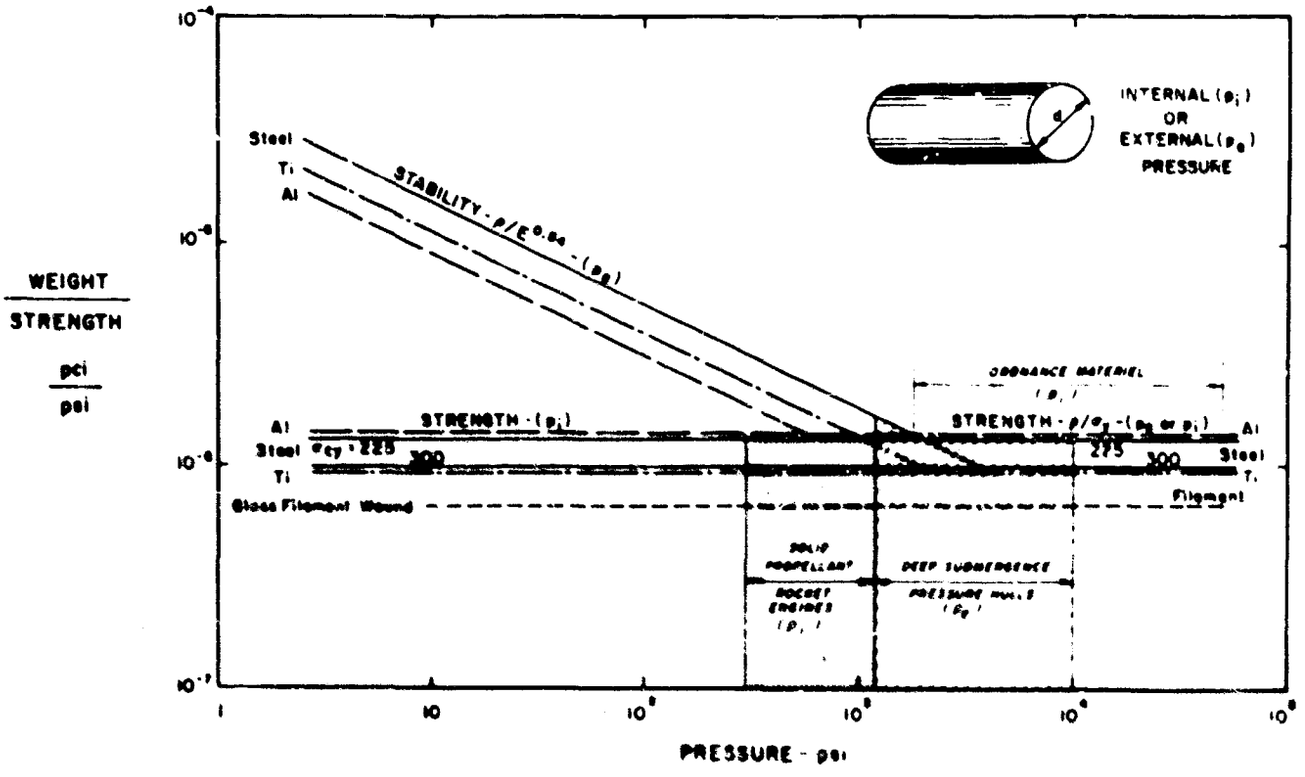

FIGURE 3. COMPARATIVE EFFICIENCIES OF MATERIALS IN PRESSURE VESSEL APPLICATIONS

It must be observed, however, that from a minimum weight standpoint, titanium alloys and glass filament wound structures do exhibit a competitive edge on the ultrahigh-strength steels. The competition is sufficiently close that minimum costs of the fabricated structure may govern the selection of materials for these applications. In this regard, steels may show to some advantage because of their lower costs in sheet form.

DEEP-SUBMERGENCE PRESSURE HULLS

Having identified ultrahigh-strength steels as being potentially competitive with other materials for deep-submergence pressure hulls, we shall consider here some of the design factors retarding its use and some design possibilities for removing such limitations. It is to be noted that although this discussion focuses on ultrahigh-strength steels, other competitive high-strength materials share many of the same difficulties.

The attainment of a deep-submergence capability for naval operations requires a sufficiently light-weight pressure hull so that a reasonable payload can be carried. The hull structure is designed primarily on the basis of compressive strength and is subject to relatively long-time loading under cyclic conditions. This design problem is illustrated in Figure 4 in terms of depth capability and buoyancy coefficient which reflects the buoyancy of the pressure hull and conversely the payload. It appears that a buoyancy coefficient of 0.5 is a reasonable upper limit for naval submersibles.

One of the important factors retarding the use of steels in this application is the insistence upon welding the relatively thick plates required for the pressure hull. The pressure hull performs at least three separate functions: it transmits and resists the external pressure, it provides the desired contour, and it provides the sealing function and other environmental protection. The use of welding is primarily associated with the sealing function since the other functions can be handled independently of welding. As shown in Figure 4, the weight penalty associated with the use of weldable steels such as HY 80, and a yet to be attained HY 150, places a distinct limitation on a deep submergence capability.

There is a design approach which has been suggested[5] and successfully tested[6,7], which can remove this limitation. The approach is to separate the three design functions of the pressure hull instead of incorporating all of them in a welded monolithic structure. By dividing the functions, ultra high-strength steel rings at the 300 ksi yield strength level can provide the load transmission and contouring function. On the outside, a relatively thin welded steel sheath chosen for its weldability rather than strength provides the sealing function and environmental protection.

The weight penalty associated with the use of the welded sheat is relatively small and permits a a significant increase in deep submergence capability. It constitutes a design approach which removes the limitations inherent in welding of thick high-strength heat-treated plating and quite possibly permits the use of ultrahigh-strength steels in the more immediate future.

PRESSURE VESSELS

The use of ultrahigh-strength steels in pressure vessel applications such as solid-propellant rocket-engine cases and ordnance materiel has been identified as competitive with other high-strength materials. We shall now examine some of the design factors retarding its use and possible design solutions.

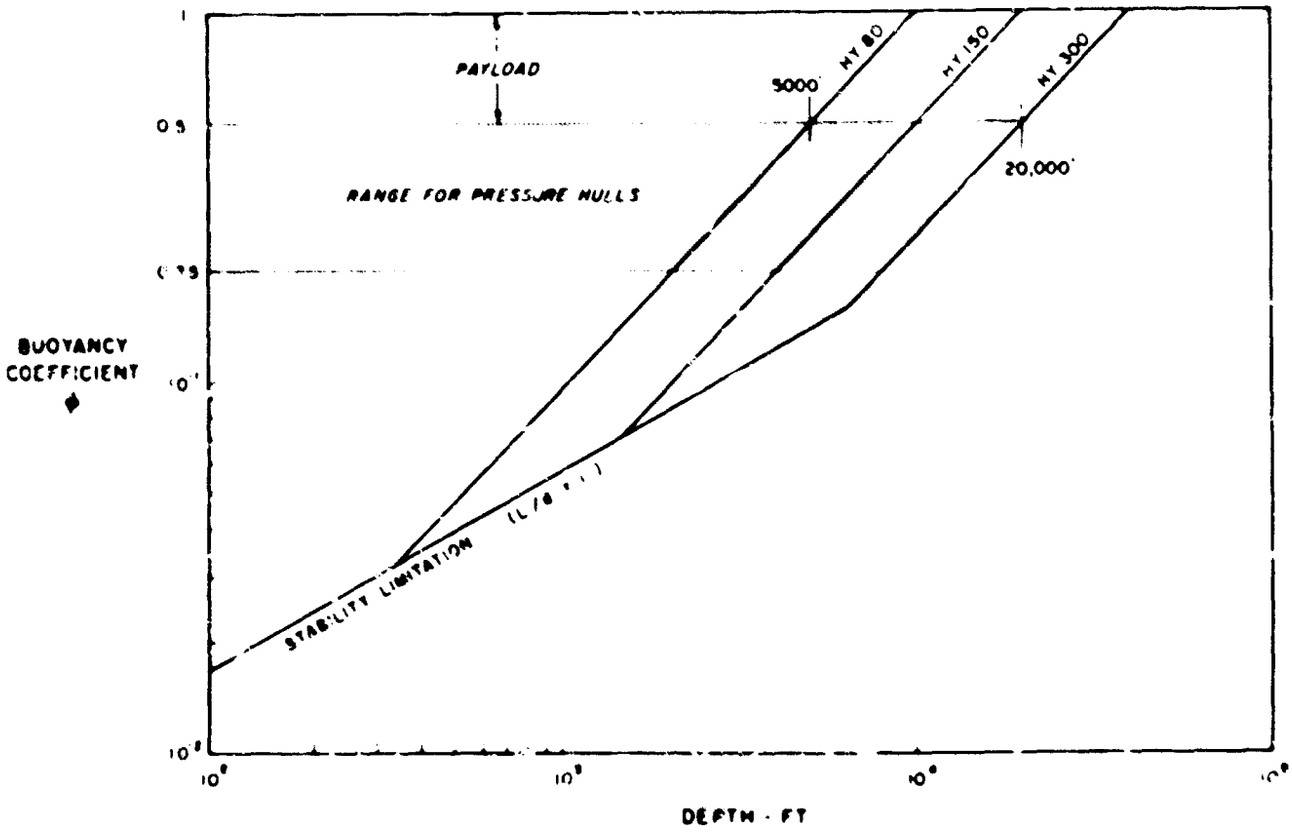

FIGURE 4. COMPARATIVE EFFICIENCIES OF VARIOUS STEELS FOR RING-STIFFENED CYLINDERS UNDER EXTERNAL PRESSURE

One of the major factors retarding the use of ultrahigh-strength steels as well as other high-strength materials in structural applications is the loss of ductility as the strength level increases. For plastic behavior, ductility is required to reduce the stress concentrations resulting from geometric discontinuities or fabrication and thus permit structural strength to approach the strength of the material used. The problem is reasonably well recognized today and areas such as fracture mechanics, notch toughness, fracture initiation, and fracture propagation are associated with various aspects of it. We shall be concerned here with the fracture initiation phase.

Ductility Ratio

In considering the use of ultrahigh-strength materials, it must be recognized that there is an essential difference between the strength of tension structures and the tensile strength of materials. A tension structure inevitably contains stress concentrations which tend to reduce the structural strength from the strength level associated with the material.

The simplest representation of a tensile structure is a flat strip similar to the smooth tensile specimen used to obtain the strength of a material, but containing a suitable stress concentration. By testing to failure specimens containing a range of elastic stress concentration factors, the plastic stress concentration factor can be determined. As shown in Reference 8, these data can be plotted in a form which yields the ductility ratio, a quantity which can be looked upon as a basic mechanical property that provides a meaningful measure of ductility in a structural sense. The ductility ratio has a value of unity for a completely brittle material and a value of zero for a completely ductile material.

Ductility ratio data obtained from such tests on various steels, titanium alloys, and beryllium are shown in Figure 5 in terms of the strength/weight ratio. The data tend to follow the line shown in the figure within 10 per cent limits and thus reflect a convenient strength/weight ductility ratio "law" that hardly could have been anticipated. Also shown in Figure 5 is an estimate of the improvement in ductility ratio that may be associated with the more recent hot-work and maraging ultrahigh-strength steels.

Structural Strength/Weight

By use of the data contained in Figure 5, calculations can be made to estimate the influence of ductility and stress concentrations upon structural strength/weight as compared to material strength/weight. Following the analytical procedures of Reference 8, the results presented in Figure 6 are obtained where structural strength/weight is plotted as a function of material strength/weight for various reference values of the elastic stress concentration factor, k_e.

It is most interesting to observe that for each value of k_e, the structural strength reaches a maximum and then declines with further increases in the material strength/weight ratio. This result is associated with the reduced ductility as the strength level of the material is increased. The results shown in Figure 6 indicate that there is an optimum σ_{tu}/ρ for each elastic stress concentration at which S/ρ has a maximum value. Departures to either side of this strength level result in a decrease in structural strength.

In order to confirm these predictions, extensive sharp notch-test data on various steel sheet materials from Reference 9 are shown in Figure 7. Also shown is the predicted trend based on the use of Figure 5 and the analysis of Reference 8. It can be observed that the trend is predicted with reasonable accuracy particularly in terms of the existence of a maximum S/ρ. For very sharp notches (k_e = 17), it is evident from Figure 7 that the optimum σ_{tu}/ρ for materials is of the order of 0.8×10^6 (psi/pci) or approximately 225 ksi ultimate tensile strength for steels.

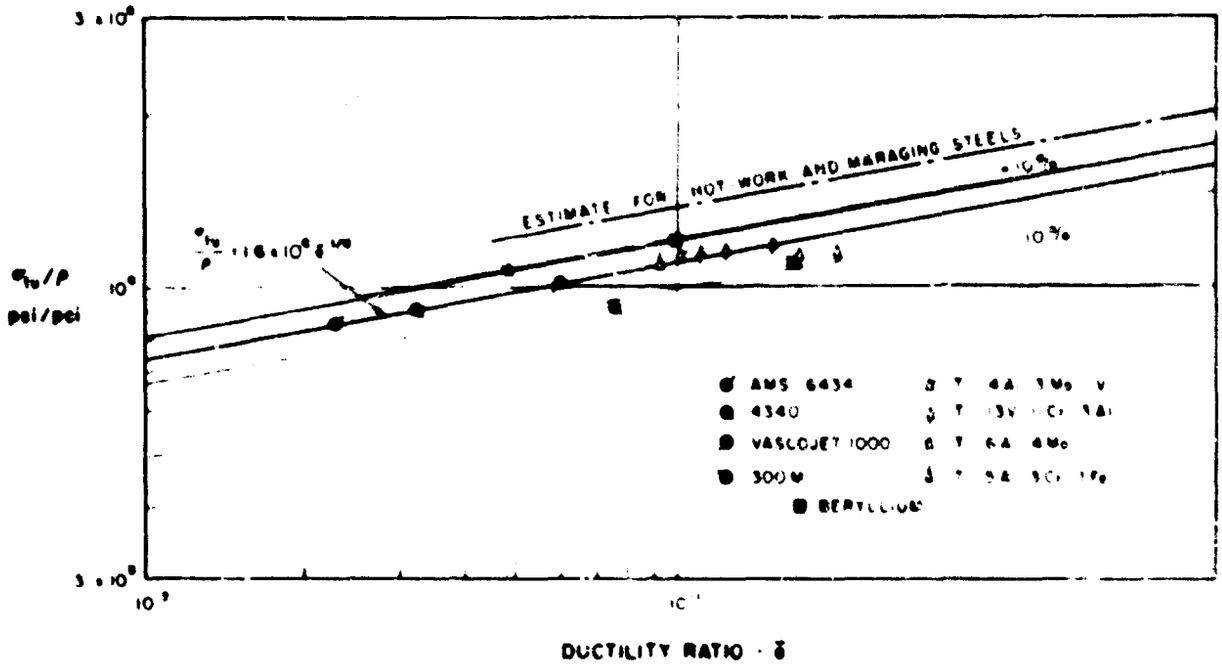

FIGURE 5. STRENGTH/WEIGHT RATIO OF VARIOUS MATERIALS AT ROOM TEMPERATURE AS A FUNCTION OF DUCTILITY RATIO

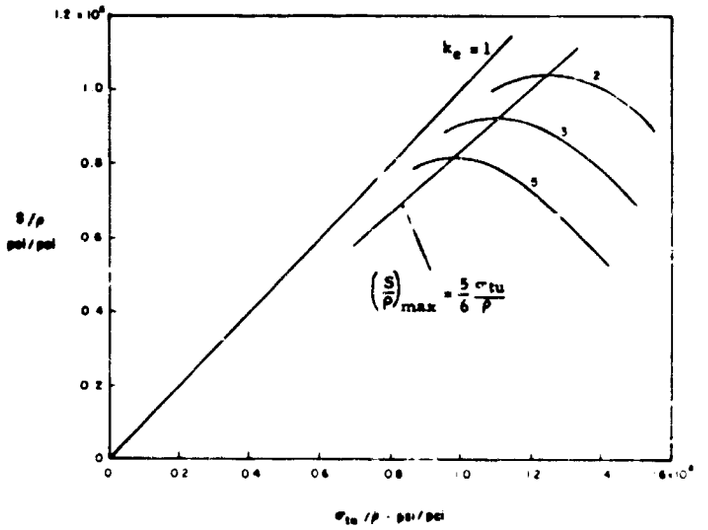

FIGURE 6. STRUCTURAL STRENGTH/WEIGHT AS A FUNCTION OF MATERIAL STRENGTH/WEIGHT FOR VARIOUS ELASTIC STRESS CONCENTRATION FACTORS

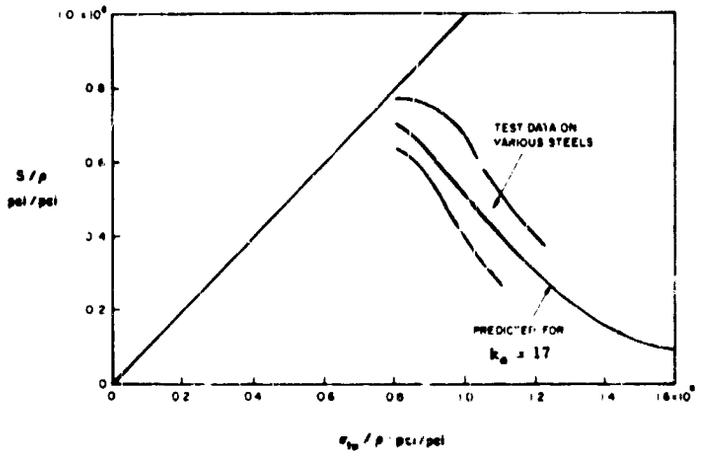

FIGURE 7. COMPARISON BETWEEN NOTCH TEST DATA AND PREDICTED TREND FOR STEELS

Design Guidelines

The results presented in Figure 6 can be synthesized to provide some approximate guideline for the use of ultrahigh-strength steels in tension structures. By using the elastic stress concentration factor as a reference value which characterizes the efficiency of the structural design and its fabrication, the results shown in Figure 8 are obtained from Figures 5 and 6. On the left scale, the optimum tensile strength of steel and the associated maximum attainable structural strength levels are shown. On the right scale, the minimum required ductility in per cent for a given elastic stress concentration factor is shown. It is to be noted that as shown in Reference 8, the ductility is associated with the zero gage-length fracture strain.

The results shown in Figure 8 are presented in terms of the elastic stress concentration factor, k_e, because it is believed that this factor can provide a meaningful characterization of the efficiency of the structural design and fabrication. For example, the maximum k_e resulting from geometric discontinuities in the structure can be established analytically or by experimental techniques such as photoelasticity, strain gages, or coatings. The stress concentrations arising from fabrication such as tolerance mismatches or the minimum detectable flaw size can also be represented in terms of an effective elastic stress concentration factor. Thus, k_e can be used as a basic design parameter to characterize the efficiency or quality of the structural design and fabrication.

It is for this reason that the horizontal scale of Figure 8 is somewhat arbitrarily divided into three "quality" regions as follows:

Region	k_e range	Requirements
Quality A	1-3	meticulous design and fabrication
Quality B	3-8	careful design and fabrication
Quality C	>8	routine design and fabrication

These regions are to be looked upon as conceptual rather than quantitative at this stage of development and were selected primarily for the purposes of providing some guidelines as to the minimum ductility that is required in each of these regions.

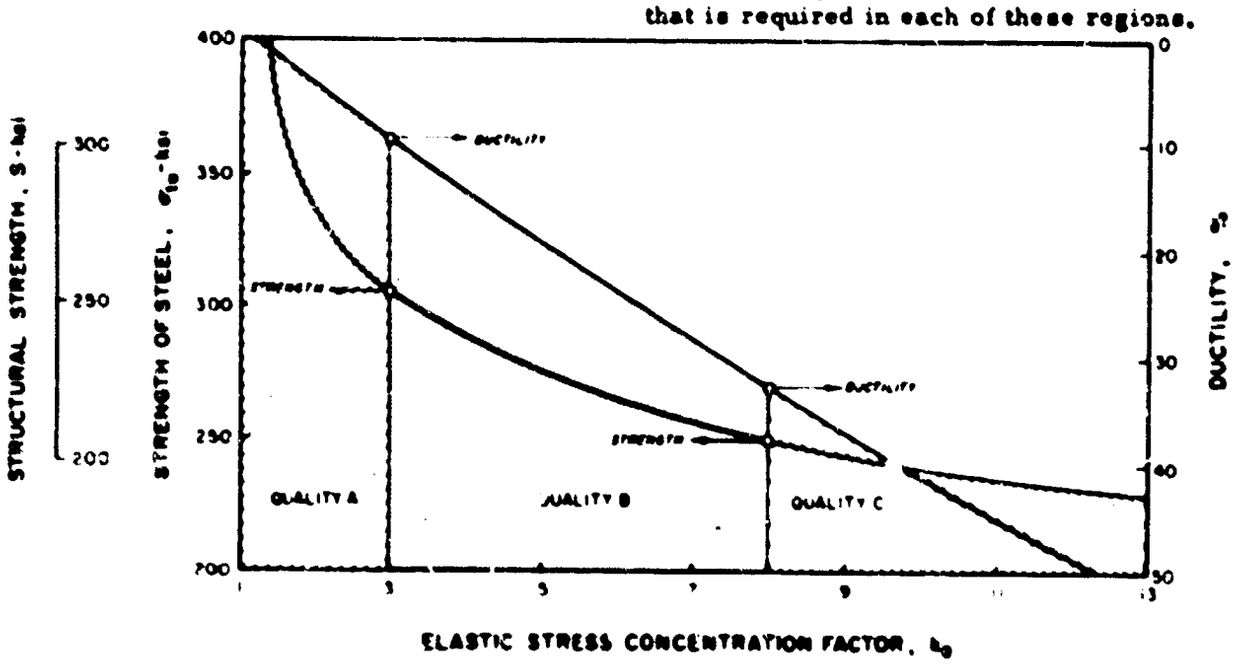

FIGURE 8. OPTIMUM STRENGTH LEVEL AND REQUIRED DUCTILITY FOR TENSION STRUCTURES CONTAINING VARIOUS ELASTIC STRESS CONCENTRATIONS

In the Quality C region which is associated with stress concentration factors greater than 8, structural strength levels of approximately 200 ksi can be realized using 240-ksi ultimate tensile strength steels of adequate ductility. A rough estimate of the minimum required zero gage-length ductility is approximately 30 per cent as indicated in Figure 8. For this region, it is anticipated that rather routine aerospace design and fabrication techniques can be employed because of the relatively large ductility requirements.

The Quality B region requires rather careful design and fabrication techniques to achieve elastic stress concentration factors in the 3 to 8 range. For k_e = 3 and 10 per cent zero gage-length ductility, 250-ksi structural strength levels appear to be attainable with 300-ksi ultimate tensile strength steels.

Meticulous design and fabrication techniques are required to operate in the Quality A region because of the relatively low stress concentration factors associated with this region. The required ductility values become quite low and the structural strength level reflects a dangerous sensitivity to small changes in stress concentration. These tentative conclusions are based upon the main trend line shown in Figure 5. It is believed that a significant improvement in this picture can be realized with the newer hot-work and maraging steel for which an estimate of improvement in ductility is shown in Figure 5.

Easing the Limitations

Having identified some of the design parameters retarding the use of ultrahigh-strength steels and other high-strength materials, we turn now to some approaches which can ease the current limitations. These approaches involve structural design, structural fabrication and testing, and the development of materials.

It is quite obvious from Figure 8 that the structural designer must strive to reduce stress concentrations in order to achieve maximum structural strength levels compatible with the materials selected. If relatively low stress concentration factors cannot be achieved, there is obviously no point in using ultrahigh-strength materials. In fact, their use could lead to lower structural strength than by use of a lower strength, more ductile material.

Minimum detectable fabrication flaws should be evaluated in terms of an effective elastic stress concentration factor. Flaws of small length relative to the size of the structure are not necessarily associated with high stress concentration values as indicated in Reference 10. Consequently, they can be related to the Quality regions shown in Figure 8 together with the structural design values of k_e.

In connection with the limitations imposed by stress concentrations, do not overtest. The data shown in Figure 7 were obtained from severely notched specimens with a k_e = 17. It is apparent from Figure 7 that if this value of k_e is truly representative of the structural application, only an upper structural strength level of approximately 200 ksi (0.7 x 10^6 psi/per) can be realized regardless of the tensile strength of the steel used. This test procedure obviously restricts the structural design to the Quality C region and clearly can represent an example of overtesting.

With regard to the development of materials, it is quite apparent that improvements in the zero gage-length ductility particularly in the Quality A and B regions are to be welcomed. More importantly, perhaps, is the concept that optimum heat-treatment procedures should not be based upon achieving the highest ultimate tensile strength of the material but upon achieving the highest tensile strength for an elastic stress concentration representative of the Quality region of interest. This concept which accounts for ductility and its effect upon stress concentrations could lead to an effective increase in the structural strength level of existing ultrahigh-strength steels.

REFERENCES

(1) Gerard, G., Minimum Weight Analysis of Compression Structures, New York University Press, New York (1956).

(2) Gerard, G., Introduction to Structural Stability Theory, McGraw-Hill Book Company, New York, 73-118 (1962).

(3) Gerard, G., "An Evaluation of Structural Sheet Material in Missile Applications", Jet Propulsion, 28 (8), 511-520 (August, 1958).

(4) Gerard, G., "Structural Interplay: Design and Materials", Aero/Space Engineering, 18 (8), 37-42 (August, 1959).

(5) Gerard, G., "Minimum Weight Design of Ring Stiffened Cylinders Under External Pressure", Journal of Ship Research, 5 (2), 44-49 (September, 1961).

(6) Krenzke, M. A., and Kiernan, T. J., "Structural Development of a Titanium Oceanographic Vehicle for Operating Depths of 15,000 to 20,000 Feet", David Taylor Model Basin Report 1677 (September, 1963).

(7) Macurdy, A. C., "Exploratory Investigation of Nonwelded Pressure Hulls For Hydrospace Vehicles", David Taylor Model Basin Report 1762 (March, 1964).

(8) Gerard, G., "Structural Significance of Ductility in Aerospace Pressure Vessels", ARS Journal, 32 (8), 1216-1221 (August, 1962)

(9) Espey, G. B., Jones, M. H., and Brown, W. F., "Sharp Edge Notch Tensile Characteristics of Several High Strength Titanium Sheet Alloys at Room and Cryogenic Temperatures", Symposium on Low Temperature Properties of High Strength Aircraft and Missile Materials, ASTM STP 287, 74-95 (1960).

(10) Gerard, G., "Residual Tensile Strength of Cracked Structural Elements", AIAA Journal, 1 (5), 1175-1177 (May, 1963).

EFFECT OF PRIMARY PROCESSING ON ULTRAHIGH-STRENGTH STEELS

by

Dr. J. C. Hamaker, Jr.*

To properly discuss the primary processing variables that affect the properties and performance of the many ultrahigh-strength steels would involve much more time than we wish to spend today. As an alternative, a description of a few outstanding examples might offer some insight into the powerful effects of these variables without, we hope, boring you with too much detail. Examples will be cited of work in our laboratories, and that of others, with respect to: (1) a change in primary processing that was made, (2) its effect on product quality or properties in both research studies and routine inspection of multiple heats, and (3) where available, actual components in which its effect on performance or reliability has been demonstrated.

In accumulating these data, statistical quality control tests from large quantities of steel were used when available to more accurately define the effects of primary processing. It is well recognized that comparisons of a few sample bars or sheets may or may not be representative of production quantities due to the statistical variations involved. Since the large quantity data were necessarily collected over a span of years, they do not always include the notch tests of more recent interest; however, notch-toughness data on quantity production are included in the paper where available. Incidentally, fracture toughness tests are still not found in many specifications and the need for their statistical evaluation in production quantities is indicated.

The conference objective of 225-ksi minimum yield strength also limited the number of comparisons available. For example, in studying the effect of vacuum melting, one finds that D6AC has been used mostly at lower strength levels and almost exclusively in the vacuum melt, rather than the air melt, condition. On the other hand, 4340 has a somewhat limited vacuum melting history compared with its extensive air-melt experience. Thus, comparisons to show effects of primary processing were necessarily limited to (1) materials with production histories in both conditions, and (2) testing techniques of the type employed in the evaluations.

Vacuum Melting

The most important recent primary processing development has been vacuum melting, making possible the extension of existing steels to higher strength levels, and introducing entirely new compositions not otherwise suitable for structures. Table 1 summarizes the characteristics of the various vacuum-melting processes and their general effects on properties. Currently, two of these processes are in greatest use for ultrahigh-strength steels; vacuum degassing and consumable-electrode vacuum melting, with double vacuum melting also used to a lesser extent.

Vacuum degassing was initially developed to remove hydrogen and prevent flaking in low-alloy steels used for large electrical rotors. Carbon deoxidation is a recent modification, in which, by incompletely deoxidizing the air melt before subsequent degassing, the carbon in the melt is used to accomplish part of the deoxidation. Since the deoxidation product of carbon is a gas, this process can be used to reduce the number of indigenous inclusions normally resulting from deoxidation of the steel, and has created considerable interest for commercial bearings that would otherwise be made from air-melt steels.

The other process, consumable-electrode vacuum melting, is being applied on a steadily increasing basis, to most of the ultrahigh-strength steels in use for aerospace and other critically stressed applications. Steels melted by this method include: (1) the aircraft bearing steels, ranging from low alloy through martensitic stainless to high-speed steels, (2) the low-, medium-, and high-alloy high-strength steels, (3) the low-carbon steels designed for carburizing or nitriding for highly stressed gearing, and (4) tool steels subjected to severe operating conditions. In addition to subjecting the steel to very low pressures and high temperatures for extensive gas removal and reduction of inclusions, the consumable-electrode process practically eliminates the ingot segregation normally present in other air- and vacuum-melting processes. By virtue of a solidification process which resembles a welding pool, center properties nearly as good as those in other portions of the cross section are obtained after subsequent hot working. Furthermore, the metallic crucible eliminates the danger of exogenous or refractory inclusions that can occur with the other processes.

Table 2 shows, in greater detail, a comparison of gas and inclusion contents resulting from consumable-electrode vacuum melting, vacuum degassing, and air melting of a typical ultrahigh-strength steel. Vacuum degassing exhibits its greatest effect on hydrogen, while consumable-electrode vacuum melting reduces all gasses extensively, and effects a major change in the inclusion rating. Magnaflux stepdown inspection shows quality improvement similar to those indicated for the J-K inclusion ratings. Figure 1, obtained from a large number of such quality-control tests on AISI 9310 for carburized helicopter gearing, shows the distribution of inclusions found in air-melted, induction-vacuum-melted, and consumable-electrode vacuum-melted material of this analysis. The freedom from magnaflux indications in the consumable vacuum-melted material is noteworthy.

*Vice President, Technology, Vanadium-Alloys Steel Company, Latrobe, Pennsylvania

TABLE 1. CHARACTERISTICS OF AIR AND VACUUM-MELTED STEELS

Melting Characteristics			Product Characteristics					
Process	Temperature, F	Pressure, microns	Gas Content, ppm: Hydrogen	Oxygen	Nitrogen	Cleanliness	Segregation	Mechanical Properties
Air melt	2500-3100	760,000(a)	4 to 20	10 to 150	30 to 500	Fair	Normal	Normal
Vacuum degas (+ carbon deoxidation)	2500-3100	500 to 10,000	1 to 4	10 to 60	40 to 200	Fair to clean	Normal	+5 to 50%
Induction vacuum melt	2500-3100	1 to 50	1	4 to 20	3 to 50	Very clean	Normal	+20 to 200%
Consumable-electrode vacuum melt (air-melt electrodes)	2500-8500	1 to 50	0.5 to 2	6 to 30	15 to 50	Very clean	Relatively free	+20 to 200%
IVM + CEVM or double CEVM (vacuum-melt electrodes)	2500-8500	1 to 50	1	1 to 5	2 to 20	Extremely clean	Relatively free	+30 to 300%

(a) One atmosphere.

TABLE 2. EFFECT OF VACUUM MELTING ON QUALITY OF AN ULTRAHIGH-STRENGTH STEEL

Property:	Consumable vacuum melt	Vacuum degassed	Air melt
Pressure:(a)	1	500	760,000
Gas Analysis:			
Hydrogen	0.8	1.5	4.5
Oxygen	17	28	48
Nitrogen	28	125	175
J-K Inclusion Rating:			
Type A	1 Thin	1-1/2 Thin	1-1/2 Thin
Type B	1 Thin	1-1/2 Thin	1-1/2 Thin
Type C	0	1-1/2 Thin	1-1/2 Thin
Type D	1 Thin	1-1/4 Heavy	1-3/4 Heavy

(a) Microns.

and the manufacturer reported that in-plant rejections and service problems have been reduced to such an extent that the additional cost of the vacuum-melt material has been more than justified.

Now let us look at the effect of these metallurgical changes produced by vacuum melting on the properties and performance of critically stressed parts. When the material is used in the form of large bars or billets for forgings or machined hog-outs, a very effective measure of material quality is obtained by cutting slices from the bars or billets, machining transverse tensile tests from them, and heat treating them to the specified strength level. Differences in quality are sharply differentiated by the ductility transverse to the principal direction of working; if still more tests sensitivity is required, notched transverse tensile tests are even more definitive. In addition to measuring material quality, these tests may also be directly related to the performance of the finished component, since large forgings, hog-outs, and biaxially stressed vessels are frequently limited by their ability to withstand stress concentrations in the cross-grain direction.

Figure 2, plotted from a large number of transverse tests on H-11 at 280-310-ksi ultimate strength level, indicates the degree of ductility improvement obtained by consumable-electrode vacuum melting. The data shown are for midradius tests; when center tests are compared, the air-melt properties

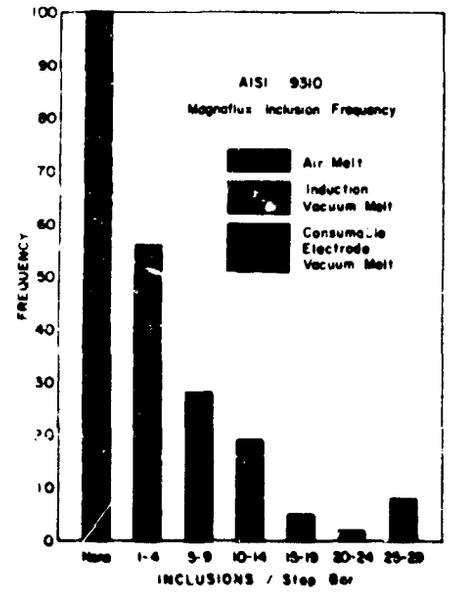

FIGURE 1. COMPARATIVE FREQUENCY OF INCLUSIONS IN MAGNAFLUX STEP-BAR INSPECTION OF AISI 9310 MELTED BY THREE METHODS (W. B. Bond, Bell Helicopter)

are frequently very low, below 5% R.A., whereas the vacuum-melt properties are very close to those shown here for the midradius location. Thus, at the center of large sections, transverse ductility and impact properties may show improvements of 10 to 1 or more by consumable-electrode vacuum melting.

Now let us see what this means in terms of an actual part. Figure 3 shows a landing-gear test forging, which was made from both air- and consumable-electrode vacuum-melted billets, and tested in the locations shown. Figure 4 plots the reduction of area values obtained at the 280-300,000-psi ultimate tensile level for the various locations throughout the forging. The superiority of the consumable-electrode vacuum-melt material was clearly indicated. Note the frequency distribution chart (inset) in which all the consumable-electrode vacuum-melted tests range around the 25% value, whereas the air-melt group segregate into two distinct regions around 25% and around 6%, corresponding to test bars parallel and transverse to the principal direction of working. In other words, consumable-electrode vacuum melting essentially

eliminated the low-ductility properties that would normally occur in unfavorable grain-flow orientations of the forging. Incidentally, this test forging was used to evaluate material for the North American B70 landing gear, which was subsequently made from consumable-vacuum-melted H-11 at this very high strength level, and to date, has met all material expectations.

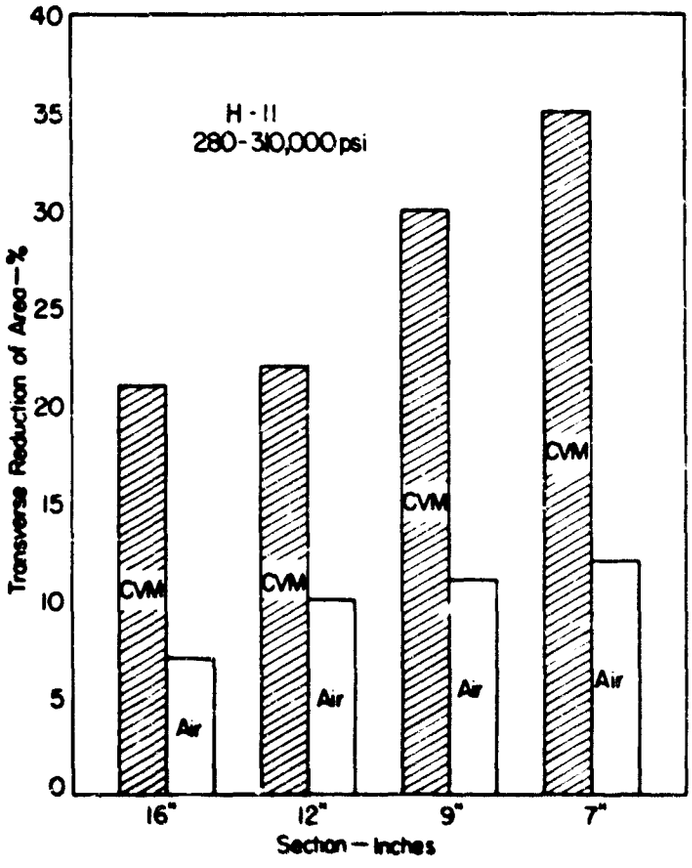

FIGURE 2. EFFECT OF CONSUMABLE-VACUUM MELTING ON TRANSVERSE DUCTILITY AT 280-310-KSI ULTIMATE TENSILE STRENGTH IN LARGE BILLETS OF H-11 FOR AEROSPACE COMPONENTS

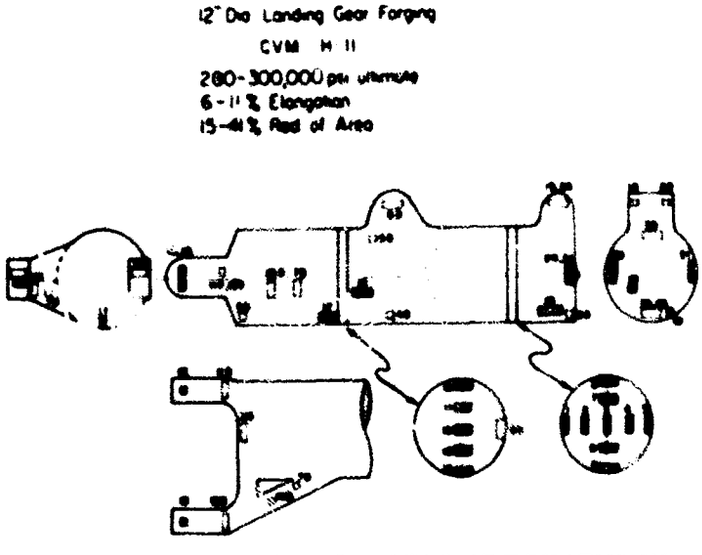

FIGURE 3. LOCATION OF TEST SPECIMENS IN DESTRUCTIVELY TESTED LANDING-GEAR FORGINGS OF H-11 AIR MELTED AND CONSUMABLE VACUUM MELTED (Ladish, Cleveland Pneumatic)

Another landing gear recently designed from consumable-electrode vacuum-melt material is that installed on the DeHavilland Buffalo, an enlarged version of the Caribou, which is a short take-off and landing aircraft that experiences extremely high landing shock loads. Figure 5 shows the consistency of ductility results, both in the parent metal and in the weld, obtained by Jarry Hydraulics, the landing-gear manufacturer, in routine testing of the 6-inch square H-11 billets and forgings going into the gear. These ductility values are a significant gain over the 14-15% minimum reduction of area values appearing in earlier landing gear specifications for air-melt material.

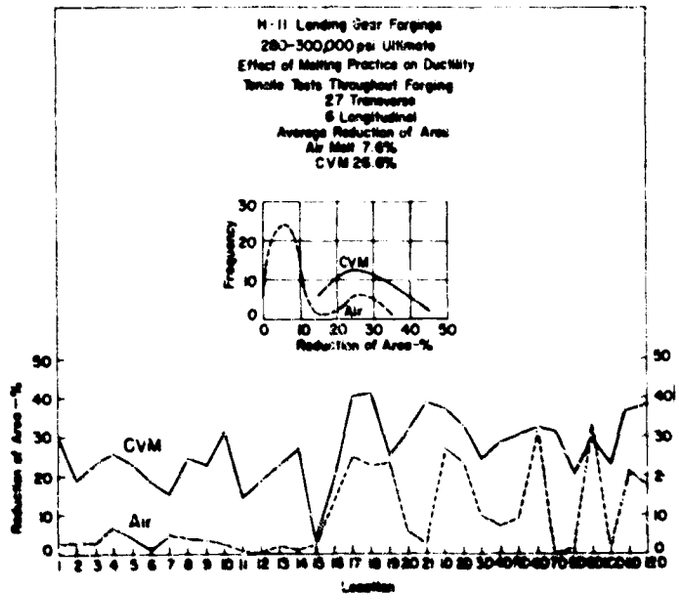

FIGURE 4. COMPARATIVE DUCTILITY OF AIR-MELT AND CONSUMABLE-VACUUM-MELT SPECIMENS FROM LOCATIONS SHOWN IN FIGURE 3. FREQUENCY DISTRIBUTION OF ALL TESTS SHOWN IN INSET (Ladish, Cleveland Pneumatic)

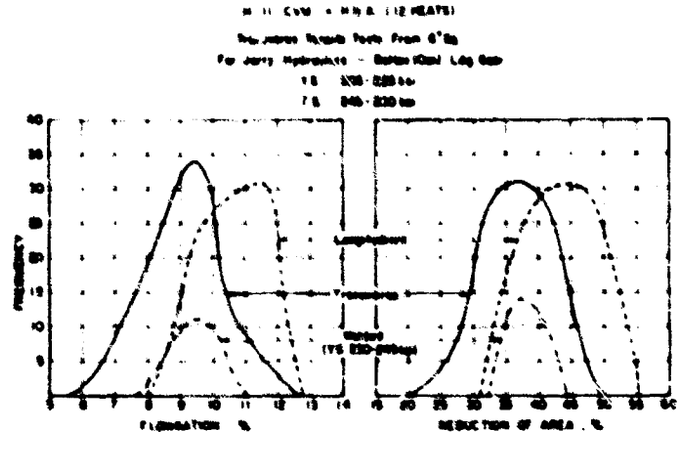

FIGURE 5. FREQUENCY DISTRIBUTION OF LONGITUDINAL, TRANSVERSE, AND WELD DUCTILITY FROM INSPECTION OF 12 HEATS OF CONSUMABLE-VACUUM-MELT H-11 FOR DE HAVILLAND BUFFALO LANDING GEAR (M. D. Brown, Jarry Hydraulics)

Unlike H-11, the acceptance of vacuum melting for AISI 4340 and other popular landing-gear steels has progressed somewhat more slowly because they contain manganese as an essential alloying element. This is the only element normally in steel which vaporizes in melting, boiling off over 50 per cent in a good vacuum, causing arc instability and less desirable macrostructural characteristics. The substitution of molybdenum for manganese to provide a good vacuum-melt analysis has been proposed, but has encountered the normal resistance to a new steel.

As might be expected, other properties besides tensile ductility show significant gains from consumable-vacuum melting. Figure 6 indicates a shift in notch tensile strength, both to higher values and with retention to higher heat-treated strength levels, from consumable-vacuum melting of H-11. This shift made it possible to meet a very stringent specification requiring transverse notch-tensile testing to a minimum of 1.0 notched-to-unnotched strength ratio in the transverse direction of 8-1/2" square billets going into the B58 elevon hinge forging shown in Figure 7. Table 3 shows typical notch-tensile ratios obtained in quality-control testing of billets to this specification.

Due to the lower inclusion content, fatigue properties are also significantly improved by consumable vacuum melting, both in notched and smooth bar tests, as shown for H-11 in Figure 8. Other fatigue tests on this material at 240-ksi ultimate tensile strength for the Jarry landing gear produced rather startling fatigue specimens that cracked around the entire periphery, reducing the effective cross section sufficiently to shut off the rotating-beam fatigue machine, but resisting complete fracture. Specimens of this type were consistently obtained in the high-stress, low-cycle portion of the curve.

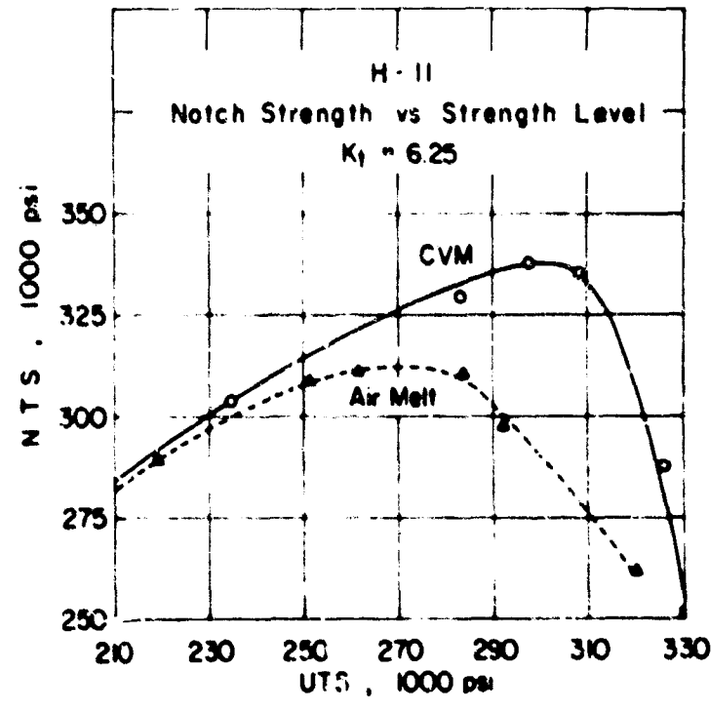

FIGURE 6. EFFECT OF CONSUMABLE VACUUM MELTING ON NOTCH-TENSILE STRENGTH OF H-11 AT VARIOUS HEAT-TREATED STRENGTH LEVELS (P. Ruff and R. Steur, Metal Progress, December, 1961)

FIGURE 7. CONVAIR B58 ELEVON HINGE, WELDED FROM CONSUMABLE-VACUUM-MELT H-11 SHEET AND DIE FORGING. BILLETS FOR LATTER INSPECTED TO TRANSVERSE NOTCH-TENSILE REQUIREMENTS SHOWN IN TABLE 3.

TABLE 3. H-11 CVM TRANSVERSE NOTCH TENSILE INSPECTION OF 8-1/2" SQUARE BILLETS

UTS = 260-270 EL = 5-8
YS = 220-225 RA = 16-30

$\frac{\text{Notch } (K_t 6)}{\text{Smooth}}$ (Transverse)

Heat	T	B
1	1.1-1.1	1.2-1.2
2	1.2-1.3	1.3-1.3
3	1.3-1.3	1.0-1.0
4	1.2-1.2	1.2-1.2
5	1.3-1.3	1.3-1.3
6	1.3-1.3	1.2-1.2
7	1.3-1.3	1.2-1.2
8	1.1-1.1	1.2-1.2
9	1.2-1.2	1.2-1.2

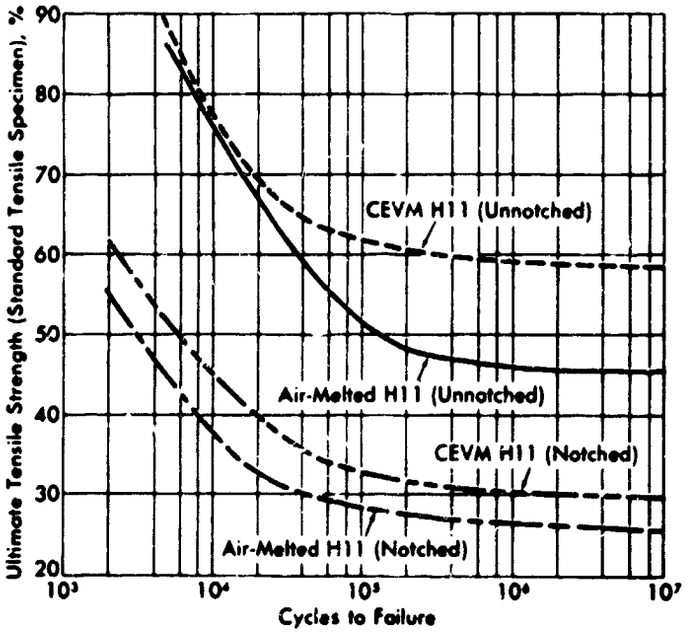

FIGURE 8. EFFECT OF CONSUMABLE VACUUM MELTING ON SMOOTH AND NOTCH FATIGUE STRENGTH OF H-11 (P. Ruff and R. Steur, Metal Progress, December, 1961)

Vacuum melting has recently assumed additional significance in the ultrahigh-strength field with the introduction of the maraging steels. Containing the reactive elements, titanium and aluminum, these steels are subject to oxide and carbo-nitride stringers in the air-melted condition which can seriously reduce their inherently good ductility and notch toughness, as well as cause splitting of plate, "delamination" as it has been named, during welding of rocket cases. Vacuum melting has successfully overcome these problems. As maraging steels have progressed to the full production stage (over 350 production heats have been made in our operations), considerable know-how has been gained in the vacuum melting and hot-working procedures for maximum properties in large sections. Table 4 shows the transverse properties which were reported two years ago and included in a number of specifications in the intervening period, together with typical properties now being obtained in sections as large as 18" x 24". The ability of maraging steel to be simply aged to these properties in large sections is increasing designers' confidence for its use in progressively larger components. Figure 9 shows flexures which are machined from 18"-diameter solid forgings of the 300-grade maraging steel. These flexures have been made in quantity for rocket test stands, providing all support through the very thin-machined webs visible in the picture. Ductility and notch toughness throughout the cross section, weldability, and the minimum distortion heat treatment were major criteria for selection of vacuum-melted maraging steel for this service.

Although these interesting new materials will be discussed further by other speakers, there is one additional point relating to primary processing that

TABLE 4. 18% NICKEL MARAGING STEEL TRANSVERSE PROPERTIES IN HEAVY SECTIONS

Size	Grade	Location	Yield Strength, ksi	Tensile Strength, ksi	Elongation, per cent	Reduction
			Typical 1962			
6" sq.	300	Center	279	283	10.0	48
6" sq.	250	Center	260	262	9.0	46
10" sq.	300	Center	275	284	8.5	40
12" sq.	250	Center	248	253	8.0	34
			1964 (Average of 65 Tests):			
18" rd.	300	Center	266	275	6.5	27
24" sq.	250	Midradius	238	247	6.0	30

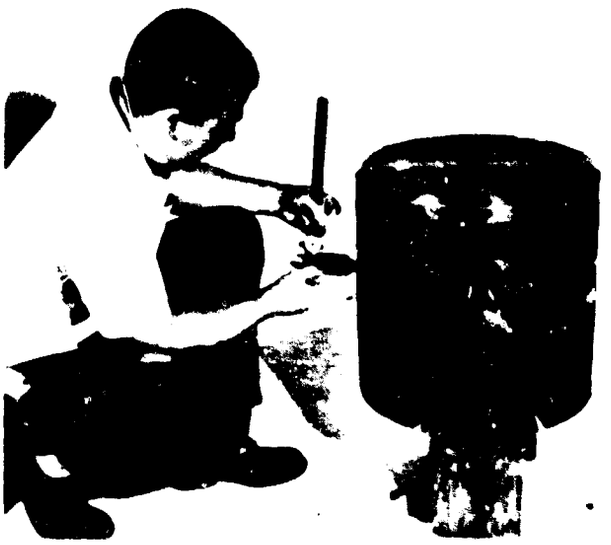

FIGURE 9. PRODUCTION 18"-DIAMETER, 1-MILLION-LB FLEXURE MADE FROM CONSUMABLE-VACUUM-MELT 18% NICKEL MARAGING STEEL. MULTIPLE STRESSES ARE TRANSMITTED THROUGH THIN WEBS, NECESSITATING FULL STRENGTH AND DUCTILITY THROUGHOUT SECTION (Allegheny Instrument Company)

should be mentioned briefly; that is the question of banding, which is frequently mentioned with respect to maraging steels. Due to a high-alloy content, banding can be quite visible and resist removal by heat treatment. However, there are all degrees of banding, ranging from that which is extremely detrimental, causing delamination, poor transverse properties, and poor notch properties, to that which satisfactorily passes all tests, even when the notches and cracks are intentionally located in various portions of the band. The reason for conflicting reports on this problem is that the bands require closer metallographic examination before their effect can be predicted. If accompanied by oxide or carbo-nitride inclusion stringers, the bands are definitely detrimental. However, if the bands are merely light and dark etching regions due to slight variations in alloy content, and not accompanied by stringers, test and performance data indicate that the material is fully satisfactory and can be used with confidence.

In addition to its ability to sharply improve existing grades of ultrahigh-strength steel, consumable-electrode vacuum melting is making possible the development of still higher strength steels that, in the air-melted condition, would be considered too brittle for structural applications. Figure 10 shows such a steel, which contains 0.55 carbon and 12 per cent alloying elements and is based on the carbide-free matrix of high-speed steel that is normally used for cutting tools. By vacuum melting this steel, usable ductility is obtained at heat-treated strength levels as hich as 360,000 psi with 325,000-psi yield strength. It is in production use for 300-ksi aircraft fasteners, high-strength gearing, small high-pressure devices, etc. When thermal mechanically worked, the consumable vacuum-melted material achieves an ultimate strength level of 460-500,000 psi, a yield strength of 425,000 psi, with 6 per cent elongation and 22 per cent reduction of area (Table 8). Thus, the former plateau of 260-300,000 psi for high-strength steels is being surpassed by new higher alloy materials designed specifically for consumable vacuum melting.

Obviously, these few examples have hit only the high points of vacuum melting and its effect on properties, but I hope it has at least indicated its potential. The shift to vacuum-melted steels is growing steadily; in many instances, the improved service and reduced in-plant rejections have more than offset the increased cost of the material. In other cases, a new vacuum-melt steel has reduced manufacturing costs; for example, maraging steels have replaced 4340 and similar steels in production parts with sharply reduced heat-treating, straightening, and finishing costs.

Hot Working

Now let us consider other primary processing steps subsequent to the melting operation. In the hot working of ultrahigh-strength steels, much is learned by trial and error; new forging procedures and grain-flow orientations are developed on the presses and hammers, and the resulting properties evaluated. Figure 11 shows typical clay models which can be used to simulate mechanical working of ingot structures and offer guide lines for developing optimum properties in these steels. Upsetting various percentages has been quite successful with some grades. In other cases, the heating and working cycles are very critical. For example, the maraging steels must be finished cold for fine grain because they cannot be refined by heat treatment.

Figures 12 and 13 show an interesting study in which a very narrow working range was determined for Udimet 700 or Astroloy, which had been strenuously resisting successful hot working. Although not strictly a high-strength steel, it illustrates the

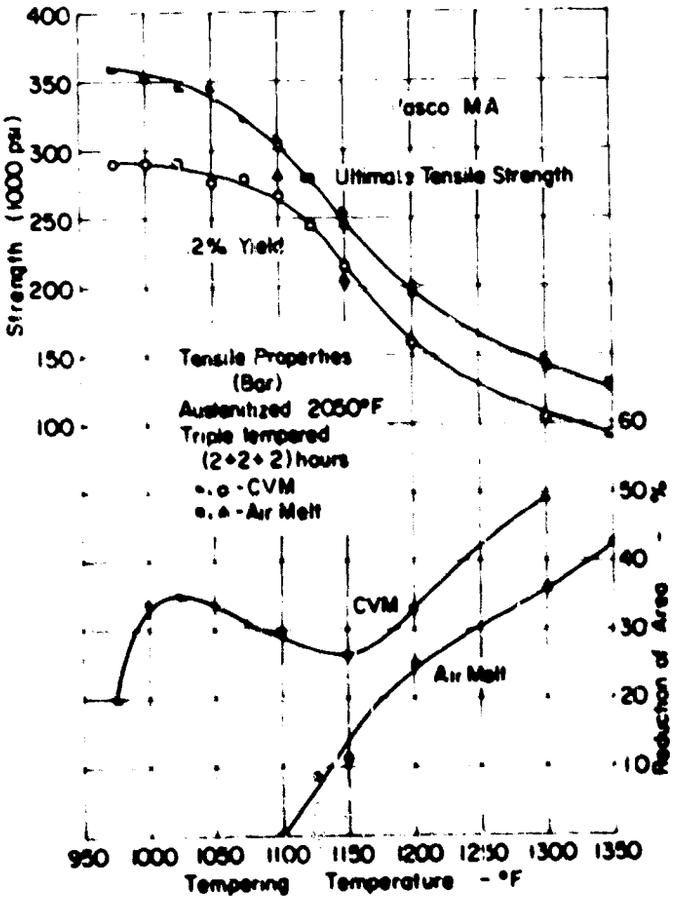

FIGURE 10. EFFECT OF TEMPERING ON PROPERTIES OF NEW HIGH-ALLOY ULTRAHIGH-STRENGTH STEEL. NOTE THAT CONSUMABLE VACUUM MELTING IS ESSENTIAL TO DUCTILITY AT HIGHER STRENGTH LEVELS

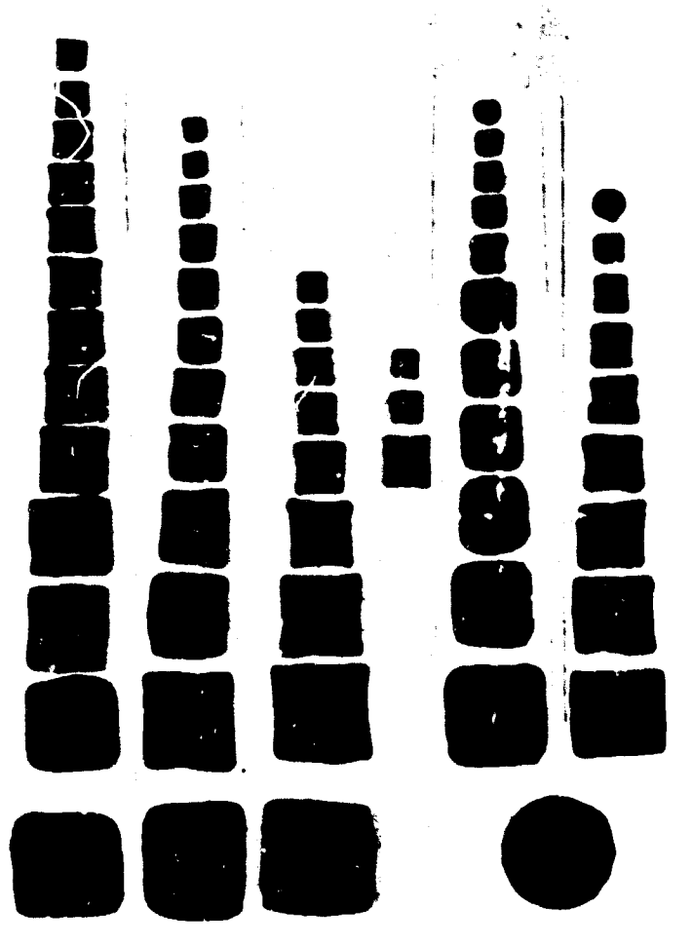

FIGURE 11. USE OF CLAY TO STUDY EFFECT OF VARIOUS HOT-WORKING PROCEDURES ON INGOT STRUCTURES

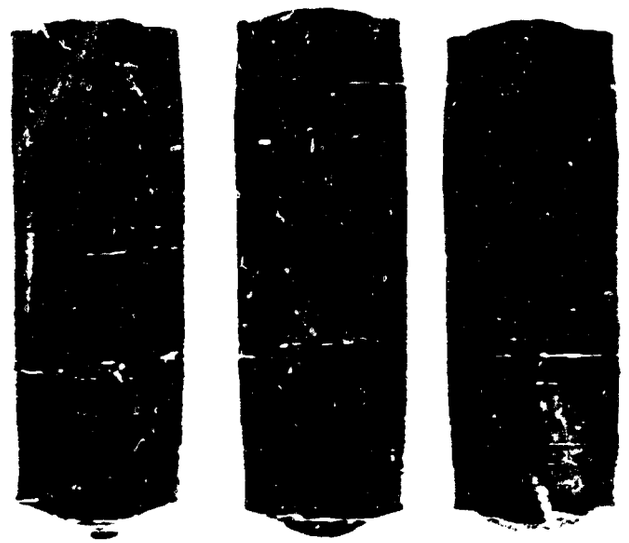

1825°F 1950°F 2000°F

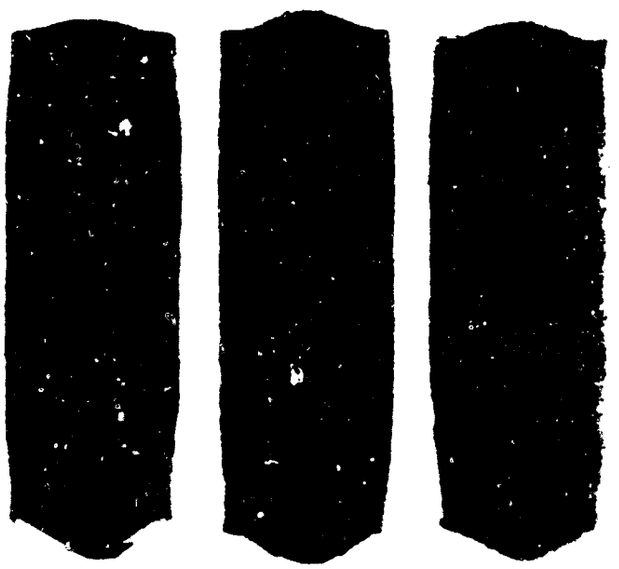

2025°F 2100°F 2175°F

FIGURE 12. EFFECT OF FORGING TEMPERATURE ON HOT WORKABILITY OF UDIMET 700. 33% REDUCTION IN A SINGLE PASS (R. J. Quigg, AIME High-Temperature Materials Conference, Cleveland, Ohio, April, 1961)

criticality of the working process as we increase alloy content and progress to higher strength and higher temperature materials. In this nickel-base alloy, the lower limit of the working range is set at 1950 F by cracking due to excessive work hardening, while the upper limit is a mere 100° higher, above which cracking reappeared. Metallurgical investigation showed that the upper limit was not due to a low melting phase or other common cause of hot shortness, but by a fine precipitate which occurs on reheating or slow cooling a structure which has been previously solution treated at higher temperatures. In fact, as shown in Figure 13, cracking even occurred at the optimum working

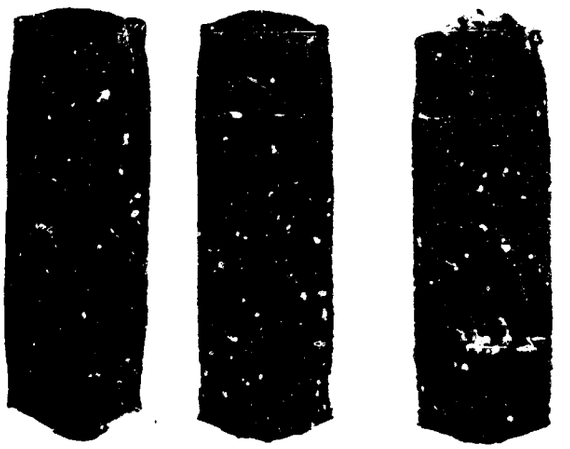

STRESS RELIEVED | FULL ANNEAL. 2 HRS AT 2150°F AIR COOL | FULL ANNEAL 2 HRS AT 2150°F WATER QUENCH

FIGURE 13. EFFECT OF SOLUTION TREATMENT ON WORKABILITY OF UDIMET 700 AT OPTIMUM FORGING TEMPERATURES. 33% REDUCTION IN A SINGLE PASS (R. J. Quigg, AIME High-Temperature Materials Conference, Cleveland, Ohio, April, 1961)

temperature of 2025 F, when the material had been previously solution treated at a higher temperature. The obvious remedy was, then, to keep the temperatures low and the particles coarse and out of solution.

Thermal Treatments

For some steels, special thermal cycles after hot working can be surprisingly effective in improving properties and performance of ultrahigh-strength steel parts. Figure 14 shows the degree of microstructure improvement attained by a special thermal cycle applied to H-11. A normal annealing cycle after hot working can produce the structure shown on the left, with carbides tending to segregate into the grain boundaries. By a subsequent heat treatment which we call "HNA" for homogenizing, normalizing, and annealing, the structure on the right is produced from this same steel (U. S. Patent No. 2,893,902). The homogenizing temperature used is 1975 F, which is below the grain-coarsening temperature but 125° above the normal hardening temperature for this steel. This is followed by a normalizing treatment at 1700 F, to obtain maximum grain refinement, followed by a normal annealing or tempering cycle. As shown in Table 5, this special thermal treatment has a major effect on properties, improving transverse reduction of area in large air-melt billets by 28 to 38 per cent and transverse impact properties to a slightly smaller extent. Another series of tests, shown in Table 6, compared this treatment with special forging practices, including single upsetting and triple upsetting in all directions. Note that for this steel, the upsetting treatments showed no significant effect, whereas the thermal treatment consistently improved properties by about 20 per cent.

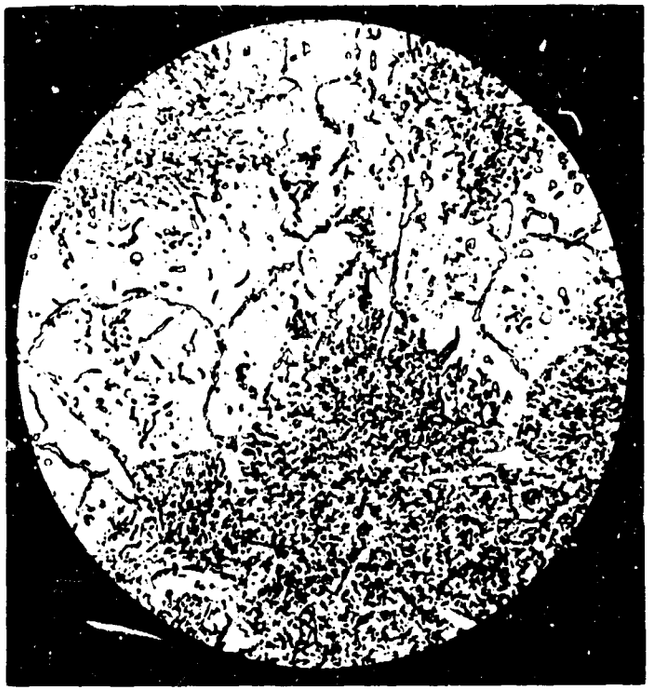

Ordinary H-11

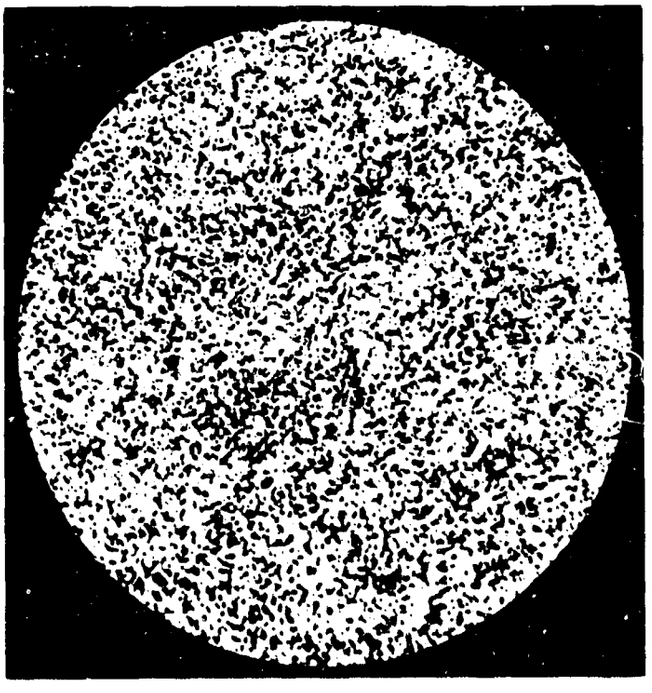

HNA

FIGURE 14. CHANGE IN MICROSTRUCTURE OF H-11 EFFECTED BY HOMOGENIZING, NORMALIZING, AND ANNEALING TREATMENT AFTER HOT WORKING

TABLE 5. EFFECT OF THERMAL TREATMENT ON TRANSVERSE PROPERTIES OF H-11

Multiple Tests at 260-ksi

Size	Location	Anneal: Conventional	Anneal: HNA	Improvement
		Transverse Reduction of Area %		
15" sq.	Midradius	12.9	16.5	28%
8" sq.	Center	10.7	14.8	38%
		Transverse Charpy-V, ft-lb		
15" sq.	Midradius	10.8	13.0	20%

TABLE 6. UPSETTING VERSUS THERMAL TREATMENT FOR H-11

16" x 7" Billets; Transverse Tensiles at 240-ksi UTS

Ingot	Forging Method	Per Cent Reduction of Area After: Conventional Anneal	HNA	Improvement
1	Conventional	24.2	29.2	+20%
2	Single upset	24.6	29.7	+20%
3	Triple upset	24.2	28.6	+18%

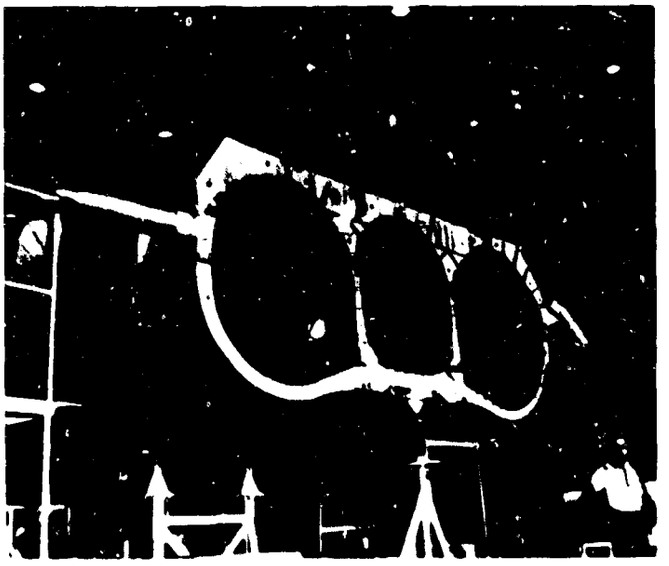

FIGURE 15. CARRY-THROUGH TAIL STRUCTURE OF NORTH AMERICAN A3J VIGILANTE WELDED FROM 280-KSI ULTIMATE TENSILE STRENGTH H-11 CVM FORGINGS, HNA THERMALLY TREATED

Figure 15 shows a very challenging ultrahigh-strength steel aircraft component in which the HNA thermal treatment played a significant role. This carry-through structure on the A3J Vigilante measures 14' across and supports the entire tail surface on the three spindles. Designed in 1956 before large sizes of consumable-vacuum-melt material were readily available, this part involved stringent transverse-property testing for air-melt material at the 280-300,000-psi level, which was the highest strength in production use at that time. The parts were made from billets as large as 28" by 8" by 38" long, which were hand forged to some degree, followed by hog-out machining to sections as thin as 1/16", some of which fell near the center line of the original billet. Some of the initial parts were hand forged on hammers of insufficient capacity, and were subjected to 47 reheats before reaching the desired configuration. As you can well suspect, this resulted in extremely coarse grain, poor microstructure, and zero ductility on coupon tests. Surprisingly, by application of the HNA thermal treat-

ment, properties were sufficiently restored to the forging to meet specifications, and it was used in a static test airplane. After that experience, the treatment was applied to all billets and forgings of H-11 subsequently furnished, either in the air-melt or vacuum-melt condition.

These were specific tests; now let us look at the effect of this HNA treatment on routine quality control of large quantities of H-11. The data in Figure 5 were obtained from material which had been both consumable vacuum melted and given the HNA treatment. Table 7 shows additional inspection data reported by an aircraft producer from transverse ductility tests on over 100,000 lbs of consumable-vacuum-melted H-11 in similar billet sizes and heat treated to the 290,000-psi tensile level. All of the material furnished by Producer X was given this thermal treatment, plus consumable vacuum melting in a production furnace that operates below one micron pressure. Producers Y and Z, to the best of their knowledge, did not use the HNA treatment and employed consumable vacuum furnaces operating in the 5- to 25-micron range. As you can see, the differences were quite significant, again indicating a major effect of primary processing on ultrahigh-strength steel properties.

TABLE 7. INSPECTION HISTORY, 100,000 LBS. OF H-11 CVM BILLET, TRANSVERSE TENSILES AT 290-KSI UTS

	Overall Average		
	Producer X (HNA)	Producer Y	Producer Z
Short Transverse			
T.S.	301 ksi	296 ksi	288 ksi
R.A.	31.8%	14.9%	23.6%
Long Transverse			
T.S.	294 ksi	287 ksi	289 ksi
R.A.	38.4%	25.3%	21.2%
Longitudinal			
T.S.	303 ksi	290 ksi	295 ksi
R.A.	42.8%	40.1%	36.6%

Texturing in Sheet Material

A recently recognized effect of primary processing, which related to the fabricability of ultrahigh-strength sheet steel, is the anisotropy associated with crystallographic texturing in sheet material. Studies in this field have been largely concentrated on low-carbon auto-body sheet and other metals, but recent experience in hydroforming Hawk missile accumulator components indicates some promise for the high-strength steels also. Since these studies are not yet complete, this must necessarily be limited to a progress report.

Figure 16 shows the accumulator which is fabricated by machining and welding from hydroformed domes and forgings of H-11. Figure 17 shows a hydroformed dome in this material. This part, hydroformed from sheet 0.170-inch thick, is very close to the drawing limit; thus, slight variations in formability are very significant. Studies are now underway to relate the actual response to hydroforming with tensile properties measured in directions 0°, 45°, and 90° to the direction of final rolling. The relationships developed by Whiteley*

FIGURE 16. ACCUMULATOR FOR HIGH-PRESSURE GAS IN CONTROL SYSTEM OF RAYTHEON HAWK MISSILE, WELDED FROM H-11 CVM FORGING AND HYDROFORMED DOME

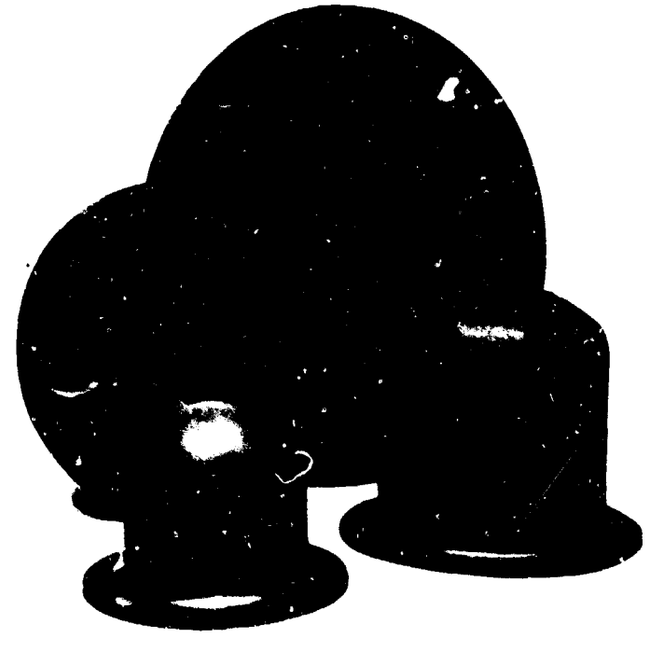

FIGURE 17. UNTRIMMED HYDROFORMED DOME FOR ACCUMULATOR IN FIGURE 16. RELATIONSHIP OF HYDROFORMING RESPONSE TO PROPERTIES SHOWN IN FIGURE 18 IS UNDER STUDY

*Whiteley, R. L., "Anisotropy in Relationship to Sheet Processing", Fundamentals of Deformation Processing, 9th Sagamore Conference, Syracuse University Press, pages 183-198, 1964.

suggest that drawability of sheet is related to these tensile properties by the formulas shown in Figure 18. The value $\bar{R}$ is the ratio of the strain in the width direction to the strain in the thickness direction on the tensile specimen. The average of the ratios for the various orientations represents the normal anisotropy of the sheet, which in turn is a function of the relative strength in the thickness direction--of major importance to deep drawing. For best drawability, average $\bar{R}$ should be as high as possible. The planar anisotropy is indicated by the second formula showing the variation in R in different orientations relative to the rolling direction. To avoid earing and nonuniform deformation during the draw, Δ R should be 0; in other words, the material should show similar width to thickness ratios in all directions. Studies are now underway to relate sheet-rolling conditions to these values, and in turn, to relate the calculated values to actual performance in the hydroforming operation.

Thermal-Mechanical Treatment

Simply to complete the record, we should mention thermal-mechanical treatment, which is a very powerful primary processing tool. Laboratory and semi-production tests indicate that it can raise the strength of ultrahigh-strength steels by 100,000 psi with no degradation in ductility; in fact, a slight increase in ductility is frequently observed. As shown in Table 8, strength levels as high as 425,000 psi have been obtained with H-11 and 460,000 psi with the aforementioned matrix steel, Vasco M-A, accompanied by usable ductility for structural purposes. The subject will be more fully covered in another paper, but it certainly should be included in this report as a significant primary processing variable.

TABLE 8. STRENGTH AND DUCTILITY ACHIEVED BY AUSFORMING OF HOT-WORK DIE STEELS

Both steels ausformed 90% and tempered at 1000-1050 F.

Material	Test Temperature, F	Ultimate Tensile, psi	0.2% Yield, psi	Elongation, per cent	Reduction in Area, per cent
Modified H-11 CVM	R.T.	420,000	400,000	6.0	3*
	1000	255,000	230,000	10.5	58
Vasco M-A CVM	R.T.	460,000	425,000	6.0	22
	1000	300,000	280,000	8.8	48

Fracture Toughness Properties

With respect to fracture toughness testing, there are, as pointed out earlier, a dearth of statistical tests showing primary processing effects. However, some interesting trends are being revealed by research studies on small sample quantities that should be noted here. Figure 19 shows a summary plot of K_{Ic} tests for a number of ultrahigh-strength materials plotted against the heat-treated strength level.* With extremely sharp notches or cracks, there is a consistent indication of smaller benefits from major differences in composition or primary processing. In other words, fracture-toughness testing appears to reduce all materials to quite similar levels, regardless of their other quality or other properties. The 18% nickel maraging types are somewhat exceptional in this respect, as shown in Figure 19.

It should be remembered, however, that an absence of significant differences in K_{Ic} or other fracture toughness parameters is not the only consideration. For example, an extremely clean vacuum-melted steel has appreciably fewer inclusions and other fracture origins so that, even though its fracture toughness may not be significantly higher than the air-melted material, the reliability of the material in an actual component may be significantly improved. It would appear that sufficient production quantities of air-melt and vacuum-melt material have now been compared in aircraft and missile structures to indicate their overall reliability in this respect. Further fracture toughness testing in quality control, as well as additional performance history, will undoubtedly further clarify the relative significance of improved cleanliness and microstructure, changes in ductility, and fracture-toughness values to actual performance of components.

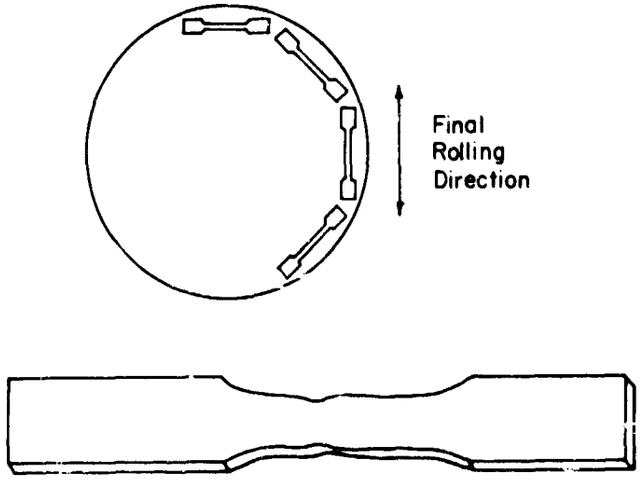

$$R = \frac{\ln w_o/w}{\ln t_o/t}$$

Normal Anisotropy (maximize): $\bar{R} = \frac{1}{4}(R_0 + 2R_{45} + R_{90})$

Planar Anisotropy (minimize): $\Delta R = \frac{1}{2}(R_0 - 2R_{45} + R_{90})$

FIGURE 18. ANISOTROPY PROPERTIES IN H-11 SHEET CIRCLES BEING STUDIED FOR: (1) RELATIONSHIP TO HYDROFORM RESPONSE (FIG. 17) AND (2) RELATIONSHIP TO PRIMARY PROCESSING IN SHEET MANUFACTURE (H. Freedman, Raytheon, and R. Colton, Watertown Arsenal)

*Masters, J. N., "Booster Case Materials Evaluation", The Boeing Company, 4th Maraging Steel Project Review, Dayton, Ohio, Volume I, pages 226-254 (July, 1964).

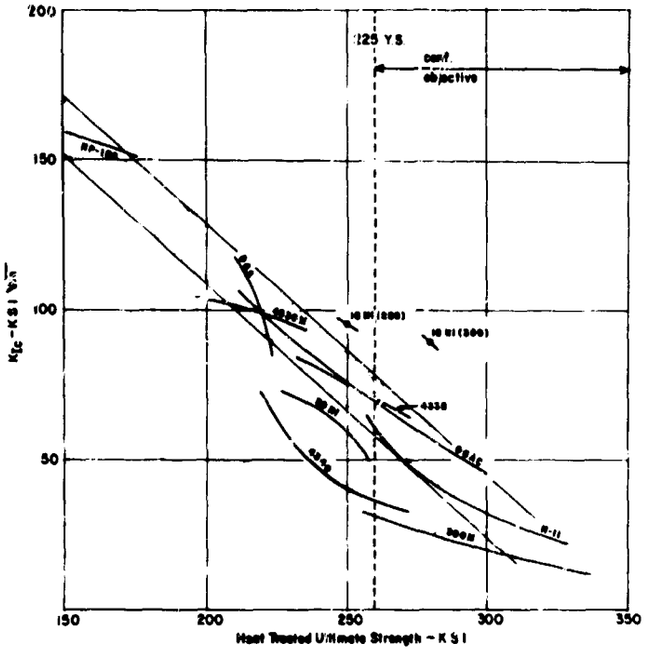

FIGURE 19. EFFECT OF HEAT TREATED STRENGTH LEVEL ON FRACTURE TOUGHNESS (K_{Ic}) OF REPRESENTATIVE ULTRAHIGH-STRENGTH STEELS (Masters. The Boeing Company, 4th Maraging Review)

Figure 20 shows an interesting comparison of the notch toughness of two ultrahigh-strength steels with the conventional titanium and aluminum alloys used for aerospace structures, when compared at equivalent strength-to-weight ratios. Note that all materials appear to decrease in notch toughness as the strength level is raised, and the steels compare favorably with the other materials on a notch-toughness basis.

In conclusion, primary processing can exert profound effects on ultrahigh-strength steels, not only on their final properties and performance, but also in some instances of their fabricability.

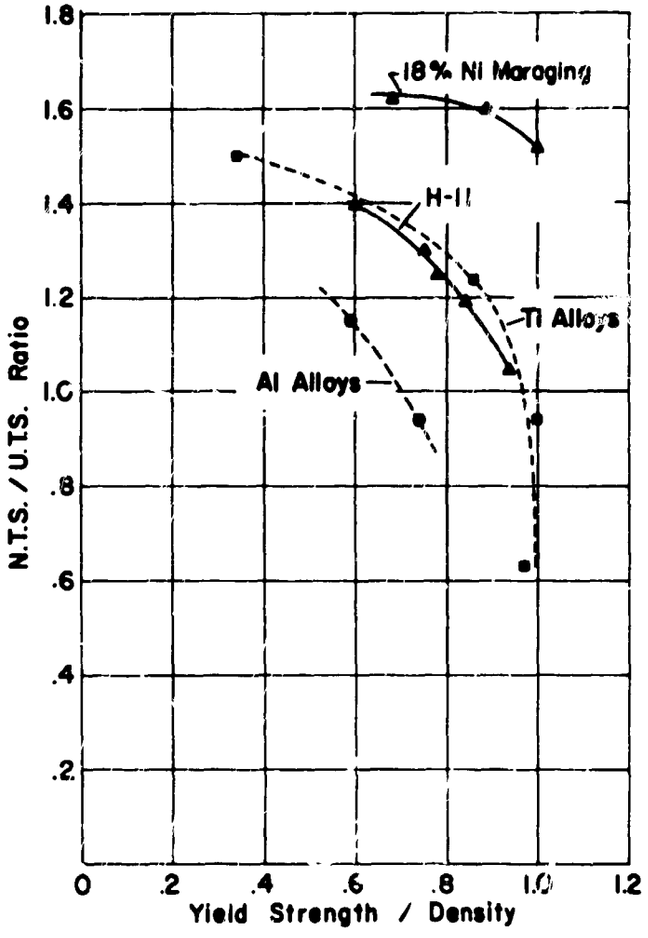

FIGURE 20. EFFECT OF STRENGTH-TO-DENSITY RATIO, ACHIEVED BY CHANGES IN COMPOSITION OR HEAT TREATMENT, ON NOTCH TOUGHNESS OF TWO STEELS COMPARED WITH AEROSPACE TITANIUM AND ALUMINUM ALLOYS

NTS = Notch tensile strength $K_t = 6.25$
UTS = Unnotched tensile strength

JOINING OF HIGH-STRENGTH STEELS

by

Warren F. Savage*

INTRODUCTION

One major obstacle to full utilization of steels with yield strengths exceeding 225,000 psi is the present status of joining technology. Both mechanical and metallurgical problems have been encountered which severely complicate the application of the available joining processes to these materials. However, joining by either adhesive bonding or brazing techniques is unlikely to introduce any novel problems other than insuring adequate load carrying capacity by suitable joint design. Thus, the extremely high design stresses constitute a mechanical problem likely to limit the application of these techniques to lap joints in relatively thin gage material.

A review of the literature on joining of high-strength steels indicates that the major problems are associated with welding of the high-strength steels and are largely metallurgical in origin. The novel metallurgical characteristics of the various types of high-performance steels, their relatively high alloy content, and the present limited metallurgical background knowledge combine to provide complex problems in welding metallurgy. Therefore, the following brief review has been specifically restricted to the welding of high-strength steels and is primarily limited to joining problems of a metallurgical nature.

METALLURGICAL CLASSIFICATION OF HIGH-STRENGTH STEELS

From a metallurgical standpoint, high-strength steels may be subdivided into four groups on the basis of strengthening mechanism as indicated in Table 1. The approximate nominal composition of the specific examples cited for each type are summarized in Table 2, while Table 3 compares typical room-temperature mechanical properties.

TABLE 1. CLASSIFICATION OF HIGH-STRENGTH STEELS ON THE BASIS OF STRENGTHENING MECHANISM

Group	Strengthening Mechanism	Example
I	Quenched and tempered steels	H-11
II	Cold-worked stainless steels	AISI 301
III	Precipitation-hardening stainless steels	PH15-7Mo
IV	Maraging steels	18Ni(250)

TABLE 2. NOMINAL COMPOSITION OF THE TYPICAL EXAMPLES OF THE FOUR TYPES OF HIGH-STRENGTH STEELS CITED IN TABLE 1

Group:	I	II	III	IV
Type:	H 11	AISI 301	PH15-7 Mo	18 Ni (250)
Strengthening Mechanism:	Quench and Temper	Cold Worked 65%	Precip. Hard	Maraged
C	0.3/0.4	0.08/0.20	0.09 max	0.03 max
Mn	0.2/0.4	2.0 max	1.0 max	0.1 max
Si	0.8/1.2	1.0 max	1.0 max	0.1 max
S	--	0.03 max	0.04 max	0.01 max
P	--	0.03 max	0.04 max	0.01 max
Cr	4.75/5.5	16/18	14/16	--
Ni	--	6/8	6.5/7.75	17/19
Co	--	--	--	7/8.5
Mo	1.25/1.75	--	2.0/3.0	4.6/5.2
Ti	--	--	--	0.3/0.5
V	0.3/0.5	--	--	--
Al	--	--	0.75/1.50	0.05/0.15
B	--	--	--	0.003
Zr	--	--	--	0.02
Ca	--	--	--	0.05
Fe	Bal	Bal	Bal	Bal

The materials in Group I, of which H-11 is typical, all derive their high strength from a microstructure of tempered martensite. The alloy content in most cases is sufficiently high to render these steels air hardenable, and therefore the high strength levels can usually be obtained in thicknesses of 1 in. or more without special quenching facilities. However, these materials tend to exhibit retained austenite, and multiple tempering operations are often employed to minimize this problem.

The materials in Group II, of which the cold-worked AISI 301 stainless steel is typical, derive their high strength from a combination of work hardening and strain-induced transformation of the metastable austenite to martensite. In general, high strength levels can only be achieved in relatively thin sheet and small-diameter wires owing to the non-uniformity of plastic straining characteristic of thicker sections.

The materials in Group III, of which PH15-7 Mo is typical, derive their high strength from a precipitation-hardening reaction following the transformation of a metastable austenite to a martensitic phase on cooling from a carefully chosen austenitizing temperature. Since the M_s temperature depends upon the alloy content of the austenite, complete solution of the alloy carbides causes stabilization of the austenite and interferes with the hardening process unless the proper austenitizing temperature is employed.

* Director of Welding Research, Rensselaer Polytechnic Institute, Troy, New York.

TABLE 3. TYPICAL ROOM-TEMPERATURE MECHANICAL PROPERTIES FOR THE FOUR TYPES OF HIGH-STRENGTH STEELS CITED IN TABLE 1

Group	I	II	III	IV
Type	H 11	AISI 301	PH15-7 Mo	18 Ni (250)
Treatment to Achieve Properties Noted	1900 F - 30 min AQ Temper 3 + 3 + 3 at 1050 F	Cold Rolled 65%	1750 F - 10 min AC -100 F - 8 hr 950 F 1 hr AC	1500 F - 1 hr 900 F - 3 hr
Section Thickness (in.)	0.125	0.020	0.020	0.5
Yield Strength 0.2% offset (psi)	232,000	244,000	225,000	250,000
Ultimate Strength (psi)	283,000	260,300	235,000	257,000
Elongation (% in 2 in.)	7.0	1.5	6.0	1.2
Hardness Rc	53	51.5	48	51

The maraging steels of Group IV provide high strength levels by what is believed to be a combination of ordering and precipitation-hardening reactions in a very low carbon iron-nickel martensite. The martensite is produced by a reversible shear mechanism which is essentially independent of the cooling rate, and therefore section size presents no limitation to the hardening process. Although the 95-110,000 psi yield strength of the "as-quenched" martensitic phase is too low to be of commercial interest, a relatively brief aging treatment at 900-950 F may be employed to increase the yield strength by a factor of 2-3 times to as high as 300,000 psi. The reversibility of the martensite reaction is unique to this family of high-strength steels, since all other commercial steels exhibit irreversible martensitic reactions.

WELDING METALLURGY OF HIGH-STRENGTH STEELS

Quenched and Tempered Steels

High strength levels can only be obtained in these steels by a post-weld quench and temper operation. Since the strength levels required are far higher than can be obtained by solid-solution hardening, filler metals utilized with the fusion welding processes must provide an as-deposited composition with heat-treating characteristics identical to those of the parent metal. This restriction, together with the extreme requirements on weld integrity imposed by the poor notch-toughness of the high-strength, quenched and tempered steels, has led to almost universal application of the tungsten-inert-gas (TIG) process using a cold wire of matching composition fed directly into the weld puddle.

Since the cooling rates associated with welding invariably exceed the critical cooling rate, the weld and those portions of the weld-heat-affected-zone heated above the critical temperature transform to a brittle, high-carbon martensite if allowed to cool through the martensite transformation range. Therefore, it is customary to utilize pre-heat and interpass temperatures slightly above the M_s temperature to avoid martensite formation during welding. The entire structure is then heat-treated immediately after welding, usually before the weldment cools below some specified minimum post-weld temperature.

The relatively high carbon content required of this family of steels makes the exclusion of all sources of hydrogen in the vicinity of the weld puddle mandatory if hydrogen embrittlement and underbead cracking are to be avoided. Thus acid pickling of the work or filler wire is inadvisable and all sources of moisture in the arc atmosphere must be eliminated.

Hot cracking in these materials is often encountered, necessitating expensive repair welding. A better understanding of the mechanism of hot-cracking and the influence of both material composition and welding variables on the hot-cracking propensity is required before this problem can be eliminated. The available evidence indicates that microsegregation of both phosphorus and sulfur contributes to the observed hot-cracking problems. However, the choice of welding variables appears to alter the microsegregation pattern for these elements and thus influence the hot-cracking tendency for a given material composition.

Cold-Worked Stainless Steels

The inherent stability of the highly alloyed austenitic phase in most of the steels falling within this category necessitates severe cold working to produce the required high strength levels by a combination of strain-induced transformation to martensite and strain hardening. Depending upon the welding process, the temperature distribution surrounding the weld causes irreversible weakening of the weld-heat-affected-zone by one or more of several mechanisms.

Solid state welding processes, such as flash welding and electric resistance butt welding, produce temperatures in the heat-affected zone sufficiently high to cause recrystallization, thus eliminating the strengthening effect due to prior cold work. The fusion welding processes, which provide temperature gradients embracing the entire range of temperatures up to the melting point, cause regions of the heat-affected zone to experience both reversion to austenite and severe grain growth in addition to eliminating the strain hardening effects. The resulting heat-affected-zone microstructure retains only the strength imparted by solution hardening effects and the high strength can only be restored by repetition of the cold working operation. The microstructure of the weld deposit is similar in this regard, and cold working is rarely possible after fabrication. Therefore, steels of this family are inherently incapable of being fabricated by any of the available welding processes without a considerable loss in strength.

Precipitation-Hardening Stainless Steels

The composition of this family of steels is adjusted to permit thermally induced transformation to martensite by appropriate heat treatment. The steels are then subjected to a precipitation treatment in the vicinity of 950 F to develop optimum strength levels. However, the desired metastability of the austenite is obtained by the proper choice of austenitizing temperature. Exposure to temperatures sufficiently high to dissolve the alloy carbides produces excessive austenite stability and thus precludes thermally induced transformation to martensite.

Weld metal closely matching the base metal in both composition and response to heat treatment can be deposited with the TIG process using a cold wire of suitable composition fed directly into the weld puddle. However, stable austenite is produced in both the as-deposited weld metal and adjacent regions of the heat-affected zone as a result of the high temperatures experienced during welding. Thus, it is necessary to subject the entire structure to the complete hardening heat treatment after the welding operation if high strength levels are to be obtained.

Microsegregation of major alloying elements in the weld deposit is difficult to homogenize during subsequent heat treatment and often makes impossible the development of full strength in the deposited metal. In addition, microsegregation of impurities such as sulfur and phosphorus may result in hot-cracking problems, so the need for additional work on the influence of welding conditions on microsegregation is again encountered.

Hydrogen-induced cold cracking does not appear to be a problem in these materials, presumably because of the inherent stability of the austenite in the heat-affected zone in the as-welded condition. However, the use of processes which minimize the access of hydrogen to the weld area is sound engineering practice.

Maraging Steels

The recently introduced maraging steels offer great promise as weldable, high-strength steels. However, in the transition from laboratory-scale weldability testing to commercial application, it is not surprising that problems have developed. Hot cracking in the weld and weld heat-affected zone during fabrication of highly restrained structures, and reduction in strength by the formation of stabilized austenitic regions constitute the major deterents to full utilization of these material at ultrahigh strength levels. Both of these problems appear to be related to the pattern of microsegregation produced by welding.

Current research in the welding laboratories at Rensselaer seeks to evaluate the hot-cracking propensity of the maraging steels and to determine the influence of process variables on microsegregation in the weld and weld-heat-affected zone. As part of the investigation, a new testing technique, called the VARESTRAINT TEST has been evolved which promises to provide a quantitative evaluation of the hot-cracking tendency in an inexpensive laboratory specimen.

Figure 1 summarizes the testing mechanism in schematic form. A pneumatically operated loading system is employed to bend a specimen to a predetermined radius while a weld bead is being deposited on the specimen. The specimen is supported as a simple cantilever beam as shown in Figure 1, and a loading yoke is located near the free end of the specimen. A longitudinal weld bead is deposited as indicated, and when the arc reaches point "b" at the left-hand end of the precision ground die block "A", the specimen is bent suddenly by a force "F". As the specimen is forced to conform to the radius of curvature of the die block, the outer fibers of the specimen, including the weld bead, heat-affected zone, and unaffected base metal, experience a uniform, suddenly applied strain. The magnitude of the strain can be calculated from the specimen geometry and the

radius of curvature of the die block, and the amount of strain can be varied by simply substituting a die block of different radius.

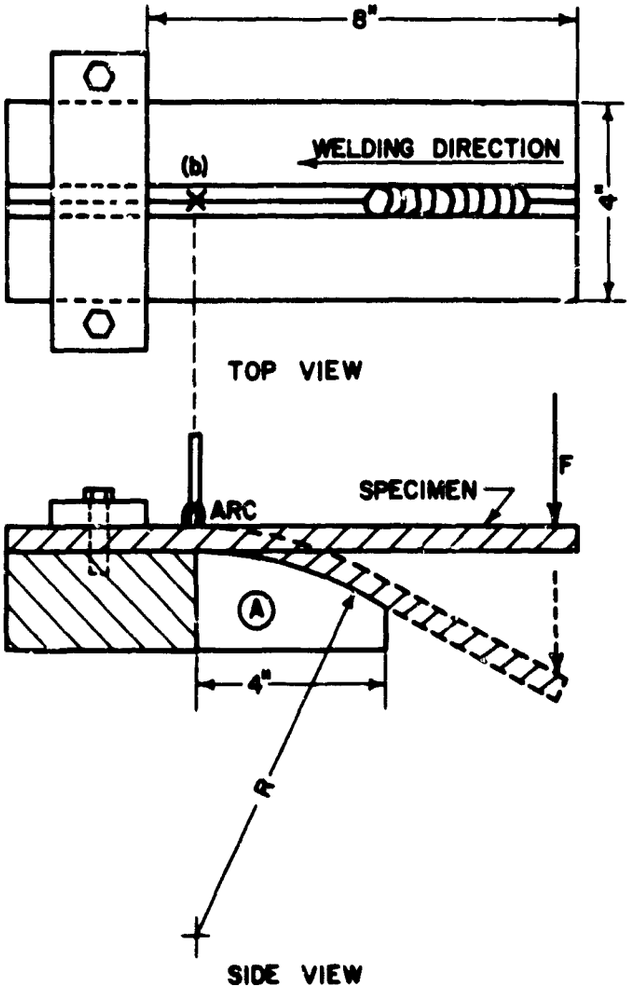

FIGURE 1. SIMPLIFIED SKETCH OF THE OPERATION OF THE "VARESTRAINT" TESTING DEVICE

The primary advantage of this method is that a constant reproducible strain, of magnitude essentially independent of the welding parameters, is applied simultaneously over a finite length of weld. Thus, the same augmented strain is suddenly applied to the actual welded composite at temperatures ranging from the melting point to far below the hot-cracking range. In addition, tungsten-tungsten-rhenium thermocouples, plunged into the weld puddle and allowed to freeze in position, have been used to establish the influence of welding variables and specimen geometry on the temperature distribution along the weld. From these data and the crack location, the temperature range over which hot cracking occurs for a given level of augmented strain can be evaluated as an additional quantitative index of the hot-cracking propensity.

Figure 2 shows typical examples of heat-affected zone microcracks observed in an as-welded 18Ni (250) maraging steel. This photomicrograph, taken at 100X, reveals intergranular microcracks ranging from 0.001-0.008 in. long located in the coarsened region of the heat-affected zone immediately adjacent to the weld fusion zone. In all cases, the cracks are essentially perpendicular to the fusion zone boundary and thus transverse to the augmented strain.

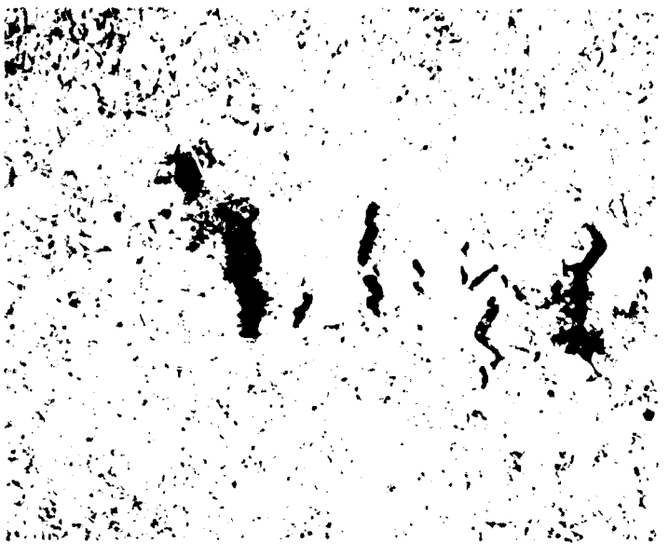

FIGURE 2. TYPICAL HEAT-AFFECTED-ZONE MICROCRACKS IN AS-WELDED 18Ni (250) MARAGING STEEL

Etched with modified Marbles Reagent; 100X (reduced approximately 20 per cent in printing).

Figure 3 shows, at 100X magnification, hot microcracks typical of those observed in the weld deposit of VARESTRAINT specimens. These cracks are always either intergranular or are located in the subgrain boundaries produced by the solidification process. The orientation of the cracks is completely dependent upon the orientation of the grain and sub-grain boundaries produced during solidification and ranges from nearly parallel to nearly perpendicular to the direction of the augmented strain.

Preliminary metallographic studies indicate that the boundary regions where cracking occurs are solute rich areas where extensive microsegregation is present. Preliminary tests have demonstrated that the nature and extent of this microsegregation can be altered by appropriate choice of welding variables, thus suggesting that the hot-cracking propensity of a given material can be minimized by the choice of optimum welding conditions. Further work is in progress to establish techniques for establishing welding parameters providing microstructures with the minimum cracking propensity.

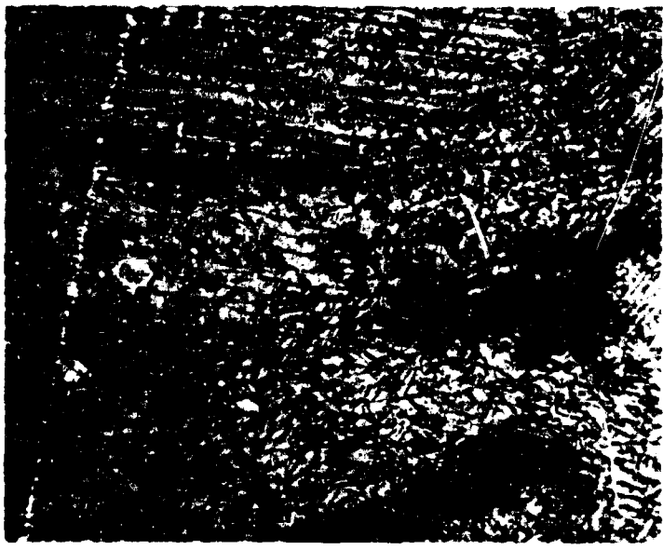

FIGURE 3. TYPICAL MICROCRACKS IN AS-DEPOSITED TIG WELD IN 18Ni (250) MARAGING STEEL

Etched with Modified Marbles Reagent; 100X (reduced approximately 20 per cent in printing).

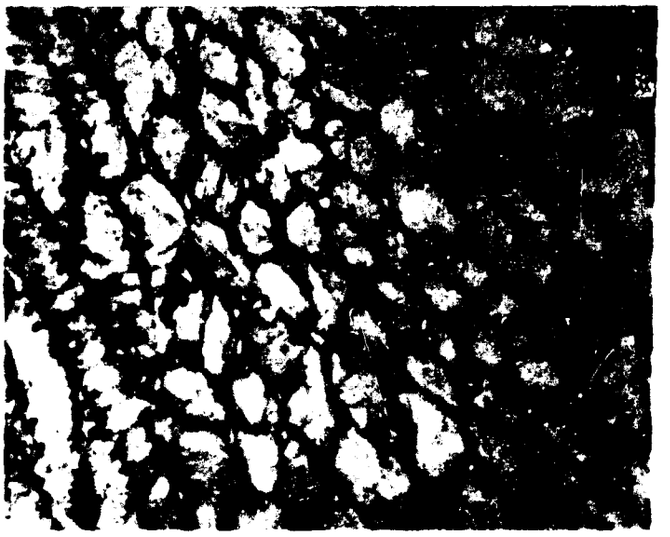

FIGURE 4. TYPICAL MICROSTRUCTURE OF TIG WELD IN 18Ni MARAGING STEEL

Aged 3 hours at 900 F; etched with Wazu's modified Frye's Reagent; 500X (reduced approximately 20 per cent in printing).

Figure 4, taken at 500X of a weld in 18Ni (250) maraging steel after aging, shows typical regions of alloy-rich retained austenite at the solidification subgrain boundaries. This high-alloy austenite is extremely stable and did not respond to the 900 F post-weld aging treatment. Unless the welding conditions are chosen to provide minimal quantities of randomly dispersed alloy-rich retained austenite, serious impairment of weld strength can result after local aging. Furthermore, the microsegregation produced during solidification exaggerates the tendency for austenite reversion in those portions of multipass welds reheated by the deposition of subsequent passes.

Although considerable joining of maraging steels has been performed using TIG welding with a cold wire feed, submerged arc-welding techniques have recently been developed which promise to provide greatly increased deposition rates. One of the major problems in developing suitable submerged arc-welding fluxes is the necessity for eliminating siliceous ingredients in order to prevent excessive silicon in the deposited metal. Although this problem has been averted by certain proprietary fluxes, additional research is necessary before consistently sound, high-quality welds are assured with routine commercial fabrication techniques.

SUMMARY OF THE CURRENT STATE OF THE ART

Numerous applications of the quenched and tempered steels at high strength levels have demonstrated that these materials can be successfully joined by fusion welding if special care is exercized and the structure can be heat treated after fabrication. The high-strength, cold-worked stainless steels appear to be unsuited to fabrication by any existing welding technique, since it is usually impossible to apply the cold-working operation required to restore the loss of strength caused by the heat of welding. The precipitation-hardening stainless steels currently available are marginal in ability to achieve the required yield strength levels. Accordingly little application has been made of these materials in the 225,000 psi range and almost no welding technology exists. The maraging steels offer the greatest promise as weldable high-strength steels, but additional research will be required to establish an adequate welding technology based upon sound welding metallurgical principles.

SECONDARY FORMING PROCESSES AND THEIR EFFECTS ON RESULTING PRODUCTS

by

William W. Wood*

ABSTRACT

The current trend toward higher usage of new high-strength materials such as the high-strength steels is posing a considerable problem in the defense industry for both the design and manufacturing engineer. In particular, the manufacturing engineer is faced, not only with deficiencies in fabrication of these new materials such as secondary forming, but also with the quality assurance of producing a sound part free of defects.

This paper is being presented to bring out the manufacturing problems associated with secondary forming of new high-strength steels, and to give indications of possible solutions for the future. The conventional forming processes to be discussed are bending, flanging, stretching, drawing, and bulging; while the advanced processes are shear spinning, high-velocity, high-temperature, and high-pressure forming.

The presentation will be centered around formability, quality of resulting parts, final shaping and sizing, process limitations, and resulting mechanical properties. Formability will be discussed for the various processes by giving relative formability of the high-strength steels to other high-strength alloys. The quality of the resulting parts will be discussed for distortions such as buckling, twisting and crippling, spring-back, thickness reductions and variations, and inspection techniques.

Methods of controlling the quality of parts by final shaping and sizing will be presented. These will include handworking, creep forming, and heat-treat fixturing. In addition, the limitations of the processes will be given. These will include friction resulting in localized thinning, heat applications, atmospheric protection, available pressures and energy, and tooling applications. Finally, resulting mechanical properties will be discussed.

FORMABILITY AND MATERIAL PROPERTIES

As shown in Figure 1, there are four basic ways of deforming sheet metal--by pulling, pushing, bending, and twisting. The first three of these are used extensively in sheet-metal forming with the various machines developed for this purpose. Pulling and pushing result in instabilities as shown and when carried beyond definite limits of the material and part shape, failure occurs by splitting and buckling, respectively. Bending also results in a splitting failure, but without the instability shown for pulling.

*Vought Aeronautics Division, Ling-Temco-Vought, Inc., Dallas, Texas.

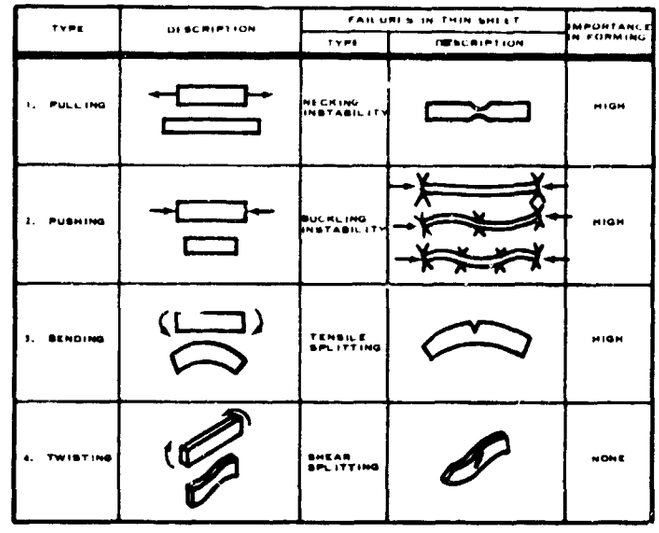

FIGURE 1. WAYS OF DEFORMING METAL

Pulling a piece of sheet metal by application of a tensile load will lead to various degrees of instability, as shown in Figure 2, depending on the relative amounts of biaxial loading in the plane of the sheet. Simple tension loading results in a highly localized neck that is at an angle of approximately 55° to the loading direction, whereas balanced biaxial loading results in a diffuse-type necking with the instability spread over a relatively large area. Plane strain loading will result in an instability between the other two.

Pushing a piece of sheet metal by the application of compressive loads will result in various types of instability and buckling, as shown in Figure 3, depending on the direction of loading and the type of edge restraint on the part. Similar types of buckling are shown for compressive end loading of an element of sheet metal, shear loading on the edges, and tensile loading on the inside edge of a circular element. Twist buckling is shown for compressive end loading of an angle section which results from spring-back and residual stresses in linear contoured parts.

These types of loading on sheet-metal parts can be related to the formability of materials by various formability indices based on the mechanical properties of the material. Figure 4 gives some indices used for predicting the formability of a few typical sheet-metal forming processes. Brake forming has been related to the 1/4-inch gage length elongation giving the bend radius to thickness ratios shown for the four materials. Stretching over a larger area, as in linear and

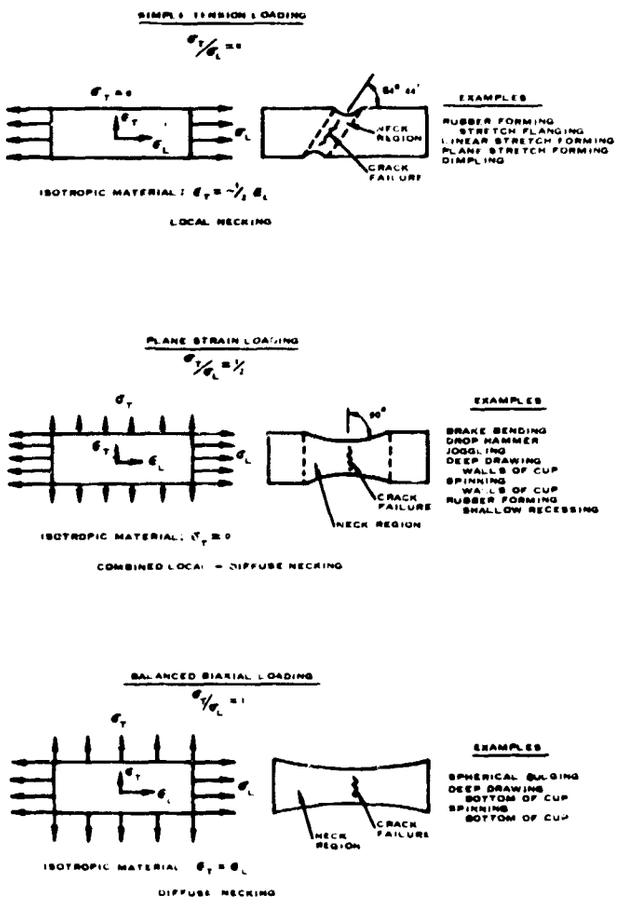

FIGURE 2. FAILURE FROM TENSILE LOADS-SPLITTING FAILURES

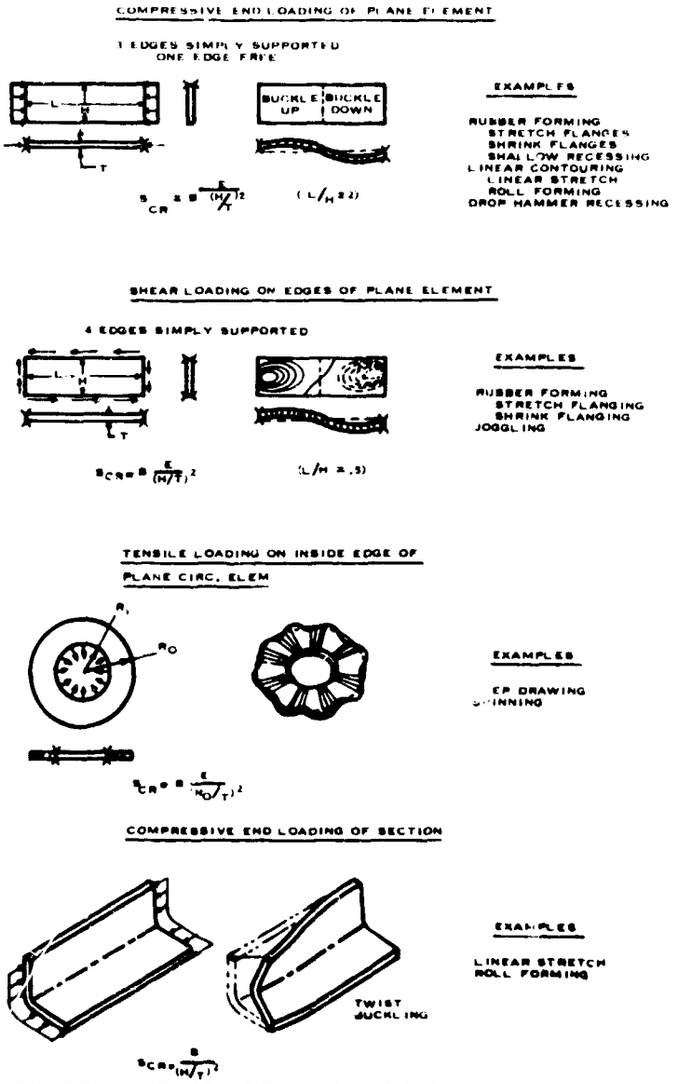

FIGURE 3. FAILURE FROM COMPRESSIVE LOADS-BUCKLING FAILURES

Material	Bending: Brake Forming, Bend Radius R/t (.23)	Stretching: Plane Stretching Linear Stretch Flanging, Elongation 2.0%	Buckling and Spring-back: Stretching Drawing Shrinking, Modulus E(10^6 psi)	Buckling and Spring-back: Roll Forming Spinning, Yield Sy(10^3 psi)	Buckling and Spring-back: Ratio E/Sy
2024 Aluminum	.30	22	10.6	11	964
H-11 Tool Steel (VJ-1000)	1.30	17	30.0	70	428
18 Nickel Maraging Steel	--	8	27.0	118	228
6Al-4V Titanium	5.40	10	15.4	120	128

FIGURE 4. FORMABILITY OF ANNEALED MATERIALS

plane stretch forming, can be predicted by formability indices based on a larger gage length such as the two-inch elongation. Both buckling and spring-back can be related to the ratio of the modulus of elasticity to the yield stress E/S. It will be shown that the high value given for aluminum and the low value for titanium represent the relative difficulty in initial and finish forming of the latter material over the former. The two high-strength steels are shown to be intermediate.

LIMITATIONS IN SHEET-METAL FORMING

All sheet-metal forming operations have restrictive limitations based on the fundamental nature of the process. In matched die forming on the hydraulic presses and drop hammer, it is principally the friction between the die and the part and the localization of heat in hot forming. In high-velocity forming, friction is virtually eliminated, but some materials become brittle when formed beyond a critical speed. In rubber forming, the limitations are primarily associated with the pressure limits with additional restrictions of friction. In the stretching operations, friction and the inability to distribute heat properly are the principal limiting factors.

In order to evaluate these limitations properly with regard to the high-strength steels, it will be helpful to analyze the pressure limitations in rubber forming for spring-back, part definition, and shrink flanging.

The relationship between pressure and spring-back for four materials is shown in Figure 5 for rubber-pad forming. It is indicated that pressure has a critical influence on the spring-back of the four materials, generally a two-to-one factor for practical pressure values. The materials properties are shown to have an even greater influence

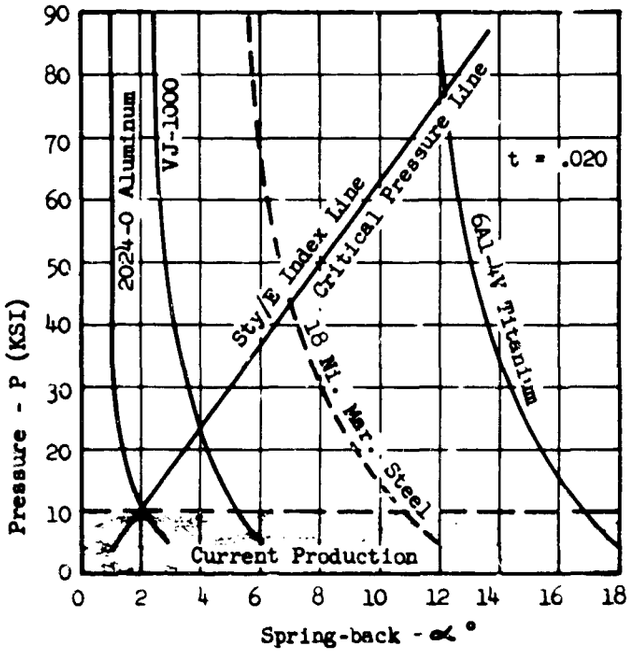

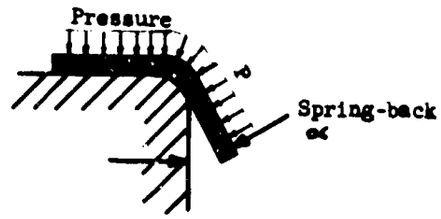

	E/Sty	Sty/E(10^4)
2024-0	964	10.4
VJ-1000	428	23.2
18 Ni. Mar.Steel	228	44.0
6-4 Titanium	128	78.0

FIGURE 5. RUBBER FORMING STRAIGHT FLANGES

on spring-back, however, which is directly related to the ratio of the tensile yield to modulus, Sty/E. Because of the fact that current production in the aircraft industry is limited to approximately 10,000 psi, the spring-back values are 18°, 11°, 5°, and 2°, respectively, for the 6Al-4V titanium, 18Ni maraging steel, VJ-1000 tool steel, and 2024-0 aluminum. The critical pressure line is shown to coincide with the index line and is defined as the pressure for each material above which little gain can be made on spring-back. It should be noticed that the two high-strength steels show intermediate spring-back values between the aluminum and titanium, indicating the relative effort required in tool development and finish forming for the four materials.

The effect of rubber forming pressure on part definition is shown in Figure 6 for Vascojet 1000 tool steel. For this typical high-strength steel, it can be seen that current production limits of 10,000 psi are inadequate. In order to obtain a reasonable value of 4t free form radius, it is necessary to maintain a 33,000-psi rubber-forming pressure for the VJ-1000, whereas only 7,000 psi is needed for 2024-0 aluminum. For this reason, the high-strength steels are virtually ruled out for current production rubber forming except for thin gages below 0.020. Most shallow recessing for the high-strength steels is accomplished on the hydraulic and drop-hammer presses with matched dies.

The effect of shrink flange limits for various pressures is given in Figure 7 for VJ-1000. It is shown that, for a fairly severe radius of curvature R of 10 inches, the maximum flange that can be formed with 15,000 psi is 0.75 inch; whereas for the larger radius of 30 inches, it is 2.25. For

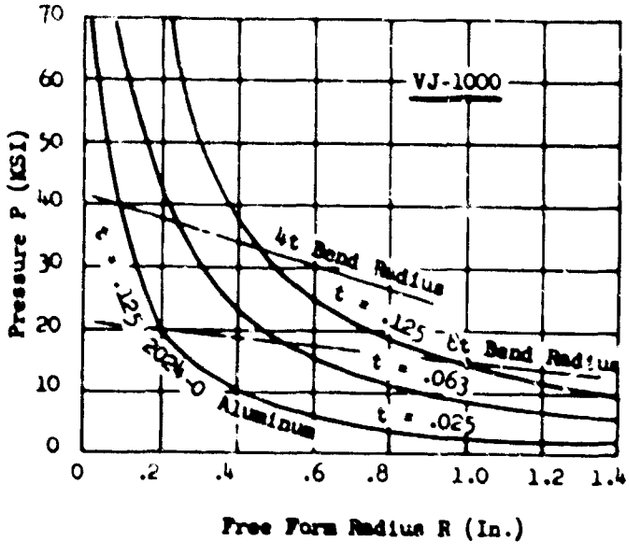

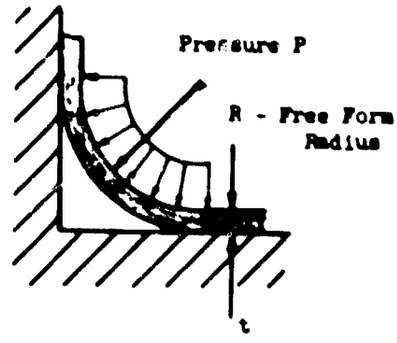

FIGURE 6. PART DEFINITION

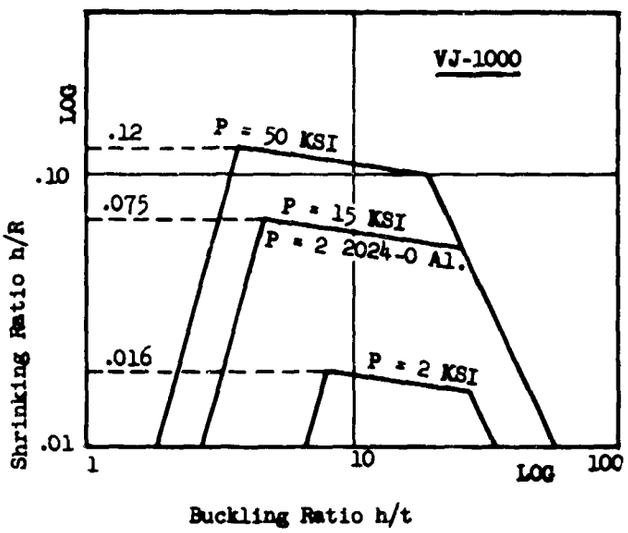

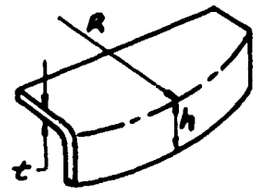

R (In.)	P (KSI)	h (In.)
10	2	.16
	15	.75
	50	1.20
30	2	.48
	15	2.25
	50	3.60

FIGURE 7. SHRINK-FLANGE LIMITS

this reason, flanging of the high-strength steels on the rubber press is generally limited to the larger radii of curvature on the order of 25 to 30 inches. More severely curved parts have to be formed on matched dies. In comparison, it is shown that the same parts requiring 15,000 psi for VJ-1000 require only 2,000 psi for aluminum.

HOT FORMING AND SIZING

The ability to control distortions such as buckles, wrinkles, spring-back, oil canning, and to a limited extent part definition, depend largely on the creep-forming temperature of the material. This is the temperature at which appreciable metal movement will occur in a reasonable time, generally less than 10 minutes.

The creep-forming temperature is given in Figure 8 for a titanium alloy and a high-strength steel. The high temperature of 1900 F required for finish forming of VJ-1000 precludes this type of operation for this material because of the low recrystallization temperature and the high tooling cost. Even though the previous charts and graphs have shown titanium to be significantly inferior in resistance to buckling, spring-back, and other distortions, the total forming costs are low in comparison with the high-strength steels largely because of almost total elimination of hand working by hot finish forming. Titanium is readily hot formable for two principal reasons: (1) the creep-forming temperature is below the recrystallization and contamination temperature, and (2) the creep-forming temperature is within the limits of current tooling materials such as cold-rolled steel and cast iron without the need for coatings.

Most of the high-strength steels are highly creep resistant, thereby eliminating them from hot-finish forming. Improvements in formability are insignificant below their recrystallization temperature, which also virtually eliminates them from the hot-forming class. For these reasons,

Material	Creep-Forming Temperature, F	Recrystallization Temperature, F	Contamination Temperature, F	Hot Tooling Requirements
6Al-4V Titanium	1100	1300-1500	1100	Steel and cast iron
H-11 Tool Steel VJ-1000	1900	1200-1300	1800*	Ceramic
18 Nickel Maraging Steel	--	1000-1300	1800**	Ceramic

*Slight oxidation. **Light surface scale.

FIGURE 8. HOT FORMING AND SIZING

these high-strength steels will require hand working and the total forming costs will reflect this requirement.

HIGH-VELOCITY FORMING

Most materials are very applicable to high-velocity forming as long as it is performed below a critical velocity above which the material behaves in a brittle manner. A number of materials exhibit a significant increase in ductility with forming velocities to 700 ft/sec, well into the high-explosive-forming range.

Figure 9 illustrates some important forming parameters for high-velocity forming of domes for an aluminum, a high-strength steel, and a titanium alloy. The chart illustrates the significant improvement in uniform elongation for aluminum and titanium over static forming values. However, both materials have a relatively low critical forming velocity in the lower range of high explosive forming, and consequently, are critical with regard to the size of the explosive charge, stand-off distance, etc. The titanium alloy is further restricted to forming at elevated temperature at the high velocities which practically necessitates forming in air with low explosives or the equivalent. The high-strength steel shows little gain in ductility, but it is important to note that there is no decrease in formability even to the high-velocity ranges of high explosive forming.

Presented in Figure 10 is a typical formability limit graph for high explosive forming of AM-350 stainless steel and 2024-T3 aluminum for three-part shapes. In contrast with static deep drawing of these part shapes, it can be seen that high-explosive deep recessing results from both a drawing and stretching action. For the heavier gage materials with an H/t below 200, good formability can be accomplished because of the large amount of draw that can be effected. Above a critical H/t, representing thin gages, the best formability can be obtained by a rigid clamping of the edges of the part, thereby restraining the drawing action. Intermediate gages in the transition region of the curves require precise control over the hold-down ring pressure in order to obtain optimum formability.

Material	Optimum Velocity and Temperature			Increase Over
	Temperature °F	Velocity F.P.S.	Uniform Elongation %	Static Room Temp. %
2024-O Aluminum	400	0-400	30	61
H-11 Tool Steel VJ-1000	R.T.	600-750	21	10
6-Al-4V Titanium	1200	0-450	15	145
Low Explosive - 50-400 F.P.S. High Explosive - 300-800 F.P.S.				

FIGURE 9. HIGH-VELOCITY FORMING OF DOMES

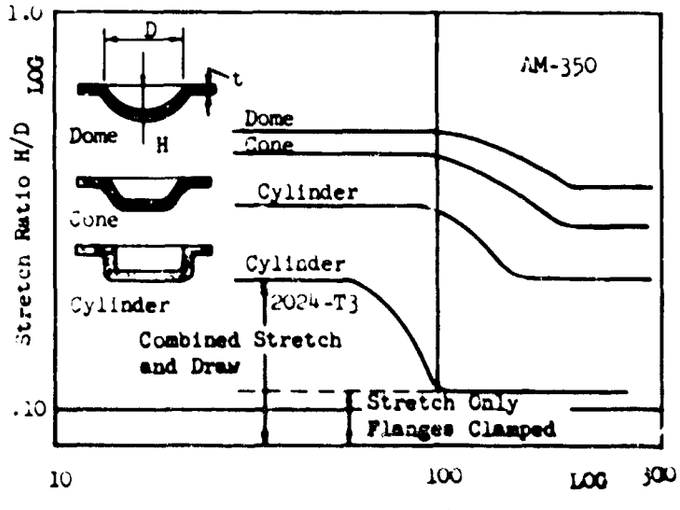

Material	Uniform Strain ϵ_u	Buckling Ratio Ec/Scy	Index I
2024-T3 Aluminum	.10	229	249
AM-350 Stain.Steel	.39	371	410
VJ-1000	.17	382	399

Index:

$$I = \frac{\text{Dynamic}}{100\epsilon_u} + \frac{\text{Static}}{Ec/Scy}$$

FIGURE 10. HIGH-EXPLOSIVE FORMING

In examining the index values shown on the table, it is evident that VJ-1000 maintains a formability comparable with AM-350, somewhat higher than the aluminum alloy, even though the uniform elongation is lower. This results from the fact that most of the forming action is accomplished by draw under conditions of good control of the pressure pad.

The strains resulting in the plane of the sheet are shown in Figure 11 for the explosive formir of domes, as an example. This type of graph will give some insight into the relative importance of drawing and stretching in explosive forming. On analysis of the two strains across the dome, it can be seen that the biaxial strain condition varies from balanced biaxial at the crown to pure shear within the flange. The original bend line at B represents the area of plane strain where the circumferential strain vanishes. When forming is below the critical velocity, failure will invariably occur in the crown at the point of highest balanced biaxial strain. Even though only diffuse-type necking has occurred in this area, the part has strained sufficiently to reduce the thickness a considerable amount. When the critical velocity has been exceeded, failure will occur circumferentially on a line between B and C.

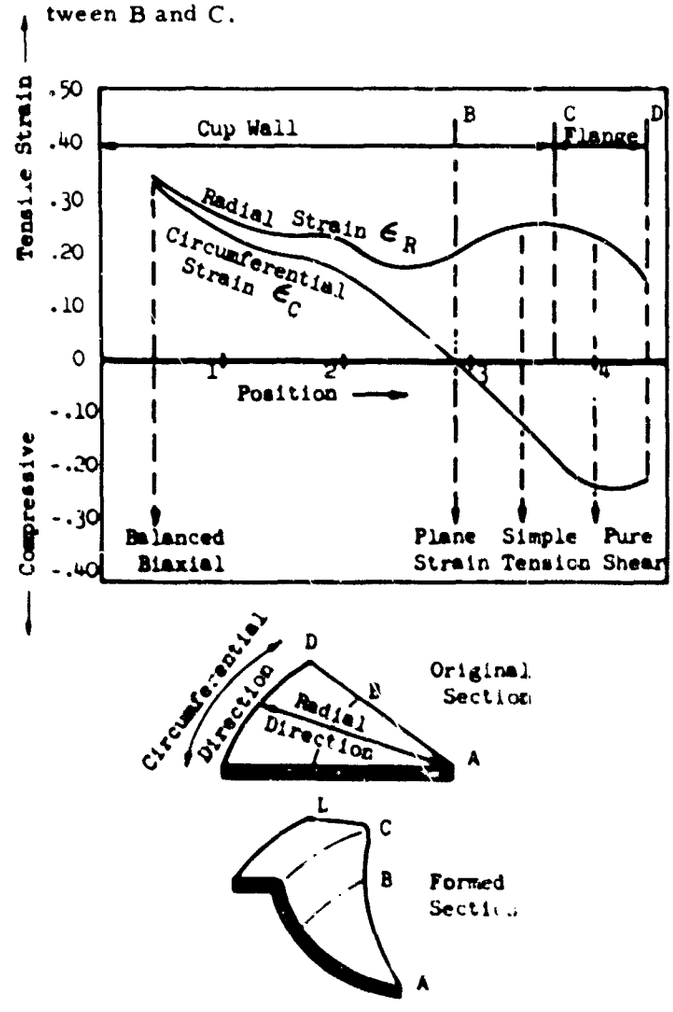

FIGURE 11. BIAXIAL STRAINS IN EXPLOSIVE FORMING OF DOME

THICKNESS STRAINS IN SHEET-METAL FORMING

Thinning of parts resulting from sheet-metal forming is often a critical problem both in design and fabrication. The design has to be such that the part, after it has been formed, will sustain the structural load. If appreciable thinning has occurred in some areas of the part and not in others, the part may be heavier and less efficient than a part with more uniform thinning. If too much thinning occurs locally during the initial forming stages, the part may become unable to sustain further loading for completion of forming.

Figures 12 and 13 illustrate the amounts and distribution of thinning that occur from forming typical aircraft parts. Drawing of the cylinder and dome illustrates the large gradients in thinning that can occur in forming these parts, particularly at the high-velocity rates. The dome, for example, can thin to as much as 60 per cent in the crown and thicken to as much as 30 per cent on the outer edge. These large amounts of thinning are not so detrimental in design as it might first appear because the areas that thin the most are the ones that generally take the least structural load.

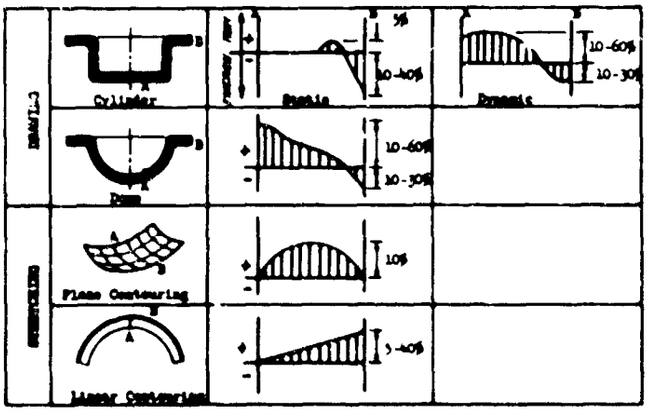

FIGURE 12. THICKNESS STRAINS IN SHEET-METAL FORMING

MECHANICAL PROPERTIES FROM SHEAR FORMING

The shear-forming process has been used extensively in the aerospace industry in the past few years, particularly in the large missile industry for the forming of conical and to a lesser extent hemispherical and cylindrical shapes. The process is a natural for the conical shapes, but problems are encountered in the forming of the other two shapes because premachined or prewelded blanks are required.

One of the most intriguing shapes to be formed by the process is a cylindrical part that can be shear formed by either a forward or back extrusion. This is the only production method available to produce these shapes free of a longitudinal weld.

Some interesting material properties result from such a heavy plastic working as shown in Figure 14. These properties were developed on a WADD contract for the Air Force in 1961 by Ling-Temco-Vought, Inc. The parts were back-extrusion shear formed at room temperature using the 18 nickel maraging steel alloy. It is evident that a 12-15 per cent increase in tensile yield can be obtained by a shear-forming and double-aging operation over the as-received material. The ductility, however, was decreased from 8.8 per cent to 2.45 per cent.

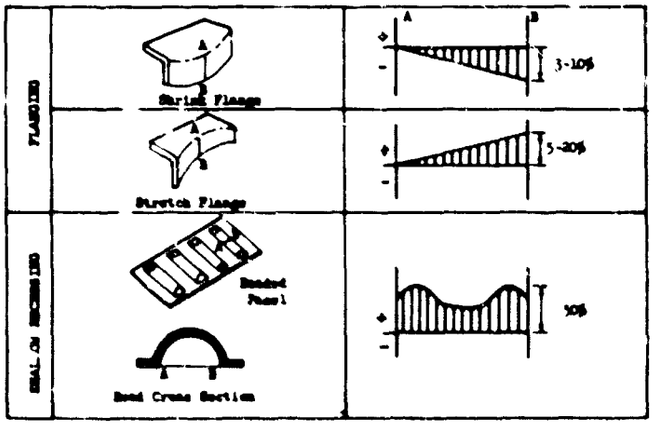

FIGURE 13. THICKNESS STRAINS IN SHEET-METAL FORMING

Condition	Age*	Direction	Tensile Yield Sty (ksi)	Tensile Ultimate Stu (ksi)	Elongation, 2.0%	Hardness, R_C	Number of Specimens
1. As received	Single	-	276.3	282.8	8.80	53.1	-
2. 73% Shear-formed	-	L	144.0	170.0	4.85	37.6	10
		T	152.0	179.2	4.50	38.0	6
3. 73% Shear-formed	Single	L	293.0	297.5	2.50	53.0	5
4. 73% Shear-formed	Double	L	307.5	309.0	2.45	54.5	13
		T	317.8	323.0	2.25	54.1	4
5. 73% Shear-formed	Triple	L	307.5	311.0	2.37	54.0	5
		T	321.0	323.9	2.12	53.9	5
6. 73% Shear-formed	Annealed and single	L,T	271.9	279.7	2.80	52.0	6

*First and Third Age - 900 ± 10 F for 3 hours. Second Age - 850 ± 10 F for 3 hours. Anneal (6) - 1525 F for 1/2 hour.

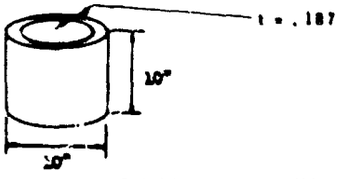

18 Nickel Maraging Steel
Back-extrusion shear forming at room temperature.
Two passes prewelded cylinder.
Ling-Temco-Vought, Inc., contract
WADD TE-7025, September 1961.

FIGURE 14. MECHANICAL PROPERTIES FROM SHEAR FORMING

THE SURFACE INTEGRITY OF MACHINED-AND-GROUND HIGH-STRENGTH STEELS

by

Michael Field and John F. Kahles*

ABSTRACT

In machining or grinding of high-strength steels, there is a strong tendency to produce significant alterations in the surface layer, such as plastic deformation, high-temperature gradients, rehardening, overtempering, and residual stress. Data are presented which show the advantages of using low-stress machining-and-grinding conditions to control these surface alterations and their resultant effects on distortion, stress corrosion, and mechanical properties, including fatigue, of high-strength steels, such as 4340 and D6AC. In using uncontrolled machining or grinding conditions, which often result in abusive shop practices, a rehardened brittle martensitic layer is developed on the surface during drilling, milling, grinding, and abrasive cutoff of 4340 and D6AC. Similar rehardened layers along with remelted surface material are observed in electrical-discharge machining. Secondary methods to impart beneficial surface characteristics to machined and ground surfaces, such as heat treating, shot peening, and tumbling, are reviewed along with methods for detection and measurement of surface changes.

INTRODUCTION

High-strength steels are being used for the manufacture of important aerospace components, such as rocket-motor cases, landing gears, spars and other primary aircraft structures. In an ever-continuing attempt to increase strength-weight ratios, cross sections of components are being decreased so that the ratio of surface layer is becoming increasingly large with respect to the overall thickness. The nature of the surface layer is thus requiring added attention in research and development, design and manufacturing.

The purpose of this paper is to call greater attention to some of the subtle, but highly significant, changes which can be affected in the surface of high-strength steels by machining and grinding processes. Heretofore most attention in consideration of these processes has been centered on rates of metal removal, tool or grinding wheel life and surface finish. Demands now call for greater surface integrity of parts since it has been found that average processing frequently produces a highly stressed and sometimes a damaged surface on the workpiece. Some companies producing aerospace components no longer allow machinists to set their own conditions in the shop. Not only are wheels and tools specified, but feed rates, cutting speeds and other pertinent cutting conditions are controlled under carefully designed specifications.

Such specifications are aimed to eliminate high residual stresses and thus distortion, as well as to reduce significantly the possibility of causing excessive surface damage resulting from metallographic changes, such as those which occur in the rehardening of tempered martensite.

A number of the new alternative metal removal processes, such as electrical-discharge machining and electron-beam machining, create a layer of melted metal. The extent of the affected surface can be controlled and should be removed for many applications involving aerospace components which are being produced under closely held specifications.

In the following discussion, various important aspects of the relationship of metal removal processes to the surface being produced are presented.

In machining and grinding of any alloy, the generated surface is subjected to varying degrees of deformation and heating. The resulting surface produced has a disturbed layer that may contain surface alterations of the following types:

1. Plastic Deformation

Surfaces produced by cutting or grinding operations are frequently plastically deformed. The material in the main body of the chip is subjected to very large strains, strain rates and temperatures under conditions of unusual restraint. These unique conditions of plastic deformation yield large amounts of strain hardening. All the conditions pertaining to the formation of chips influence the characteristics of the finished surface, since before the newly formed surface is generated it is physically connected with the chip. The extent to which the deformed zone extends below the cutting edge in front of the tool determines the extent of deformation in the finished surface. In addition to the plastic deformation associated with chip formation, a newly cut surface may be burnished by dull cutting tools or loaded grinding wheels. Subsurface plastic deformation and strain hardening can be

*Michael Field, President, and John F. Kahles, Vice President, Metcut Research Associates, Inc., Cincinnati, Ohio.

detected by metallographic examination and by a microhardness survey.

2. Temperature Gradient

The surface temperature of a machined part will reach very high values during cutting with temperatures over 1500 F being possible. The fact that the bulk of the material immediately below a machined surface will be at a low temperature gives rise to temperature gradients that are unusually severe.

3. Residual Stress

The presence of large amounts of plastic strain in a freshly machined surface, together with high surface temperatures and temperature gradients, results in residual stress patterns in the surface layer. The residual stresses may be principally confined to a depth of only .001 or .002", while in other cases the stresses may exist to a depth of .020", depending upon the type and severity of the material removal process. The residual stress pattern may be principally tensile or compressive. It may be compressive at the immediate surface and may change to become predominantly tensile at a layer .001 to .002" below the surface.

4. Metallurgical Transformation

When steel is ground, the surface temperature may reach a value sufficiently high to cause a thin layer to transform to austenite. Due to the extremely high rate of cooling associated with the large temperature gradient that normally exists at a surface being machined or ground, the austenitic layer transforms to hard martensite, bainite and other decomposition products.[1, 2]* The volume changes associated with these transformations induce residual stresses. Steels are not unique in this respect for similar transformations occur in many other alloy systems.

5. Overtempering

When hardened and tempered steel surfaces are machined or ground, the heat generated during these operations may develop temperatures considerably higher than the original tempering temperature and thus cause a softening of the surface due to overtempering of martensite.

6. Spattered Molten Metal

In some metal removal operations, such as electrical-discharge and electron-beam machining, a layer of molten metal may be formed on the surface.

7. Macrosurface Cracks

Some metals, such as hardened steels or tungsten, when abusively ground, may actually form visible cracks at the surface.

8. Tears, Voids and Inclusions

In some cases, the inherent defects within the metal, such as inclusions and voids, are uncovered by the machining process and are then located at or near the surface. Many of these defects can be detected by visual examination or by surface penetrant inspection.

9. Surface Finish or Surface Texture

The actual surface finish or surface texture has, in most cases, a pronounced effect upon fatigue. The sharp notches associated with a rough finish tend to act as stress risers and promote the nucleation of fatigue cracks.

All of the above surface characteristics have an influence to varying degrees on physical properties. Since fatigue failures tend to originate at or near the surface, it is evident that any discontinuity or unusual surface condition will have the greatest influence on the fatigue strength of the material. This tendency is furthermore aggrevated by the fact that in general the maximum applied strength in a component tends to be concentrated at the surface.

There is a growing amount of evidence that residual surface stresses play an important role on fatigue strength and on stress corrosion of steels. Residual stress induced in the surface of a component also has a very marked effect on the distortion of a component, especially in the very thin section components that are commonly used in today's carefully designed aerospace systems.

SURFACE EFFECTS IN MACHINING AND GRINDING HIGH-STRENGTH STEELS

Rehardened Surface Layer

In machining and grinding of 4340 and D6AC steels, in both the annealed or quenched and tempered states, it has been found that there is a tendency for untempered martensite to be produced on the surface. The untempered martensite is present in small quantities in almost all of the operations, and the amount and depth of the hard untempered martensitic layer is greatest where abusive machining or grinding conditions are used. Figures 1 and 2 show the typical white layer formation on the bottom of a blind hole produced by a dull drill on 4340 and D6AC steels. The hardness of this layer was 65-67 R_C, even though the base hardness of the steels was 37-44 R_C.

*References are given on pages 76 and 77.

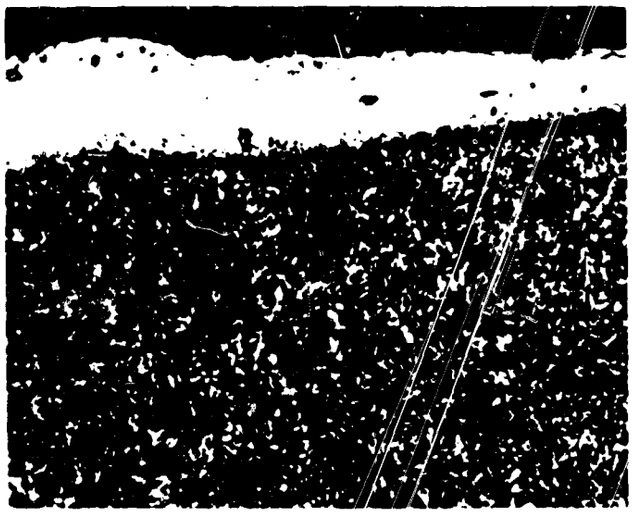

FIGURE 1. WHITE UNTEMPERED MARTENSITIC LAYER ON SURFACE OF DRILLED HOLE; 4340 STEEL, Q&T TO 44 R_C

Drilled with dull high-speed steel drill; white layer is .001" thick and 65-67 R_C; Nital etch; 500X (reduced approximately 20 percent printing).

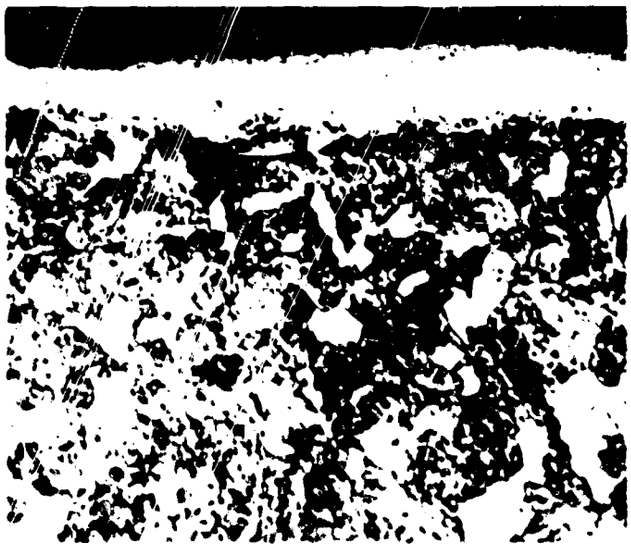

FIGURE 2. WHITE UNTEMPERED MARTENSITIC LAYER ON SURFACE OF DRILLED HOLE; D6AC STEEL, ANNEALED TO 37 R_C

Drilled with dull high-speed steel drill; white layer is .0009" thick and 65-66 R_C; Nital etch; 500 X (reduced approximately 20 percent in printing).

A cross section through the hole shows that the "white" untempered martensitic layer was not continuous throughout the entire drilled hole, Figures 3 and 4. The depth of the white layer is

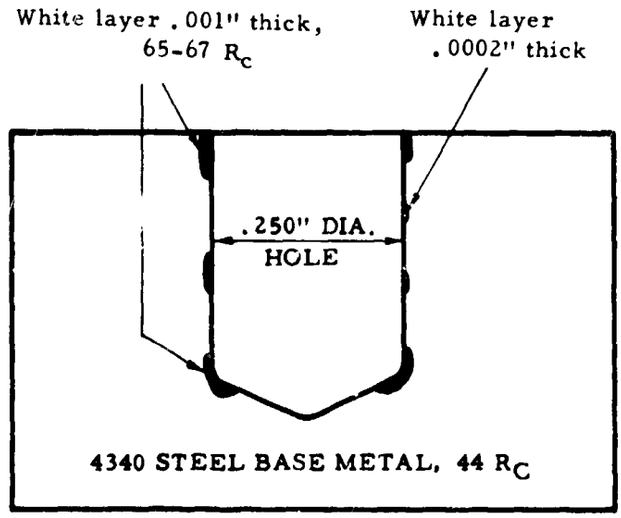

FIGURE 3. WHITE UNTEMPERED MARTENSITIC LAYER ON SURFACE OF DRILLED HOLE; 4340 STEEL, Q&T TO 44 R_C

Drilled with dull high-speed steel drill; white layer occurs in scattered areas over surface of hole.

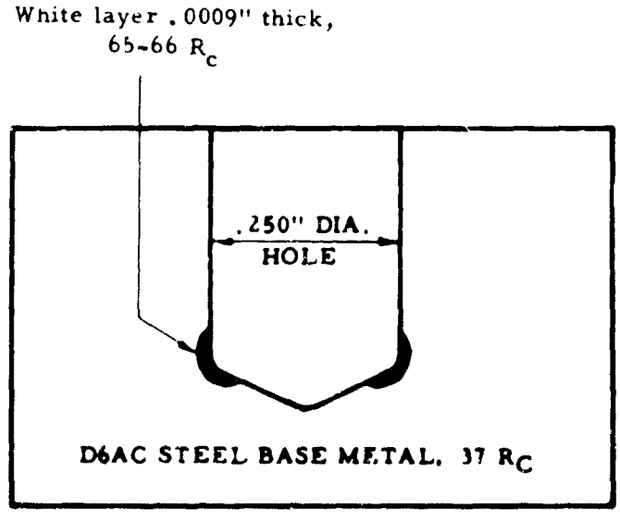

FIGURE 4. WHITE UNTEMPERED MARTENSITIC LAYER ON SURFACE OF DRILLED HOLE; D6AC STEEL, ANNEALED TO 37 R_C

Drilled with dull high-speed steel drill; white layer occurs only on bottom of hole where drill lip failed.

seen to be as great as .001", but in some cases the depth was only .0002". These holes were drilled with a high-speed steel drill that dulled during the drilling operation. The drilling was stopped in the blind hole when the wear on the drill margin became excessive, and at this point the drill dwelled at the bottom of the hole momentarily. As might be expected, the greatest concentration

of the hard white layer is found at the bottom of the hole where the drill margin meets the drill point, Figure 4. It should be noted that this "white" layer is different from the white layer sometimes produced in the nitriding process in which the chemistry of the surface is changed significantly.

Holes drilled in 4340 and D6AC over a hardness range of 37-55 R_C produced varying amounts of the white layer when drilled with dull high-speed steel drills. The more abusive the drilling, the larger the quantity and greater the depth of the white layer. However, holes drilled in the same steels under proper drilling conditions with sharp drills show an absence, or occasionally just a trace, of the untempered martensitic layer. Good conditions include the use of the correct speeds, feeds, drill material, drill geometry, drilling machine and cutting fluids. Recommendations for proper drilling conditions, as well as for other proper machining and grinding conditions, for high-strength steels are given in References 3 and 4.

Strict observance must be made to insure that all of the important facets of the drill condition are met to avoid the white layer. For example, in carbide drilling of 4340 steel, 52 R_C, an untempered martensitic layer .001" thick was obtained using a hand feed, Figure 5a, whereas in using a power feed .002 in./rev. this white layer was avoided, Figure 5b. The hand feed permitted uncontrollable feed rates and at times the 4340 steel workpiece was overheated producing scattered areas containing a white layer.

An untempered martensitic layer can also be obtained in carbide milling if conditions are abusive. Figures 6a and 6b illustrate the presence and nonpresence of a white layer in carbide milling of 4340 steel at 50 R_C. The white layer was produced when the wearland on the cutting edge of the carbide mill became excessive, Figure 6a. In milling under the same conditions, however, with a sharp carbide mill, the white layer was practically nonexistent, Figure 6b. A similar situation is observed in surface grinding of high-strength steels. While grinding under abusive conditions tends to produce this white layer, Figure 7a, grinding under gentle conditions leaves the surface practically free of the untempered martensitic layer, Figure 7b.

An extremely deep untempered martensitic layer can be obtained by abrasive cutoff of the high-strength steels. Figure 8 shows the surface hardness distribution after an abrasive cutoff operation using a proper cutoff wheel and water-soluble fluid in cutting through a 1/2 x 3" section of 4340 steel at 53 R_C and D6AC steel at 55 R_C. The 4340 steel had a surface hardness of 57 R_C. The hardness decreased to a low of 46 R_C at a depth of .005" below the surface. The hardness then increased gradually and returned to a value of 53 R_C at about .020" below the surface. The D6AC steel had a surface hardness of 65 R_C. The hardness decreased rapidly to a low value of 46 R_C .007" below the surface. The hardness then increased to the matrix hardness of 55 at about .040" below the surface. In both cases, the high hardness in the surface is that of an untempered martensitic layer. An actual marked softening in each case was noted at an intermediate zone .005 to .010" below the surface which existed in a zone of overtempered martensite. These zones of untempered martensite at the surface and overtempered martensite at the intermediate position below the surface have been observed in hardened tool and

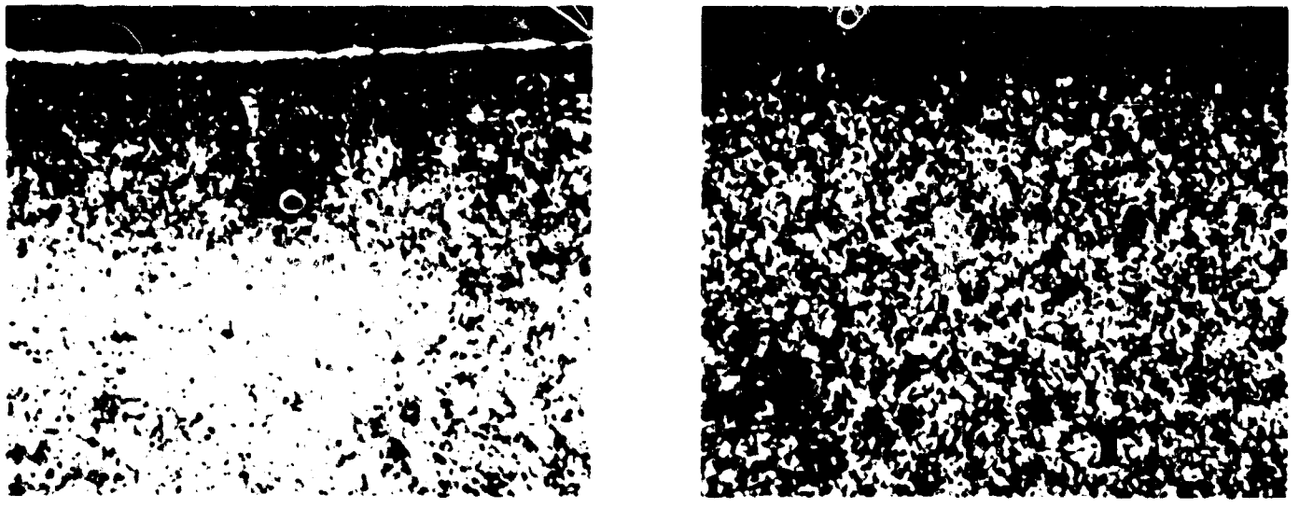

5a 5b

FIGURE 5. SURFACE OF HOLE CARBIDE DRILLED IN 4340 STEEL, 52 R_C

(5a) white layer on hole drilled with hand feed; (5b) no white layer on hole drilled with power feed; Nital etch; 250X (reduced approximately 20 percent in printing).

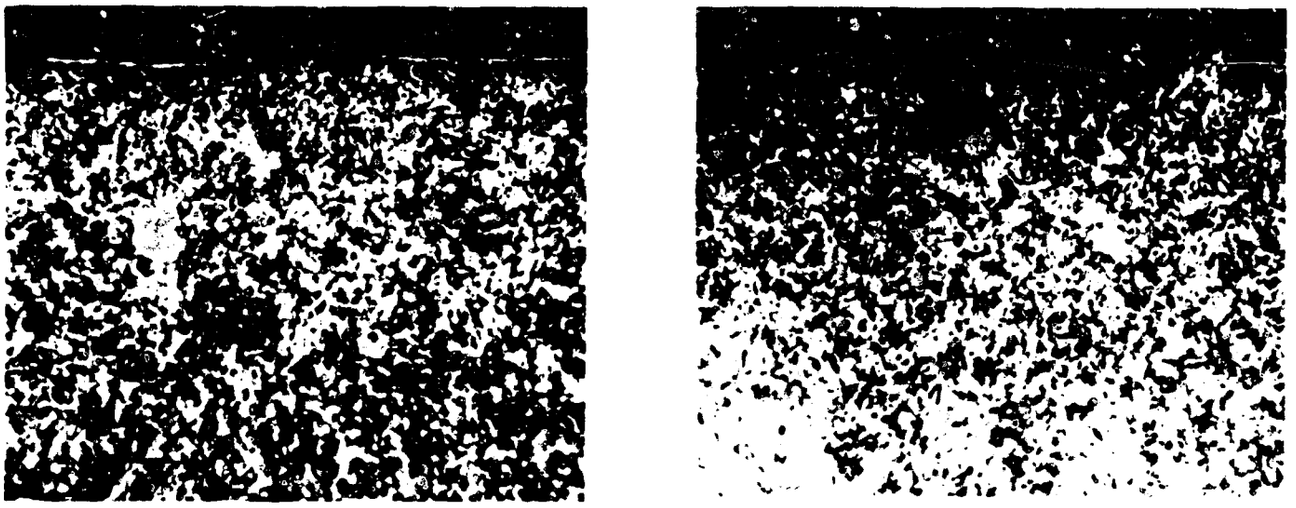

6a 6b

FIGURE 6. CARBIDE MILLED SURFACE ON 4340 STEEL, 50 R_c

(6a) milled with dull tool, .0001" white layer on surface; (6b) milled with sharp tool, no white layer on surface; Nital etch; 500X (reduced approximately 20 percent in printing).

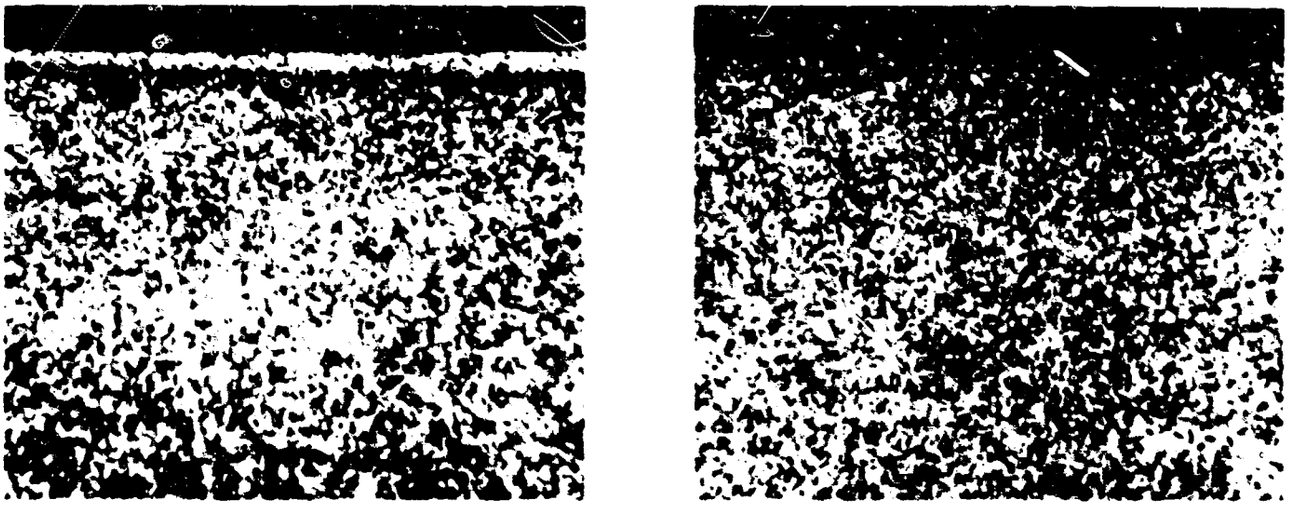

7a 7b

FIGURE 7. GROUND SURFACE ON 4340 STEEL, 53 R_c

(7a) abusively ground, .0002" white layer on surface; (7b) gently ground, no white layer on surface; Nital etch, 250X (reduced approximately 20 percent in printing).

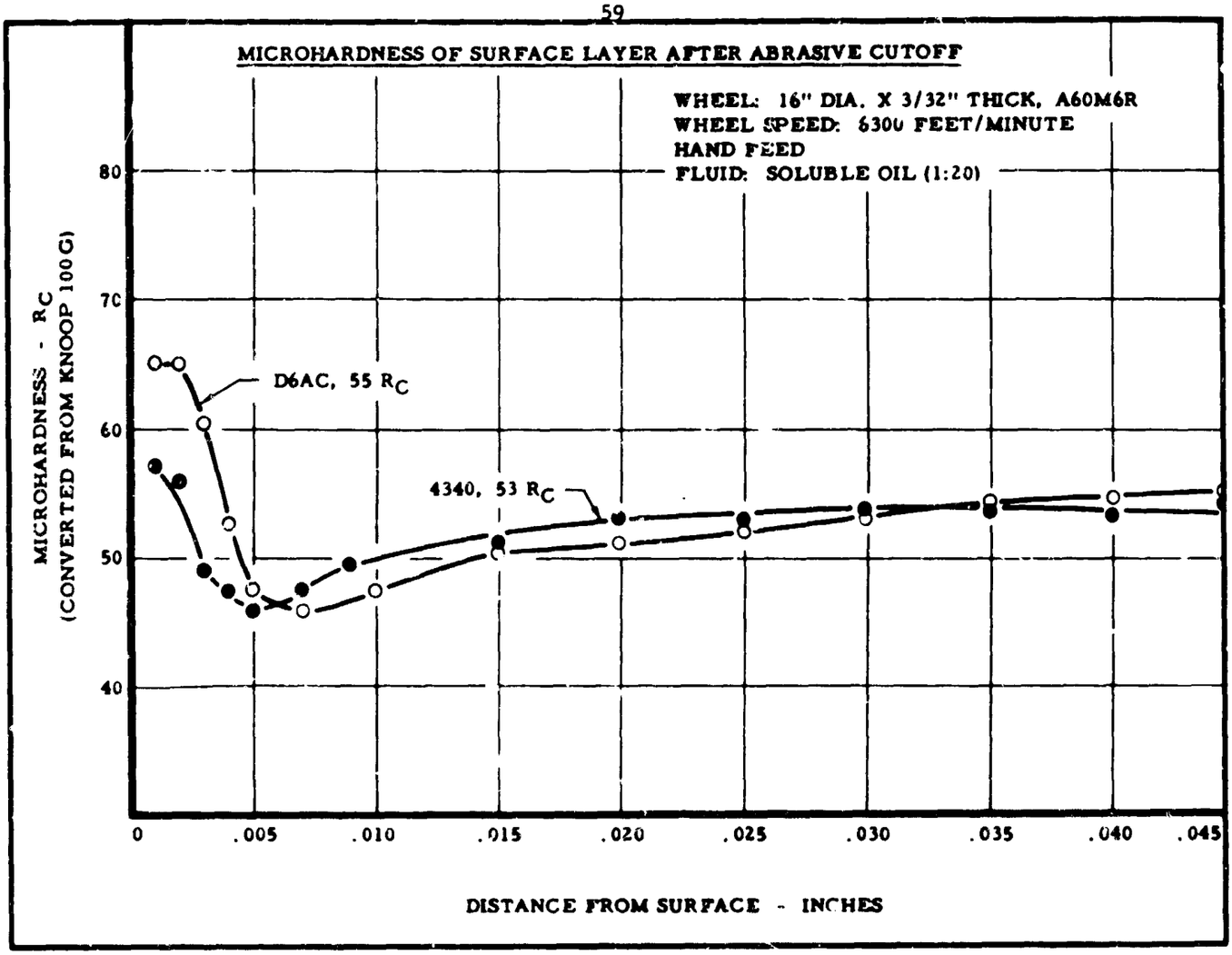

FIGURE 8. MICROHARDNESS OF SURFACE LAYER AFTER ABRASIVE CUTOF OF D6AC STEEL, 55 R_C, AND 4340 STEEL, 53 R_C

bearing steels and reported previously by Tarasov[5] and others.

The same untempered martensitic layer is obtained in electrical-discharge machining (EDM) of high-strength steels, Figures 9, 10 and 11. EDM drilling of holes under rough conditions, that is, at high feed rates with low frequency and high amperage, tends to produce a surface covered with spattered molten metal below which is a zone of untempered martensite, Figure 10. The spattered remelted metal layer is seen to be about .0016" thick and has a hardness of 4° R_C, Figures 10 and 11. Below the spattered metal is an untempered martensitic white layer about .0012" thick having a hardness of 58 R_C. The base metal of the 4340 steel was 54 R_C. EDM machining of the same material under finish conditions, namely, light feed, high frequency and low amperage, will produce a hole with very little spattered molten metal and only a very thin untempered martensitic layer, Figure 12.

It is extremely important to use machining and grinding conditions which do not develop untempered martensitic areas on the surface. These layers are inherently brittle and often crack almost immediately. Changes in these structures, such as further decomposition of some retained austenite present along with the martensite, often lead to delayed cracking when parts are in service. A number of components, such as landing gears, longerons, etc., have reportedly failed as a result of the white layer developed in drilling. Grinding cracks or checks are well recognized as the cause of failure of many parts. Some of these were either nonexistent at the time of inspection or too small for detection by average quality-control procedures. Therefore, it appears imperative to set up processing procedures which will virtually eliminate the possibility of parts going into the type of service where design safety factors are very low.

Residual Stresses in Machined and Ground Surfaces

Residual stresses are produced in the surface of a part after any and all machining and grinding operations. The residual stress layer is generally confined to a relatively shallow depth within a .005 to .010" layer. Recently considerable work

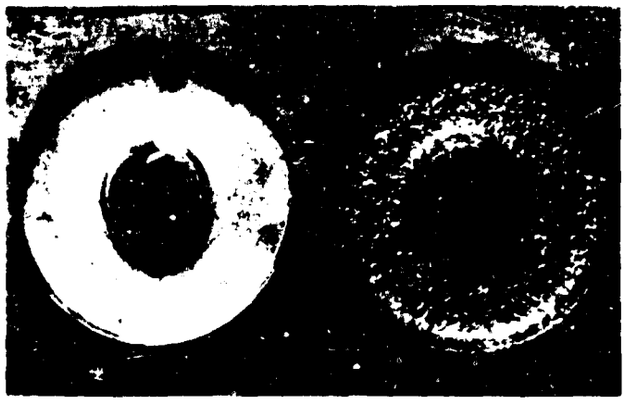

FIGURE 9. VIEW OF BOTTOM OF HOLES EDM DRILLED IN 4340 STEEL, 54 R_C, UNDER ROUGHING AND FINISHING CONDITIONS

Rough drilled hole (on right) drilled at 5 kc with 20 amps.; finish drilled hole (on left) drilled at 200 kc with 1 amp.; 5X (reduced approximately 44 percent in printing).

FIGURE 10. SURFACE OF HOLE ROUGH DRILLED BY EDM, SHOWING SPATTERED MOLTEN METAL AND UNTEMPERED MARTENSITIC LAYERS, 4340 STEEL, 54 R_C

See Figure 11 for further description; Nital etch; 500X (reduced approximately 44 percent in printing).

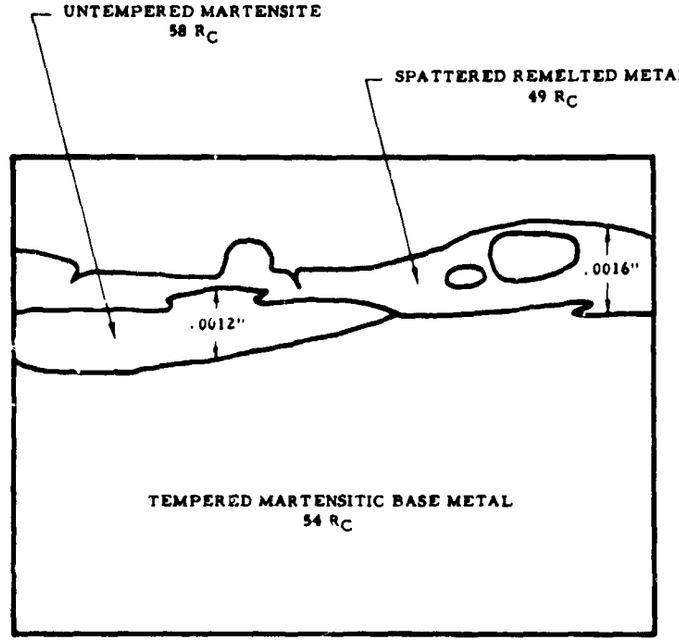

SURFACE OF HOLE ROUGH DRILLED BY EDM
4340 STEEL, 54 R_C

COPPER ELECTRODE
LOW VOLTAGE
5 K_C
20 AMPS

FIGURE 11. SKETCH OF SURFACE LAYERS OF PHOTOMICROGRAPH OF FIGURE 10

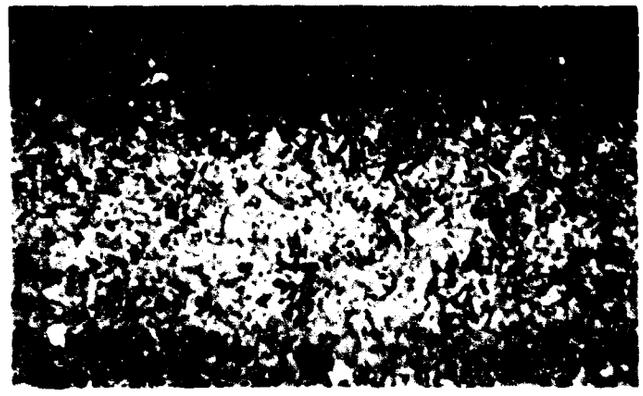

FIGURE 12. SURFACE OF HOLE FINISH DRILLED BY EDM, 4340 STEEL, 54 R_C

High voltage, 200 kc, 1 amp.; only a thin white layer (approx. .0001" thick) was present; Nital etch; 500X (reduced approximately 41 percent in printing).

has been done in measurement of these stresses using surface dissection methods and X-ray techniques.[6, 7] A typical residual stress pattern is shown in Figure 19. It should be noted that the stress at the actual surface is not indicative of the overall stress distribution in the surface layer. What is most important is the actual stress pattern within the surface layer, such as that shown by a single curve in Figure 19. The two most significant factors in the stress pattern or stress distribution curve are: first, the integrated area under the curve; and second, the maximum stress, be it tensile or compressive.

The integrated area under the curve in the surface layer is extremely important in that it gives an indication of the total stress in the surface layer that tends to produce distortion in the workpiece. Thus, a large tensile stress on a workpiece will tend to produce a concave curvature of the workpiece, whereas a large compressive stress will tend to produce a convex curvature of the workpiece when viewed from the machined-or-ground surface. The maximum value of the stress, be it tensile or compressive, appears to have some influence on the fatigue strength of the component.[8, 9]

The depth of the stress layer is also of importance since it determines the degree of penetration of the surface disturbance and also gives an indication of how much material would have to be removed from the surface by some secondary means to remove the surface effect.

The origins of residual stresses may be thermal, chemical or mechanical, but are often combined as follows:[10]

a. Plastic deformation from nonuniform thermal expansion or contraction produces residual stresses in the absence of phase deformation.

b. Volume changes from chemical reactions, precipitations, or phase transformations produce residual stresses.

c. Mechanical working which produces nonuniform plastic deformation may result in undesirable or favorable residual stress patterns.

Matson[11] states that "residual stresses are introduced or altered when a localized phase transformation occurs as it entails a specific volume change or when a localized plastic flow occurs. Localized plastic flow occurs when temperature differences exist producing a three-dimensional internal force system (because of thermal expansion and/or contraction) in such a manner that locally some forces exceed the limit of elastic deformation. Localized plastic flow can also occur if a system of externally applied forces is such that localized force exceeds the limit of elastic deformation.

"Phase transformations occur locally when temperature, stress conditions, and time conditions are satisfied. The transformation from austenite to martensite is of particular interest in steel because of the specific volume increase associated with this transformation.

"Machining and grinding operations are important stress introducers. It is conceivable that temperature differences are high enough to cause plastic flow, that phase transformation might occur, and that mechanical forces occur, all simultaneously producing a triaxial residual stress state. Processes involving superficial cold work at a surface, such as shot peening, tumbling, etc., are generally not regarded as having high temperatures existing or phase transformation occurring, although these cannot be ruled out entirely. In this instance, the dominating factor is the localized high stress system applied by external means."

It is of interest to note that the surface cold-working processes represented by shot peening and surface rolling are processes for which fairly accurate predictions can be made of residual stresses. Heat treating, machining and grinding stresses are not too predictable. For example, in shot peening, the residual stress is compressive with the maximum residual compressive stress occurring at some depth below the surface and at a lower value at or near the surface, Figure 13.

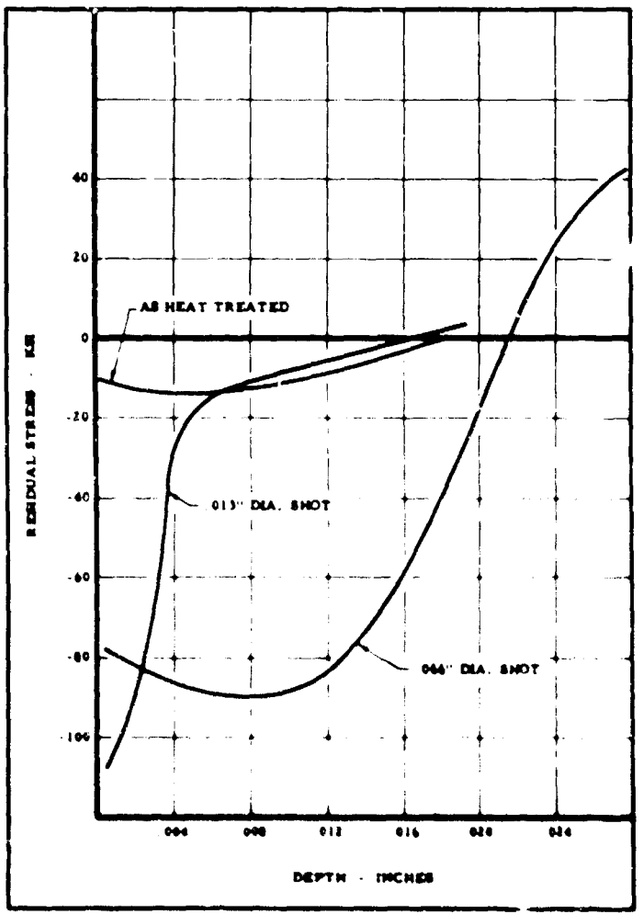

FIGURE 13. RESIDUAL STRESS INTRODUCED BY SHOT PEENING 5147 STEEL, 48 R_C, BY VARIOUS SHOT-PEENING TREATMENTS[11]

The maximum residual compressive stress is reasonably constant and independent of shot peening treatment apart from coverage. As the hardness of material increases, the peak residual

compressive stress introduced by shot peening also increases, Figure 14.

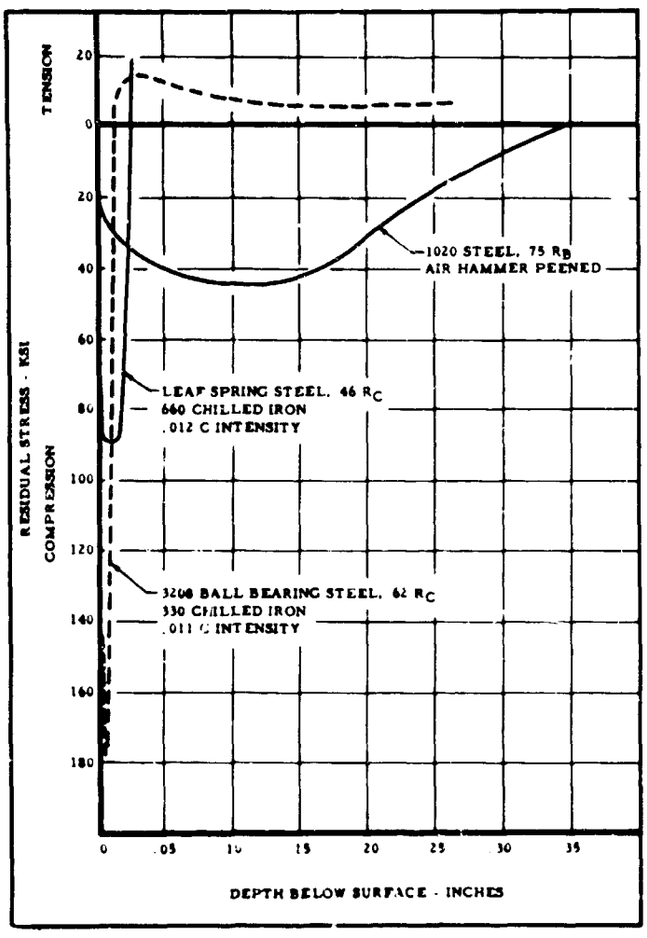

FIGURE 14. EFFECT OF HARDNESS AND INTENSITY OF COLD WORKING ON THE MAGNITUDE AND DEPTH OF COMPRESSIVELY STRESSED LAYER[11]

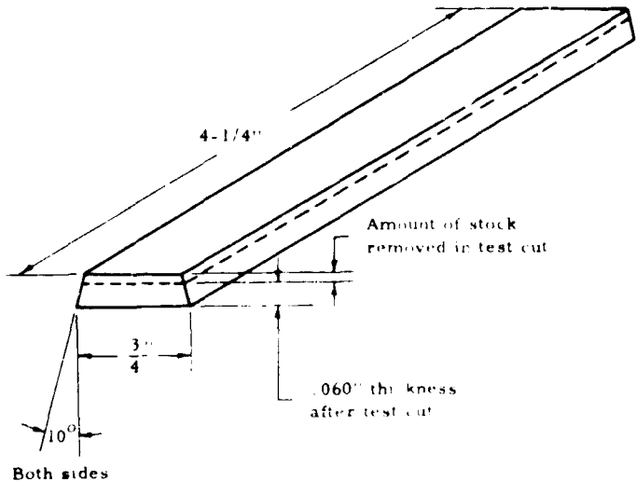

FIGURE 15. TEST SPECIMEN USED FOR DISTORTION AND RESIDUAL STRESS STUDIES

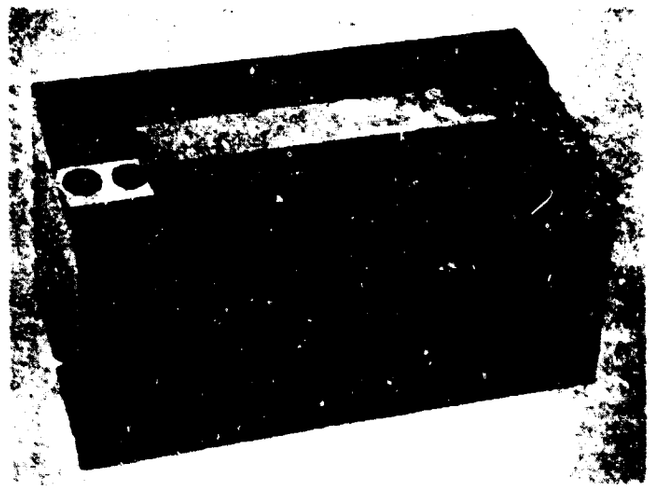

FIGURE 16. FIXTURE USED FOR HOLDING SPECIMEN IN MILLING AND GRINDING

Residual Stresses and Distortion Resulting From Machining and Grinding High-Strength Steels

The residual stresses induced in grinding and milling of high-strength steels have been investigated recently.[3, 4, 15] In these studies, a specimen was originally prepared 3/4" wide by 4-1/4" long. The thickness was such that all specimens were .060" thick after testing, Figure 15. A special test fixture was used to hold the specimen for the grinding and milling test, Figure 16. The 10° taper ground on the sides of each specimen was used to clamp the specimen in the fixture. The grinding and milling tests were performed on one side of the specimen only, leaving the bottom or wider surface for the gaging surface. The flatness or deflection of the test specimen was measured using the fixture shown in Figure 17. The deflection was read on the .0001" dial indicator.

The procedure used to determine the residual stresses was one of progressively etching the ground or machined surface and noticing the change in deflection of the test strip. The change in deflection versus depth of stock removed data was then used to calculate the residual stress at any depth below the test surface using the procedures and equation developed by Frisch and Thomsen[12] and Stablein.[13] This method determines the uniaxial stress in the longitudinal direction of the test specimen. The biaxial surface stress distribution in both the longitudinal and transverse directions can also be measured by curvature measurement methods.[14]

The residual stress patterns produced in surface grinding of 4340 steel, quenched and tempered to 52 R_C, are shown in Figures 18, 19 and 20. Figure 18 shows the effect of grinding wheel

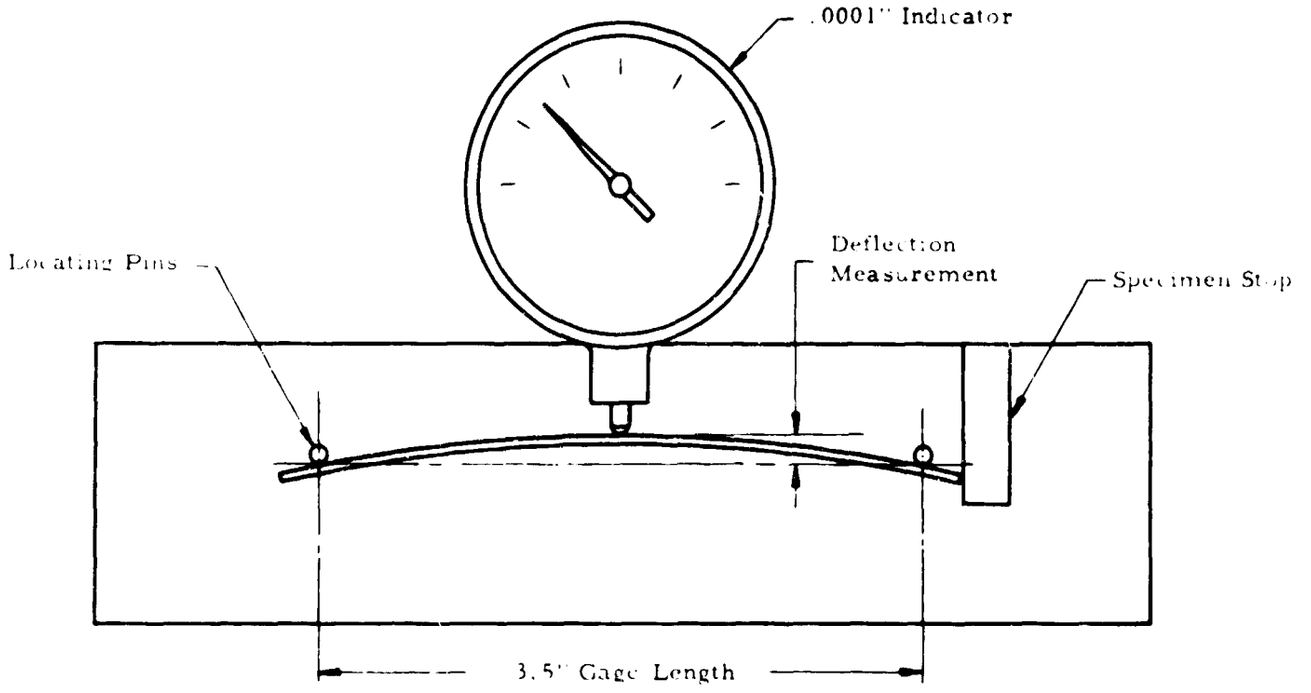

The above fixture is used to measure deflection of the test specimen in both the distortion and the residual stress analyses

FIGURE 17. FIXTURE FOR DEFLECTION MEASUREMENT

speed on residual stress. It is observed that the conventional wheel speed of 6000 feet/minute tends to produce very high tensile stresses, compared to the low speeds of 4000 or 2000 feet/minute. Likewise, the 6000 feet/minute tends to produce a stress layer about .004" deep, whereas the stress layer with the low speeds tends to be much shallower, .001 to .002" deep. Figure 19 indicates the effect of down feed per pass, which is equivalent to depth of cut in grinding. The heavy depth per pass, .002" down feed, tends to produce a high tensile stress and a greater depth of stress layer, whereas a very gentle "low stress" down feed tends to confine the stress layer to a shallow depth approximately .001". In the "low stress" down feed the last .010" of metal is removed as follows: .008" is removed at .0005 inch/pass, and the last .002" is removed at .0002 inch/pass. By selection of "low stress grinding techniques," it is possible to produce shallow compressive stresses in the ground surface, Figure 20. Here a wheel speed of 2000 feet/minute, a soft grinding wheel such as "H" hardness, and the gentle "low stress" down feed produced a compressive stress confined to a .001" surface layer.

In general, it has been found that the following factors are the major ones determining the nature and magnitude of the residual stress produced in grinding high-strength steels:

a. Wheel speed – low wheel speeds tend to produce low residual stresses.

b. Grinding wheel – sharp, soft, friable wheels tend to produce low residual stresses.

c. Depth per pass – shallow depths per pass tend to produce low stresses.

d. Grinding fluid – high chemical reactive grinding fluids, such as sulphurized oil, tend to reduce surface stresses.

Although the exact residual stress distribution cannot be entirely predicted in grinding, it is possible to select conditions which will tend to produce either high tensile stresses with a deep penetration or compressive stresses with a shallow penetration, Figure 29.

The grinding studies on SAE 4340 steel, quenched and tempered to 52 R_C, indicate that distortion is very closely related to the residual stress imposed on a specimen. The relative distortion under various grinding conditions could be measured on the test specimen previously described in Figure 15. The distortion was measured by noting the change in deflection within the 3.5" gage length as measured in the distortion measuring fixture, Figure 17. Typical relationships of distortion to grinding variables are shown

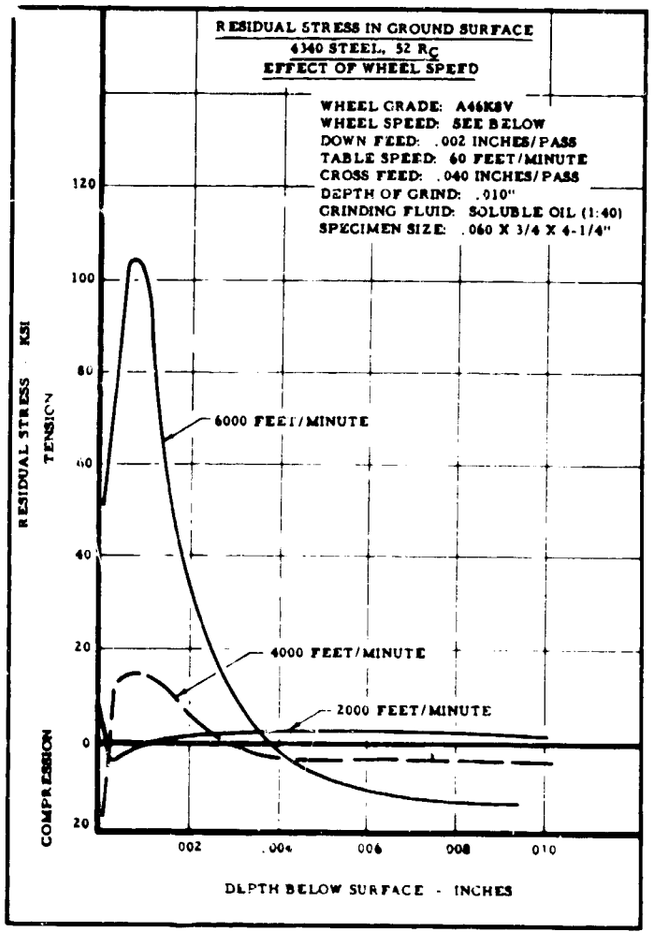

FIGURE 18. EFFECT OF WHEEL SPEED ON RESIDUAL STRESS IN SURFACE GRINDING 4340 STEEL, 52 R_C

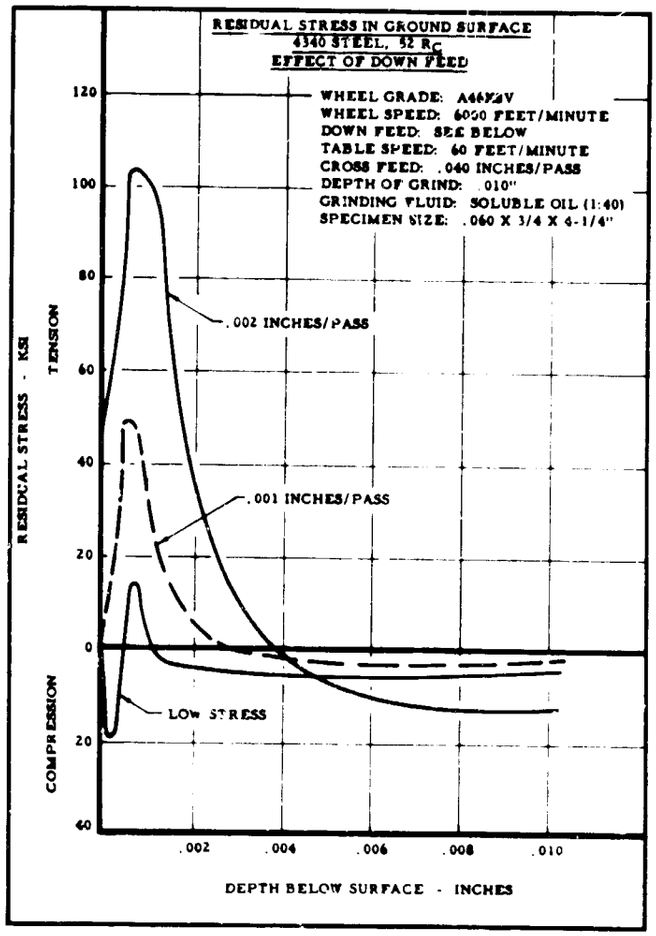

FIGURE 19. EFFECT OF DOWN FEED ON RESIDUAL STRESS IN SURFACE GRINDING 4340 STEEL, 52 R_C

in Figures 21, 22, and 23. In Figure 21, it is observed that distortion increases as the wheel speed increased and as the wheel hardness increases. (Note the "H" hardness wheel is the softest and the "N" wheel is the hardest abrasive.) The distortion is also greater for the heavier down feeds, Figure 22, with the "low stress" down feed producing the minimum distortion. Also it should be noted that the distortion is minimized by using very low speeds combined with low down feeds. The effect of grinding fluid on distortion is illustrated in Figure 23. Here it can be seen that the chemically active highly sulphurized oil reduces distortion significantly.

Comparison of the residual stress patterns, Figures 18, 19, and 20, with the distortion patterns, Figures 21, 22, and 23, verify that the low distortion is associated with the low reridual stress. Furthermore, it has been found that the direction of curvature of the specimen is determined by the integrated area under the residual stress curve, be it tensile or compressive.

The residual stress patterns in carbide milling of 4340 steel, 52 R_C, are shown in Figure 24. In carbide face milling, the most significant factor that induced residual stress is the sharpness of the tool. Thus, it can be seen that the ultrasharp tool with zero wearland produced the minimum stress, whereas the dullest tool with .016" wearland produced the maximum residual stress. The residual stress in the surface layer is predominantly compressive, although the stress at the surface seems to be practically zero with a sharp tool and 50,000 to 100,000 psi tensile for the dull tools.

The distortion in milling is governed by the induced residual stress. The distortion is seen to be practically independent of the cutter speed, Figure 25, but is primarily dependent on the tool wearland or tool sharpness. The distortion is influenced somewhat by the depth of cut, Figure 26. Thus, a light finishing cut .010" deep is seen to produce less distortion than the heavy cuts.

The residual stress produced in surface grinding of D6AC steel, quenched and tempered to 56 R_C, shows the same general patterns as with the 4340 steel. The effect of wheel hardness on the residual stress in surface grinding D6AC steel, 56 R_C, is shown in Figure 27. Here at a wheel speed of 6000 feet/minute and with a .002 inch/pass down feed, the residual stresses are seen to be predominantly tensile with the softest wheel ("H" hardness) producing the

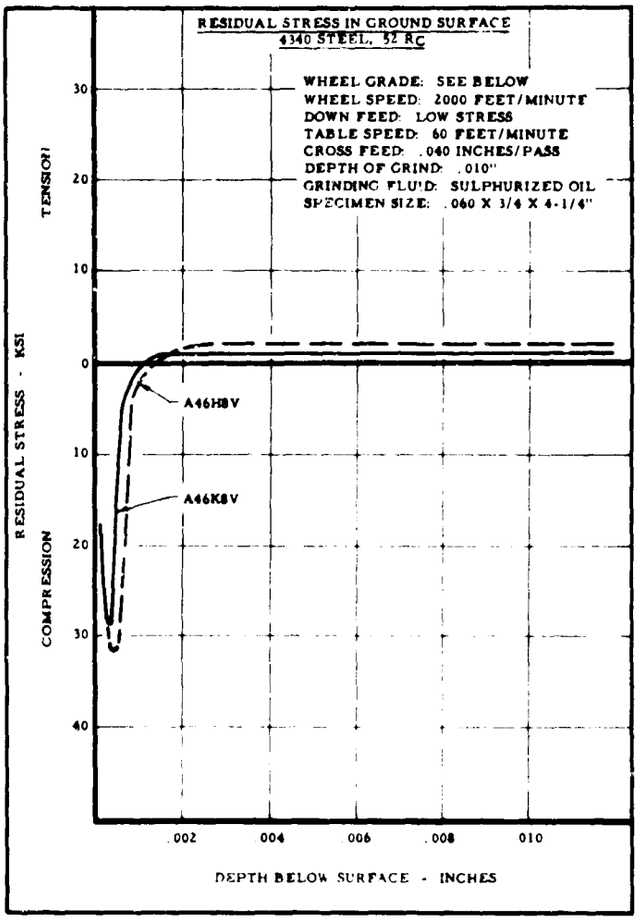

FIGURE 20. CONDITIONS WHICH PRODUCE A LOW COMPRESSIVE RESIDUAL STRESS IN SURFACE GRINDING 4340 STEEL, 52 R_c

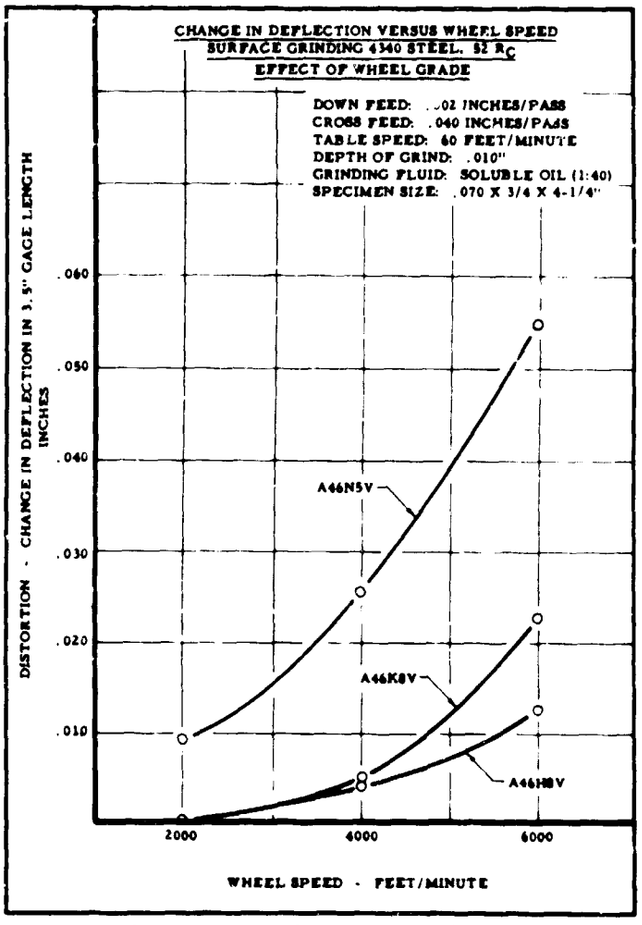

FIGURE 21. EFFECT OF WHEEL GRADE AND WHEEL SPEED ON DISTORTION IN SURFACE GRINDING 4340 STEEL, 52 R_c

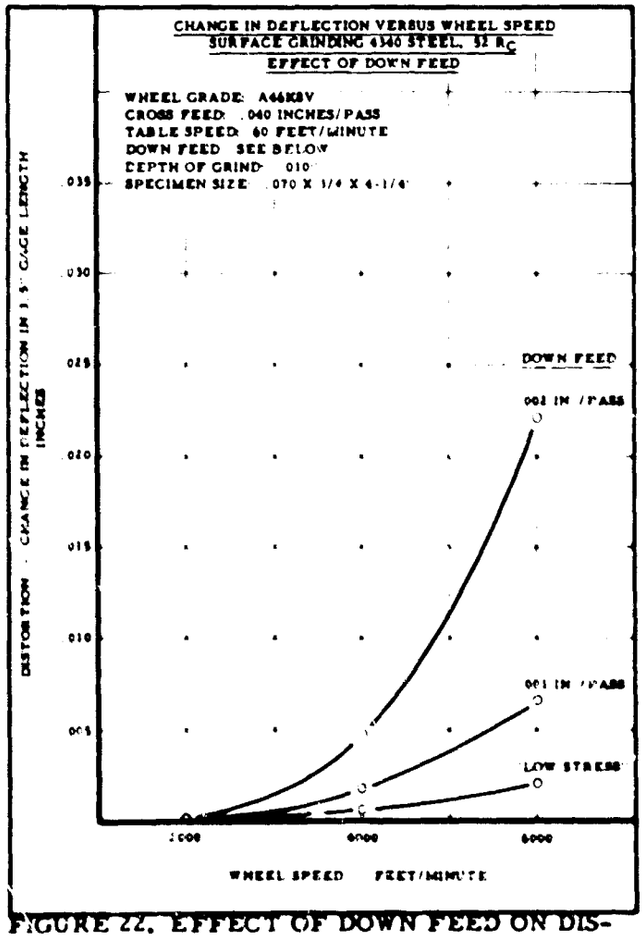

FIGURE 22. EFFECT OF DOWN FEED ON DISTORTION IN SURFACE GRINDING 4340 STEEL, 52 R_c

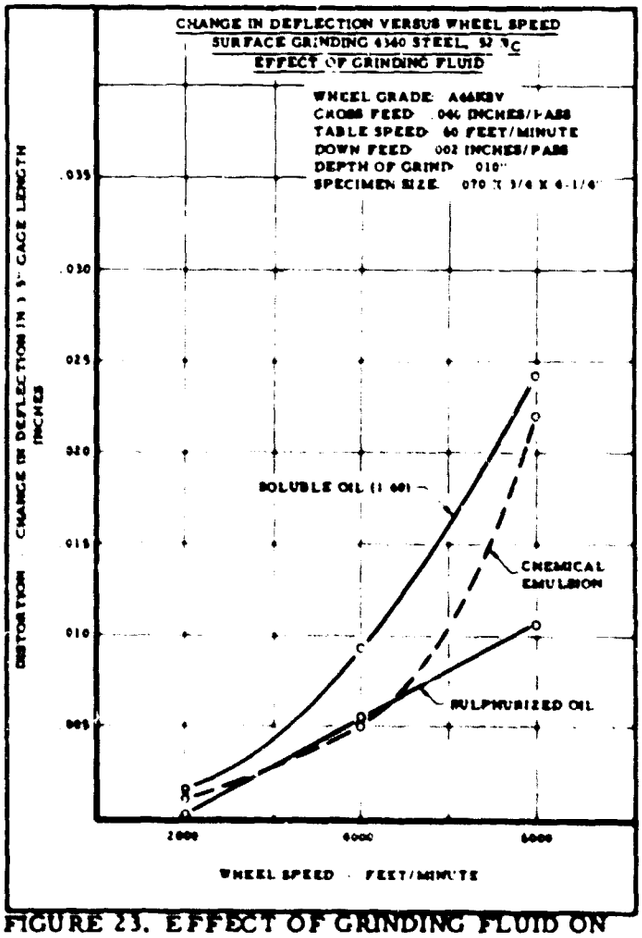

FIGURE 23. EFFECT OF GRINDING FLUID ON DISTORTION IN SURFACE GRINDING 4340 STEEL, 52 R_c

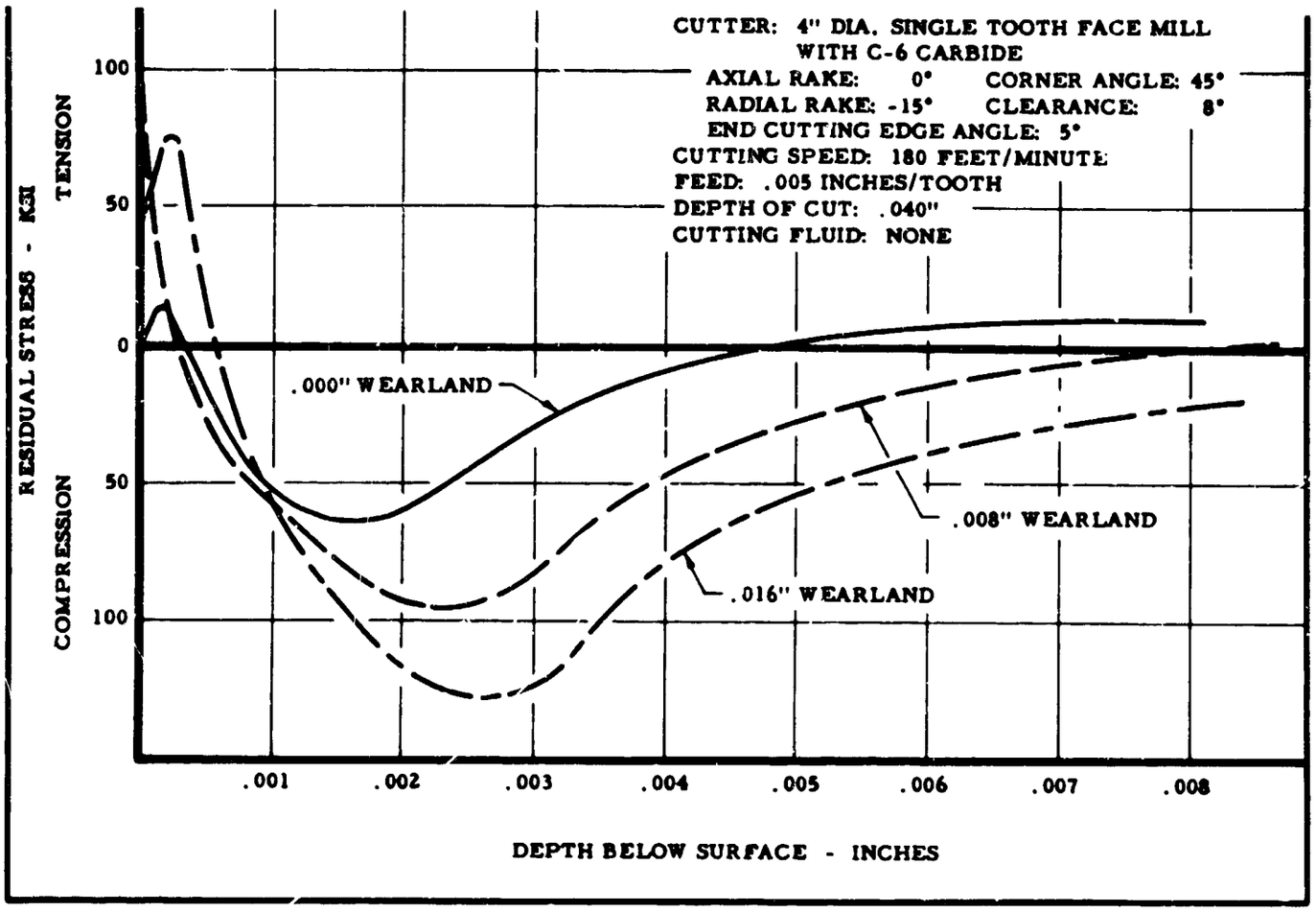

FIGURE 24. RESIDUAL STRESS IN CARBIDE FACE MILLING 4340 STEEL, 52 R_C

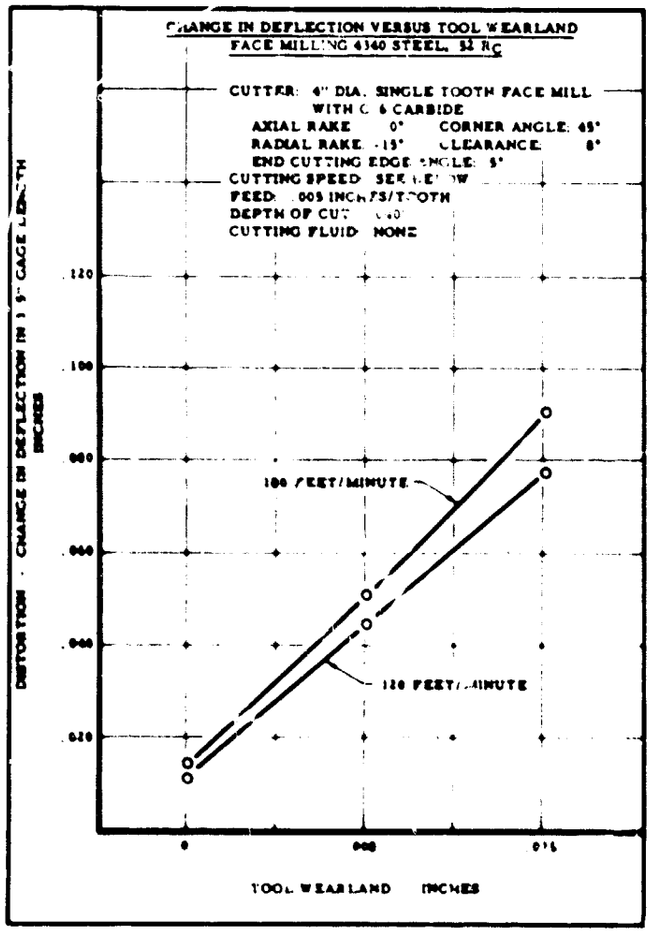

FIGURE 25. EFFECT OF TOOL SHARPNESS ON DISTORTION IN CARBIDE FACE MILLING 4340 STEEL, 52 R_C

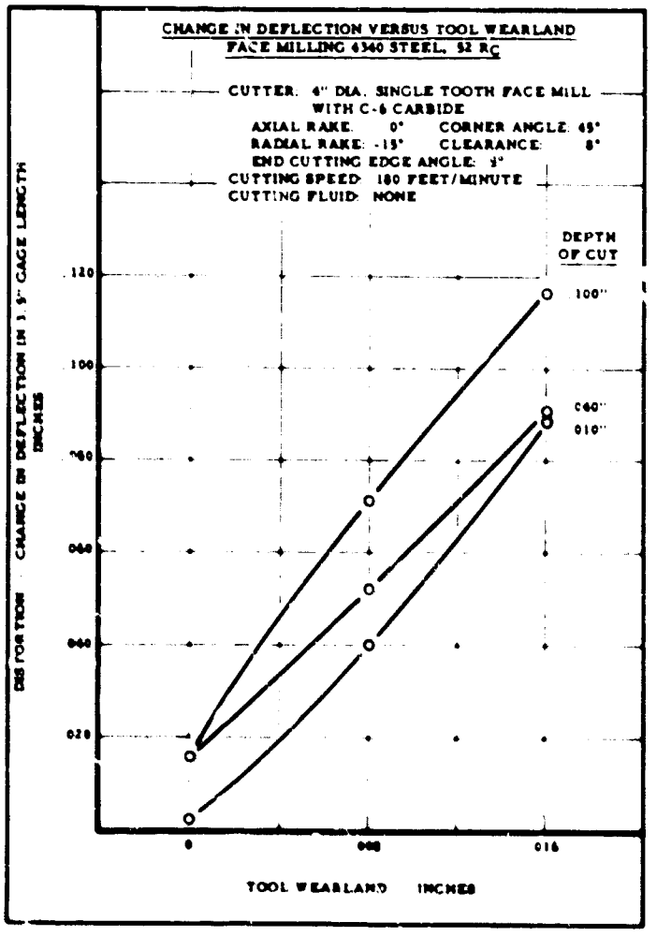

FIGURE 26. EFFECT OF TOOL SHARPNESS AND DEPTH OF CUT ON DISTORTION IN CARBIDE FACE MILLING 4340 STEEL, 52 R_C

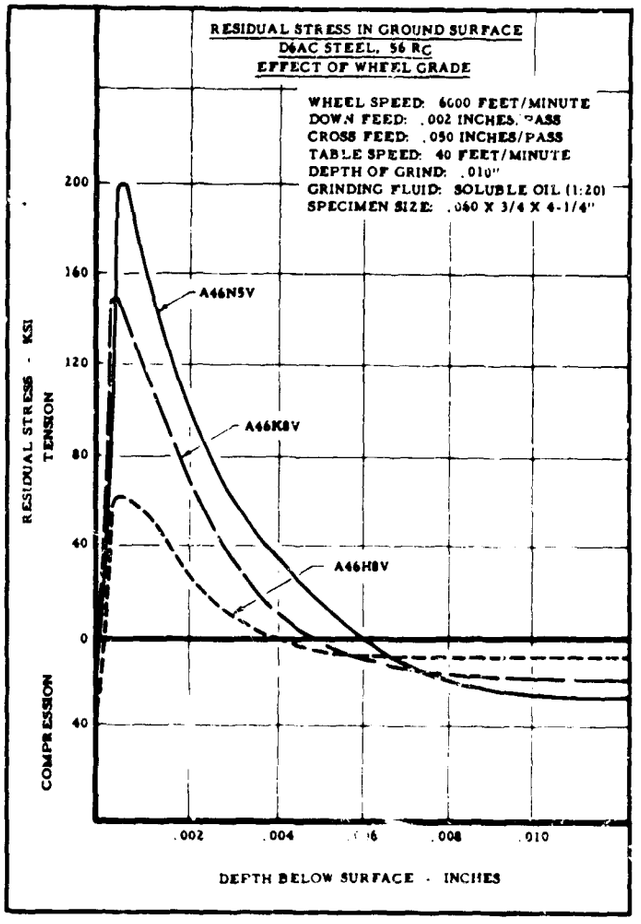

FIGURE 27. EFFECT OF WHEEL GRADE ON RESIDUAL STRESS IN SURFACE GRINDING D6AC STEEL, 56 R_c

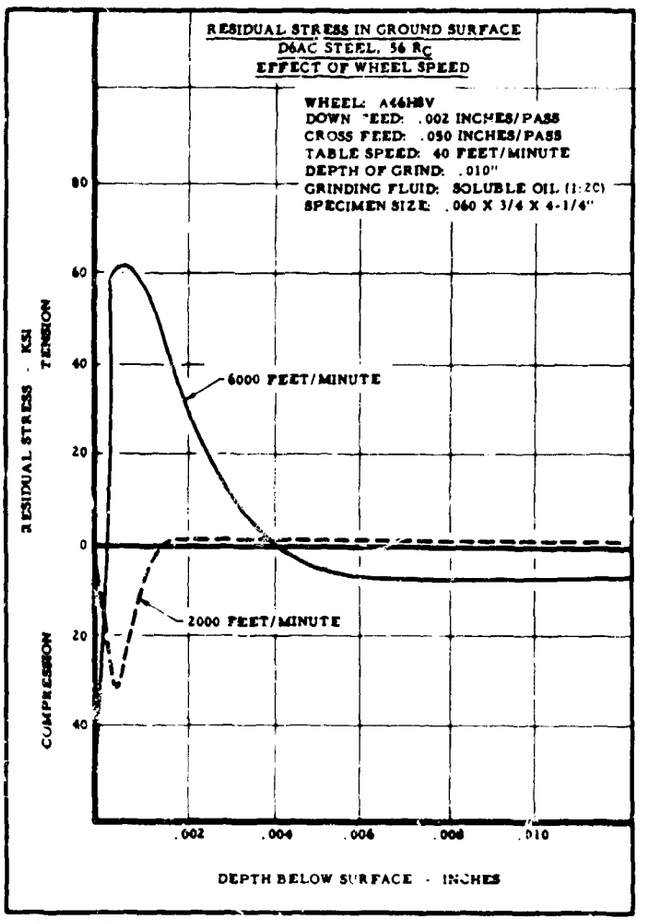

FIGURE 28. EFFECT OF WHEEL SPEED ON RESIDUAL STRESS IN SURFACE GRINDING D6AC STEEL, 56 R_c

minimum stress and the hardest wheel ("N" hardness) producing the maximum stress. Notice that with the "N" hardness wheel a peak tensile stress of 200,000 psi was produced approximately .0005" below the surface. It is also interesting to note that the residual stress at the surface with the "K" and "N" wheels was practically zero, while that of the "H" wheel was 40,000 psi in compression. The effect of grinding wheel speed on the residual stress pattern for the soft ("H") wheel, .002 inches/pass down feed, is shown in Figure 28. The high wheel speed of 6000 feet/minute produced a predominant tensile stress to a depth of .004", while the low speed of 2000 feet/minute produced compressive stress to a depth of about .001". The down feed in grinding is again seen to have a tremendous effect on the residual stress pattern, Figure 29. The gentle "low stress" down feed technique produced a negligible amount of residual stress compared to the .001 or .002 inches/pass down feed.

The distortion produced in surface grinding D6AC steel, quenched and tempered to 56 R_c, is governed by the residual stress in like manner to that of the 4340 steel. A soft wheel, grade "H", produced far less distortion than the harder wheels, Figure 30. The combination of low stress down feed with low wheel speed is seen to produce the minimum distortion, Figure 31. The significant effect of highly sulphurized oil over soluble

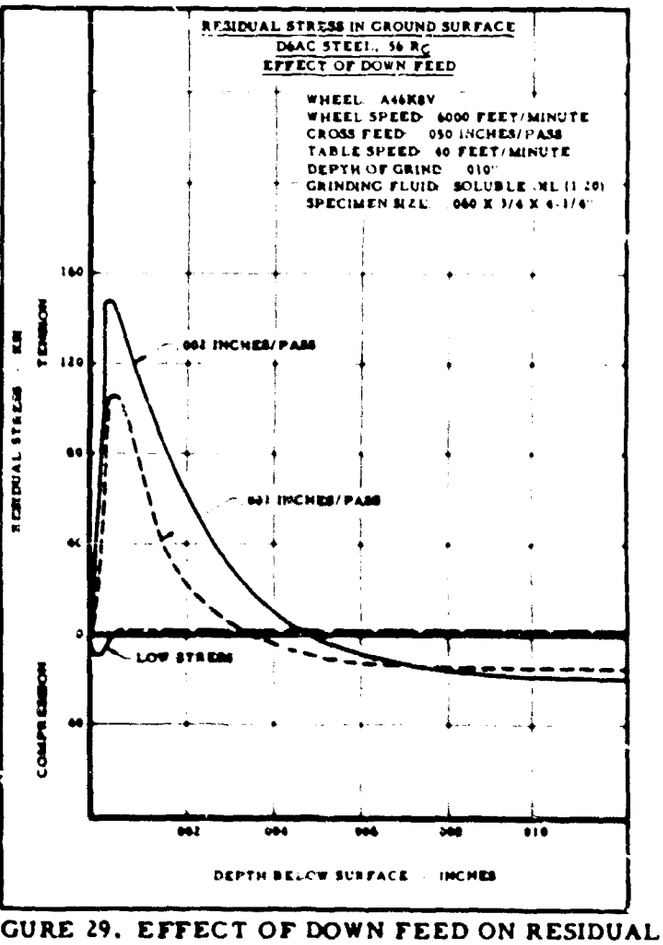

FIGURE 29. EFFECT OF DOWN FEED ON RESIDUAL STRESS IN SURFACE GRINDING D6AC STEEL, 56 R_c

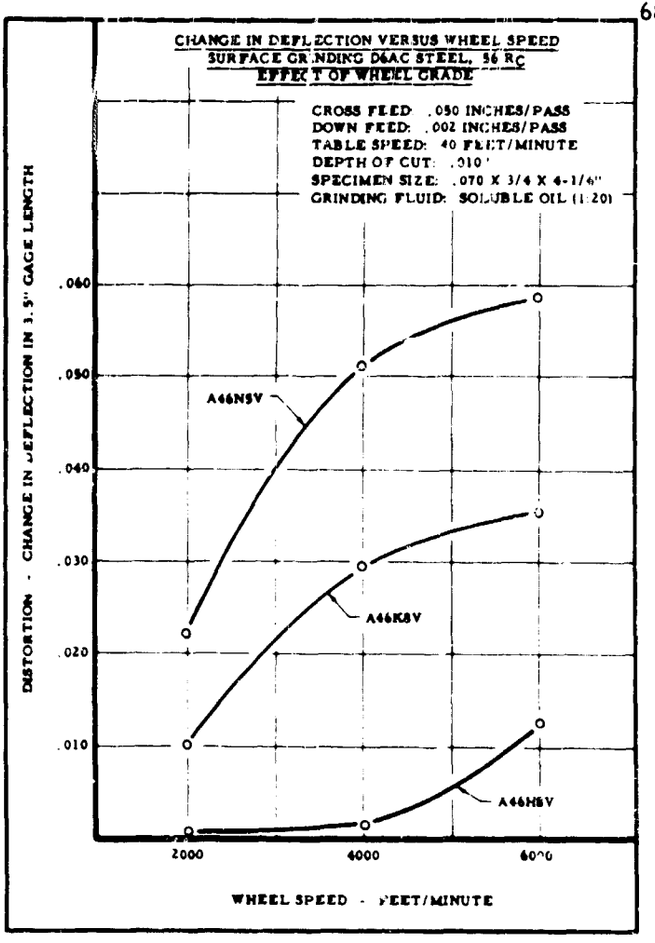

FIGURE 30. EFFECT OF WHEEL GRADE ON DISTORTION IN SURFACE GRINDING D6AC STEEL, 56 R_C

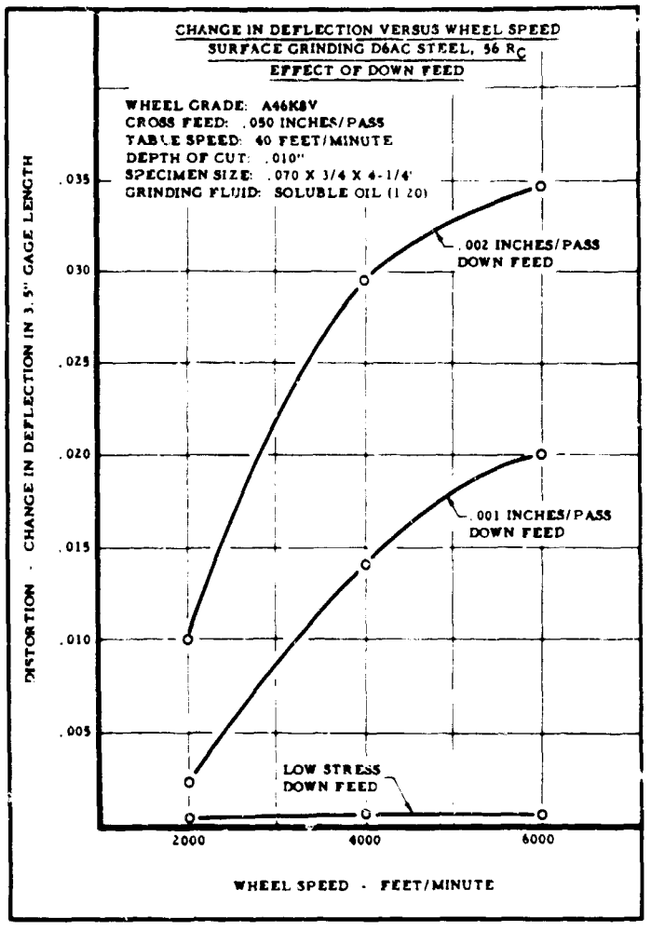

FIGURE 31. EFFECT OF DOWN FEED AND WHEEL SPEED ON DISTORTION IN SURFACE GRINDING D6AC STEEL, 56 R_C

oil on distortion is illustrated in Figure 32. Here it can be seen that at the conventional high wheel speed of 6000 feet/minute there was no difference in distortion in using the two fluids. However, at 2000 and 4000 feet/minute, there was a drastic reduction in distortion by the use of highly sulphurized oil over soluble oil.

The residual stress and distortion produced by carbide milling of D6AC steel, 56 R_C, is shown in Figures 33 and 34. The sharpness of the milling cutter is again seen to be the predominant factor in controlling the residual stress and distortion.

EFFECT OF MACHINING AND GRINDING ON THE MECHANICAL PROPERTIES OF HIGH-STRENGTH STEELS

It has been seen that residual stresses produced in milling and grinding of high strength steels can reach extremely high values. For example, stresses of 100,000 psi are frequently observed in both grinding and milling, and a residual tensile stress of 200,000 psi was observed in abusively ground D6AC steel, 56 R_C, Figure 27. It should also be noted that the residual stress layer tends to be quite shallow on the order of the magnitude of .002 to .010". It would seem logical to assume that such high residual stresses should affect certain properties of steels, such as fatigue strength or stress corrosion strength.

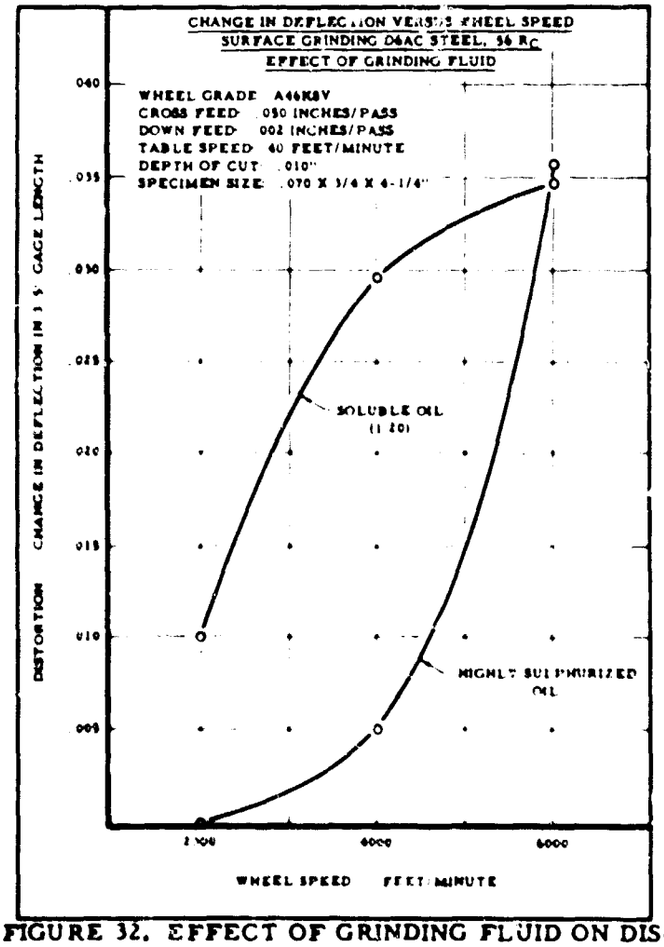

FIGURE 32. EFFECT OF GRINDING FLUID ON DISTORTION IN SURFACE GRINDING D6AC STEEL, 56 R_C

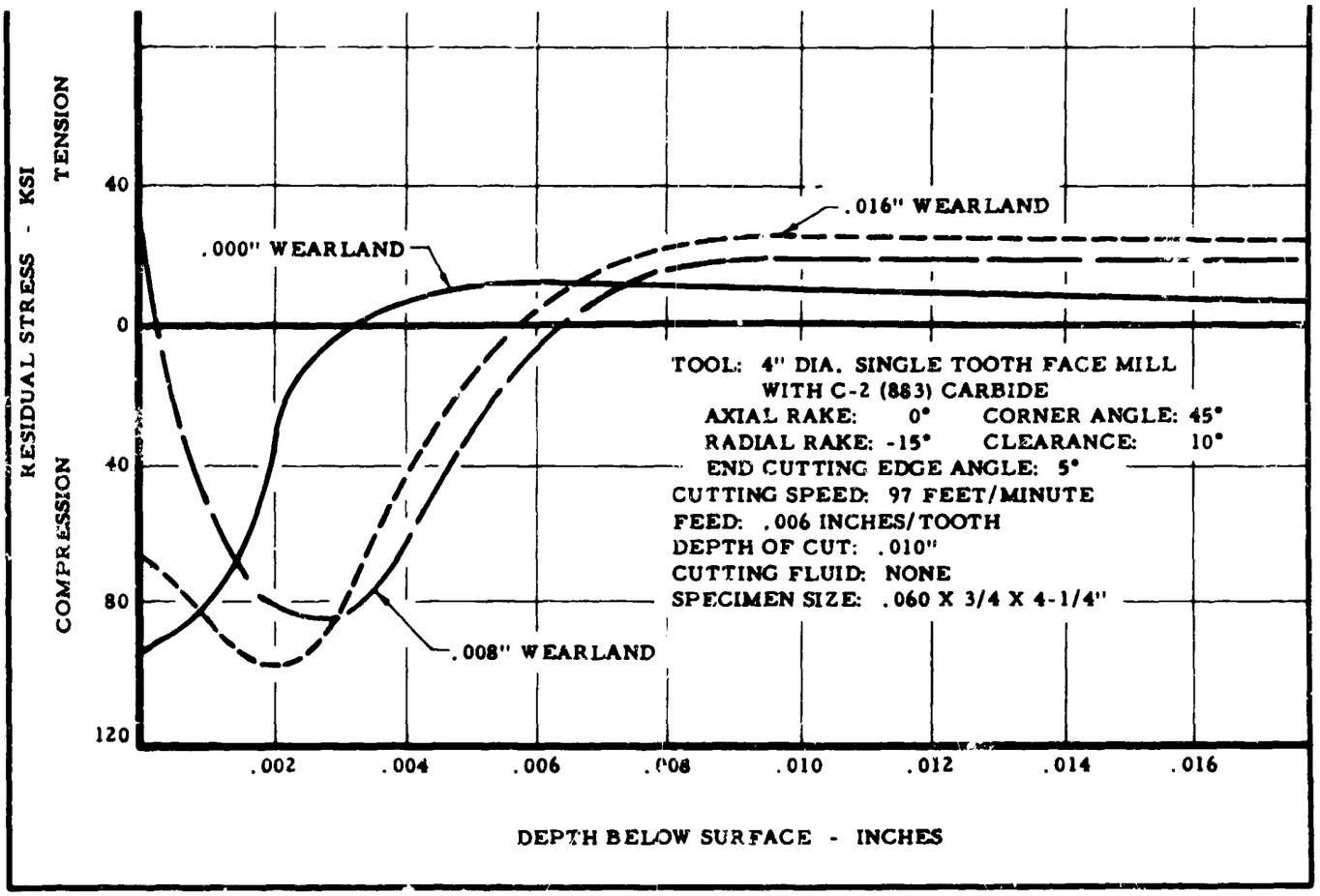

FIGURE 33. RESIDUAL STRESS IN CARBIDE FACE MILLING D6AC STEEL, 56 R_c

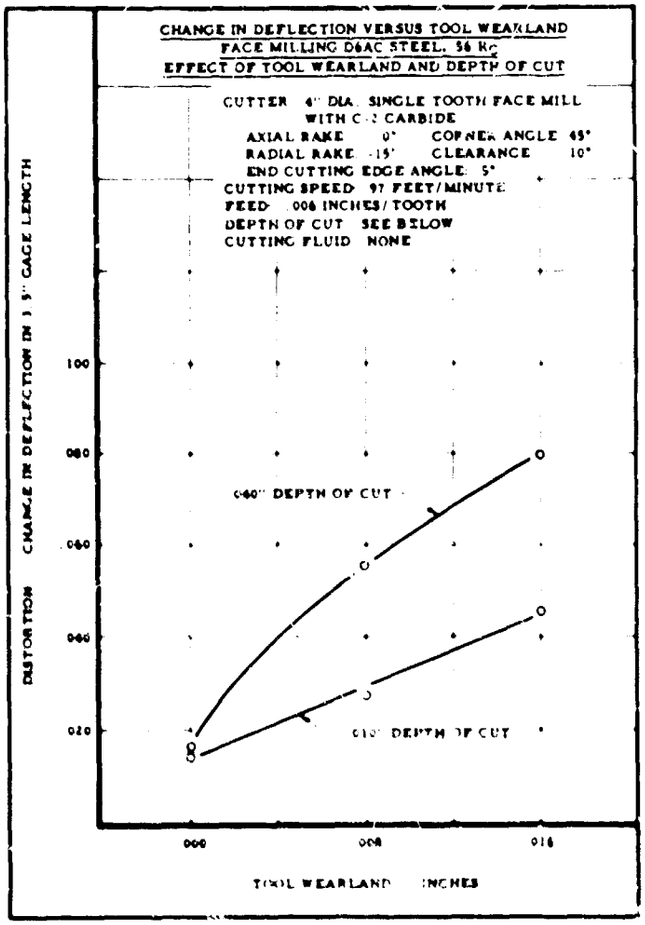

FIGURE 34. EFFECT OF TOOL SHARPNESS AND DEPTH OF CUT ON DISTORTION IN CARBIDE FACE MILLING D6AC STEEL, 56 R_c

A series of studies were made on the effect of residual stress in grinding 52100 steel, quenched and tempered to 59 R_c by Tarasov, Hyler and Letner.(8) Their results are summarized by Gormly(16) as follows:

1. "Specimens which had been ground under conventional or gentle grinding practice, that is, with "H" or "I" grade wheels with down feed rates of .001 inch/pass or less using either soluble straight grinding oil as the grinding fluid, exhibited fatigue strengths comparable to specimens which were stress free even though residual stresses range from 107,000 psi in compression to 49,000 psi in tension.

2. "Those specimens which had been ground severely, that is, with a "M" grade wheel at a down feed rate of .002 inch/pass, using a water soluble fluid, exhibited fatigue strengths about 13 percent below that of the first group.

3. "Three sets of specimens, all of which were ground with an "I" grade wheel, at a down feed rate of .001 inch/pass using sulfochlorinated oil, exhibited fatigue strengths up to 38 percent higher than the value for stress free specimens. Since the residual stress distributions were not significantly different from some of those in the first group above,

it was concluded that the increase in fatigue strength was due to a greater benefit from cold work."

Vitovec and Binder[17] indicate that a rough turned surface resulted in a 20 percent lower fatigue strength compared with mechanically polished specimens while ground specimens were 10 percent lower. In all cases, electrolytic polishing reduces the fatigue strength of mechanically polished specimens. There are a number of effects caused by the preparation process which occur simultaneously, and their effects are superimposed. The relative magnitude of the various effects may produce either a gross increase or decrease in fatigue strength. These effects are plastic deformation, strain hardening, tool marks, internal stress, heating of the material and metallurgical changes and reorientation of the grains at the surface. Mechanical polishing in a direction parallel to maximum principal stress results in the highest fatigue strength apparently due to the lack of notch effects and strain hardening.
Table 1[17, 18, 19] shows the effect of material condition on the fatigue strength of several high-strength steels.

TABLE 1. EFFECT OF MACHINING AND POLISHING ON FATIGUE STRENGTH OF STEEL

Steel	Tensile Strength, psi	Fatigue Strength, percent: Highly Polished	Polished	Ground	Rough Surface	Reference
Ni-Cr (.32C, 3-6Ni, .75Cr)	264,000	100 (117,500 psi, 0000 emery cloth)	96 (00 emery cloth)		19 (as forged)	(18)
D. T. D. 331 (.3C, 4.0Ni, 1.0Cr, .6Mo	179,000 to 200,000	100 (about 35,000 psi, super-finished)		99		(19)
Ni-Cr-Mo (.41C, 2.5Ni .6Cr, .6Mo	308,600	100% (145,000 psi 0000 emery cloth)	76 (00 emery cloth)		13 (as forged)	(17)

Since the surface effects in high-strength steels caused by metal removal processes have not been thoroughly evaluated with respect to mechanical properties, work by investigators, such as Forsyth and Carreker; Frankel, Bennett and Pennington; and Borik, Chapman and Jominy, are helpful. Their studies are important because they relate to bulk changes which can also occur in the surface as a result of machining and grinding.

Forsyth and Carreker[20] have studied the effect of microstructure on fatigue strength of SAE 1095 steel, 53 R_c. They found that the resistance to fatigue failure (rotating cross fatigue tests at room temperature) depends markingly on the heat treatment used to obtain that hardness. Conventional water quenching and tempering gave lowest fatigue limits of 124,000 psi. Austempered specimens produced a higher value of 130,000 psi, and the highest of 160,000 psi was produced with martempering. They reported that microcracks existed in these steels after quenching in water or oil. These microcracks are caused by very high thermal and transformation stresses in that area during quenching and formation of martensite. Austempering reduces both thermal and transformation stresses which lead to these microcracks. In martempering, it is possible to produce a martensitic structure without producing the high stresses accompanying the transformation. The specimen temperature is essentially uniform throughout so that transformation can occur randomly throughout the material, instead of preferentially at the periphery. Thus, the volume changes accompanying transformation are uniformly distributed.

Frankel, Bennett and Pennington[21] report that the fatigue strength on R. R. Moore testing of 4340, 52100 and two tool steels at hardness range of 46 R_c and higher was lowered by increasing amounts of retained austenite up to about 10 percent. This deleterious effect was apparently due to transformation of some of the austenite which was observed to take place during fatigue stressing.

Borik, Chapman and Jominy[22] show that a small percentage of nonmartensitic structures has a deleterious effect on fatigue strength of 4340 steel and several other medium carbon steels.

In an investigation of fatigue properties of thin-gage PH15-7Mo, .163" thick, at 217,000 UTS and 210,000 yield point, it was found that intergranular attack from pickling results in a slight loss of fatigue strength.[13] The static tensile strength of the PH15-7Mo sheet was noticeably affected by chem-milling striations and intergranular attack. In addition, ductility was reduced by chem-milling. Apparently selective etching by the chem-milling solution causing continuous transverse striations has a more serious effect on the static properties of the PH15-7Mo and on ductility than does shallow intergranular attack, see Table 2.

TABLE 2. MECHANICAL PROPERTIES OF PH15-7Mo .061" THICK[13]

Condition of Sheet	Ultimate Tensile Strength, psi	Yield Point, psi	Elongation, percent	Surface Roughness, rms
.061" As Rolled	217,000	210,000	5.5	72
.020" Chem. Milled from .061"	203,000	197,000	1.0	71
.020" As Rolled	204,000	201,000	4.0	
.020 Polished	196,000	191,000	3.0	

A systematic and extensive investigation showing relation of residual stress to fatigue strength has been done using shot peening, and the information collected is worthy of careful consideration for the relationship of residual stress on fatigue. Attention is given to these matters in this paper since surface studies involving peening have been studied more extensively than for machined and ground surfaces and because peening is an important subsequent method for treatment of machined and ground surfaces (see page 62).

Evans and Millan[24] reported fatigue tests run on notched 86B45 steel specimens in bending at three hardness levels, 20, 35, and 50 R_C, to determine the influence on fatigue of X-ray measuring parameters of microstrain and particle size. Changes in these quantities were produced by shot peening. The attendant macro residual stresses were shown to be equivalent to mechanically applied stresses and were compensated for by appropriate values of mean mechanical stress. Peening of the soft material produced large changes in microstrain and particle size and enhanced the fatigue limit. Peening did not alter the microstrain and particle size in the hard materials. Variable microstrain produces rms strain deviations from the mean strains which can be determined by X-ray line broadening analysis. Small particle or subgrain size can also cause X-ray line broadening analysis. Figure 35 shows the separate effects of residual stress and line broadening as a function of the steel hardness.[24] The upper curve shows the percent increase in fatigue limit due to macro residual stress in peening. The lower curve shows the percent increase in fatigue limit due to rms strain deviations and smaller particle size, both of which are measured by X-ray line broadening. Thus, it can be concluded that at 50 R_C the increase in fatigue limit is due mainly to the high level of induced compressive macro residual stresses, while at low hardness levels the fatigue limit of steel is enhanced by large changes in rms microstrain and particle size.

Morrow and Millan[9] reported on the influence of residual stress on fatigue of steels with hardness greater than 25 R_C. Their investigation showed that:

1. "Residual stresses have a similar effect on fatigue behavior of materials as do mechanically imposed static stresses of the same magnitude.

2. "Thus, the significant residual stresses are beneficial if compressive and detrimental if tensile, particularly in 'hard' materials.

3. "Near the fatigue limit (i.e., long fatigue life) the residual stress remains practically unchanged by the fatigue load.

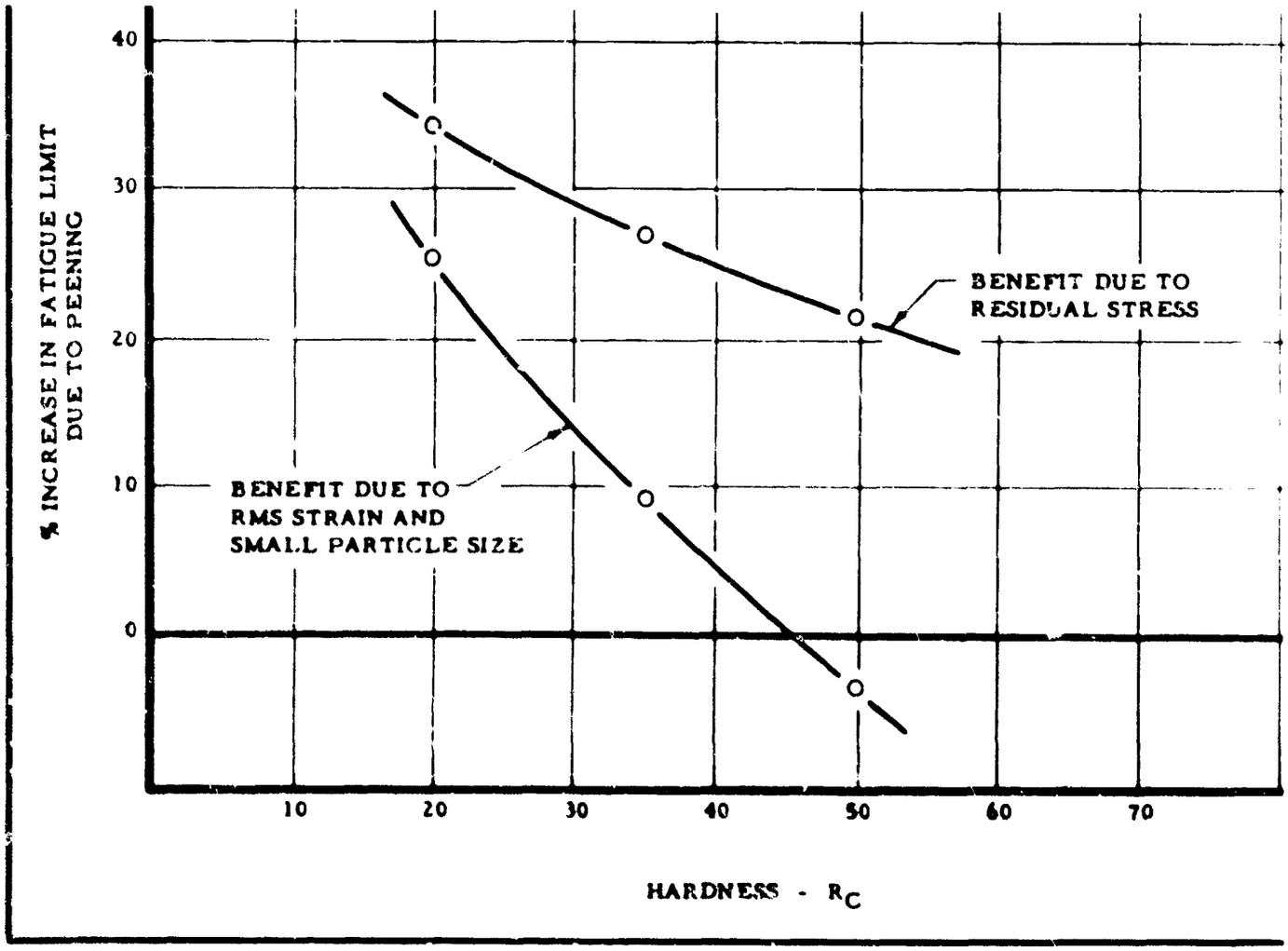

FIGURE 35. PERCENT INCREASE IN FATIGUE LIMIT DUE TO PEENING AS A FUNCTION OF HARDNESS FOR SAE 86B45 STEEL[24]

4. "At stresses above the fatigue limit, residual stresses may relax as an accompaniment of the fatigue processes, this effect being greater in 'soft' materials and at stresses well above fatigue limit.

5. "As a result of Conclusion 4, the fatigue life at high applied stresses depends very little on the initial residual stresses.

6. "The significant residual stress in bending is the peak value near the surface whether it is tensile or compressive."

Examples of data which support these conclusions are given in Figures 36, 37 and 38.[10] Fatigue diagrams are shown in Figures 36 and 37 for strain-peened specimens with the corresponding residual stress distributions obtained by beam dissection techniques and corroborated by X-ray diffraction measurements. Microstrain effects as indicated by line broadening were confirmed as being similar because the variation in residual stress was achieved by various conditions of applied elastic strain during similar shot peening treatments.

A mean stress-alternating stress diagram, Figure 38, was constructed from the data of Figure 37 demonstrating that the effect of the peak residual stress near the surface is like that of a static stress superimposed on the externally applied dynamic stresses. Confirmation is provided for this interpretation by the fact that the endurance limit for the "as heat treated" specimen fits equally well with the other points from sample groups having widely different levels of residual stress, see Figure 38. The broken line in Figure 38 represents data from another investigation from Reference 9 and was obtained by combination of an external steady stress on an alternating applied stress in order to simulate the effect of different levels of residual stress. The similar results illustrated in Figure 38 for different steels treated to similar hardness levels reinforces the conclusion that residual stresses have the same effect as similar static stresses imposed in other ways.

SUBSEQUENT PROCESSING OPERATIONS TO COUNTERACT RESIDUAL STRESS PRODUCED IN MACHINING AND GRINDING OF HIGH-STRENGTH STEELS

It has been found possible to relieve considerably the grinding stresses on hardened steels by brief low-temperature annealing without significant effect on metal hardness.[16] For example, a 90-second immersion in a salt bath at 550°F followed by a water quench produced a 50 percent decrease in tensile residual stress on hardened

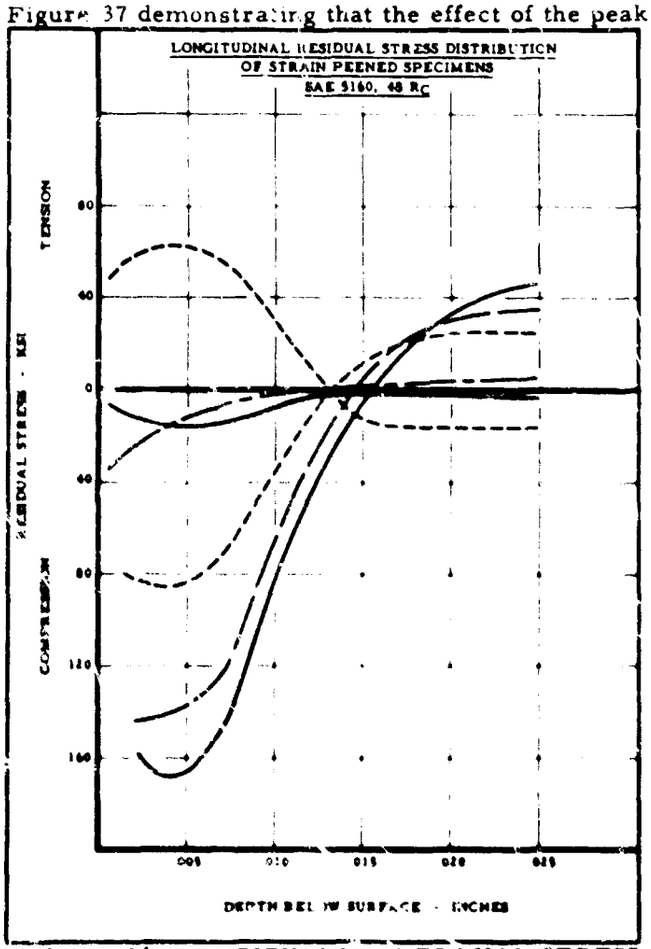

FIGURE 36. LONGITUDINAL RESIDUAL STRESS DISTRIBUTION OF STRAIN-PEENED SAE 5160 STEEL, 48 R_c[9]

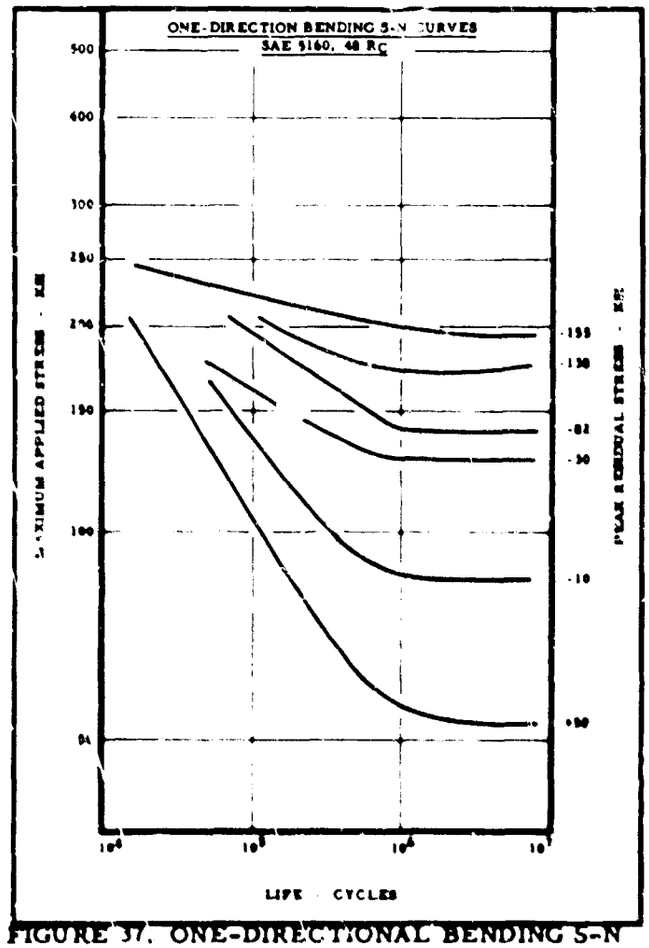

FIGURE 37. ONE-DIRECTIONAL BENDING S-N CURVES FOR SPECIMENS OF FIGURE 36[9]

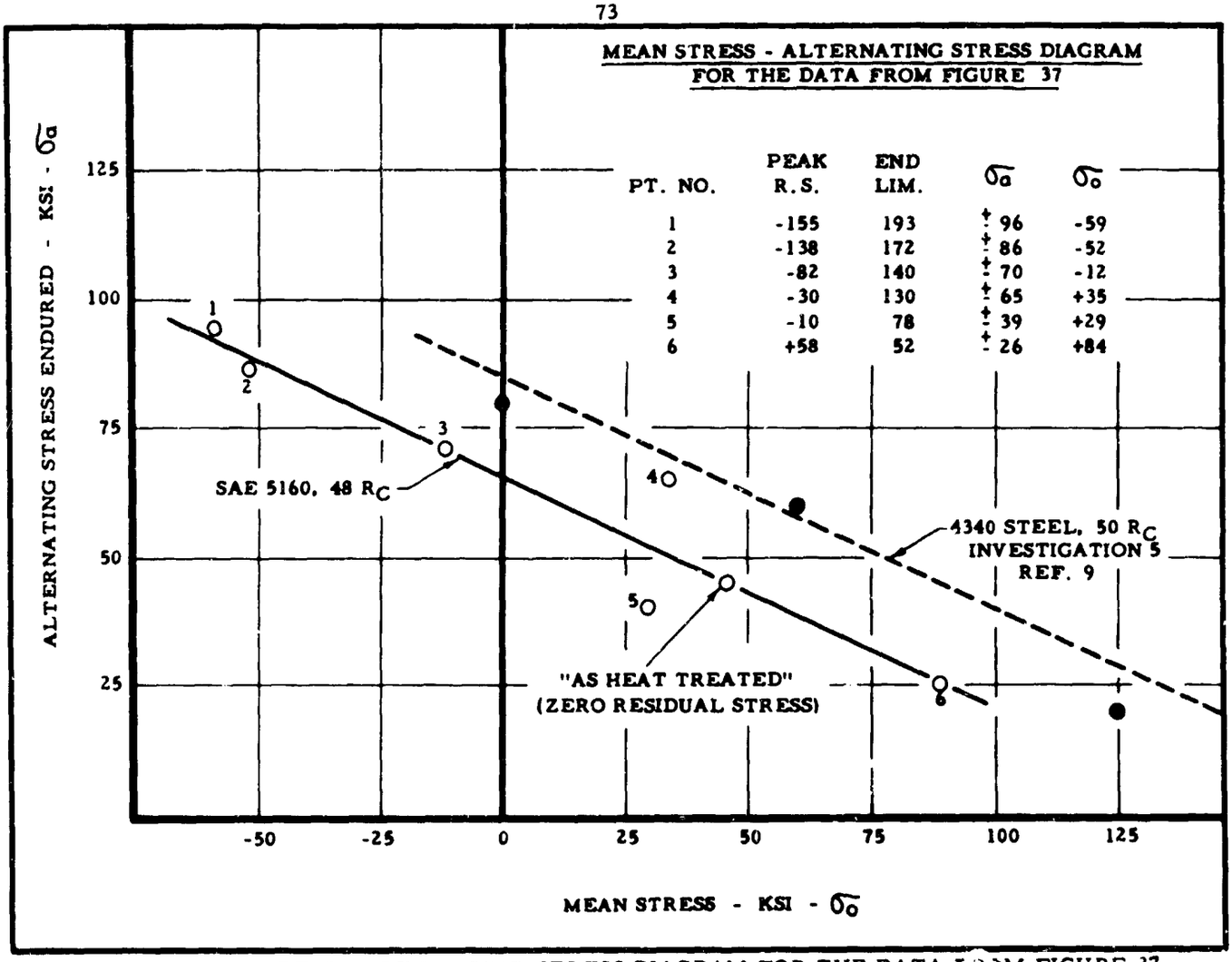

FIGURE 38. MEAN-STRESS ALTERNATING-STRESS DIAGRAM FOR THE DATA FROM FIGURE 37. BROKEN LINE IS FROM INVESTIGATION 5,[9] SIMILAR EFFECT OF RESIDUAL STRESS TO THAT OF EXTERNAL STRESS IS SHOWN[9]

steel. It would be valuable to perform a systematic study on residual stress-relieved or machined and ground high-strength steels.

Tumbling can be used to alter the grinding stresses by superimposing a new stress distribution.[25] The as-ground tensile residual stress of 120,000 psi on 64 R_c tool steel was reduced to 20,000 psi by subsequent tumbling, Figure 39. Abrasive tumbing of 52100 steel, 59R_c, ground previously with either tensile or compressive residual stresses moderately raised the fatigue strength. The tumbled surfaces with their high compressive stresses caused the fatigue failures to nucleate below the surface.[26]

As previously discussed, shot peening is used quite widely on high-strength steel components, such as landing gears, for imposing a definite compressive residual stress which supersedes any previous residual stress imposed by machining or grinding.

EFFECT OF MACHINING AND GRINDING OF HIGH-STRENGTH STEELS ON STRESS CORROSION

It again seems logical to presume that the high residual stresses imposed by machining and grinding of high-strength steels will affect their stress corrosion properties. It has been demonstrated by Tarasov[27] that etching of abusively ground hardened steel in hydrochloric or sulphuric acid of suitable concentration will produce almost instantaneous "etch cracks".

Several tests were run recently at Metcut Research Associates, Inc., to investigate the effect of gentle and abusive grinding on the stress corrosion of 4340 steel and D6AC steel at 50 R_c. In this test, steel strips were prepared 3/4" wide by 3.9" long, and one of the flat surfaces of the 4340 and D6AC specimens was ground by gentle and abusive methods as follows:

Type Grind	Grinding Wheel	Wheel Speed
Gentle	A46H8V	2000
Abusive	A46K8V	6000

Grinding Fluid	Down Feed
Sulphurized oil	Low stress
Dry	.002 in./pass

The specimens, after grinding, were then bent so that the ground side was put in tension.

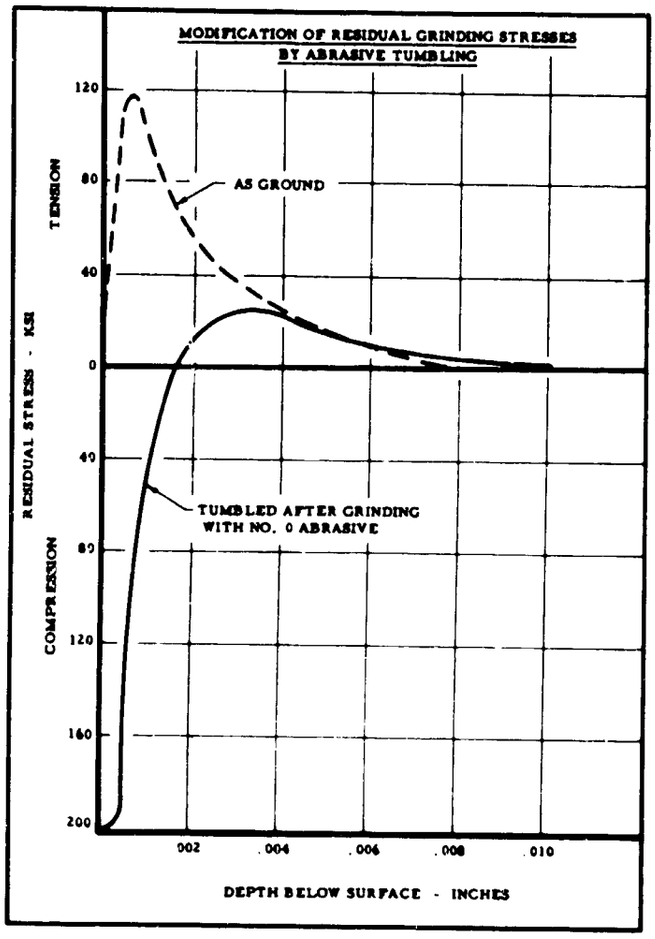

FIGURE 39. MODIFICATION OF RESIDUAL STRESSES BY ABRASIVE TUMBLING(25)

The tensile stress applied was 110,000 psi which is approximately 50 percent of the yield strength of both the 4340 and D6AC steels. The specimen was held in its bent position by means of a simple fixture, Figure 40, which in turn was placed in a salt-spray cabinet. The salt-spray conditions used were those corresponding to ASTM B117-62. The solution consisted of 95 parts distilled water and 5 parts sodium chloride with the chamber temperature maintained at 95 F. The salt-spray fog was directed into the chamber containing both the gentle and abusively ground specimens.

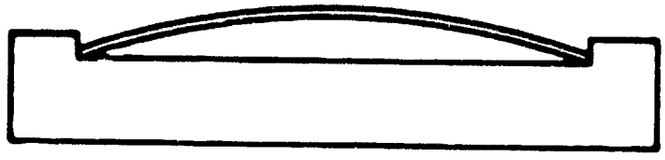

FIGURE 40. FIXTURE FOR STRESSING SPECIMEN IN SALT-SPRAY STRESS-CORROSION TEST

The results of the salt-spray test are shown in Table 3. The abusively ground 4340 steel failed after 70 hours, while the gently ground 4340 steel lasted 435 hours before failure. The abusively ground D6AC steel failed after 16 hours, whereas the gently ground D6AC did not fail after 768 hours. The photomicrographs of the abusively ground D6AC and 4340 steels after stress-corrosion failure are shown in Figures 41 and 42. Figure 41a shows typical stress-corrosion cracks which indicate tendencies toward an intergranular type of failure progression in D6AC. Figure 41b shows an etched surface at a magnification of 500X. Figure 42 shows a similar type of failure surface for 4340 steel.

TABLE 3. STRESS-CORROSION TESTS IN SALT SPRAY

Spec. No.	Material	Hardness, Rockwell C	Type Grind	Applied Bending Stress on Specimen	Time to Failure in Salt Spray
1	4340	53	Gentle	110,000 psi	435 hours
2	4340	53	Abusive	110,000 psi	70 hours
3	D6AC	50	Gentle	110,000 psi	768+ hours*
4	D6AC	50	Abusive	110,000 psi	16 hours

*Test still running after 768 hours.

FIGURE 41a. UNETCHED PHOTOMICROGRAPH OF D6AC STEEL ABUSIVELY GROUND AND SUBJECTED TO SALT-SPRAY TEST; FAILURE IN 16 HOURS; 150X (REDUCED APPROXIMATELY 40 PERCENT IN PRINTING)

FIGURE 41b. ETCHED PHOTOMICROGRAPH OF D6AC STEEL SHOWN IN FIGURE 41a; CRACKS APPEAR TO FOLLOW GRAIN BOUNDARIES OF PRIOR AUSTENITE; NITAL ETCH; 500X (REDUCED APPROXIMATELY 20 PERCENT IN PRINTING)

FIGURE 42. UNETCHED PHOTOMICROGRAPH OF 4340 STEEL ABUSIVELY GROUND AND SUBJECTED TO SALT-SPRAY TEST; FAILURE IN 70 HOURS; 100X (REDUCED APPROXIMATELY 20 PERCENT IN PRINTING)

There apparently has not been a systematic study of the effects of machining and grinding variables on stress corrosion. However, it has been established that the stress corrosion of high strength steels is a function of the strength level of these steels.[28] Three steels, H-11, 4340 and 9Ni-4Co, were tested on creep machines by loading specimens to a constant stress at room temperature and recording time to failure. The test specimens were alternately immersed in a 5 percent sodium chloride solution for five minutes and then in air for fifteen minutes while under constant load at particular stress levels. Round, smooth specimens were used and were, for the most part, stressed at 200,000 psi, which was equivalent to approximately 70 to 75 percent of the ultimate strength of the 265,000 to 280,000 psi materials. The stress corrosion properties of all the materials were improved by lowering the ultimate strength as shown in Figure 43 for the H-11 steel.

Holshouser[29] has reported on service failures in a number of aircraft parts made of 4340 steel heat treated to 260,000 to 280,000 UTS. Some of these failures have been attributed to delayed cracking as a result of hydrogen embrittlement or to stress corrosion.

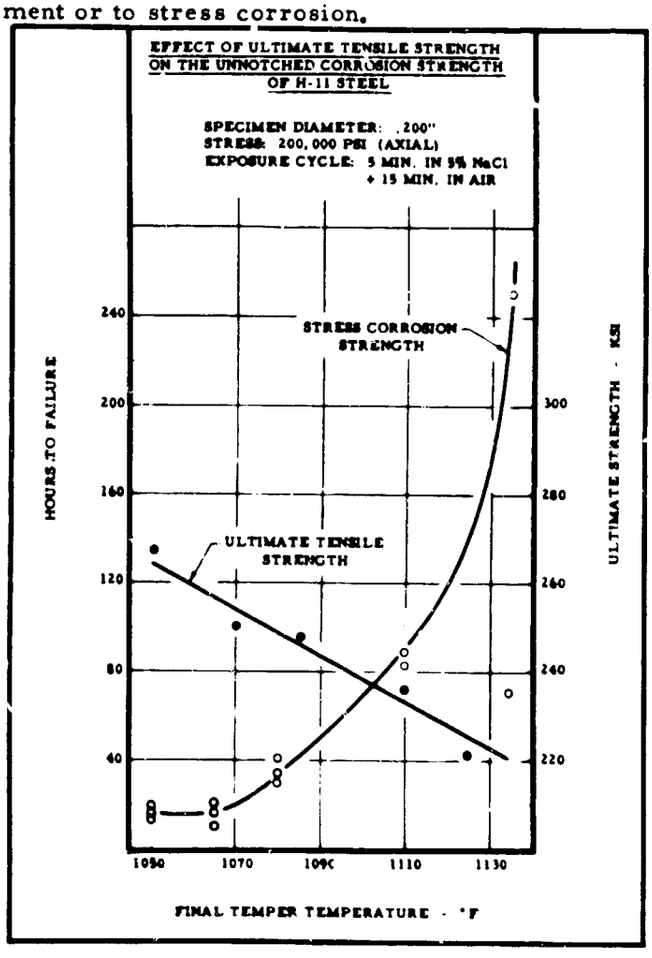

FIGURE 43. EFFECT OF ULTIMATE TENSILE STRENGTH ON THE STRESS CORROSION OF H-11 STEEL

The presence of high residual stress within a part is conductive to hydrogen embrittlement and stress-corrosion cracking. High-strength steels have a propensity for delayed brittle fracture or static fatigue.[30] These brittle fractures may occur when parts are subjected to static loads far below the yield point for considerable lengths of time, sometimes for months. There is a general agreement that hydrogen is necessary for these failures to occur and that hydrogen from plating or pickling is the most likely cause of these delayed failures. It had been demonstrated[31] that it is hydrogen in solution and not hydrogen occluded in internal voids that is damaging. It has been further demonstrated that hydrogen will diffuse to the maximum triaxiality of stress. Thus, the process involved is not the one of classical diffusion, but rather diffusion in the presence of a stress gradient. After the crack is started, its growth is discontinuous. Further cracking growth must await diffusion of hydrogen to the new region of maximum triaxiality of stress beyond the crack tip. This process is repeated until a crack length is reached which is critical at which time failure

occurs. Thus, stress concentration in a component plays an important part in hydrogen embrittlement, cracking and delayed failure in steel. To initiate fracture, hydrogen must reach a very high level in a local area. This high level is reached in the presence of a stress concentration by stress induced diffusion of hydrogen to the area of maximum triaxiality of stress.

INSPECTION AND DETECTION OF SURFACE LAYERS PRODUCED BY MACHINING AND GRINDING OF HIGH-STRENGTH STEELS

The surface texture produced in machining and grinding can first be inspected by means of a surface finish analyzer which measures the surface roughness. Surface burns, if sufficiently severe, can be detected visually by discoloration. Surface burns and cracks produced in grinding can furthermore be detected by lightly etching in Nital.(27)

Highly stressed surfaces produced in abusive machining or grinding can be detected by destructive etching in hydrochloric or concentrated sulphuric acid. If the residual tensile stresses are high enough, etching cracks will be produced.(27) Surface voids and excessive tears and cracks can be detected by magnetic particle or dye penetrant inspection methods.

The residual surface stress induced in machining and grinding can be detected nondestructively by X-ray diffraction techniques.(6, 7) Portable X-ray equipment using special techniques has been used to determine residual stresses nondestructively on high-strength steel parts, such as main landing gears.(32) One company is using X-ray diffraction techniques to set up machining methods in manufacturing jet engine discs. Favorable residual stress patterns are purposely machined into both sides of the disc so that the residual stress on both sides are matched, which in turn tends to produce flat discs.(33)

A study is under way to investigate possible use of ultrasonic methods in the measurement of residual stress in steels and other alloys by nondestructive means.(34) It has been observed that the velocity and attenuation of ultrasonic waves through solid materials are unusually stress dependent. Ultrasonic equipment is also being used to detect nondestructively the combined effects of the presence of surface discontinuities and the presence of untempered martensite.

In conclusion, it would appear that there is need for a wider recognition of the fact that surfaces generated in all types of metal removal processes can be altered considerably from the base metal and often in a deleterious fashion. Furthermore, serious damage sometimes occurs after considerable delay especially when stress corrosion environments are encountered.

In gathering data for this paper, it was apparent that considerably more work is needed to help designers and manufacturing engineers make parts more accurately by control of distortion and to make parts more reliable in service through control of their fatigue and stress corrosion characteristics.

REFERENCES

(1) Tarasov, L. P., "Some Metallurgical Aspects of Grinding in Machining", Machining Theory and Practice, ASM, 409-464 (1950).

(2) Littmann, W. L., and Wulff, J., "The Influence of the Grinding Process on the Structure of Hardened Steel", ASM Trans., Vol 47, 692-714 (1955).

(3) "Machining Characteristics of High Strength Thermal Resistant Materials", USAF Machinability Report, Curtiss-Wright Corporation, Vol 4 (1960).

(4) "Final Report on Machining Refractory Materials", USAF Technical Documentary Report No. ASD-TDR-581, Contract AF 33(600)-42349 (July, 1963).

(5) Tarasov, L. P. and Lundberg, C. O., "Nature and Detection of Grinding Burn in Steel", ASM Trans, Vol 41, 893-939 (1949).

(6) Martin, D. E., "Evaluation of Methods for Measurement of Residual Stress", SAE TR-147 (1960).

(7) Christenson, A. L., et al, "The Measurement of Stress by X-Ray", SAE TR-182 (1960).

(8) Tarasov, L. P., Hyler, W. S., and Letner, H. R., "Effect of Grinding Conditions and Residual Stresses on the Fatigue Strength of Hardened Steel", ASTM Proceedings, Vol 57, 601-622 (1957).

(9) Morrow, J. D., and Millan, J. F. (Editors), "Influence of Residual Stress on the Fatigue of Steel", SAE Handbook Supplement J 783 (1961).

(10) Littmann, W. E., "Measurement and Significance of Residual Macrostresses in Steel", SAE 793A (January, 1964).

(11) Mattson, R. L., "Fatigue, Residual Stresses and Surface Cold Working", International Conference on Fatigue of Metals, Institute of Mechanical Engineers, Session 7, Paper 5.

(12) Frisch, J., and Thomsen, E. G., "Residual Grinding Stresses in Mild Steel", ASME Paper No. 50-F-10 (1950).

(13) Stablein, F., "Spannungsmessen An Einseitig Abgeloschten Knuppeln", Kruppsche Monatshefte, Vol 12 (1931).

(14) Letner, H. R., and Snyder, H. J., "Grinding and Lapping Stresses in Manganese Oil Hardening Tool Steel", ASME Trans, 873-882 (July, 1953).

(15) Nowikowski, L. J., Maranchik, J., and Field, M., "Distortion and Residual Surface Stress in Grinding and Milling of High Strength Steels", SAE 340L (1961).

(16) Gormly, M. W., "Residual Grinding Stresses", Grinding Stresses Collected Papers Published by Grinding Wheel Institute.

(17) Vitovec, F. H., and Binder, H. F., "Effects of Specimen Preparation on Fatigue", WADC Technical Report 56-289 (August, 1956).

(18) Hankins, G. A., Becker, M. L., and Mills, M. L., "Further Experiments in the Effect of Surface Conditions on the Fatigue Resistance of Steels", J. Iron & Steel Inst., 128 (1), 399 (1936).

(19) Roberts, A. M., and Grayshon, R. J., Science Technical Memo No. 6/43, British Ministry of Aircraft Production.

(20) Forsyth, A. C., and Carreker, R. P., "Fatigue Limit of SAE 1095 After Various Heat Treatments", Metal Progress, 683-685 (November, 1948).

(21) Frankel, H. E., Bennett, J. A., and Pennington, W. A., "Fatigue Properties of High Strength Steels", ASM Trans, Vol 52, Preprint 121 (1958).

(22) Borik, F., Chapman, R. D., and Jominy, W. E., "The Effect of Percent Tempered Martensite on Endurance Limit", ASM Trans, Vol 50, Preprint 16 (1957).

(23) "Effect of Intergranular Attack and Pitting on the Fatigue Properties of Thin Gage PH15-7Mo and 17-7PH Sheet Materials", North American Aviation Report No. TTD-61-651-SST, ASTIA No. AD 283091 (July 7, 1961).

(24) Evans, W. P., and Millan, J. F., "Effect of Microstrains and Particle Size on the Fatigue Properties of Steel", SAE No. 793B (January, 1964).

(25) Letner, H. R., "Stress Effects of Al ive Tumbling", ASME Trans, 51, 402-42(19 3).

(26) Tarasov, L. P., Hyler, W. S., and Letner, H. R., "Effects of Grinding Direction and Abrasive Tumbling on the Endurance Limit of Hardened Steel", ASTM Preprint 71 (1958).

(27) Tarasov, L. P., "Detection, Causes and Prevention of Injury in Ground Surfaces", ASM Trans, 36, 389-439 (1946).

(28) Jones, R. L., and Nordquist, F. C., "An Evaluation of High Strength Steel Forgings", USAF Technical Documentary Report No. RTD-TDR-63-4050 (May, 1964).

(29) Holshouser, W. L., "Failure in Aircraft Parts Made of Ultra High Strength Steel", ASM Technical Report No. 11-1 (1963).

(30) Slaughter, E. R., "Review of the Effects of Hydrogen in Steel", J. of Metals, 430-431 (April, 1956).

(31) Shank, M. E., Spaeth, C. E., Cooke, V. W., and Coyne, J. E., "Solid-Fuel Rocket Chambers for Operation at 240,000 psi and Above - II", Metal Progress, 84-92 (December, 1959).

(32) Bolstad, D. A., Davis, R. A., Quist, W. E., and Roberts, E. C., "Measuring Stress in Steel Parts by X-Ray Diffraction", Metal Progress, 88-92 (July, 1963).

(33) Malerich, J. B., "Use of X-Ray Diffraction Analysis of Residual Stress in the Development of Production Materials and Methods of Machining Flat Discs", ASME Paper No. 62-PROD-13 (March, 1962).

(34) Rollins, F., "Ultrasonic Methods for Nondestructive Measurement of Residual Stress", WADD Technical Report No. 61-42, Part I (May, 1963).

CORROSION PROTECTION OF HIGH-STRENGTH STEELS

by

S. Goldberg*

Since high-yield-strength steels are primarily used for aerospace articles, this paper is confined to corrosion protection from this viewpoint. Although other papers are concerned with stress-corrosion cracking, hydrogen embrittlement, and corrosion fatigue, these facets are also considerations in serviceable corrosion protective systems. The environmental conditions are -65 F to approximately 1000 F in marine environments of the spray type with intermittent bold exposure. Although 12 per cent type chromium steels have been widely used without protective coatings, these materials require protection for many applications. Higher chromium-content materials although not requiring corrosion protection when used alone, require coatings where they may contact other materials or are mechanically joined with themselves. Although successful protective schemes are being used, substantive advances are needed to simplify application and maintenance. Also required are nondestructive test methods to evaluate corrosion damage which may occur.

INTRODUCTION

There is an advantage favoring the use of steel alloys, up to about 1000 F, which has been extensively exploited. In consideration of the notch effects of corrosion pits, complete protection is required against deterioration for reasonable periods in environments which can be very aggressive. The environment of interest can be the ocean environment with heavy salt spray or a completely protective environment. Other environmental conditions involve ship stack gas deposits--engine, both turbo-jet and piston engine exhaust deposits--rocket blast impingement and deposits--exposure to runway de-icing materials, cleaning materials; fluids and other materials used in various systems such as synthetic lubricating oils, hydraulic fluids, greases, etc. Not to be overlooked is exposure to corrosive water-soluble materials in coatings such as neoprene and resins used in composite insulating blanket materials. Beach and desert sand can be significant environmental factors. Although the wear factor in the usually understood sense is outside the scope of this paper, it cannot be overlooked in connection with the aforementioned deteriorating factors. Interaction with the stress field of applied and assembly loads; pressure and radiation environment are factors of significance in many applications. Design for use in a completely corrosion-free environment has no basis in the practical world. Equipment designed for use in a temperature-humidity controlled environment can only be considered laboratory equipment.

* Bureau of Naval Weapons, Department of the Navy, Washington, D. C. 20360

Since steels are generally used with other materials, consideration must be given to their behavior in contact with other materials--high-strength aluminum alloys, magnesium alloys, other compositions of steels and titanium alloys, and with brazing materials. Included in this factor is compatability with mechanical attachments which are usually of the high-strength type steels, including stainless compositions and titanium alloys. A substantial proportion of these fasteners are of proprietary design, non-reusable with special retention features and use proprietary dry-film lubricants to achieve high clamping force necessary for successful use in shear applications.

Cost of ownership provides the limiting frame of reference in considering the approach to prevention of deterioration. This frame of reference is further limited in the case of the subject discussion in that alternate material choices are excluded. In considering cost of ownership, in addition to the obvious elements of original cost and life, less obvious elements such as accessibility for inspection, rework, and replacement and availability of tools, materials, and processing equipment become significant. Unfortunately, instances of penalities involving these features are not rare. A current problem in this category is illustrative.

A landing-gear trunion designed and fabricated of tapered high-strength steel tubing included a flash weld to join the large diameter center section; the weld flash was allowed to remain and the open ends inadequately sealed and the interior inadequaly protected. Atmospheric condensate build-up occurred with resulting corrosion and crack initiation at corrosion pits with subsequent failure and extensive physical damage during landing. Inspection for corrosion and mechanical damage required disassembly of the gear. Rework required the development of special tools which could only be used by skilled personnel to preclude the possibility of introducing other unfavorable conditions.

Let us now consider in some detail the consequences of deterioration in high-strength steel parts. The situation where a more or less uniform corrosion pitting type of attack which results in reduction in section size, which as is well known, is the usual effect of a corrosive environment on low-alloy steels of the 4340 type, is the most common situation. Where the material was selected for reasons other than static and dynamic mechanical properties, such as stiffness, the effect of the deterioration is least troublesome and a modicum of corrosion protection generally is adequate. The same kind of deterioration can be catastrophic where significant static or dynamic loads or combinations thereof are significant. Hildebrand[1]*

*References are given on page 90.

shows that corrosion pits developed during pre-treatments in a laboratory evaluation of stress-corrosion cracking of high-strength steels with varying nickel content for aircraft application appear to influence the behavior of the 4340 material. The pits were developed during phosphate coating pre-treatment in solutions of two concentrations; the more concentrated solution resulting in a greater loss in life. Figure 1 shows the effect of black oxide treatment of nitrided steel. It is to be noted that the specified treatment temperature for this process is 285-295 F.

FIGURE 1. PHOTOMICROGRAPH OF NITRIDED NITRALLOY STEEL SHOWING THE GRAIN STRUCTURE OF THE NITRIDED AREA AND CORE

The nitrided steel surface had been coated with black oxide under abnormal conditions at a solution temperature of 295 F. The photograph shows the pitting and possible intergranular corrosion attack on the nitrided area of the nitralloy.

(Etchant: 5% Nital, Magnification: 150X, reduced approximately 35 per cent in printing.)

Figures 2, 3, and 4 show the same kind of behavior to have been exhibited by a 4340 steel, landing-gear part heat treated to 260,000-280,000-psi tensile strength. In this failure, the corrosion deterioration is of the type described as "filoform"; stress-corrosion cracking has been established to have developed which precipitated the final failure; the pit acting to provide a stress-concentration point which was acted on by a fairly high level of residual tensile stress; heat treating was the source of the residual tensile wherein the normally compressively stressed surface material was removed as the final machining operation.

Figures 5, 6, and 7 illustrate the deterioration of turbojet engine compressor vanes which were investigated after an engine failure. The severity of the pitting attack is to be noted. Also to be noted is the deterioration which occurred under an apparent intact paint film.

Tests of corroded blades, which appear to have only superficial corrosion damage, have established that a loss of approximately 50 percent in fatigue strength is the consequence of the corrosion damage. During investigation of a failed steel-helicopter component, it was found that sometimes fatigue cracks develop at the bottom of a corrosion pit.

Figures 8, 9, and 10 show evidence of corrosion damage which led to premature failure of an expensive jet-engine afterburner fuel-spray-bar assembly manufactured from Type 321 stainless steel. The intergranular corrosion and pitting were sites for thermal fatigue failure.

METHODS OF CORROSION PROTECTION

Unavoidable interaction with hydrogen embrittlement exists in considering methods of corrosion protection. In this respect, this treatment will be confined to consideration of the metal-coating interface.

The ideal coating and coating process would have the following characteristics:

(a) Economical to apply to complex shapes

(b) Free from defects

(c) Thickness and range of thickness capable of precise control

(d) Inert to the usual chemical environments

(e) Resistant to wear and erosion

(f) When damaged mechanically, will not induce hydrogen embrittlement as the result of galvanic effects

(g) Retention of characteristics in the temperature range to which the material is exposed

(h) No damaging effect on the mechanical properties, both static and dynamic, of the materials to which they are applied

(i) Compatible corrosion-wise with other materials which they contact in assemblies

(j) Easily inspected for required characteristics and interpose no restrictions for inspection of materials to which they are applied

(k) Receptive to the application of organic finish systems

(l) Resistant to organic coating strippers.

Since metallic coatings generally meet these requirements to the required degree and the characteristics of aqueous electroplating processes meet the process requirements, this area will be discussed initially. The hydrogen embrittlement factor is introduced thereby.

Although no unequivocal mechanism exists at this time to account for the varying characteristics of various electroplating baths, the results of past and continuing studies are providing data which provide a clearer insight.

Reference (2) reports the results of tests showing that aliphatic amino acids in cadmium electroplating solutions significantly affect hydrogen-

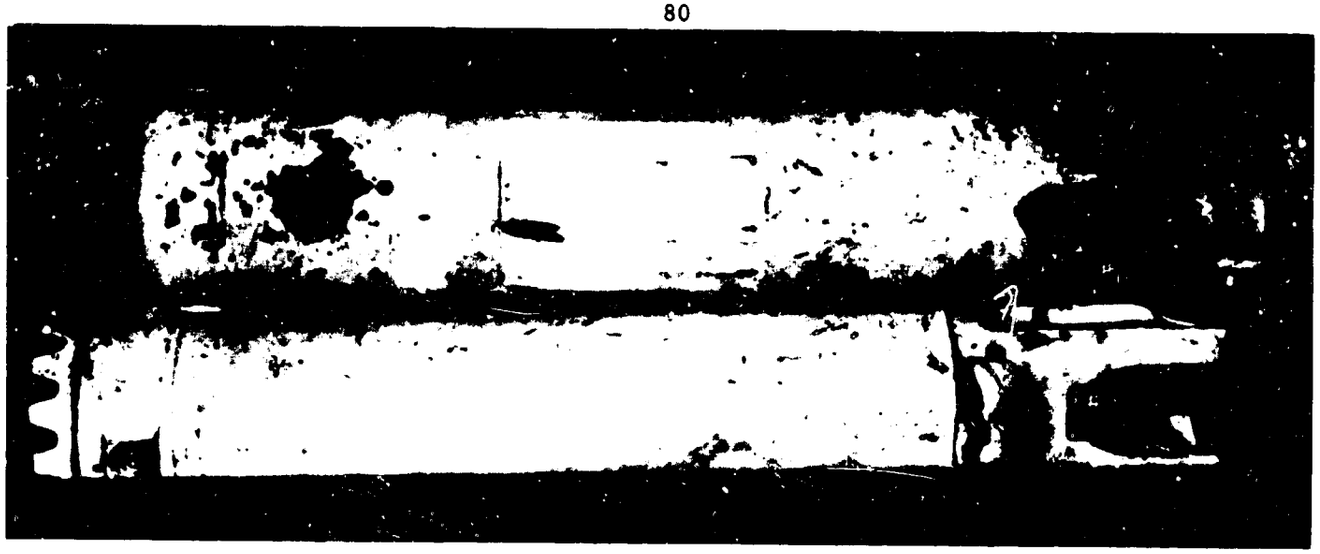

FIGURE 2. No. 1 ORIGINAL FACTORY PAINT FINISH, No. 2 PAINT FINISH APPLIED DURING OVERHAUL

(Note flaking and peeling of paint on No. 1.)

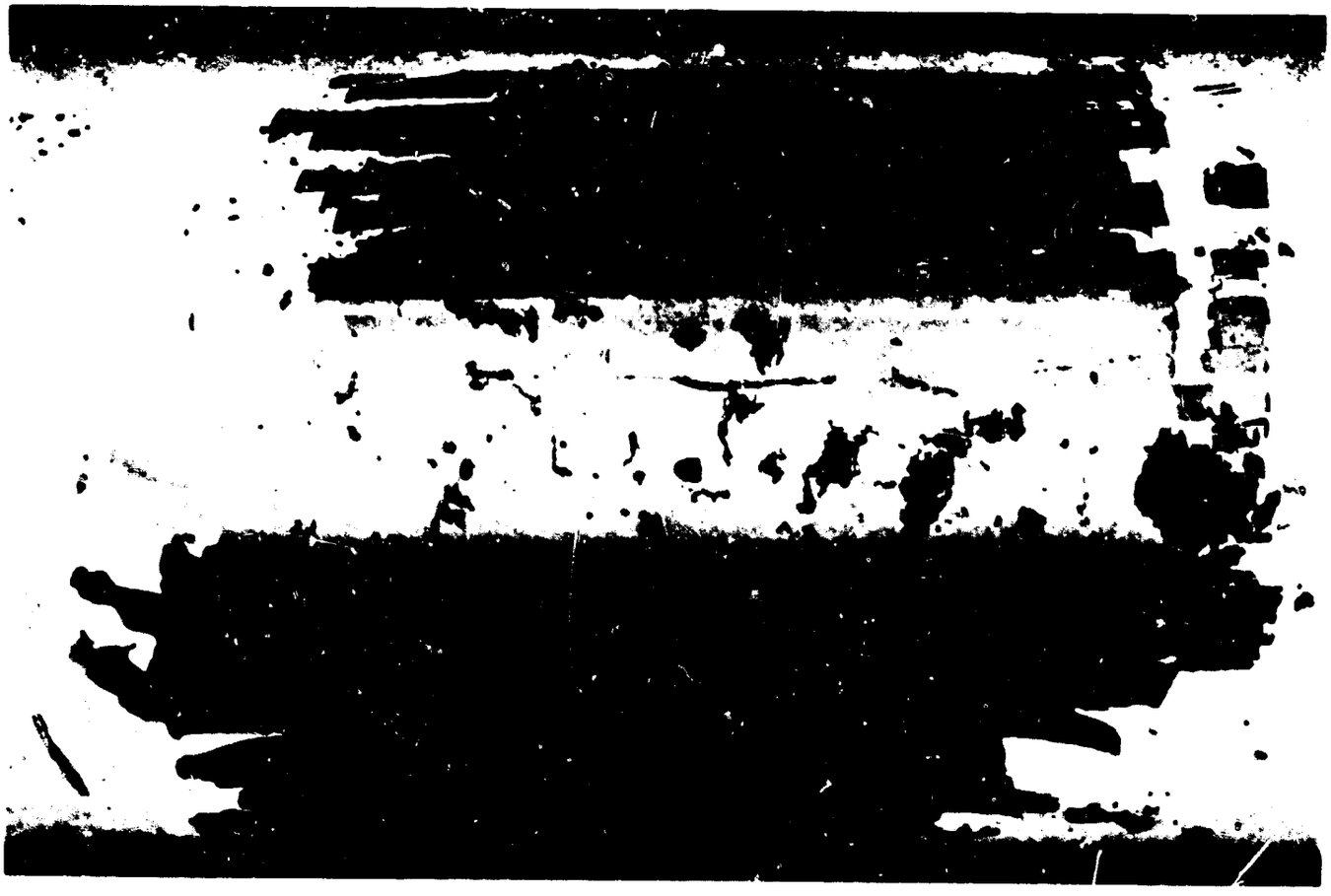

FIGURE 3. FILOFORM TYPE OF CORROSION FOUND UNDER PAINT COATING ON STRUT No. 1, 1X

(Reduced approximately 20 percent in printing.)

embrittlement behavior; α-amino-n-butyric a[illegible] appears to essentially prevent hydrogen-embrittlement damage when used as complexing agent in place of cyanide.

FIGURE 4. AN AREA FROM FIGURE 3 AT HIGHER MAGNIFICATION TO SHOW THE NATURE OF THE FILOFORM CORROSION, 10X
(Reduced approximately 20 percent in printing.)

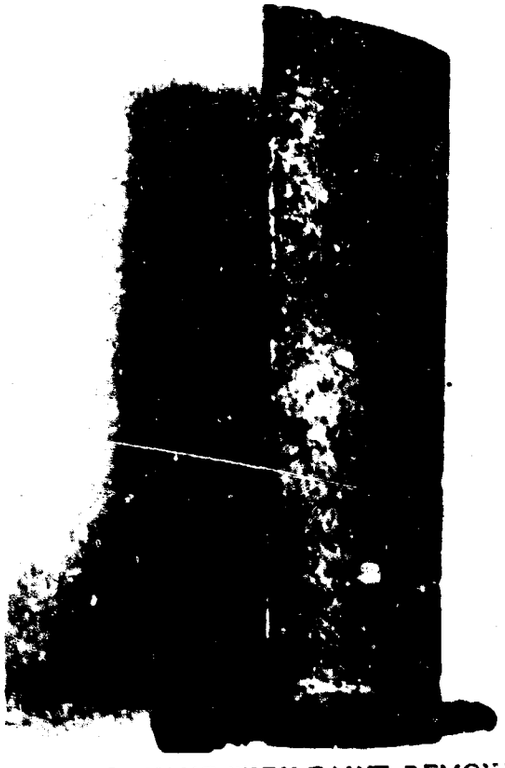

FIGURE 5. VANE WITH PAINT REMOVED, TYPE 403 STAINLESS STEEL, 345 HOURS, 4X
(Reduced approximately 20 percent in printing.)

FIGURE 6. CORROSION PIT ON TYPICAL UNETCHED VANE FROM FAILED SEGMENT, 100X
(Reduced approximately 20 percent in printing.)

FIGURE 7. VANE PITS ON LEADING EDGE, 250X
(Reduced approximately 20 percent in printing.)

FIGURE 8. INTERGRANULAR CORROSION AT AN ORIFICE, UNETCHED, 500X
(Reduced approximately 20 percent in printing.)

FIGURE 9. INTERGRANULAR CORROSION AT AN ORIFICE, ETCHED ELECTROLYTICALLY, 10% OXALIC ACID, 500X
(Reduced approximately 20 percent in printing.)

FIGURE 10. PITTED AREA ADJACENT TO AN ORIFICE, ETCHED ELECTROLYTICALLY, 10% OXALIC ACID, 200X
(Reduced approximately 20 percent in printing.)

The Naval Air Engineering Center, Aeronautical Materials Laboratory, has demonstrated that the presence of the cyanide anion in alkaline solutions results in the increase of the hydrogen potentials. This was thought to be due to formation of a cyanide compound with the atomic hydrogen on the cathode. The existence of a cyanide film was established by radiochemical means (Cyanide C-14) and calculations indicated that a film is a monomolecular layer.[3] Using the same technique with radioactive α-amino-n-butyric acid,[4] it was established that the maximum surface coverage of the absorbed layer is considerably less than the calculated theoretical value for a monolayer; the uncoated "free" area, it is postulated, contains many "active sites" where recombination occurs of the atomic hydrogen released at the cathode to form molecular hydrogen and pass out of solution as a gas.

Other empirical data indicate that the aforementioned model may have some validity.

(a) Brightening addition agents aggravate hydrogen embrittlement. These are organic materials such as aldehydes, ketones, alcohols, furfural, dextrin, gelatin, milk sugar, molasses, piperonal, coumarin, etc. These materials form complexes with the electrolyte in cyanide baths and influence the orientation and growth of the crystals, resulting in the formation of fine longitudinal crystals. It may be postulated that such agents contribute to the formation of a more continuous cathode film on the metal surface than solutions not containing such agents. Further, this film provides many uniform sites for deposit nucleation and elimination of influence of the substrate to establish significant epitaxial effects.

(b) Porosity in deposits appears to mitigate hydrogen embrittlement.[5] Deposits applied at high current density (70 amps/ft^2) from cyanide baths have been shown to have little hydrogen embrittlement effects when followed by 23 hours baking at 350–400 F. This behavior appears to be similar to the behavior of parts plated from α-amino-n-butyric baths. Further, it is to be noted that the characteristics of the deposits are also similar--matte in appearance and lacking somewhat in adherence.

Other evidence is available to indicate some merit to this postulation. A technique described in Reference (6) is capable of measuring the quantity of hydrogen permeating a thin (0.77 mm) iron or steel membrane during any type of cathodic treatment. With readout in permeation rate in terms of $\mu a/cm^2$ (microamps/cm^2), the data show a significant difference between the aminobutyrate cadmium-plating bath and the cyanide-cadmium bath (see Figure 11). Figures 11, 12, and 13, show that the presence of the cyanide ion in alkaline electrolytes for cathodic charging increases hydrogen permeation tremendously. To be noted also is the barrier effect of cadmium for hydrogen as the coating thickness builds up. This study, which is continuing, has also shown some other interesting results.

(a) The effect of sustained tensile stress is much greater for 4340 steel at 260,000-psi tensile strength than Armco iron.

(b) Stress has been found to increase permeation independently both of the pH of the catholyte and the presence of capillary active substances therein (see Figures 13 and 14).

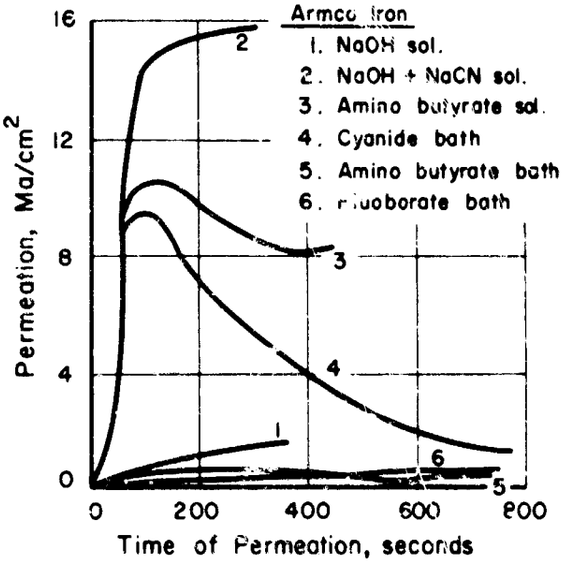

FIGURE 11. DEPENDENCE OF PERMEATION ON TIME OF CATHODIC CHARGING AND ELECTROLYTE (CURVES 1, 2, AND 3); ON TIME OF ELECTRODEPOSITION OF Cd FROM VARIOUS BATHS (CURVES 4, 5, AND 6)

Cathodic Current Density = 8.1 ma/cm²
Membrane Thickness = 0.77 mm

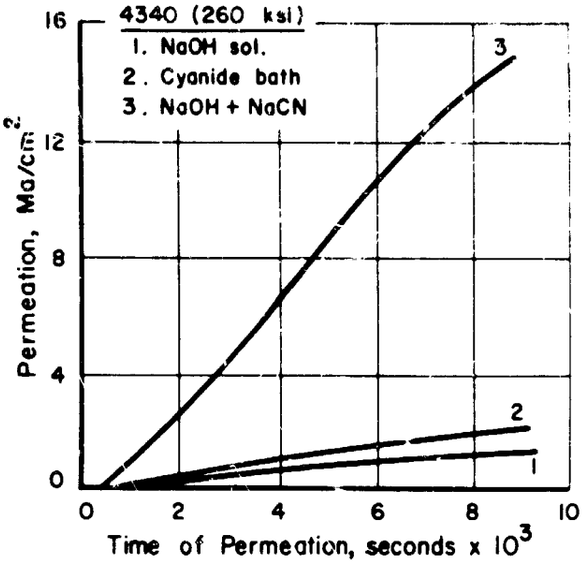

FIGURE 12. DEPENDENCE OF PERMEATION ON TIME WITH (CURVE 2) AND WITHOUT (CURVES 1 AND 3) Cd PLATING

Cathodic Current Density = 8.1 ma/cm²
Membrane Thickness = 1 mm

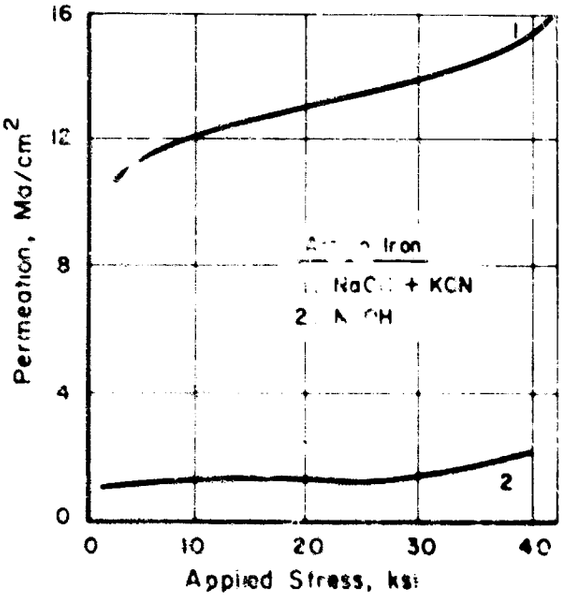

FIGURE 13. DEPENDENCE OF PERMEATION ON APPLIED STRESS

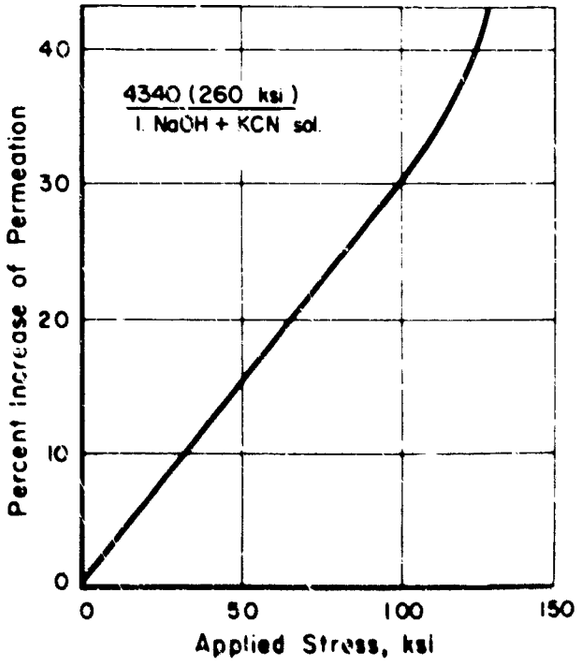

FIGURE 14. PERCENTAGE INCREASE IN PERMEATION WITH INCREASED APPLIED STRESS

(c) A negligible effect of trace impurities has been shown as the result of studies with zone-refined iron in comparison with Armco iron, whereas drastic effects of alloying has been shown in studies with H-11 type steel.

LAWRENCE HYDROGEN-DETECTION GAUGE

A recent development, the Lawrence Hydrogen-Detection Gauge, provides a new approach in the study of processes involving hydrogen. The results of an investigation in progress at the Naval Air Station, Alameda Materials Laboratory, Alameda, California, indicate this promise.

The gauge (Figure 15) comprises a metal probe which is essentially a metal electron tube and an instrument for measuring electron-beam current, internal probe pressure, oven temperature, plating current density, and polarity, with necessary function switches.

The sensing element of the gauge is a metal-shelled vacuum tube with electronic means for measuring variations in the low pressures within this sealed probe when subjected to exposure to hydrogen ion emission sources and to baking. The shell material is metallurgically controlled aluminum-killed 1010 steel, 0.016-inch thick. Hydrogen ions, resulting from chemical or electrochemical processes ap-

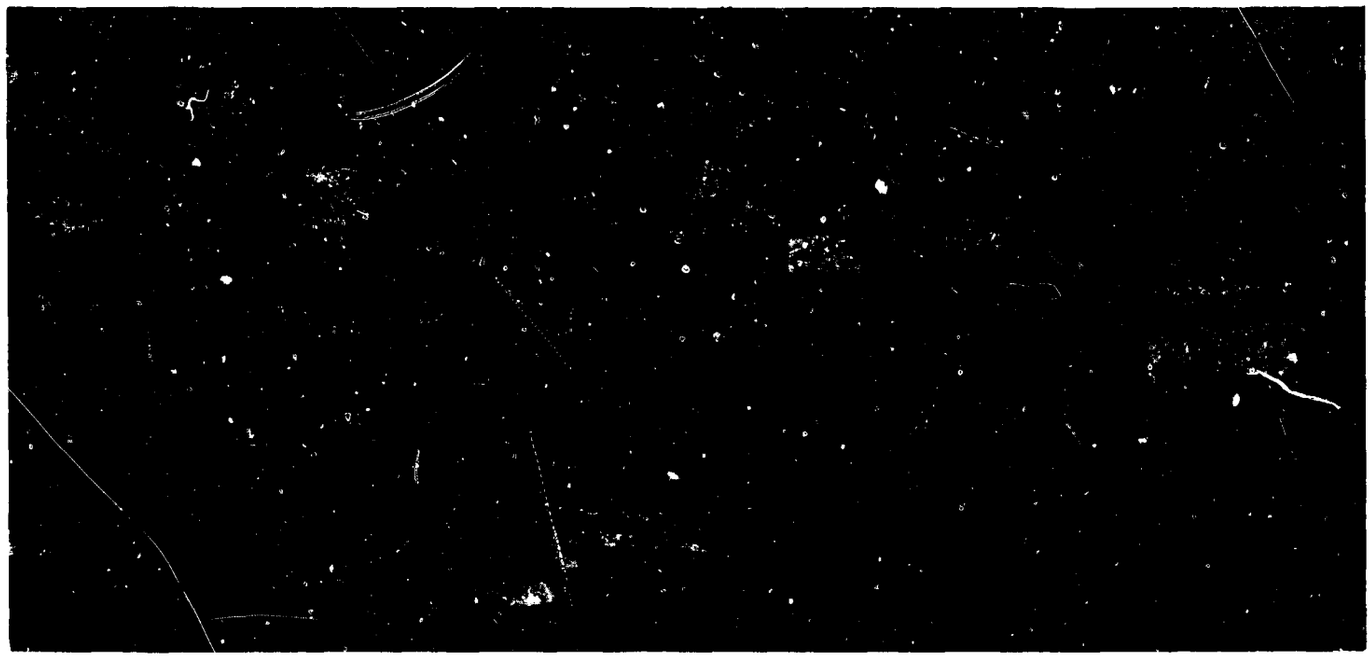

FIGURE 15. LAWRENCE HYDROGEN-DETECTION GAUGE BEING USED TO MONITOR HYDROGEN INPUT FROM SHOP ELECTROPLATING SOLUTION, ALL RELATED ACCESSORIES ARE SHOWN

plied to the immersed probe, are sorbed on the probe shell and diffuse rapidly through this thin shell.

The diffused hydrogen ions recombine at the probe inner wall to form hydrogen molecules which migrate into the low-pressure vacuum area (10^8 torr) and change the pressure within the probe which is electronically measured by an ionization gauge. As with all such devices, the gas pressure is continually pumped (gettered) by the active ionization gauge, so that the pressure that is shown by the meter on the gauge (or by the strip chart recorder attached to the hydrogen-detection gauge) is an equilibrium measurement, being a balance between hydrogen entering the probe and hydrogen being pumped (or gettered) within the probe.

Following hydrogen exposure, the probe is inserted into a special analog oven which is an integral part of the gauge. The probe is heated in a 200 C atmosphere while the hydrogen pressure is measured. Pressure within the probe increases rapidly as the heated hydrogen is driven from the applied plate into and through the steel probe shell. This hydrogen is representative of that which is driven into production parts processed similarly to the probe and then baked. The hydrogen which is "boiled off" from the plate during baking and does not enter the probe will not contribute to the embrittlement of the plate or be measured by the gauge. The pressure increases to a peak value rapidly and then decreases as the pumping rate within the probe exceeds the rate at which hydrogen is being released by the plating on the shell. By measuring the time, in seconds, for the probe pressure to fall from the peak reading (HP) to a value of one-half of the peak ($\frac{1}{2}$ HP), called the Lambda Value (λ), the hydrogen permeability of the electrodeposited coating is measured. The numerical results of the gauge are expressed in terms of two related quantities, heat peak (HP) and lambda (λ). A meter reads in units called hydrogen index (HI). These units can be thought of as units of pressure. The greater the amount of hydrogen exposed to the surface of the tube, the greater the pressure within the tube and an increased HI reading will result. Decreasing the amount of hydrogen exposed to the tube surface will result in lower readings. Exposing the probe to hot or cold solutions during processing will also register on the meter as greater or lesser HI. After processing of the probe is completed, it is placed in the gauge analog oven. A rapid rise in HI is noted on the total hydrogen index (THI) meter and on the recorder as hydrogen is driven out of the plated coating and shell and as the temperature of the probe approaches maximum. As the pressure and temperature increase, the cleanup rate also increases and the HI reaches a maximum reading, followed by a sharp drop in HI. This maximum HI reading is called the heat peak (HP). This measures the total amount of hydrogen sorbed during the complete processing. The second quantity (λ) is the measure in seconds of the amount of time required for the HP value to decrease to one-half its numerical value.

Knowing the HP and (λ) values, limits can be set to control the embrittlement by controlling postplate bake times. The lower the value, the more hydrogen permeable is the plate, and hence for a fixed HP value, the shorter is the postplate bake time required.

A set of curves plotting HP versus limits, for various bake times for 4340 steel heat treated to 260-280,000 psi, is shown in Figure 16. These limits are derived from correlation studies made between notch tensile specimens made from 4340 steel, heat treated to 260-280,000 psi having 0.01-inch notch radius and subject to 75 percent ultimate load for 200 hours.

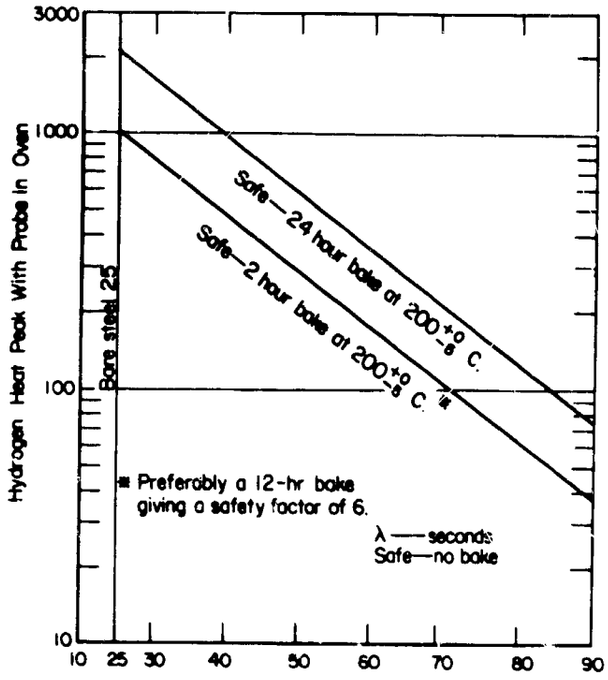

FIGURE 16. DATA OBTAINED FROM HDP-1A PROBES AND NOTCH-TENSILE SPECIMENS MADE FROM 4340 STEEL, HEAT TREATED TO 260-280,000 PSI

(Having 0.01-inch notch root radius and subjected to 75 percent ultimate load for 200 hours to pass test requirements.)

Figure 17 illustrates the read-out obtained when bright cyanide cadmium electrodeposit was examined. The curves on the right-hand side represent the effect of various pre-plate operations; the inflections in the central portion reflect changes in recorder scale to accommodate buildup in hydrogen heat peak. Figure 18 shows that Wood's nickel strike may be satisfactory. Figure 19 shows that hard sulfamate nickel may be applied over Wood's nickel.

Preliminary experiments indicate that this technique can be used to study corrosion reactions. An experiment with spray-metallized aluminum indicated a surprisingly high degree of hydrogen input during exposure for 15 minutes in a 10 percent sodium chloride solution at room temperature. Similar experiments with cadmium coatings indicated a significant advantage in use of conversion coatings.

As is well known, the major significant effect of hydrogen in steel is reduction in capability to resist sustained tensile loads. Of lesser significance generally is reduction in ductility. Tests have shown that an almost constant reduction in ductility results under given plating conditions for the same steel composition and heat treated to various strength levels (see Figure 20). Tests involving high strain rates and fatigue tests of smooth bars do not show any significant effect of hydrogen. However, if a sharp notch exists, the effect of hydrogen embrittlement is shown. In Reference (7), Beck has shown that a

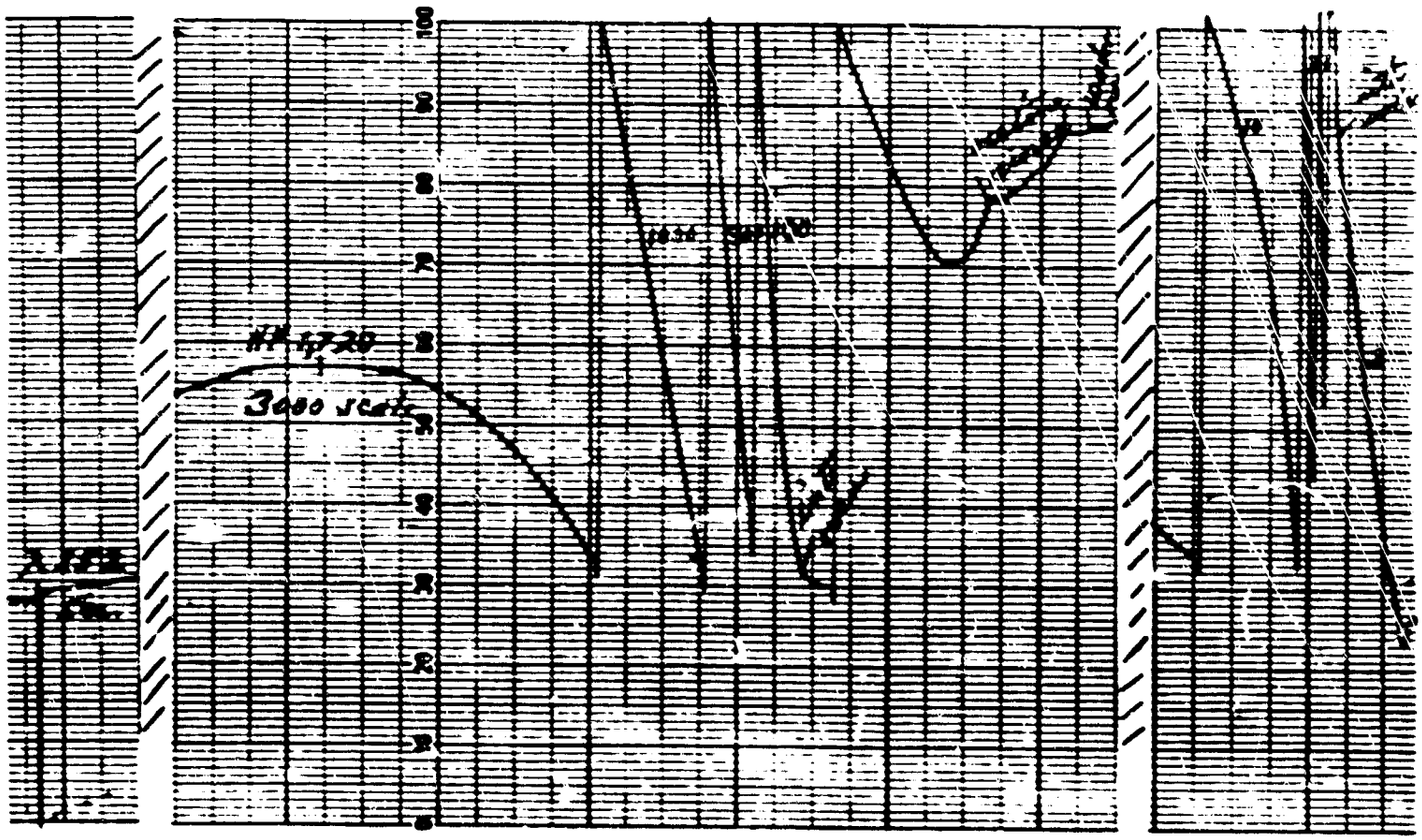

FIGURE 17. BRIGHT CONVENTIONAL CADMIUM, 5-MINUTE PLATE AT 20 AMPS/SQ FT [Test No. 31, Probe No. N129, Calibration 0.9 (1.15), To 1.52, Corrected Reading Heat Peak 1670, Lambda 258; Readings indicate bright conventional cadmium is not safe on 4340 steel.]

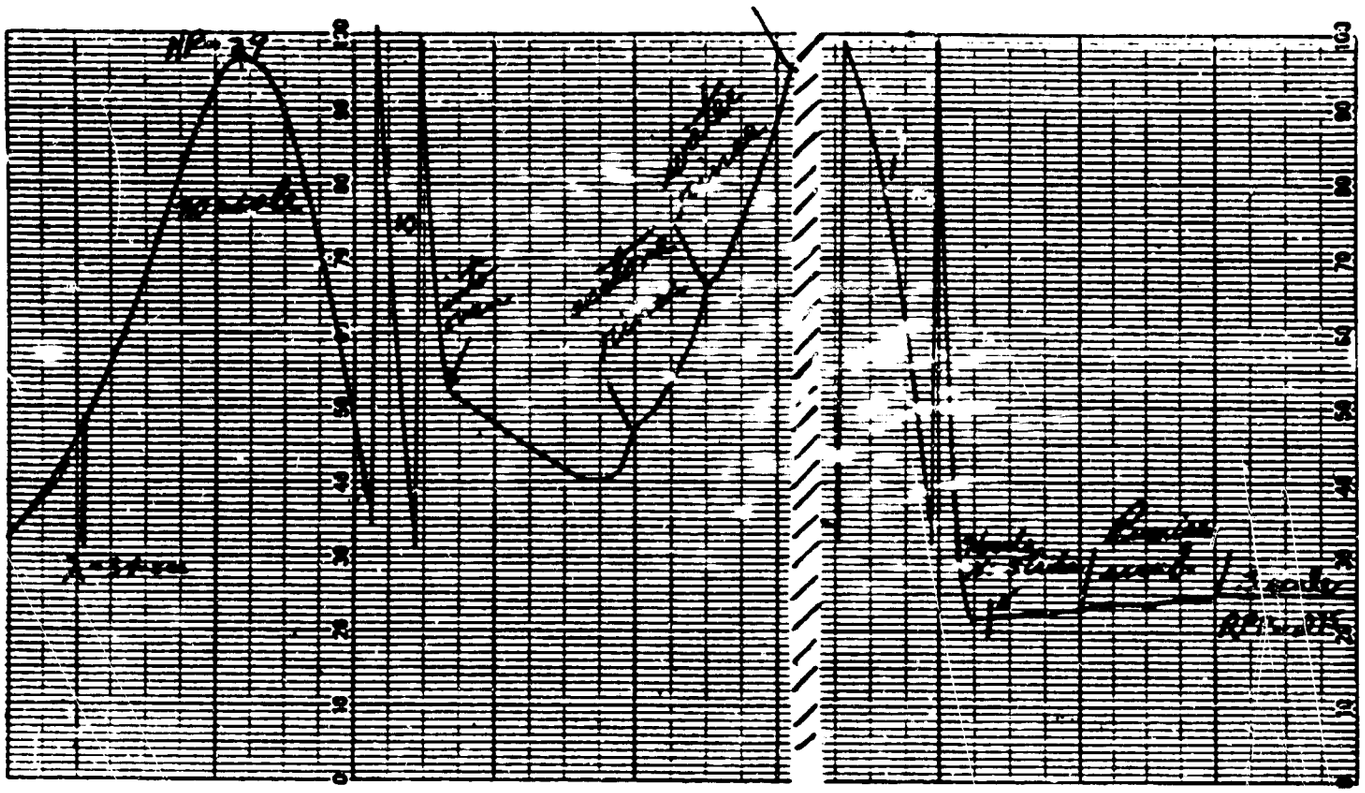

FIGURE 18. WOOD'S NICKEL STRIKE, 3-MINUTE PLATE AT 100 AMPS/SQ FT [Probe No. N71, Calibration 0.67 (1.52), To 1.52, Corrected Readings Heat Peak 37, Lambda 26; Readings indicate Wood's nickel strike is safe on 4340 steel.]

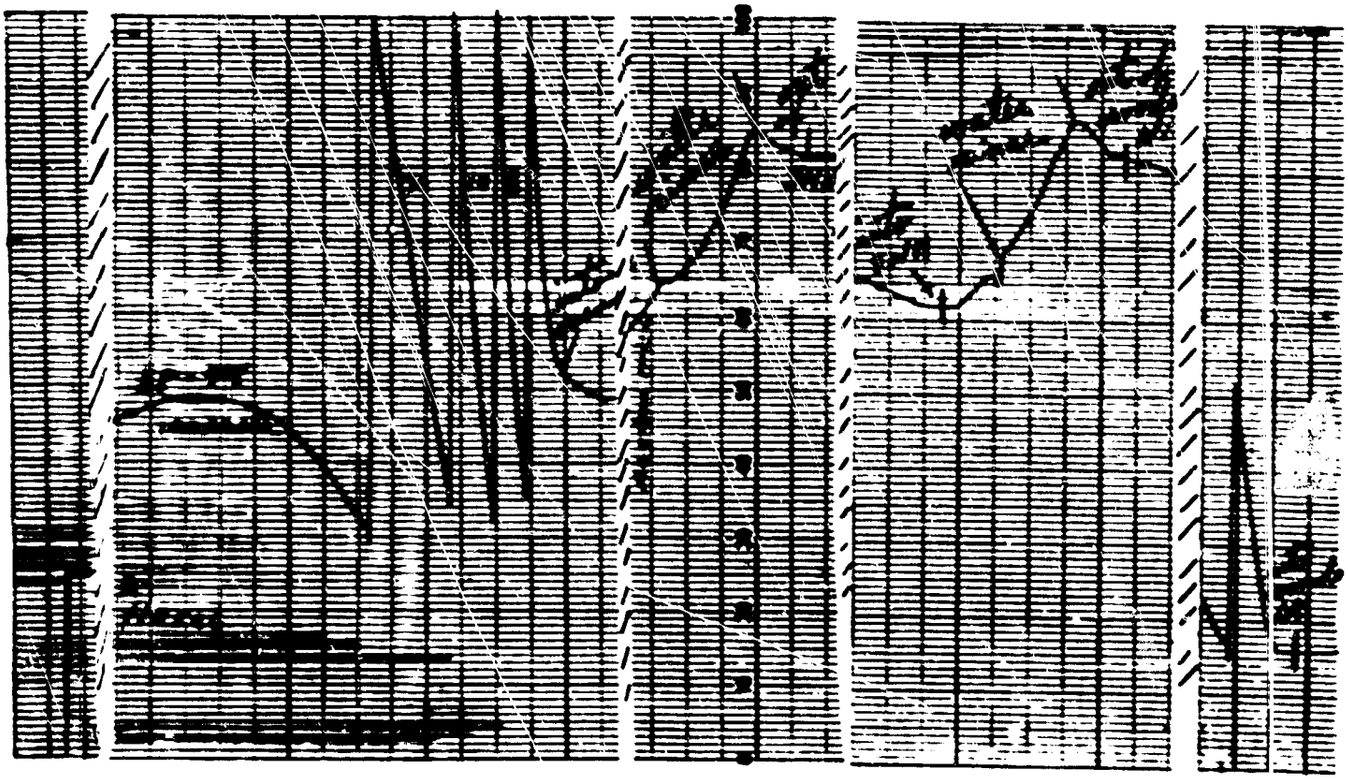

FIGURE 19. HARD SULFAMATE NICKEL, 15-MINUTE PLATE AT 50 AMPS/SQ FT AND WOOD'S NICKEL STRIKE, 3-MINUTE PLATE AT 50 AMPS/SQ FT [Probe No. 148, Calibration 0.28 (2.6), To 151, Corrected Heat Peak 157, Lambda 46; Readings indicate hard sulfamate nickel with Wood's nickel strike is safe on high-strength 4340 steel.]

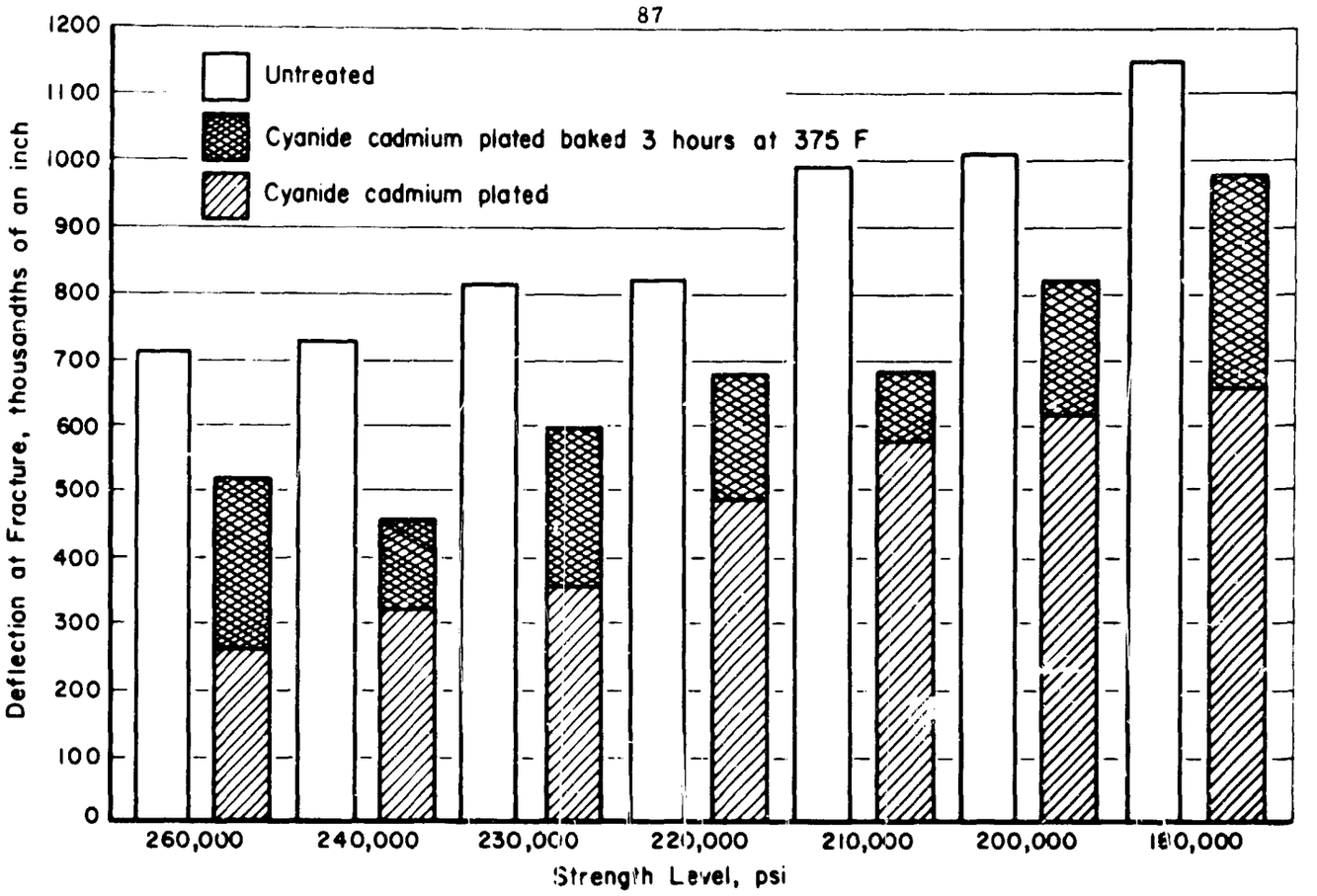

FIGURE 20. EFFECT OF CYANIDE CADMIUM PLATING ON 4340 STEEL AT VARIOUS STRENGTH LEVELS

notch significantly reduces fatigue strength; for SAE 4340 (280,000 psi) sheet-flexure specimens, cathodic charging in (0.025N NaOH with 0.20N NaCN) reduced the notched fatigue strength to 45 percent of the untreated notched control (35 ksi to 19 ksi), whereas no effect was found in unnotched specimens. A lesser effect (30 percent loss) of cadmium deposited from a cyanide bath was shown for H-11 type steel (280,000 psi). A lesser effect on rotating-beam fatigue test H-11 (280,000 psi) specimens was shown, the deposit from a cyanide cadmium bath caused a reduction of about 20 percent (45 ksi to 33 ksi). It appears that the effect of the notch is to induce local yielding with accompanying residual tensile stress which provides the stress condition for crack initiation in the presence of hydrogen with growth as the result of load applications.

RESIDUAL TENSILE STRESSES

Experience has indicated that it is impractical to insure that all areas of a part are free from residual tensile stresses which, although they might be of sufficiently low magnitude so as not to induce cracking during exposure to chemical and electrochemical pretreatment and plating processes, with superimposed service stresses could result in hydrogen embrittlement failure. Processes such as stress relief prior to processing and mechanical working such as shot peening appear to eliminate this factor. But this is not necessarily the case.

Considering thermal stress relief, the maximum temperature at which this can be accomplished is obviously the tempering temperature; however, for complex parts, the maximum may not be entirely adequate and other factors become important.

(1) In many cases, the stress analysis used in design of the part does not adequately reflect all of the critical load conditions, so that minor deformation may take place with attendant sustained stresses.

(2) In the case of aircraft, hard landings can also induce minor deformation with areas developing sustained tensile stress.

(3) Mismatch of mating parts is not an uncommon situation to add to the problem.

Considering shot peening and other mechanical methods of surface work; although the condition of the surface resulting is optimized with regard to hydrogen effects, a balancing sub-surface residual tensile stress exists. Although generally this condition may not be sufficient to cause hydrogen embrittlement, when significant stresses are induced for the reasons discussed in connection with residual stress, they may also be factors.

The significance of surface and sub-surface sustained tensile stresses is further enhanced by another intrinsic factor; namely, the extreme notch sensitivity of the materials under concern. As others will note, the critical crack size for catastrophic failure being of such small size, existing crack detection methods make their detection essentially impractical. In view of this situation, it appears to be prudent to adopt pretreatment and coating methods for ultrahigh-strength steels which avoid such an array of problems, which approach has been taken by the Bureau of Naval Weapons.

Dry mechanical blasting methods are prescribed to prepare surfaces where either spray-metallized aluminum or vacuum-deposited cadmium are specified as the metallic coating. Generally, parts are required to be coated with an organic finish system. Where the coating is functionally acceptable, the spray-metallized system comprises a thickness of 0.003-0.005 inch followed by a chemical conversion coating, one coat of wash primer, one coat of epoxy primer, and one or two coats of epoxy topcoat. The cadmium vacuum deposit is specified to be 0.0003- to 0.0005-inch thick, and the same organic finish system as the spray-metallized aluminum is used, except that the chemical conversion coating is omitted. Experience to date indicates that adhesion problems can develop if scrupulous cleanliness is not obtained.

With regard to vacuum-deposited cadmium coatings, it is noteworthy to report that significant extension in usage has occurred not only for steels heat treated above 240,000-psi tensile strength but to steel parts of lower strength level. Current requirements in Federal Specification QQ-P-416 require that for parts which require a baking treatment (minimum four hours 375 ± 25 F), hardness Rockwell C 40 and above, that sustained load tests of parts shall be accomplished to insure freedom from hydrogen embrittlement damage. In consideration of these requirements, a number of manufacturers have found it to be economical to adopt vacuum-cadmium for parts in the 220-240,000-psi tensile strength range. In fact, experience in one installation indicates costs close to electrodeposition. Problems associated with spray-metallized coatings appear to be more difficult to cope with, since geometric factors are of greater significance; optimum adhesion is obtained when the coatings are applied to the exterior surface of regular cylindrical parts; flat surfaces can be expected to present adhesion problems. There is, however, a good solution to the adhesion problem; namely, the use of an undercoat of spray-metallized molybdenum of the order of 0.0001- to 0.0003-inch thick. For reasons as yet unknown, the molybdenum establishes what is in effect a solid-state bond with the substrate and promotes a solid-state bond with metals subsequently applied. There is, however, a penalty paid in that a severe reduction in fatigue properties results (30-40 percent reduction). Fortunately, shot peening prior to application of the molybdenum avoids this loss. There are indications that significantly better coating characteristics may be obtained using other application methods such as plasma-spray. This technique is currently being examined by the Bureau of Naval Weapons.

There is another significant advantage in the use of the spray-metallized aluminum; currently 450 F is the temperature limitation imposed on cadmium usage, whereas aluminum coatings generally can be used up to about 900 F. This limitation is applicable to aluminum applied by the vacuum method. Insofar as is known, the upper limit for use of the molybdenum-aluminum coating system has not been investigated.

Aluminum deposited by other methods, such as decomposition of metallo-organic compounds and in pigments in inorganic and organic binders is also receiving attention. As pigments in silicone resins the coatings have been used with questionable success; cycling from ambient to operating temperature apparently affects adhesion, and flaking results. Applications which experience minimum thermal shock have greater prospect of success.

Recent developments in the ceramic-type binders appear to offer much greater prospect of avoiding the deficiencies that exist in organic and other inorganic type aluminized coatings.

Aluminum coatings applied by thermal decomposition of metallo-organic compounds are also being investigated. Results to date appear very promising. The most interesting developments in these areas are proprietary processes and have application temperatures which are closely compatible with tempering temperatures for ultrahigh-strength steels.

Ceramic coatings should not be overlooked as an area of future development. The major deficiency that exists in this area is the comparatively high firing or maturing temperature. Recently developed coatings which have satisfactory properties have the capability of being applied at about 1000 F. In connection with ceramic coatings and metallo-ceramic coatings, electrophoretic and electrostatic application of the uncured material in uniform and precisely controlled thicknesses appears to be promising.

DISSIMILAR METALS

It is fortunate that the metallic coatings which are satisfactory, galvanic-wise, for the protection of high-strength steels are generally compatible to an acceptable degree with the materials with which they are generally in contact. However, as is the case with coated high-strength steels themselves, if a reasonable life is expected, there should not be any attempt to use them in contact with these materials in any application where continuous exposure to liquid corrosive media is expected. Further, articles which are part of an exterior structure should have a suitable elastomeric installed at faying surfaces and at joints to preclude entry and retention of fluids; fasteners should be installed with wet zinc chromate primer to accomplish the same objective. It is to be noted also that the same procedures should generally be followed when even similar materials are used, including corrosion-resistant steels, although in the case of the latter where mechanical features and temperatures preclude use of available organic materials, nickel coating of the order of 0.0005-inch thickness is generally satisfactory. However, for specific compositions, tests simulating the temperature-corrosion environment should be conducted to insure adequacy. For example, in the case of AM-355, electroless nickel has been found to prevent corrosion of the substrate which would otherwise occur.

In connection with nickel deposits, including electroless nickel, if fatigue properties are important, the exposure of coated parts to elevated temperature can reduce fatigue strength, even though room-temperature properties before exposure are unaffected.

Although this paper is intended to cover only corrosion protection, it is fitting to mention briefly a related area; namely, wear protection. The most commonly used material is electrodeposited chromium, 0.002-inch minimum thickness. It appears to be the only electrodeposited or electroless coating which can be applied to high-strength steel which responds to the usual four hours at 375 ± 25 F hydrogen-relief baking treatment. However, as with nickel coatings, chromium can significantly affect fatigue properties. Shot peening prior to plating is effective in preventing such loss. Tests conducted at the Aeronautical Materials Laboratory have also shown that shot peening after plating has the same beneficial effect. Figure 21 shows the effect of plating and of shot peening on the S-N curves. It is worthy of note that two other significant benefits have been derived from post-plate peening:

(a) Corrosion protection afforded by the chromium is significantly improved
(b) Where the coated surface is a seal surface in a high-pressure fluid system, a significant reduction is obtained in the incidence of leakage, which is found frequently and is attributed to cracks in the deposit which exist and grow or develop when the system is pressurized.

Recent tests indicate that post-plate peening of electroless nickel coatings also prevents loss in fatigue properties.

In past investigations of cleaning, friction, adhesion, corrosion prevention, and other studies, or uses of the surface properties of metals, it usually was assumed that a final solvent cleaning or degreasing of a surface was satisfactory, provided that a sufficiently pure or volatile solvent was used. Bewig and Zisman,[8] show that this supposition is incorrect even if the solvent is nonpolar, and is capable of greatly confusing the experiments. Where complete freedom from absorbed organic material is desired, it is better to avoid using any organic solvent in the last stage of cleaning the solid surfaces.

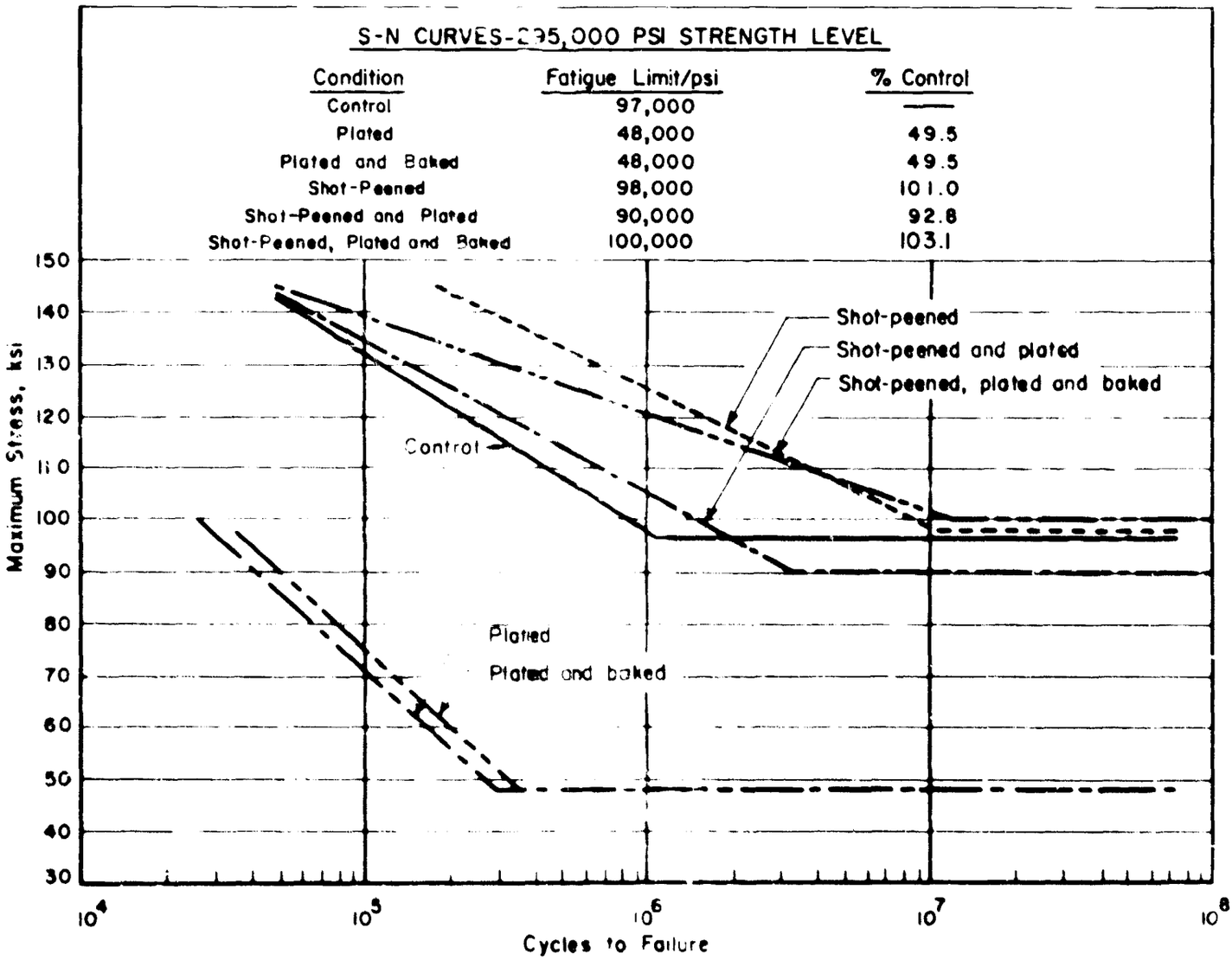

FIGURE 21. THE EFFECT OF SHOT PEENING ON THE FATIGUE STRENGTH OF PLATED HIGH-STRENGTH 4340 STEEL

In general, the neglect of the effects of: (a) the polarization induced in the solvent by the metal absorbing surface, (b) the retention of a residual film by the solid surface after evaporation of a pure solvent, and (c) the conditions required to avoid mixed film formation, are all sources of difficulty to be avoided in research in this area.

From the scientific viewpoint, the kind of knowledge needed for understanding corrosion processes is directly dependent upon knowledge of solid surfaces. Problems in the corrosion area may be expected to have solutions benefitted from this knowledge. The attention this field is receiving from physicists using field-ion and field-electron microscopy and low-energy electron diffraction provides this promise. Although results to date are fragmentary, they are providing information not previously available. For example, Reference (9) reports that using field-electron emission microscopy, G. Ehrlich at General Electric Company and Robert Gomer at the University of Chicago have investigated what happens when a hydrogen atom attaches itself to a surface, for example, when the gas is allowed to be selectively absorbed on one side of the tip of a silicon surface and the temperature is raised, it migrates across the tip; these studies show that the temperatures for migration vary with the crystal plane over which the atoms move; on some planes the atoms move easily, on others they migrate only at temperatures close to the desorption temperature.

Low-energy electron-diffraction studies are providing an even more impressive insight to the nature of solid surfaces. H. E. Farnsworth and his associates at Brown University have found that the arrangement of atoms on the surface of semiconductors is not the same as that in the bulk material; the regular atomic lattice apparently stops about two atomic layers below the surface; the top layers have another structure which is different for each crystal face and depends on the method used to clean the surface; absorbed oxygen, however, eliminates this disarray.

L. H. Germer and A. U. MacRae of Bell Laboratories in similar studies with nickel have shown that absorbed oxygen promotes disarray; absorption of a fractional monolayer of oxygen caused the nickel atoms in the surface to migrate to new positions, which took place at room temperature. When Farnsworth studied absorption of oxygen on nickel, he found that when the surface oxygen reached a certain concentration, the surface is essentially nickel and the oxygen apparently diffused inward. Other studies indicate that the atomic spacing between surface atoms and the second layer is about 5 percent greater than the spacing between bulk atoms.

If one may be so bold as to extrapolate this information to the heterogeneous materials under consideration, a possibly more satisfying insight may be presented. The findings by Farnsworth with regard to rearrangement of structure and the differences noted for each crystal face suggest that upon exposure to a corrosive environment, such a condition will add to the usual heterogenity to permit the establishment of local anode-cathode cells, and the nickel may also be useful in explaining the requirement for insuring ready access of stainless steel to a ready source of oxygen to maintain corrosion resistance.

REFERENCES

(1) Hildebrand, J. F., "Stress Corrosion Cracking of High Strength Nickel Alloys for Aircraft Applications", Materials Protection, 9 (3), 36 (1964).

(2) Vlannes, P. N., Strauss, S. W., and Brown, B. F., "Electroplating Baths for Ultra High-Strength Steels, Part I, Use of Aliphatic Amino Acids in Cadmium Baths to Reduce Hydrogen Embrittlement", U. S. Naval Research Laboratory Report 4906 (March 1, 1957).

(3) Glass, A. L., "A Radiochemical Investigation of the Mechanisms of Formation of Cyanide Films on Steel Components in Alkali-Cyanide Electroplating Baths", U. S. Naval Air Engineering Center, Aeronautical Materials Laboratory, Part I, Report NAMC AML 1137 (August 23, 1960); Part II, Report NAMC AML 1253 (June 26, 1961); and Part III, Report NAMC AML 1664 (April 22, 1963) (with E. Taylor).

(4) Glass, A. L., and Taylor, E., "A Radiochemical Investigation of the Absorption of Amino-n-Butyric Acid on Steel Components in Ammoniacal Electroplating Baths", U. S. Naval Air Engineering Center, Aeronautical Materials Laboratory, Report NAMC AML 1970 (June 10, 1964).

(5) American Society for Metals, Metals Handbook Volume 2, Appendix II, 416 (1964).

(6) Devanathan, M. A. V., Stachurski, Z., and Beck, W., "A Technique for the Evaluation of Hydrogen Embrittlement Characteristics of Electroplating Baths", J. Electrochem. Soc., 110, 886 (1963).

(7) Beck, W., "Effect of Cathodic Charging and Cadmium Plating on the Fatigue Behavior of High Strength Steels", Electrochem. Tech., 2, 74 (1964).

(8) Bewig, K. W., and Zisman, W. A., "Surface Potentials and Induced Polarization in Nonpolar Liquids Absorbed on Metals", U. S. Naval Research Laboratory Report 6068 (June 19, 1964).

(9) Lynch, C. J., "Solid Surfaces", International Science and Technology, No. 20 (August, 1963).

STRESS-CORROSION CRACKING AND CORROSION FATIGUE OF HIGH-STRENGTH STEELS

by

B. F. Brown*

ABSTRACT

Stress-corrosion cracking is a problem with low-strength steels only in a very few special environments; it is seldom a problem with austenitic steels at room temperature, and even at elevated temperatures it is a problem only if halides or caustic solutions are present. By contrast, many high-strength steels are highly susceptible to stress-corrosion cracking at room temperature in many "wet" environments, including humid argon and distilled water. Substantial advances are needed to properly evaluate the susceptibility of high-strength steel to stress-corrosion cracking, but the indications from present test methods are that many heat-treated steels are susceptible at strength levels as low as 150-175 ksi yield strength, in reasonable environments, and that the susceptibility increases with increasing yield strength. In approximately the same strength range, these steels also begin to exhibit susceptibility to hydrogen embrittlement, so that cathodic protection against stress-corrosion cracking cannot be used in seawater, and inorganic zinc coatings are unsuitable. A new requirement is thus imposed upon coatings for at least some of these steels: the coatings must be more than corrosion barriers, they must be vapor barriers as well.

Cathodic protection measures (even where they are otherwise feasible) are not attractive to combat corrosion fatigue in high-strength steels, again because of the intrusion of hydrogen embrittlement. In the atmosphere, fatigue-crack propagation rates of the AISI 4340 type steel are sensitively affected by humidity. This environmental effect may also be accompanied by a tendency for the periodic fatigue markings to be replaced by an intergranular-cracking mode resembling that of hydrogen embrittlement or stress-corrosion cracking in this type of steel.

The general approach is outlined which is believed necessary to design studies of stress-corrosion cracking and corrosion fatigue in a way which is both manageable experimentally and meaningful in terms of results.

INTRODUCTION

We tend to be conditioned, largely by experience with austenitic stainless steels and with aluminum alloys, to assume that stress-corrosion cracking (SCC) is typically a slow process and that its effect, however inconvenient or costly, are not expected to be sudden and violent. By way of illustration, SCC in an austenitic stainless steel pressure vessel will lead typically to a leaking vessel. But in high-strength steels such as are used for or are contemplated for rocket-motor cases, SCC can cause very small flaws to grow during hydrostatic testing to produce thumbnail-shaped cracks such as in Figure 1, and the consequence of such a crack in these steels under high stress is not merely a leaking pressure vessel but a shattered one (Figure 2).

FIGURE 1. STRESS-CORROSION CRACK (THUMBNAIL-SHAPED AREA) FORMED DURING HYDROSTATIC TESTING OF A THIN-WALLED PRESSURE VESSEL OF HIGH-STRENGTH STEEL, NUCLEATING FAST RUNNING FRACTURE (CHEVRONS)

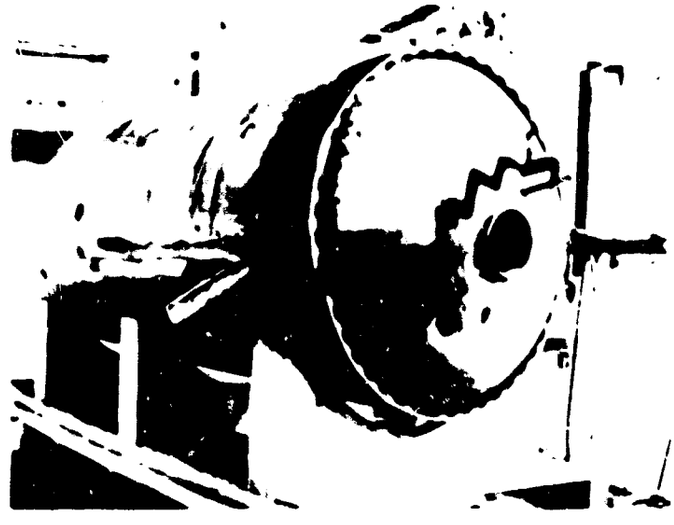

FIGURE 2. PRESSURE VESSEL SHATTERED IN HYDROSTATIC TEST

In terms of fracture mechanics, the size of a stress-corrosion crack or a corrosion-fatigue crack required to cause catastrophic shattering of a typical austenitic stainless steel component under a reasonable working stress is enormous,

*U. S. Naval Research Laboratory, Washington, D. C.

whereas the corresponding critical-size crack for a structure made of high-strength steel may be only a small fraction of an inch. Because of this, SCC and corrosion fatigue may play a critical role in the utilization of high-strength steels, as contrasted to the essentially maintenance-economy role which wastage corrosion plays in the utilization of conventional structural steels.

Corrosion fatigue is far more complex than stress-corrosion cracking, but since all the concepts of SCC are applicable to corrosion fatigue, both phenomena are covered in the present review.

STRESS-CORROSION CRACKING

Introduction

The rate at which the surfaces of unalloyed or low-alloy steel recede by general corrosion or by pitting in quiescent seawater is thought to be limited by the rate of diffusion of oxygen in the water. The rate at which the advancing edge of a stress-corrosion crack in high-strength steel in salt water recedes from the original surface is faster by some 6 orders of magnitude than the rate of pitting or general corrosion, and the phenomenon must, therefore, be regarded as a separate one and not merely the general process restricted to a narrow zone. The rate of propagation of stress-corrosion cracks in the high-strength steels is comparable to that for austenitic stainless steels, and the processes in the two classes are believed to involve electrochemical reactions. Here the similarity largely ends, and the differences in the phenomena in the two steels are noteworthy:

(1) The austenitic stainless steels rarely crack at room temperature, whereas the high-strength steels do so readily.

(2) Specific ionic species (halides or hydroxides) are believed necessary to crack the austenitic steels, but not the high-strength steels.

(3) The austenitic stainless steels are not susceptible to hydrogen embrittlement in the same sense that the high-strength steels are.

(4) The austenitic stainless steels are notch-tough, whereas the high-strength steels are notch-sensitive.

Points (1) and (2) are self-explanatory. Points (3) and (4) will be discussed in subsequent sections. Considerable progress has been made in the development of concepts of fundamental mechanisms[1,2]* and of remedial measures for SCC of the austenitic stainless steels, but because of the four important differences cited, it would appear unwise at this time to assume that these concepts apply to the high-strength steels.

*References are given on page 102.

Basic Concepts

If a specimen of high-strength steel undergoing stress corrosion has impressed upon it very small electrical currents, the cracking behavior is altered. This can be explained by the mechanism shown in Figure 3, which depicts metal dissolving anodically at the advancing tip of the crack and a cathodic reaction (the reduction of hydrogen in this illustration) occurring at another location. For these reactions to occur, electrons must move from the anodic area through the metal to the cathodic area, and there must be a movement of ions in the electrolyte to complete the electrical circuit. The fact that small extraneously impressed electrical currents (not shown in Figure 3) either accelerate or retard cracking, depending upon their direction, is interpreted as either intensifying or opposing the natural electrochemical process.

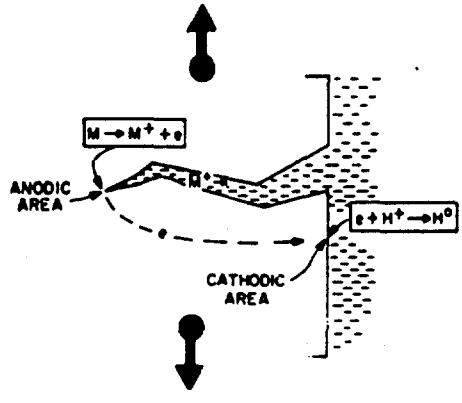

FIGURE 3. STRESS-CORROSION CRACKING (SCHEMATIC)

The hydrogen which is shown being reduced in Figure 3 introduces a serious impediment to the practical use of the high-strength steels in aqueous solutions. This is the phenomenon of hydrogen embrittlement, to which the high-strength steels tend to be acutely susceptible. Hydrogen embrittlement may take many forms, but perhaps one of its simplest and most characteristic forms is that of delayed fracture (sometimes unfortunately called "static fatigue"). This is illustrated by an experiment in which sharply notched round bars were simultaneously charged with hydrogen and electroplated with cadmium (which effectively seals in the hydrogen). The specimens were removed from the electroplating bath, thoroughly rinsed and dried, and stressed in stress-rupture racks at various percentages of the tensile strength of the unplated notched bar. In the triaxial zone just under the root of the notch, a hydrogen-embrittlement crack nucleates and grows (under constant load) until it achieves critical size and the remaining section ruptures. The time for this slow crack growth to critical size (time-to-fracture) as a function of stress is shown in

Figure 4. Note that in sharply notched bars this form of hydrogen embrittlement is observed at a low nominal stress for this moderately high-strength steel.

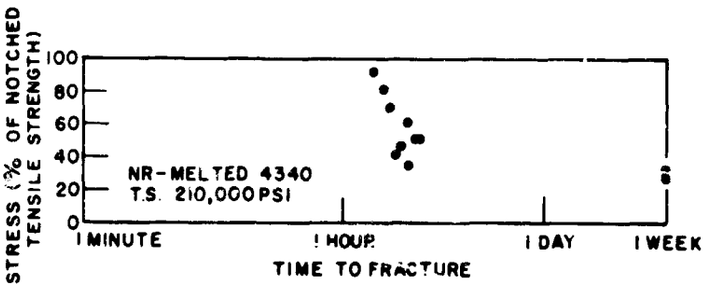

FIGURE 4. DELAYED FRACTURE OF STEEL CONTAINING HYDROGEN FROM A CADMIUM ELECTROPLATING PROCESS[3]

The present state of the theory of hydrogen embrittlement has been reviewed recently by Tetelman in a paper[4] which is recommended to the interested reader.

Steel corroding in an aqueous environment can absorb hydrogen which may presumably cause the steel, if under suitable stress and if sufficiently susceptible, to crack not directly from the anodic reaction but from the hydrogen reduced at the cathodic areas, as depicted in Figure 5. The cathodic reaction in Figure 3 is depicted as occurring outside the stress-corrosion crack, but there is no reason why it could not occur within the crack, and in fact this has been demonstrated to occur.[5] This suggests the possibility that under the right electrochemical conditions, SCC may be accompanied by hydrogen-embrittlement cracking to produce a dual cracking process, as depicted in Figure 6. (It is conceivable that this dual process can be further complicated by purely mechanical fracturing of limited areas of uncracked salients or islands of metal partially or wholly surrounded by a stress-corrosion crack.) Because of the possibility of either or both cracking modes in many aqueous solutions, the non-committal term "environmental cracking" has been used by some to cover either or both SCC and hydrogen embrittlement, and it appears to be an admirable choice of terms at the present stage.

We are thus dealing with a more complicated situation on a microscopic scale in the cracking of high-strength steel than is the case with other metals, particularly the austenitic steels. The situation is also more complicated on the macroscopic scale because of the notch-sensitivity effect, for reasons which will become evident in the following discussion.

Several procedures are in current use to evaluate the notch sensitivity (or its inverse, notch toughness) of high-strength steels, but one which is particularly instructive to the present subject makes use of a strip tensile specimen into which

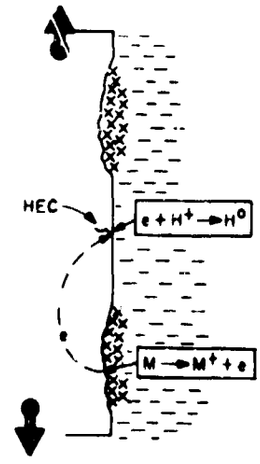

FIGURE 5. HYDROGEN-EMBRITTLEMENT CRACKING (HEC) FROM AQUEOUS CORROSION (SCHEMATIC, CONJECTURAL)

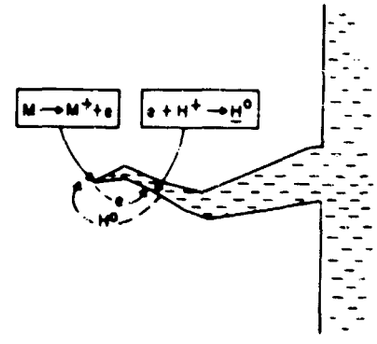

FIGURE 6. DUAL CRACKING PROCESS (SCC AND HYDROGEN EMBRITTLEMENT), (SCHEMATIC, CONJECTURAL)

a sharp transverse crack is inserted. Such specimens may be pulled to rupture over a range of temperatures and the data may then be reported as the net fracture stress. Typical data for a steel heat treated to be brittle in one case and tougher (at room temperature) in the other case are shown in Figure 7. Note that with decreasing temperature there is a transition from high toughness (high net-fracture stress) to low toughness. Not only can this transition from ductile-to-brittle behavior be shifted by changes in heat treatment, as shown by the two curves of Figure 7, but it is also shifted by changes in thickness of specimen for purely mechanical reasons: An increase of 20 mils in thickness caused the ductile-to-brittle transition of one steel to increase 100 Fahrenheit degrees.[7]

Let us now see what the foregoing extracts from notch-sensitivity technology imply to macroscopic phenomena in SCC testing:

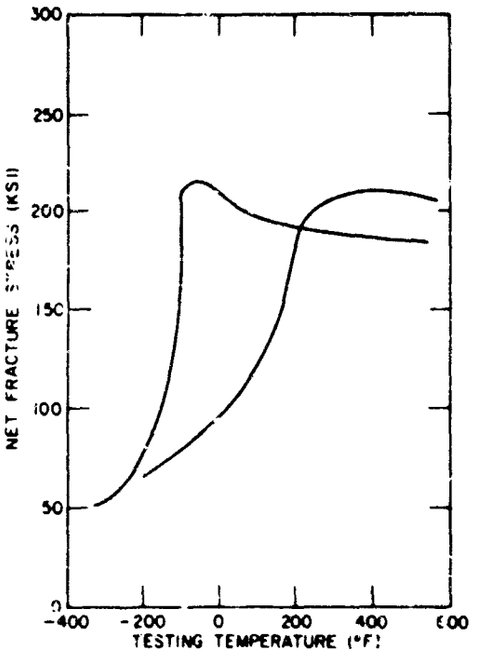

FIGURE 7. EFFECT OF TESTING TEMPERATURE ON THE NET FRACTURE STRESS OF MODIFIED TYPE 422 STEEL TEMPERED AT 900 F (482 C) (CURVE ON RIGHT) AND AT 1050 F (566 C) (CURVE ON LEFT)

After Reference 6.

(1) If one steel is more notch sensitive than another (under test conditions), a small corrosion crack (or even a pit or crevice-corrosion area with no stress-corrosion crack at all) may trigger the fast fracture (brittle fracture) in the notch-sensitive steel, whereas a much larger stress-corrosion crack would be necessary to cause the tougher steel to rupture. Thus the more notch-tough steel may require a longer time to rupture, not necessarily because of a slower rate of SCC but because the SCC process must produce a longer crack before it is of the critical size to set off the terminal, purely mechanical, fracture. (The separation of the nucleation, stress corrosion, and 'fast' fracture of a specimen is clearly evident in Figure 8. These are the two halves of a single specimen having a notch on one side which was extended by fatiguing before the test to the point marked by the smaller arrow. This fatigue crack provided sufficient stress intensity to cause the stress-corrosion crack to propagate to the second, larger, arrow; at this point the remainder of the specimen ruptured by fast fracture. Careful study will reveal poorly defined chevron markings in the fast-fracture area pointing back to the origin of fast fracture. These are similar to those which appear more clearly in Figure 1, and they positively identify fast, purely mechanical, fracture. The borders on either side of the fast fracture are known as shear lips or shear borders, and they are formed by purely mechanical rupturing, although under some circumstances a stress-corrosion crack may tunnel a long way, invisible on the surface until the surface layers tear apart to form the shear lips.)

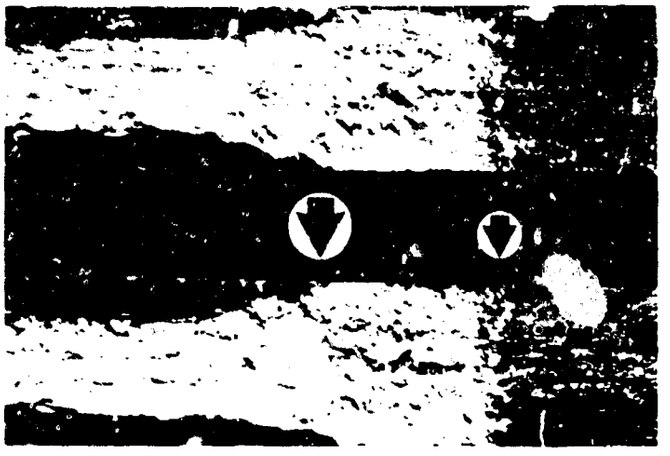

FIGURE 8. STRESS-CORROSION TEST FRACTURE SURFACES (MACHINING HALVES OF ONE SPECIMEN)

Specimen was fatigue-cracked to the smaller arrow before testing; stress-corrosion crack propagated to larger arrow, remainder of section ruptured by fast fracture. Specimen thickness, 1/8 inch.

(2) From a purely geometric cause, a stress-corrosion crack may not have to be nearly as extensive to set off fast fracture in a thick specimen as in a thin one. Furthermore, there is some evidence that a stress-corrosion crack may be very difficult to propagate in a very thin specimen of high-strength steel, again for a purely geometric reason.

(3) Because of the transition temperature effect, the length of crack required to trigger fast fracture is increased as the test temperature is increased in the transition range. If one attempts to measure a temperature coefficient of SCC by noting only total time-to-rupture, the two factors of SCC growth rate and notch-sensitivity effect oppose each other, and the data are meaningless at best.

The foregoing has been discussed at considerable length in order to emphasize for the newcomer to the subject the facts that hydrogen embrittlement can play an important role in the

micro-mechanism of cracking, and notch-sensitivity effects can play an equally important role in macroscopic phenomena in SCC tests of high-strength steels, whereas they can be safely ignored in most other metals, including the austenitic stainless steels.

Conventional Experimental Methods Used in SCC Tests

Most SCC testing of high-strength steels makes use of specimens of thin sections because these are usually available as mill products, they place small demands on loading fixtures, and they are very much like the specimens widely used for the testing of other metals. The specimens are, with exceptions which are as important as they are rare, unnotched. Typically, under exposure the specimens begin to develop pits or other localized attack*, and when one of these surface irregularities develops to sufficient depth and is in the right location with respect to the stress field, a stress-corrosion crack nucleates in the pit, or irregularity, and commences to grow at right angles to the maximum principal stress. Meanwhile other pits may initiate other cracks, the growth of which alters the stress field around every other growing crack in a complex manner. Eventually one crack will achieve critical size and the remaining section snaps in fast fracture (brittle fracture). A complete description of the cracking process would require a statement of the rate of nucleation and rate of growth of the stress-corrosion cracks, which would be a formidable task indeed where more than one crack is growing, and even more formidable if the specimen is "self-stressed" and therefore subject to relaxation during growth of the cracks. In view of the enormity of a complete description, therefore, it is not surprising that the results of such tests are reported simply as the total-time-to-rupture.

Let us see what this parameter means: The rate of propagation of fast (brittle fracture) is something like 10^{10} times the rate of propagation of a stress-corrosion crack, which in turn is roughly 10^{5} times as fast as the rate of pit growth. Even taking into consideration a wide difference in the total growth of a pit and a stress-corrosion crack (if indeed there is much difference, and in many instances seen by the author, there was very little difference), the total-time-to-rupture parameter is heavily weighted in terms of pitting rate rather than stress-corrosion-cracking susceptibility. The fact that multiple nucleation of stress-corrosion cracks is not a common occurrence is another hint that the total-time-to-rupture parameter is tending to measure the pitting rate, and that once the pit of favored location forms, the SCC and fast-fracture processes are so fast by comparison that the second-most-favored pit seldom has a chance to nucleate a stress-corrosion crack before the specimen has ruptured from the first crack.

Customarily the specimens used are strips bent in their most flexible direction, and as the fast fracture runs under the prevailing stress pattern, the chevron markings such as are evident in Figure 1 are not evident on the specimen fracture surface, and there may be no means whatever to distinguish between the extent of the stress-corrosion crack and the fast fracture.

Turning now to the sort of data which are being collected using the total-time-to-rupture parameter, Figure 9 shows all the SCC data on high-strength steels which the author found readily available for "reasonable" corrosive media (seawater, tap water, distilled water, and humid air or humid argon). The ordinate is plotted as time-to-failure, and the abscissa is the yield strength. From such a plot, in spite of (or because of) the scatter, we can draw certain conclusions: (1) Many tests are being run for hundreds or thousands of hours. (2) Either the susceptibility to SCC is not overwhelmingly controlled by yield strength, or the test procedure is faulty, or both. (Figure 9 includes data for

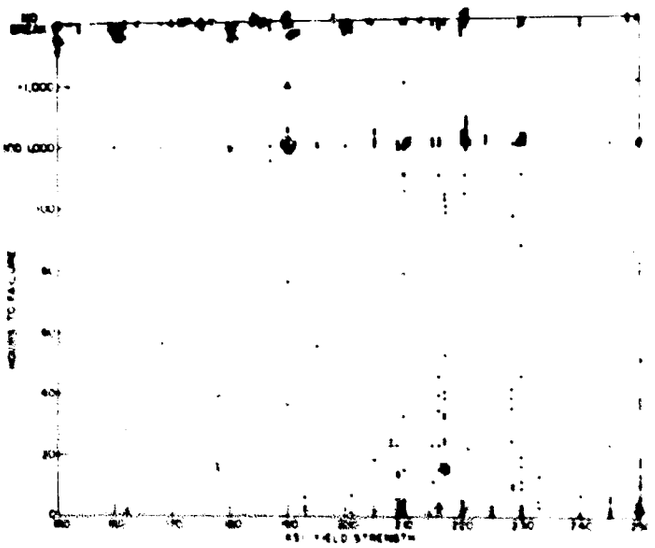

FIGURE 9. SUMMARY OF DATA ON STRESS-CORROSION CRACKING OF ALL CLASSES OF HIGH-STRENGTH STEEL USING TRADITIONAL PROCEDURES

Corrodents include seawater, NaCl solutions, tap water, distilled water, humid air, and humid argon.

*In the case of the stress-corrosion crack of Figure 1, small intergranular intrusions of oxide which probably formed during heat treatment apparently acted to nucleate the stress-corrosion crack.

martensitic, maraging, and precipitation-hardening steels, both stainless and non-stainless, but even identifying points on the graph according to steel class, no pattern emerged, with the possible exception that the stainless steels were somewhat more prone to show cracking. This is possibly due to their greater tendency to form pits.) (3) At yield strengths of about 175 ksi, many steels begin to show some tendency to cracking, and at 200 ksi and above their susceptibility may be acute.

There is no one corrodent which occupies the position in SCC tests of high-strength steels that boiling 42% $MgCl_2$ occupies in tests of austenitic stainless steels. Tap water, or 3% or 3-1/2% NaCl solution, distilled water, humid air or argon, and acetic acid solutions with or without NaCl and with or without poisons such as H_2S are among the more common corrodents.

Mechanisms

The first procedure used in attempting to distinguish SCC from hydrogen embrittlement was based on the position that the term SCC would be reserved for cracking which necessarily involved corrosion at anodic areas at the advancing tip of the crack, that is, the mechanism of Figure 3. Figure 10 shows the effect of small extraneously impressed electrical currents on the time-to-fracture for Type 410 stainless steel under the indicated conditions. The fact that a low level of cathodic current very greatly extends the breaking time was taken to indicate that the "natural" cracking process (in the absence of impressed current) is properly classified as SCC. At high current densities the specimens also failed after a short time; this was taken to be hydrogen-embrittlement cracking. (Note that one must work in the microampere/sq cm current density range to observe the effect. Note also in this and in similar plots reproduced in the present paper that at currents or potentials plotted toward the right, the specimen is more cathodic, which is opposite from the convention which Phelps and Loginow[9] used when they adopted this procedure to distinguish between the two cracking modes.)

Figure 11 shows the results of a similar study in a different medium. Here impressing even a small cathodic current decreases the breaking time, whereas anodic currents greatly extend life; this response was taken to indicate that in the "natural" case the failure occurred by hydrogen embrittlement.

Figure 12 shows the results of a similar study in still another medium; here impressed currents failed to change the cracking time, which might be interpreted as indicating either a dual process (cf. Figure 6) or that the process was not an electrochemical one.

These foregoing electrochemical analyses must be regarded as highly simplified. The

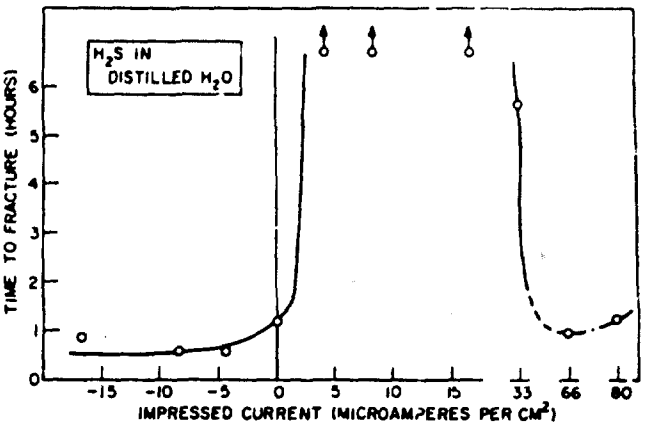

FIGURE 10. EFFECT OF IMPRESSED CURRENTS ON TIME-TO-FRACTURE OF A MARTENSITIC STEEL, CORRODENT AS NOTED[8]

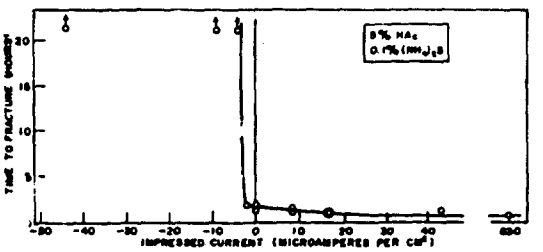

FIGURE 11. EFFECT OF IMPRESSED CURRENTS ON TIME-TO-FRACTURE OF A MARTENSITIC STEEL, CORRODENT AS NOTED[8]

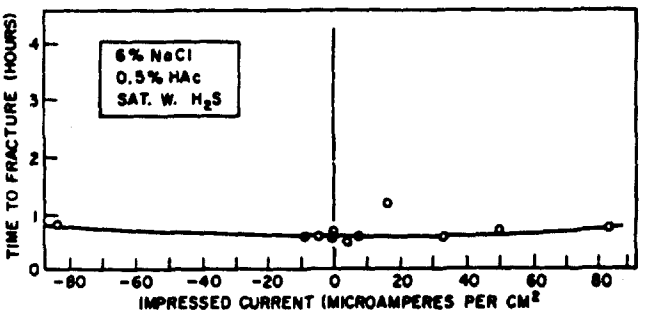

FIGURE 12. EFFECT OF IMPRESSED CURRENT ON TIME-TO-FRACTURE OF A MARTENSITIC STEEL, CORRODENT AS NOTED[8]

conclusions from them, however, are consistent with two subsequent observations: Conditions presumed by these analyses to cause SCC caused the measured potential to behave during cracking as if the cracking was occurring along an active path;[10] and conditions presumed to cause

hydrogen-embrittlement cracking caused hydrogen to permeate a thin membrane.[11] There is one somewhat disturbing note which must be added here, however. The most painstaking metallography, including fractography with the electron microscope, has thus far failed to disclose a metallographic difference between "pedigreed" fractures in high-strength steels produced by SCC, hydrogen embrittlement, and (in some instances) fast fracture, all of which tend to be intergranular with respect to the prior austenite. Not only has this been somewhat less than satisfying as far as looking for sharply different mechanisms is concerned, but it also sometimes impedes the satisfactory analysis of a service failure of a high-strength steel part.

Another set of experiments was performed somewhat similar to those of Figure 10 but with the following differences: The steel used was the hot-work die steel designated H-11 heat treated to a yield strength of 225 ksi, the corrodent was flowing seawater, the specimens were sharply notched bars, and they were carefully maintained under potential control (rather than current density control). The nominal stress on the notched section was 100 ksi which produces a stress intensity parameter K of about 21 ksi$\sqrt{\text{in.}}$. The results are plotted in Figure 13, from which the following can be concluded:

(1) Cracking in the "natural" condition was by SCC.

(2) Cathodic polarization to a moderate extent increased the life of the specimens; but somewhat more negative potentials (toward the right of the plot) caused rapid cracking by hydrogen embrittlement.

(3) Even with a geometry as simple as a notched cylindrical bar prepared in a machine shop with long experience in quality control over the notch acuity, and tested by personnel long experienced in electrochemical instrumentation, there was bad scatter on the two edges of the central "protected" zone. Furthermore, this zone is narrow, and it does not include the point (slightly to the right of -1.00 volts) which a sprayed or otherwise applied coating of zinc would cause any exposed area of steel to assume. One would conclude from this particular "map" that cathodic protection would not afford an engineering solution to the problem of using this steel in seawater

Such electrochemical mapping as in Figure 13 may well provide the quickest and easiest way to find whether cathodic protection methods are useful for service in a given bulk electrolyte

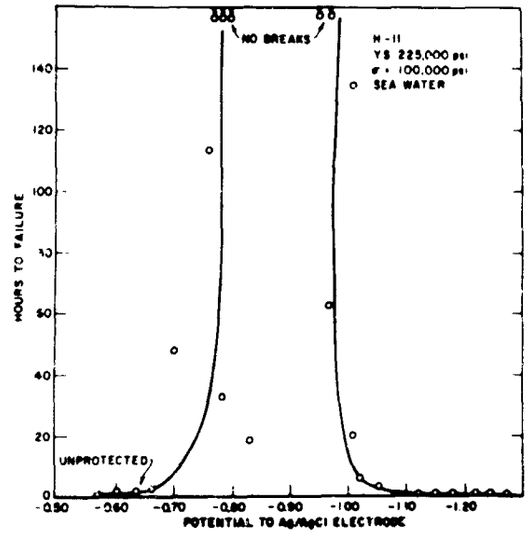

FIGURE 13. EFFECT OF ELECTROCHEMICAL POTENTIAL ON THE TIME-TO-RUPTURE (WALDRON)[12]

Unlike high-strength steels, ship-plate steels and submarine-hull steels now in use are not susceptible to either SCC or hydrogen embrittlement in the same sense that the high-strength steels are, and we can therefore apply cathodic protection to them to great economic advantage by combatting "wastage corrosion". This probably makes an additional desirable contribution which will be mentioned under the section on corrosion fatigue.

So much for stress corrosion cracking as it has been studied by more or less conventional means. We will return to the subject in a section on "Outlook" in order to get a preview of the problem as it appears in studies using recently developed test concepts, after a brief review of corrosion fatigue.

CORROSION FATIGUE

Corrosion fatigue might be regarded as the most general of all deterioration or failure modes because, if one wishes to be pedantic, he could point out that by going to various extremes of combinations of corrosion and fatigue conditions, one could get straight corrosion, straight SCC, straight fatigue, or anything in between. For the purposes of the present review, however, corrosion fatigue will be approached from the standpoint of stress-corrosion cracking. To all the complexities of this cracking mode, corrosion fatigue adds the further complication of the load-time profile, which can assume an infinite number of forms. Even if this profile is kept sinusoidal, there remain the variables of maximum load, average load, and frequency; and all the complexities of SCC--electrochemical potential effects, hydrogen embrittlement, and notch-sensitivity effects--are added to these. This formidable array of variables has undoubtedly been partly

responsible for the meager amount of traditional corrosion-fatigue data available on high-strength steels. From a practical point of view, there is limited justification for studying corrosion fatigue of a metal under conditions in which it fails rapidly under even static stress. The corrosion fatigue which is therefore of practical concern in the utilization of the high-strength-steels is not that experienced in the traditional bulk media such as salt water or tap water, but either that experienced in much more benign media (such as the atmosphere) or else in conditions of extremely low-cycle high-stress fatigue, as in repeatedly hydrostatically testing a pressure vessel. The fairly recent review[13] of conventional corrosion fatigue in general, while excellent for the low-strength steels, gives little guidance for the problem with the high-strength steels.

The purist might take the position that essentially all the fatigue data which have been taken in air are actually corrosion-fatigue data, because particularly for the high-strength steels the fatigue behavior in air of uncontrolled but reasonable humidity is appreciably different from that in a carefully controlled inert environment. That this difference is appreciable may be seen in the curves of Figure 14. This shows the crack-propagation rate in inches per cycle for specimens of AISI 4340 at a yield strength of 225 ksi fatigued in tension-tension at 6,000 cycles per minute. Note that at low-stress intensity (K = 20 ksi$\sqrt{\text{in.}}$) there is an order of magnitude difference in the rate in very dry air and the rate in air at about 80% relative humidity; but there is less of a difference at high-stress intensity (K = 60). The reason for this may be inferred from the macrographs of Figure 15. The fatigue crack initiated at the left of this figure and propagated toward the right of these Kahn-type (single-edge notch) specimens. The shear borders indicate approximately the end of the fatigue and the start of fast fracture. The "flame-shaped" central areas of the specimens fatigued in humid air are seen by electron fractography to be intergranular, whereas the lighter areas of the fatigue fracture tend to be transgranular. This is attributed to environmental cracking from atmospheric moisture occurring in the zone of maximum triaxiality. The gradual disappearance of this transgranular cracking mode toward the right is attributed to the inability of the environmental processes to keep pace with the fatigue fracturing as the lengthening crack raises the stress intensity.

Turning from atmospheric "corrosion fatigue" to the more conventional conditions of bulk electrolyte, we find that for mild steel undergoing high-speed rotate bending in salt water, the application of cathodic current of sufficient magnitude could in effect restore the air fatigue life, as shown in Figure 16. This might appear to offer a possible way to the utilization of high-strength steels under corrosion-fatigue conditions in an electrolyte of sufficiently high conductivity by

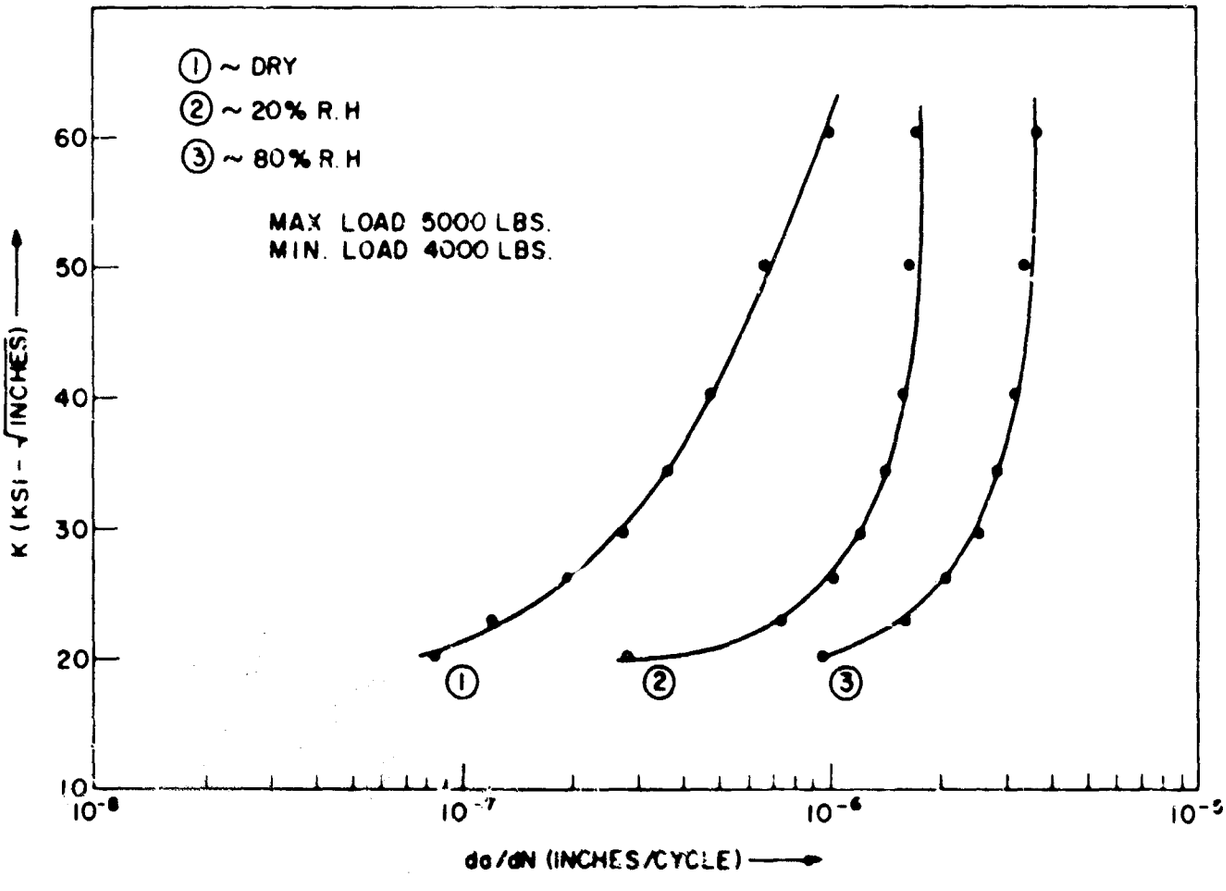

FIGURE 14. CRACK GROWTH RATE PER CYCLE (da/dN) FOR THREE SPECIMENS TESTED IN AIR OR DIFFERENT HUMIDITIES[14]

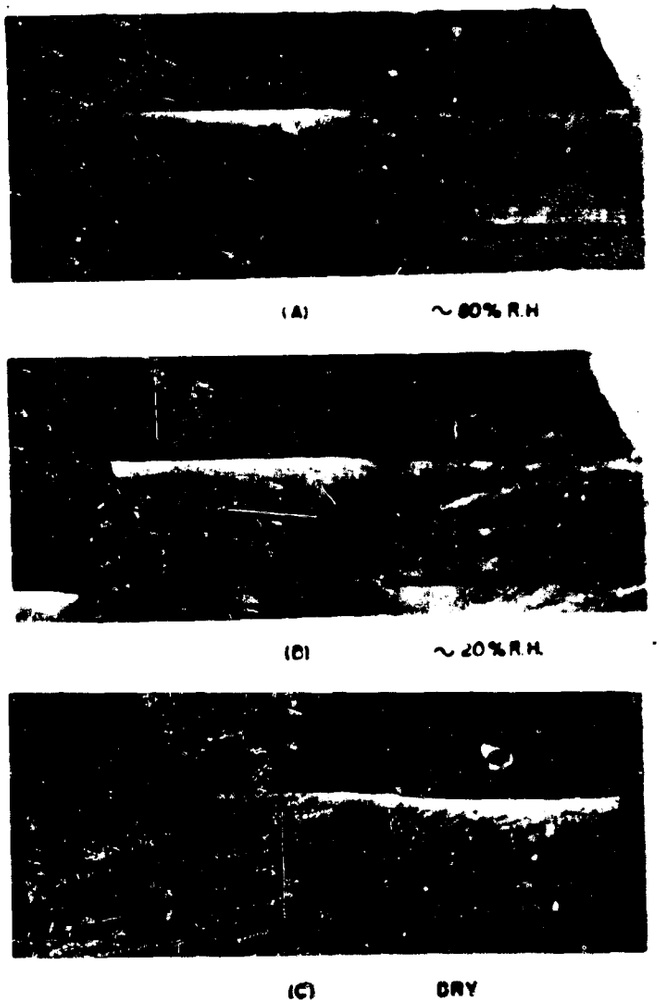

FIGURE 15. MACROSCOPIC APPEARANCE OF FRACTURES WHOSE GROWTH RATES ARE PLOTTED IN FIGURE 14[14]

Magnified 2.5X but reduced approximately 38 percent in printing.

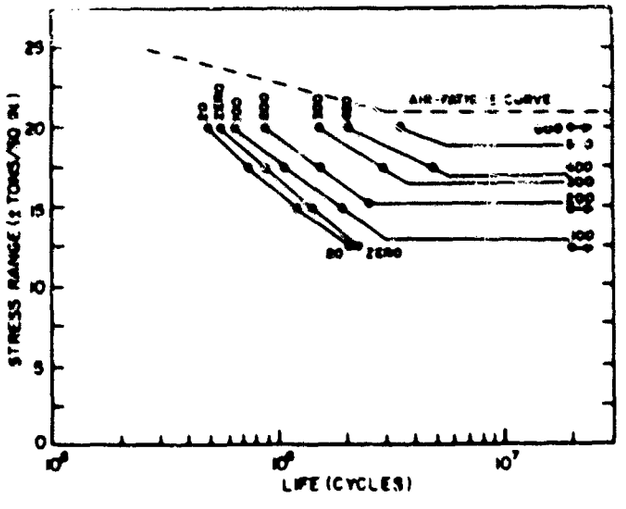

FIGURE 16. EFFECT OF IMPRESSED CURRENTS OF VARIOUS MAGNITUDES (NUMBER OF CURVES) ON THE CORROSION FATIGUE OF STEEL[15]

application of cathodic protection. This however, only succeeds if both the following conditions are met:

(1) There must be a full reversal of stress.

(2) The cycle rate must be high, something of the order of one or two thousand cycles per minute.

If both these conditions are not met, the cathodic currents to prevent the corrosion component of corrosion fatigue must, as a consequence of the thermodynamics of the $Fe-H_2O$ system, reduce hydrogen from the water, and the consequence of this is hydrogen embrittlement. This is not observed under complete reversal at high cycle rate because (according to present models of hydrogen embrittlement) there must be sufficient time for hydrogen to diffuse in the zone of triaxial tension ahead of the advancing crack front in order for it to contribute to the cracking process, and the compression half of the cycle must then in effect counteract the tension half. Under either (a) tension-tension programming (high or low speed, but lacking the compression half of the cycle), or (b) slow tension-compression, allowing time for the damage to be done during the tension portion of the cycle, hydrogen embrittlement is seen if hydrogen has access to the steel.

Figure 17 shows data on steel fatigued in reverse bending at 90 cycles per minute in salt solution. The stress-time profile was the same for all specimens, and the electrochemical potential was fixed at various levels ranging from the unprotected to the point of vigorous evolution of hydrogen; the number of cycles to complete failure was then recorded. These data show that for the limited number of conditions studied, the application of a small degree of cathodic protection (to, say, 0.8 volts to Ag/AgCl) improves the fatigue life to equal, or to at least approach, the fatigue life in air; but that at higher levels of cathodic protection the life falls off, in accordance with the model discussed above. (The same qualitative behavior has also been seen in mild steel which cannot have been much different in strength from that used in the study of Figure 16, but the cycle rate made the difference.)

The effect of potential on corrosion fatigue has not been thoroughly explored with all the other pertinent variables, but the behavior seen in Figure 17 has been confirmed in so many steels at various strength levels that it must be a widespread phenomenon. The important point is that one should not assume too confidently that cathodic protection provides as easy a way out of corrosion fatigue as the study of Figure 16 (or several similar more recent high-speed studies) might be thought to imply. Although gross over-

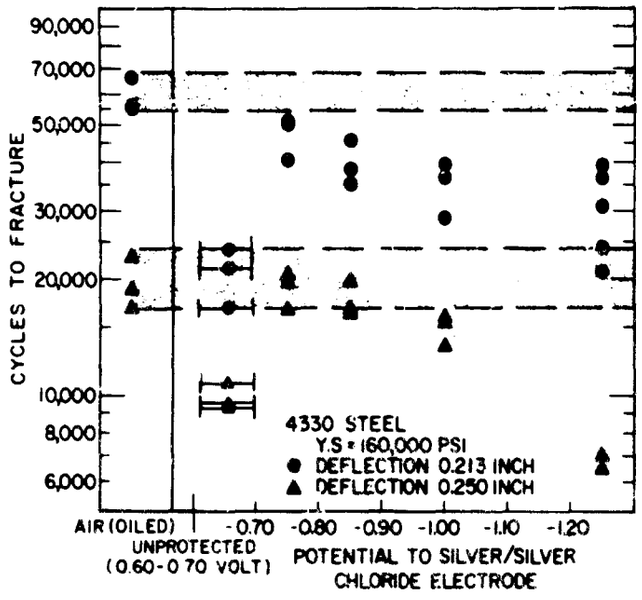

FIGURE 17. EFFECT OF POTENTIAL ON CYCLES TO FAILURE ON MEDIUM-STRENGTH STEEL FATIGUED IN REVERSE BENDING AT TWO MAXIMUM STRESS LEVELS[16]

protection can cause a loss in fatigue life, in point of fact the cathodic protection systems now in use for hulls of (low-strength) steel probably contribute to resisting corrosion fatigue for two reasons: These systems probably do not polarize the hull much beyond the optimum potential range, if at all; and even minimal cathodic protection appears to prevent the formation of pits which otherwise would invite the nucleation of corrosion-fatigue cracks. Hence the cathodic protection systems now in use for underwater structures of low-strength steels not only contribute to maintenance economy but may additionally mitigate corrosion fatigue with little chance of any adverse effects from hydrogen.

OUTLOOK

Learning how to use high-strength steels under stress-corrosion cracking conditions and corrosion-fatigue conditions requires that we learn how to exclude the environment by suitable coatings, or that we learn how to identify with confidence steels which are resistant to these cracking modes. (With the high-strength steels, one seldom has the possibility freely at his disposal of removing the stresses, for high-temperature stress relieving of heat-treated components would, in all too many cases, degrade the required strength properties before it would relieve the stresses. It is not uncommon therefore to find environmental cracking of heat-treated shapes as simple as flat plates and hollow cylinders.) There is ample evidence that organic coatings which are perfectly adequate to prevent general corrosion may not be adequate to prevent SCC of a susceptible steel, so that a new criterion of adequacy--perhaps impermeability to humid air--may have to be established and met. If we are to learn how to characterize with confidence the response of high-strength steels to stressing in a corrosive environment, it is necessary to modernize our concepts of testing for both SCC and corrosion fatigue. The need to modernize SCC testing is due to the long time which must elapse before one can characterize a metal even tentatively as "resistant", and to the fact that there is not much we can do with total time-to-failure data on initially smooth specimens. It is known that the stress-corrosion process is relatively rapid, and that it is sensitive to stress intensity. Why then does one not start with a high stress intensity, provided by a pre-existing crack, and then characterize the cracking behavior. The data are not only taken rapidly, but in principle they can be related to the stress and crack size needed to cause a stress-corrosion crack to grow in a real structure.

At least three different methods have been used to do just this: (a) Monitoring the crack length by measuring the electrical resistance of the specimen[17] (which unfortunately introduces some potential complications in a SCC test using a highly conductive electrolyte such as salt water), (b) observing the time-to-failure of a notched specimen under known initial stress intensity K_{I_i} (18); or (c) mechanically gauging the crack opening (19). These methods have not been applied enough yet either to sort out the most advantageous for all purposes, or to characterize the response of various steels. There does, however, appear to be an enormous difference in response of a given martensitic steel depending upon heat treatment, and there appears to be a large difference between some of the classes of steels studied so far. Some of the most interesting published data using the pre-cracked specimen are shown in Figures 18 and 19. Here the author stresses pre-cracked specimens to an initial stress intensity K_{I_i} and exposes them until they rupture. He then divides the stress intensity at exposure K_{I_i} by the notch toughness of the steel K_{I_c} and reports the time-to-failure as a function of this ratio. As the ratio approaches unity, one approaches the condition under which the specimen must in effect be torn apart in the test. In Figure 18 it appears that this ratio reaches an asymptote of roughly 0.9 for an 18%-nickel maraging steel plate but that the asymptote, if any, must be less than about 0.6 for the weld center. (By contrast, a ratio of about 0.15 was observed in a Type 4340 steel heat treated to a yield strength of 200 ksi (19). In a similar study on a precipitation-hardening stainless steel with about 17% chromium and 7% nickel, the ratio appears to be about 0.8-0.9 (Figure 19). Thus there is a real incentive to take a searching look for resistance to cracking in the various steels.

Learning to use high-strength steels under corrosion-fatigue conditions requires, even more than the case of SCC, a modernization of test concepts. Again the general approach of making use of the most practical pertinent concepts of fracture

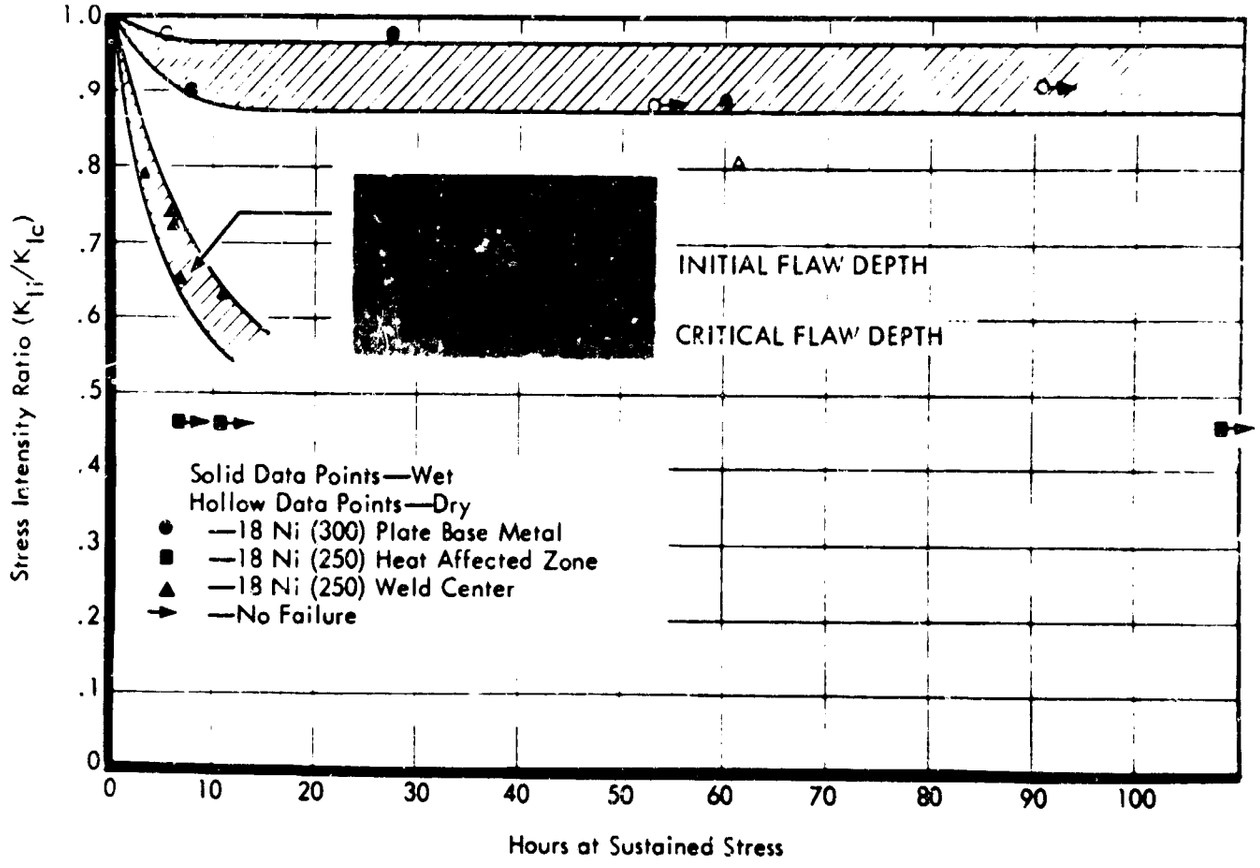

FIGURE 18. EFFECT OF STRESS INTENSITY TO NOTCH-TOUGHNESS RATIO ON TIME-TO-FRACTURE OF PRE-CRACKED SPECIMENS OF A MARAGING STEEL(18)

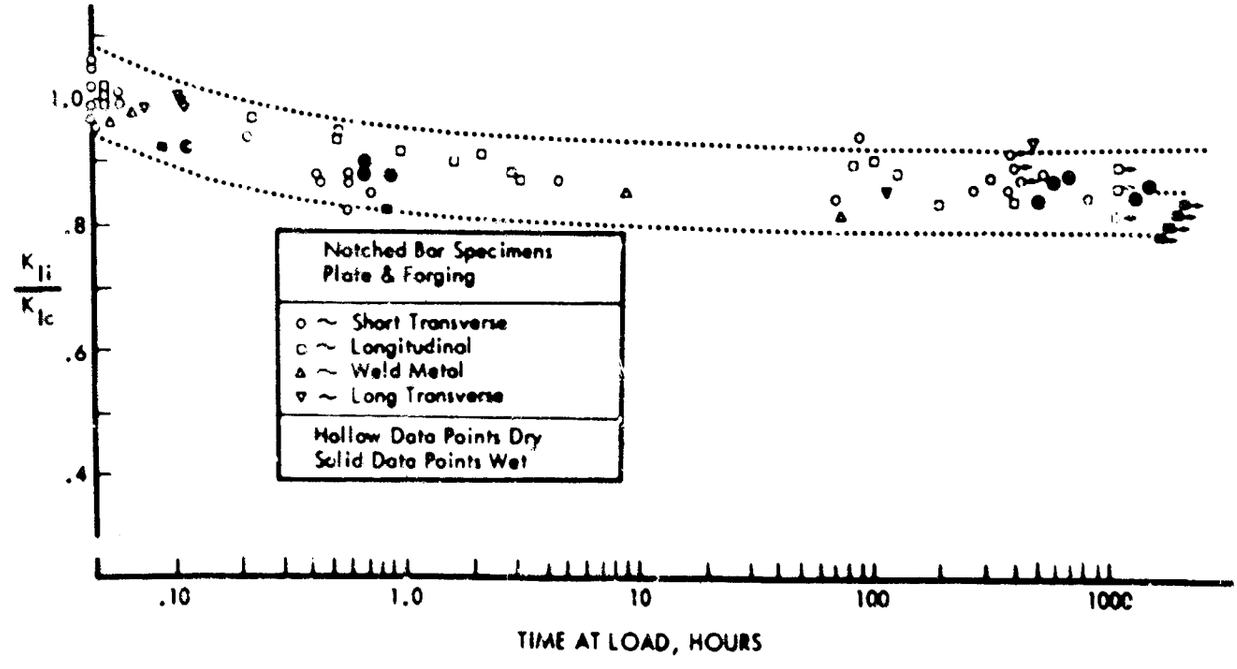

FIGURE 19. EFFECT OF STRESS INTENSITY – NOTCH-TOUGHNESS RATIO ON TIME-TO-FRACTURE OF PRE-CRACKED SPECIMENS OF A PRECIPITATION-HARDENING STEEL(18)

mechanics is indicated where these concepts promise real helpfulness in streamlining an otherwise impossibly demanding task, both in conducting experimental research and in retrieving the findings when needed.

Unless and until we find otherwise, we must assume that electrochemical processes are necessarily involved in both SCC and corrosion fatigue. Modernization of testing must of course reckon with this. As a barest minimum, one must measure and control the potential wherever this can be done in a significant way, rather than to try to investigate electrochemical processes by control or measurement of currents alone. For the metallurgist, this represents a difference analogous to controlling or measuring the temperature inside an electrically heated furnace rather than merely controlling or measuring the current through the windings, even though the current is responsible for creating the temperature: It is the intensive parameter which is fundamental in both cases. Controlling the chemical environment is of course not as simple as potentiostating the specimen. The stress-corrosion crack or the corrosion-fatigue crack must surely represent a type of chromatography column, sorting out the chemical species from the mouth of the crack to the advancing tip, and so, for a long time to come, even using the best concepts of fracture mechanics and electrochemistry, there will remain enough complexities to keep the subjects of stress-corrosion cracking and corrosion fatigue challenging.

REFERENCES

(1) Hoar, T. P., "Stress-Corrosion Cracking", Corrosion, 19, 331t (1963).

(2) Barnartt, S., "General Concepts of Stress-Corrosion Cracking", Corrosion, 18, 322t (1962).

(3) Rinebolt, J. A., and Raring, R. H., "The Effect of Gases in Steel", NRL Report 4683 (January, 1956).

(4) Tetelman, A. S., "The Hydrogen Embrittlement of Ferrous Alloys", Metallurgical Society Conferences, 20, 671 (1963).

(5) Brown, B. F., "Stress-Corrosion Cracking and Related Phenomena in High Strength Steels, A Review of the Problem, With an Annotated Bibliography", NRL Report 6041 (November, 1963).

(6) Srawley, J. E., and Beachem, C. D., "Crack Propagation Tests of Some High-Strength Sheet Steels", NRL Report 5263 (January, 1959).

(7) Beachem, C. D., and Srawley, J. E., "Crack Propagation Tests of High Strength Sheet Materials, Part V", NRL Report 5507 (August, 1960).

(8) Brown, B. F., "Cracking of Martensitic, Type 410, Stainless Steel in Corrosive Environments", Report of NRL Progress, 40-42 (May, 1958).

(9) Phelps, E. H., and Loginow, A. W., "Stress Corrosion of Steels for Aircraft and Missiles", Corrosion, 16, 325t (1960).

(10) Scharfstein, L. R., and Eisenbrown, C. M., "Potential-Time Curves Obtained During the Stress Cracking of Metals", Nature, 188, 572 (1960).

(11) Bhatt, H. F., and Phelps, E. H., "Effect of Solution pH on the Mechanism of Stress Corrosion Cracking of a Martensitic Stainless Steel", Corrosion, 17, 430t (1961).

(12) Brown, B. F., et al, "Interim Report of Progress on Marine Corrosion Studies", NRL Memorandum Report 1549 (July 1, 1964).

(13) Gilbert, P. T., "Corrosion Fatigue", Metallurgical Reviews, 1, 379 (1956).

(14) Dahlberg, E. P., and Lytle, D. B., "Fatigue Crack Propagation in High Strength 4340 Steel", NRL Memorandum Report 1471 (November, 1963).

(15) Evans, U. R., and Simnad, M. T., "The Mechanism of Corrosion Fatigue of Mild Steel", Proc. Roy. Soc., 188, 372 (1947).

(16) Smith, J. A., et al, Research at NRL, Submitted to NACE for publication.

(17) Johnson, H. H., and Willner, A. M., "Environment and Fracture of High Strength Steel", U. S. Naval Research Laboratory Mechanics Division, Technical Memorandum No. 240 (October, 1963) [Report of research conducted at Cornell University under Contract No. NOnr-3286(00)(X), quoted with the author's permission].

(18) Tiffany, C. F., and Masters, J. N., "Applied Fracture Mechanics", Instruction Notes for Workshop in Fracture Mechanics (August, 1964).

(19) Brown, B. F., Unpublished research at NRL.

PROTECTION AGAINST CORROSION, HYDROGEN EMBRITTLEMENT

by

H. G. Cole *

GENERAL

Hydrogen embrittlement is still a major problem restricting the use of very strong steels and confidence in them. Even the recent 5% chromium and maraging steels which seem to be less sensitive to embrittlement by cleaning and protective process are subject, perhaps severely, to stress corrosion in which hydrogen embrittlement may play a large part.

In most technologies, scientific understanding lags behind technical achievement, but the technologist, though paying lip service to the value of the work of his academic brethren, is not thereby held back from further empirical practical conquests. In the hydrogen-embrittlement field, however, behaviour of components and of specimens in systematic tests can be so erratic and unpredictable that we feel a strong need for a better fundamental understanding.

THEORIES OF HYDROGEN EMBRITTLEMENT

It is generally agreed that hydrogen moves through steel in the atomic form, and that in some way it reduces the cohesive strength of the steel lattice. Professor Troiano's observations on crack initiation and propagation suggest strongly that the atoms move to regions under tensile stress, perhaps merely because there is more room in the lattice there, though I know of no direct observation of this movement, e.g., by analysis or radiography. These two accepted phenomena are about the total of our certain knowledge. The areas of uncertainty are threefold. The first concerns the nature and location of hydrogen in steel, and the effect of temperature. There seem to be at least two different forms with different rates of diffusion. One is undoubtedly atomic and interstitial, the other may be locked to some extent at dislocations or other lattice defects, or at foreign atoms, but we do not know the proportions between the two forms, the effect of temperature on the proportions, or whether the locked form includes gas molecules, or whether gas is yet a third form in which hydrogen can be present. Of the interstitial atomic form we do not know the magnitude or even the sign of the electric charge on the atom or ion, hydrogen dissolved in steel can behave as negatively charged and the Russians claim to have observed this. The second area of uncertainty concerns which of the two or more forms of hydrogen is responsible for embrittlement. Here we have two opposed theories. The first comes from Professor Troiano's experiments in which he charged, refrigerated and strained his steel specimens, and then measured their ductility after aging. from these experiments he concluded that hydrogen in lattice imperfections was harmless, and that it was the hydrogen in the lattice which caused embrittlement. The second theory stems from Hewitt's still unfortunately unpublished work on internal friction, from which he concluded that below about 120 C hydrogen is present at lattice defects and causes embrittlement whereas above 120 C it is present in the lattice where it causes no harm.

The third area of uncertainty follows closely from the second, and is concerned with the actual mechanism whereby hydrogen reduces the cohesive strength of the steel. Zapffe many years ago postulated that hydrogen gas was formed at lattice defects in the steel and burst the steel apart. This theory accounts satisfactorily for blistering after acid pickling, but seems an unlikely explanation for the embrittlement of very strong steel caused by a mobile hydrogen content of one atom per 200,000 atoms or more of iron. Kazinczy modified Zapffe's theory by postulating that the lattice rifts at which hydrogen gas is formed are of the nature of Griffiths cracks; expansion of gas in them would provide energy to promote crack propagation at an applied stress lower than in the absence of gas. Petch also calls up Griffiths crack , but postulates that embrittlement is caused by hydrogen atoms, not gas. He suggests that atoms condensed on the crack surface reduce the external energy required to extend the surface, i.e., to propagate the crack. Recently there has been a revival of belief that molecular gas plays a part in causing embrittlement, but it is difficult to see how a gas theory can account for embrittlement by such minute quantities of hydrogen and its disappearance at temperatures above about 120 C.

A better understanding of the nature and location of harmless and damaging hydrogen seems essential if control methods based on detection or estimation of hydrogen are to be used to declare a steel safe from embrittlement.

COMPOSITION OF STEEL

Turning now to more practical and empirical knowledge, there seems no doubt of the value of cleanness and of low sulphur and phosphorus content, not only for improved mechanical properties, but also for raising the threshold hydrogen content below which embrittlement does not occur. 270,000 psi steel should be vacuum melted and of low sulphur and phosphorus content as a matter of course and should be free from retained austenite which can transform on straining to untempered martensite. Incidentally, the more academic research workers might note that embrittlement by hydrogen is so strongly dependent on impurity content that it may properly be considered as an interaction between hydrogen and impurities.

*Principal Scientific Officer, Directorate of Materials & Structures R&D, Ministry of Aviation, London, England.

SURFACE STRESSES

There is much evidence of the damaging interaction between hydrogen and surface tensile stresses, and very fair evidence of the benefit of surface compressive stresses. It is essential to give stress relief after any process liable to introduce tensile stresses into the surface. If compressive stresses are to be introduced into the surface, as by shot peening, then it must be arranged that the inevitable balancing tensile stresses are in a location in the component where they can do no harm.

CLEANING PROCESSES

It is generally agreed that anodic pickling in strong sulphuric acid solution does not itself cause hydrogen embrittlement, but there is an inevitable potentially damaging short period of plain pickling when the components are withdrawn for washing. Abrasive blasting, dry rather than wet, is to be preferred, and is acceptable on close tolerance areas.

PROTECTIVE PROCESSES

It is widely accepted that cadmium plate plus paint is the best protective for steel, though some hold the view that phosphate treatment plus paint is as good or even better. Much work has been devoted to finding safe ways of depositing cadmium. So far as aqueous processes are concerned, this work has been reasonably successful in that processes of relatively low embrittlement have been made available, and conditions leading to a high degree of embrittlement are known and can be avoided. Vacuum plating is an obvious but expensive solution to the problem; hitherto the adhesion of vacuum-plated cadmium has been poor unless the surface of the steel was first appreciably roughened, but R. A. E. Farnborough have recently developed a process which they think gives much better adhesion on smooth surfaces.

Much further work is being devoted to the passage of hydrogen through cadmium films, into the steel during plating and out during baking. Perhaps one day we shall know whether high and low embrittling plating processes are associated solely with the porosity of the plate and if so, whether we want high or low porosity, and if high porosity, then the degree of porosity which can be tolerated without loss of protection.

There is increasing laboratory evidence, however, that vacuum-melted high-purity steel is not difficult to electroplate without dangerous embrittlement.

HYDROGEN CONTENT

In the U.K. we have tried to evaluate processes applied to very strong steel in terms of hydrogen absorbed by the steel, and then to correlate hydrogen content with degree of embrittlement as shown by a sustained load notched tensile test. A fair degree of correlation has been found between embrittlement and hydrogen extractable at 200 to 300 C, and an exercise between a number of laboratories has shown that concordant and reproducible analytical results can be obtained on standard specimens. There is now evidence from several laboratories that 0.03 to 0.05 ppm hydrogen extractable at 200 to 300 C is the threshold quantity which causes embrittlement in low-alloy, high-strength steels of normal impurity content. For high-purity steels the threshold may be 0.3 to 0.5 ppm, i. e., ten times as high. There is evidence, too, that a further constant 0.1 ppm is extractable at 650 C irrespective of the quantity extracted at the lower temperature.

PRACTICAL CONCLUSIONS

The U. K. were the first to be bold enough, or foolish enough, to publish a specification, D. T. D. 934, for the protection of very strong steels. Recent work suggests that on normal purity steels the specification goes in the right direction but not far enough, while for high-purity steels of strengths up to 280,000 psi the specification is adequate. It may not be adequate for steels of yet higher strength, even when they are of high purity.

HYDROGEN AND FATIGUE

There has been some doubt in the past as to whether or by how much fatigue properties are reduced by hydrogen. The author believes that much of the confusion has arisen from lack of appreciation of the large influence of surface stresses on fatigue properties. A recent investigation in the U. K. led to the conclusion that hydrogen had no effect on the axial load fatigue properties of a properly machined test piece even when the maximum load exceeds the sustained load limit. If the specimen surface contains large compressive stresses, hydrogen will nullify the expected benefit and reduce fatigue properties down to, but not below, an intrinsic value, but if the surface contains tensile stresses, hydrogen can cause a catastrophic drop in fatigue properties. There is room for a lot more work on the surface stresses left by machining and grinding operations and their effect, coupled with that of hydrogen, on fatigue properties.

STRESS CORROSION

The problem of applying protective treatment to low-alloy steel without damage to mechanical properties is, though far from fully resolved, at least reasonably under control. The same may not be true of the danger of stress corrosion failure in service.

Until recently it was possible to regard stress corrosion failure as due to corrosion-induced hydrogen embrittlement. We now, however, have two steels, the 5% chromium steel and the 18% Ni maraging steel, which are relatively insensitive to hydrogen, but apparently strongly susceptible to stress corrosion. Carbon and nonstainless steels of low strength have not hitherto been found susceptible to stress corrosion in atmospheric environments. Here, then, is a new and important problem requiring research at all levels.

THE NOTCH TOUGHNESS OF ULTRAHIGH-STRENGTH STEELS IN RELATION TO DESIGN CONSIDERATIONS*

by

R. C. A. Thurston**

INTRODUCTION

During the last ten years, rapid strides have been taken in the development and application of ultrahigh-strength steels. For the purposes of the present paper, ultrahigh-strength steels will be arbitrarily defined as those steels having a yield strength (0.2%) in excess of 200 ksi. Such steels are generally available in the form of sheet, plate, bar and forgings, and their major applications are aircraft undercarriages, pressure vessels, solid-propellent rocket-motor cases, and machine parts, with perhaps many additional lesser known uses. At the present time, the use of ultrahigh-strength steels is restricted almost entirely to those applications where the strength/weight ratio of the component or product is of prime importance, and their success or failure in these specialized fields will determine the extent of their contribution to the manufacture of engineering items of a more general nature.

The properties of the ultrahigh-strength steels which are of particular interest to the user include tensile strength at various temperatures, ductility and toughness, fatigue strength, corrosion resistance, and weldability. While these are all probably of equal importance, and to some degree interrelated, the following discussion will be restricted to the notch-toughness characteristics, by which is meant the reaction of the steels to the presence of stress concentrations, whether these be design discontinuities, surface cracks or internal flaws. It is an established but unfortunate fact that as the tensile strength increases, the ductility and toughness tend to diminish. Consequently, any ultrahigh-strength steel development programme involves the generation not only of conventional smooth tensile test data, but also of data from notched tensile tests and V-notch Charpy impact tests. The uniaxial elongation given by the standard tensile test may be a satisfactory criterion for a medium-strength steel, but show no correlation with the performance of an ultrahigh-strength steel. Cottrell[1]*** has reported the results obtained from burst tests on two welded rocket motor cases of a 3% Cr-Mo-V steel. Tensile specimens heat-treated with the cases gave tensile strengths of 231 ksi and 237 ksi respectively, and the same elongation, 9-1/2%. When hydraulically pressurized to failure, the first case burst in a ductile manner at a hoop stress of over 235 ksi, whereas the second case burst in a brittle manner at 159 ksi. Hence, it is essential for the ultrahigh-strength steels to supplement the normal tensile data with the results of some type of notched test.

This necessity was recognized at an early stage and numerous tensile and impact tests were carried out on specimens containing a relatively mild stress raiser before it was realized that any meaningful material evaluation must include specimens with high stress concentrations, preferably a natural crack. The development of a suitable specimen was assisted by the notable work of Irwin and his collaborators[2-5], who extended the Griffith theory and derived expressions for K, the stress intensity factor, and G, the crack extension force or strain energy release rate, based on the principles of linear elastic fracture mechanics. A knowledge of the fracture toughness of a material, obtained from suitable tests, should enable a designer to determine the size of crack the material will tolerate without fracture, when loaded to a level approaching that at which it would fail by excessive plastic deformation.

In a series of reports[6-10], the ASTM Special Committee on Fracture Testing of High-Strength Materials has detailed the requirements for suitable tests on both sheet and rounds, and more recently a very clear exposition of the present state of the art was presented by Srawley and Brown[11]. Basically, there are two types of flat specimen used for fracture-toughness tests in tension - the through-crack type, either centre-notched or edge-notched, and the partial or surface-cracked type. Satisfactory tests have also been made using a single-edge-cracked specimen in tension or in bending, but the amount of data available is still relatively small. For round bars, a circumferentially notched and cracked specimen is recommended with a minor diameter/major diameter ratio of 0.70/.

Prior to the development of fracture mechanics, the majority of notched tensile tests were carried out on round specimens with a machined notch, and an indication of the notch toughness was given by the ratio of the notched tensile strength to the smooth tensile strength or the yield strength. With a very sharply notched

**Head, Engineering Physics Section, Physical Metallurgy Division, Mines Branch, Department of Mines and Technical Surveys, Ottawa, Canada

***References are given on pages 122-124.

specimen, root radius less than 0.001 in., this test still has many adherents and is often used for screening purposes. The recommended fracture-toughness tests, though intended for the estimation of plane-stress or plane-strain values of K and G, will also give values of the notched tensile strength.

In addition to the foregoing, there are several arbitrary empirical procedures for evaluating notch toughness which have been proved by correlation with service-failure studies. Prominent among these are the explosion-bulge and drop-weight tests developed at the U. S. Naval Research Laboratory, the pre-cracked Charpy impact test and the Allison instrumented bend test. Reference will be made to their particular merits in the course of the text.

REVIEW OF NOTCH-TOUGHNESS DATA

The ultrahigh-strength steels presently available can be broadly classified in the following categories:

(1) Low-alloy structural steels
(2) Hot-die and tool steels
(3) Nickel alloy steels
(4) Precipitation-hardening steels.

Table 1 gives typical chemical composition of those steels for which sufficient data of a satisfactory nature were available to the writer.

In an attempt to obtain a realistic appraisal of the notch-toughness characteristics of the available alloys, the data contained in over 100 publications were critically examined and analyzed. Much of the data was regrettably incomplete or failed to comply with the necessary requirements for a satisfactory test, e.g., the specimen width was too small or the notch root radius too large. This criticism is not meant to imply that the tests were not perfectly adequate for the purpose for which they were intended. The remaining data were averaged for the particular steel and strength level, and are presented in Table 2.

It will be observed that the notch-toughness level is expressed by two values:

(a) The notch-strength ratio (notched tensile strength/ultimate tensile strength), derived from tensile tests on notched or cracked sheet or rounds, the notch root radius being less than 0.001 in.

TABLE 1. CHEMICAL COMPOSITION OF SELECTED ULTRAHIGH-STRENGTH STEELS

Steel	Composition, per cent							
	C	Mn	Si	Ni	Cr	Mo	V	Other
Class (1)								
AISI 4340	0.4	0.75	0.3	1.8	0.8	0.25	--	--
300 M	0.4	0.75	1.6	1.85	0.85	0.4	0.08	--
Airsteel X-200	0.4	0.85	1.5	--	2.0	0.5	0.05	--
AMS 6434	0.36	0.7	0.3	1.8	0.8	0.35	0.2	--
4137 Co	0.4	0.7	1.0	--	1.1	0.25	0.15	1.0 Co
MBMC No. 1	0.4	0.8	1.7	--	0.8	--	0.05	--
Class (2)								
H-11	0.4	0.35	1.0	--	5.0	1.3	0.5	--
Vascojet 1000								
D6Ac	0.44	0.8	0.2	0.55	1.0	1.0	0.05	--
Class (3)								
18% Ni Maraging	0.02	0.08	0.08	18.0	--	4.8	--	7.5/9.0 Co
9 Ni - 4 Co	0.44	0.3	0.1	8.5	0.3	0.3	0.1	4.0 Co
Class (4)								
PH 15 - 7 Mo	0.07	0.5	0.35	7.0	15.0	3.0	--	1.0 Al
AM 355	0.14	0.7	0.3	4.3	15.5	2.75	--	--

TABLE 2. SUMMARY OF NOTCH-TOUGHNESS DATA

Steel	Ultimate Tensile Strength, psi	Notch Strength Ratio 300	280	260	240	Ultimate Tensile Strength, ksi	Critical Stress Intensity Factor, K_c – ksi$\sqrt{in.}$ 300	280	260	240
AISI 4340	Sheet	--	0.65 (1)	0.54	0.63	Sheet	--	86 (1)	200	180 (1)
	Rounds	--	1.06	1.12	1.27	Plate	--	35 (1)	47 (1)	57 (1)
	Cracked	--	0.34	0.66	--	Rounds	--	[92] (1)	[61] (1)	--
300 M	Sheet	0.37	0.50 (1)	0.70	0.62	Sheet	--	133	194	--
	Cracked	0.29	0.40	0.58	0.55	Rounds	[73] (1)	[72]	[69] (1)	[70] (1)
Airsteel X-200	Sheet	0.27	--	0.47 (1)	--	Sheet	85*	105	90*	125*
	Rounds	--	0.61	--	0.98					
	Cracked	--	0.55	--	--	Rounds	[70]*	[55]*	--	[80]*
AMS 6434	Sheet	--	--	0.68	0.84	Sheet	>90 (1)	>120 (1)	>120 (1)	200
	Cracked	0.47 (1)	0.64 (1)	0.66 (1)	0.69		[82] (1)		[54]	
4137 Co		--	--	--	--			[42]		
MBMC No. 1	Sheet	--	0.35	0.38	--	Sheet		74*	83* (1)	
H-11	Sheet	0.35	0.29	0.49	--	Sheet	20/100	47	90	106 (1)
Vascojet 1000	Cracked	0.32	0.34	0.35	0.86 (1)		[34] (1)			
D6 AC	Sheet	0.30 (1)	0.49 (1)	0.44 (1)	0.64 (1)	Sheet	77* (1)	112* (1)	98* (1)	130* (1)
	Rounds	--	0.74	0.35 (1)	1.05					
	Cracked†	0.56 rd. (1)	0.75 rd. (1)	--	1.00 rd. (1)	Rounds	[49]	[57]	[42] (1)	[80]
18% Ni	Sheet	0.78	0.87	0.90	0.92	Sheet	175	217* (1)	160 (1)	203* (1)
Maraging	Plate			1.40	1.48 (1)	Plate	20/190	213 (1)	109	--
	Cracked	0.53	0.54 (1)	0.77 (1)	0.81 (1)		[97]	[84]	[85]	
9 Ni – 4 Co						Sheet		[47] (1)	[96] (1)	[88] (1)
						Plate			[110] (1)	[112] (1)
PH 15 – 7 Mo	Sheet	--	0.80 (1)	0.94 (1)	0.68	Sheet	--	--	--	77
	Cracked	--	--	0.95 (1)	.25/.71					
AM 355	Sheet	0.91 (1) (CR 40%)	--	0.86 (1) (CR 15%)						

* indicates that the fracture toughness values were obtained from notched specimens which had not been pre-cracked.
(1) indicates that the value tabulated is believed to be the result of a single test - or a small number of tests made in one laboratory on a single heat.
[ ] indicates a K_{Ic} value.
† indicates that the cracked NSR values were obtained from round specimens; the remainder were derived from tests on sheet specimens.

(b) The critical stress intensity factor (K_c or K_{Ic}) derived from tensile or bend tests on pre-cracked sheet or rounds.

No data from V-notch Charpy impact tests are included since, in the ultra high-strength range, the test is insufficiently discriminatory. Furthermore, the results obtained from small experimental heats were neglected.

The results of the survey of available data were neither very satisfactory nor conclusive. They showed the expected trend of decreasing notch toughness with increasing tensile strength (Figure 1), though even here there were some peculiar inconsistencies, presumably due to composition or processing variables or to an insufficient number of tests. The 18% Ni maraging steel, which has been the subject of intensive investigation, is seen to possess a definite superiority over the earlier steels (Figures 1 and 2), and should obviously be of particular interest to the designer of high-strength minimum-weight hardware. The more recently developed 9Ni-4Co alloy also appears to have desirable characteristics, but unfortunately, insufficient reliable information was available to the writer for a more accurate assessment. The behaviour of the remaining ultrahigh-strength steels is far from consistent and varies with the strength level and parameter considered. The best of the group would appear to be 300 M alloy, and the poorest H-11 (Vascojet 1000) and MBMC #1 alloys.

A comparison of the steels is best obtained by reference to those investigations in which similar tests have been made on specimens of the same form cut from sheets of the same, or approximately the same, thickness. Espey[12] has stated that the alloy having the lowest notch sensitivity varies somewhat with the strength level considered, and has reported the superiority of 300 M and D6AC steels over Vascojet 1000 at a yield strength of about 230 ksi. Davis[13] has tested a number of ultrahigh-strength steels in plate form (0.3 in.) and, in addition to confirming the higher fracture toughness of the 18% Ni (250) steel, has shown D6AC alloy to be superior to H-11 alloy at a strength level of 280 ksi.

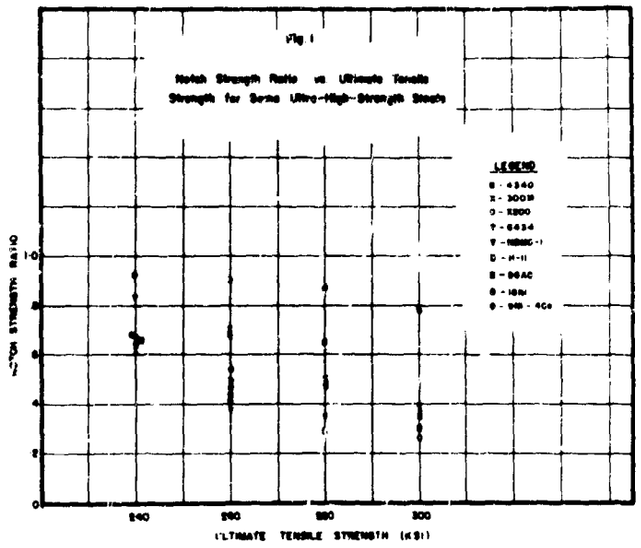

FIGURE 1. NOTCH STRENGTH RATIO VERSUS ULTIMATE TENSILE STRENGTH FOR SOME ULTRAHIGH-STRENGTH STEELS

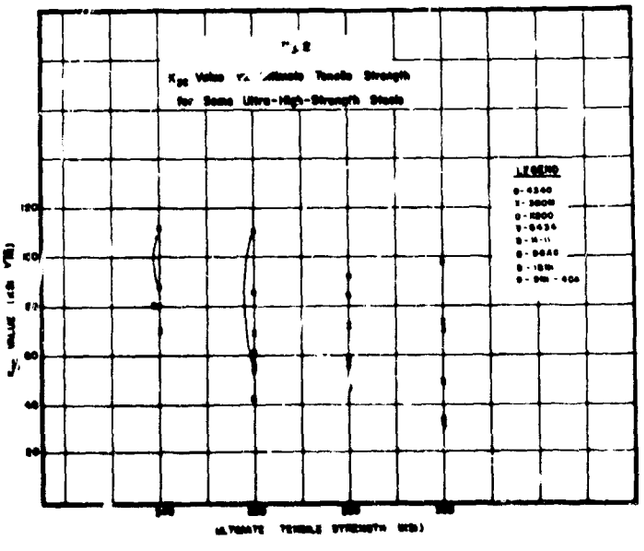

FIGURE 2. K_{Ic} VALUE VERSUS ULTIMATE TENSILE STRENGTH FOR SOME ULTRAHIGH-STRENGTH STEELS

Matas, Hill, and Munger[14] compared several of the alloys in the form of 0.080 in. sheet, and tentatively classified them into three groups in terms of notch strength and fracture toughness. The most desirable qualities were shown by the 18% Ni alloy (Group III); the 9% Ni - 4% Co alloy (Group II) was somewhat inferior, and the older alloys, D6AC, 4340, 300 M and H-11 Group I) gave the lowest values. Jones[15] carried out a similar investigation on 0.180-inch specimens, and reported his results in terms of the notch strength. At a strength level of 280 ksi, both 18% Ni and 9% Ni - 4% Co steel were found to be superior to 4340 (air-melt) steel, which in turn was superior to H-11 steel. An additional observation of particular interest was that vacuum-melted 4340 steel was comparable to both the high nickel steels, which raises the question of the importance of processing variables.

EFFECT OF PROCESSING VARIABLES

As the design requirements of the various types of hardware are raised and the alloys have to be fabricated to meet the higher strength levels, the beneficial or deleterious effects of processing variables tend to become of greater significance. Those variables which have a degrading influence on the toughness of the steel must be more closely controlled, while those which appear to be advantageous must be utilized to their fullest extent. Processing in the present context covers all stages of the manufacture of the steel from the melt to the finished stock, sheet, plate or bar, and includes in particular, melting practice, composition, cold or warm reduction, decarburization and banding. The respective effects of these variables are outlined below.

Melting Practice

While there is a general belief that melting under vacuum should produce a superior grade of steel, due to a reduction in gas content and nonmetallic inclusions, this belief is not consistently substantiated by the data from notch-toughness tests of a number of alloys. The effect of vacuum melting will be seen to vary with the alloy composition and with the tensile strength level, and is not always beneficial. The results reported by Gilbert and Brown[16] for AMS 6434 alloy are typical in their trend of those obtained in several investigations in which vacuum melting produced an improvement. The net fracture strength of transverse centre-notched specimens was increased by about 100 percent, whereas that of longitudinal specimens was increased by about 50 percent. The marked directionality of the air-melted sheet was almost completely removed by vacuum melting.

Cottrell[1] has investigated the effect of consumable electrode vacuum melting on the surface strain to failure in a wide bend test using a 3% Cr-Mo-V steel in the ultrahigh-strength range. He reported that vacuum melting of this steel increased the tensile strength for a given surface strain to failure by about 20 ksi.

On the other hand, Reference (1) reports somewhat different results obtained with 9% Ni - 4% Co steel. Vacuum remelting reduced the directionality, but gave no increase in the nominal notch strength of longitudinal, centre-cracked, sheet specimens (0.08 and 0.180 in.) from a Si/Al deoxidized heat. Vacuum carbon

deoxidation practice, however, resulted in a significant improvement for 0.180-inch sheet in the lower part of the ultrahigh-strength range.

Additional evidence concerning the effect of vacuum melting on the notch-strength ratio and the fracture toughness of several steels has been compiled in Table 3.

Referring to Table 3, it will be seen that alloys H-11 and 300 M showed little improvement with vacuum melting. The 4340 steel gave some improvement, particularly with the vacuum induction treatment. The 18% Ni maraging alloy and AMS 6434, also showed some improvement, this being more marked at the 290-ksi level for the maraging alloy.

It would appear that the case for vacuum melting is by no means resolved. While it can do no harm, its general effect is a reduction in directionality with possibly some upgrading of notch toughness. Since the latter varies with the alloy and its strength level, any specific application would have to be considered on its merits, and the controlling factor may well be the economic aspect.

Composition

No attempt will be made to discuss the effect of alloying elements in detail, but some comments may be of interest on the particular effects of variation between heats, carbon content, sulphur content, decarburization and purity. Campbell, Barone, and Moon[24] have reported the results of notch-toughness tests on two heats of 18% Ni steel (300 grade), one being a low chemistry heat and the other a high chemistry heat. In the case of bar stock, the former gave a notch strength ratio (K_t = 12) of 1.49, and the latter gave 1.26. In the case of 0.115 in. sheet, the former gave a K_{Ic} value of 230 ksi $\sqrt{in.}$, whereas the latter gave 119 ksi $\sqrt{in.}$. Melville[25] carried out tests on surface-cracked sheet specimens from three heats of the 300-grade material, and his results are presented in Figure 3 in terms of net strength vs. crack length. Though the chemistry was similar, the difference in

TABLE 3. EFFECT OF VACUUM MELTING ON NOTCH TOUGHNESS

Steel	Form of Material	Type of Test-Piece	Ultimate Tensile Strength, ksi	Notch Strength Ratio K_c — ksi $\sqrt{in.}$				Reference
				Air Melt	Vacuum Melt	Air Melt	Vacuum Melt	
H-11	0.063 in. sheet	Edgenoteh	250	0.65	0.70	120	135	17
			300	0.24	0.26	45	45	
300 M	0.063 in. sheet	Edgenotch	250	0.40	0.50	80	95	
			300	0.26	0.31	65	78	
4340	0.180 in. sheet	Centre-cracked	280	0.31 (0.37)	0.64* (0.37)			15
300 M	0.07 in. sheet	Centre-cracked	250	0.37	0.33			18
			300	0.37	0.36			
18% Ni	0.3 in. dia.	K_t > 15	260	1.46	1.52			19
			290	1.06	1.46			
18% Ni	0.3 in. dia.	K_t > 10	270	≈1.39	≈1.45			20
4340	0.067 in. sheet	Centre-cracked	285	0.35 (0.24)		100 (60)		21
			300		0.36		108	
			270		0.73†		220†	
18% Ni	0.625 in. plate	K_t > 10	260	(1.44)	(1.44)			22
	0.5/1.0 in. plate	K_t > 10	265	(1.25)	(1.43)			
	0.063 in. sheet	K_t > 15	275	0.92	0.96			
AMS 6434	0.063 in. sheet	Centre-cracked	250	0.89 (0.85)	0.97 (0.96)			23

Notes on Table 3:

* The individual values showed considerable scatter.

† These values apply to vacuum induction melted and vacuum induction remelted heats; the remainder apply to CEVM heats.

( ) Values in parentheses are for transverse specimens; the remainder are essentially for longitudinal specimens.

fracture toughness behaviour is readily apparent. An inspection of the individual analyses revealed some correlation with nickel only, the respective contents being 18.63%, 18.43%, and 17.80%.

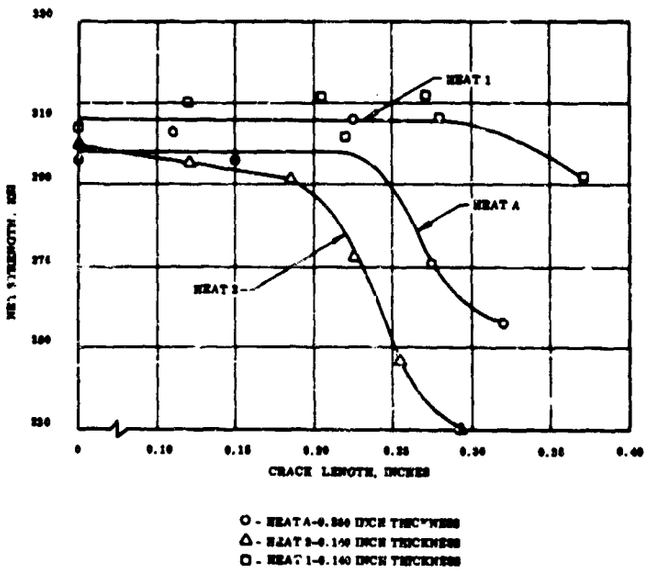

FIGURE 3. RELATIVE CRACK RESISTANCE OF THREE MARAGING STEEL HEATS[25]

As regards the effect of carbon content, it is generally accepted that the toughness increases as the carbon percentage is reduced, and the lower limit of carbon is usually determined by the yield strength requirement. Cottrell, Langstone, and Rendall[26] have investigated the effect of carbon content on the toughness of a 1% Cr-Mo steel of ultrahigh purity. As the carbon content was increased from 0.30% through 0.37% to 0.44%, both the Charpy energy absorbed and the biaxial ductility in a wide bend decreased. Klier's[27] findings from edge-notch tensile tests on a series of 43xx (V-modified) steels were similar. Espey and his co-workers[17,28] made an extensive study of the sharp-edge-notch characteristics of H-11 and 300 M sheet steel (0.063 in.). The notch strength ratio for the 300 M alloy in the ultrahigh-strength range decreased steadily for a given tensile strength with increasing levels of carbon (0.28%, 0.34%, 0.40%, and 0.46%), in agreement with the results quoted above. The results obtained with the H-11 alloy, however, were quite the reverse, the ratio increasing with increasing carbon (0.23%, 0.26%, 0.29%, 0.39%, and 0.43%). The effect was less pronounced and tended to fade-out at 0.39% C. This behaviour was confirmed by Hamaker and Vater[29] with Charpy impact tests on an H-11 type alloy, and it appears that the alloy is an exception to the general rule.

High sulphur and phosphorus, as in other steels, are detrimental to the properties of the 18% Ni maraging alloys (ref. 1). The Charpy value for the 250 grade was reduced from 20 ft-lb at a level of 0.002% S to 10 ft-lb at the 0.014% S level. Wei[30] recently reported the results of plane-strain fracture-toughness tests on a series of AISI 4345 steels containing four levels of sulphur and prepared by carefully controlled melting procedures. The K_{Ic} value (Figure 4) increased steadily as the sulphur content was reduced from 0.049% to 0.008%, at all ultrahigh-strength levels. It is of interest to note that the same reference confirmed that silicon, though increasing the tempering resistance of these steels, does not yield improved fracture toughness at a given strength level.

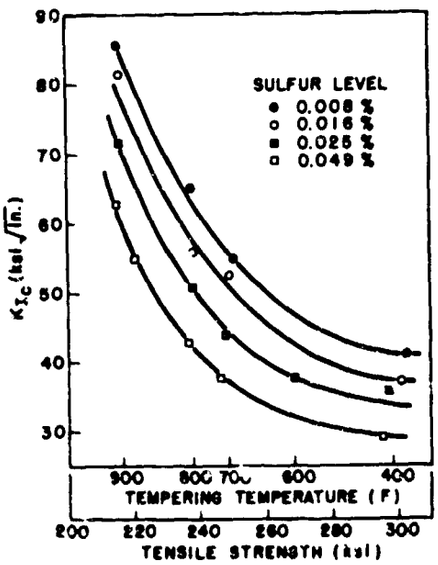

FIGURE 4. EFFECT OF SULPHUR LEVEL ON CHARPY-V ENERGY ABSORBED AT ROOM TEMPERATURE--AISI 4745 STEEL[30]

Surface decarburization, though generally regarded as a deleterious influence, has been found to give a striking improvement in the fracture toughness behaviour of certain steels. Nevertheless, it must be remembered that decarburization can be quite harmful to the fatigue properties of ultrahigh-strength steels, and its usefulness in any particular application will depend upon the extent to which the hardware is subject to cyclic or repeated loading in service. Warke and Elsea[31] have prepared a comprehensive review of the subject to which reference should be made for detailed information. Figure 5, based on an investigation by Manning, Murphy, Nichols, and Caine[32], shows the marked increase in burst strength of

12 in. diameter pressure vessels, of X-200, 300 M and MBMC-1 steels with an increase in depth of decarburization from 0.005 to 0.015 in. The increase was accompanied by a reduction in the tensile strength of about 30 ksi. The reviewers also report that Pratt and Whitney recommend decarburization for solid-propellent rocket-motor cases of H-11, D6AC, and 300 M alloys.

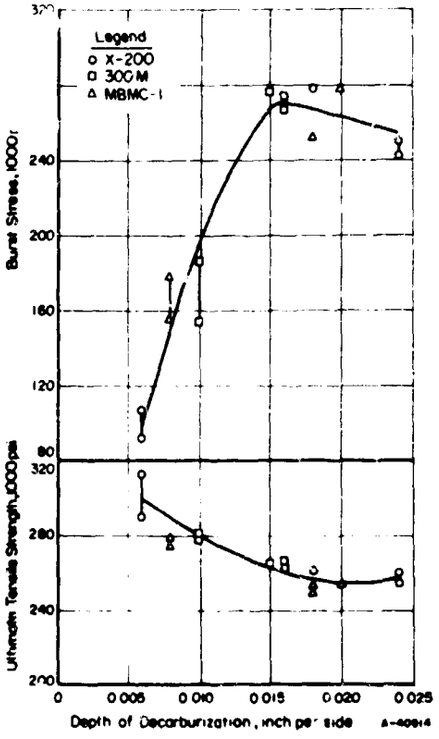

FIGURE 5. EFFECT OF DECARBURIZATION ON BURST STRESS AND TENSILE STRENGTH[31]

Similar results have been reported by Cottrell and Turner[33], and Langstone[34] from burst tests on 17 in. diameter tubes and motor cases of RS 140 (3% Cr-Mo-V) steel. The strength level of the material was in the lower part of the ultrahigh-strength range and the depth of decarburization varied from 0.001 in. to 0.008 in. The results were expressed in terms of the burst hoop stress/tensile strength ratio, and the consistently beneficial effect of the decarburization was evident in all tests, but more particularly for the motor cases, where biaxial ductility is important. According to Langstone, the surfaces of motor cases made by Bristol Aerojet Ltd., are partially decarburized during heat treatment.

Sheehan and Manning[35] have measured the fracture toughness of X-200 sheets, from experimental heats containing four levels of carbon, by means of the centre-notch tension test, and have studied the effect of surface decarburization. They concluded for this material that decarburization was beneficial only insofar as it decreased the yield strength, and that above 240 ksi, the fracture toughness was poor even though the sheet was decarburized. Nevertheless, it might still be better than that of the undecarburized material.

In general, therefore, it may be said that decarburization should be advantageous for such items as rocket-motor cases, but should be applied with caution to items such as landing gear until further information as to its effect on the fatigue properties is available.

Thermomechanical Treatment

Thermomechanical treatment in the present context is intended to cover those processes which result in metal reduction at low, room, or elevated temperatures, e.g., cold-rolling, marforming, ausforming. The majority of the information available on the effects of cold-rolling was developed in connection with liquid-propellent rocket tanks or the skin for a supersonic transport, and relates to a variety of stainless steels. In general, however, the strength level at room temperature of the materials investigated is below the lower limit of the ultrahigh-strength range and in several cases the notch was insufficiently sharp. Appropriate data for several stainless steels were presented in Table 4.

It will be noted that the notch strength ratios, based on edge-notch tests, are remarkably high, even at the 280 ksi level. Alloys AM 350 and 355 appear to be closely comparable and somewhat superior to AISI 301, in which directionality is more pronounced as shown by the transverse notched tests. More recently, test results were reported by Alper[40] for cryogenically stretch-formed AISI 301. Fourteen-in.-diameter spherical pressure vessels, stretched at -320°F with or without aging, gave an increase in burst strength at -320°F of more than 25%. The technique obviously shows promise for the lightweight cryogenic pressure vessel field.

The effect of cold rolling has also been studied on 18% Ni maraging steel, although here it is called marforming and is carried out between the annealing and aging treatments. The results, however, are contradictory. Decker, Eash, and Goldman[19] made tests on small experimental heats with 50% marforming, and reported an increase in yield strength, tensile strength, and notch strength with a slight increase in the notch strength ratio. The figures they reported for the K_c value of 50% marformed sheet, 0.039 in. to 0.079 in., were also relatively high, ranging from 170 to >245 ksi $\sqrt{in}$. Data given in Reference 22, on the other hand, indicates a

TABLE 4. NOTCH TOUGHNESS OF COLD-ROLLED STAINLESS STEEL SHEET

Steel	Thickness, inch	Cold Reduction, per cent	Direction	0.2% Yield Strength, ksi	Ultimate Tensile Strength, ksi	Notch Strength Ratio	Type of Test	Reference
AM 355	0.025	15++	L	255	256	0.86	Edge-notch	36
			T	255	265	0.64		
	0.024	20++	L	218	239	1.01		
			T	186	233	0.95		
	0.024	30++	L	257	262	0.98		
			T	243	281	0.86		
	0.026	35++	L	286	289	0.96		
			T	258	286	0.80		
	0.024	40++	L	289	294	0.91		
			T	270	297	0.71		
AISI 301 (CEVM)	0.025	50	L	215	220	1.00(.73)	Edge-notch	37
		60	"	230	235	0.87(.64)		
		70	"	245	255	0.84(.59)		
		80	"	270	275	0.57(.33)		
AISI 301	0.063	70	L	220	250	0.80	Edge-notch	38
			T	220	265	0.64		
AISI 301	0.063	70	L	218	248	0.81	Edge-notch	36
			T	220	261	0.45		
	0.031	70	L	260	>263	<0.72		
			T	--	287	0.37		
AISI 301	0.043	67	L	249	264	0.56	Centre-crack	21
			T	264	288	0.26		
		67*	L	268	280	0.65		
			T	299	315	0.22		
AM 350 (CEVM)	0.025	30+	L	239	245	1.04	Edge-notch	39
			T	222	244	0.94		
		30‡	L	241	243	1.07		
			T	228	247	0.94		
		45+	L	274	280	0.98		
			T	274	280	0.82		

1. L = longitudinal; T = transverse.
2. Figures in parenthesis refer to transverse tests.
* Aged at 750°F for 8 hr.
\+ Aged at 825°F for 3 hr.
‡ Aged at 700°F for 3 hr.
++ Aged at 800°F for 3 hr.

steady reduction in the K_c value for 0.115 in. sheet as the degree of marforming increases from 0 to 50% for both the 250 and 300 grade.

Reference 22 also reports the effect of 50% hot-working in the austenitic range, followed by quenching, on the notch strength (centre-crack specimens) of 9% Ni - 4% Co steel sheet. When tempered at 400 F, the yield and tensile strengths in both directions and the longitudinal notch strength increased, but the transverse notch strength decreased. Matas, Hill, and Munger[14] report a similar effect, though no details are given. After the above treatment, tensile strengths as high as 370 ksi, were obtained with a K_c value of 150 ksi $\sqrt{in}$. The transverse fracture toughness was stated to be only 70-80% of the longitudinal value, but it would appear that the process should have some specialized applications. Kula and Dhosi[41] have applied the treatment to SAE 4340 steel plate tempered at 450 F, and found a corresponding improvement. Reductions up to 50% at 1550 F had no effect on the tensile strength, but tended to raise the Charpy energy absorbed vs. temperature curve and translate it in the direction of lower temperatures. Unfortunately, no data on the notched or cracked tensile strength are available for comparison.

The effect of mar-straining, in which the quenched and tempered steel is plastically deformed and subsequently re-tempered or aged, was investigated by R. E. Yount[42] with regard to its possible use for solid-propellent rocket-motor cases. Centre-notch tension tests were made on two alloys, D6AC and modified S-5 (.5 C, 1.8 Si, .5 Mo, .25V) in the form of sheet. In all cases, the specimen blanks were pre-strained up to 1.0% and aged before notching.

Results for both steels showed that 0.2% mar-strain lowered the K_c value to about 90 ksi $\sqrt{in.}$, but that this value remained substantially unchanged up to 1.0% mar-strain. Yount states that this value is still higher than that of H-11 steel, which has been successfully used in pressure vessels. Furthermore, the pre-straining process would be expected to reduce the effects of sub-critical defects already present in the material by the addition of compressive stresses and/or notch blunting. Tests were also made on 6 in. diameter cylinders from ring forgings, pre-strained by pressurizing, and then aged. The burst strengths for both alloys were equivalent to the tensile strength of the mar-strained material, the highest value obtained being 362 ksi.

Similar results were reported by Steigerwald[43] from edge-notch and centre-crack tests on H-11 sheet (UTS 290 ksi) after warm pre-stressing. In this treatment, the specimen blanks were pre-stressed at various levels at 80 F or 600 F before notching and testing at room temperature. The results showed, as above, a general decrease in the notch tensile strength, independent of the pre-stressing temperature and more marked as the pre-stress level was raised. Similar tests, however, made on specimens pre-stressed after notching showed a beneficial effect which tended to increase with the pre-stress level. The increase appeared to be limited only by the notch strength at the pre-stressing temperature. A much smaller improvement was observed in tests on another steel, 300 M alloy, presumably due to its low notch strength at the pre-stressing temperature (550 F). The investigator pointed out that the treatment was most effective when applied to materials of fairly high notch sensitivity; H-11 steel at a lower strength level was less improved. Its principal application would appear to be to hardware containing local potential trouble-spots, such as welds with micro-cracks.

Before leaving this section, some reference should be made to the effect of banding which may be found in rolled products and has been particularly prevalent in the 18% Ni steel. Fracture toughness tests on the 250 grade have generally given higher values (about 30%) from surface-crack specimens than from edge or centre-crack specimens. To investigate this effect further, Pellissier[44] carried out single-edge-crack tests on 0.14 in. thick specimens cut from 1-1/8-in. plate in four principal orientations. The orientations, with respect to the rolling direction, and the average G_{Ic} values obtained are shown in Figure 6. The G_{Ic} values in the longitudinal(A) and transverse(B) directions are closely similar, but the G_c value for the C orientation, simulating the surface-crack specimen, is about 25% greater. The much lower toughness observed in the D orientation demonstrates the harmful effect of banding in those conditions under which a crack can develop in the plane of the bands. This deleterious effect must obviously be taken into account in any application involving material which is known to be subject to banding. Pellissier also reported that the banding could be essentially eliminated by annealing at 2300 F for 16 hours prior to heat treatment. Unfortunately, homogenization reduced the longitudinal notch-tensile strength of round specimens from 319 ksi to 253 ksi.

ORIENTATION	G_{Ic}, lpsi
A	245
B	230
C	310
D	150

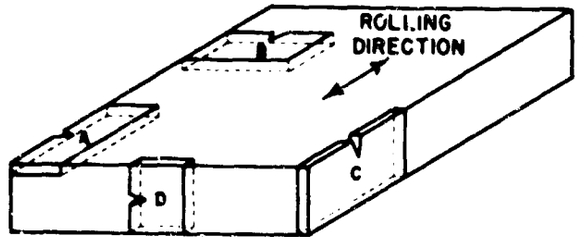

FIGURE 6. EFFECT OF ORIENTATION ON G_{Ic} VALUE - 18% Ni STEEL[44]

EFFECT OF ENVIRONMENT

Fracture mechanics concepts provide the designer with a relationship between defect or crack size and the stress at the moment of catastrophic failure. The slow growth of the original defect to its critical value is obviously a matter of some importance, and several investigations have been carried out to shed some light on the effect of the environment on this problem. The time-dependent delayed failure of rocket-motor cases at constant pressure when exposed to aqueous environments led Steigerwald[45] to examine their effect on centre-crack specimens of 300 M and H-11 sheet (UTS 290 ksi). At about 85% of the notch tensile strength, failure did not occur in 100 hours with 300 M steel and no liquid environment. The same steel in the presence of aqueous solutions of different pH values (4.8 to 9.0) gave failures in a matter of minutes; non-aqueous solvents and lubricating oil extended the time required considerably. H-11 tool steel gave similar results in distilled water. One other observation of interest was that the K_c value remained constant over the delayed failure range.

Saperstein and Whiteson[46] and Bennett[47] reported the results of fracture toughness tests on cracked sheet specimens of 4340 steel in distilled water. Delayed failure was again observed, due to slow crack growth, within 30 minutes at stresses as low as 40% of the tensile strength. The latter author, however, reported satisfactory behaviour in oil saturated with water. Saperstein and Whiteson made comparison tests on 18% Ni maraging steel and demonstrated its clear superiority on the basis of 30 minutes exposure, to stresses over 90% of the net fracture stress in air. Similar results for 4340 steel sheet (UTS 265 ksi) in distilled water have been presented by Yen and Pendleberry[48] who showed that the gross strength was proportional to the logarithm of the holding time for a given initial shallow-crack length.

Tiffany and Masters[49] recently reported the results of sustained-load tests on welded shallow-crack specimens of 18% Ni steel plate in a water environment. Little effect was observed with the base metal up to 100 hours, but the initial-to-critical stress intensity ratio decreased rapidly with holding time in the weld metal. Tests on notched bar specimens of 17-7 PH also showed only a small effect of a wet environment on slow crack growth, but data for surface-crack specimens of 4330 M steel showed a significant effect and indicated a threshold stress intensity level of about 30% of the critical value.

Slow crack growth is also effected by cyclic loading, and the combined effect of water vapour plus repeated loading on the fracture toughness of 4340 steel (UTS 260 ksi) has been studied by Van der Sluys[50]. Tests were made on pre-cracked round specimens in an argon atmosphere containing various amounts of water vapour. The data indicated that, though the presence of moisture only reduced G_{Ic} slightly, there was an increase in slow crack growth with increasing humidity. The addition of cyclic loading produced a further increase. When the results were compared on the basis of the stress required to cause either slow crack growth or failure in less than 100 cycles, it was found that a condition of 100% relative humidity reduced the "dry" stress level by nearly 50%.

Additional confirmation of the effect of moisture is provided by the work of Tiffany and Lorenz[51] on D6AC steel plate. The endurance of pre-cracked round specimens under cyclic loading was reduced by a factor of more than ten in an atmosphere of high humidity. As above, they too reported no significant effect of moisture on fracture toughness.

Although the data are still relatively sparse, it is evident that the environment, in particular water or water vapour, can have a profound effect on slow crack growth, more so with some alloys than with others. The designer must therefore pay due attention to this factor, whether his hardware is subject to sustained or to cyclic loading conditions.

EFFECT OF LOADING RATE

Even less experimental information is available on the effect of loading rate on the toughness of ultrahigh-strength steels, which are not generally regarded as being strain-rate sensitive. Since the hardware may be exposed to high loading rates due to shock or impact, this is a matter of considerable importance and merits further investigation. Srawley and Beachem[52] carried out centre-crack tests on a martensitic stainless steel, 422 M (UTS 250 ksi), over a range of temperatures. With rapid loading, from 500 to 1000 X normal rate, the net-fracture-stress transition temperature (NFSTT) was hardly affected. Below the NFSTT (e.g., at room temperature) however, the net fracture stress was lowered slightly, while above the NFSTT, it was raised (Figure 7). Additional work by the same investigators, reported by Marschall[53], showed a greater decrease (about 43%) in the net fracture stress at room temperature for a higher strength steel (UTS 290 ksi). The rapid loading rate was from 200 to 300 X normal rate; other details were not available.

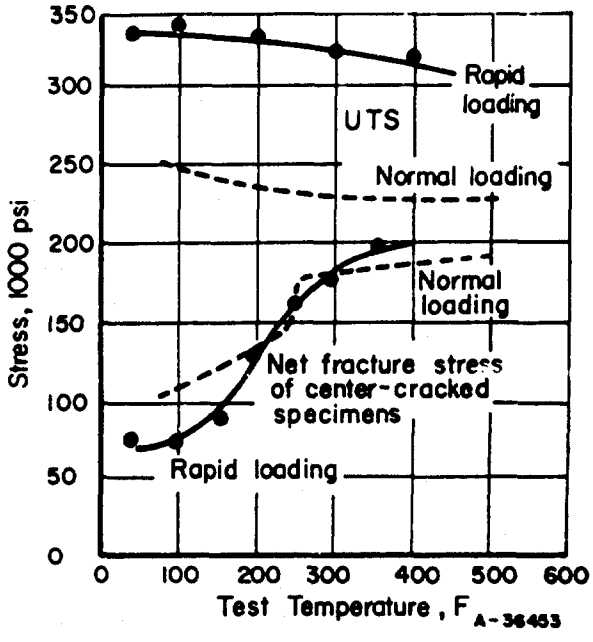

FIGURE 7. EFFECT OF LOADING RATE ON NET FRACTURE STRESS TRANSITION TEMPERATURE – 422 M STEEL[53]

A few test results were presented by Raring et al[39] for AM 355 stainless steel sheet

(UTS 230/240 ksi). The specimens were large, centre-notch panels, 24 in. wide with an 8 in. notch, and the loading time varied from 0.2 to 200 sec. For tests lasting between 2 and 200 sec, the net fracture stress and G_c showed little effect of loading rate, but at the higher rates both values decreased, about 25% and 40%, respectively.

Some tests reported by Yen and Pendleberry[48] on shallow-crack specimens of 4340 steel sheet (UTS 265 ksi) indicated a similar effect. Two series of tests were carried out with three crack lengths at stress rates of 100 and 12 ksi/min. Tests at the slower rate gave consistently higher values of the fracture strength, though the effect was slight (maximum 3%).

Evidence for an improvement in notch toughness due to rapid loading was given in reference 22, in which the results of G_c determinations were presented for 4340, D6AC and 18% Ni (250 and 300 grade) alloys. The tests were made at strain rates of 0.00005, 0.05 and 0.15 in./in./sec. At the two lower rates, the G_c values for each steel were closely comparable. At the highest rate, the 4340 and D6AC values showed no change, whereas the 18% Ni values showed a marked increase.

In the present state of the art, it would appear that materials for hardware for which high strain rates are a service condition or a potential hazard should preferably be evaluated under comparable loading rates. Failing this, some additional factor of safety might well be incorporated.

TESTS ON TYPICAL HARDWARE

Having reviewed the available notch toughness data and discussed the effects of some of the more important parameters, it is desirable to pay some attention to the results of tests on actual or sub-scale hardware before considering the question of design requirements. The great majority of the data in the literature relates to internal pressure tests on tubes, cylinders or spheres, and a summary of the results for ultrahigh strength steels is presented in Table 5.

Considering first the hoop burst stress data, it is apparent that values in excess of 300 ksi can be obtained with a number of ultrahigh-strength alloys (MBMC No. 1, Mod. S-5, D6AC, 300 M, H-11 and 18% Ni) in vessels ranging from 3-1/2 in. to 24 in. diameter. The highest values reported are 354 ksi for a 9-1/2 in. diameter vessel of H-11 steel with slight decarburization, and 362 ksi for a 6 in. diameter vessel of Mod. S-5 steel, pre-strained 0.30% and pre-cycled. At the other end of the scale, the lowest value (100 ksi) was obtained with a welded 12-inch diameter vessel of X-200 steel. Unfortunately, the literature is not always too clear regarding the method of manufacture, but at least three alloys, 300M, D6AC, and 18% Ni, gave burst stresses exceeding 300 ksi when welding was involved.

The majority of the results are shown plotted in Figure 8 in terms of hoop burst stress/yield strength ratio versus yield strength. The plot is very similar to that presented by Manning et al[32], and confirms their conclusion that satisfactory performance, burst stress exceeding yield strength, can be expected for pressure vessels fabricated from steels with yield strengths up to 220 ksi. The sole exceptions to this conclusion are two results for the 3Cr-Mo-V alloy. Above a yield strength of 220 ksi, the scatter becomes most pronounced, and the only alloy giving consistent satisfactory performance is the 18% Ni maraging steel. It is in this range that methods, previously discussed, for improving the notch toughness might most efficiently be employed. For example, the pre-straining of vessels of Mod. S-5 and D6AC steels in all cases gave burst stress/yield strength ratios greater than one at yield strengths well above 220 ksi. Similar experiments with 301 vessels were not quite as effective.

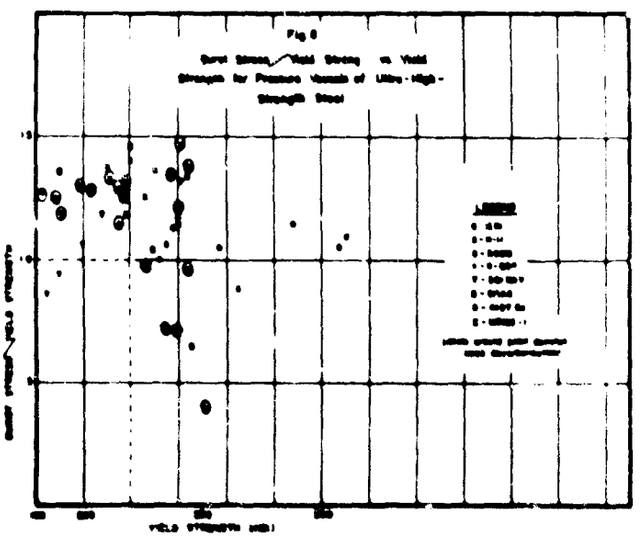

FIGURE 8. BURST STRESS/YIELD STRENGTH VERSUS YIELD STRENGTH FOR PRESSURE VESSELS OF ULTRAHIGH-STRENGTH STEEL

It is interesting to note that the beneficial effects reported for a small amount of surface decarburization on notch tensile specimens are confirmed by burst tests on actual vessels. It has been suggested that decarburization is beneficial only in so far as it reduces the yield strength, and there is considerable evidence to

TABLE 5. SUMMARY OF RESULTS OF BURST TESTS ON PRESSURE VESSELS

Steel	Form of Specimen	Thickness, in.	0.2% Yield Strength, ksi	Ultimate Tensile Strength, ksi	K_c, ksi$\sqrt{in.}$	Hoop Burst Stress, ksi	Depth of Decarburization, in.	Type of Fracture	Ref.	Remarks
AISI 4130	12 in. dia cylinder	.08	186	226	>290	247(3)	0.019	Full shear	32	Longitudinal weld: NSR > .88
	3-1/2 in. dia cylinder	.08	207	250	60.6*	258	--	Ditto	54	Draw and spin manufacture: pre-cracked vessel gave burst stress of 208 ksi (1/4 in. crack) K_{Ic} after test = 56.0 ksi$\sqrt{in.}$
MBMC No. 1	11-1/2 in. dia cylinder	.10	216	253	--	281(4)	0.011	--	55	Drawn vessel
	16 in. dia cylinder	.06	237	280	--	318(32)	0.011	--	55	Forged and spun vessel
	16 in. dia cylinder	.05	240	271	--	289(23)	0.004	--	55	Rolled and welded vessel
	12 in. dia cylinder	.08	204	243	>209	261(3)	0.019	Mainly shear	31	Rolled and welded vessel: NSR = .70
	12 in. dia cylinder	.08	234	276	80	167(2)	0.008	Mixed		Rolled and welded vessel: NSR = .43
Mod. S-5	6 in. dia cylinder	.06	≈300	--	≈87	354	--	Full shear	42	Non-welded manufacture: .26% pre-strain
	6 in. dia cylinder	.06	≈310	--	--	360	--	Ditto	42	Non-welded manufacture: .30% pre-strain
	6 in. dia cylinder	.06	≈310	--	--	362	--	--	42	Non-welded manufacture: .30% pre-strain and pre-cycled 9 times.
4137 Co	6 in. dia cylinder	.05	238	273	--	268(2)	--	--	56	Non-welded manufacture
	6 in. dia cylinder	.05	235	270	--	250	--	--	56	Girth weld
	12 in. dia cylinder	.10	240	275	--	286	--	--	56	Rolled and welded vessel
	54 in. dia vessel	.08	240	275	--	280	--	--	56	Deep drawn, longitudinal weld: pre-cycled 3 times.
D6AC	6 in. dia cylinder	.08	≈280	--	≈92	313(2)	--	Full shear	42	Non-welded manufacture: .34% pre-strain and pre-cycled 9 times.
	9-1/2 in. dia cylinder	.04	243	277	--	326(2)	0.005	--	55	Girth weld
	10 in. dia cylinder	--	220	270	--	322(2)	--	--	55	Forge-extruded
	10 in. dia cylinder	--	218	235	--	257(2)	--	--	55	Forge-extruded
	24 in. dia cylinder	--	229	264	--	235(2)	--	--	55	Forge-extruded and ring-rolled.
	24 in. dia cylinder	.08	190	215	--	256(4)	--	--	57	Forged and girth welded: Allison parameter 150 ksi.
	24 in. dia cylinder	.02	245	286	--	157	--	--	57	Forged and girth welded: Allison parameter 45 ksi.
	40 in. dia cylinder	.08	199	219	150†	Service test satisfactory	--	--	58	Girth weld: K_{Ic} = 66 ksi$\sqrt{in.}$
	3-1/2 in. dia cylinder	.08	234	264	40.5*	>168	--	Flat	54	Draw and spin manufacture: K_{Ic} after test = 28.9 ksi$\sqrt{in.}$ Pre-cracked cylinder gave burst stress of 102 ksi (1/4 in. crack).
	17 in. dia cylinder	.25	247	280	50*	169	--	--	51	Roll and weld manufacture: pre-cracked (1/4 in.)
	17 in. dia cylinder	.25	247	280	50*	73	--	--	51	Roll and weld manufacture: pre-cracked (1/2 in.)
3Cr-Mo-V	17 in. dia tube	.07	208	260	--	245(4)	(None)	--	33	Helical welding
	17 in. dia tube	.07	199	248	--	259(6)	0.005	--	33	Ditto
	17 in. dia tube	.07	200	244	--	212(2)	(None)	--	33	"
	17 in. dia tube	.07	191	231	--	226(4)	0.004	--	33	"
	17 in. dia cylinder	.07	190	230	--	178	(None)	--	33	"
	17 in. dia cylinder	.07	189	231	--	235(3)	0.003	--	33	"
	17 in. dia cylinder	.07	185	238	--	193	(None)	Brittle	33	Helical welding: Allison parameter = 0 ksi
	17 in. dia cylinder	.07	183	231	--	236	0.004	Full shear	33	Helical welding: Allison parameter = 33.6 ksi
AMS 6434	3-1/2 in. dia cylinder	.07	225	270	58.5*	295	--	Full shear	54	Draw and spin manufacture: K_{Ic} after test = 44.4 ksi$\sqrt{in.}$ Pre-cracked cylinder gave burst stress of 167 ksi (1/4 in. crack).
AISI 4340	3-1/2 in. dia cylinder	.07	214	254	62.0*	290	--	Full shear	54	Draw and spin manufacture: K_{Ic} after test = 49.7 ksi$\sqrt{in.}$ Pre-cracked cylinder gave burst stress of 195 ksi (1/4 in. crack).
X-200	3-1/2 in. dia cylinder	.08	246	286	31.6*	>205	--	Mixed	54	Draw and spin manufacture: K_{Ic} after test = 26.1 ksi$\sqrt{in.}$ Pre-cracked cylinder gave burst stress of about 105 ksi (1/4 in. crack).
	12 in. dia cylinder	.07	219	259	>197	278	0.018	Mainly shear	31	Roll and weld manufacture: NSR = .60
	12 in. dia cylinder	.07	215	259	>171	246(2)	0.024	Ditto	31	Roll and weld manufacture: NSR = .71
	12 in. dia cylinder	.07	251	291	102	100(2)	0.006	--		Roll and weld manufacture: NSR > .37

TABLE 5. (Continued)

Steel	Form of Specimen	Thickness, in.	0.2% Yield Strength, ksi	Ultimate Tensile Strength, ksi	$K_{c/}$ ksi $\sqrt{in.}$	Hoop Burst Stress, ksi	Depth of Decarburisation, in.	Type of Fracture	Ref.	Remarks
Rocoloy 270	3-1/2 in. dia cylinder	.08	256	313	30.1*	204	--	Mixed	54	Draw and spin manufacture: K_{Ic} after test = 52.1 ksi$\sqrt{in.}$ Pre-cracked cylinder gave burst stress of 113 ksi (1/4 in. crack).
AISI 4330V (Mod. + Si)	3 in. dia cylinder	--	206	248	115*	171(2)	--	--	58	Ring forgings with external notch (.15 in.) pre-cycled to leak.
	3 in. dia tube	--	206	248	115*	165(2)	--	--	58	
300-M	9 in. dia cylinder	.06	244	290	--	329	0.007	--	55	Girth weld
	12 in. dia cylinder	.08	216	261	>177	272(3)	0.016	Mainly shear	31	Roll and weld manufacture: NSR = .63
	12 in. dia cylinder	.08	237	280	144	170(2)	0.010	--	31	Roll and weld manufacture: NSR = .53
	40 in. dia cylinder	.08	232	282	150†	232	--	Full shear	56	Hot-cupped and cold drawn; pre-cycled: K_{Ic} = 86 ksi$\sqrt{in.}$
	3-1/2 in. dia cylinder	.08	242	286	53.3*	324	--	Full shear	54	Draw and spin manufacture: K_{Ic} after test = 43.2 ksi$\sqrt{in.}$ Pre-cracked cylinder gave estimated burst stress of 200 ksi (1/4 in. crack).
H-11	11-1/2 in. dia cylinder	.10	211	255	--	279(4)	0.008	--	55	Drawn
	9-1/2 in. dia cylinder	.07	241	291	--	354	0.0005	--	55	Flow-turned
	6 in. dia cylinder	.05	226	255	--	284(78)	--	--	55	Roll and weld manufacture
	6 in. dia cylinder	.05	≈230	286	--	312(3)	--	--	55	Drawn
	6 in. dia cylinder	.05	≈220	263	--	308(3)	--	--	55	Drawn
	6 in. dia cylinder	.05	≈210	243	--	287(3)	--	--	55	Drawn
	12 in. dia cylinder	.08	226	256	80	219(3)	0.009	5% shear	32	Roll and weld manufacture: NSR = .41
	12 in. dia cylinder	.08	244	297	97	233(2)	0.007	--	32	Roll and weld manufacture: NSR = .42
	3-1/2 in. dia cylinder	.08	265	303	34.5*	235	--	Flat (fragmented)	54	Draw and spin manufacture: K_{Ic} after test = 31.5 ksi$\sqrt{in.}$ Pre-cracked cylinder gave estimated burst stress of 185 ksi (1/4 in. crack).
301	13-1/2 in. dia sphere	.03	≈195	≈220	--	207	--	--	40	Hydroformed and welded: pre-strain at -32 F, .06
	13-1/2 in. dia sphere	.03	≈ 175	≈280	--	258**	--	--	40	Hydroformed and welded: pre-strain at -32 F = .06
	(14-1/2 in. dia after stretching)	.08	≈275	≈280	--	287**	--	--	40	Hydroformed and welded: pre-strain at -32 F = .075
		.08	≈260	≈270	--	248**	--	--	40	Hydroformed and welded: pre-strain at -32 F = .06
						**Aged after pre-straining				
18% Ni	6 in. dia cylinder	--	--	≈290	--	324(2)	--	--	55	Forged and welded
	6 in. dia cylinder	.14	310	315	--	338(3)	--	Full shear (fragmented)	25	Draw and spin manufacture
	24 in. dia cylinder	.13	288	291	--	320(2)	--	Ductile	59	Roll-formed and welded; pre-cycled.
	3-1/2 in. dia cylinder	.09	[illegible]	267	59.1*	268	--	Full shear	54	Draw and spin manufacture: K_{Ic} after test = 59.4 ksi$\sqrt{in.}$ Pre-cracked cylinder gave estimated burst stress of 250 ksi (1/4 in. crack)
	3-1/2 in. dia cylinder	.09	[illegible]	310	63.6*	322	--	Full shear	54	Draw and spin manufacture: K_{Ic} after test = 55.8 ksi$\sqrt{in.}$ Pre-cracked cylinder gave estimated burst stress of 300 ksi (1/4 in. crack).

Notes:

1. K values:
   † indicates K_c value obtained from a centre-crack tension test.
   * indicates K_{Ic} value obtained from a centre-crack tension test.
   The remaining data represent K_c values obtained from centre-notch tension tests.
2. Figures in parentheses indicate the number of specimens tested when greater than one.
3. The chemical compositions of the following alloys were not included in Table 1:

   Mod. S-9: 0.50 C, 0.80 Mn, 1.8 Si, 0.50 Mo, 0.25 V.
   3Cr-Mo-V: 0.40 C, 0.60 Mn, 0.25 Si, 3 Cr, 1 Mo, 0.20 V.
   Rocoloy 270: 0.45 C, 0.55 Mn, 1.2 Si, 1.7 Cr, 1.3 Ni, 0.5 Mo, 0.20 V, 0.30 W.

support this argument. The results of the burst tests on 3Cr-Mo-V steel vessels[33], however, are directly contradictory. The small amount of decarburization (0.003/0.004 in.) had little effect on the yield strength, admittedly somewhat low, but a significant effect on the burst stress of 17 in. diameter cylinders.

Table 5 also gives results obtained from burst tests of pre-cracked vessels of a number of alloys. These tests were essentially carried out in one laboratory[54] on 3-1/2 in. diameter cylinders of draw-and-spin manufacture, and were supplemented by K_{Ic} determinations from centre-cracked tensile tests. The results for both uncracked and cracked cylinders are shown plotted in Figure 9 in terms of burst hoop stress/yield strength versus K_{Ic} value. The data for the uncracked vessels suggest that a K_{Ic} value of 45-50 ksi $\sqrt{in.}$ is required to give a burst stress exceeding the uniaxial yield strength. In the presence of a 1/4 in. crack, which presumably would not escape detection but might develop during service, a K_{Ic} value of about 60 ksi $\sqrt{in.}$ would probably give a burst stress within 10% of the yield strength.

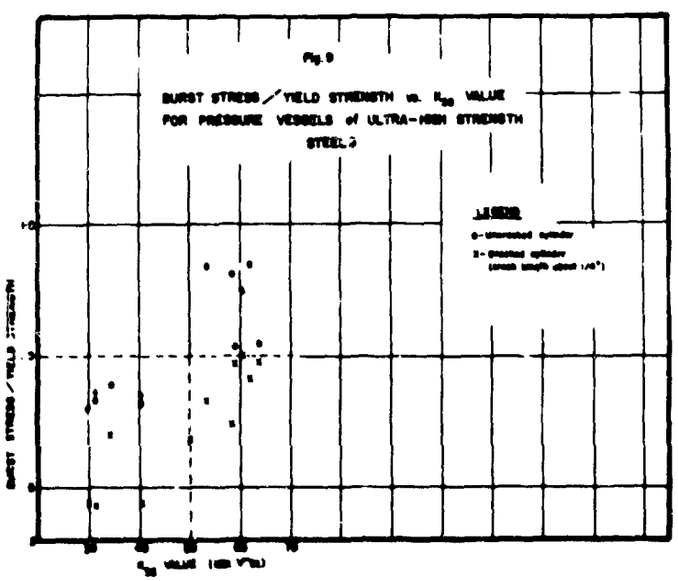

FIGURE 9. BURST STRESS/YIELD STRENGTH VERSUS K_{Ic} VALUE FOR PRESSURE VESSELS OF ULTRAHIGH-STRENGTH STEELS

Additional notch toughness data included in Table 5 are values of the Allison parameter, obtained from instrumented bend tests, of K_C, obtained from centre-notch tensile tests, and of the notch strength ratio, obtained from edge-notch tensile tests. Data for the former is rather meagre and is available only for vessels of D6AC and 3Cr-Mo-V alloys. In both cases, a lower value of the parameter is associated with a burst stress below the yield strength, and a higher value with a burst stress above the yield strength. Apart from showing the discriminatory nature of the test, the results do not warrant any further conclusions.

The K_C and NSR data were obtained from a series of tests on specimens taken from burst vessels of AISI 4130, M3MC No. 1, X-200, 300 M and H-11 steels, carried out in one laboratory[32]. The results are shown plotted in terms of hoop burst stress/yield strength ratio versus K_C and NSR in Figures 10 and 11, respectively, taken from the author's publication. Manning et al suggested that minimum values for K_C of 150 ksi $\sqrt{in.}$ and NSR of about 0.57 are required for satisfactory performance, but pointed out that their data were derived from specimens which had undergone a certain amount of plastic deformation.

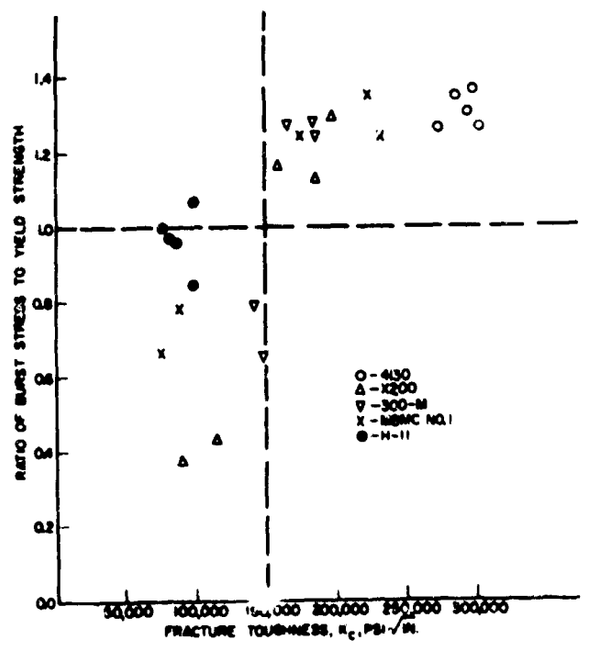

FIGURE 10. BURST STRESS/YIELD STRENGTH VERSUS K_C VALUE FOR PRESSURE VESSELS OF ULTRAHIGH-STRENGTH STEEL[32]

Apart from the information available and discussed above on pressure vessels, a few results have been reported for recoilless rifles[60] and aircraft landing gear[61]. In the case of the recoilless rifles, the requirement was for a steel with a minimum yield strength of 220 ksi, and good notch toughness. The alloy selected was 4330 V (Mod. + Si) steel, and at the specified yield strength, the NSR value was about 0.9 and the K_{Ic} value about 85 ksi $\sqrt{in.}$ The data were obtained from notched round specimens (no details of notch given). Centre-notch sheet specimens were used to determine K_C, the value obtained being 290 ksi $\sqrt{in.}$ Hydrostatic tests were carried out on 3-1/2 in. diameter cylinders, and gave full shear failures

with the combined yield stress very close to the uniaxial yield strength. Firing tests on actual rifles were also satisfactory. It will be apparent that these results are in agreement with the conclusions arrived at earlier in this section.

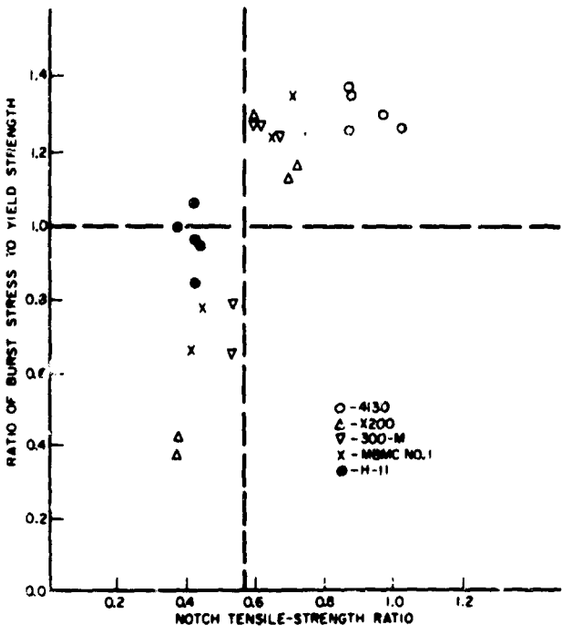

FIGURE 11. BURST STRESS/YIELD STRENGTH VERSUS NOTCH STRENGTH RATIO FOR PRESSURE VESSELS OF ULTRAHIGH-STRENGTH STEELS[32]

The information regarding landing gear is contained in an article analyzing the service failure of three aircraft parts made of AISI 4340 steel, quenched and tempered to a tensile strength of about 270 ksi with a yield strength of about 235 ksi. Although no data pertinent to the present discussion were given, the investigation was of some importance since it stressed the dangers of hydrogen embrittlement in ultrahigh-strength steel. All three failures were attributed basically to this cause, and the necessity of extreme care in processing and fabrication, and in the design and maintenance of the hardware was emphasized. It is not proposed to review this particular aspect of the notch toughness problem here, but reference may be made to a related study of solid-fuel rocket chambers carried out by Shank et al[62]. The authors stressed the beneficial effects of surface decarburization, and concluded that it was necessary with present alloys to design to notch strength ratios of less than 1.0 to secure minimum feasible weight.

DESIGN REQUIREMENTS

Examination of structures and structural components of ultrahigh-strength steels, which have failed in service, generally reveals that the origin of failure was a small crack or crack-like flaw. Presumably the initial flaw size was insufficient to cause fracture in the proof test or upon initial loading, and required a number of load cycles and/or time under sustained load to attain the critical size for failure. The flaws normally encountered can be classified as surface flaws, embedded flaws and through-the-thickness cracks[10,49]. For surface and embedded flaws, the conditions are generally those of plane strain. The initial flaws may or may not reach the critical size before growing through the thickness depending upon the K_{Ic} value, the applied stress level and the material thickness. For through-the-thickness cracks in relatively thin material, plane stress conditions normally predominate, and K_c is the important parameter. As the thickness increases the fracture appearance changes from full shear to flat, and the K_{Ic} value should be used.

It will be apparent from the foregoing that three of the principal factors controlling the performance of ultrahigh-strength hardware are the initial flaw size, flaw growth and critical flaw size. These factors in turn are dependent upon a number of others, notably the material, its processing and heat treatment, the fabrication procedure, the service temperature, the type of loading, the environment, and the accuracy and extent of the nondestructive inspection. The effect of the majority of the factors on the notch toughness of various materials has already been discussed, but some additional comments are desirable at this point.

Firstly, with regard to the inherent toughness of the material, a number of investigators[25,63] have reported significant variations from heat to heat and from vendor to vendor with no obvious connection with the chemistry. Such a situation is to be regretted, but also accepted in the present state of the art, and is an additional reason for the incorporation of some form of fracture toughness test, other than the standard Charpy test which is insufficiently sensitive, into material specifications.

Secondly, the effect of temperature has so far been largely ignored. The operating temperature is undoubtedly an important factor, and must be taken into consideration for such applications as cryogenic tankage and those involving aerodynamic heating. It is not intended in the present review, however, to deal with this aspect in detail, but references are provided for those who are specifically interested. In general, the notch-toughness parameters (NSR, K_c and K_{Ic}) of the ultrahigh-strength steels decrease as the test temperature is lowered from room temperature to cryogenic

temperatures. References 60, 64, 65, 66 and 67 present data for 4330V (Mod. + Si), Vascojet 1000 and 300 M, 4340, X200 and AMS 6434 alloys, respectively. In contrast, limited tests on both grades of 18% Ni alloy[24] indicate little effect, if anything a slight increase, down to -45 F. The information available on the effect of elevated temperatures (up to 400 F) on the toughness is less consistent. References 16, 24 and 68 indicate a decrease for AMS 6434, 18% Ni, and 4340 alloys respectively, when the temperature is raised, whereas references 64 and 66 show an increase for Vascojet 1000 and 300 M, and X200 alloys, respectively.

Thirdly, there is the question of the degree and extent of the non-destructive inspection. The adequacy of the inspection procedure, since it controls the magnitude of the initial flaw size, is a major factor in determining the performance of the hardware. The difficulties involved in the adequate inspection of certain items such as large rocket-motor cases, however, must be appreciated. It has been reported that the smallest flaw known to cause a failure was 1/32 in. long and 1/32 in. deep[69]. An additional control in the case of pressure vessels is supplied by the conventional proof test which, if successful, actually defines the maximum possible initial flaw size that exists in the vessel.

The three primary factors controlling service performance, as mentioned earlier, are initial flaw size, flaw growth and critical flaw size. With the aid of fracture mechanics and a knowledge of the fracture toughness, the critical flaw size can be derived for the operating conditions. In order, then, to determine the limiting initial flaw size, and hence the level of inspection, data must be obtained on the rate of flaw growth, whether this be due to cyclic or sustained loading, or both. Tiffany, et al,[49,51] have utilized the reverse approach to predict with reasonable accuracy the life of a 17 in. diameter cylinder of D6AC, subjected to low cycle fatigue. The cyclic flaw growth was determined using notched bars and surface-cracked specimens, and cycling them to failure at various percentages of the critical stress intensity. The curve obtained was then used to predict the life of pre-flawed cylinders. Data were also presented on the cyclic flaw growth of 17-7 PH and 18% Ni steels and the flaw growth under sustained loading, by a similar procedure, of 17-7 PH, 4330M and 18% Ni steels. Under sustained loading, crack growth does not normally occur when the stress intensity is less than about 80% of the critical value, but both types of growth may have to be taken into account in any given application. An exception to this behaviour has been noted for certain alloys in the presence of water, when crack growth may take place at considerably lower stress intensities.

One test on a surface-cracked specimen of 18% Ni steel is of particular interest, since it supports Irwin's so-called "second line defence" suggestion[70]. The plane stress fracture toughness of an ultrahigh-strength steel is much higher than the plane strain value, which governs the onset of instability, and may be sufficient to arrest the running crack. In the test on a 1/4 in. thick specimen of 18% Ni steel, the surface crack was observed to pop through the thickness at 173 psi and was arrested until the stress was raised to 178 ksi, at which level the specimen fractured.

It will be apparent that this aspect of the problem, cyclic flaw growth, has overlapped into the field of fatigue, and some consideration may usefully be given to a tentative approach from this field[71]. The method, proposed by Kuhn, is designed for the prediction of the effect of flaws on both the static and the fatigue strength. Briefly, the static strength of a cracked component is predicted from the theoretical stress concentration factor corrected for size effect, by the Neuber constant, and for the effect of plasticity. For fatigue loading near the fatigue limit, the plasticity correction is omitted. The method appears to have been applied with reasonable accuracy to the prediction of the fracture stress of cracked aluminum and titanium alloy sheet, and the notch fatigue factor of low-alloy steel shafts, but no corresponding applications have been presented for ultrahigh-strength steels. Some data are given for H-11 steel in which the method is used satisfactorily to predict the notch strength ratio for a limited range of root radii based on a value of Neuber's constant derived from tests of cracked specimens. Further examination of this approach is warranted and might be quite rewarding.

Numerous other design procedures and design criteria, both theoretical and experimental have been proposed during the last few years. One of the earlier criteria was suggested by Srawley[72], and involved the fracture appearance transition temperature (FATT) and the net fracture stress transition temperature (NFSTT). The former was defined as the lowest temperature at which a centre-crack specimen would exhibit full shear, and the latter as the temperature at which the net fracture stress is equal to the yield strength. If, for the particular thickness and condition of the material, either the FATT or the NFSTT were above the lowest operating temperature, the author contended that the steel should not be used. Of the alloys studied at that time, only two gave a FATT below room temperature (75°F) with a yield strength above 200 ksi, as can be seen in Figure 12. Unfortunately, no service data were available to check the operational validity of this approach.

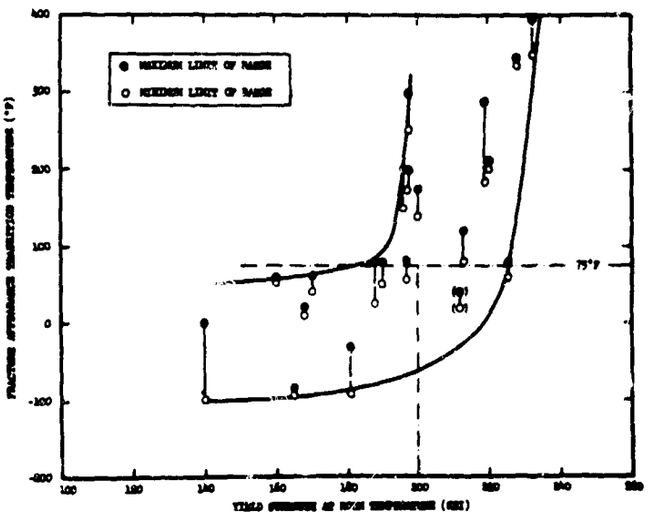

FIGURE 12. FRACTURE APPEARANCE TRANSITION TEMPERATURE VERSUS YIELD STRENGTH FOR SOME HIGH-STRENGTH STEELS(72)

A design criterion, based on fracture mechanics and associated with the foregoing, was proposed by Irwin(3) for pressure vessels, and is known as the leak-before-burst criterion. It is based upon the parameter β_c, which is proportional to the ratio between the plastic zone size ahead of the crack tip and the plate thickness (B).

$$\beta_c = \frac{K_c^2}{B\sigma_\gamma^2} \quad (\sigma_\gamma = 0.2\% \text{ yield strength})$$

Irwin suggested that β_c should be equal to or greater than 2π, which is equivalent to stating that the material should be able to arrest a through-crack of length equal to 2B when the stress equals the yield strength. This relationship corresponds experimentally(73) to test-pieces containing more than 80% shear on the fracture surface, hence the connection with Srawley's criterion. Experimental justification is afforded by burst tests on pressure vessels carried out by Carman, et al(58). From the results for several alloys, the authors concluded that a value of 2π for β_c was, at least, desirable, and that extreme care in fabrication and inspection was necessary below this value. They also pointed out that under certain conditions, K_c/K_{Ic} ratio of less than two, the fracture behaviour is governed by the plane strain fracture toughness. Additional verification is provided by the data for pressure vessels summarized in Table 5. For all those tests for which the necessary information is available, the behaviour of the pressure vessel could essentially be predicted by the β_c criterion. Furthermore, the condition proposed by Manning, et al(32), of a minimum K_c value of 150 ksi $\sqrt{\text{in.}}$ at yield strengths up to 220 ksi for vessels of about 0.08 in. wall thickness corresponds to a minimum β_c value of about 2π(4).

Other design criteria have been suggested which are not based directly on fracture mechanics, in particular a critical value of the notch-strength-ratio (NSR). A value of unity has been proposed and, as a less conservative criterion, a notch tensile strength exceeding the yield strength(12). Unfortunately, the notch strength is dependent upon the specimen size, notch depth and root radius, and much of the available data does not meet the current requirements for a sharp notch. Experimental data from pressure vessel tests by Manning et al(32) led to the conclusion that a NSR value of about 0.57 was sufficient for satisfactory performance, as mentioned earlier. Very little additional information is available in Table 5 to check this conclusion. Klier(65) has carried out tests on fatigue-cracked, round specimens of 4340 steel and has concluded that the temperature at which NSR = 1 corresponds to the nil ductility transition (NDT) temperature as measured in the drop-weight test. This point will be returned to later in the discussion.

Another possible criterion, which has been shown to correlate well with the behaviour of pressure vessels, is based on the instrumented bend test. In this test, developed by Hanink and Sippel(74), the specimen dimensions are designed to produce a biaxial stress field similar to that in a cylindrical pressure vessel, and no artificial notch is required. The bend test parameter is the difference between the maximum fibre stress and the stress at which rapid crack propagation begins, and has been shown to correlate with the per cent shear and the G_c value for centre-crack tests. The results of tests by Cottrell and Turner(33) would suggest a critical parameter value of more than 30 ksi, since their bend tests were made on material from burst vessels. The only other data available(57) indicates a value in excess of 45 ksi. The important point is that this simple test does reproduce pressure vessel conditions, and can discriminate between satisfactory and unsatisfactory material. Cottrell, et al(26), have also used a wide bend test to evaluate the biaxial ductility of low-alloy steel for rocket-case construction. If the specimens can be bent through 180° without failure around a former of radius equal to four times the sheet thickness, the ductility is considered to be satisfactory.

The consideration of design criteria would not be complete without a reference to the extensive work of Pellini and his collaborators. In order to study the response of thicker material, suitable for submarine hulls and hydrofoils, to a crack, these investigators developed the drop-weight test and the explosion bulge test, and more recently the tear versions of these tests. The drop-weight test was designed

to evaluate the resistance of the material to crack propagation in a stress field of yield strength level, and leads to the determination of the NDT. The drop-weight tear test differs essentially in the direction of crack propagation relative to the motion of the impacting load, and in the magnitude of the initial crack velocity which is higher when it reaches the test material. The explosion bulge and explosion bulge tear tests are similar insofar as the loading method is concerned, but in the latter the crack propagates from a 2 in. flaw in a direction of essentially uniform loading. The explosion bulge tear test may be regarded as establishing an extreme upper limit to the severity of loading conditions in a structure.

Pellini and Puzak have drawn attention to the "low energy shear" characteristics of the ultrahigh-strength steels, and have discussed the implications[75,76]. At yield strength levels above 200 ksi, the Charpy V upper shelf or plateau energy may drop to very low values (15 to 20 ft lb), as indicated schematically in Figure 13. In effect, the ductile energy absorption of such steels is comparable to the energy absorption for brittle fracture of lower strength steels. Hence, fracture with no sign of cleavage may initiate from small flaws at elastic stress levels close to the yield strength, and large flaws may be disastrous. Typical failures from service were quoted to illustrate this point. Explosion bulge tear tests of a number of steels demonstrated that a high level of fracture toughness was associated with a shelf energy in excess of 50 ft lb. A maraging steel of 220 ksi yield strength, however, gave a "flat break" of full width at 30 F. Similarly, in the drop-weight tear test, the energy absorbed by the maraging steel was very low. Presumably, other ultrahigh-strength steels would have shown much the same behavior. The authors conclude that maraging steels of the 260 ksi strength level, which are not subject to quench-and-temper treatments, are acceptable for large booster casings, despite the fact that the flaw size for fracture initiation at yield strength levels is of the order of 3/8 in. for a 3/4 in. thick plate. This conclusion is based upon inspectability and the nature of the service, and obviously the same considerations would not apply to submarine hulls.

The difference in the requirements for motor cases and submarine hulls has been stressed by Manning and Martin[77]. The latter, in particular, must be capable of withstanding shock wave loading, and it is desirable that the material should absorb the applied energy by distributing the plastic deformation through as large a volume of metal as possible. If it is accepted that the explosion bulge tests evaluate this characteristic, and if the correlation with the Charpy V shelf energy is maintained, then it is apparent that the

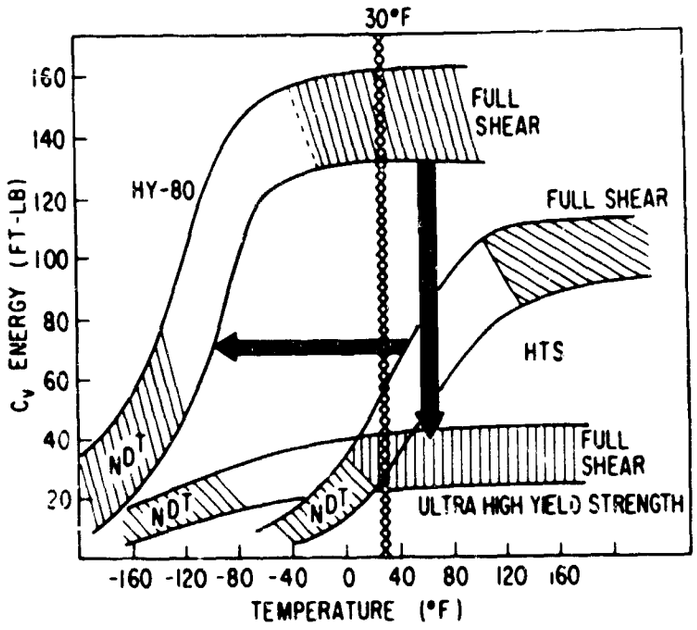

FIGURE 13. REPRESENTATIVE CHARPY-V TRANSITION CURVES FOR HIGH-STRENGTH AND ULTRAHIGH-STRENGTH STEELS[75]

application of ultrahigh-strength steels to hulls may be limited entirely by the extent and level of the inspection procedure.

To summarize the foregoing discussion, a number of criteria are now available to the designer of ultrahigh-strength steel hardware. For conditions involving essentially static "one-shot" loading, the β_c criterion has been found to correlate well with service performance. When the conditions are such that a fair degree of cyclic loading is involved, allowance must be made for possible slow crack growth, and here the environment may be an important factor. For those applications in which shock loading is likely or even possible, and in the present state of the art, it would appear that more severe tests are necessary, such as those developed at NRL, particularly if failure of the hardware involves a hazard to personnel. Nevertheless, it is suggested that for certain applications more use might profitably be made of simpler tests, such as the instrumented bend test, which have also shown good correlation with performance.

REFERENCES

(1) Cottrell, C. L. M., "High-Strength Steels", Iron and Steel Inst., Special Report 76, 1-6 (1962).

(2) Irwin, G. R., "Fracturing of Metals", ASM, Cleveland, Ohio (1948).

(3) Irwin, G. R., and Kies, J. A., Metal Progress, 73-78 (August, 1960).

(4) Irwin, G. R., Applied Materials Research, 3, 65-81 (April 1964).

(5) Irwin, G. R., Kies, J. A., and Smith, H. L., Proc. ASTM, 58, 640-657 (1958).

(6) ASTM Special Cttee, ASTM Bulletin 29-39 1960.

(7) ASTM Special Cttee, ASTM Bulletin, 18-28 (1960).

(8) ASTM Special Cttee, Materials Research and Standards, 389-393 (May, 1961).

(9) ASTM Special Cttee, Materials Research and Standards, 196-203 (March, 1962).

(10) ASTM Special Cttee, Materials Research and Standards, 4, 107-119 (March, 1964).

(11) Srawley, J. E., and Brown, W. F., Jr., NASA Tech. Memo, NASA TMX-52030 (1964).

(12) Espey, G. B., Metal Progress, 78, 83-88 (August, 1960).

(13) Davis, R. A., 3rd Maraging Steel Project Review, 527-535 (November, 1963).

(14) Matas, S. J., Hill, M., and Munger, H. P., ASM Metals Engineering Quarterly, 3, 7-16 (August, 1963).

(15) Jones, R. L., 3rd Maraging Steel Project Review, 483-501 (November, 1963).

(16) Gilbert, L. L., and Brown, J. A., High Strength Steels for the Missile Industry, ASM, 3-39 (1961).

(17) Shannon, J. L., Espey, G. B., Repko, A. J., and Brown, W. F., Proc. ASTM, 60, 761-777 (1960).

(18) Srawley, J. E., and Beachem, C. D., NRL Report 5771 (May 31, 1962).

(19) Decker, R. F., Eash, J. T., and Goldman, A. J., ASM Trans. Quarterly, 55, 58-76 (March, 1962).

(20) Haynes, A. G., and Blower, R., "High-Strength Steels", Iron and Steel Inst. Special Report 76, 40 (1963).

(21) Anonymous, Technical Documentary Report No. ASD-TDR-62-1034, Pt I (April, 1963).

(22) Republic Steel Corp., Interim Eng. Progress Report (September 1-November 1, 1963).

(23) Beachem, C. D., and Srawley, J. E., NRL Report 5507 (August 19, 1960).

(24) Campbell, J. E., Barone, F. J., and Moon, D. P., DMIC Report 198, Battelle Memorial Institute, Columbus, Ohio (February 24, 1964).

(25) Melville, A., 3rd Maraging Steel Project Review, 327-368 (November, 1963).

(26) Cottrell, C. L. M., Langstone, P. F., and Rendall, J. H., J. Iron and Steel Inst., 201, 1032-1037 (December, 1963).

(27) Klier, E. P., ASTM Special Technical Publication No. 287, 196-207 (1961).

(28) Espey, G. B., "High-Strength Steels for the Missile Industry", ASM, 129-152 (1961).

(29) Hamaker, J. D., and Vater, E. J., Proc. ASTM, 60, 691-717 (1960).

(30) Wei, R. P., ASTM Preprint, June, 1964, Annual Meeting.

(31) Warke, W. R., and Elsea, A. R., DMIC Memo 154, Battelle Memorial Institute, Columbus, Ohio (June 18, 1962).

(32) Manning, R. D., Murphy, W. J., Nichols, H. J., and Caine, K. E., Materials Research and Standards, 2, 392-395 (May, 1962); 469-475 (June, 1962).

(33) Cottrell, C. L. M., and Turner, M. J., J. Iron and Steel Inst., 200, 380-388 (May, 1962).

(34) Langstone, P. F., Metallurgia, 64, 107-115 (September, 1961).

(35) Sheehan, J. P., and Manning, R. D., ASTM Special Technical Publication No. 345, 89-97 (1963).

(36) Barone, F. J., and Hall, A. J., DMIC Memo 164, Battelle Memorial Institute, Columbus, Ohio (January 31, 1963).

(37) Espey, G. B., Jones, M. H., and Brown, W. F., Jr., ASTM Special Technical Publication 302, 140-165 (1962).

(38) Espey, G. B., Jones, M. H., and Brown, W. F., Jr., National Academy of Sciences, Report MAB-156-M, 93-157 (1959).

(39) Raring, R. H., Freeman, J. W., Schultz, J. W., and Voorhees, H. R., NASA Tech Note D-1798 (May, 1963).

(40) Alper, A. H., ASTM Advance Copy, Annual Meeting, June, 1964.

(41) Kula, E. B., and Dhosi, J. M., Trans ASM, 52, 321-338 (1960).

(42) Yount, R. E., Technical Documentary Report No. ASD-TDR-62-230 (August, 1962).

(43) Steigerwald, E. A., ASM Trans., 54, 445-455 (1961).

(44) Pellissier, G. E., 3rd Maraging Steel Project Review, RTD-TDR-63-4048, 407-437 (November, 1963).

(45) Steigerwald, E. A., Proc. ASTM, 60, 750-760 (1960).

(46) Saperstein, Z. P., and Whiteson, B. V., 3rd Maraging Steel Project Review, RTD-TDR-63-4048, 1-42 (November, 1963).

(47) Bennett, G. V., Materials Protection, 2, 16, 19-21, 23, 24, and 26 (October, 1963).

(48) Yen, C. S., and Pendleberry, S. L., ASM Trans., 55, 214-229 (March, 1962).

(49) Tiffany, C. F., and Masters, J. N., ASTM Advance Copy, Annual Meeting, June, 1964.

(50) Van Der Sluys, W. A., University of Illinois, T and A.M. Report No. 245 (May, 1963).

(51) Tiffany, C. F., and Lorenz, P. M., Technical Documentary Report ML-TDR-64-53 (May, 1964).

(52) Srawley, J. E., and Beachem, C. D., NRL Report 5127 (April 9, 1958).

(53) Marschall, C. W., DMIC Report 147, Battelle Memorial Institute, Columbus, Ohio, (February 6, 1961).

(54) Bhat, G. K., Mellon Institute, Final Report on Project 4396 (June 25, 1963).

(55) Campbell, J. E., DMIC Report 178, Battelle Memorial Institute, Columbus, Ohio (November 20, 1962).

(56) Bhat, G. K., Metal Progress, 77, 75-79 (June, 1960).

(57) Sippel, G. R., Vonnegut, G. L., and Hanink, D. K., National Academy of Sciences Symposium, Report MAB-156-M, 273-305 (February, 1959).

(58) Carman, C. M., Armiento, D. F., and Markus, H., ASME Preprint No. 63-WA-138, Annual Meeting, 1963.

(59) Sippel, G. R., and Vonnegut, G. L., 3rd Maraging Steel Project Review, RTD-TDR-63-4048, 213-273 (November, 1963).

(60) Carman, C. M., Armiento, D. F., and Markus, H., Metal Progress, 82, 86-89 (July, 1962).

(61) Holhouser, W. L., Preprint ASM National Metal Congress (1963).

(62) Shank, M. E., Spaeth, C. E., Cooke, V. W., and Coyne, J. E., Metal Progress, 76, 74-82 (November, 1959) and 84-92 (December, 1959).

(63) Payne, W. F., Preprint ASTM Annual Meeting, 1964.

(64) Sachs, G., and Sessler, J. G., ASTM Special Technical Publication No. 287, 122-135 (1961).

(65) Klier, E. P., NRL Report No. 6012 (December 16, 1963).

(66) Srawley, J. E., and Beachem, C. D., ASTM Special Technical Publication No. 302, 69-80 (1962).

(67) Srawley, J. E., Lupton, T. C., and Kenton, W. S., NRL Report No. 5895 (February 13, 1963).

(68) Hays, L. E., and Wessel, E. T., Applied Materials Research, 2 (2), 99-108 (1963).

(69) Hendron, J. A., ASTM 4th Pacific Area National Meeting, October 2, 1962.

(70) Anonymous, ASTM Special Bulletin (January, 1960).

(71) Kuhn, P., SAE-ASME Preprint No. 843C, April, 1964, Meeting.

(72) Srawley, J. E., National Academy of Sciences Symposium, Report MAB-156-M, 189-201 (February, 1959).

(73) Kies, J. A., Smith, H. L., Romine, H., and Bernstein, H., NRL Report No. 5521 (October 20, 1960).

(74) Hanink, D. K., and Sippel, G. R., Metal Progress, 78, 89-92 (August, 1960).

(75) Pellini, W. S., and Puzak, P. P., NRL Report No. 5892 (December 5, 1962).

(76) Pellini, W. S., and Puzak, P. P., NRL Report No. 6030 (November 5, 1963).

(77) Manning, G. K., and Martin, D. C., DMIC Memo 175, Battelle Memorial Institute, Columbus, Ohio (August 16, 1963).

FACTORS AFFECTING THE FRACTURE OF HIGH-STRENGTH STEELS

by

C. L. M. Cottrell*

SUMMARY

Factors affecting the fracture of thin-walled high-strength steel rocket-motor cases of welded construction are studied. A line of reasoning is proposed which leads to the conclusion that those factors which affect crack initiation and slow propagation are of prime importance. Using this approach, the factors governing fast propagation assume secondary importance and are, therefore, not discussed at length.

It is known that in a welded structure, fracture can be initiated either in the weld zone or in the parent metal outside the weld zone. In this paper, a special distinction is made between these two forms of initiation, since measures for their control may well differ.

Weld-zone fracture initiation may be prevented by using steel with a high resistance to hot cracking. Results are presented which show that the hot crack resistance of low-alloy steels can be calculated from a knowledge of the steel composition.

The likelihood of fracture initiation in the parent metal outside the weld zone can best be determined by some form of bend test which gives conditions of biaxial stress on the surface. This test ensures that fracture is initiated by a parent-metal defect. Steel composition, surface condition, and test environment are shown to have an effect on fracture initiation, steel purity being of the utmost importance.

Finally, a significant correlation is shown to exist between the performance of welded rocket cases and tubes and instrumented bend test results. This correlation should be of use in design, since results are shown as a function of material tensile strength.

INTRODUCTION

It is well known[1,2] that high-strength steels suffer from embrittlement in the presence of stress concentrations when heat treated to tensile strengths above about 224,000 psi (100 tons sq/in.) and the situation in the USA has recently been summarized by A. Q. Mowbray.[3] This property has been demonstrated in notched tensile tests of various types and has also been observed in service where cracks were present.[4]

The importance of prior crack length on the liability of the crack to propagate in an unstable manner has been fully dealt with by Irwin and Kies,[5] who also demonstrated the effect of material thickness on crack propagation. This work has led to the conclusion that for high-strength rocket-motor cases and other similarly stressed components, only material which will tolerate a certain crack length without giving rise to unstable fracture can be used. This crack length would, of necessity, be such that could be observed by known inspection techniques such as radiography.

The result of this approach is that relatively low-strength materials have become approved, and the very high-strength materials are not considered suitable because the crack size, which would lead to unstable fracture, would be too small to be measured by conventional inspection techniques. There also tends to be a dislike of welding because, in the past, weld defects in the form of cracks have been quite numerous and the normal method of inspection is by radiography which, as mentioned before, can only detect defects down to a certain limiting size.

When considering this approach, which relies on a limiting crack size, it is interesting to speculate on what advantage could be obtained by reducing the inherent defects in both the weld metal and the parent material. Some earlier work carried out on a number of different steels[6] indicated that a strict control over the composition of the weld zone could markedly restrict the amount of hot cracking during welding. At the same time, the liability of the parent material to contain a defect of a given size is likely to be a function of the melting technique used in its manufacture and this could also be controlled. Bearing in mind these two factors, it should be possible to control both the weld zone and the parent material so that neither is prone to initiate failure. If this can be done, it is evident that considerably higher usable tensile strengths could be achieved in steels.

This approach has been used in the work described in this paper and the investigation was first concentrated on those factors which promote weld-zone hot cracking (weld-zone weakness) and latterly on factors governing the initiation of cracks in the parent material (inherent material defects) under conditions of biaxial stress.

WELD-ZONE CRACK INITIATION

The adverse effects of the impurity elements sulfur and phosphorus[7,8] on hot cracking in the weld zone are now well known and the effect of these elements in combination with carbon has also been noted.[9] More recently, the relationship between certain impurity elements and certain alloying elements in steel and their combined effect on hot cracking has been studied.[6] It would appear from these

*Bristol Aerojet, Limited, Banwell, Weston-Super-Mare, Somerset, England.

earlier results, that in the presence of phosphorus, elements which favour solidification of the steel as austenite are adverse, whereas those which favour solidification as ferrite appear beneficial.

This work has now been greatly extended and a large number of steels have been examined using the Huxley hot-cracking test.(10)

The principle of the test is the initiation of a crack in a melt run, made by the tungsten inert-gas (TIG) process, and measurement of the extent to which the crack propagates along the melt under decreasing strain. Consistent thermal conditions, and consequently a consistent pattern of decreasing strain within the melt, is ensured by making the melt run at a constant speed, by certain features in the design of the specimen and jig, and by using specimens of a standard thickness.

The test specimen takes the form of a strip 16 inches long by 1-1/2 inches wide, having opposing slots approximately 1/32-inch wide cut into the sides to a depth of 0.6 inch. The distance between each pair of slots is 1-1/2 inches.

The slots in the specimen, while acting as thermal insulators between each test section (a test section being the area of metal between each pair of opposing slots), have the additional function of simulating an "edge starting" effect for the initiation of a crack.

This test gives a quantitative measure of the hot-cracking tendencies of steels and has been shown to correlate with production welding experience over some hundreds of welds.(10) The liability to cracking is expressed in terms of a crack susceptibility factor (CSF). The relationship between this factor and cracking in production welding is shown in Figure 1 from which it will be seen that when the factor falls below about 20, the percentage of cracking in production is very low.

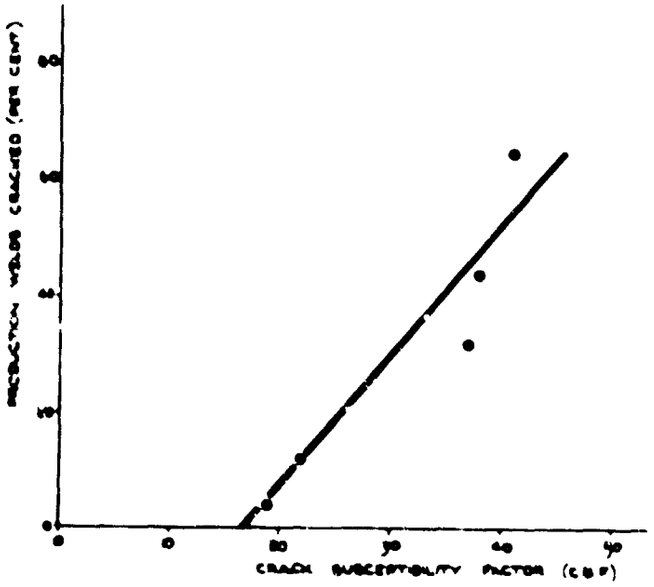

FIGURE 1. CORRELATION OF HOT-CRACK TEST RESULTS WITH CRACKING ON PRODUCTION COVERING 782 WELDS

The Huxley cracking test has been used to evaluate the hot-crack resistance of over 50 steels shown in Table 1. The results have been expressed in terms of steel composition based on the combined effect of phosphorus on ferrite stabilizers and austenite stabilizers, as mentioned earlier. In order to get the best possible relationship, the test results were analysed by means of a computer and a factor obtained for each element. The results are shown plotted in Figure 2 from which it will be seen that there is a most significant correlation between the crack susceptibility factor and steel composition, when expressed in this way.

The steels shown in Figure 2 have been made by various melting techniques, and there does not appear to be any marked effect of melting processes, bearing in mind that in most cases, standard melting techniques were used.

The indications are, from the results shown in Figure 1, that when the crack susceptibility factor is reduced to well below 20, all tendencies to hot cracking will be avoided, but it is also considered that there may still be some weakness in the weld zone even when cracks are not present. However, if this factor is reduced to almost zero, then there is every likelihood that this zone of weakness will also be reduced to a minimum which should remove any sources of fracture initiation.

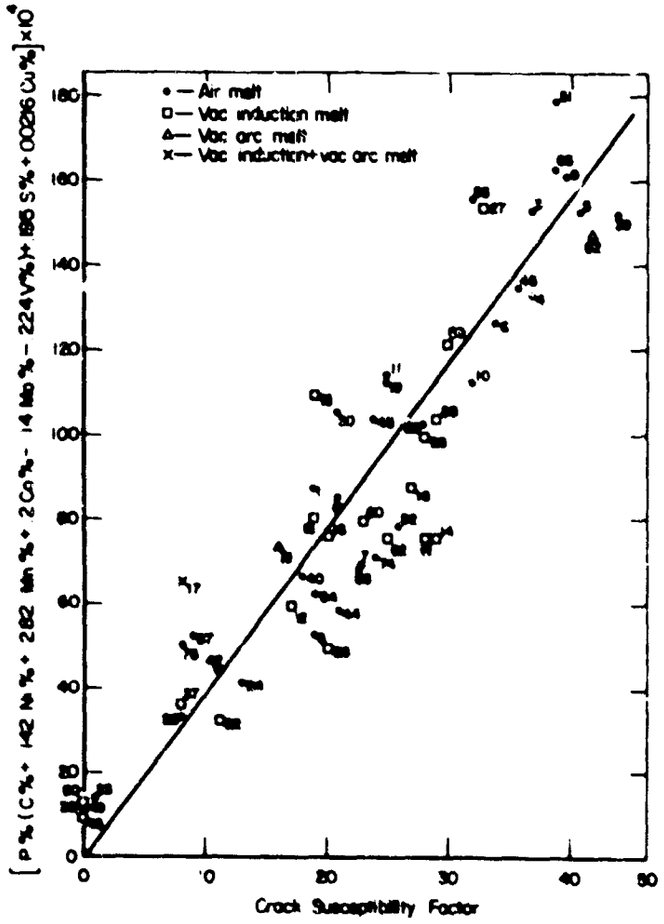

FIGURE 2. EFFECT OF STEEL COMPOSITION ON HOT-CRACK SUSCEPTIBILITY

TABLE 1. HOT CRACK TEST RESULTS

Material	Steel No.	Batch Number or Identification and Specification	Composition, per cent C	Mn	Si	S	P	Ni	Cr	Mo	V	Cu	Co	W	C.S.F.	Average Crack Length, inch	Melting Process
1% Chromium-Molybdenum	1	B/USSE. 6 RS. 120	.30	.49	.29	.009	.016	.18	.96	.19	-	-	-	-	19	.280	Air melted
	2	5916 RS. 120	.295	.44	.24	.011	.015	.13	.90	.24	-	-	-	-	21	.321	Air melted
	3	5855 RS. 120	.315	.41	.19	.015	.030	.09	.85	.245	-	-	-	-	37	.554	Air melted
	4	A. 675 RS. 120	.30	.51	.14	.016	.023	.16	.95	.195	-	-	-	-	37	.560	Air melted
	5	5654 RS. 120	.315	.41	.19	.013	.031	.09	.82	.245	-	-	-	-	41	.615	Air melted
	6	6469 RS. 120	.31	.49	.29	.014	.023	.09	.88	.215	-	-	-	-	34	.514	Air melted
	40	BU. 340 RS. 120	.285	.51	.23	.006	.013	.10	1.02	.17	-	-	-	-	18	.277	Air melted
	48	35 ADSI Ex. NPL	.30	.52	.20	.00065	.002	.17	.99	.20	-	-	-	-	0	0	Vacuum induction melted (pure base)
	49	36 ADSI Ex. NPL	.37	.52	.20	.0008	.002	.17	.98	.21	-	-	-	-	0	0	Vacuum induction melted (pure base)
	50	37 ADSI Ex. NPL	.44	.52	.20	.0009	.002	.17	.99	.21	-	-	-	-	0	0	Vaccum induction melted (pure base)
	65	5851 RS. 120	.285	.46	.22	.010	.031	.08	.95	.23	-	-	-	-	39	.580	Air melted
	74	BU. 295 RS. 130	.30	.56	.26	.007	.013	.11	.99	.21	-	-	-	-	24	.365	Air melted
	75	BU. 342 RS. 130	.30	.53	.285	.003	.010	.12	1.02	.16	-	-	-	-	8	.126	Air melted
	92	Ex. SAAB	.31	.70	.38	.006	.014	trace	1.19	.255	-	-	-	-	26	.393	Air melted
3% Chromium-Molybdenum-Vanadium	7	B/FR. 49 RS. 140	.38	.72	.24	.005	.014	.14	3.08	.97	.20	-	-	-	23	.342	Air melted
	21	J. 8 H. 27	.345	.60	.31	.005	.018	.14	2.88	.94	.22	-	-	-	16	.238	Vacuum arc remelted
	26	GV. 26 Ex. Brown Firth	.39	.27	.03	.014	.007	.10	2.93	.86	.22	-	-	-	20	.300	Vacuum induction melted
	27	GV. 27 Ex. Brown Firth	.315	.86	.04	.045	.015	.28	2.99	.84	.205	-	-	-	33	.496	Vacuum induction melted
	28	GV. 28 Ex. Brown Firth	.37	.47	.24	.029	.012	.13	2.93	.85	.205	-	-	-	28	.421	Vacuum induction melted
	30	G. 8946	.375	.68	.11	.020	.016	.08	2.89	.86	.195	-	-	-	21	.314	Air melted
	44	BU. 354 RS. 140	.42	.57	.20	.009	.010	.115	3.31	1.06	.185	-	-	-	21	.309	Air melted
5% Chromium-Molybdenum-Vanadium	8	B/ZFI. MOG. 510	.37	.41	1.110	.011	.016	.21	4.84	1.41	.56	-	-	-	19	.278	Air melted
	37	BU. 227 H. 50	.40	.52	.88	.009	.012	.34	5.13	1.29	1.15	-	-	-	8	.122	Vacuum induction melted
	42	Canadian Vascojet 1000	.435	.34	.92	.008	.010	.11	5.31	1.16	.44	-	-	-	11	.158	Air melted
2% Nickel	9	B/ICI. 115 SAE. 4335	.375	.63	.15	.010	.018	1.82	.82	.23	-	-	-	-	40	.594	Air melted
	10	L. 744 Ex. Brown Bayleys.	.46	.41	.11	.009	.011	2.10	.83	.46	.26	.55	-	-	32	.483	Air melted
	11	L. 778 Ex. Brown Bayleys.	.53	.48	.19	.009	.011	2.15	.90	.87	.25	.43	-	-	25	.369	Air melted
	39	B/ICI. 163 SAE. 4335	.35	.72	.24	.012	.017	1.70	.97	.29	-	.12	-	-	44	.664	Air melted
	45	"JBS" Ex. JBS Lees.	.73	.42	-	.009	.010	2.21	-	-	-	-	-	-	36	.534	Air melted
	51	63780 Ex. Brown Bayleys.	.435	.63	.28	.009	.023	1.82	1.31	.93	.20	-	-	-	39	.582	Air melted
	52	CAV. 57	.42	.51	.28	.009	.020	1.83	1.28	.96	.20	-	-	-	42	.629	Vacuum arc remelted
Silicon-Copper Ex. RARDE	12	W/GYN.	.24	.40	1.53	.008	.015	trace	.04	1.44	.33	1.49	-	-	17	.261	Vacuum induction melted
	13	W/GYM.	.37	.49	1.86	.007	.015	trace	trace	.85	.25	2.12	-	-	19	.278	Vacuum induction melted
	14	W/HGN.	.34	.93	1.91	.008	.005	.01	.03	.75	.33	1.75	-	-	29	.438	Vacuum induction melted
	15	W/HGO.	.29	.68	2.12	.009	.009	.01	.04	.84	.35	1.76	-	-	20	.304	Vacuum induction melted
	16	W/HCP.	.35	.68	2.12	.011	.009	.01	.02	.80	.27	1.75	-	-	27	.406	Vacuum induction melted
	17	W/HCN.	.32	.62	2.10	.008	.005	<.01	.02	.80	.36	1.74	-	-	8	.126	Double vacuum melted
	18	A. 119	.23	1.36	1.89	.012	.008	<.01	.05	1.58	.66	1.73	-	-	19	.282	Vacuum induction melted
	19	A. 121	.40	.54	1.58	.008	.014	<.01	.04	.77	.25	1.94	-	-	25	.375	Air melted
	58	A. 518	.34	1.04	1.87	.019	.006	.03	.04	.77	.35	1.80	-	-	29	.439	Vacuum induction melted
	59	A. 522	.375	1.0	1.62	.018	.007	.04	.03	.73	.30	1.05	2.1	-	30	.456	Vacuum induction melted
	60	A. 549/1	.325	1.49	1.74	.014	.004	.03	.03	1.74	.76	1.80	-	-	23	.345	Vacuum induction melted
	62	HAB. 113	.40	1.30	1.86	.005	.006	-	-	.91	.56	1.99	-	-	25	.379	Vacuum induction melted
X. 200	22	WIL. 2	.385	.92	1.43	.007	.003	.24	2.05	.47	.06	-	-	-	11	.159	Vacuum induction melted
	29	G. 9082 Ex. Brown Firth.	.46	.62	1.59	.004	.017	trace	2.06	.58	.07	-	-	-	28	.421	Air melted
	43	BU. 421	.42	.68	1.16	.009	.016	.09	1.99	.54	.06	-	-	-	26	.395	Air melted
12% Chromium Ex. Brown Firth. Research Laboratories	54	FV. 532	.095	.84	.27	.008	.013	1.09	11.6	.57	.22	-	-	-	19	.279	Air melted
	55	FV. 535	.085	.94	.54	.002	.011	-	10.22	.80	.23	-	5.94	-	32	.478	Air melted
	56	FV. 566	.095	.79	.31	.011	.011	2.32	11.73	1.38	.14	-	-	-	23	.342	Air melted
	57	FV. 607	.14	.82	.33	.009	.012	.61	10.92	.82	.26	-	-	-	9	.133	Air melted
Miscellaneous	23	B/AEDU. 7 14V5	.15	.52	.29	.004	.007	.15	.42	1.13	.29	-	-	-	1	.014	Air melted
	24	HAB. 43 HST. 140	.445	.63	.30	.007	.011	.15	9.10	2.12	.43	-	-	-	13	.195	Air melted
	25	HAB. 44 HST. 120	.365	.63	.35	.008	.009	.16	3.04	2.0	.39	-	-	-	8	.113	Air melted
	32	BU. 144 K. K. 3	.81	1.25	.12	.004	.014	.17	4.06	5.06	1.96	-	-	6.68	0	0	Air melted
	61	A. 671 Ex. RARDE	.625	.55	.08	.013	.004	.01	2.76	.88	.28	-	2.01	-	28	.416	Vacuum induction melted

It would appear that by using this approach, it should be possible to design a steel to give a marked degree of safety against liability to crack initiation in the weld zone. Further, if fabrication of rocket cases is carried out by the helical welding process, this will--because of the weld alignment relative to the principal stress--allow the weld to be slightly softer and thus give an additional degree of safety.

PARENT-METAL CRACK INITIATION

It is considered that, in the absence of a mechanical notch, crack initiation occurs at a point of weakness in the parent material such as an inclusion or some other defect. It, therefore, follows that some form of test which initiates a crack from one of these points is necessary to evaluate truly this property of the material. The most suitable form of test is, therefore, a wide bend test, since it provides a degree of biaxial stress on the surface without recourse to notching. In this manner, fracture is allowed to initiate at the weakest point in the material within a certain area.

A large number of tests have been carried out[11] using a wide bend test in which test pieces were bent over formers of different radii. The results have been reported in terms of the smallest former radius which will just avoid cracking when the material is bent through 180°. These results are shown in Figure 3, and it is apparent that the purity of the steel has a marked effect on its resistance to crack initiation, since this form of test essentially measures this property and takes no account of fast crack propagation. It is also interesting to note that the embrittlement of the material when tempered at 570 F (300 C) is much reduced when the purity is increased. In the case of the most pure steel, 0.001% sulfur-0.002% phosphorus, this material has bend properties similar to a steel containing 0.004% sulfur and 0.009% phosphorus with an addition of 0.005% cerium. It appears, therefore, that the cerium addition is beneficial in reducing the adverse effects of sulfur and phosphorus, and hence, the liability of the material to initiate cracks.

The instrumented bend test[12] which also evaluates the liability of material to initiate cracks, has been carried out on a number of steels. In this test, the test specimen is bent as a simple beam supported at two points and loaded at the center. The change in load as the specimen is bent is detected by a load cell, the signal from which is passed to an amplifier and then to a high-response recorder. As the test proceeds, the load increases to a maximum and then falls at a flow rate until rapid failure occurs, at which point the load falls to zero. The results are expressed as the difference between the maximum outer fibre stress and the outer fibre stress at which rapid failure occurs.

The results for 1% chromium-molybdenum steel, 2% nickel-chromium-molybdenum, and 18%

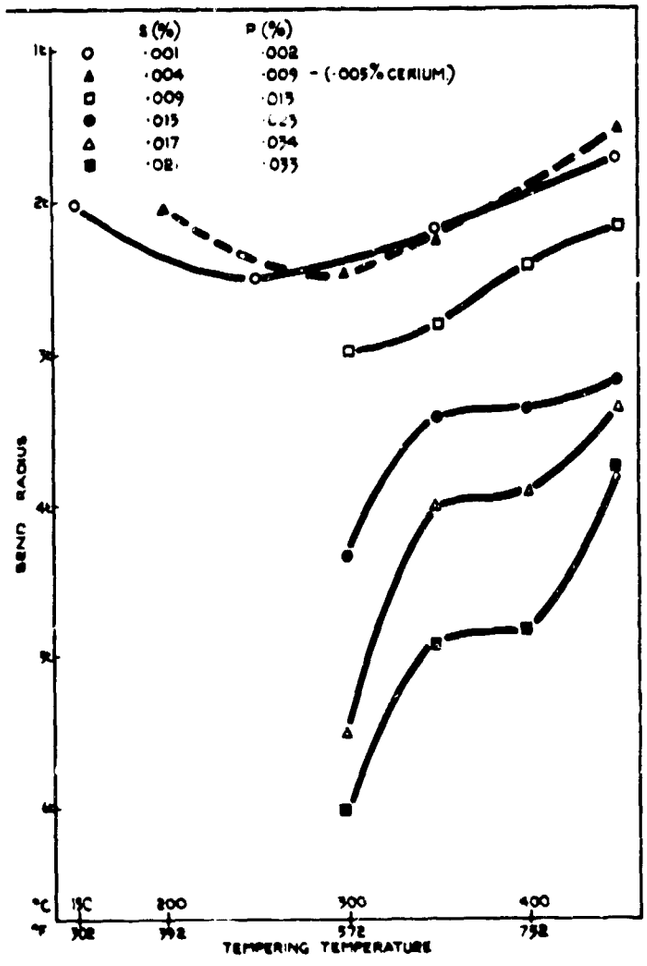

FIGURE 3. WIDE BEND TEST PROPERTIES, 1% CHROMIUM-MOLYBDENUM STEEL

nickel-cobalt-molybdenum maraging steel are given in Figure 4, the analyses of the materials being given in Table 2.

In order to enable different materials to be compared more easily, the bend parameter is related to the material tensile strength which gives a dimensionless function. This is defined as the crack initiation susceptibility of the material, i.e.,

$$\text{CIS} = \frac{\text{Tensile Strength}}{\text{Bend Parameter}}.$$

It will be observed in Figure 4 that there is a considerable decrease in crack initiation susceptibility when the steels are made from higher purity material and vacuum induction melted, this decrease being very marked at high strength levels irrespective of steel type.

Some earlier work which has been reported[13] on the 2% nickel-chromium-molybdenum steel indicated that in one batch of material there was a variation of about 30 per cent in crack initiation susceptibility at a tensile level of about 265 ksi (118 tons/sq in.). After a thorough microscopical examination of the various bend test specimens, it was noted that the one having the greatest CIS contained irregular inclusions up to 0.002-inch long, whereas the inclusion size for the good material was below

TABLE 2. STEEL COMPOSITIONS AND SPECIFICATIONS

Melting Process and Base	C	Mn	Si	S	P	Ni	Cr	Mo	Co	Ti	V
					Compositions*						
Air, normal purity	0.31	0.74	0.26	0.014	0.010	1.69	0.95	0.29	-	-	-
Vacuum induction, high purity	0.38	0.59	0.21	0.004	0.001	1.96	0.77	0.28	-	-	-
Air, normal purity	0.32	0.51	0.22	0.006	0.014	0.08	1.17	0.25	-	-	-
Vacuum induction, high purity	0.30	0.52	0.20	0.001	0.002	0.17	0.99	0.20	-	-	-
Air, normal purity	0.02	0.04	0.18	0.005	0.006	18.1	-	4.8	7.9	0.52	-
Vacuum induction, high purity	0.03	0.02	N.D.	0.005	0.006	19.5	-	4.8	8.9	0.98	-
Vacuum induction, high purity	0.03	0.05	0.02	0.005	0.003	18.7	-	5.2	9.4	1.3	-
					Specifications*						
RS.140 Min.	0.38	0.50	0.10	-	-	-	2.90	0.90	-	-	0.15
RS.140 Max.	0.43	0.70	0.35	0.010	0.015	0.30	3.30	1.10	-	-	0.25

* Per cent.
Note: N.D. = not detectable.

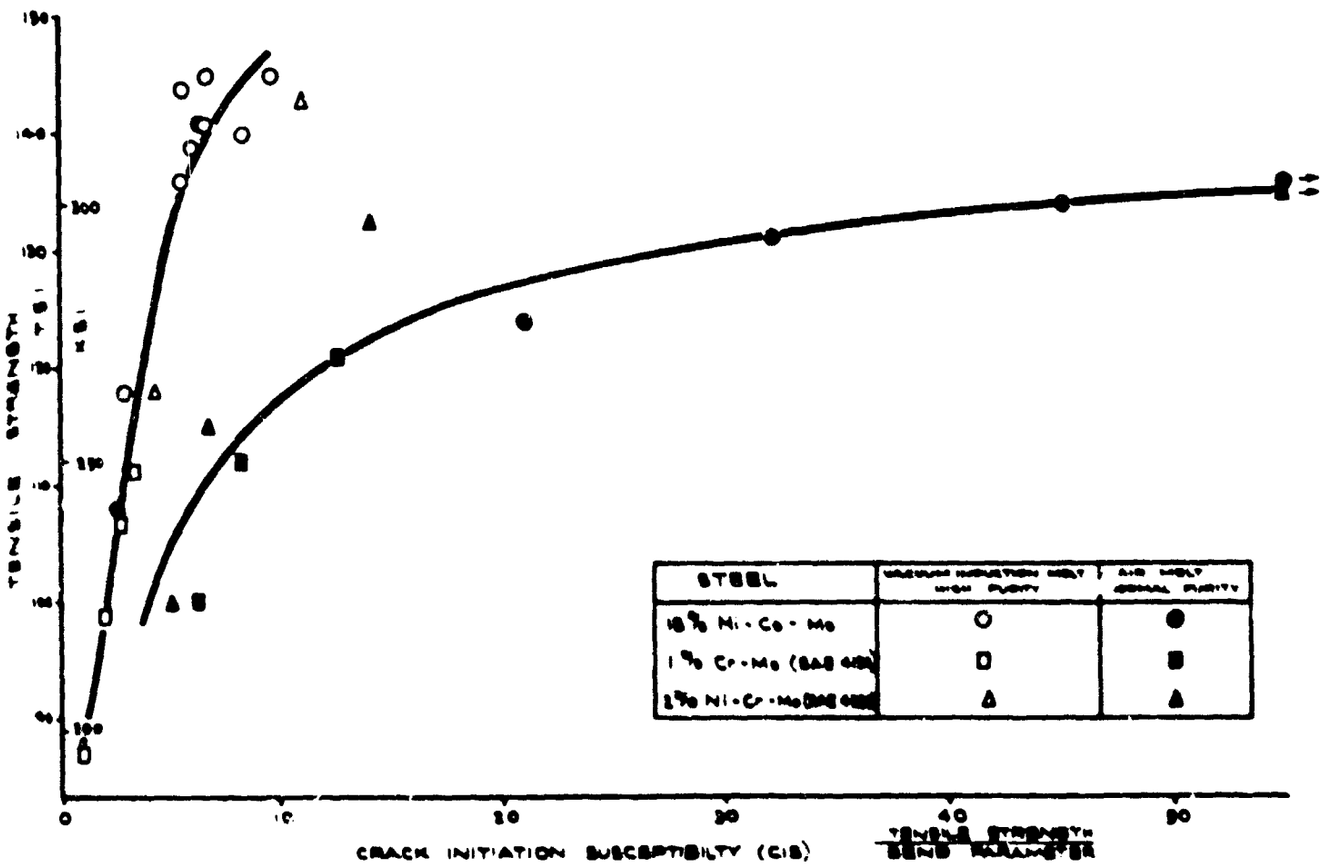

FIGURE 4. EFFECT OF MELTING PROCESS AND STEEL PURITY ON CRACK INITIATION

0.0005 inch. This was considered adequate evidence of the ability of the instrumented bend test to measure the effect of inherent steel defects on crack initiation.

The instrumented bend test has also been used to study the effect of tempering temperature and degree of decarburization on the crack initiation susceptibility of air-melted 3% chromium-molybdenum-vanadium steel. The results are given in Figure 5. It will be noted that there is a tendency for the nondecarburized material to be brittle when tempered in the region of 660-930 F (350-500 C), and that a considerable decrease in crack initiation susceptibility is evident when decarburization is applied. This effect extends over the whole tempering temperature range and there is no evidence of embrittlement.

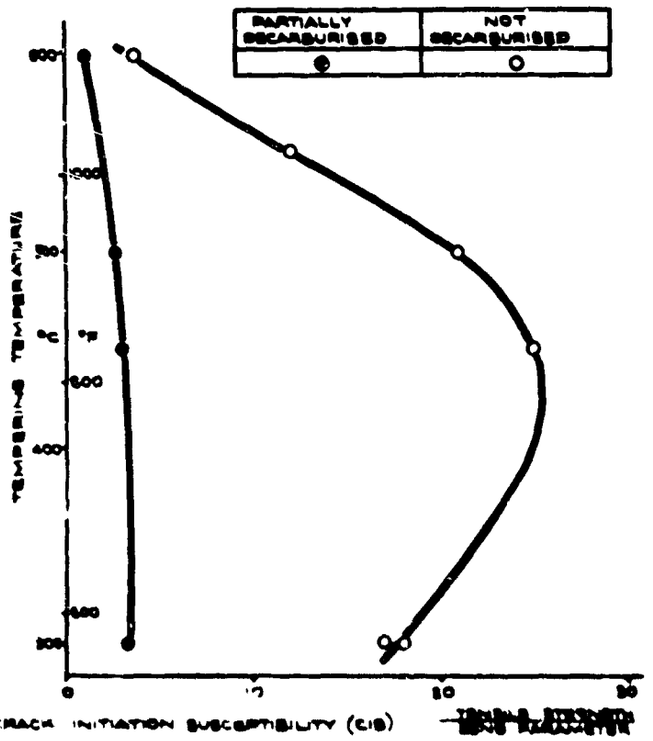

FIGURE 5. EFFECT OF TEMPERING AND DECARBURIZATION ON CRACK INITIATION IN 3% Cr-Mo-V STEEL

The effect of surface treatment on crack initiation susceptibility, as measured by the instrumented bend test, has also been investigated. In these tests, 3% chromium-molybdenum-vanadium and 18% nickel-cobalt-molybdenum maraging steels were examined. Specimens were tested with no surface treatment, after vacublasting and phosphating, and finally, after vacublasting, phosphating, and baking for four hours at 390 F (200 C). The results of these tests are given in Tables 3 and 4, and it will be observed that the greatest susceptibility to crack initiation is produced by vacublasting and phosphating the material. Baking after vacublasting and phosphating generally restores the original crack initiation susceptibility.

Tests were also made on the maraging steel at -94 F (-70 C) with no surface treatment, and also on both steels at room temperature after immersion in water daily for seven days. The tests, after immersion, were done both under water and in air with the specimen wet. The results are included in Tables 3 and 4 and indicate that, in the case of maraging steel, no increase in crack initia-

TABLE 3. EFFECT OF SURFACE TREATMENT AND TEST CONDITIONS ON CRACK INITIATION SUSCEPTIBILITY OF AIR-MELTED 3 PER CENT Cr-Mo-V STEEL

Surface Treatment After Heat Treatment	Test Temperature*	C.I.S. Tensile Strength** Bend Parameter
None	In air	8.3
Immersed in water and dried each day for seven days	Under water In air, specimen wet	7.8 10
Vacublast	In air	7.8
Vacublast and phosphate	In air	18
Vacublast, phosphate, and bake 4 hrs. 390 F (200 C)	In air	9.7

* Tested at room temperature.
** Tensile strength 262 ksi (117 tons/sq.in.).

TABLE 4. EFFECT OF SURFACE TREATMENT AND TEST CONDITIONS ON CRACK INITIATION SUSCEPTIBILITY OF VACUUM INDUCTION MELTED 18% Ni-Co-Mo MARAGING STEEL CONTAINING 1% Ti.

Surface Treatment After Aging	Test Conditions[a]	C.I.S. Tensile Strength[b] Bend Parameter
None	In air	7.1
	Dry ice and meths[c]	7.1
Immersed in water and dried each day for seven days	Under water	7.4
	In air, specimen wet	8.8
Vacublast	In air	8.3
Vacublast and phosphate	In air	8.8
Vacublast, phosphate bake 4 hrs. 390 F (200 C)	In air	7.1

(a) Tested at room temperature.
(b) Average of four tests in most cases tensile strength 318 ksi (142 tons/sq.in.)
(c) Tested at -94 F (-70 C).

tion susceptibility is obtained by testing at -94 F (-70 C). There is, however, a slight increase with both steels when the specimen is given the water-immersion treatment and tested in air with the specimen wet.

From a consideration of the two forms of test, the standard wide bend and the instrumented bend, it would appear that both tests measure the crack initiation susceptibility of the material and that the instrumented bend test, apparently, also measures the ease of slow crack propagation up to the stage of unstable fast fracture. In the case of the instrumented bend test, certain curves produced have shown two distinct zones with a change in slope of the load-time curve taking place at a certain point, this occurring prior to the onset of unstable fracture. It would appear that these two zones may relate to the deformation before crack initiation and to the slow propagation of the crack. If this can be substantiated, then the instrumented bend test should fulfill a very useful purpose as it appears to be sensitive to steel purity, surface condition, surface treatment, and also test environment.

CORRELATION OF CRACK INITIATION SUSCEPTIBILITY WITH TUBE AND CASE BEHAVIOUR

In order to establish whether the instrumented bend test could differentiate between satisfactory and unsatisfactory rocket cases, which was suggested in an earlier paper,[13] a large number of tests were made on different materials, the results of which are given in Tables 5 and 6. The

TABLE 5. RESULTS OF HYDRAULIC BURST TESTS AT ROOM TEMPERATURE AIR-MELTED 3% CHROMIUM-MOLYBDENUM-VANADIUM STEEL

Component	Heat Treatment	Decarburization, (in. x 10^3)	Tensile Strength		Bend Parameter		Ultimate Hoop Stress		Structural Efficiency UHS/TS	Crack Initiation Susceptibility (CIS) Tensile Strength / Bend Parameter	K_c psi $\sqrt{in.}$
			ksi	tsi	ksi	tsi	ksi	tsi			
Tube	Oil quench and temper 570 F (300 C)	0	260	116	15	6.7	241	108	0.93	17	-
			258	115			250	112	0.98	17	-
			260	116			248	111	0.96	17	-
			264	118			235	105	0.90	18	-
		2-5	250	112	76	34	262	117	1.04	3.3	-
			250	112			264	118	1.05	3.3	-
		6-8	246	110	146	65	266	119	1.08	1.7	-
			246	110			253	113	1.03	1.7	-
			24	118			258	115	1.04	1.7	-
			246	110			250	112	1.02	1.7	-
	Oil quench and temper 840 F (450 C)	0	241	108	9.6	4.3	199	89	0.82	25	-
			246	110			224	100	0.91	25	-
		6-8	228	102	116	52*	222	99	0.97	1.9	-
			228	102			226	101	0.99	1.9	-
	Oil quench and temper 1020 F (550 C)	0	244	109	21	9.2	226	101	0.92	12	-
			244	109				103	0.94	12	-
		2-5	224	100	T.S.	T.S.	235	105	1.05	1.0	-
			235	105	T.S.	T.S.	244	109	1.04	1.0	-
			224	100	T.S.	T.S.	233	104	1.04	1.0	-
			224	100	T.S.	T.S.	230	103	1.03	1.0	-
	Oil quench and temper 1110 F (600 C)	0	235	105	63	28	250	112	1.06	3.7	-
			237	106	63	28	253	113	1.06	3.8	-
		2-5	215	96	T.S.	T.S	230	103	1.07	1.0	-
			217	97	T.S.	T.S.	237	106	1.09	1.0	-
	Marquench and temper 570 F (300 C)	2-5	253	113	110	49	270	121	1.07	2.3	88,000
			258	115	110	49	282	126	1.09	2.3	89,000
			260	116	110	49	268	120	1.03	2.3	89,000
			282	117	110	49	280	125	1.07	2.4	89,000
Case	Oil quench and temper 840 F (450 C)	2-5	240	107	83	37	246	110	1.03 (1.01)	2.9	-
	Oil quench and temper 930 F (500 C)	0	237	106	11	5	150	67	0.63 (0.81)	21	-
		2-5	230	103	90	40	235	105	1.02 (1.01)	2.6	-
	Oil quench and temper 1020 F (550 C)	2-5	226	101	T.S.	T.S.	258	115	1.13 (1.06)	1.0	-
			222	99	T.S.	T.S.	258	115	1.16 (1.08)	1.0	-
			226	101	T.S.	T.S.	258	115	1.13 (1.06)	1.0	-
			226	101	T.S.	T.S.	260	116	1.15 (1.07)	1.0	-
	Marquench and temper 570 F (300 C)	0	295	132	7	3	164	73	0.56 (0.78)	44	-
		2-5	264	118	110	49	293	131	1.11 (1.05)	2.4	89,000
			260	116	110	49	295	132	1.14 (1.07)	2.3	89,000
			264	118	110	49	289	129	99 (1.04)	2.4	89,000
			264	118	110	49	298	133	1.12 (1.06)	2.4	89,000

* Tempered at 750 F (400 C).

TABLE 6. RESULTS OF HYDRAULIC BURST TESTS AT ROOM TEMPERATURE 18% NICKEL-COBALT-MOLYBDENUM STEEL

Steel	Component	Heat Treatment	Tensile Strength ksi	Tensile Strength tsi	Bend Parameter ksi	Bend Parameter tsi	Ultimate Hoop Stress ksi	Ultimate Hoop Stress tsi	Structural Efficiency UHS/TS	Crack Initiation Susceptibility (CIS) Tensile Strength / Bend Parameter	K_c psi. √in.
Air melt, 0.5% Ti	Tube	3 hours at 680 F (360 C)	241	108	99	44	250	112	1.04	2.4	-
		3 hours at 805 F (430 C)	293	131	9	4	273	122	0.93	32	-
		3 hours at 895 F (480 C)	305	136	4.5	2	278	124	0.91	68	-
Vacuum induction melt, 1.0% Ti	Tube	3 hours at 805 F (430 C)	264	118	92	41	264	118	1.00	2.9	-
		3 hours at 895 F (480 C)	305	136	56	25	309	138	1.01	5.4	-
		3 hours at 930 F (500 C)	311	139	52	23	313	140	1.00	6.0	140,000
		3 hours at 930 F (500 C)	315	141	52	23	313	140	0.99	6 1	140,000
		1510 F (820 C) + 3 hours at 895 F (480 C)	317	142	58	26	309	138	0.97	5.	-
		1510 F (820 C) + 3 hours at 930 F (500 C)	315	141	48	22	320	143	1.01	6.4	-
		1510 F (820 C) + 3 hours at 970 F (520 C)	313	140	38	17	309	138	0.98	8.2	-
	Case	3 hours at 895 F (480 C)	315	141	56	25	336	150	1.06 (1.03)	5.6	-
		3 hours at 930 F (500 C)	313	140	52	23	338	151	1.07 (1.03)	6.1	140,000
		1510 F (820 C) + 3 hours at 895 F (480 C)	305	136	58	26	336	150	1.10 (1.05)	5.2	-
		1510 F (820 C) + 3 hours at 930 F (500 C)	307	137	48	22	336	150	1.09 (1.04)	6.2	-
Vacuum induction melt, 1.3% Ti	Tube	3 hours at 930 F (500 C)	325	145	34	15	334	148	1.02	9.7	-
		1510 F (820 C) + 3 hours at 930 F (500 C)	325	145	49	22	331	149	1.03	6.6	-
	Tube*	3 hours at 930 F (500 C)	317	142	-	-	329	147	1.03	-	-
		1510 F (820 C) + 3 hours at 930 F (500 C)	325	145	-	-	331	149	1.03	-	-

* Tests at -13 F (-25 C).

materials tested included three types of 18% nickel-cobalt-molybdenum maraging steels with different levels of titanium, and 3% chromium-molybdenum-vanadium steel to Specification RS. 140 (see Table 2) in both decarburized and non-decarburized conditions.

In order to enable the different materials to be compared more easily, the crack initiation susceptibility has been related to the structural efficiency of the rocket case or tube, defined as the ratio of ultimate hoop stress to tensile strength. For a satisfactory structural efficiency, according to Mises Hencky, this ratio should be greater than 1.0 for a complete rocket case. A large number of the tests were, however, made on open-ended tubes, and these were tested with end plugs held with tie rods thus reducing the end load. Because of this method of testing, the Mises Hencky effect does not apply and a satisfactory structural efficiency is obtained with a ratio of about 1.0. It has also been observed[13] that when a complete case is unsatisfactory, it has a lower ratio than the equivalent open-ended tube.

In order to enable the results for cases and tubes to be combined on the same graph, a correction factor has been applied to the case ratios and the corrected values are shown in brackets in Tables 5 and 6. The empirical correction applied is as follows:

$$\text{S. E.}_{\text{tube}} = \left(\frac{\text{S. E.}_{\text{case}} - 1}{2} \right) + 1.$$

The results are plotted in Figure 6 from which it will be seen that there is a good correlation, satisfactory burst test results lying within the hatched area. It is also apparent that the crack initiation susceptibility factor should be less than 10 for satisfactory structural efficiency.

Some points are also included in Figure 6 for a titanium alloy containing approximately 15% molybdenum. The fact that these points fit the relationship is attributed to the use of parameters which are functions of tensile strength.

The results included in Figure 6 cover a wide range of material tensile strengths, the highest hoop burst strength being 336 ksi. Results of tests carried out at -13 F (-25 C) are also given in Table 6.

Some of the unsatisfactory structural efficiencies shown in Figure 6 have been achieved by using 3% chromium-molybdenum-vanadium steel without surface decarburization and the good results have been achieved from correctly decarburized material. In the case of 18% nickel-cobalt-molybdenum maraging steel, the low results have been obtained from air-melted material and the good results from high-purity vacuum-induction-melted material.

In order to provide a comparison of previous results with crack propagation properties, plane stress fracture toughness K_c values were obtained on the 3% chromium-molybdenum-vanadium steel and the 18% nickel-cobalt-molybdenum steel. These results are included in Tables 5 and 6 and are average values.

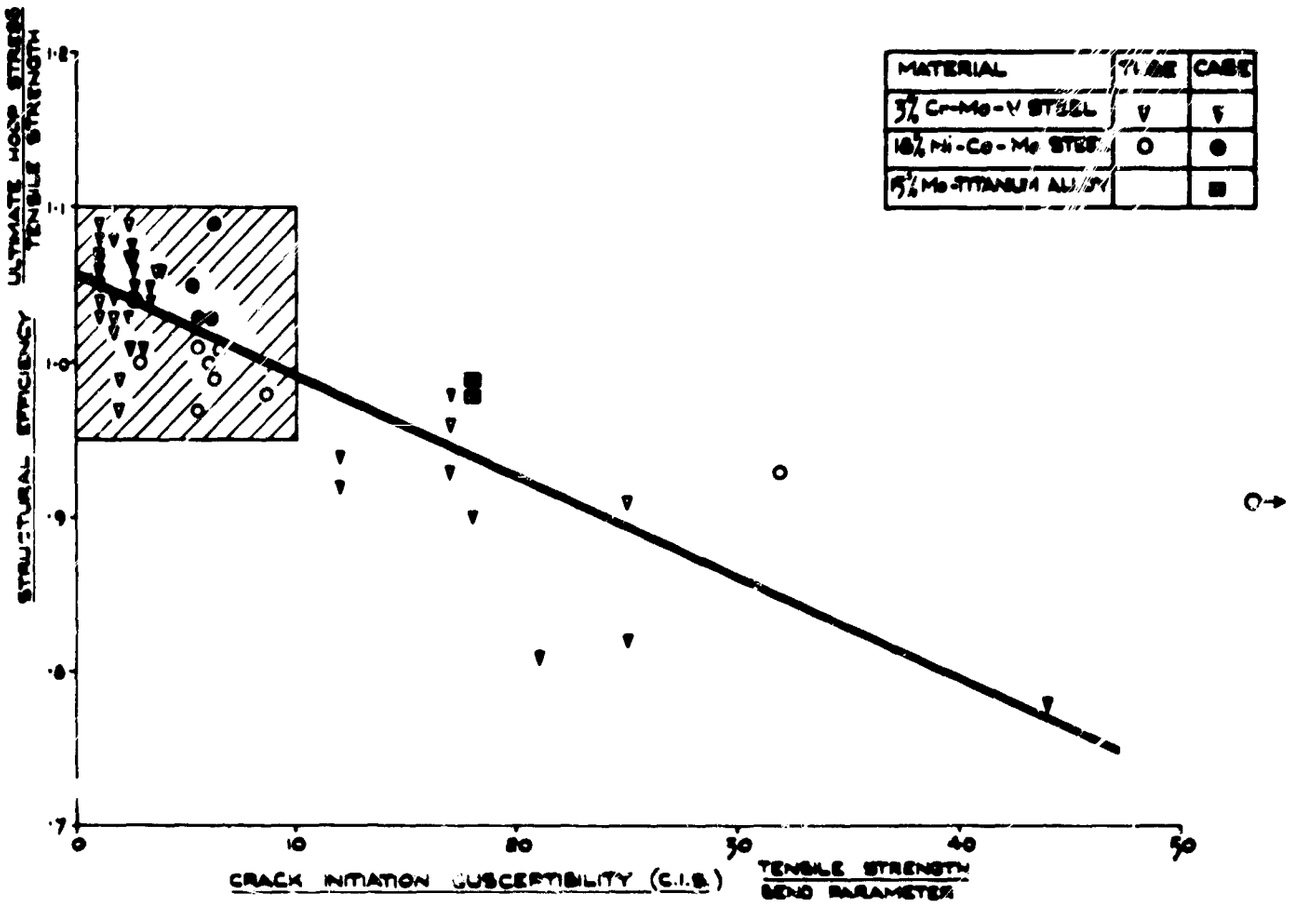

FIGURE 6. CORRELATION OF BEND TEST RESULTS WITH STRUCTURAL EFFICIENCY OF TUBES AND CASES

The K_c values quoted were obtained from 2-inch wide, edge-notched specimens with a notch depth of about 0.3 inch. The notch roots were both fatigue cracked and eroded in the 3% chromium-molybdenum-vanadium steel and the specimen thickness was 0.077 inch. The notch roots were fatigue cracked in the 18% nickel-cobalt-molybdenum steel, and the specimen thickness was 0.058 inch. All the results were corrected to actual K_c values.

DISCUSSION

When full consideration is given to the results obtained from the large number of hot-crack tests carried out on the various materials, it appears that a solution to the welding problem with respect to liability to crack initiation in the weld zone is becoming closer. It is also apparent that if an extremely low crack susceptibility factor is obtained on the parent material (i.e., a CSF well below 20 and approaching zero), then there is little likelihood of minute hot tears or grain-boundary weakness of a similar nature occurring in the welded zone, thus fracture initiation points in this zone will virtually be absent. It is, of course, assumed that the welding techniques will be under close control to avoid porosity, slag inclusions, and lack of penetration, which is practicable provided the necessary precautions are taken.

When the helical welding process is used for the manufacture of rocket-motor cases, some reduction in weld-zone strength can be tolerated compared with the parent-metal strength. This reduction in weld strength confers somewhat greater ductility on the weld zone. When sound welds are achieved by closely controlled material, as described earlier, and some general increase in ductility is obtained by the use of the softer helical weld, then there is little likelihood of fracture initiating in the weld zone. This satisfactory state of affairs is well illustrated in Figure 7 which shows a rocket-motor case which failed at a hoop stress of 336 ksi (150 tons/sq in.). This case was fabricated by helical welding, and it will be observed that after failure, two parts of the case are being held together by an uncracked weld.

It is also of interest to note that of four motor cases of this type tested, all failed within the range 336-338 ksi (150/151 tons/sq in.), indicating that there was no lack of consistency in the weld zone. These four cases were fabricated from steel made using the best possible melting techniques, i.e., high-frequency vacuum melting using high-purity base materials. The steel gave a crack susceptibility factor (CSF) of zero and a crack initiation susceptibility (CIS) of 5.2-6.2.

It would appear from the investigation of weld hot-crack susceptibility that it should be possible

FIGURE 7. MARAGING STEEL MOTOR CASE SHOWING WELD UNBROKEN, ULTIMATE HOOP STRESS 150 TONS/SQ IN. (336,000 psi)

to design a steel composition specifically to give the best possible welding properties with respect to hot cracking. The liability of a steel to cold cracking, although not mentioned in detail in this paper, has not been forgotten, but it is considered that provided the hydrogen level of the weld zone is kept low and/or a certain minimum level of pre- and post-heat is applied during welding, cracks of this nature can be avoided completely.

When crack initiation is prevented in the weld zone, the crack initiation sites within the parent metal assume major significance. Work in this paper has shown how bend tests can evaluate the crack initiation susceptibility of the parent material and has indicated which factors affect crack initiation.

The marked adverse effect of impurities in the steel on crack initiation in both the wide bend and instrumented bend tests has been demonstrated and it would appear, as in the case of hot cracking, that the impurity level of the steel should be maintained as low as possible. It is also likely that the addition of certain elements may counteract impurities in the steel and one such case is the addition of cerium. By using pure materials, even higher strengths appear possible; an example being an 18% nickel-cobalt-molybdenum maraging steel containing 2.2% titanium which gave a tensile strength of 374 ksi (167 tons/sq in.) and reduction in area of 55 per cent. The broken test piece is shown in Figure 8, and a ductile cup and cone fracture was obtained.

FIGURE 8. MARAGING STEEL TEST PIECE, TENSILE STRENGTH 167 TONS/SQ IN. (374,000 psi)

Other factors which affect the crack initiation susceptibility of the steel are the surface condition and treatment of the material, and the test environment, all of which may have an effect, depending upon the type of steel used.

A satisfactory correlation between crack initiation susceptibility and structural efficiency has been demonstrated for rocket cases and tubes fabricated by helical welding. This correlation indicates that the instrumented bend test is an effective means of evaluating material for rocket-case manufacture. It is also considered that a bend test could well be incorporated with every fabrication in order to determine that the heat treatment, level of decarburization, and any other surface treatment had been carried out in a satisfactory manner.

The bend parameter is shown as a function of the tensile strength in the correlation with case and tube properties shown in Figure 6, and this method of plotting is used in order to enable different metals other than steel to be compared. In view of this, it is considered that when a sufficient amount of testing has been carried out, it should be possible to use crack initiation susceptibility (CIS) as a design criterion for thin-wall cases.

Finally, some mention should be made of crack propagation and in this connection, it is interesting to compare the results of burst tests with both crack initiation and crack propagation properties for the 3% chromium-molybdenum-vanadium and 18% nickel-cobalt-molybdenum steels. This comparison is made in Table 7, and it will be observed that a high K_c value does not necessarily give a high structural efficiency, since the higher efficiencies were obtained with the lower K_c values. In fact, the crack initiation susceptibility (CIS) gives a better indication of structural efficiency in this instance.

It is apparent from Table 7 that the steel having the higher resistance to crack propagation also has the greater susceptibility to crack initiation, whereas

TABLE 7. EFFICIENCY OF CASES AND TUBES WITH CORRESPONDING CRACK PROPAGATION AND CRACK INITIATION PROPERTIES

Steel	Yield Strength ksi	Yield Strength tsi	Structural Efficiency, Ultimate Hoop Stress, Tensile Strength Tube	Structural Efficiency, Ultimate Hoop Stress, Tensile Strength Case	K_c psi. $\sqrt{in.}$	Crack Initiation Susceptibility (CIS), Tensile Strength Bend Parameter
3% Cr-Mo-V, air melted	205	92	1.03-1.09	1.09-1.14	85,000	2.3-2.4
18% Ni-Co-Mo-1.0% Ti vacuum induction melted	278	124	1.00-1.01	1.03-1.09	140,000	6.0-6.1

the ideal steel should have a high resistance to crack propagation combined with a low crack initiation susceptibility. This could be an important result, since it highlights the need for more work on those factors affecting crack initiation and suggests that an evaluation of high-strength steel in terms of K_c only may not be adequate.

CONCLUSIONS

The effect of steel composition on the liability of high-strength steels to weld hot cracking has been demonstrated for low-alloy high-strength steels. A formula based on material composition has been proposed which allows accurate calculation of material hot-crack resistance. It is concluded that when the hot crack susceptibility of steel approaches zero, there is little likelihood of crack initiation in the weld zone from this cause.

Crack initiation in the parent material is shown to be markedly affected by steel purity, in addition to the general alloy content of the steel. The effect of surface condition of the material on crack initiation is quite marked especially with respect to decarburization in 3% chromium-molybdenum-vanadium steel. The effect of other surface conditions is not so marked, although the need for baking after phosphating has been demonstrated.

In the case of the 18% nickel-cobalt-molybdenum maraging steel, reducing the test temperature to -94 F (-70 C) has no effect on crack initiation susceptibility. Testing steels after immersion in water and in the wet condition in air produces a slight increase in crack initiation susceptibility.

A satisfactory correlation has been established between the crack initiation susceptibility (CIS) using the instrumented bend test, and the efficiency of helically welded rocket cases and tubes. This has been demonstrated for certain steels and a titanium alloy. It is concluded that this test constitutes a reliable means of establishing rocket-case performance and could, therefore, be used as a design criterion. It is proposed that the CIS should be less than 10 for satisfactory thin-wall case behavior.

From the limited number of crack propagation tests made, it appears that a steel with a high plane-strain fracture toughness (K_c value) may have a relatively high crack initiation susceptibility (CIS). It is considered, therefore, that further work should be carried out on factors affecting crack initiation in high-strength steel, since the CIS of a steel is not included in its K_c value. Furthermore, a steel with a low CIS may not necessarily require a high K_c to give a satisfactory performance.

ACKNOWLEDGMENTS

The author wishes to thank Dr. C. E. Turner of Imperial College, London, for providing the K_c test results.

REFERENCES

(1) Shank, M. E., Spaeth, C. E., Cooke, V. W., and Coyne, J. E., Metal Progress, 74 (November, 1959); 84 (December, 1959).

(2) Hays, L. E., and Wessel, E. T., Appl. Mat. Res., 99 (April, 1963).

(3) Mowbray, A. Q., Matls. Res. & Stds., ASTM, 103 (March, 1964).

(4) Fifth Report of a Special ASTM Committee, Matls. Res. & Stds., ASTM, 107 (1964).

(5) Irwin, G. R., and Kies, J. A., Metal Progress, 73 (August, 1960).

(6) Huxley, H. V., Welding and Metal Fabrication, 29 (January, 1963).

(7) Mishler, H. W., Monroe, R. E., and Rieppel, P. J., Welding Journal, 1B (January, 1961).

(8) Wilkinson, F. J., Cottrell, C. L. M., and Huxley, H. V., British Welding J., 557 (December, 1958).

(9) Bollenrath, F., and Cornelius, H., Stahl und Eisen, 569 (May, 1963).

(10) Huxley, H. V., British Welding J., 514 (November, 1961).

(11) Cottrell, C. L. M., Langstone, P. F., and Rendall, J. H., J. Iron & Steel Inst., 1032 (December, 1963).

(12) Hanink, D. K., and Sippel, G. R., Metal Progress, 89 (August, 1960).

(13) Cottrell, C. L. M., and Turner, M. J., J. Iron & Steel Inst., 380 (May, 1962).

A SURVEY OF THE FATIGUE ASPECTS IN THE APPLICATION OF ULTRAHIGH-STRENGTH STEELS

by

S. R. Swanson*

SUMMARY

The fatigue strength of many ultrahigh-strength steels will be presented as found in the literature, together with a discussion of the shortcomings of the present state-of-the-art method of expressing fatigue strength; i.e., the "endurance limit". The increased importance of fatigue strength or weakness in the application of such steels demands the use of a sounder criterion, especially in the light of recent statistical discoveries regarding the bimodal behaviour of constant amplitude fatigue endurance in the region of the "endurance limit".

A new criterion is put forward, namely, the fatigue strength (in terms of Root Mean Square Stress) for 1 million cycles of a Rayleigh distribution of stress amplitudes. Such a test is statistically unique, quite simply obtained by exciting a single-degree-of-freedom system containing the specimen with random noise, and can often be applied directly to service problems without resorting to tenuous cumulative damage theories. An example of the application of this criterion (from a small number of Rayleigh tests) to assess the fatigue life of the DHC Hydrofoil main foil (to be made from 250 ksi Y.S. maraging steel) will be presented.

A brief comparison of the fatigue strength of maraging steels manufactured by different methods will be given for various test conditions (e.g., air, saltwater corrosion, butt welded, etc.) to indicate what compromises in the selection of manufacturing processes can be made if the ultimate application is kept in mind. Some findings on notched specimen fatigue will be given in the appendix. A short discussion of scale effect in the fatigue of maraging steels will also be included in the presentation.

INTRODUCTION

A natural starting point for any discussion of the fatigue strength of steels is Bullens' famous figure, shown as Figure 1a of this report.[1]** This figure shows the "fatigue ratio" for what are now considered the "soft" steels.[2] In earlier days, one could almost rely on any steel having a basic endurance limit of about half the ultimate tensile strength, with appropriate reductions due to notching or hostile environments.

The upper limit of Bullens' range of ultimate tensile strength represents the minimum yield strength for the class of steels we are concerned with today. I have just completed a survey similar to Bullens' (Figure 1b) for steels with 0.2 percent proof strengths greater than 220,000 psi. The data and their source are listed in Table 1. While this figure is no doubt incomplete, it does show the presence of a "fatigue barrier". Regardless of the static strength, the endurance limit appears to be limited to about 120,000 psi.

Why should we be worried about this barrier? To begin with, these modern steels represent what might be considered as the designer's "high-priced help". He would be foolish to go to the increased expense of calling up such materials if they were not going to be efficiently utilized. Such utilization involves high stress levels. While there are certain applications (such as in undercarriage design) which result in predominantly compressive stress histories, there are a growing number of applications involving symmetrical, or even predominantly tensile load histories. Because these load histories are usually of a cyclic or variable nature, the fatigue strength is an all-important quantity.

One such application is the Canadian FHE-400 hydrofoil vessel shown in Figure 2. This application not only benefits from the use of ultrahigh-strength steel, its use is mandatory if the structural design is to be feasible at all, from the fabrication viewpoint.

The most vital load-carrying component in this structure is the main foil, shown in Figure 3. This member is hydrodynamically loaded in a manner similar in many respects to an aircraft wing. There is, for instance, a steady tensile "1-g" loading supporting the vessel when foil-borne in calm water. Superimposed on this steady load is the variable load history which results from passage through turbulent seas, which is similar to the flight of an aircraft through a patch of atmospheric turbulence.

Figure 4 shows the structural details of the centre section of the main foil. The material chosen for this foil is 18% nickel maraging steel heat treated to obtain a yield strength of 250,000 psi. (See the Appendix.) The use of such a steel is a typical example of the sort of situation for which this symposium is being held. It is a relatively new material, and confidence in its wide-

* The author is associated with The De Havilland Aircraft of Canada Limited, Malton, Ontario, Canada

** References are given on page 142.

Note: Tables start on page 143, Figures on page 150.

spread use is being delayed or hampered by lack of information on its load-carrying limitations.

In order to assess the fatigue behavior of this material, an extensive test program described briefly in Figures 5a and 5b was undertaken. All tests thus far have been carried out at room temperature. The air tests have been carried out in rooms where the relative humidity varied in a normal fashion. (7) A number of additional test programs were carried out which are not shown in Figure 5 for clarity. Many of these have already been described in References 7 and 8. The test program to study Inconel 718 (Figure 14), the material chosen for the leading edge of the foil, was also omitted but will be discussed in this paper.

A CRITERION FOR FATIGUE STRENGTH

The Use of the Criterion "Endurance Limit"

The endurance limit is traditionally defined as the greatest stress amplitude which can be sustained in constant amplitude sinusoidal loading by a material, without causing failure. While there were a significant number of 'soft' steels (and a few other materials) in the past which could be represented as having a definite endurance limit, the vast majority of modern practical materials do not possess such a definite demarcation in their S-N curves. The criterion is usually qualified, to cater to this situation, by referring to a specific endurance, such as 10 million cycles.

There are, unfortunately, other characteristics of 'hard' steels aside from the continuously sloping S-N curve which render the accurate establishment of the quantity almost impossible, at least from an economic viewpoint.

From the preliminary rotating beam tests carried out in Reference 7, it was soon noted that the scatter of test results at low stress levels could be consistently greater than 100 to 1, for 18% nickel maraging steel.

A second, more intriguing observation, discussed in both References 7 and 8 and also by Thomson in Reference 2, is that the test results do not appear to belong to a "single-humped" statistical population. It is becoming increasingly evident from both statistical and physical metallurgical studies(10) that more than one mechanism of fatigue is involved in causing failure in the region of the endurance limit. From our studies in Canada, we have observed statistical grouping into two distributions in a wide variety of materials.(8) Cicci used 50 maraging steel specimens at each of five stress levels to show that at each stress level there was a definite division of endurances into two groups.(7)

Recently, Thomson(2) has observed three separate groups in the endurances for another hard steel, (52100) shown in Figure 16. He also found similar behavior in 5160 steel (Rockwell C54) and in EN 31 (C-Cr) steel (Rockwell C62). Examining the statistical behavior of the component distributions, he found (as did Cicci) that they could individually be well represented by the log-normal distribution.

Factors Affecting the Endurance Limit

As one might expect from the data of Figure 1b, the manipulating of normal metallurgical process variables has yielded surprisingly little improvement on the fatigue strength of hard steels.(2) I would suggest that a better approach might be to examine as closely as economically possible the statistical grouping discussed above as it occurs in the steel. One would then separate out and isolate the fatigue processes responsible for the different groups, and attack each process separately to prevent its action in the metal.

a) Relative Humidity

Cicci observed that when the test results were separated into the two groups, relatively few failures were attributable to the first-encountered distribution when the test was carried out in a dry atmosphere (Figure 5j).(7)

Thomson also presents results which show that the mean life moves to greater endurances under dry conditions. However no information is given as to the effect on the grouping of test results (Figure 2b).(2)

b) Refractory (hard) Inclusions

In the appendix of this paper, information on the inclusion counts is given for maraging steel obtained from three separate manufacturing processes:

1. Consumable-electrode vacuum remelt, with vacuum casting.
2. Air melt, with vacuum stream degassing during pouring.
3. Air melt and air cast.

It was found that while the three methods all resulted in comparatively clean steel, they are listed above in order of decreasing cleanliness. It will be evident in the test results presented later that the inclusion count (for hard inclusions) often has a significant effect on the fatigue strength of hard steels.

Thomson(2) also found that refractory inclusions can be a major source of fatigue

weakness in hard steel (tested in air). It is unfortunate that in both Thomson's work and ours, that not enough raw data was generated to establish the effect of cleanliness on the individual component distributions of endurances. The inclusions thought to influence fatigue behavior the most are the titanium carbonitride inclusions (E rating on the Jernkontoret chart).

The probability behavior of axial load constant amplitude fatigue tests carried out with the unnotched specimen shown in Figure 6 is shown in Figures 7 and 8, for both zero and 50,000 psi tensile mean stress, for the first process (consutrode vacuum-remelt, vacuum-cast material). The resulting mean S-N relations are presented in Figure 9 obtained by at least squares linear regression of the mean endurances (see the appendix). Figure 9 also shows, for comparison, a few single test results obtained for a rough assessment of the fatigue life of the 'as received' mill-annealed material (Table 3). The data for the constant amplitude tests are given in Tables 2 and 3.

Establishment of a New Criterion

Since most fatigue load histories involve variable stress interaction, there are strong arguments to replace the endurance limit with a new criterion, the "Rayleigh fatigue strength". I have outlined these arguments in previous papers[8] and I will not labour the points here. It is quite feasible these days to quickly put together fatigue test equipment which will apply a narrow-band stationary Gaussian fatigue loading to a given test specimen. By keeping the frequency bandwidth reasonably narrow, specifying the resulting Root Mean Square stress amplitude and measuring the clipping ratio (maximum stress amplitude in terms of the RMS) one has a unique repeatable test configuration which can be of great value in assessing fatigue strength under variable (service) loadings. In the present application, such a test is a very good simulation of the load history developed on the lightly-damped main foil, as the hydrofoil speeds through a given sea state (which is in itself a stationary random process). It will be evident shortly that this type of test control is inherently less scatter than constant amplitude test results, and there is no evidence of sub-groups in the endurances obtained.

Using the same axial load machine (described in the appendix) and the specimen shown in Figure 6, material from the same melt as used in the constant amplitude tests was studied (for two mean stresses) under stationary Rayleigh loadings. The probability behavior of the test results (Tables 4 and 5) is shown in Figure 10. The S-N relations resulting from least squares regression of the mean endurances are shown in Figure 11. Also plotted on Figure 11 are the predicted Rayleigh curves using linear cumulative damage theory and the cumulative damage theory proposed by Freudenthal.[11]

USE OF THE RAYLEIGH CRITERION

Assessing the Effect of Manufacturing Process

The three different levels of quality or cleanliness referred to in Section 3b represented the first variable to be studied using the new criterion. A constant RMS of 40 ksi was used, superimposed on the '1-g' mean stress of 50 ksi. The resulting endurances are given in Table 6 and are plotted using probability paper in Figure 12. As one might expect, the use of vacuum techniques not only resulted in a greater mean endurance, but reduced the variability or scatter in the test results appreciably. Not much improvement came about by using vacuum stream degassing during pouring.

Effect of a Transverse Weld

The second variable to be examined with this criterion was the relative fatigue performance of welded maraging steel. The axial-load specimens, made from each of the three processes referred to above, were manufactured from butt welded plate in the manner shown in Figure 6. The test results (Table 10) are plotted on log-normal probability paper in Figure 13. One can certainly say that the expense of obtaining very clean steel is not justified from these test results. Tests carried out at other RMS levels and reported in Table 13 reveal that the quality of the weld results in greater variability than the primary process used to create the parent metal. The welding details are given in the Appendix. The effect on the RMS endurance relation of these welds is shown in Figure 16.

Further Tests to Study Weld Fatigue

In order to shed more light on the fatigue behavior of maraging steel containing welds, a program of constant amplitude repeated flexure tests at zero mean stress was carried out using 0.050 in. thick sheet specimens machined from 0.080 in. thick plate. All specimens were made from vacuum melt and vacuum cast material. Figure 15 shows the results which are tabulated in Tables 7 and 8. As expected, the tests results for the plain specimens grouped into two distributions. These control data are given in Reference 8. The so-called endurance limit is approximately 90-95 ksi.

Specimens were then tested which had a longitudinal weld running along the main axis of the specimen, resulting from the butt welding of two 0.080 in. sheets. In a similar manner, transverse weld specimens were manufactured. All specimens were then heat treated and machined equally on both surfaces to result in a 0.050 in. thick specimen.

From Figure 15, one can see that the direction of weld did not have much effect on the fatigue life.

The metallurgical notch formed by the weld itself appears to be the overriding factor. The endurance limit appears to drop to about 85 ksi and there is a half-log-cycle decrease in life compared with the first distribution of the control data.

EFFECT OF SURFACE CONDITION

Unmachined Specimens

The repeated flexure test program described above was extended to obtain some information on the seriousness of not machining off the scale formed on the surface of the maraging steel sheet when the steel is aged at 900 F for 3 hours. The specimens were in all other respects similar to the control specimens. These tests (Table 9) showed that the notch effect which results is of a similar magnitude to that obtained using weld specimens.

FATIGUE STRENGTH OF A 200 KSI MATERIAL INCONEL 718

A program of fatigue tests to investigate the rotating beam fatigue strength of unnotched (longitudinal) Inconel 713 alloy was also performed. This program was primarily conducted to compare the fatigue behavior of Inconel 718 with identical tests carried out using transverse and longitudinal specimens of 18% Maraging Steel. These latter tests are discussed in Reference 7. Further details of this material are given in the appendix.

The final values of endurance at each stress level investigated are given in Table 11. The test results are plotted in Figure 14.

A study of Figure 14 reveals that the fatigue strength of Inconel 718 is certainly comparable to that obtained for the 18% Maraging Steel. This is particularly significant when one considers that the UTS of the Inconel 718 is only 200 ksi compared with 250 ksi for the maraging steel. Even though the comparison is between longitudinal 718 and transverse maraging steel specimens, longitudinal maraging steel specimens show no improvement in mean endurance over transverse specimens of the same material.[7] The increased ratio of fatigue strength to tensile strength of Inconel 718, combined with its corrosion-resistant properties make this material attractive, at least in the unnotched condition. Of course the expense, and difficulties in fabrication preclude its widespread use.

A further study of the grouping of test results for Inconel 718 in Figure 14 reveals the two distribution behavior, at least at the two lowest levels of testing. While no tests were carried out using Inconel 718 in a salt water environment, information available in Reference 13 shows that 181 ksi UTS Inconel 718 exhibits an endurance limit of 86.8 ksi at 10 million cycles.

THE INFLUENCE OF 'SIZE EFFECT'

In order to determine whether 'size effect' would be an important consideration in the practical evaluation of fatigue life for the main foil from the relatively small laboratory specimens, several large-scale specimens shown in Figures 17 to 20 were manufactured and tested in a UHS 100 ton Losenhausen axial-load fatigue machine. First, control specimens using the unnotched configuration shown in Figure 17 were tested to obtain direct comparison with the axial load constant amplitude test results described earlier, using the specimen shown in Figure 6. The material was taken from the same melt of consumable electrode vacuum melt and vacuum cast plate as used for the earlier tests.

As one can see comparing the fatigue performance of 18% nickel maraging steel shown in Figure 21 with the S-N test results in Figure 9, there is an appreciable size effect in this material. This is consistent with the general predictions for hard steels made by Kuhn and Figge.[12] The test data are presented in Table 14.

Further tests, using a salt-water environment are contemplated for the subject material using the large scale specimens.

EFFECT OF POOR FABRICATION PRACTICE

As part of the test program using the large scale specimens, it was decided at an early stage in the main foil design to obtain an assessment of the relative virtues of two different fabrication techniques. These were: joining the metal by plug (MIG spot) welds, or joining the metal by fillet welds. Accordingly, specimens with transverse welds (Figure 18) and longitudinal welds (Figure 20) were tested at a given stress amplitude, against the fatigue performance of specimens containing a row of plug welds (Figure 19) at the same stress level. The results, contained in Table 14, are plotted in Figure 21.

The fillet design proved superior largely because of the difficulty encountered in preventing excessive corrosion from occurring at the inaccessible plug weld joint (see Table 14) in interdendritic fissures within the weld. These weld processes are described in more detail in the Appendix.

The occurrence of corrosion fatigue in inaccessible welds was shown to be a significant problem from a design standpoint. Grinding operations are usually used in fabrication and the coolant can penetrate into these joints. The subsequent heat treatment of the welded part aggravates the problem. The longitudinal fillet weld specimen shown in Figure 20 behaved similarly to the plug weld specimens, with many failures in the welded grips, where it was impossible to clean up the weld

surfaces. From these observations, the decision was made to employ accessible fillet welds. (Compare Figure 20 and Figure 4.)

ENVIRONMENTAL EFFECTS – CORROSION FATIGUE

None of the other high-strength steels which were considered for the main foil (such as 5Cr-Mo-V and 17-4 Ph) possess inherent corrosion resistance. The Inconel 718 to be used at the leading edge is known to have good corrosion properties. Since erosion is likely to be an even greater problem than corrosion at the leading edge no coating protection would be feasible there in any case. For the maraging steel skin, however, the steel must be protected from the salt water, since indications were that its corrosion fatigue strength would be low (Figure 25).

But just how badly would this maraging steel perform if this coating were damaged? Also what difference would the cleanliness of quality of the steel make if it were subjected to corrosion fatigue?

Simulating exposure to a salt water environment is another area where, traditionally, simplifying assumptions are made. Often as long as the water enveloping the specimen contained the correct percent NaCl in solution this was taken to be adequate simulation. But is this really the case?

In order to investigate the validity of this compromise, actual samples of salt water were obtained from both Pacific and Atlantic coast Naval Laboratories in Canada. These waters were then compared with an artifically prepared seawater, in their ability to induce corrosion fatigue failure. All three salt waters are described in the appendix.

A schematic view of the corrosion rig is shown in Figure 22, with an inset photograph of the transparent plastic tubing chamber fitted over a specimen (Figure 6) in the random load fatigue machine. From a study of corrosion fatigue life as it varied with the flow rate of the seawater through the tubing, it was soon established (Figure 23) that the greater the circulation, the more severe would be the corrosion fatigue. (Table 15.) The final flow rate decided upon, 2 knots, corresponds to 1956 cubic centimeters of water flowing over the specimen per minute.

Comparative Performance of Sea Waters

The three different sea waters were used in turn in corrosion fatigue tests performed on the cleanest grade of maraging steel. The first set of tests was performed using constant amplitude axial loading, in order to provide a comparison with American test results shown in Figure 25. Since the latter tests were obtained using rotating beam equipment, our axial load tests included zero mean stress as well as the hydrofoil mean stress. (Figure 24.) The mean endurances were superimposed on the American data in Figure 25, and show good agreement. They also show that the type of seawater has a rather small effect on the mean endurances. It was also interesting to note the low scatter obtained under constant amplitude testing in salt water. Possibly the subsequent mechanisms of failure are not present due to the overwhelming influence of the first (corrosive) mechanism of fatigue. The mean values for the constant amplitude corrosion fatigue test were:

Mean Stress	Artificial cycles	Atlantic cycles	Pacific cycles
Zero	210,000	203.000	163,000
48 ksi tension	84,000	63,000	72,000

In general the natural sea waters appear more corrosive than the artificial salt water, but the differences are admittedly small (Table 16).

For the random amplitude tests using the same two values of mean stress, a single RMS stress level of 33 ksi was chosen. This level of intensity corresponds closely to the conditions prevailing in the hydrofoil skin when the craft is foilborne. The test data are given in Table 17 and are plotted in Figure 26. The mean endurances for the unnotched specimens were, in effective cycles to failure:

Mean Stress	Artificial cycles	Atlantic cycles	Pacific cycles
Zero	320,000	315,000	300,000
48 ksi tension	140,000	125,000	140,000

Now an RMS stress of 33 ksi corresponds to an RMS peak stress of 46.7 ksi for the Rayleigh distribution. Comparison with the fatigue endurance in air obtained earlier (Figure 11) shows that the random load fatigue performance drops to one-third to one-tenth its value in air, when the specimens are immersed in circulating seawater. The difference in using different seawaters appears to be negligible.

Comparative Performance of Manufacturing Processes

A further series of corrosion fatigue tests was carried out using specimens of the same type as shown in Figure 6, made from the other two manufacturing processes as well as the consumable electrode vacuum melt technique. These test results shown in Table 18, and plotted in Figure 27 were obtained using the artificial seawater only, to permit easier comparison. It can be seen that the fatigue behavior is relatively insensitive to the cleanliness of the specimen material (in contrast to the situation in air, Figure 12) due to the overriding effect of the corrosive environment.

An identical series of corrosion fatigue tests was carried out, in which specimens were made

from butt-welded plate. (See Figure 6.) The material from which these specimens were manufactured came from the three different manufacturing processes involved in this study. The test results (Table 12) are plotted in Figure 13. Again the overriding effect of the weld and the environment negate the advantage in cleanliness of the more expensively produced material. In fact, one gains the impression that, for weld applications, relatively speaking, the dirtier the material the better. This is probably a spurious conclusion due to the wide variation in quality of weld. However, further work is necessary to clarify this point.

FATIGUE LIFE OF THE MAIN FOIL – SAMPLE CALCULATION

From information given in Reference 13 one might safely conclude that an impervious coating will yield fatigue test results which will be quite similar to those obtained for the metal in air. For this reason the most pertinent fatigue data would be the random load fatigue test results obtained for the plate material in air. If we assume that chordwise welds are avoided, the data for the plain specimen will apply, as shown in Figure 11. The mean stress 50 ksi was deliberately chosen to correspond to the operating mean stress of the foil. This mean stress was subsequently altered, slightly, to 48 ksi.

In order to avoid considerations of cumulative damage, it will be assumed that the fatigue life may be based on the percentage of time that the vessel is foilborne. Since the lightly damped main foil has a stress output spectrum which is essentially a rather narrow-band one may assume the Rayleigh distribution of stress peaks obtained in tests is a good simulation of the random process. Let us assume that the mean frequency of the stress cycles is estimated at 0.50 cps. If the vessel is foilborne 100 hours per year, 180,000 cycles will be encountered. For five years of operation, therefore, the material must be capable of about one million cycles before failure.

Let us assume that the "stationary" sea state which is of interest corresponds to an RMS stress amplitude of 33 ksi. From consideration of the scatter in the test results (Figure 10), and extrapolating slightly below the tests carried out at 35 ksi (Figure 11), one obtains somewhat greater than one million cycles for 10% probability of failure.

This fatigue strength was considered satisfactory for the intended application at the early stages of the project. The tests to study size effect and also the numerous tests with weld specimens have pointed out the need to test the full-scale completed foil in a fatigue test which will simulate the variability of the loading. Work is in progress toward that end.

CONCLUSIONS

After reviewing the general fatigue behavior of ultra-high strength steels, the author has presented the results of an intensive study of the fatigue properties of one member of this group; namely 18 percent nickel maraging steel heat treated to a yield strength of 250,000 psi.

It is quite evident that these materials are highly sensitive to scale effects, fabrication details such as weld defects, and environment. This sensitivity places a grave responsibility on the manufacturer of the end product to simulate the service conditions as closely as possible, if he is to place any reliance on the absolute 'numbers' he obtains from laboratory fatigue test. He must also pay meticulous attention (using for example non-destructive test techniques) to fabrication details to ensure that the structure is of a dependable quality.

While the traditional constant amplitude type of fatigue test is discredited, on statistical and economic grounds, in its use to determine the 'endurance limit' it may prove highly useful in fundamental studies to isolate the different failure processes which seem to exist in metal fatigue.

The prediction of the Rayleigh fatigue life using the linear law of cumulative damage was not far from the actual mean values obtained in test, especially at zero mean stress. This is consistent with the trend in work by others which show similar agreement for random load tests using notched specimens. However unnotched data usually results in gross over-estimates using this cumulative damage rule. This may be another manifestation of the notch sensitivity of this high strength material.

The use is advocated of a stationary random process type of fatigue test to supersede constant amplitude testing for comparative fatigue strength evaluation. The narrow band Rayleigh test pattern which results from the Gaussian excitation of a single degree of freedom system containing the specimen results in low scatter and good random stress interaction histories. Such a test can often provide a finer screening more economically (especially at low stress levels) than constant amplitude testing since 'runouts' cannot occur at the usual levels of RMS stress which are of interest.

From the results of the Rayleigh test criterion as applied in this paper, it is evident that if the material is not notched and is well protected from hostile environments such as salt water, there is a definite advantage to the use of high purity metal.

If however, the high strength metal contains weld defects greater than (an apparently quite

small) given threshold size, or if it is exposed to salt water, any advantage presented by cleaner material can be quickly nullified.

It would appear that much more testing must be done to obtain definite conclusions as to the degree to which artificial salt water successfully simulates natural seawater. For practical engineering purposes, it appears to provide adequate simulation in corrosion fatigue, to natural seawater.

REFERENCES

(1) Bullens, D. K., Steel and Its Heat-Treatment, Wiley Publications, 37 (1938).

(2) Thomson, R. F., "Fatigue Behavior of High-Carbon High-Hardness Steels", 196[illegible] Campbell Memorial Lecture, Transactions of the ASM, 56 803 (December, 1963).

(3) Weiss, V. and Sessler, J. G. (Editors), Aerospace Structural Metals Handbook, Volume 1, Ferrous Alloys, Syracuse University Press (March, 1963).

(4) Brodrick, R. F., "Fatigue and Dynamic Creep of High-Strength Steels", Technical Documentary Report No. ASD-TDR-62-480 (May, 1962).

(5) Justusson, W. M., and Zackay, V. F., "Engineering Properties of Ausformed Steel", reprinted from Metal Progress (December, 1962).

(6) Melcon, M. A., "Ultra High Strength Steel for Aircraft Structures", Product Engineering.

(7) Cicci, F., "An Investigation of the Statistical Distribution of Constant Amplitude Fatigue Endurances for a Maraging Steel", UTIAS Technical Note 73 (July, 1964).

(8) Swanson, S. R., "Practical Fatigue Loadings for Aeronautical Structures", Paper No. 64-568, presented at International Council of the Aeronautical Sciences, Fourth Congress, Paris, France, August 24-28, 1964.

(9) Gideon, D. N., et al., "Investigation of Notch Fatigue Behavior of Certain Alloys in the Temperature Range of Room Temperature to -423 F", Technical Documentary Report No. ASD-TDR-62-351 (August, 1962).

(10) Swanson, S. R., "The Dual Nature of the Fatigue Process", Proceedings of Canadian Industrial Research Conference, Engineering Institute of Canada, September 2 and 3, 1964.

(11) Freudenthal, A. M., and Heller, R. A., "On Stress Interaction and a Cumulative Damage Rule", Journal of the Aero-Space Sciences (July, 1959).

(12) Kuhn, P., and Figge, I. E., "Unified Notch-Strength Analysis for Wrought Aluminum Alloys", NASA TN D-1259, (May, 1962).

(13) Heitzmann, R. J., "Corrosion Fatigue Properties of Structural Materials", Grumman Aircraft Corp., Adv. Dev. Program, Progress Report and Final Report ADR-02-09-64.1 (1962).

TABLE 1. SURVEY OF FATIGUE STRENGTHS OF ULTRAHIGH-STRENGTH STEELS, ZERO MEAN STRESS

Item	Type of Steel	Type of Fatigue Test	Stress Concentration	Ultimate Tensile Strength, ksi	0.2% Proof Stress, ksi	Endurance Stress at 10^5 kc	Reference
1	4140	Rotating Beam	1.0	240	225	100	3
2	52100	Rotating Beam	1.0	270	240	120	3
3	USS Strux	Rotating Beam	1.0	290	250	122	3
4	300-M	Axial	1.0	300	250	110	3
			3.0			60	3
5	Vasco MA	Rotating Beam	1.0	360	290	130	3
6	9% Maraging	Rotating Beam	1.0	260	230	125	3
7	D6AC	Axial	1.0	270	237	100	4
			3.0			50	4
8	Labelle H. T.	Axial	1.0	291	237	90	4
			3.0			50	4
9	Peerless 56	Axial	1.0	297	252	80	4
			3.0			40	4
10	Thermold J	Axial	1.0	338	275	100	4
			3.0			60	4
11	H. 11 Modified	Rotating Beam	1.00	300	250	130	5
12	H. 11 Modified and Deformed 90%	Rotating Beam	1.00	400	360	160	5
13	4340	Axial	1.00	280	240	120	6
			3.00			50	6
14	18% Ni Maraging	Rotating Beam	1.00	275	260	100	7
			2.00			65	8
15	18% Ni Maraging Air Melt (250)	Rotating Beam	1.00	257	250	115	3
16	18% Ni Maraging Vacuum Melt (300)	Rotating Beam	1.00	286	280	122	3
17	Type 301 Stainless	Repeated Flexure	1.00	240	222	72	9
			3.00			25	

TABLE 2. CONSTANT AMPLITUDE FATIGUE ENDURANCES

Axial Loading
18% Nickel Maraging Steel
Zero Mean Stress

Alternating Stress, ksi	Specimen	Life, kilocycles
125	AZF 50L	61.8
	AZF 52L	63.3
	AZF 51L	69.5
	AZF 54L	91.2
	AZF 53L	142.9
116	AZF 60L	73.4
	AZF 57L	93.0
	AZF 56L	186.7
	AZF 59L	191.8
	AZF 55L	200.1
	AZF 151L	517.5
108	AZF 91L	208.9
	AZF 62L	331.6
	AZF 61L	344.2
	AZF 63L	1,066.7
105	AZF 152L	201.7
	AZF 90L	228.4
	AZF 150L	251.8
	AZF 85L	294.5
	AZF 89L	295.0
	AZF 88L	618.0
	AZF 87L	781.4
102	AZF 235L	257.6
	AZF 242L	368.8
	AZF 153L	394.0
	AZF 241L	950.5
	AZF 237L	2,089.6
	AZF 240L	2,866.0

TABLE 3. CONSTANT AMPLITUDE FATIGUE ENDURANCES

Axial Loading; 18% Maraging Steel; S_m = 50 ksi

Alternating Stress, ksi	Specimen	Life, kilocycles
(a) Heat Treated to 250 ksi		
150	AZF 1L	11.1
135	AZF 36L	16.7
	AZF 65L	19.5
	AZF 66L	19.5
	AZF 35L	20.6
	AZF 64L	21.5
	AZF 38L	22.9
	AZF 37L	26.7
125	AZF 16L	20.2
	AZF 18L	23.87
	AZF 19L	24.6
	AZF 68L	28.2
	AZF 42L	28.9
	AZF 15L	30.2
	AZF 43L	33.3
116	AZF 32L	25.3
	AZF 33L	29.3
	AZF 69L	32.9
	AZF 71L	35.8
	AZF 31L	49.1
	AZF 30L	49.6
	AZF 70L	66.2
115	AZF 20L	25.3
108	AZF 29L	39.8
	AZF 76L	45.9
	AZF 28L	47.2
	AZF 24L	48.6
	AZF 25L	71.4
	AZF 26L	82.5
	AZF 73L	83.1
100	AZF 23L	44.7
	AZF 5L	76.1
	AZF 6L	83.9
	AZF 39L	100.9
	AZF 3L	101.7
	AZF 40L	149.1
	AZF 2L	169.6
90	AZF 77L	104.8
	AZF 81L	144.4
	AZF 82L	172.4
	AZF 79L	286.9
	AZF 27L	552.5
	AZF 41L	666.6
	AZF 45L	734.1
85	AZF 67L	60.6
	AZF 34L	150.9
	AZF 78L	152.1
	AZF 80L	268.1
	AZF 74L	318.3
	AZF 47L	345.9
	AZF 72L	630.7
	AZF 44L	1,413.6
80	AZF 14L	873.5
	AZF 22L	4,050.0
(b) As-Received Mill-Annealed.		
100	AZF 7L-A	9.6
80	AZF 9L-A	22.4
	AZF 8L-A	58.3
60	AZF 10L-A	188.7
50	AZF 12L-A	195.9
40	AZF 11L-A	5,608.2

TABLE 4. STATIONARY RANDOM AMPLITUDE TEST RESULTS

Axial Loading, 18% Nickel Maraging Steel,
Zero Mean Stress

RMS, ksi	Specimen Number	Equivalent Cycles to Fail (2,000 cpm)
52	AZF 123L	72,799
	AZF 102L	73,832
	AZF 98L	76,932
	AZF 126L	80,833
	AZF 124L	93,765
	AZF 119L	122,400
	AZF 120L	136,864
45	AZF 99L	178,300
	AZF 100L	184,167
	AZF 118L	196,733
	AZF 95L	206,100
	AZF 101L	209,865
	AZF 96L	250,346
	AZF 97L	263,898
40	AZF 122L	299,865
	AZF 94L	300,932
	AZF 127L	351,000
	AZF 128L	353,765
	AZF 92L	370,033
	AZF 93L	470,000
	AZF 121L	772,100

TABLE 5. STATIONARY RANDOM AMPLITUDE TEST RESULTS

Axial Loading, 18% Nickel Maraging Steel,
Zero Mean Stress

RMS, ksi	Specimen Number	Equivalent Cycles to Fail (2,000 cpm)
45	AZF 107L	50,466
	AZF 108L	53,432
	AZF 106L	59,499
	AZF 109L	65,665
	AZF 111L	70,966
	AZF 112L	74,000
	AZF 110L	88,766
40	AZF 136L	98,966
	AZF 133L	107,166
	AZF 135L	115,399
	AZF 134L	118,666
	AZF 137L	141,931
	AZF 138L	148,599
	AZF 139L	153,233
35	AZF 104L	373,265
	AZF 103L	518,533
	AZF 105L	614,100
	AZF 116L	614,400
	AZF 114L	693,232
	AZF 115L	1,706,899
	AZF 140L	1,760,366

TABLE 6. EFFECT OF MANUFACTURING PROCESS ON STATIONARY RAYLEIGH-TYPE FATIGUE ENDURANCE

RMS Stress = 40 ksi; S_m = 50 ksi

Specimen Identification	Test Endurance hours	minutes	seconds	Equivalent Cycles to Fail (33.3 cps)
(a) Vacuum Melt, Vacuum Cast - Supplier - Vanadium-Alloys Steel				
AZF 141L	0	43	20	86,580
AZF 143L	0	47	02	93,970
AZF 136L	0	49	29	98,966
AZF 144L	0	51	30	102,897
AZF 133L	0	53	35	107,166
AZF 135L	0	57	42	115,399
AZF 134L	0	59	14	118,466
AZF 137L	1	10	58	141,931
AZF 138L	1	14	18	148,599
AZF 139L	1	16	37	153,233
(b) Vacuum Melt, Vacuum-Stream Degassing - Supplier - Bethlehem Steel				
AYF 10L	0	23	00	45,954
AYF 2L	0	29	03	58,042
AYF 3L	0	34	36	69,130
AYF 7L	0	34	52	69,664
AYF 8L	0	46	50	93,573
AYF 6L	0	58	40	117,216
AYF 9L	1	10	30	140,859
AYF 1L	1	22	56	165,700
(c) Air Melt, Air Cast - Supplier - U. S. Steel				
AXF 5L	0	21	00	41,958
AXF 7L	0	27	48	55,544
AXF 3L	0	29	44	59,407
AXF 4L	0	34	53	69,697
AXF 10L	0	38	24	76,723
AXF 1L	0	39	36	79,121
AXF 8L	0	46	38	93,173
AXF 6L	1	00	25	120,712
AXF 9L	1	11	30	142,857
AXF 2L	1	25	21	170,529

TABLE 7. REPEATED FLEXURE CONSTANT AMPLITUDE TEST RESULTS

Longitudinal Weld Specimens "B"
0.045-in. Thickness
18% Maraging Steel Sheet

Alternating Stress Amplitude, ksi	Specimen Identification	Cycles to Fail	Machine Number
90	AZF 40L	208,800	2
	AZF 44L	1,769,200	1
	AZF 43L	5,192,700	2
100	AZF 28L	70,600	2
	AZF 27L	259,100	2
	AZF 39L	259,300	2
	AZF 38L	814,600	1
110	AZF 35L	91,700	1
	AZF 25L	134,500	1
	AZF 37L	136,500	1
	AZF 26L	147,000	2
120	AZF 36L	77,800	1
	AZF 24L	81,900	1
	AZF 33L	83,900	2
	AZF 34L	86,400	1
	AZF 23L	99,700	1
130	AZF 30L	38,200	1
	AZF 31L	63,100	1
	AZF 29L	72,100	2
	AZF 32L	74,200	1

TABLE 8. REPEATED FLEXURE CONSTANT AMPLITUDE TEST RESULTS

Transverse Weld Specimens "C"
0.0425-in. Thickness
18% Maraging Steel Sheet

Alternating Stress Amplitude, ksi	Specimen Identification	Cycles to Fail	Machine Number
90	AZF 63T	218,000	2
	AZF 64T	258,000	2
	AZF 62T	292,000	2
	AZF 65T	739,600	2
	AZF 61T	8,484,600	1
100	AZF 56T	112,400	1
	AZF 53T	192,200	1
	AZF 54T	275,100	2
	AZF 55T	308,600	2
110	AZF 52T	52,600	2
	AZF 49T	91,100	1
	AZF 50T	105,800	2
	AZF 51T	128,700	1
120	AZF 48T	60,700	2
	AZF 47T	67,400	1
	AZF 45T	78,700	1
	AZF 46T	79,200	2
130	AZF 60T	38,700	2
	AZF 58T	45,000	2
	AZF 59T	45,500	1
	AZF 66T	57,100	2
	AZF 57T	168,700	1

TABLE 9. REPEATED FLEXURE CONSTANT AMPLITUDE TEST RESULTS

Plain Specimens – Heat Treat Scale "D"
0.050-in. Thickness
18% Maraging Steel Sheet

Alternating Stress Amplitude, ksi	Specimen Identification	Cycles to Fail	Machine Number
90	AZF 84L	482,600	1
	AZF 87L	3,154,600	2
	AZF 68L	36,193,200*	2
	AZF 86L	37,845,200*	1
100	AZF 67L	104,900	2
	AZF 83L	109,300	1
	AZF 72L	113,200	1
	AZF 69L	140,100	1
110	AZF 73L	73,800	1
	AZF 75L	80,600	1
	AZF 74L	95,300	1
	AZF 76L	105,200	1
	AZF 82L	108,700	1
120	AZF 80L	81,100	1
	AZF 88L	83,800	2
	AZF 77L	85,700	1
	AZF 81L	119,400	1
	AZF 78L	159,200	1

* No failure (runout).

TABLE 10. EFFECT OF MANUFACTURING PROCESS ON THE RANDOM LOAD FATIGUE LIFE OF SPECIMENS CONTAINING A TRANSVERSE WELD (SEE FIGURE 6)

18% Nickel Maraging Steel
RMS Alternating Stress = 33 ksi
S_m = 40 ksi tension

Specimens Tested in Air

Specimen Identification	Effective Cycles to Failure	Remarks
Consumable Electrode Vacuum Melt and Vacuum Cast		
AZF 250W	60,460	Good weld
AZF 249W	64,128	Good weld
AZF 257W	82,944	Two large gas holes
AZF 248W	87,744	Good weld
AZF 253W	92,736	Small inclusions
AZF 256W	98,880	Good weld
AZF 251W	128,832	Two large holes
Air Melt, With Vacuum Stream Degassing During Pouring		
AYF 26W	33,957	Large inclusion
AYF 27W	37,456	Large gas hole
AYF 33W	99,607	Small gas hole
AYF 35W	123,860	Good weld
AYF 28W	125,744	Gas hole
AYF 34W	141,279	Good weld
AYF 32W	256,427	Good weld
Air Melt Air Cast		
AXF 49W	39,102	Large gas hole and inclusion
AXF 53W	100,636	3 small gas holes
AXF 37W	110,103	1 large gas hole
AXF 36W	148,500	Good weld
AXF 54W	185,632	Good weld
AXF 39W	340,393	Good weld
AXF 30W	426,623	Good - failed in HAZ

Note. All failures were in the weld metal unless otherwise noted.

TABLE 11. UNNOTCHED CYLINDRICAL SPECIMEN, INCONEL 718, ROTATING BEAM FATIGUE TESTS

Zero Mean Stress

Stress Amplitude, ksi	Specimen Identification	Kilocycles to Failure	Machine Number
95	BWF 11L	900	1
	BWF 33L	13,080	1
	BWF 34L	18,175	3
	BWF 35L	478,604*	4
	BWF 23L	493,517	2
	BWF 12L	667,117*	3
97.5	BWF 57L	896	1
	BWF 54L	8,634	1
	BWF 55L	77,321	2
	BWF 56L	91,924	3
	BWF 53L	109,750*	4
100	BWF 29L	509	4
	BWF 2L	711	2
	BWF 3L	735	3
	BWF 27L	800	1
	BWF 1L	895	1
	BWF 8L	3,338	1
	BWF 10L	3,477	3
	BWF 9L	33,244	2
	BWF 4L	101,801	4
105	BWF 50L	294	1
	BWF 7L	417	3
	BWF 51L	572	2
	BWF 6L	807	2
	BWF 18L	935	3
	BWF 17L	1,216	4
	BWF 19L	1,879	2
	BWF 20L	2,577	1
	BWF 5L	3,875	1
110	BWF 16L	280	4
	BWF 22L	406	4
	BWF 21L	423	3
	BWF 49L	466	4
	BWF 48L	534	3
	BWF 26L	594	1
	BWF 15L	736	3
	BWF 14L	860	2
	BWF 13L	1,213	1
115	BWF 36L	196	3
	BWF 28L	233	1
	BWF 46L	275	1
	BWF 25L	292	4
	BWF 47L	314	2
	BWF 45L	326	4
	BWF 37L	347	1
	BWF 38L	367	2
	BWF 24L	391	1
120	BWF 30L	189	1
	BWF 41L	191	1
	BWF 32L	199	4
	BWF 40L	201	2
	BWF 44L	252	3
	BWF 42L	273	1
	BWF 39L	340	3
	BWF 31L	378	3
	BWF 43L	438	2

*No Failure (runout).

TABLE 12. EFFECT OF MANUFACTURING PROCESS ON THE RANDOM LOAD FATIGUE LIFE OF SPECIMENS CONTAINING A TRANSVERSE WELD (SEE FIGURE 6)

18% Nickel Maraging Steel
RMS Alternating Stress = 33 ksi
S_m = 48 ksi Tension

Specimen Identification	Effective Cycles to Failure	Remarks
Consumable-Electrode Vacuum Melt and Vacuum Cast		
AZF 263W	58,430	Good weld
AZF 264W	82,908	Good weld
AZF 262W	103,240	Good weld
AZF 267W	153,938	Good weld
AZF 265W	156,202	Good weld
AZF 266W	157,023	Good weld
Air Melt, With Vacuum-Stream Degassing During Pouring		
AYF 29W	17,081	Porosity and segregation
AYF 25W	17,905	Porosity and segregation
AYF 30W	50,833	Porosity in weld
AYF 24W	51,719	Good weld
AYF 31W	70,178	One small hole in weld
AYF 23W	75,012	Good weld
Air Melt Air Cast		
AXF 30W	41,983	Many gas holes
AXF 28W	9 ,331	Good weld
AXF 29W	96,529	Good weld
AXF 27W	107,583	Good weld
AXF 31W	131,506	Good weld
AXF 32W	136,857	Good weld

Note All failures were in the weld metal unless otherwise noted. Specimens tested in artificial sea water (Figure 22).

TABLE 13. EFFECT OF MANUFACTURING PROCESS ON THE RANDOM LOAD FATIGUE LIFE OF SPECIMENS CONTAINING A TRANSVERSE WELD AND TESTED IN AIR ATMOSPHERE

18% Nickel Maraging Steel; S_m = 48 ksi

Specimen Identification	Effective Cycles to Failure	Remarks
RMS Stress Amplitude = 23 ksi		
Consumable-Electrode Vacuum Melt and Vacuum Cast		
AZF 245W	148,416	Good weld
AZF 246W	202,176	Good weld
AZF 244W	292,224	Good weld
AZF 243W	356,736	Good weld
Air Melt Air Cast		
AXF 41W	90,552	Very large gas hole
AXF 43W	232,960	Good weld
AXF 42W	1,389,356	Good - failed in HAZ
AXF 44W	1,632,611	Good weld
RMS Stress Amplitude = 20.8 ksi		
Consumable-Electrode Vacuum Melt and Vacuum Cast		
AZF 259W	491,904	Good weld
AZF 258W	915,072	One large hole in centre
AZF 269W	2,331,920	Good weld
Air Melt, Vacuum-Stream Degassing During Pouring		
AYF 36W	34,368	Very poor weld - lack of penetration
AYF 38W	480,543	Five small holes
AYF 39W	4,402,062	Good weld
AYF 37W	5,704,159	Good weld
Air Melt Air Cast		
AXF 45W	258,896	Small holes on edge
AXF 46W	283,181	Good weld
AXF 47W	5,667,732	Not failed
AXF 48W	6,120,000	Not failed
RMS Stress Amplitude = 18.3 ksi		
Consumable-Electrode Vacuum Melt and Vacuum Cast		
AZF 268W	1,761,236	Hole on circumference
AZF 260W	4,154,496	One large hole
AZF 261W	7,401,984	Not failed
Air Melt Air Cast		
AXF 50W	451,731	Good weld
AXF 52W	558,335	Large gas hole
AXF 51W	9,549,120	Not failed

Note All failures were in the weld metal unless otherwise noted.

TABLE 14. AXIAL LOAD CONSTANT AMPLITUDE FATIGUE TESTS USING THE LARGE-SCALE FATIGUE SPECIMENS

S_m = 50 ksi

Specimen Identification	Reference Figure	Alternating Stress, ksi	Endurance Kilocycles	Remarks
		(a) Plain Unnotched Waisted Plate Specimen		
A-B	17	90	31.8	Good failure
A-C	17	60	80.9	Good failure
A-A	17	60	92.3	Fracture near fillet
A-D	17	60	104.6	Good failure
A-E	17	60	107.1	Good failure
		(b) Specimen With Transverse Fillet Welded Stub at Mid-Length		
B1	18	60	17.3	Cracks usually developed on both sides of stub with one side finally causing failure. Must hand-grind weld to avoid failures at boundary between weld and ground surfaces.
B2	18	60	18.8	
B3	18	60	19.1	
B4	18	60	24.1	
B6	18	60	26.3	
B5	18	60	29.6	
		(c) Specimen With Three Equally Spaced Plug Welds Along Axis		
C1	19	90	0.96	All fractures passed thru an end plug weld. Significant corrosion appeared at the fracture at the plug weld. Possibly due to trapped water during grinding, between specimen and backing block.
C2	19	60	2.5	
C6	19	60	2.9	
C3	19	60	3.1	
C4	19	60	3.7	
C5	19	60	7.75	
		(f) Specimen With Longitudinal Fillet Welded Stub		
F3	20	60	33.9	Only failure in parallel section. Grips shot peened and minimum area reduced.
F1	20	60	20.7	First test – failure in weldment at grips.
F4	20	60	30.2	Failed in grips – grips extensively hand-ground to remove weld notches.
F2	20	60	31.1	Failed in grips – minimum area reduced and material removed from grips.
F5	20	60	40.2	Failed in grips, which were shot peened before test.

TABLE 15. EFFECT OF SALT WATER FLOW RATE

Fatigue Stress 0 ± 60 ksi
Pacific Sea Water

Flow Rate	Specimen Identification	Cycles to Failure	Log Cycles to Failure
0.5 fpm	AZF 146L	217,500	5.3374
	AZF 147L	246,600	5.3920
	AZF 148L	258,600	5.4126
	AZF 131L	292,700	5.4664
	AZF 149L	367,200	5.5649
	AZF 130L	469,100	5.6894
1 knot	AZF 158L	114,900	5.0603
	AZF 154L	197,800	5.2962
	AZF 156L	205,500	5.3128
	AZF 159L	216,100	5.3347
	AZF 157L	237,900	5.3764
	AZF 155L	299,000	5.4757
2 knots	AZF 164L	149,900	5.1758
	AZF 162L	151,400	5.1801
	AZF 160L	159,600	5.2030
	AZF 165L	171,600	5.2345
	AZF 163L	181,200	5.2582
	AZF 161L	249,200	5.3965

TABLE 16. CORROSION FAGITUE PROGRAM - CONSTANT AMPLITUDE FATIGUE TESTS

Stress Amplitude = 60 ksi
Line Flow Rate = 2 knots

Artificial Sea Water		Atlantic Sea Water		Pacific Sea Water	
Specimen Number	Life Cycles	Specimen Number	Life Cycles	Specimen Number	Life Cycles
(a) Zero Mean Stress					
AZF 180L	153,800	AZF 207L	190,900	AZF 164L	149,900
AZF 192L	169,000	AZF 204L	198,200	AZF 162L	151,400
AZF 194L	220,700	AZF 211L	199,200	AZF 160L	159,600
AZF 179L	234,100	AZF 210L	210,900	AZF 165L	171,600
AZF 176L	245,300	AZF 216L	229,200	AZF 163L	181,200
AZF 181L	250,600	AZF 215L	271,100	AZF 161L	249,200
(b) Mean Stress - 48 ksi Tension					
AZF 188L	60,900	AZF 205L	57,600	AZF 170L	60,700
AZF 191L	75,500	AZF 206L	59,000	AZF 166L	67,800
AZF 187L	85,500	AZF 208L	59,500	AZF 168L	71,000
AZF 189L	87,300	AZF 202L	65,600	AZF 167L	72,700
AZF 190L	90,800	AZF 209L	73,500	AZF 171L	80,600
AZF 193L	100,700	AZF 203L	75,300	AZF 169L	85,200

TABLE 17. CORROSION FATIGUE PROGRAM - RANDOM (RAYLEIGH) AMPLITUDE TESTS

RMS Stress Amplitude = 33 ksi
Line Flow Rate = 2 knots

Artificial Sea Water		Atlantic Sea Water		Pacific Sea Water	
Specimen Number	Life Cycles	Specimen Number	Life Cycles	Specimen Number	Life Cycles
(a) Zero Mean Stress					
AZF 234L	304,500	AZF 214L	279,150	AZF 175L	235,460
AZF 233L	311,600	AZF 220L	236,250	AZF 182L	264,750
AZF 228L	315,650	AZF 219L	299,550	AZF 173L	269,200
AZF 229L	327,550	AZF 217L	345,800	AZF 174L	319,500
AZF 232L	386,500	AZF 221L	394,350	AZF 172L	376,300
AZF 225L	670,000	AZF 218L	644,300	AZF 181L	506,300
(b) Mean Stress - 48 ksi Tension					
AZF 223L	119,250	AZF 200L	107,500	AZF 184L	110,800
AZF 212L	135,750	AZF 199L	114,050	AZF 196L	120,000
AZF 227L	136,900	AZF 198L	126,900	AZF 186L	141,500
AZF 230L	140,350	AZF 212L	127,300	AZF 195L	142,850
AZF 231L	171,450	AZF 213L	129,200	AZF 197L	144,000
AZF 224L	173,400	AZF 201L	172,200	AZF 185L	149,950

Note: Effective cycles based on 32 cps and time readings.

TABLE 18. EFFECT OF MANUFACTURING PROCESS - AXIAL FATIGUE TESTS IN ARTIFICIAL SEAWATER - UNNOTCHED FATIGUE SPECIMENS

18% Maraging Steel

Machine R1

Loading: 48 ksi Tension, 33 ksi RMS (Rayleigh)

Specimen Identification	Time to Failure, minutes	Effective Cycles, 32 cps
(a) Vacuum Melt, Vacuum Cast - Supplier - Vanadium-Alloys Steel		
AZF 223L	62.1	119,23[illegible]
AZF 232L	70.7	135,744
AZF 227L	71.3	136,896
AZF 230L	73.1	140,352
AZF 231L	89.3	171,456
AZF 224L	90.3	173,376
(b) Vacuum Melt, Vacuum-Stream Degassing - Supplier - Bethlehem Steel		
AYF 19L	83.4	160,128
AYF 17L	84.5	162,240
AYF 20L	89.7	172,224
AYF 16L	108.1	207,552
AYF 18L	127.9	245,568
AYF 15L	165.8	318,336
(c) Air Melt, Air Cast - Supplier - U. S. Steel		
AXF 18L	71.2	136,704
AXF 14L	78.3	150,336
AXF 13L	80.7	154,944
AXF 15L	88.8	170,496
AXF 17L	106.1	203,712
AXF 16L	177.7	341,184

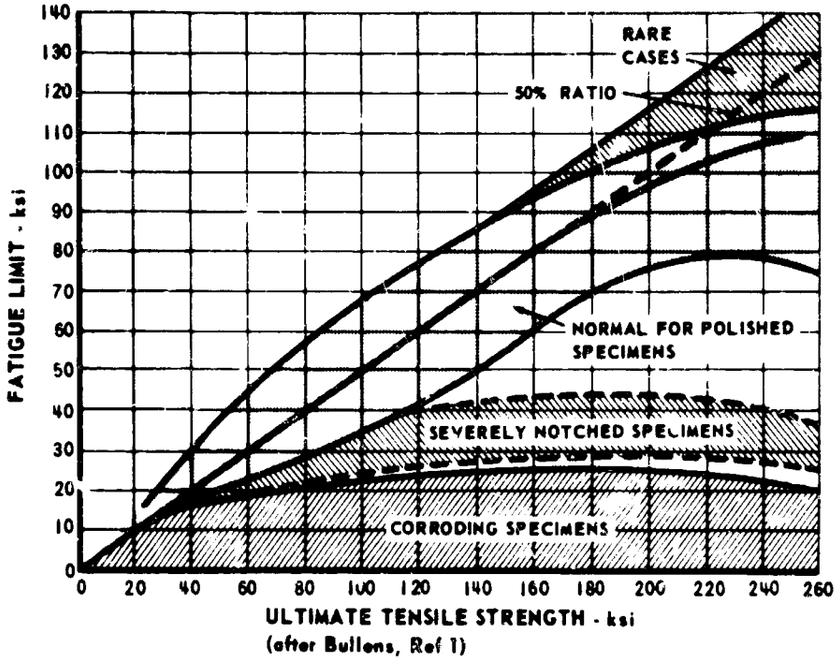

FIGURE 1a. BEHAVIOUR OF WROUGHT STEEL IN FATIGUE

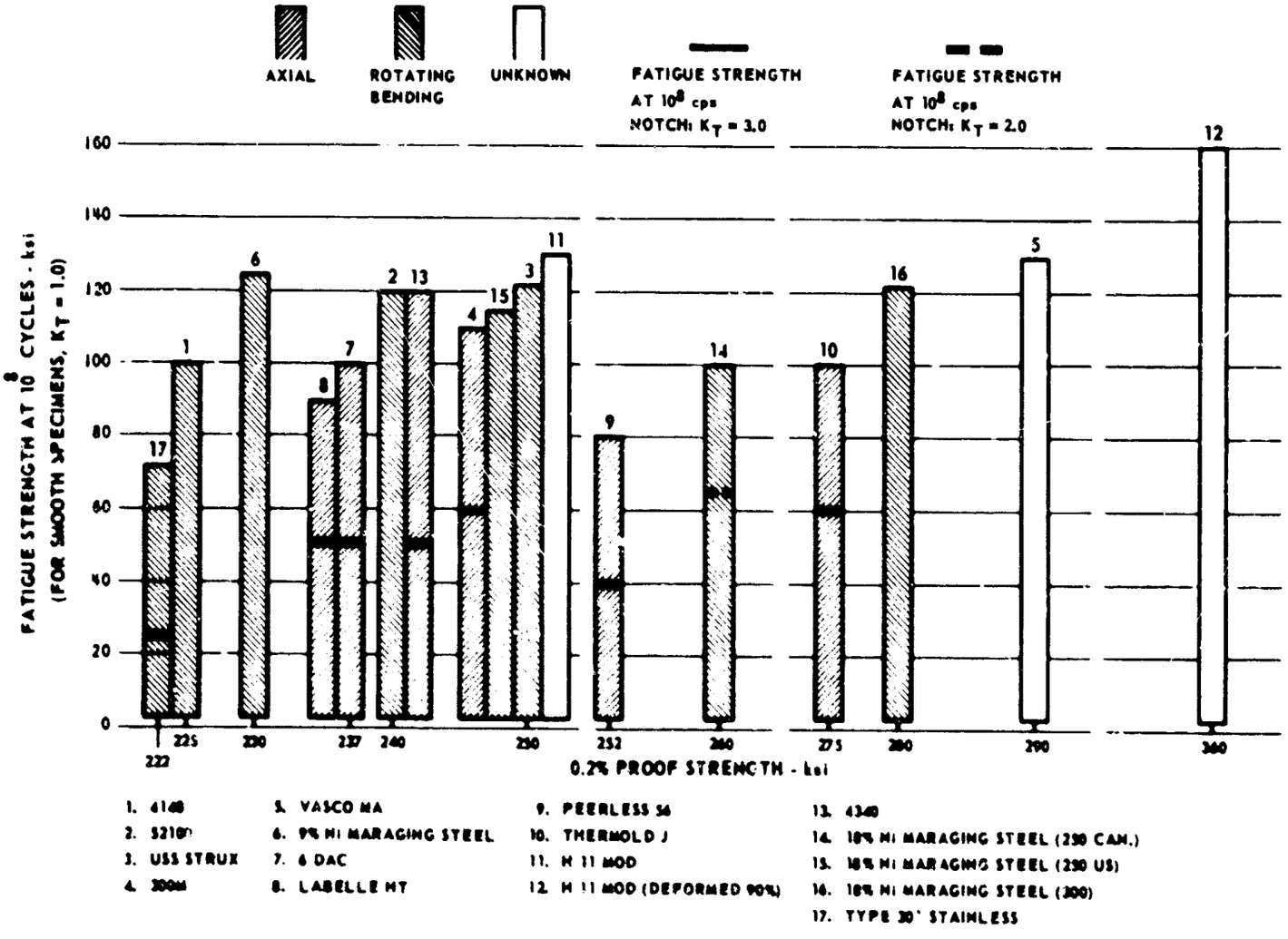

FIGURE 1b. FATIGUE STRENGTHS OF ULTRAHIGH-STRENGTH STEELS

Yield Strength Greater than 225,000 lb/sq in.

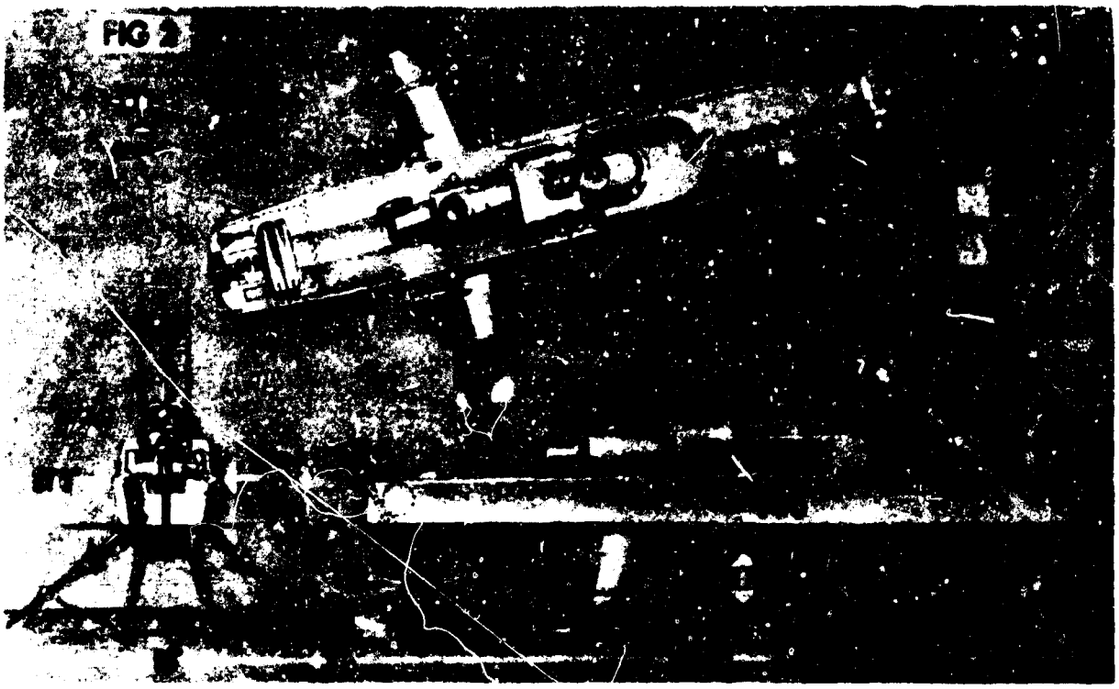

FIGURE 2. THE FHE 400 RCN PROTOTYPE ASW HYDROFOIL SHIP
(Plan and Profile Views)

FIGURE 3a. MAIN FOIL OF THE FHE 400 RCN PROTOTYPE ASW HYDROFOIL SHIP

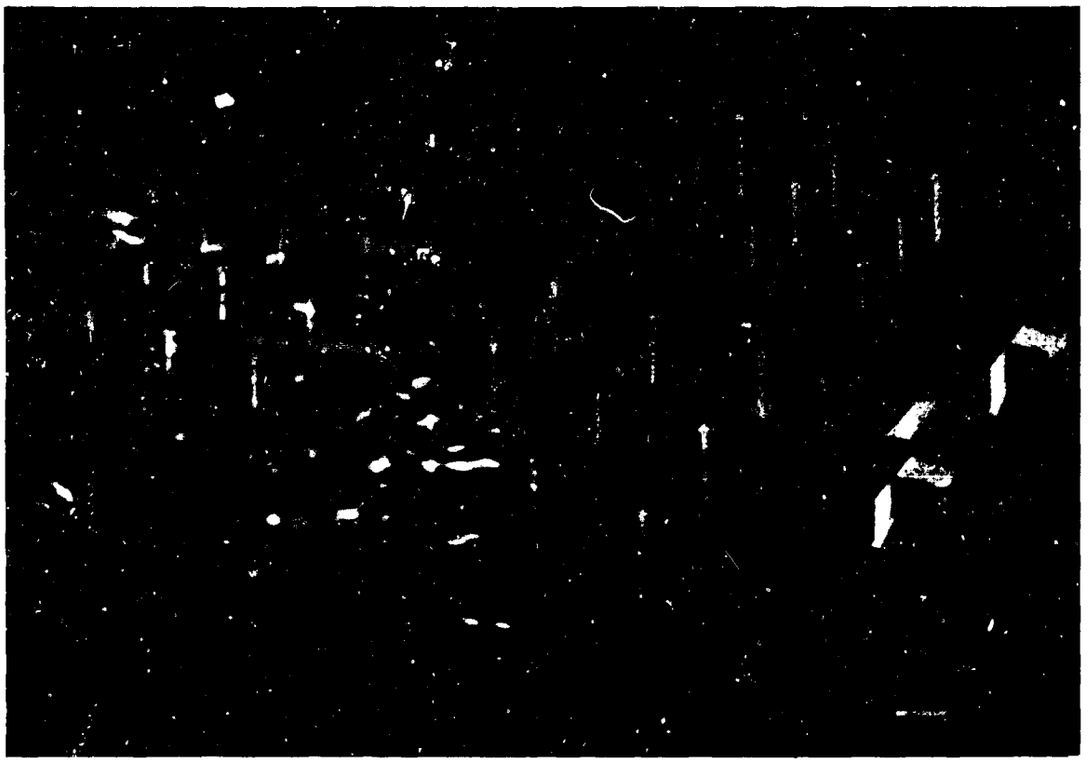

FIGURE 3b. DISTRIBUTION OF LOADS IN MAIN FOIL OF THE FHE 400

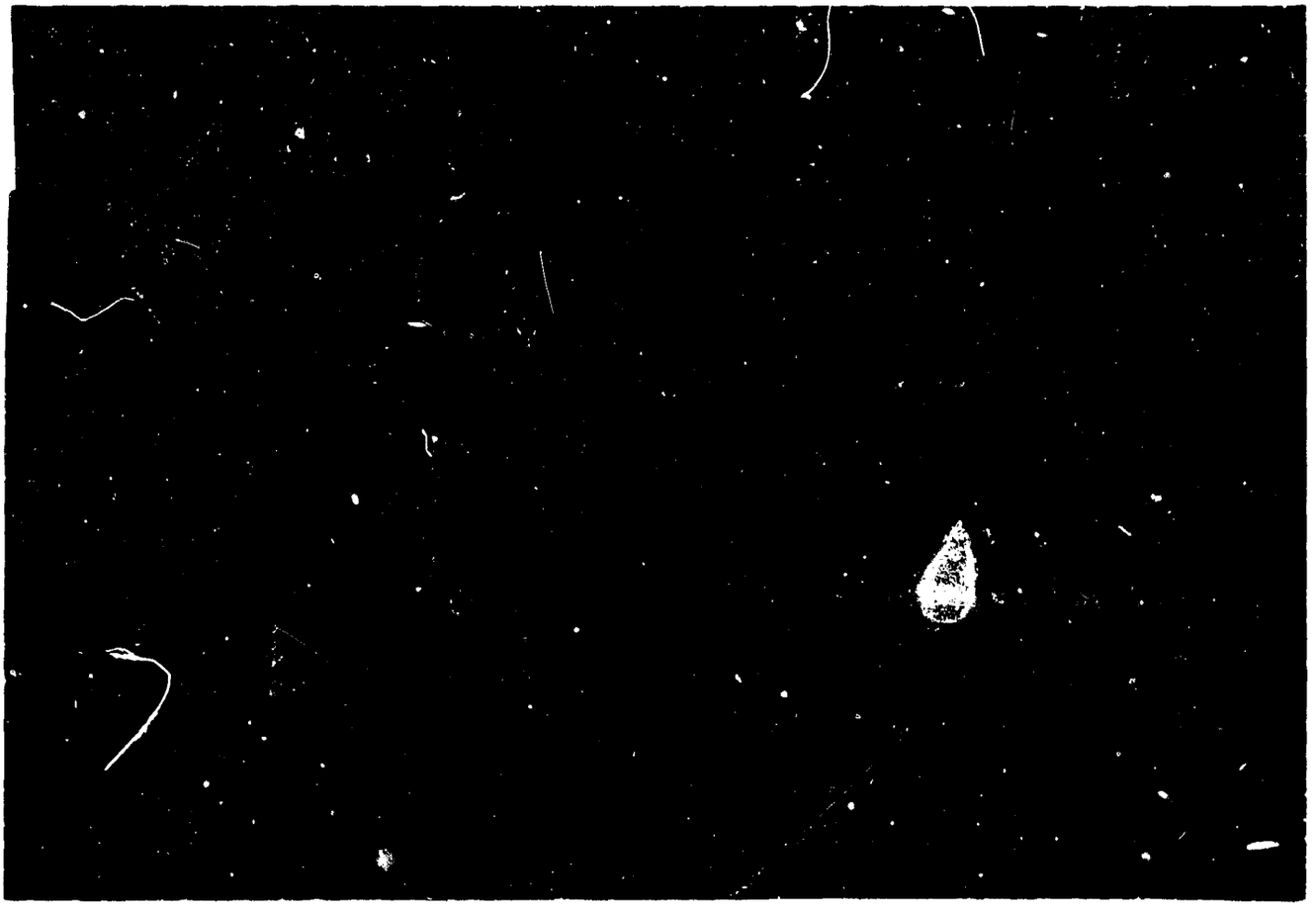

FIGURE 4. STRUCTURAL DETAILS OF THE CENTER SECTION OF THE MAIN FOIL OF THE FHE 400

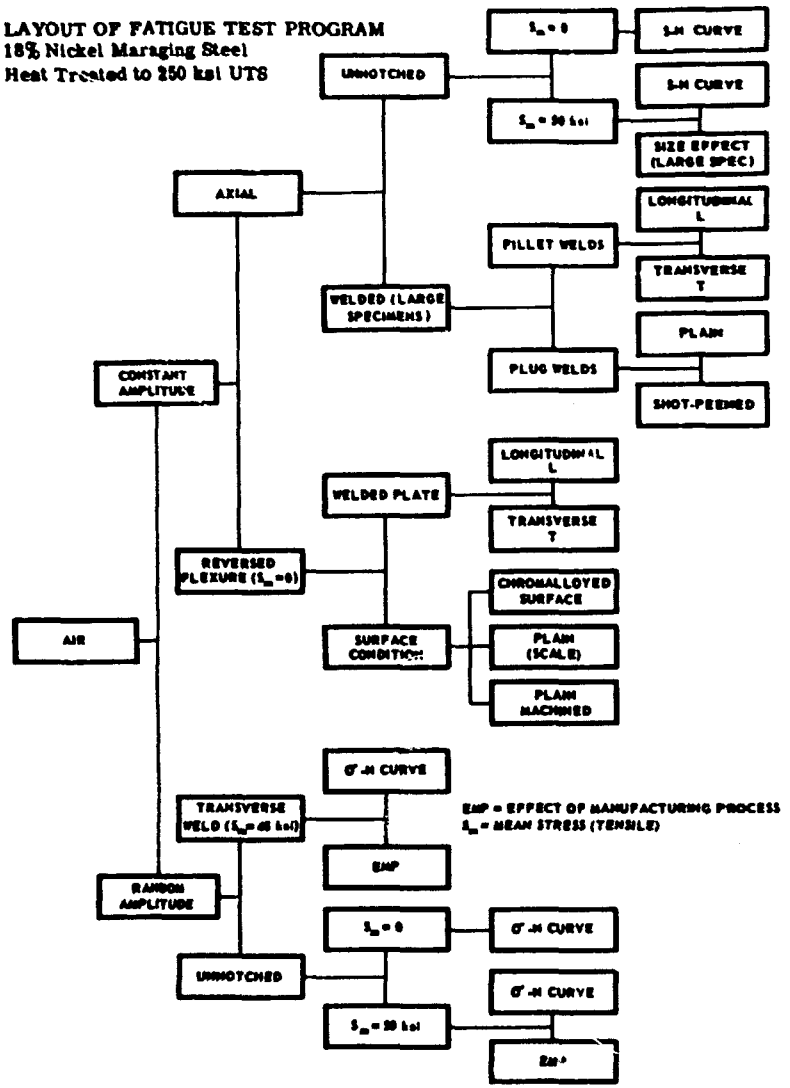

FIGURE 5a. LAYOUT OF FATIGUE TEST PROGRAM FOR 18 PERCENT NICKEL MARAGING STEEL HEAT TREATED TO 250 KSI UTS

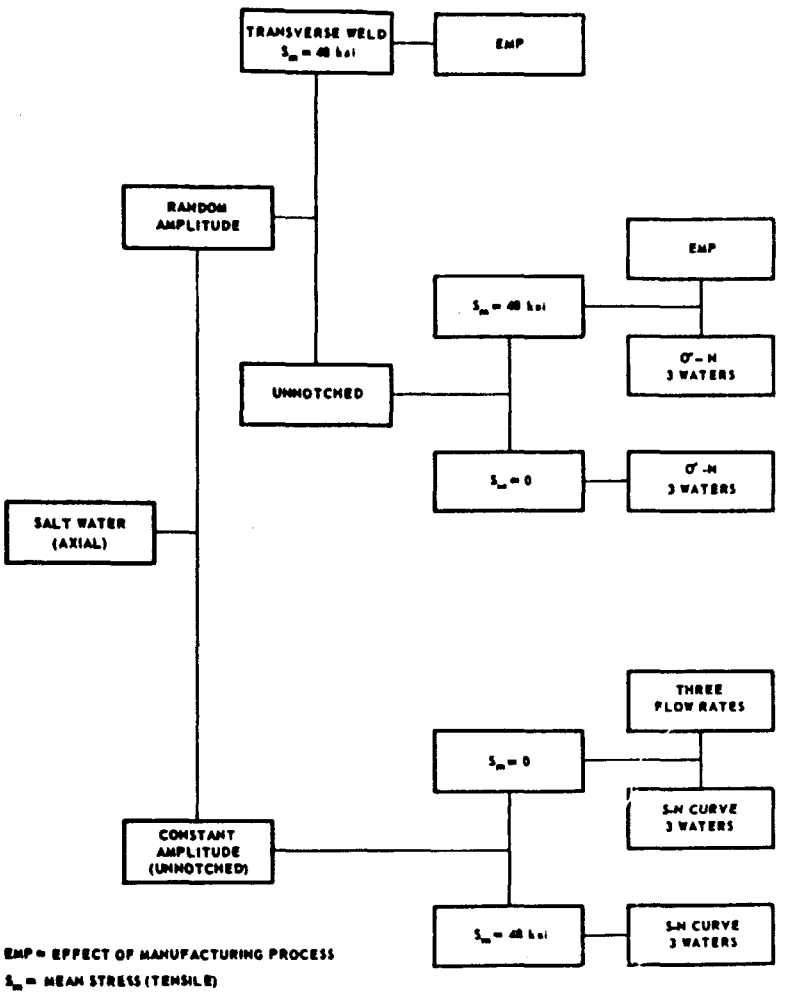

FIGURE 5b. LAYOUT OF FATIGUE TEST PROGRAM FOR 18 PERCENT NICKEL MARAGING STEEL HEAT TREATED TO 250 KSI UTS

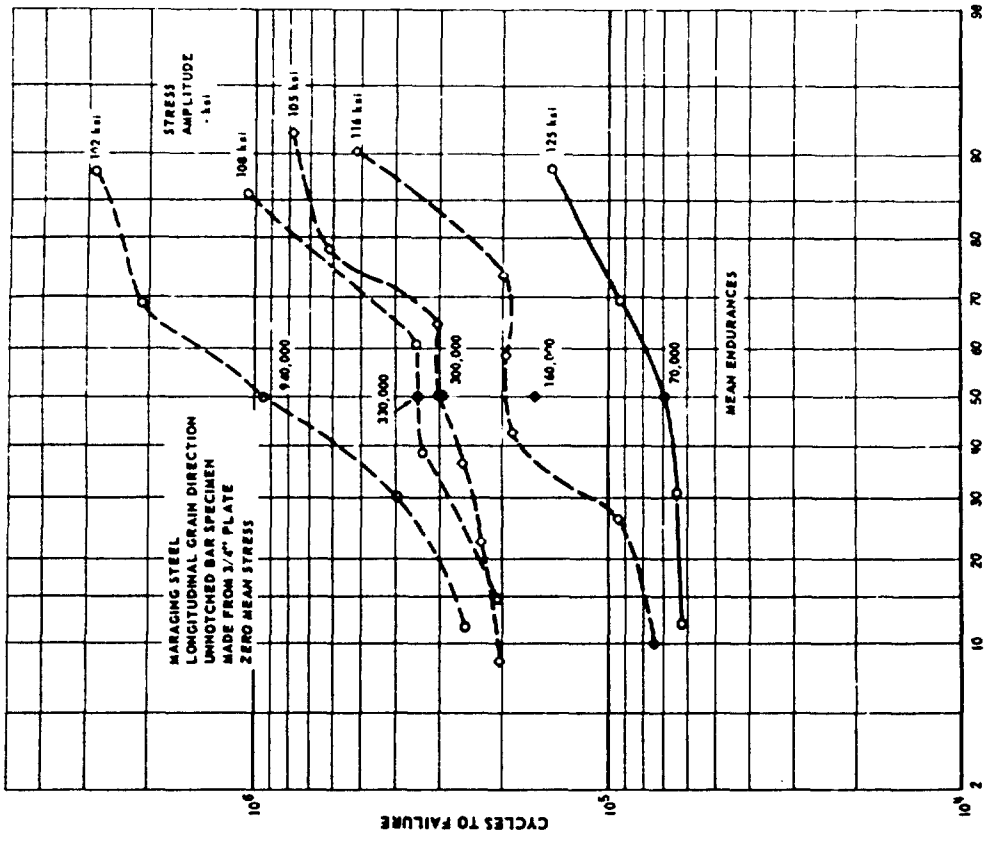

FIGURE 7. PROBABILITY OF CONSTANT AMPLITUDE SINGLE LEVEL TEST RESULTS

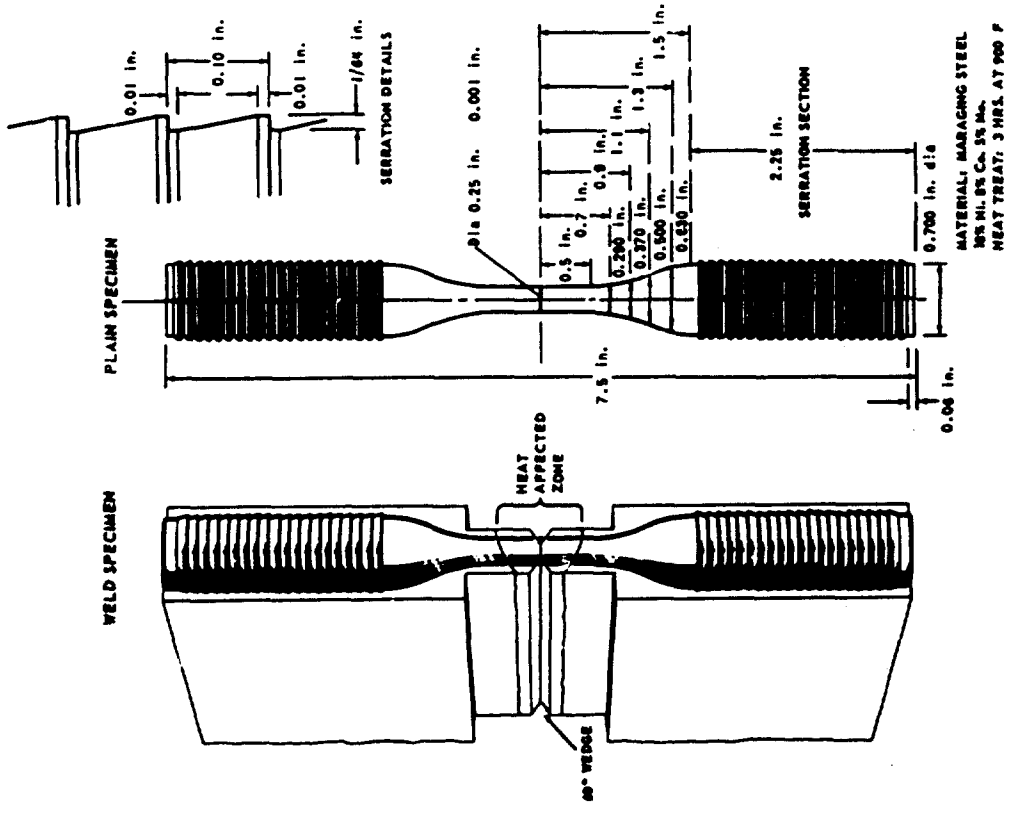

FIGURE 6. FATIGUE SPECIMENS FOR AXIAL TESTS

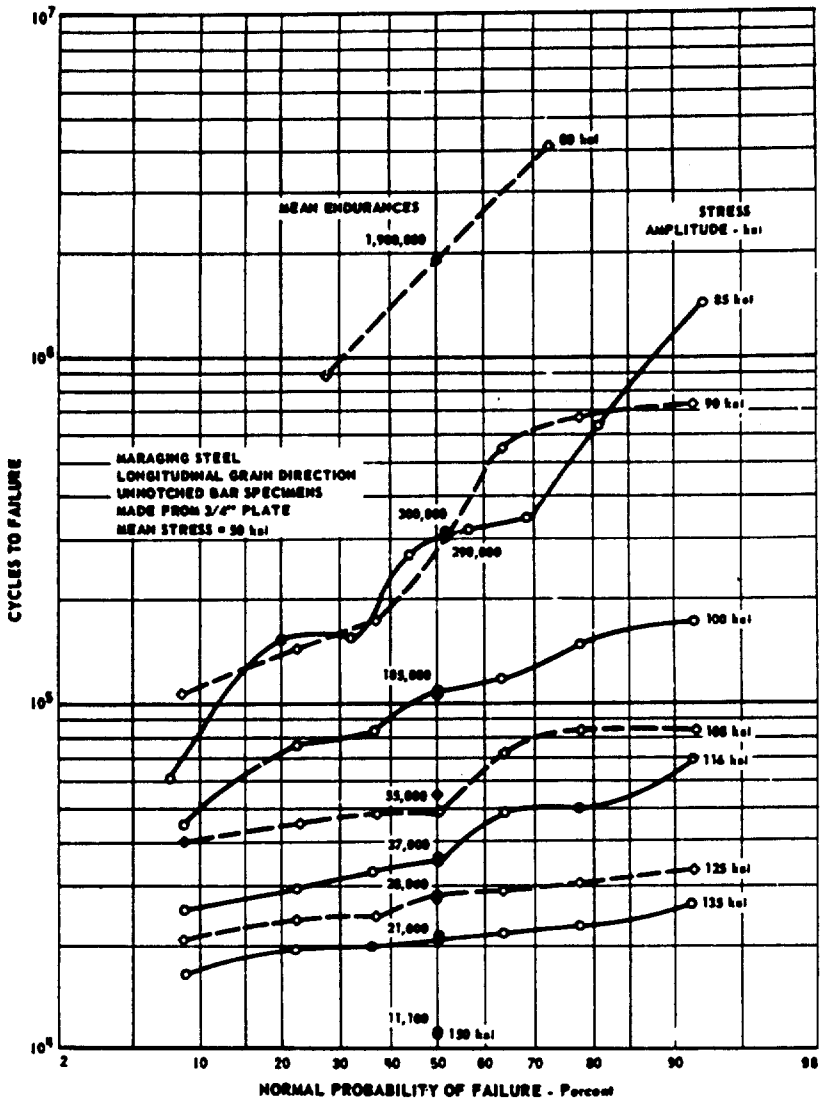

FIGURE 8. PROBABILITY BEHAVIOR OF CONSTANT AMPLITUDE SINGLE-LEVEL TEST RESULTS

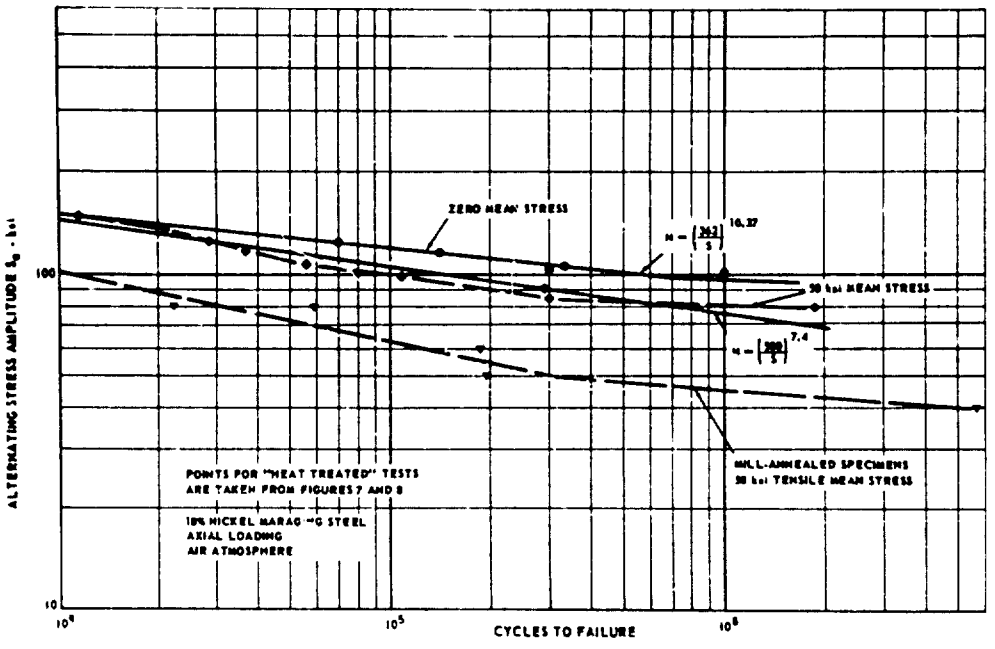

FIGURE 9. FATIGUE S-N CURVES FOR CONSTANT AMPLITUDE TESTS

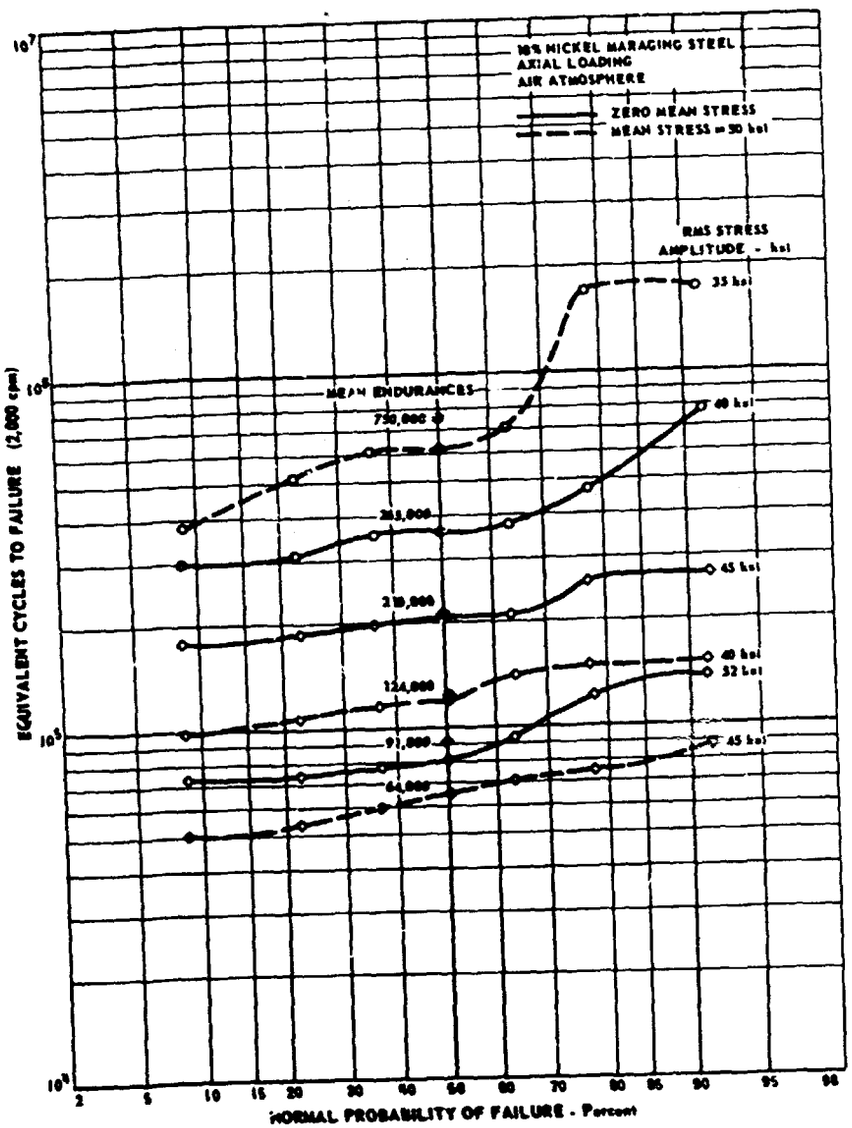

FIGURE 10. STATIONARY RANDOM AMPLITUDE TEST RESULTS

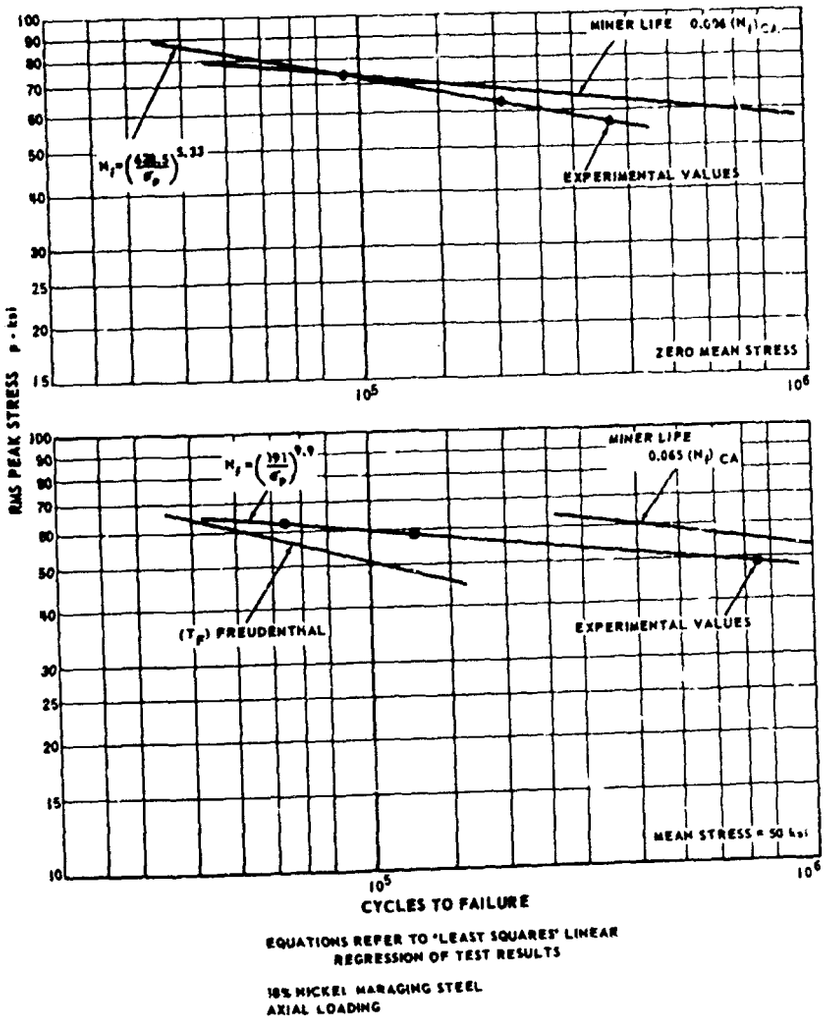

FIGURE 11. COMPARISON OF TEST RESULTS WITH PREDICTIONS FROM CUMULATIVE DAMAGE THEORY

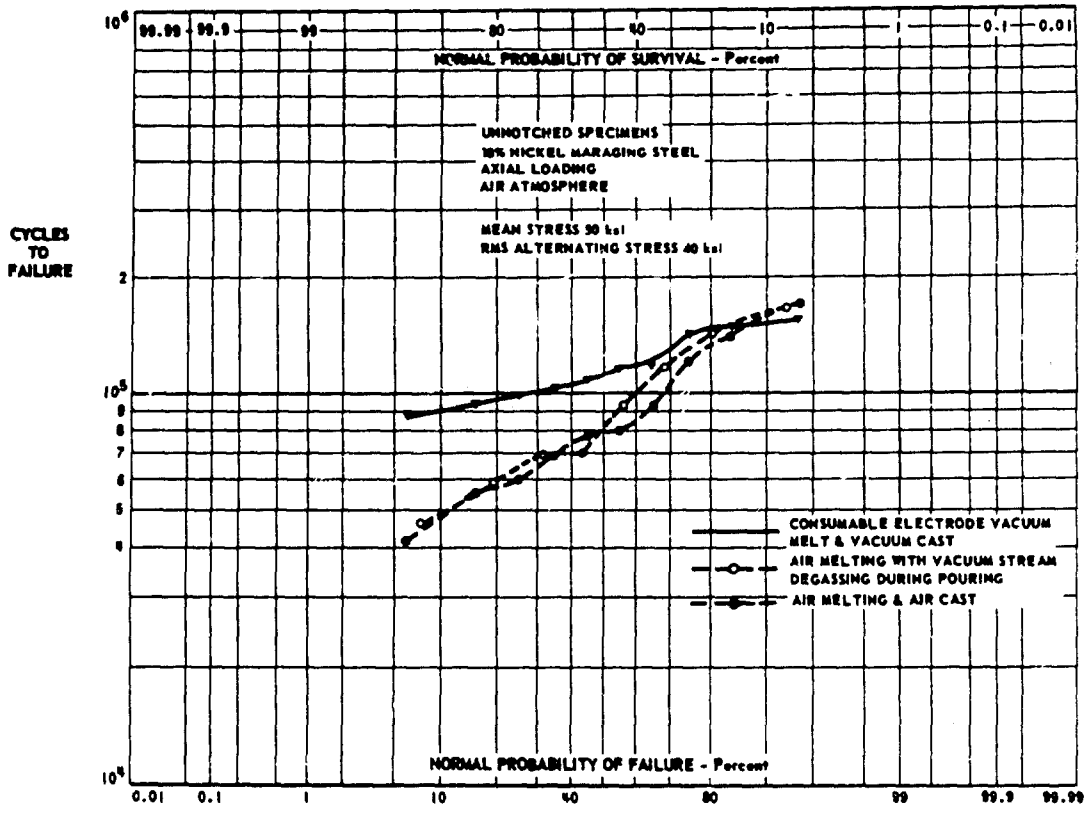

FIGURE 12. EFFECT OF MANUFACTURING PROCESS ON RANDOM FATIGUE LIFE

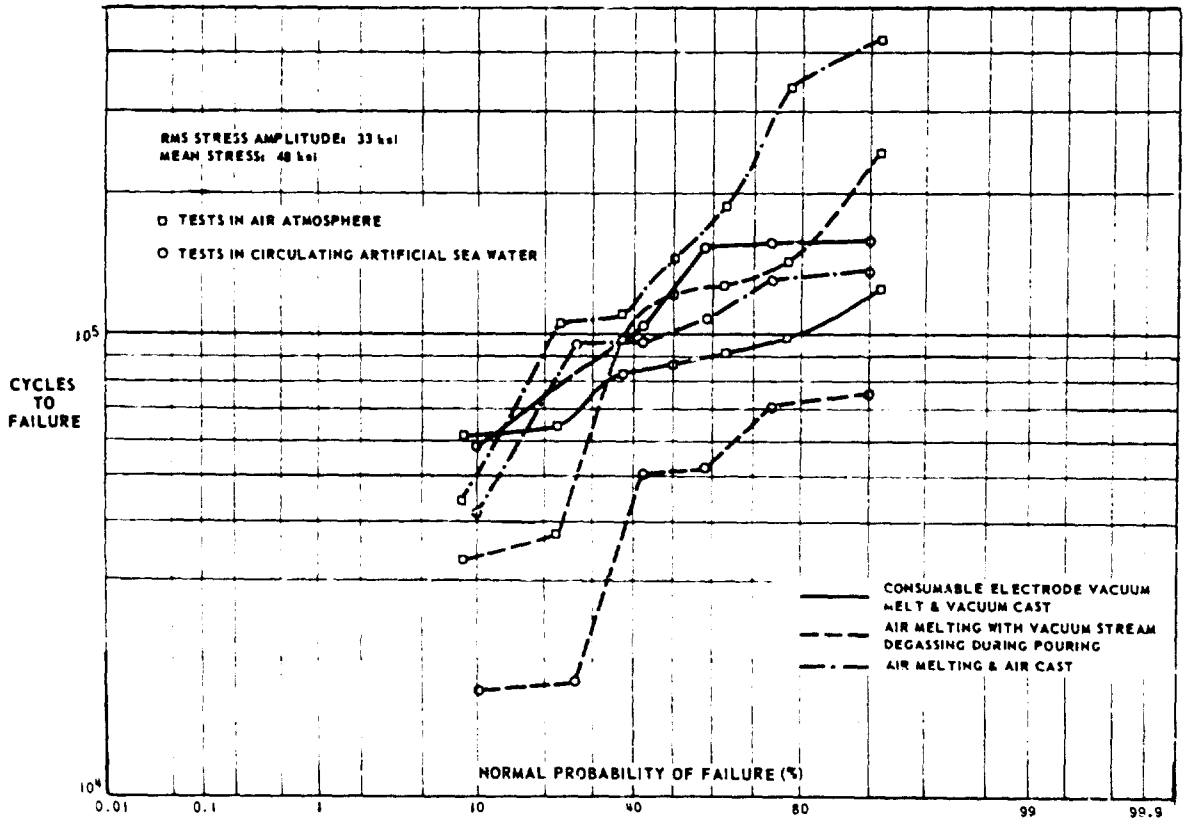

FIGURE 13. AXIAL LOAD FATIGUE TESTS USING THE STANDARD SPECIMEN WITH A TRANSVERSE WELD

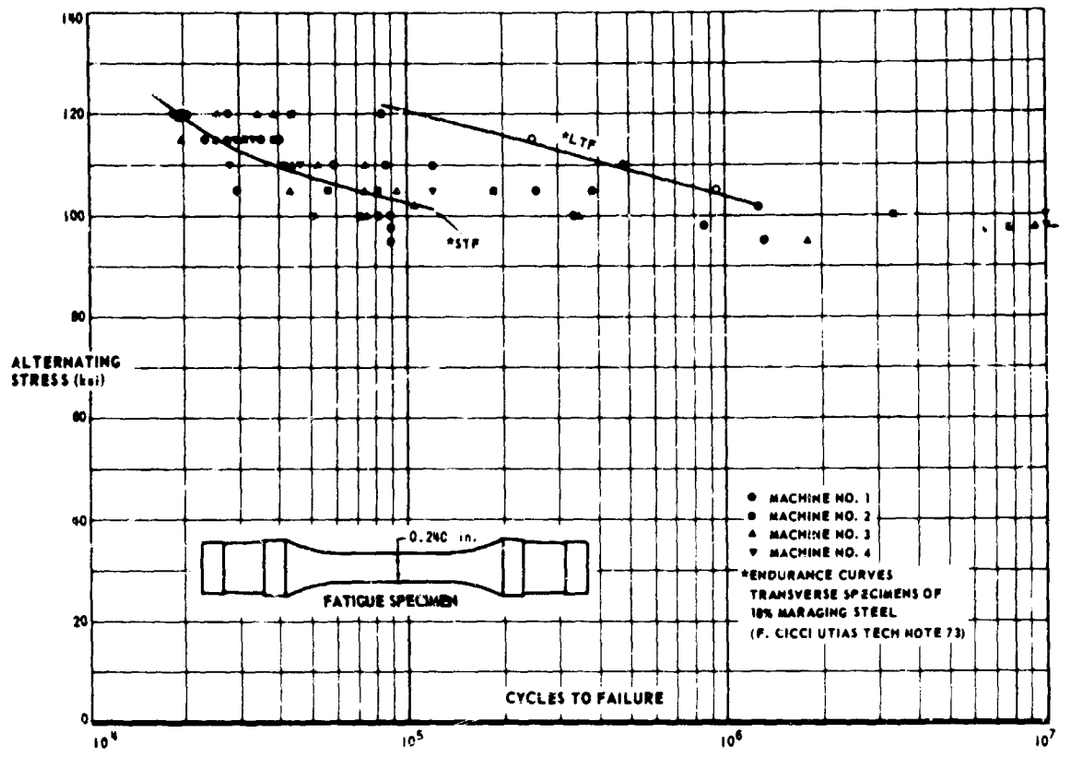

FIGURE 14. R.R. MOORE TOTATING BEAM FATIGUE TEST RESULTS (AIR)
Longitudinal Specimens - Inconel 718

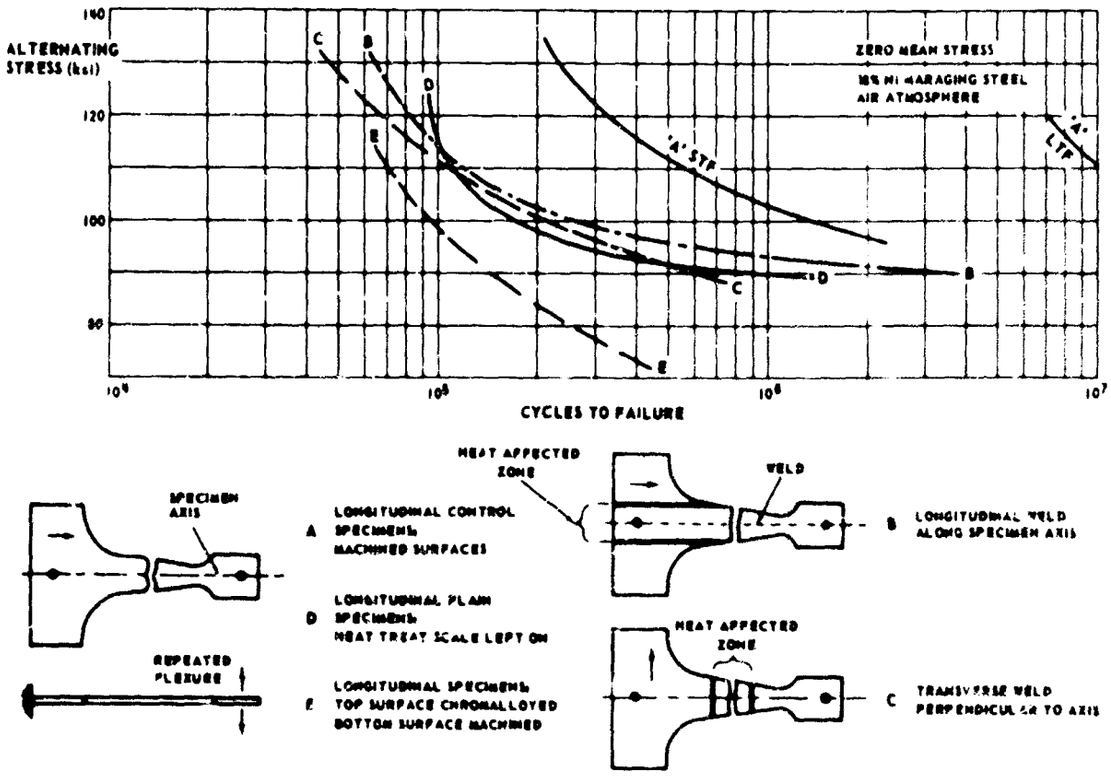

FIGURE 15. CONSTANT AMPLITUDE FATIGUE S-N CURVES REPEATED FLEXURE EFFECT OF WELDS AND VARIOUS SURFACE TREATMENTS

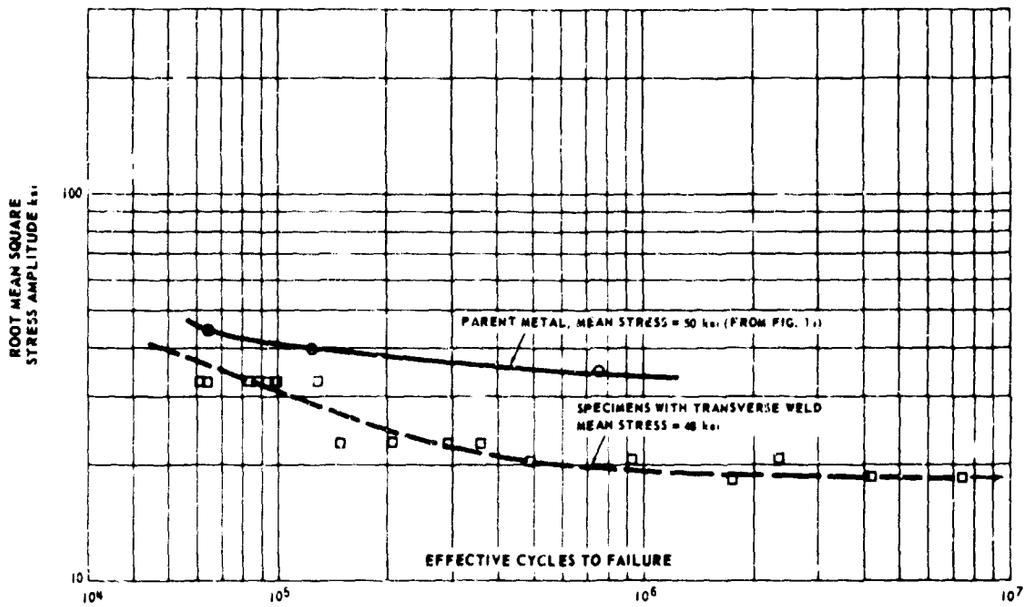

FIGURE 16. RANDOM LOAD FATIGUE σ-N CURVES FOR AIR TESTS USING CONSUMABLE ELECTRODE VACUUM-MELT AND VACUUM-CAST MARAGING STEEL

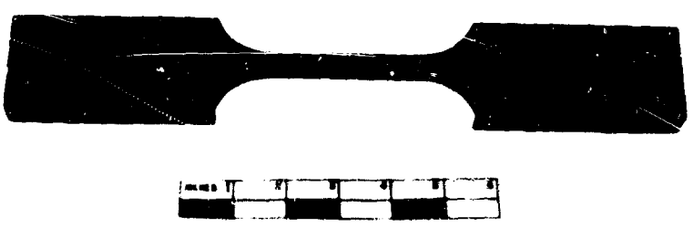

LARGE-SCALE AXIAL FATIGUE TEST SPECIMEN (A)
UNNOTCHED (CONTROL)

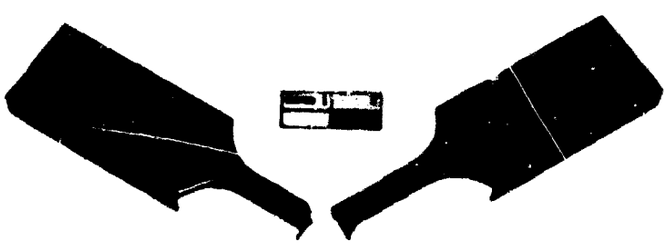

18% NICKEL MARAGING STEEL, AIR ATMOSPHERE

FIGURE 17. LARGE-SCALE AXIAL FATIGUE TEST SPECIMEN(A)

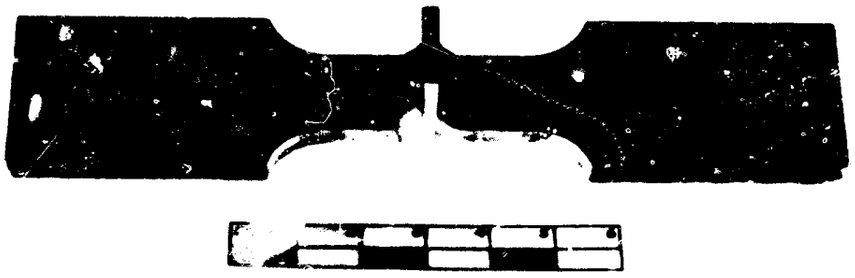

LARGE-SCALE FATIGUE TEST SPECIMEN (B)
CONTAINING TRANSVERSE FILLET WELD

18% NICKEL MARAGING STEEL, AIR ATMOSPHERE

FIGURE 18. LARGE-SCALE FATIGUE TEST SPECIMEN (B)

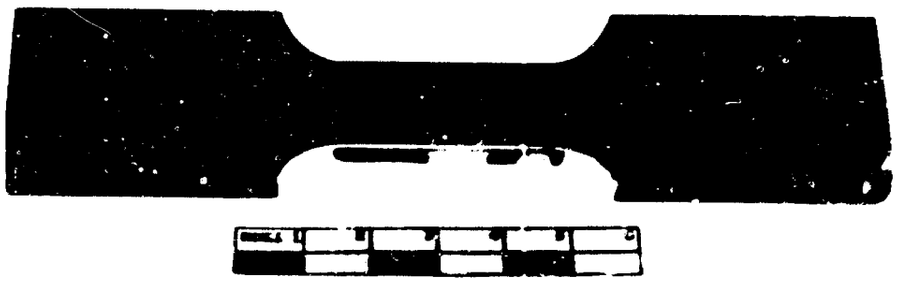

LARGE-SCALE FATIGUE TEST SPECIMEN (C)
CONTAINING 3 PLUG WELDS

18% NICKEL MARAGING STEEL, AIR ATMOSPHERE

FIGURE 19. LARGE-SCALE FATIGUE TEST SPECIMEN (C)

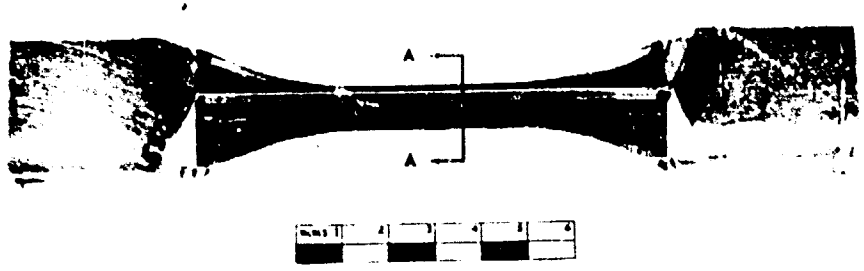

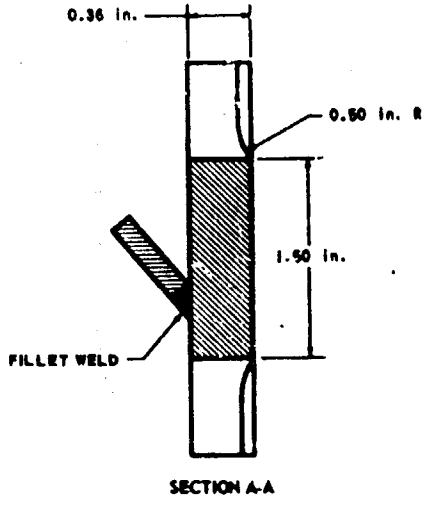

FIGURE 20. LARGE-SCALE SPECIMEN "F" WITH LONGITUDINAL FILLET WELD

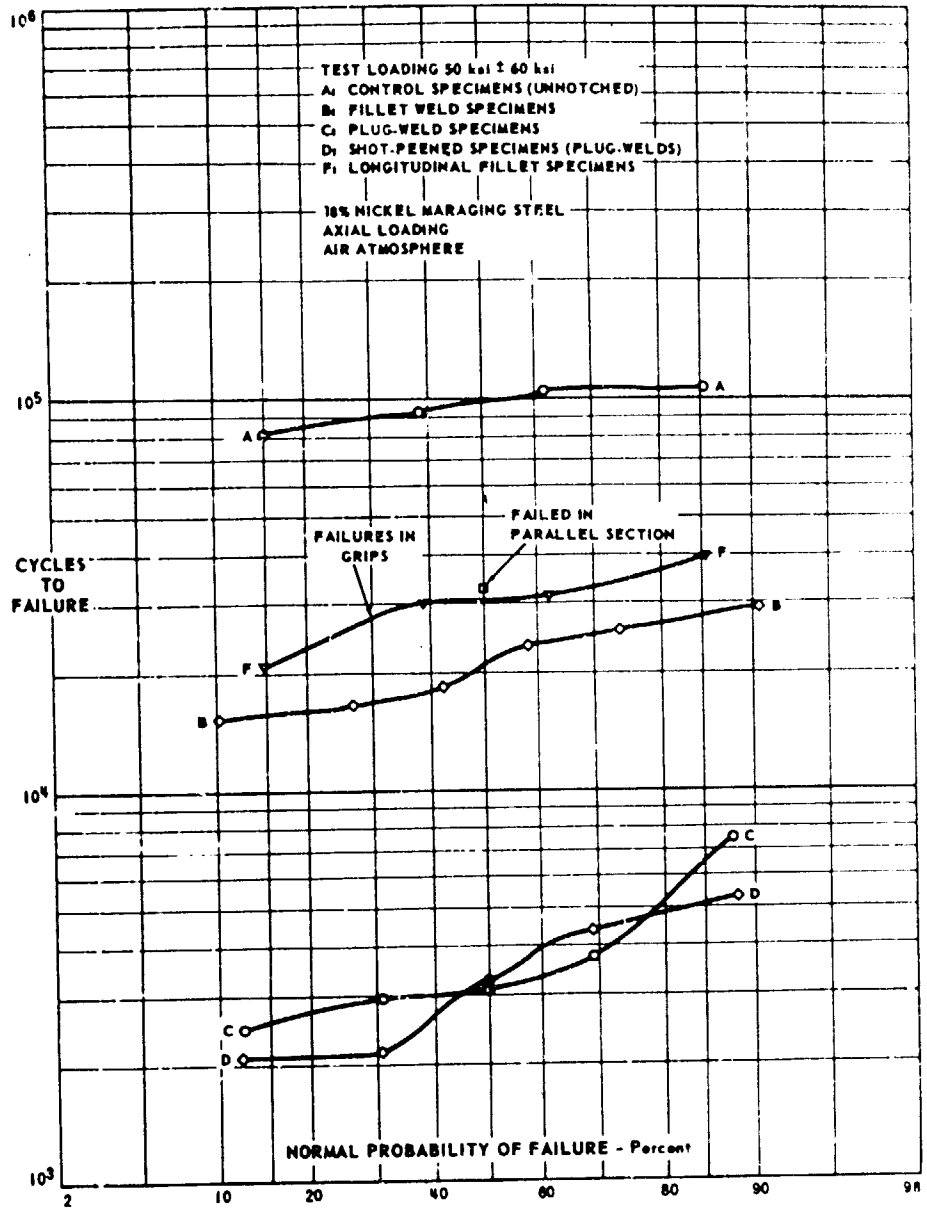

FIGURE 21. PROBABILITY BEHAVIOR OF LARGE-SCALE TEST SPECIMENS

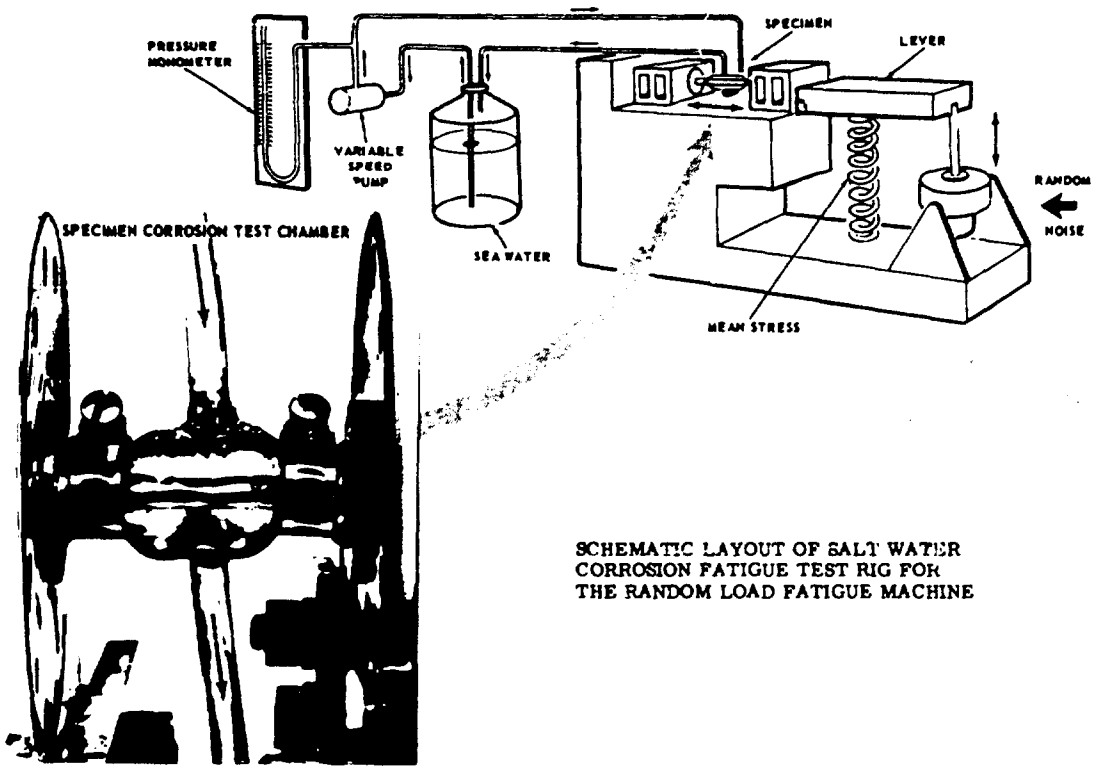

SCHEMATIC LAYOUT OF SALT WATER CORROSION FATIGUE TEST RIG FOR THE RANDOM LOAD FATIGUE MACHINE

FIGURE 22. SCHEMATIC LAYOUT OF SALT WATER CORROSION FATIGUE TEST RIG FOR THE RANDOM LOAD FATIGUE MACHINE

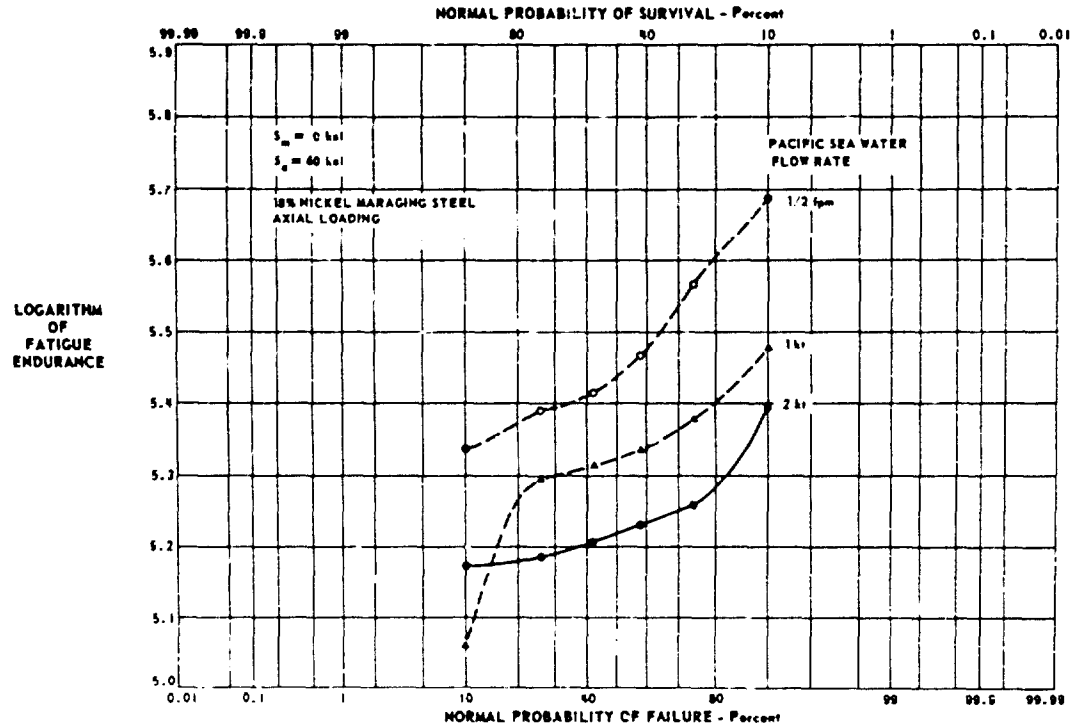

FIGURE 23. EFFECT OF FLOW RATE ON CORROSION FATIGUE CONSTANT AMPLITUDE TESTS

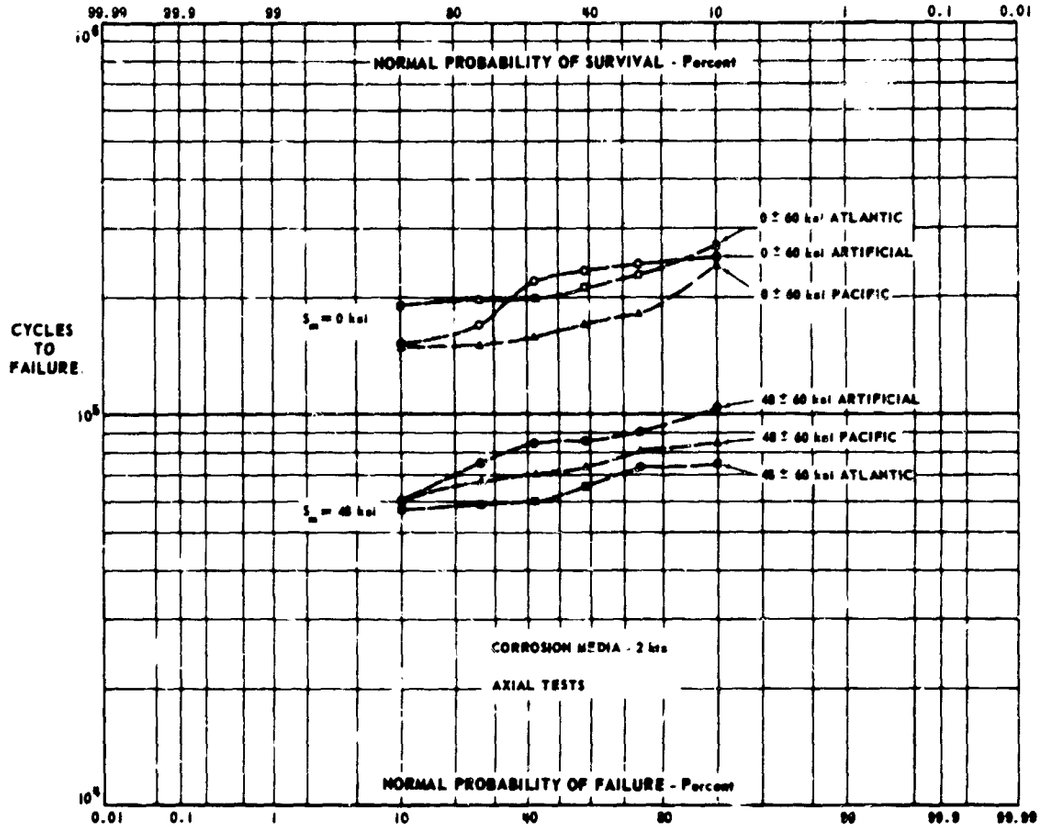

FIGURE 24. EFFECT OF VARIOUS SALT WATERS ON THE CONSTANT AMPLITUDE FATIGUE LIFE OF 18 PERCENT NICKEL MARAGING STEEL

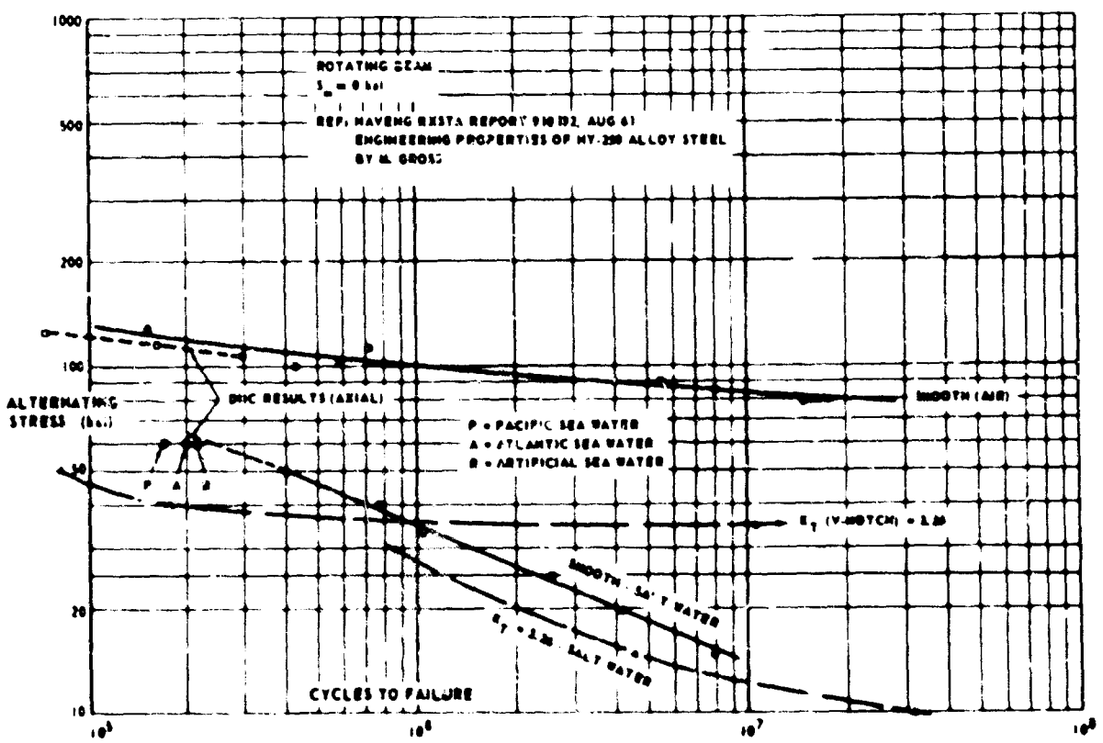

FIGURE 25. COMPARISON OF DH FATIGUE TEST RESULTS WITH THOSE OF M GROSS

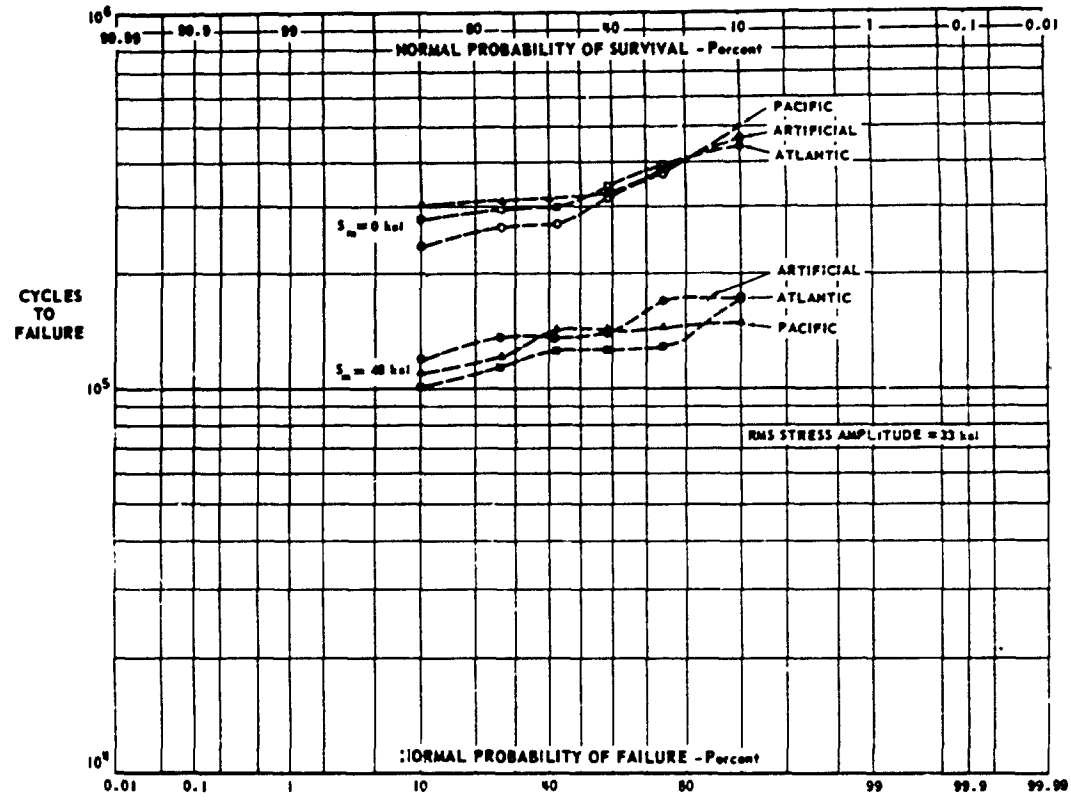

FIGURE 26. EFFECT OF VARIOUS SALT WATERS ON THE RAYLEIGH RANDOM AMPLITUDE FATIGUE LIFE OF 18 PERCENT NICKEL MARAGING STEEL

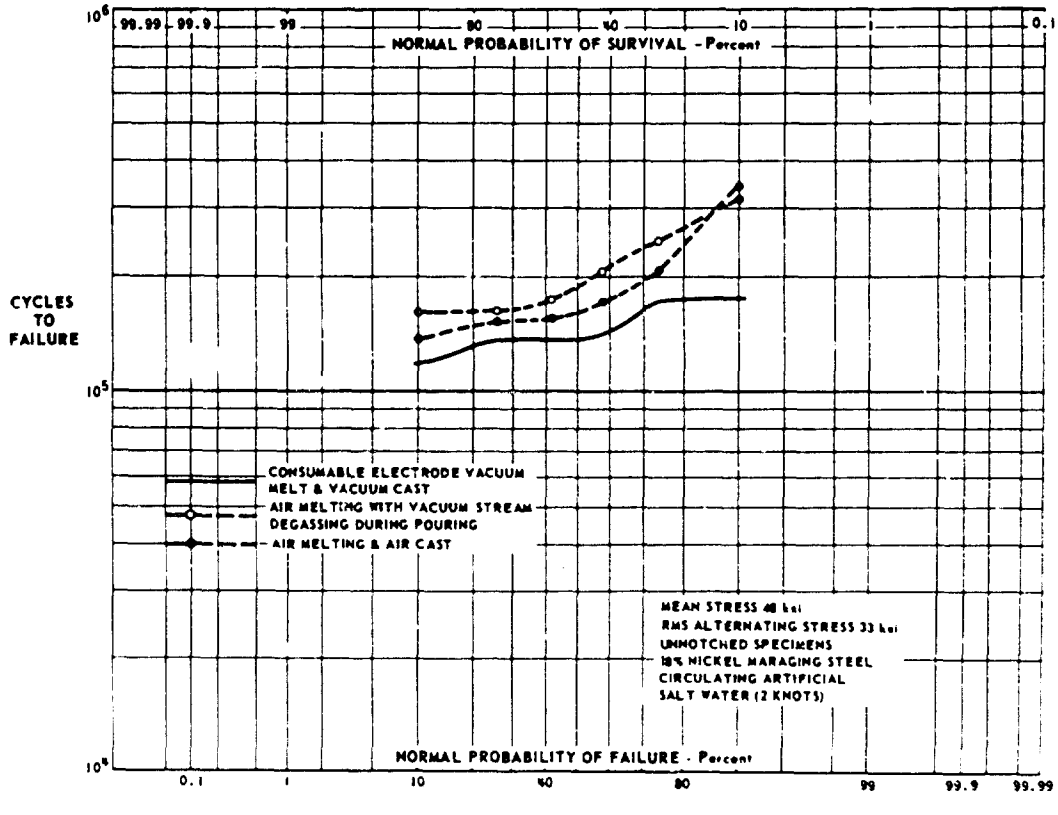

FIGURE 27. EFFECT OF MANUFACTURING PROCESS ON STATIONARY RAYLEIGH FATIGUE RESULTS IN ARTIFICIAL SALT WATER

APPENDIX

INTRODUCTION

In this appendix, several details pertinent to the fatigue test results obtained in our laboratory will be presented in abbreviated form, to complete the information necessary to appreciate the test results.

THE MATERIALS USED IN THE TESTS

Maraging Steel

This steel was developed by INCO from the early work of Bieber on iron-nickel martensites and was publicized as a commercially feasible alloy system in 1960. The basic composition consists of iron, nickel, cobalt, molybdenum and titanium in amounts which will allow the formation of a tough, iron-nickel martensite under slow cooling rates in air, the martensite then being aged at a moderately low temperature to increased hardness by the coprecipitation of what are thought to be Ni_3Mo and Ni_3Ti compounds. The role of cobalt is not understood at this time. The prime advantage of such a material is that high yield strengths of the order of 250 ksi can be obtained in large sizes without distortion and with an accompanying toughness greater than most other alloys at that strength level. In addition, the alloy can be fabricated in large sections by welding without preheat or postheat and with little resultant distortion using a filler wire of approximately matching composition.

The composition range of the alloy is as follows:

Ni	Co	Mo	Ti	C	Mn
18.0/19.0	7.0/8.5	4.6/5.1	0.3/0.5	0.01/0.03	0.1 max

Si	S	P	Al	Ca	Zr	B
0.1 max	0.01 max	0.01 max	0.1	0.05	0.02	0.003

Austenitisation, or solution treatment, for one hour at 1500 F is recommended for maraging steel. Subsequent cooling may be slow, with no risk of incomplete martensite transformation. Due to the carbon content, no protection against decarburization is required. The aging treatment is performed at 900 F for 3 to 6 hours. Negligible dimensional change has been encountered on heat treating this steel. Although an annealing temperature of 1500 F is generally specified, a great deal of controversy has raged over the correct finishing temperature for hot rolling and the optimum subsequent annealing temperature for maximum toughness. It is now generally agreed that the lowest finishing temperature should be used (1400 - 1500 F) and that the annealing temperature should be the minimum temperature at which full recrystallization occurs. The reader is referred to reports on the U.S.A.F. Maraging Steel Project Reviews for a full discussion of this problem.

Maraging steel, because of its low carbon content and relatively tight chemistry, must be produced from good-grade charging materials and has been melted in sizes up to 75-ton heats by air melting, consumable-electrode vacuum remelting and by induction vacuum melting. Ingot casting has been in air, with or without vacuum degassing and in vacuo. Ingot sizes have been up to 43 in. octagons and to some extent the problems of banding resulting from ingot segregation are influenced by ingot practice.

In this project the maraging steel used was in sheet and plate sizes up to 1 in. thick. All of the specimens of the type shown in Figure 6 originated in 3/4 in. thick plates taken from single melts of steel obtained for three different suppliers.

The maraging steel used in this study was supplied in the mill-annealed state, and after rough machining of the specimens, heat treated to approximately 250-ksi ultimate tensile strength. The heat treatment for this material consists of heating for three hours at 900 F in an air furnace, followed by air cooling. Each batch of twenty-five fatigue specimens included a control tensile test specimen. The specimens were then machined through the final stages, excluding the gripping portion. The results obtained from static tensile tests using these control specimens are shown in Table A-1. Little difference in static strength properties has been found between specimens taken longitudinal and transverse to the plate direction.

The percent compositions for the 3/4 in. steel plates used in this program are:

Element	Consumable Electrode Vacuum Remelt Vacuum Cast	Air Melt Vacuum Stream Degassed	Air Melt Air Cast
C	0.017	0.016	0.02
Mn	0.070	0.60	0.03
P	0.006	0.006	0.005
S	0.004	0.009	0.005
Si	0.16	0.070	0.09
Ni	18.04	18.12	17.73
Mo	4.70	4.77	4.80
Co	8.10	7.88	7.40
Ti	0.50	0.49	0.39
Al	0.12	0.10	0.07

A comparison of the stress-strain behavior of maraging steel with 4340 steel is given in Figure A-1.

The specimen configuration employed for the axial small-scale tests (Figure 6) was essentially that used for the 2024 aluminum alloy program described in Reference A-1. However, it was found in the early stages that the serrated gripping edges of the collets used in the jaws of the machine would not give a satisfactory grip for smooth

TABLE A-1. ROOM-TEMPERATURE STATIC TENSILE-STRENGTH PROPERTIES

250 si Yield Strength Maraging Steel

(a) As-Received Material:

Grain Direction	0.2% Yield Stress, ksi	Ultimate Tensile Strength, ksi	Elongation percent	Reduction of Area, percent	E, 10^6 psi
i) Consumable-Electrode Vacuum Melt, Vacuum Cast					
Longitudinal (L)	110.25	141.2	16.4	72	25.4
Transverse (T)	113.1	147.5	14.3	69	25.0

(b) Heat Treated Three Hours at 900°F:

Tensile Specimens	Fatigue Specimens Heat Treated With Tensile Specimen	0.2% Yield Strength, ksi	Ultimate Tensile Strength, ksi	Elongation, percent	Reduction of Area, percent	E, 10^6 psi
i) Consumable Electrode Vacuum Melt, Vacuum Cast						
AZ 30L	AZF 14L to AZF 38L	235.05	247.56	11.4	52.5	27.3
AZ 31L	AZF 39L to AZF 63L	240.37	250.16	10.9	52.0	27.9
AZ 32L	AZF 64L to AZF 88L	241.33	251.0	10.9	55.0	26.9
AZ 36L	AZF 89L to AZF 113L	240.94	252.14	12.0	56.2	28.2
AZ 37L	AZF 114L to AZF 138L	241.29	251.15	10.9	55.3	27.1
AZ 38L	AZF 139L to AZF 163L	236.36	248.37	10.8	53.0	28.7
AZ 39L	AZF 164L to AZF 188L	245.03	254.37	10.8	55.0	28.0
AZ 40L	AZF 189L to AZF 213L	236.19	246.17	10.3	52.0	26.6
AZ 94L	AZF 214L to AZF 242L	240.04	249.34	9.7	49.0	25.8
A-F	(Large-scale specimen) (Figure 17)	236.7	247.3	13.5	42.0	31.1
AZF 178L	Used as tensile	238.3	249.5	13.0	59.0	27.1
AZF 177L	Used as tensile	243.9	254.0	12.0	54.0	26.1
AZF 254L-W	(Transverse weld)	231.7	243.9	3.0*	8.0	26.5
AZF 255L-W	(Transverse weld)	233.3	247.5	7.0	29.0	29.5
ii) Air Melt, Vacuum-Stream Degassing During Pouring						
AY 110L	AYF 1L to AYF 20L	259.53	269.22	8.57	38.0	27.1
AYF 21L-W	(Transverse weld)	246.4	254.6	0**	5.5	25.8
AYF 22L-W	(Transverse weld)	253.1	256.1	2.0	8.0	32.2
iii) Air Melt, Air Cast						
AX 109L	AXF 1L to AXF 20L	256.35	262.7	8.0	37.0	27.1
AXF 11L	Used as tensile	255.6	259.7	12.0	39	26.2
AXF 12L	Used as tensile	254.6	261.8	9.0	41.5	27.0
AXF 25L-W	Transverse weld	227.6	238.8	6.0	34.0	25.7
AXF 26L-W	Transverse weld	228.1	238.3	7.0	35.0	27.4

* Large gas hole in fracture.
** Dirt in weld.

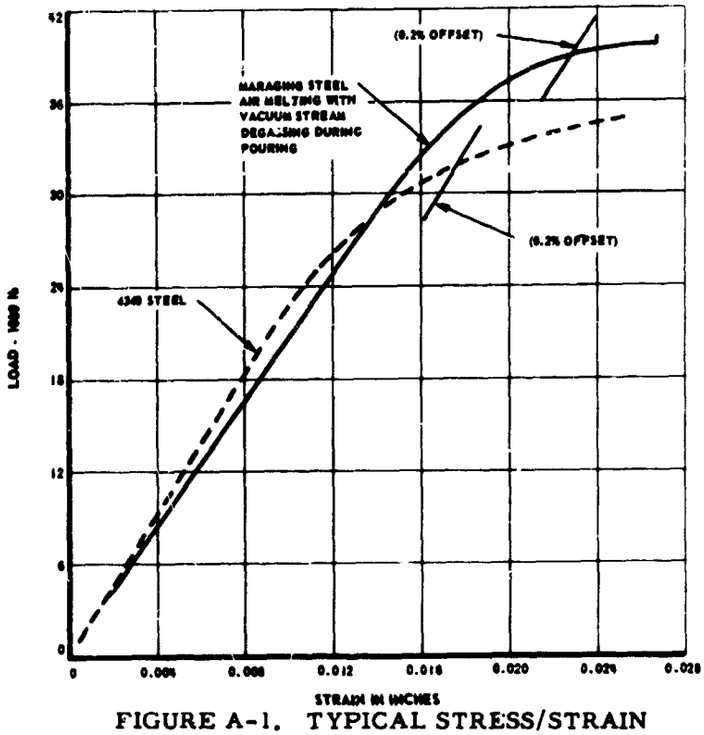

FIGURE A-1. TYPICAL STRESS/STRAIN CURVES OF MARAGING STEEL VERSUS 4340 STEEL

high-hardness steel specimens. Because of this it was necessary to incorporate machined serrations in the gripping portions of the specimen to match the serrations in the collets. This provided a very positive gripping action over the complete load range using the axial load fatigue machine.

Samples of the steels produced by each of the three primary manufacturing processes were examined metallographically and by magnetic particle inspection for cleanliness. The results were, using the Jernkontoret inclusion rating system:

Process	Numerical Designation	Inclusion Type
a) Consutrode Vacuum Melt, Vacuum Case	2 - thin	D (oxide)
b) Air Melt, Vacuum Stream degassed	2 - thin 2 - thin	D (oxide) B (alumina)
c) Air Melt Air Cast	3 - thin	D (oxide)

Thus all steels were very clean with the air melt, air cast yielding slightly dirtier microstructure. There is a definite improvement with the use of vacuum techniques, as one might expect.

The results of Charpy V-Notch Impact tests carried out at room temperature are listed below:

Process	Condition	Average Values	Grain Direction
1. Air Melt, Vacuum Stream Degassed	As Received	80 foot lbs. 50 foot lbs.	L T
2. Air Melt, Vacuum Stream Degassed	Heat Treated	14 foot lbs. 17 foot lbs.	L T
3. Consumable electrode Vacuum remelt, vacuum cast	As Received	120 foot lbs. 75 foot lbs.	L T
4. Consumable electrode Vacuum remelt, vacuum cast	Heat Treated	22.5 foot lbs. 17.5 foot lbs.	L T

There is a significant improvement in the "as-received" condition using cleaner metal. This improvement is much less with heat treatment.

The fatigue testing of the "as-received" material at the highest level of constant stress amplitude (50 ± 100 ksi) was quite interesting. While the test frequency was only 30 cps the specimen soon became extremely hot leaving a bluish oxide coating on the parallel section on both sides of the fracture. This heating can only be ascribed to damping within the material which must be very great when one begins with annealed material. This test lasted 9, 600 cycles.

Inconel 718

Inconel 718 was originally developed for gas turbine applications as an alloy with a high strength (up to 190 ksi U. T. S.) which could be obtained after a sluggish aging treatment in order to avoid transformation problems which might be encountered in fabrication. The alloy is of a nickel base and contains the titanium and aluminum additions common in these alloys. An appreciable amount of columbium is added for the slow aging reaction by precipitation of what is thought to be Ni_3Cb. The composition range is as follows:

Ni	Cr	Cb	Mo	Al	Ti
50.0/55.0	17.0/21.0	4.5/5.75	2.8/3.3	0.2/1.0	0.3/1.3

C	Si	Mn	S	Cu	Fe
0.1 max.	0.75 max.	0.50 max.	0.03 max.	0.75 max.	bal.

Although the alloy is not available in large plate, is expensive and difficult to machine, sufficient is known of the alloy's resistance to seawater corrosion to recognise that it is possibly the only high strength alloy which can be used in seawater without a protective coating. It would therefore have great value in some parts of high strength marine structures such as the leading edges of foils or as a supercavitating propeller material.

Above a temperature of 1550 F, the alloying elements responsible for the hardening mechanism are in solid solution. Annealed material may be aged for 16 hrs. at 1325 F to achieve strength by what is thought to be the precipitation of Ni_3Cb. The precipitation is very slow compared to other alloys of this type but has the advantage that many of the problems of annealing, welding and pickling associated with precipitation-hardenable nickel base superalloys are alleviated.

Annealing is performed at 1700 - 1800 F for 1 hr. Aging to optimum properties is carried out at 1325 F for 16 hrs for hot-rolled or annealed material and 1275 F for 16 hrs for cold-rolled material. No protective atmosphere is required.

A contraction of 0.05% is experienced upon aging. A recent modification of the aging treatment has been recommended this being 1325 F/8 hr furnace cool to 1150 F long enough to make the total aging time (1325 F + furnace cool to 1150 F) equal to 18 hrs, followed by air cooling.

Material used in this study originated from a 2-1/2 in. x 1/2 in. x 4 ft bar supplied by the Huntington Alloys Division of INCO.

The mechanical properties of the control tensile specimen for the fatigue tests were:

(a)	Ultimate Tensile Strength	200,800 psi
(b)	0.2% Proof Stress	165,700 psi
(c)	Percent Elongation	25.5
(d)	Percent Reduction of Area	44.5
(e)	Modulus of Elasticity	29.6×10^6

THE RANDOM LOAD FATIGUE MACHINE

This machine used for the axial load small-scale tests is capable of applying any type of fatigue loading consistent with the frequency response of the structure, since the drive is essentially electronic. This machine was also the first machine able to apply random loads with a non-zero mean stress. A complete discussion of the load envelope for this machine is contained in Appendix 'A' of Reference A-1. For the tests carried out on maraging steel, the machine was strain calibrated for stress levels under dynamic conditions using:

(i) A standard maraging steel specimen fitted with four strain

(ii) The standard eight-gauge load transfer plate connecting the lever the (movable) gripping head.

(iii) A two-channel oscillograph, with two bridges and amplifiers.

The procedure for this calibration is described in Reference A-1. *

The dynamic load capability of the fatigue machine had to be increased substantially (3,800 lb peak to 10,000 lb) in order to use a reasonably large specimen of maraging steel. For the standard specimen shown in Figure 6, the average ultimate tensile stress shown in Table 1, corresponds to a breaking load of about 12,000 lb. However, since fatigue lives less than 10,000 cycles were not desired, the maximum alternating load required in the fatigue tests was approximately 7,000 lb. This loading in the compressive sense does not present a stability problem for the specimen configuration used in these tests. In order to obtain 7,000 lb load capability, therefore, the basic machine was also modified from its former configuration by:

(i) Adding weight to the main lever.

(ii) Lowering the stiffness of the main stress spring.

(iii) Improving the gripping of the specimen.

It was also necessary, after these modifications were carried out, to re-align the gripping heads of the machine to minimize the occurrence of bending loads in the specimen. By connecting the strain bridge on the specimen to record the strain differences and hence bending in the specimen, it was possible to substantially remove bending in both the vertical and horizontal planes, by re-adjustment of the gripping head alignment.

For the random load fatigue tests, certain additional calibrations were required:

(i) In order to ensure that the input random process was sufficiently "white" a frequency analysis had to be carried out. (See Figure A-2.) The RMS voltage from the random noise generator was found to be of uniform value, on the average, over the frequency spectrum of interest.

CORROSION MEDIA

(a) Artificial Salt Water – On the recommendation of Mr. R.C.A. Thurston, D.M. & T.S. a small quantity of "Sea-Rite" Salt was obtained from Lake Products Company, Inc., 1254 Grover Road, St. Louis 25, Missouri, U.S.A. "Sea-Rite" salt is a simulated sea salt mix containing elements found in natural sea salt in quantities greater than % 0.004. "Sea-Rite" salt is granular and colorless; the particles are no larger than those that will pass a 24 mesh screen. Composition of "Sea-Rite" salt is based on 77 composite analyses of seawater with average total solids content of 35,600 parts per million. This salt is made according to Formula A, ASTM Specification D1141-52.

Na	Mg	Ca	K	Sr	B	Cl
30.577	3.725	1.178	1.099	0.0382	0.0135	55.035

SO_4	Bromide	HCO_3	Fluoride
7.692	0.1868	0.405	0.0039

The density of Sea-Water equals 1.025 at 15 C. Approximately 4-1/2 ounces of "Sea-Rite" salt per gallon of water equals this density of Sea-Water. Since most Public water supplies contain less than 500 parts per million total dissolved solids they may be used in place of distilled water. Tap water was used.

(b) Pacific Sea Water – In order to study the effect of using natural seawater, it was arranged with the Pacific Naval Laboratory that a carboy of P.N.L. seawater be sent to the Materials Laboratory. This water was collected on Jan. 6, 1964, from a depth of 10 feet from the surface.

*References are given on page 171.

TYPE 1390-B GR RANDOM NOISE GENERATOR
USING A TYPE 2107
BRUEL AND KJOER FREQUENCY ANALYSER

RANDOM NOISE RMS VOLTS .9V
PEN DAMPED TO 2MM/SEC 20 CPS TO 100 CPS
PAPER SPEED 0.2MM/SEC

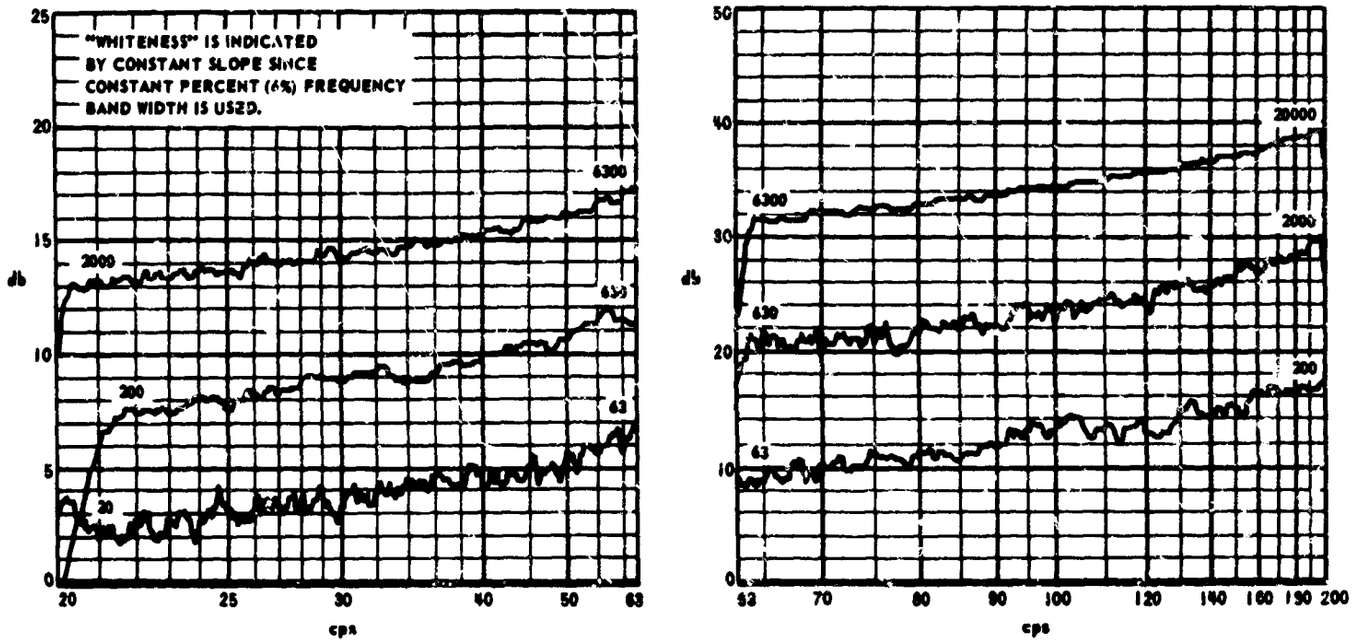

FIGURE A-2. FREQUENCY SPECTRUM ANALYSIS FOR INPUT TO THE RANDOM LOAD FATIGUE MACHINE

(c) Atlantic Sea Water – A similar arrangement was carried out with the Naval Research Establishment, Halifax, and a carboy of dockside water was despatched by N. R. E. on Jan. 10, 1964.

The results of analyses of the seawaters, as carried out in the D. H. Materials Laboratory, Malton, are given in the following table:

Type of Salt Water	"Sea-Rite"	Atlantic	Pacific
Salinity Parts per thousand or g/Kg	33.98 Feb. 12	27.09 Feb. 4	30.02 Feb. 4
Density (gm/cc)	1.023 Feb. 12	1.017 Feb. 4	1.019 Feb. 4
*O_2 Content (mg/l)	6.55 Feb. 18	6.25 Feb. 18	6.96 Feb. 18
Elect. Cond. (mhos/cm)	0.0482 Feb. 12	0.0395 Feb. 10	0.0429 Feb. 10
pH Level	8.15 Feb. 12	7.86 Feb. 12	7.86 Feb. 12

*The sample of Pacific water was taken whilst water circulating, while "Sea-Rite" and Atlantic samples were taken from the carboy.

Change of dissolved oxygen lever after bubbling air through the solution was as follows:

	"Sea-Rite"	Atlantic	Pacific
Air bubbled 1/2 hr	6.96 February 20		
Air bubbled 1/2 hr		7.31 February 21	
Air bubbled 2 hr	6.96 February 21		

All analyses performed at 23 C ± 1 C.
Lowest velocity used – 0.00493 knots.

All analyses performed at 23 C ± 1 C

Lowest velocity used – 0.00493 knots.

These natural seawaters were not filtered to remove traces of marine life.

WELDING PROCESSES

(a) Spray arc welding the 3/4 in. plate material (Figure 6)

For these welds, the Metal Inert Gas (MIG) process of spray-arc weld is used, where the electrode is consumed in a continuous feed of liquified metal to the joint. The work is enveloped in a 99% argon-1% oxygen gaseous mixture. Titanium content for these welds was found to be about 0.4% (both parent metal and wire).

(b) Short-arc welding of 0.080 in. sheet (Figure 15)

Here the wire is consumed in a helium (shield) atmosphere. The arc is short-circuited at a high frequency (eg 60 cps), and the weld bead is built up of the metal joined during these short bursts of arc. This is also a MIG process.

(c) MIG spot welds for heavy gauge material

In the fatigue tests of spot-welds (Figure 19), it was soon apparent that the lack of control available in the MIG spot weld technique rendered

it impossible to avoid tight interdendritic shrinkage cracks. These cracks formed sites for corrosion, and resulted in very short fatigue levels (Figure 21).

ANALYSIS OF TEST RESULTS

(a) Probability Plots

The plotting relation used for the numerous normal probability plots presented in this paper is

$$Pi = \frac{i-3/8}{n+1/4}$$ Equation 1, Reference A-1

where i is the order of the ranked observation (ranked by increasing endurance) and n is the total number of individual tests making up the sample.

(b) The Rayleigh-Miner Endurance Predictions

(i) 50 ksi Tensile Mean Stress

Using the analysis of Section 3.3.1, Reference A-1, the predicted endurance relation from the constant amplitude relation

$$N_f = \left(\frac{500}{Sa}\right)^{7.4} \qquad r = .976$$

for a linear accumulation of fatigue damage with the Rayleigh peak stress distribution, is given by:

$$N_{f_r} = \left[\Gamma\left(1+\frac{7.4}{2}\right)\right]^{-1}\left(\frac{500}{\sigma_p}\right)^{7.4} = .065\left(\frac{500}{\sigma_p}\right)^{7.4}$$

For the RMS peak stress levels used in the random load tests the predicted endurances are:

σ_p	N_{f_r}
49.5 ksi	1,760,500 cycles
56.6 ksi	651,800 cycles
63.6 ksi	274,700 cycles

All these results grossly over-estimate the Rayleigh test results.

(ii) Similarly for zero mean stress, the equation for the linear accumulation of damage using the constant amplitude relation

$$N_f = \left(\frac{362}{Sa}\right)^{10.37}$$

is given by

$$N_{f_r} = \left[\Gamma\left(1+\frac{10.37}{2}\right)\right]^{-1}\left(\frac{362}{\sigma_p}\right)^{10.37}$$

$$= .006\left(\frac{362}{\sigma_p}\right)^{10.37}$$

The endurances at the RMS peak stress levels tested are:

σ_p ksi	$N_{f_r} = 0.006\,(N_f)_{CA}$
56.6	1,353,800 cycles
63.6	404,400 cycles
73.5	90,345 cycles

The result at the highest stress level shows an excellent prediction, while the linear damage law becomes more and more unsafe for stress levels below this level.

(c) Predictions Using Freudenthal's Analysis

(i) 50 ksi Mean Stress

From the regression equation for the constant amplitude test results, the value of stress amplitude S_1 at 10,000 cycles endurance is 144 ksi. Using this value as the operative peak stress for cumulative damage (as suggested by Freudenthal in Reference 11), we have:

$$\frac{T_F}{(N_{f_r})_{miner}} = \left(\frac{RMS}{S_1}\right)^{\sigma_p}\frac{\Gamma\left(1+\frac{\delta}{2}\right)}{\Gamma\left(1+\frac{p}{2}\right)}$$

(of equation 19, Ref A-1)

where

$$p = 4.0$$

$$S_1 = 144 \text{ ksi}$$

$$\delta = 7.4$$

Thus $$T_F = 0.354 \quad 10^{-6} \times \sigma^{3.4} \times (N_{f_r})_{MINER}$$

ksi	(N_{f_r}) Miner	T_F	T experimental
35	1,760,525 cycles	110,860 cycles	750,000 cycles
40	651,795 cycles	64,606 cycles	176,000 cycles
45	274,683 cycles	40,582 cycles	64,000 cycles

These values are plotted in Figure 11. It can be seen that this analysis involves a rotation of the previously obtained Rayleigh-Miner straight line (on log - log format) about an RMS peak stress of about 111.0 ksi to form a new straight line with slope equal to 4.0. The use of this analysis is slightly conservative for the higher stress levels, and too severe for the lower stress levels, at least in the range of the test results.

(ii) Zero Mean Stress

Similarly, the value of constant stress amplitude which yields a regressed mean endurance of 10,000 cycles is 149 ksi. Thus:

$$\frac{T_F}{(N_{f_r})_{miner}} = \left(\frac{RMS}{149}\right)^{6.37} \frac{\Gamma(1+5.18)}{\Gamma(1+2)}$$

$$= 1.2 \times 10^{-12} \times \sigma^{6.37}$$

The results appear only in the table below, since it is obvious that the predictions are very poor, resulting in less than one-tenth the experimental mean values. Use of this damage calculation would be inadmissible in the present form.

σ_2	σ	N_{f_r}	T exp.	T Freudenthal
56.6 ksi	40 ksi	1,353,800 cycles	365,000 cycles	25,722 cycles
63.6 ksi	45 ksi	404,400 cycles	210,000 cycles	16,297 cycles
73.5 ksi	52 ksi	90,345 cycles	91,000 cycles	9,134 cycles

(d) Effect of Mean Stress

(i) Considering the results of the constant amplitude axial load tests, we have the following information:

$(S_a)_{50}$	$*(N_f)_{50}$	Approximate (S_{ao}) for same N_f	$(S_a)\,50/S_{ao}$
ksi	kcs	ksi	
85	300	106.5	0.80
90	290	107	0.84
95	170	113.5	0.84
100	105	119.5	0.84
105	67	125	0.84
110	49	130	0.85

*Obtained from drawing a smooth curve through the mean endurances established in Figure 8.

Thus the average value of the ratio of stress amplitudes is 0.84. Referring to Refence A-2, the value of m in the equation

$$\left(S_a\right)_{50} = S_{a_o}\left[1 - \left(\frac{SM}{UTS}\right)^M\right]$$

is 1.14, which places the result close to the modified Goodman mean stress relation. For the Modified Goodman relation, m = 1. For the Gerber relation m = 2. If the average yield strength (240 ksi) is substituted for the average ultimate tensile strength (250 ksi), the exponent m has the value 1.17. From this it can be seen that the experimental results can also be represented by the Soderberg mean stress relation (m = 1.10 with yield stress in place of UTS in the above formula). This is a natural consequence when the ratio of yield strength to ultimate strength approaches unity (0.96 in this case).

(ii) Turning to the results of the random amplitude tests, the selection of RMS stress levels was deliberately made to facilitate comparison of fatigue strengths within the same range of endurances. Using a graphical interpolation (on a semi-log plot) we have:

$(\sigma)_{50}$ ksi	$(N_f)_{50}$ kcs	$(\sigma)_o$ for the same N_{f_r}	σ_{50}/σ_o
45	64.0	55.0	0.82
40	124.0	49.5	0.81
37.5	210.0	45.0	0.83
36	365.0	40.0	0.90

Assuming the last value to represent a change in slope as the endurance limit is approached, and not representative of the effect of mean stress in the intermediate stress levels, we have an average value for the ratio of 0.82 using the RMS stress amplitudes. Thus m, the generalized mean stress exponent equals 1.065.

From a comparison of the above variation in stress amplitude (for given endurance) with mean stress, it can be seen that the same empirical relations as were developed for the constant amplitude results can be applied to the random load results, within the rather limited range of stress amplitudes considered. This finding is not unexpected if the stress regime is one of constant stress ratio $(S_a)\,50/S_{ao}$ for given endurances, since the random loading constitutes a mixing of all the stress levels (and lower ones as well) investigated in the constant amplitude testing.

(e) Notch Sensitivity 'g'

A series of tests using groove-notch rotating beam specimens, and described in Reference 8, is compared with the mean lives for the tests carried out by Cicci in Reference 7. The notch sensitivity as shown in Figure A-3, varies from about 0.5 to 0.6, depending on the component distribution. Possibly the "notch factor" determined by rating the stress levels for the same proportion of components (described in Reference 8) for both notched and unnotched data, is equivalent to the fatigue factor K_f. This latter quantity is the ratio of alternating strengths for a given fatigue life, using unnotched and notched fatigue data for the same material.

REFERENCES

(A-1) Swanson, S. R., "An Investigation of the Fatigue of Aluminum Alloy Due to Random Loading", UTIA Report 84 (February, 1963)

(A-2) "The Effect of Mean Stress on Fatigue Strength (Plain Test Piece)", R. Ae. S. Data Sheet, Fatigue A. 00. 01 (June, 1958).

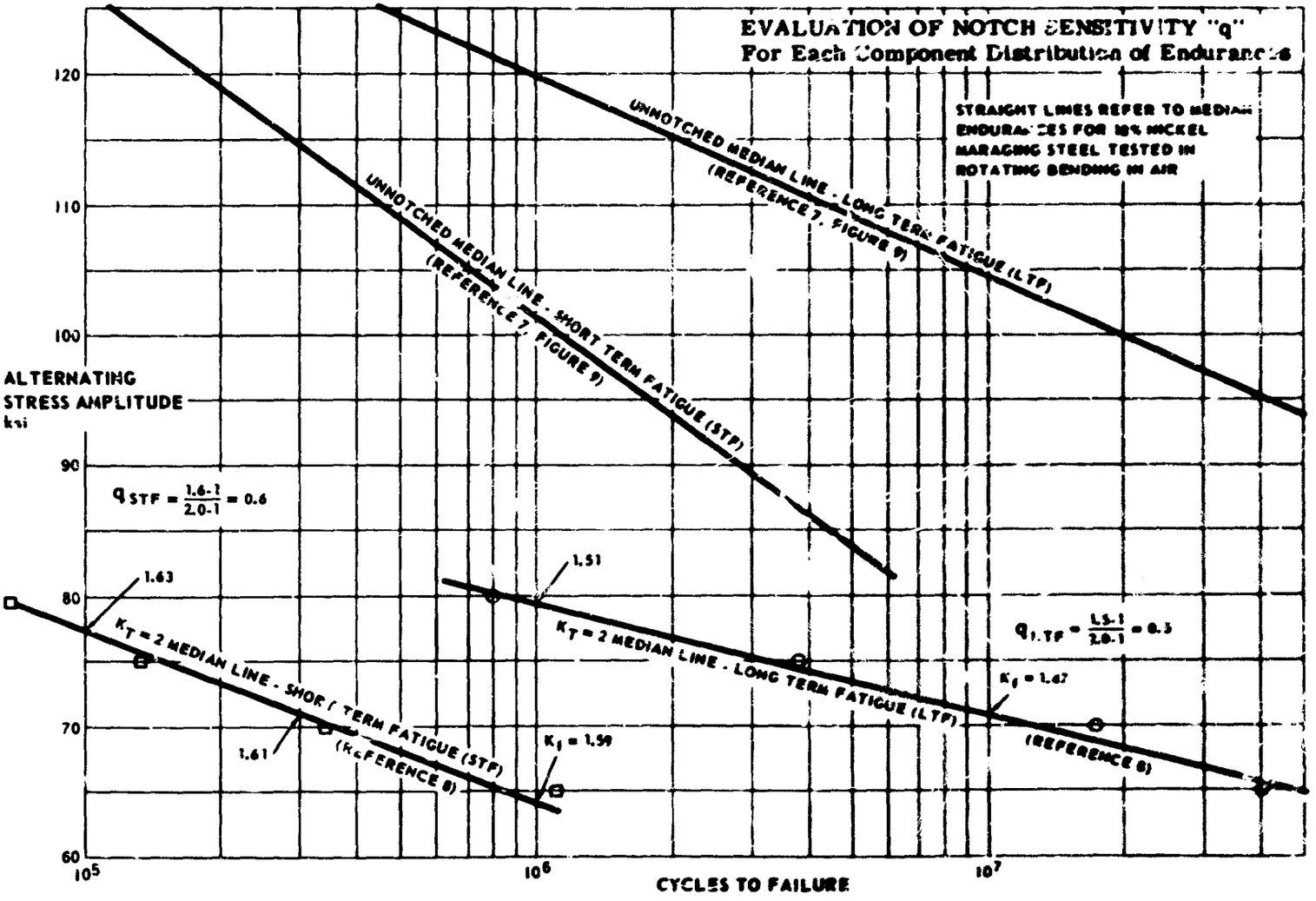

FIGURE A-3. EVALUATION OF NOTCH SENSITIVITY "q" FOR EACH COMPONENT DISTRIBUTION OF ENDURANCES

THE PHYSICAL METALLURGY AND PROPERTIES OF MARAGING STEELS

by

G. E. Pellissier*

The maraging steels are a relatively new class of ultrahigh-strength steels that derive their high strengths from hardening mechanisms other than the classical ones associated with carbon martensite, bainite, or carbide precipitation during tempering. These steels have engendered a great deal of interest as constructional alloys, particularly in extreme-duty applications requiring high strength-to-weight ratios because of their markedly superior resistance to low-stress fracture, even in relatively thick sections, as compared to conventional 0.3 to 0.5 per cent carbon, quenched-and-tempered lower alloy steels, as typified by AISI 4340 steel. The plane-strain fracture toughness (K_{Ic}) of the 18 per cent nickel maraging steels, at yield strength levels of 240 to 280 ksi, is more than twice that of the best AISI 4340 type steels, and hardenability, in the conventional sense, is not a limiting factor in the heat treatment of thick sections. Furthermore, the maraging steels possess the important practical feature of being relatively weak, ductile, and tough after the initial high-temperature (1500 to 1650 F) portion of the heat-treatment cycle, so that they can be more readily and safely fabricated into large structures prior to the final low-temperature aging at 800 to 900 F that develops the ultimate high strengths with considerably lower toughness.

The group of maraging steels originally developed by the International Nickel Company comprised a 25Ni-Ti-Al-Cb alloy, a 20Ni-Ti-Al-Cb alloy, an 18Ni-8Co-5Mo-0.4Ti alloy, and an 18Ni-9Co-5Mo-0.8Ti alloy, all capable of developing yield strengths in the range 250 to 280 ksi. As a result of subsequent engineering property and fabrication evaluations, the latter two 18Ni steels, now more commonly known as the (250) grade and the (280) grade, respectively, have assumed greater engineering importance and commercial prominence than the two steels containing more nickel. In addition, INCO has devised more recently two lower strength maraging steels, having yield strengths in the range 180 to 210 ksi, that are of interest for structural applications demanding considerably greater crack toughness, but at lower strength levels. One is an 18Ni-8Co-4Mo-0.2Ti steel, of the same type as the (250) grade and the (280) grade, and the other is a 14Ni-5Cr-3Mo-0.2Ti-0.3Al steel.

In the few years since these steels were first announced, a large body of detailed and more or less empirical information about the engineering properties of these steels has evolved which would be difficult to properly assess and adequately summarize in this brief review. It seems more appropriate, therefore, to present what is known of the basic features of their physical metallurgy in the context of their more important and unusual mechanical characteristics. The scope of this discussion, furthermore, is limited to the 18 per cent nickel maraging steels, in view of their current engineering importance, and because the present state of knowledge of their metallurgical and mechanical characteristics is considerably more advanced than for the other types of maraging steel. Qualitatively, the physical metallurgy and mechanical behavior of the three 18Ni maraging steels are very similar, as might be expected from their similar chemical compositions. They differ mainly in respect to their Ti, Mo, and/or Co contents, which are believed to exert only a quantitative influence on the strengthening reactions and on the resulting combinations of strength, ductility, and toughness attainable in these alloys. Thus, it is feasible and more convenient in the following discussion of the 18Ni maraging steels to draw primarily upon specific illustrations pertaining to the (250)-grade alloy, for which most information is available, with secondary reference to the (280)-grade alloy, and only occasional mention of the (200)-grade alloy.

MECHANICAL PROPERTIES

The recommended composition ranges for the (250) grade and the (280) grade of 18Ni maraging steel, together with actual compositions of two steels used as illustrations in describing the mechanical properties of these steels, are listed in Table 1. Steel A was from a 20-ton, air-melted, electric-furnace heat, and Steel B was from a 10-ton, consumable-electrode, vacuum-arc-furnace heat. The tensile properties of the two steels, after annealing for 1 hour at 1500 F, and aging for 3 hours at 900 F, are shown in Table 2. The values of the stress intensity parameter, K_{Ic}, as determined from fatigue-cracked, notched-round tension test specimens, provide a quantitative measure of the plane-strain fracture toughness of Steels A and B, in the form of relatively thick plates (0.8 inch and 0.9 inch, respectively). Complete true stress-true strain-tension test curves for the two steels in the aged condition appear in Figure 1. These steels, in both the annealed and aged conditions, exhibit a relatively low rate of work hardening at large strains (above about 0.5 per cent), as compared to the AISI 4340 type steels, and plastic instability or necking occurs at a relatively low level of strain (about 1.5 per cent), compared to the total nominal strain at fracture (about 10 per cent). Thus, cold rolling may be performed rather easily at these high strength levels, but deep drawing may be more difficult. Charpy V-notch impact curves for Steels A and B appear in Figure 2. Although these curves do not exhibit a clear-cut transition temperature, the energy absorbed does decrease rather markedly with decrease in temperature.

* United States Steel Corporation
Applied Research Laboratory
Monroeville, Pennsylvania

TABLE 1. CHEMICAL COMPOSITIONS OF TWO GRADES OF MARAGING STEEL*

Element	18Ni(250) Recommended Range	Steel A	18Ni(280) Recommended Range	Steel B
Ni	17-19	17.46	18-19	18.83
Co	7-8.5	7.66	8.5-9.5	9.01
Mo	4.6-5.2	4.82	4.6-5.2	4.81
Ti	0.3-0.5	0.43	0.5-0.8	0.80
Al	0.05-0.15	0.054	0.05-0.15	0.046
C	0.03 max	0.017	0.03 max	0.010
Mn	0.10 max	0.046	0.10 max	0.022
Si	0.10 max	0.077	0.10 max	0.061
S	0.010 max	0.005	0.010 max	0.009
P	0.010 max	0.002	0.010 max	0.005
B	0.003 added	0.0040	0.003 added	0.0033
Zr	0.02 added	--	0.02 added	--
Ca	0.05 added	--	0.05 added	--
N	--	0.003	--	0.002
H	--	0.000011	--	0.000009
O	--	<0.001	--	<0.001

* In weight per cent.

TABLE 2. TENSILE PROPERTIES OF TWO GRADES OF MARAGING STEEL[a]

Grade	Specimen Orientation	Yield Strength,[b] ksi	Tensile Strength, ksi	Elongation in 2 Inches, %	Reduction of Area, %	K_{Ic} ksi√in.
Steel A (250)[c]	L	254	263	10.3	42.7	75
Steel A (250)[c]	T	256	261	7.8	45.0	73
Steel B (280)[d]	L	285	294	5.5	27.0	67
Steel B (280)[d]	T	287	298	5.0	25.0	67

(a) 0.505-inch-diameter specimens.
(b) 0.2 per cent offset.
(c) 0.80-inch-thick plate.
(d) 0.875-inch-thick plate.

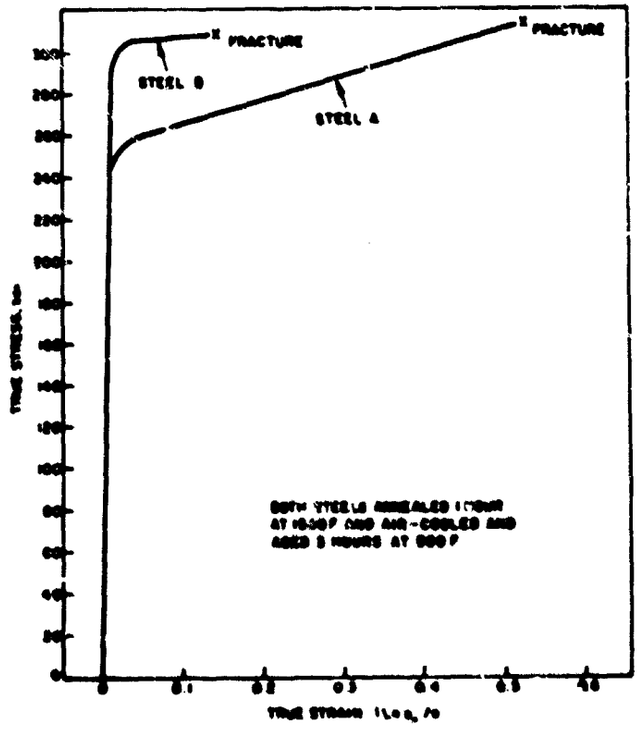

FIGURE 1. TRUE-STRESS TRUE-STRAIN CURVES FOR MARAGING (250) STEEL A AND MARAGING (280) STEEL B

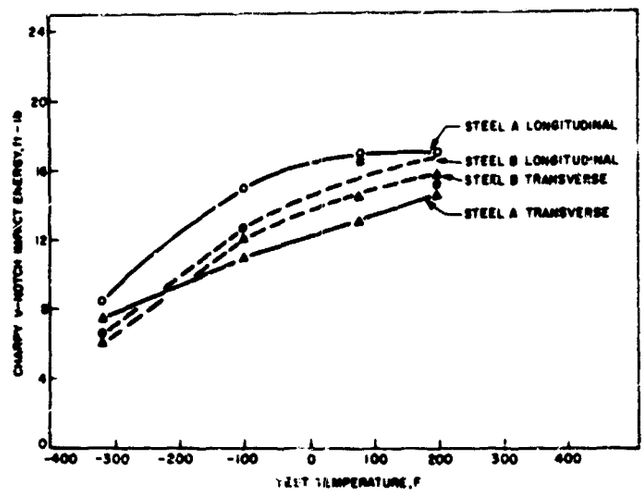

FIGURE 2. CHARPY V-NOTCH IMPACT TEST CURVES FOR MARAGING (250) STEEL A AND MARAGING (280) STEEL B

TRANSFORMATION CHARACTERISTICS, UNAGED PROPERTIES AND MICROSTRUCTURE

A transformation diagram for binary iron-nickel alloys, according to Pumphrey and Jones, is reproduced in Figure 3. The notable features of this diagram are: first, the marked depression in the alpha<-->gamma transformation temperatures with increase in nickel content; and second, the increasing hysteresis between the cooling and heating transformation temperature, as the nickel content is increased. The vertical intersecting lines drawn at a nickel content of 18 per cent indicate only roughly the martensite transformation temperature (500 F) and the austenite reversion temperature (1100 F) for the 18Ni maraging steels. The continuous air-cooling transformation curves for Steels A and B, shown in Figure 4, more accurately indicate the martensite transformation temperatures of the 18Ni grades of maraging steel; that is, about 400 F for the (250)-grade steel and 325 F for the (280)-grade steel. These curves were determined by simultaneously measuring the temperature and the magnetic permeability of 3/4-inch diameter by 5-inch long cylindrical specimens of each steel during continuous cooling in air from the annealing temperature (1500 F). The lower transformation temperature of Steel B evidently is a reflection of its somewhat higher nickel content (18.8 versus 17.5 per cent) and higher titanium content (0.80 versus 0.46 per cent). In this same chart, curves for three experimental steels also are shown: Steel C is an 18Ni-8Co-5Mo alloy containing no titanium or aluminum, whereas Steel D is an 18Ni-8Co-0.5Ti alloy, and Steel E is an 18Ni-8Co-0.5Al alloy, both containing no molybdenum. A comparison of curves for Steels A, B, and C with those for Steels D and E reveals the marked influence of molybdenum in lowering the martensite transformation temperature of these steels.

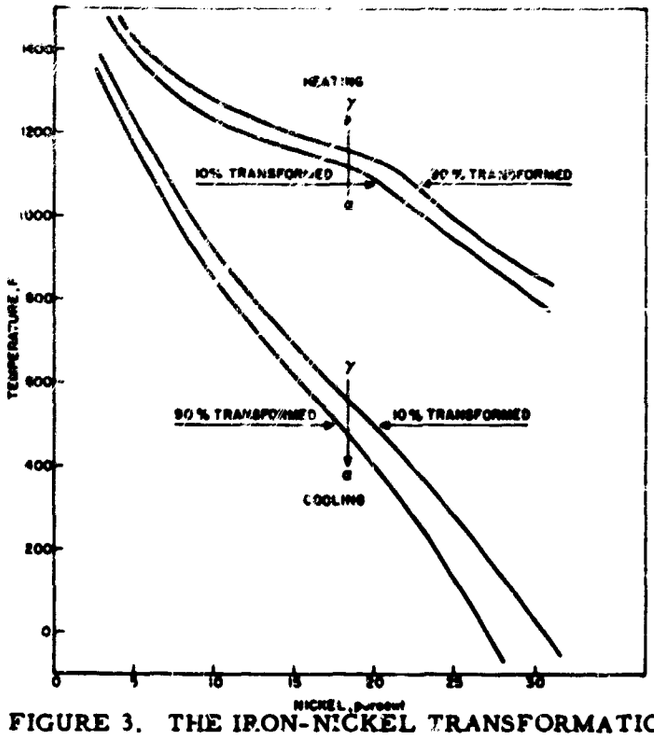

FIGURE 3. THE IRON-NICKEL TRANSFORMATION DIAGRAM (PUMPHREY AND JONES)

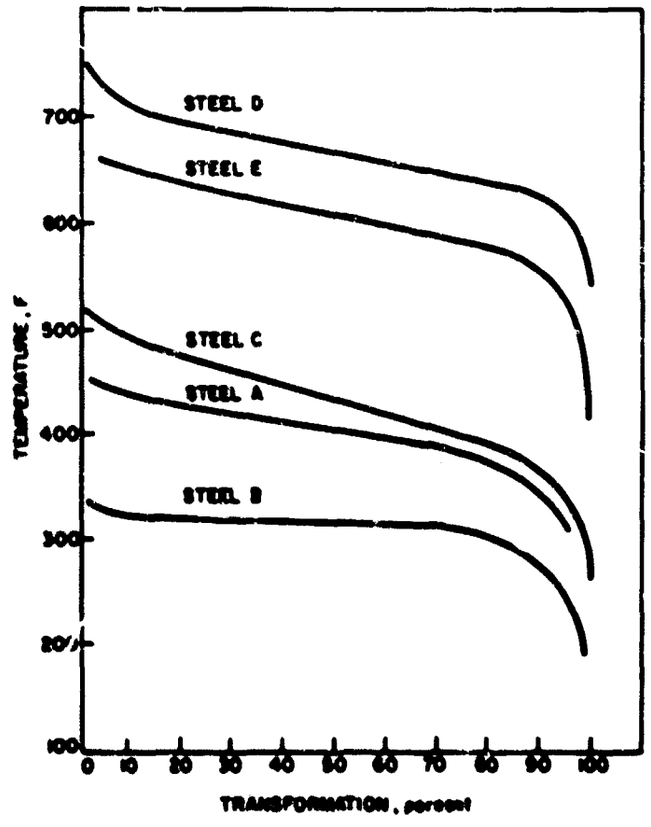

FIGURE 4. CONTINUOUS AIR-COOLING TRANSFORMATION CURVES FOR TWO COMMERCIAL MARAGING STEELS (A AND B) AND THREE EXPERIMENTAL MARAGING STEELS (C, D, AND E)

Examples of the mechanical properties obtained in rolled plates of the 18Ni(250) and 18Ni(280) grades of maraging steel, in the annealed condition, are given in Table 3. By comparison with Table 2 and Figure 2, it is clear that the strengths of the annealed materials are considerably lower, but the levels of ductility and notch toughness are markedly greater than for similar steels in the aged condition.

TABLE 3. MECHANICAL PROPERTIES OF TWO MARAGING STEELS IN ANNEALED CONDITION

Identification	Grade	Specimen Orientation	Yield Strength, ksi	Tensile Strength, ksi	Elongation, per cent	Reduction of Area, per cent	CVN Impact Energy (R.T.), ft-lb
Steel 471[a]	18Ni(250)	L	114	143	16.0	72.5	100
		T	120	145	16.0	65.0	97
Steel 822[b]	18Ni(280)	L	135	154	18.0	60.6	43
		T	129	150	18.0	63.6	44

(a) 0.75-inch-thick plate annealed at 1525 F and air cooled.
(b) 0.50-inch-thick plate annealed at 1650 (A.C.) + 1510 (A.C.).

The microstructure of an 18Ni(250)-grade steel (Steel A), in the annealed condition, is shown in Figure 5; the cubic nickel-martensite grains appear to be equiaxed platelets, containing several subgrains and a very high density of dislocations. Little evidence of microtwins, such as are commonly observed in carbon martensites and in higher nickel martensites, could be found in this martensite; in occasional, isolated areas, possibly constituting regions of microsegregation of carbon and/or nickel, a few such twins were observed (see Figure 6).

FIGURE 5. EQUIAXED MARTENSITE GRAINS IN MARAGING (250) STEEL A, ANNEALED AT 1500 F FOR 1 HOUR AND AIR COOLED

X100,000, Reduced approximately 44 percent in printing

FIGURE 6. MARTENSITE IN MARAGING (250) STEEL SHOWING DISLOCATIONS AND TWINS. TRANSMISSION ELECTRON MICROGRAPH

X160,000, Reduced approximately 44 percent in printing

AGING RESPONSE AND AGED MICROSTRUCTURES

The increase in hardness that occurs with increasing aging time, or the aging response, for different aging temperatures ranging from 750 to 900 F, is charted for the 18Ni(250) maraging steel (A) in Figure 7, and for the 18Ni(280) maraging steel (B) in Figure 8. It will be noted that the lower aging temperatures provide higher peak hardness than aging at the conventional temperature of 900 F, but the aging times required are considerably longer; furthermore, it has been found that the ductility and toughness values associated with these higher hardness (and strength) levels are significantly lower. The aging time required to achieve peak hardness in both alloys, for the 900 F aging temperature, is about 30 hours.

The first sound clue to the major mechanism of age strengthening in these alloys, whereby the strength of the annealed alloy is more than doubled by the aging treatment, was obtained by means of high-magnification electron-microscope examination of extraction replicas prepared from the aged steels, coupled with electron diffraction and electron microprobe analyses. The age-hardening precipitate, detected and identified in this way, is shown in Figure 9. Utilizing even higher resolution transmission electron microscopy to examine extremely thin sections of the aged alloys, it is possible to clearly observe and measure the individual particles, and to distinguish two different types of precipitate, as shown in Figure 10. The predominant precipitate is ribbon shaped and appears to have nucleated and grown along dislocation lines in the matrix in a partially coherent fashion; the secondary precipitate consists of smaller spherical or disc-shaped particles that appear to have nucleated homogeneously in the matrix and to have grown coherently.

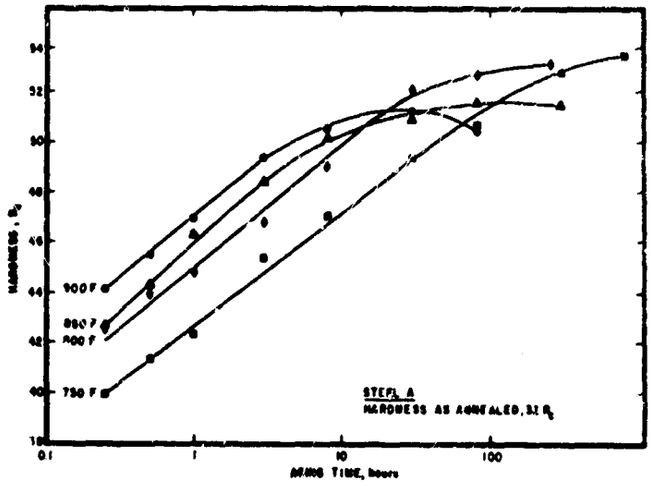

FIGURE 7. AGING RESPONSE OF MARAGING (250) STEEL A

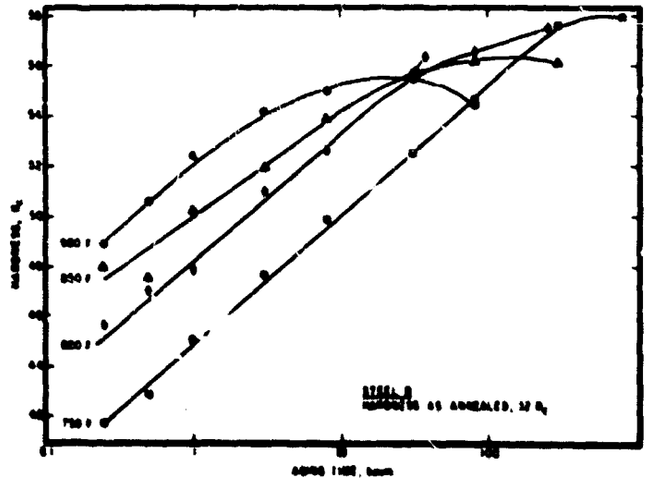

FIGURE 8. AGING RESPONSE OF MARAGING (280) STEEL B

Early electron-diffraction analyses indicated that the major precipitate was the intermetallic compound, Ni_3Mo, and that the minor precipitate probably was Ni_3Ti. To test this hypothesis, an experimental 18Ni-8Co-5Mo alloy, containing aluminum in place of titanium, was examined in the same manner, with the result that only the ribbon-shaped precipitate was observed, as shown in Figure 11. Furthermore, when a (211) diffraction spot of the Ni_3Mo diffraction pattern was utilized to obtain a transmission, dark-field, electron micrograph of the precipitate, the ribbon-shaped particles all appeared in bright contrast (Figure 12), indicating that these particles were the source of the (211) reflections of the Ni_3Mo pattern; the image of the microscope objective

FIGURE 9. AGE-HARDENING PRECIPITATE IN MARAGING (250) STEEL. ELECTRON MICROGRAPH OF EXTRACTION REPLICA

X70,000, Reduced approximately 44 percent in printing.

FIGURE 11. AGE-HARDENING PRECIPITATE IN MARAGING (250) STEEL CONTAINING ALUMINUM IN PLACE OF TITANIUM. TRANSMISSION ELECTRON MICROGRAPH

X200,000, Reduced approximately 44 percent in printing.

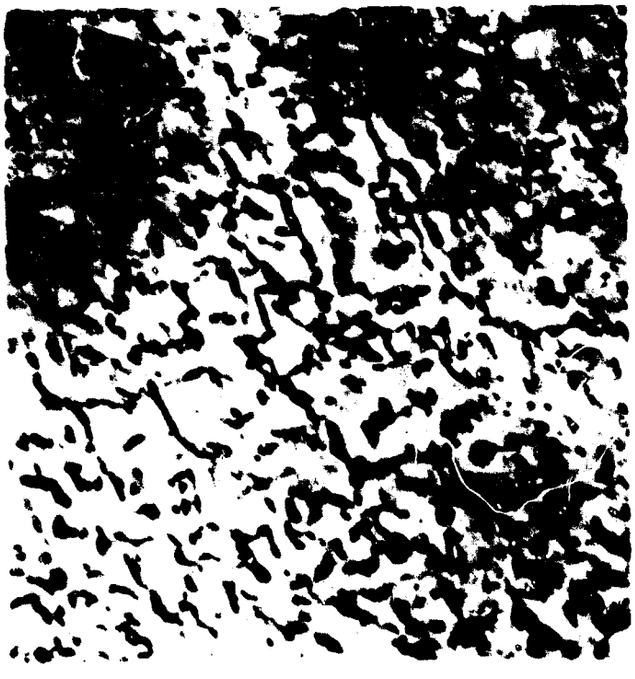

FIGURE 10. AGE-HARDENING PRECIPITATES IN MARAGING (250) STEEL. TRANSMISSION ELECTRON MICROGRAPH

X280,000, Reduced approximately 44 percent in printing.

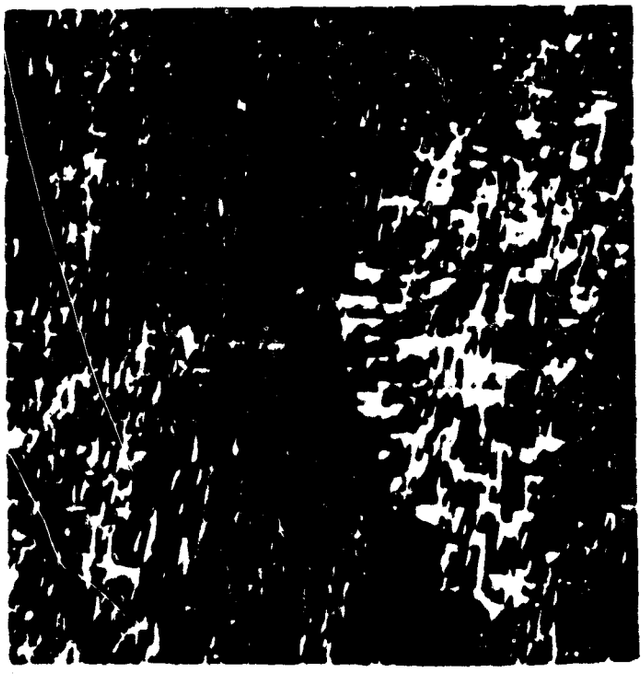

FIGURE 12. AGE-HARDENING PRECIPITATE IN MARAGING (250) STEEL. TRANSMISSION ELECTRON MICROGRAPH (DARK FIELD)

X160,000, Reduced approximately 44 percent in printing.

aperture is shown centered on the (211) reflection of the Ni_3Mo diffraction pattern in Figure 13. Electron diffraction patterns (in terms of interplanar spacings) obtained from both extraction replicas and thin sections of the aged 18Ni(250) maraging steel appear in Table 4, together with standard diffraction patterns for the two intermetallic compounds, Ni_3Mo and Ni_3Ti. These data provide convincing evidence that the primary precipitate is Ni_3Mo, but the identification of the secondary precipitate as Ni_3Ti is less certain because of the coincidence of some of the strong reflections of this diffraction pattern with those of the Ni_3Mo pattern.

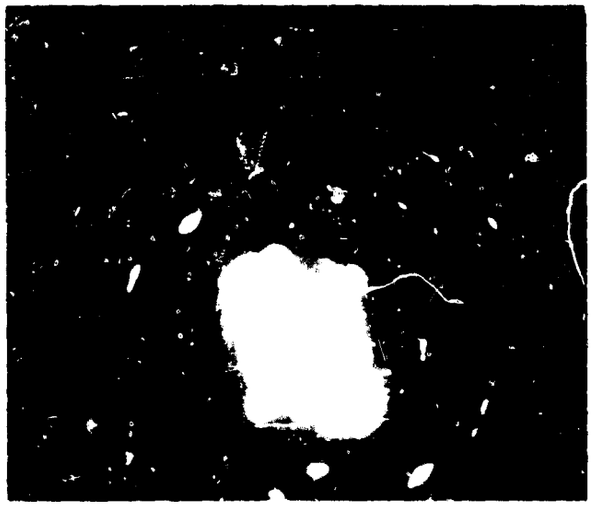

FIGURE 13. ELECTRON DIFFRACTION PATTERN OF MARAGING (250) STEEL SHOWING IMAGE OF OBJECTIVE APERTURE ON (211) REFLECTION OF Ni_3Mo USED FOR DARK-FIELD MICROGRAPH OF FIGURE 12

The results of quantitative electron microprobe analyses of precipitates extracted from the 18Ni (250) maraging steel A and the 18Ni(280) maraging steel B, after progressively longer times of aging at 900 F, are listed in Table 5. The elements involved in the precipitated phases evidently are nickel, iron, molybdenum, titanium, and aluminum; the amounts of cobalt contained in the extracted precipitates are considerably less than the average cobalt content of the alloy, and probably represent matrix contamination of the replica. Although these analyses alone cannot establish the stoichiometry and crystalline identity of the precipitate phases, the results are compatible with the findings of Ni_3Mo and Ni_3Ti, and suggest further that iron replaces nickel to a considerable extent in these phases; that is, the compounds are more properly represented by $(Ni,Fe)_3Mo$ and $(Ni,Fe)_3Ti$. No microscopic or diffraction evidence of an aluminum-bearing precipitate was found; the amount of such a precipitate obviously would be quite small, so that, if it occurs in these alloys, it might not be detectable in the presence of the larger amounts of Ni_3Mo and Ni_3Ti. Alternatively, aluminum may substitute for titanium in the Ni_3Ti precipitate.

TABLE 4. INTERPLANAR SPACINGS OF PRECIPITATES AND INTERMETALLIC COMPOUNDS

Ni_3Mo[a]		Extracted Precipitate		Thin Film	Ni_3Ti[b]	
d(A)	I/Io	d(A)	I/Io	d(A)	d(A)	I/Io
-	-	2.46	W	2.49	2.56	10
2.224	W	-	-	-	-	-
2.220	M	2.20	W	2.21	2.21	20
2.112	S	-	-	2.12	2.13	50
-	-	2.08	W	-	2.07	50
1.969	S	-	-	-	-	-
1.951	VS	1.96	S	1.95	1.95	100
-	-	-	-	-	1.72	20
1.553	VW	-	-	-	1.54	10
1.523	M	1.51	W	1.52	1.51	20
-	-	-	-	-	1.330	20
1.280	M	1.28	W	1.28	1.276	50
1.267	W	-	-	-	-	-
1.191	W	-	-	-	-	-
1.186	M	1.18	VW	1.19	1.173	20
1.113	VVW	-	-	-	-	-
1.101	VVW	-	-	-	-	-
1.094	M	1.09	W	1.10	1.095	10
1.085	W	-	-	-	1.087	50
1.076	VW	-	-	-	-	-
1.064	M	-	-	1.06	1.068	50
1.056	VW	-	-	-	1.046	20
-	-	-	-	-	1.038	20

(a) See Reference 5.
(b) ASTM X-Ray Powder Data File.

TABLE 5. ELECTRON-PROBE ANALYSES OF EXTRACTION REPLICAS

Steels A and B

Steel	Aging Treatment 900 F, hours	Composition, per cent Ni	Fe	Mo	Co	Ti	Al
A	3	46	15	34	2	3	1
	8	37	16	37	3	4	3
	30	34	22	38	3	2	0.5
	80	43	36	15	2	5	0.4
B	3	47	13	31	2	6	0.4
	8	47	14	31	3	5	0.3
	30	40	17	35	2	4	1
	80	46	27	15	2	10	0.3

The decrease in molybdenum content of the extracted precipitates that occurs upon overaging these alloys (80 hours at 900 F) is believed to signify some resolution of the Ni_3Mo precipitate in the matrix, whereas the increase in titanium content may be the result of increased precipitation of Ni_3Ti.

STRENGTHENING MECHANISMS AND ROLES OF THE ALLOYING ELEMENTS

Approximately one half of the yield strength of the fully heat-treated 18Ni maraging steels can be ascribed to the strength of the iron-nickel martensite formed upon cooling from the annealing temperature. Recently, Speich and Swann[1]* have concluded that the proposal of Winchell and Cohen[2], namely that the strength of carbon martensites is primarily a result of solid-solution hardening, can be extended to the iron-nickel martensites. They estimate that about three-quarters of the overall strength of an Fe-25Ni alloy stems from solid-solution hardening, and that the remaining portion of the strength arises from transformation substructure in the martensite.

The large incremental strengthening (more than double) of the annealed 18Ni maraging steel that occurs upon aging is believed to be the result of the precipitation of the intermetallic compounds, Ni_3Mo and Ni_3Ti, previously described. The precipitate particles range in size from 100 to 500 Å and are uniformly distributed in the matrix, with an average interparticle spacing of about 500 Å. Presumably, these particles have a very high elastic modulus, and consequently a very high fracture strength. They are large enough to be above the size likely to be sheared easily, and in addition, they exhibit some coherency with the matrix (strain-field contrast effects), which would increase their dislocation resistance. Furthermore, since their crystal structures differ significantly from that of the matrix, their slip systems probably are incompatible with that of the matrix.

Thus, it appeared that the simple Orowan analysis, which relates the shear strength of a particle-hardened alloy to the shear strength of the matrix and a term involving the shear modulus of the alloy, the Burger's vector and the interparticle spacing, should be applicable to these 18Ni maraging steels. Using this analysis, calculations of the interparticle spacing required to account for the increase in yield strength of an 18Ni maraging (250) steel upon aging, provide values of 400 to 550 Å, which agree well with the observed spacing of about 500 Å; sample calculations are shown in Table 6. Further evidence of the validity of this mechanism of strengthening is provided by (1) the fact that the initial strain-hardening rates (below about 0.5 per cent strain) in these steels are very high, irrespective of their aged condition, and (2) the observation that the dislocation-precipitate particle interactions in the deformed steels are of the type to be expected if the particles did not shear initially; an example of the latter effect is shown in the central area of Figure 14, for an 18Ni-7Co-5Mo maraging steel strained 2 per cent.

The roles of the alloying elements--Ni, Mo, Ti, and Al--in the strengthening mechanisms postulated for these steels are believed to be rather well established. The effect of cobalt, however, remains an enigma. Although Fe-20Co and Fe-18Ni-20Co alloys undergo considerable strengthening upon aging, reportedly as a result

* References are given on page 188

TABLE 6. CALCULATION OF AVERAGE INTERPARTICLE SPACING IN AGED 18Ni(250) MARAGING STEEL A

Treatment	Proportional Limit, ksi	Yield Strength (0.02%), ksi	Yield Strength (0.2%), ksi
Annealed 1 hour - 1500 F + aged 30 hour - 900 F	177	218	258
Annealed 1 hour - 1500 F	-	62	111

Orowan Relation

$\tau = \tau_o + \frac{\mu b}{L}$, where $b = 2.54$ Å, $\mu = 1.35 \times 10^7$ psi

for 0.02% criterion: $\tau = 110$ ksi; $\tau_o = 30$ ksi; L 400 Å

for 0.2% criterion: $\tau = 130$ ksi; $\tau_o = 55$ ksi; $L \sim 400$ Å

FIGURE 14. DISLOCATION TANGLES AROUND PRECIPITATE PARTICLES IN AN 18Ni-7Co-5Mo EXPERIMENTAL MARAGING STEEL STRAINED 2 PER CENT. TRANSMISSION ELECTRON MICROGRAPH

X130,000, Reduced approximately 44 percent in printing.

of matrix order hardening, an Fe-18Ni-8Co alloy does not exhibit any significant age-hardening response. However, the strength of an Fe-18Ni-5Mo alloy is increased by about 40 ksi by aging. The addition of 8 per cent cobalt to this latter alloy provides an additional strengthening increment of 40 ksi upon aging. Thus, the molybdenum is essential to the age strengthening of these alloys, and to the enhancement of strengthening provided by cobalt, whereas the cobalt alone is not effective; in this respect, cobalt also differs from aluminum and titanium. Several efforts to detect order hardening in aged 18Ni(250) maraging steels, by electron, X-ray, and neutron diffraction have not been successful. Of the several hypotheses so far advanced to account for the strengthening influence of cobalt in the 18Ni maraging steels, the most plausible one seems to be that the cobalt may provide a more dense and uniform distribution of dislocations in the martensitic matrix of the annealed alloys, which, in turn, creates many more easy nucleation sites for the more rapid precipitation of finer and more uniformly spaced particles of Ni_3Mo and Ni_3Ti.

In addition to its role in strengthening, it has been found that small amounts of titanium, or possibly some other strong carbide-forming element, are needed to scavenge the residual carbon in these alloys, and so prevent precipitation of the M_6C-type carbide, $(Fe,Mo)_6C$, upon cooling from the annealing temperature; this reaction may seriously interfere with the normal, primary age-hardening reaction by effectively reducing the amount of molybdenum available for the formation of Ni_3Mo.

OVERAGING AND AUSTENITE REVERSION

It is evident from the 900 F aging response curves of Figures 7 and 8, that overaging occurs in the 18Ni(250) maraging steel A and the 18Ni(280) maraging steel B for aging times longer than 30 hours. Microscopic and X-ray diffraction studies have shown that this phenomenon is different from that usually implied by the term "overaging", namely, excessive coarsening of the strengthening precipitate. Instead, clusters of precipitate particles redissolve locally in the matrix to form small patches of austenite, which are sufficiently enriched in Mo, Ni, and Ti to remain stable upon subsequent air cooling from the aging temperature. An example of the resulting microstructure, showing light patches of austenite, in an 18Ni(250) maraging steel that was aged at 1000 F for 10 hours, is shown in Figure 15. The amounts of reverted austenite formed in this steel for aging times up to 100 hours, at each of three aging temperatures, were determined by means of X-ray diffraction and are plotted in Figure 16. It was rather surprising to find evidence of appreciable austenite reversion for aging times shorter than the 30 hours required to attain peak hardness at 900 F, but this may be a result of localized segregation of some of the alloying elements. Although the presence of cobalt in these alloys tends to minimize this softening effect by raising the A_s temperature, higher peak hardnesses are attained at aging temperatures below 900 F, possibly because less austenite reversion occurs before the precipitation-hardening reaction reaches maturity.

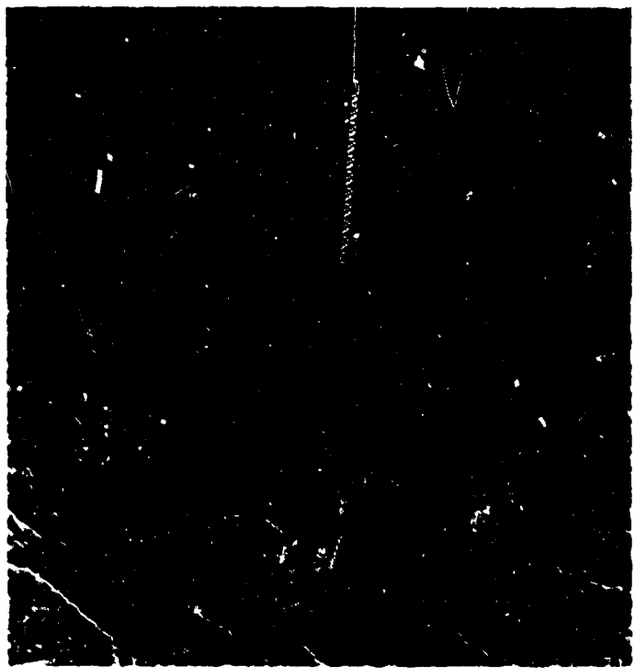

FIGURE 15. REVERTED AUSTENITE IN MARAGING(250) STEEL OVERAGED FOR 10 HOURS AT 1000 F. ELECTRON MICROGRAPH OF PLASTIC REPLICA

X32,000, Reduced approximately 44 percent in printing.

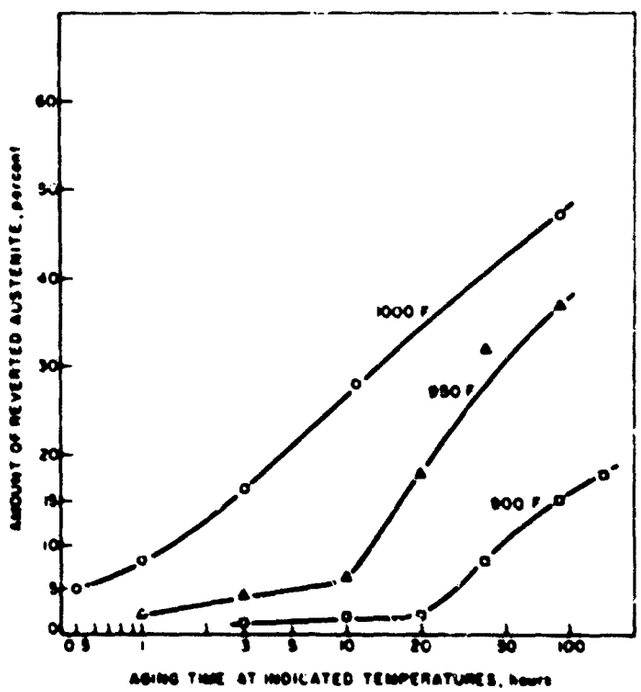

FIGURE 16. AMOUNT OF REVERTED AUSTENITE IN MARAGING (250) STEEL FOR VARIOUS AGING TIMES AND TEMPERATURES

INTERDENDRITIC SEGREGATION, BANDING, AND RETAINED AUSTENITE

Metallographic examination of longitudinal sections of plates rolled from the earliest production heats of 18Ni(250) maraging steel revealed rather pronounced segregation banding and layers of retained austenite, as shown in Figure 17. Electron-microprobe analyses of the dark segregated bands and of the austenite layers revealed that they contained considerably greater amounts of nickel, molybdenum, and titanium (also sulfur) than the surrounding matrix, as indicated in Table 7; X-ray diffraction measurements indicated that this steel contained more than 6 per cent retained austenite. This heterogeneity manifested itself mechanically as longitudinal "splits" in fractures of smooth tension-test specimens, and as "internal shear lips" in fractures of fatigue-cracked, notched-round tension-test specimens that were used to determine plane-strain fracture toughness (Figure 18). When longitudinal sections cut through these fractured specimens were investigated metallographically, it was found that the splits or shear lips intruded a considerable distance below the fracture surface, along the austenite layers, as shown in Figure 19. The possible influence of this condition on directional differences of plane-strain fracture toughness (G_{nc}) in such plates also was investigated by preparing and testing single-edge-notch, fatigue-cracked, tension test specimens of four different orientations from a single plate, as indicated in Figure 20. The test results (Figure 20) clearly demonstrated that when the crack plane and direction were oriented normal to the planes of banding (C), the fracture toughness was considerably greater than when the crack plane was normal to the bands, but the crack direction was parallel to the bands, either parallel to the rolling direction (B) or perpendicular to the rolling direction (A); furthermore, when the crack plane and direction both were parallel to the planes of banding (D), the measured fracture toughness was decidedly inferior.

To obtain some direct, visual evidence of the effects of banding on the microscopic path of fracture in these variously oriented test specimens, the fracture surfaces were electroplated with nickel, and polished-and-etched longitudinal sections were metallographically examined to determine the fracture profiles in the regions corresponding to plane-strain fracture. The fracture profile of the A-oriented specimen (or of the B-oriented specimens) did not exhibit any pronounced influence of the banding on the microscopic path of fracture (Figure 21), but the profile of the C-oriented specimen (Figure 22) showed quite clearly that the fracture frequently "detoured" abruptly from its main course, upon encountering segregation bands at approximately normal incidence, creating a rough, jagged surface. Thus, the segregation bands and residual austenite laminae appear to act as minute "internal crack arrestors" which tend to impede and divert the main propagating crack, forcing it to follow a rather circuitous path involving more plastic deformation, and thus effectively raising the fracture toughness of the material in this test orientation. In the case of the D-oriented specimen (Figure 23), the fracture occurred predominantly along the bands, occasionally stepping up or down from one band to another through interconnecting bands; this type of fracture involves considerably less plastic deformation and energy absorption. The overall effect of this banding generally is considered to be undesirable because the strength, ductility, and toughness in the through-thickness direction of plates is impaired, and low-energy fractures can occur under certain loading conditions involving combined stresses.

The segregation pattern visible in the micrograph of Figure 23 represents the vestiges of microscopic interdendritic segregation that occurred upon solidification of the ingot. The local enrichment in nickel, molybdenum, and titanium of the last, low-melting liquid to freeze in the interstices between dendrite cores and branches evidently is sufficient to cause the segregation to persist through thermal soaking and hot-working operations normally used in the production of plate. This condition is a difficult one to rectify by alloy modification, or changes in melting or casting practice. However, recent alterations in plate processing by U. S. Steel have succeeded in minimizing the segregation to the point where no residual austenite is found, banding as revealed by etching is relatively light (Figure 24), and electron-microprobe analyses indicate a marked reduction of alloying element segregation (compare Table 8 with Table 7). Furthermore, the fracture surfaces of smooth and notched tension-test specimens, Charpy V-notch impact test specimens, and slow notch-bend fracture-toughness test specimens, cut from recent production plates, do not exhibit splits or internal shear lips; an example of the notched-bend test fracture surface appearance is shown in Figure 25.

DIRECTIONALITY OF TENSILE PROPERTIES

Differences between the longitudinal and transverse tensile properties of the 18Ni(250) and 18Ni(280) grades of maraging steel plate generally are observed after the conventional annealing treatment (1500 F for 1 hour). Such directionality of mechanical behavior may be of concern in deep-drawing applications because of earing tendencies. These differences exist even though the cross-rolling ratios used in plate rolling exceed unity, and they are not necessarily a reflection of the banding referred to earlier, but rather appear to be associated with anisotropy of prior austenite grain shape and orientation, as indicated in the micrograph of Figure 26. Recently it had been found that a double-annealing treatment consisting of austenitization at 1650 F, followed by a second austenitization at about 1500 F, results in equiaxed prior austenite grains of larger size (Figure 27), and in considerably smaller differences between

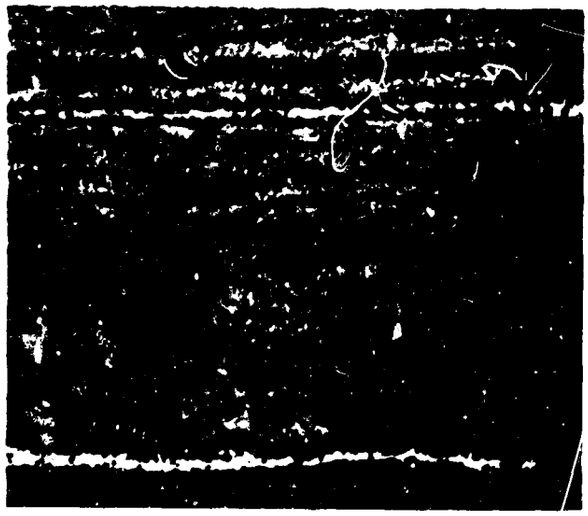

FIGURE 17. AUSTENITE AND SEGREGATION BANDS IN ROLLED PLATE OF MARAGING (250) STEEL. LIGHT MICROGRAPH OF POLISHED AND ETCHED LONGITUDINAL SECTION.

X200, Reduced approximately 21 percent in printing.

TABLE 7. ELECTRON-MICROPROBE ANALYSES THROUGH THICKNESS OF EARLY PRODUCTION PLATE (3/4-inch-thick)

Area Analyzed	Element Concentration, per cent		
	Ni	Mo	Ti
Austenite bands (white)	20.2	6.3	0.81
Dark bands	19.4	5.0	0.56
Light bands (matrix)	17.6	4.3	0.38
	17.6/20.2	4.3/6.3	0.38/0.81

Note: Greater than 6 per cent retained austenite by X-ray diffraction.

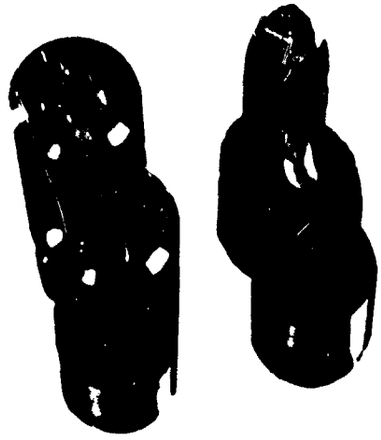

FIGURE 18. FRACTURE APPEARANCE OF SMOOTH AND NOTCHED TENSION-TEST SPECIMENS OF MARAGING (250) STEEL SHOWING LONGITUDINAL "SPLITS" AND "INTERNAL SHEAR LIPS"

FIGURE 19. FRACTURE PATH THROUGH AUSTENITE BANDS IN SMOOTH TENSION-TEST FRACTURE SHOWN IN FIGURE 18. LIGHT MICROGRAPH OF POLISHED AND ETCHED LONGITUDINAL SECTION.

X200, Reduced approximately 21 percent in printing.

ORIENTATION	G_{N_c}, ipsi
A	245
B	230
C	310
D	150

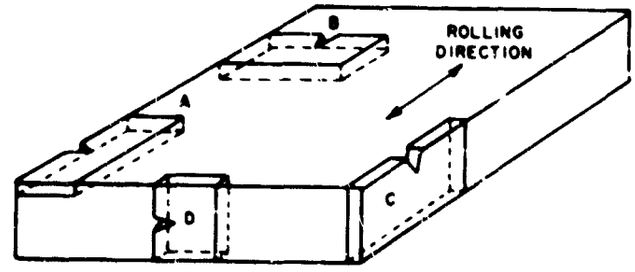

FIGURE 20. VARIATIONS IN FRACTURE TOUGHNESS (G_{n_c}) WITH SPECIMEN ORIENTATION IN MARAGING (250) STEEL PLATE (1-1/8-INCH-THICK)

FIGURE 21. FRACTURE PROFILE OF "POP-IN" REGION OF SPECIMEN "A". LIGHT MICROGRAPH OF POLISHED AND ETCHED SECTION

X200, Reduced approximately 21 percent in printing.

FIGURE 22. FRACTURE PROFILE OF "POP-IN" REGION OF SPECIMEN "C". LIGHT MICROGRAPH OF POLISHED AND ETCHED SECTION

X200, Reduced approximately 21 percent in printing.

FIGURE 23. FRACTURE PROFILE OF "POP-IN" REGION OF SPECIMEN "D". LIGHT MICROGRAPH OF POLISHED AND ETCHED SECTION

X200, Reduced approximately 21 percent in printing.

TABLE 8. ELECTRON-MICROPROBE ANALYSES THROUGH THICKNESS OF RECENT PRODUCTION PLATE (3/4-inch-thick)

Area Analyzed	Element Concentration, per cent		
	Ni	Mo	Ti
Light	18.1	5.0	0.30
Dark	17.4	4.6	0.28
Light	18.5	4.9	0.32
Dark	17.6	4.5	0.29
Light	18.5	5.1	0.33
Dark	17.7	4.5	0.30
	17.4/18.5	4.5/5.1	0.28/0.33

Note: No retained austenite detected by X-ray diffraction.

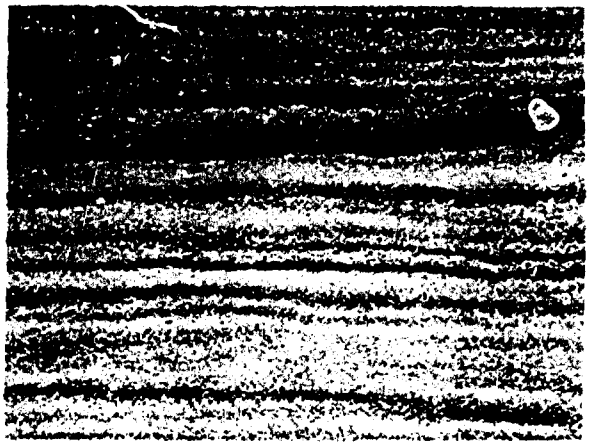

FIGURE 24. LIGHT BANDING IN MARAGING (250) STEEL PLATE (0.73-INCH-THICK) OF RECENT PRODUCTION. LIGHT MICROGRAPH OF ETCHED LONGITUDINAL SECTION

X100, Reduced approximately 21 percent in printing.

A. Longitudinal

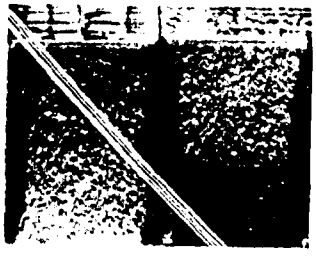

B. Transverse

FIGURE 25. FRACTURE APPEARANCE OF FATIGUE-CRACKED, SLOW-NOTCH-BEND, FRACTURE-TOUGHNESS TEST SPECIMENS OF MARAGING (250) STEEL PLATE (0.73-INCH-THICK) OF RECENT PRODUCTION

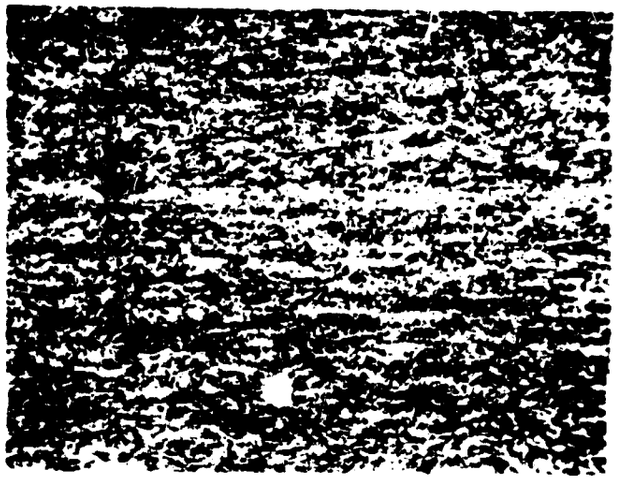

FIGURE 26. GRAIN STRUCTURE OF MARAGING (250) STEEL PLATE (0.22-INCH-THICK) ANNEALED AT 1500 F FOR 1 HOUR. LIGHT MICROGRAPH OF ETCHED LONGITUDINAL SECTION

X100, Reduced approximately 21 percent in printing.

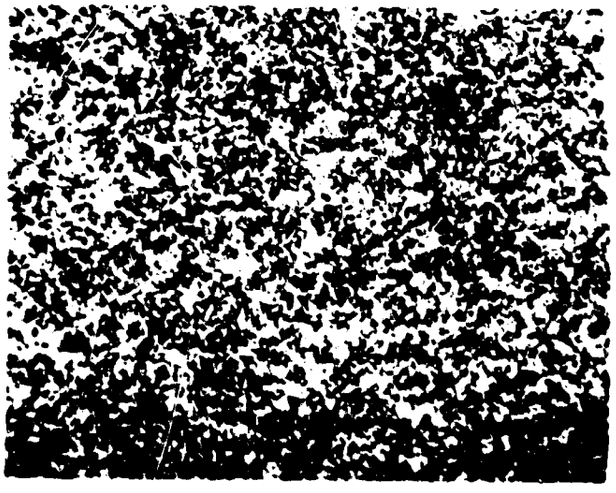

FIGURE 27. GRAIN STRUCTURE OF MARAGING (250) STEEL PLATE (0.22-INCH THICK) ANNEALED AT 1650 F FOR 1 HOUR AND THEN AT 1500 F FOR 1 HOUR. LIGHT MICROGRAPH OF ETCHED LONGITUDINAL SECTION

X100, Reduced approximately 21 percent in printing.

the longitudinal and transverse tensile properties (Table 9). The mechanism responsible for the effect has not been established, but it is conjectured that the first higher temperature anneal may redissolve some boundary precipitate at the surfaces of the elongated austenite grains in the hot-rolled plate, permitting equiaxed grain growth during the second anneal.

THERMAL EMBRITTLEMENT

In some early exploratory work on the austenitization and homogenization of the 18Ni(250) maraging steel, it was found that heating at 2200 to 2300 F for extended periods of time greatly reduced segregation and banding, but caused considerable austenitic grain growth, and marked impairment of ductility and notch toughness after subsequent conventional heat treatment. Fracture of impact test specimens of the fully heat-treated material occurred, with low-energy absorption, almost exclusively along prior austenite grain boundaries; an example of the fracture profile of such a specimen is shown in Figure 28. Electron-microscope examination of this fracture profile at higher magnification (Figure 29) revealed that the plastic deformation which had occurred during intergranular fracture, was extremely localized, indicating a weak boundary situation. Upon subsequent investigation of the fine-scale microstructure of this homogenized steel, by means of high-resolution transmission electron microscopy of extremely thin sections, a pattern of interconnecting "canals" corresponding to grain boundaries was observed, within which there was practically no fine precipitate, but instead, a thin, almost continuous film of some segregate phase, as shown in Figure 30. The identity of this film has not been established, although it is suspected to be titanium carbide, or possibly agglomerated precipitate phase. This microstructural phenomenon has been observed in other age-hardening systems, and evidently it does account for the occurrence of the low-energy intergranular fracture.

TABLE 9. EFFECT OF DOUBLE ANNEALING TREATMENT ON DIRECTIONALITY OF TENSILE PROPERTIES (0.46-inch-thick plate)

Direction	Yield Strength (0.2% Offset), ksi	Tensile Strength, ksi	Elongation in 2 Inches, per cent	Reduction of Area, per cent
	Single Anneal[a]			
L	252	263	10	46
T	270	277	8	30
	Double Anneal[b]			
L	257	266	10	45
T	261	271	9	38

(a) 1510 F + 900 F--3 hours.
(b) 1650 F + 1510 F + 900 F--3 hours.

This thermal embrittlement effect is believed to be closely related to the isothermal embrittlement of 18Ni maraging steels discussed by Novak.[3] It is to be noted that this thermal embrittlement resulted from thermal treatment alone; when hot-working operations are performed between the high-temperature homogenization treatment and the lower temperature austenitization treatment, such embrittlement usually is not evident.

THERMAL STRESS AND WELD CRACKING

When high heat input cutting processes, such as plasma-arc cutting, are used to cut heavy sections of 18Ni maraging steels, fine hairline cracking occurs at some distance behind the cut edge. In these cases, it generally is observed that the cracks originate near the interface between the high-

FIGURE 28. INTERGRANULAR FRACTURE IN MARAGING (250) STEEL THAT HAD BEEN HOMOGENIZED AT 2300 F FOR 16 HOURS PRIOR TO NORMAL HEAT TREATMENT. LIGHT MICROGRAPH OF POLISHED AND ETCHED SECTION CUT NORMAL TO PLANE OF FRACTURE

X200, Reduced approximately 21 percent in printing.

FIGURE 29. SEVERE LOCALIZED DEFORMATION ALONG PRIOR AUSTENITE GRAIN BOUNDARIES OF FRACTURE SHOWN IN FIGURE 28. ELECTRON MICROGRAPH OF REPLICA OF POLISHED AND ETCHED SECTION

X10,000, Reduced approximately 44 percent in printing.

FIGURE 30. GRAIN-BOUNDARY REGIONS DENUDED OF PRECIPITATE AND CONTAINING "STRINGERS" OF A SEGREGATE PHASE IN STEEL OF FIGURE 28. TRANSMISSION ELECTRON MICROGRAPH

X140,000, Reduced approximately 44 percent in printing.

temperature zone, which undergoes complete reaustenitization during cutting, and the adjacent lower temperature zone, where only partial reversion to austenite takes place. The cracks usually propagate in a direction normal to the cut edge, and are located mainly near the midthickness, where thermal stresses normal to the plate surfaces would be expected to be high. On a microscopic scale, this cracking follows prior austenite grain boundaries, as shown in the electron micrograph of Figure 31; these cracks started at a point about 1/4 inch behind the plasma-arc-cut edge of a 4-inch-thick plate and ran a distance of about 1/8 inch.

Electron metallographic examination of the microstructure of the steel near the point of origin of the cracks revealed an almost continuous thin network of reverted austenite at the prior austenite grain boundaries, and somewhat less continuous films at the martensite grain boundaries (Figure 32). In addition, extraction replicas prepared from the same region exhibited long, branching dendritic particles, also located at grain boundaries, as shown in Figure 33, these particles were identified as titanium carbide (TiC) by means of electron diffraction. Thus, this microstructural situation is quite similar to that previously discussed in connection with thermal embrittlement and is believed to account for the cracking which occurs upon plasma-arc cutting. Remedial processing measures recently have been developed to minimize or prevent such cracking.

FIGURE 31. CRACKS ALONG PRIOR AUSTENITE GRAIN BOUNDARIES IN PLASMA-ARC CUT MARAGING (250) STEEL PLATE (4-INCH-THICK)

X10,000, Reduced approximatey 44 percent in printing.

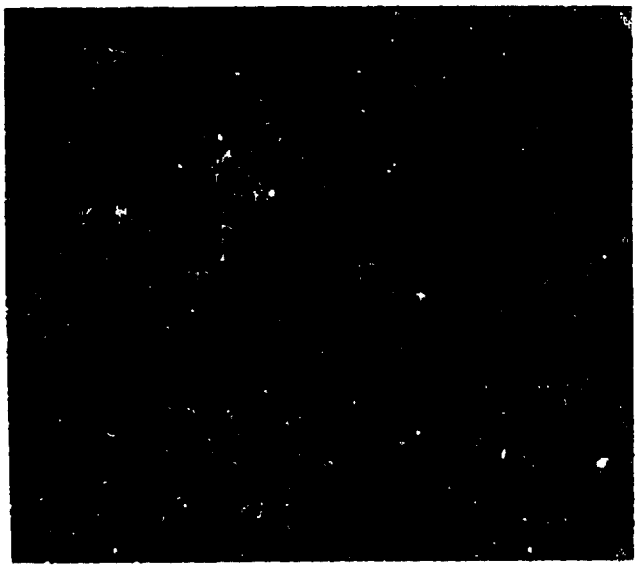

FIGURE 32. REVERTED AUSTENITE AND TITANIUM CARBIDE PARTICLES ALONG GRAIN BOUNDARIES IN VICINITY OF CRACK IN PLASMA-ARC CUT MARAGING (250) STEEL PLATE

X10,000, Reduced approximately 44 percent in printing.

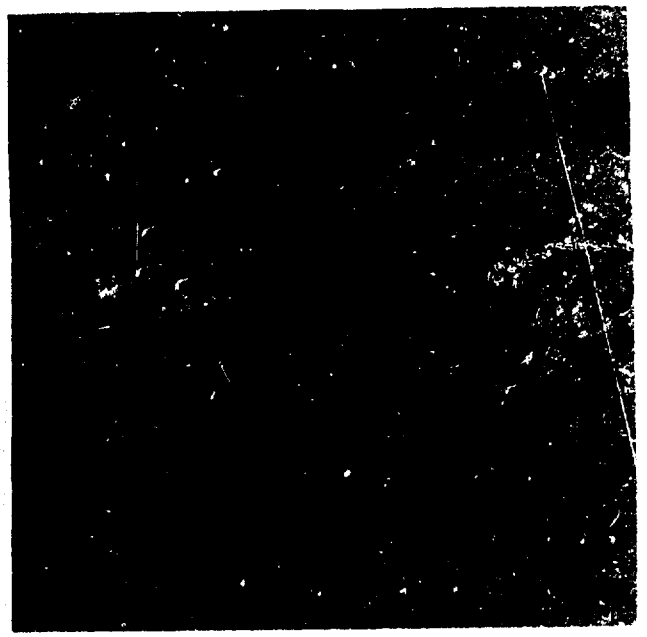

FIGURE 33. DENDRITIC TITANIUM CARBIDE PARTICLES IN EXTRACTION REPLICA OF AREA SHOWN IN FIGURE 32

X70,000, Reduced approximately 44 percent in printing.

A similar investigation of cracking in the weld metal of a submerged-arc weld in a 2-inch-thick plate also indicated that the cracks were intergranular and were associated with a small degree of austenite reversion at prior austenite grain boundaries coupled with precipitation of almost continuous chains of titanium carbide. In the schematic diagram of this weldment (Figure 34), the crack is shown near the quarter-thickness; it appeared to have originated near the interface between the weld-deposited metal and the fusion zone of the parent plate. Electron-metallographic examination of the region near this crack revealed a microstructure similar to that shown in Figure 32; an X-ray diffraction determination of the amount of reverted austenite in this same area yielded a value of about 7 percent. Extraction replicas prepared from this region exhibited almost continuous chains of fine particles along grain boundaries, as shown in Figure 35; these particles were identified as titanium carbide (TiC) by means of electron diffraction. The microstructure in Region C of the weld metal was found to be about the same. In contrast to this condition near the quarter thickness, the microstructure near the center of the weld (Region A) consisted of a cored, dendritic structure containing about 50 per cent austenite, whereas near the surface (Region B), the microstructure closely resembled that of the slightly aged parent plate steel and contained less than 2 per cent austenite.

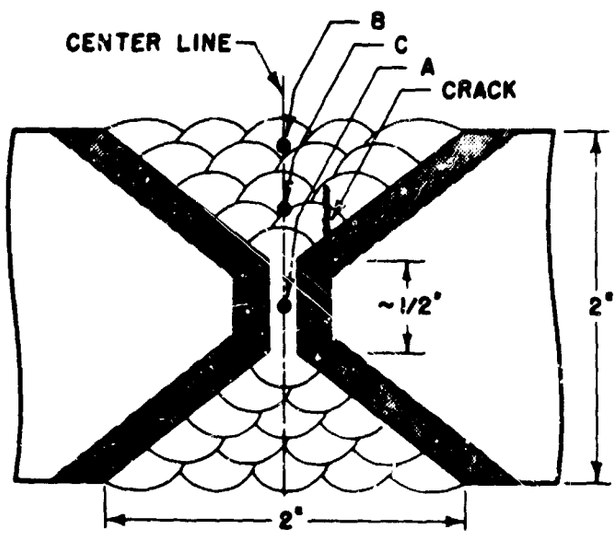

FIGURE 34. SCHEMATIC DIAGRAM OF WELD IN MARAGING (250) STEEL PLATE (2-INCH THICK)

FIGURE 35. TITANIUM CARBIDE PARTICLES ALONG GRAIN BOUNDARIES IN MARAGING STEEL WELD-METAL NEAR CRACK. EXTRACTION REPLICA

X10,000, Reduced approximately 44 percent in printing.

EFFECTS OF MINOR AND RESIDUAL ELEMENTS

The influence of residual elements on the notch toughness of 18Ni(250) maraging steel has been reported in some detail by Novak and Diran.[4] In general, later experience has confirmed those findings. Sulfur evidently is quite detrimental to toughness, as it forms platelets of titanium sulfide (TiS), and possibly iron sulfide, which, upon rolling, become flattened out into thinner but more extensive plates. In these maraging steels, the relatively high level of titanium, coupled with the rather low levels of manganese and silicon, preclude formation of the iron-manganese-silicon-sulfur inclusions that normally occur in most other types of steel. The addition of small amounts of calcium to these steels does not seem to effect any significant desulfurization. Carbon also appears to have a deleterious influence on notch toughness especially in amounts over 0.03 percent, since it forms titanium carbide (TiC) particles, both in the form of rather large particles in the as-produced material and as very fine particles which subsequently precipitate and redissolve in grain-boundary regions during certain heat treatments. Diffraction information generally has indicated that the coarse particles are titanium carbonitride (TiCN), rather than the simple carbide. The small amounts of boron and zirconium added to these alloys, presumably to retard carbide agglomeration at grain boundaries as in nickel-base alloys, do not seem to be beneficial. Both the TiS and TiCN particles frequently are observed in fracture surfaces. They are shown together, in close association, in the light micrograph of Figure 36a. X-ray fluorescence microscan images, obtained with an electron-microprobe analyser, of this same area are shown in Figure 36b for sulfur radiation, in Figure 36c for titanium radiation, and in Figure 36d for iron radiation. The large grey platelets evidently are TiS containing some iron, whereas the smaller, dark, chunky particles are believed to be TiCN.

Silicon also impairs the toughness of these steels, especially in amounts over 0.1 per cent. However, at low silicon levels, manganese in amounts up to about 0.3 percent does not appear to be harmful.

CONCLUSION

In conclusion, it may be stated that the maraging steels represent a major and important advance toward the goal of achieving ultrahigh-strength steels for use in constructional applications requiring high integrity. The physical metallurgy of this new class of steels differs considerably from that of the 0.3 to 0.5 percent carbon martensitic alloy steels of comparable strength, and this may account for some of the difficulties that have been experienced in early applications of these materials. It is equally clear, however, that the art-and-science of producing, fabricating, and utilizing these steels has been developing rapidly in recent months, as more knowledge and experience have been gained as a result of broadening use.

ACKNOWLEDGEMENT

A portion of the information contained in this review was obtained under United States Air Force Contract No. AF 33(657)-11149.

(a) Light Micrograph of Inclusions in Polished Section

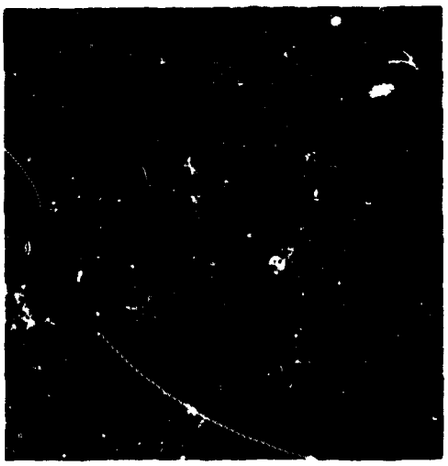

(b) X-Ray Scan Image— Sulfur Radiation

(c) X-Ray Scan Image— Titanium Radiation

(d) X-Ray Scan Image— Iron Radiation

FIGURE 36. LIGHT MICROGRAPH AND X-RAY MICROSCAN IMAGES OF TiS AND TiC PARTICLES IN POLISHED SURFACE OF A DELAMINATION IN MARAGING(250) STEEL PLATE

X750, Reduced approximately 44 percent in printing.

REFERENCES

(1) Speich, G. R., and Swann, P. R., "The Yield Strength and Transformation Substructure of Quenched Fe-Ni Alloys", to be published.

(2) Winchell, P. G., and Cohen, M., "Electron Microscopy and Strength of Crystals", Interscience, 995 (1962).

(3) Novak, C. J., "Isothermal Embrittlement of Maraging Steel", U.S. Air Force Materials Laboratory Fourth Maraging Steel Project Review, Dayton, Ohio, (June 10, 1964).

(4) Novak, C. J., and Diran, L. M., "The Influence of Residual Elements in Maraging Steels", AIME Proceedings of the Electric Furnace Conference, 20, 294 (1962).

THE POTENTIALS OF QUENCHED-AND-TEMPERED HIGH-STRENGTH STEELS

by

S. W. Hollingum*

SUMMARY

The majority of very high-strength steels currently employed are quenched and tempered steels. In their development use has been made of alloying elements which strengthen the ferrite and carbides, retard martensite breakdown, suppress transformation volume changes, and promote secondary hardening. Martensitic and secondary hardening are also controlled during heat treatment, or microstructures may be transformed isothermally, to give properties to suit a wide range of designs.

The chief steels in this group are (1) low alloy (Ni-Cr-Mo-V-Si, Cu-Si-Mo-V, Ni-Si-Mo-V, and low Cr-Mo-V), (2) modified die steels (5Cr-Mo), and (3) high-alloy steels (9Ni-4Co). They possess 0.2 per cent proof stress values up to about 280 ksi, combined with adequate toughness, good ductility, and high resistance to fatigue; also, they can be used at temperatures below the tempering temperature, say up to 1000 F (540 C).

These inexpensive steels are readily produced by conventional methods and factors likely to retard their use are being overcome. High purity was required to enhance transverse ductility, impact resistance, fatigue strength, and weldability; and, therefore, improved refining and vacuum melting and casting techniques have been introduced. The usual care is needed during heat treatment to avoid serious decarburisation, distortion, and quench cracking. Some final machining operations carried out after heat treatment have presented difficulties, but satisfactory techniques have been evolved. Problems of hydrogen embrittlement during pickling and cadmium plating were experienced, and modified or alternative protection processes are now in use. Research into factors influencing fracture toughness is required, although steels in this group can now be produced with fracture toughness properties comparable with those of maraging materials.

The success achieved in rocket-motor bodies, aircraft undercarriages, engine mountings, and other structural components, has encouraged development and stimulated extension of their use in other fields. Improvements in power-to-weight ratio, mobility, transportability, and efficiency in design, are possible in weapons, carriages, tanks, and vehicle components, particularly springs.

* Ministry of Defence, Royal Armament Research and Development Establishment, Fort Halstead, Sevenoaks, Kent, England.

Hitherto, these steels have been used in wrought forms, but recent research has lead to the production of castings with strengths in excess of 225 ksi. Quenched and tempered steels also have a great potential for ausforming to give strengths in excess of 400 ksi.

INTRODUCTION

When surveying the potentiality of very high-strength steels, it is appropriate to recall that the quenched-and-tempered steels have been the basis for engineering development over the past eighty years. At the turn of the century, alloying elements were being considered for the first time, and it is interesting to note that in 1905 Dr. Harold Moore of the Chemical Research Department, Woolwich, England, arranged for the preparation of a series of steels with between 0.25 to 6.4 per cent chromium, having uniform low carbon content and with all other elements kept to the minimum then possible.[1]* Since then, on both sides of the Atlantic, there have been classical researches into the effects of alloying elements on temper brittleness, time-temperature relationships for austenite transformation, hardening, hardenability, and many other phenomena which have prepared the way for the development of modern high-strength steels.

The gun steels of the 1914-18 war had a yield strength of about 43 ksi, and now gun designers are contemplating the use of steels five times as strong. In the aircraft and missile fields more than a decade of experience has been gained in the use of steels with 0.2 percent proof stress values in excess of 200 ksi. As designs become more complex and more demanding with respect to the combination of desired properties, metallurgists still look to the quenched and tempered steels as being capable of further development to satisfy the needs of the greatest variety of applications.

Before proceeding to summarise the properties and discuss the problems affecting their use, it is proposed to define the "quenched and tempered" class of steels.

DEFINITION OF CLASS OF STEEL

The quenched-and-tempered steels may be classified as those steels which rely on the formation of martensite which is hardened through lattice distortion by interstitial atoms of carbon, generally in combination with other alloying elements.

* References are given on page 200.

This excludes the maraging steels in which the martensite is very low in carbon and hence relatively soft.

DEVELOPMENT OF QUENCHED-AND-TEMPERED STEELS

The hardness of the martensite has a major influence on the properties which can be developed in quenched-and-tempered steels. Carbon is the most effective martensite hardener. Alloying elements permit a small additional increase in hardness, and martensite hardness can be further enhanced by ausforming (Figure 1). Because many operations involve welding, and to avoid excessive brittleness, it is desirable to keep the carbon content as low as possible, consistent with strength.

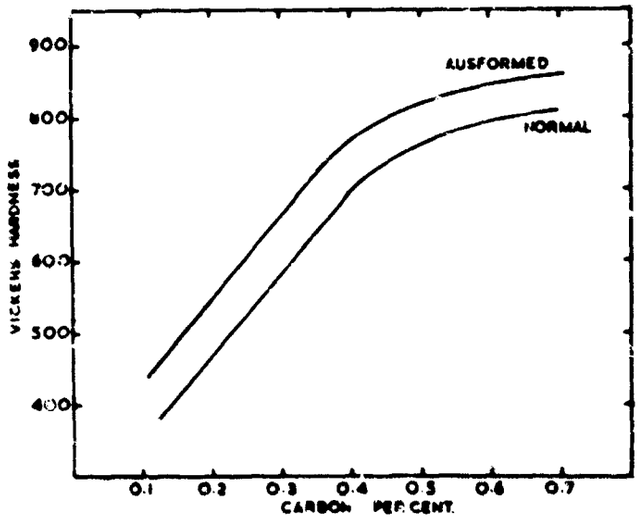

FIGURE 1. HARDNESS OF MARTENSITE

Nickel, chromium, manganese, molybdenum, and vanadium have been the alloying elements most commonly used to improve hardenability and impart strength and toughness. Each element contributes to the development of properties, either by strengthening ferrite, forming carbides, controlling the temperature and rate of transformation, or by promoting secondary hardening. In achieving the desired properties at strengths in excess of 200 ksi, it has been necessary to modify the composition of some conventional high-strength steels, notably by the addition of silicon, vanadium, or boron.

The manner in which properties may be designed into a medium carbon steel by the addition of common alloying elements is well illustrated by the series of researches by Kenneford[2] of the Royal Armament Research and Development Establishment. The quench cracking of parts having complex shapes and the crase cracking of gun bores are influenced largely by the mart transformation volume changes and Kenneford found that these could be drastically reduced by additions of up to 2.75 per cent silicon (Figure 2). The excellent thermal fatigue properties of RARDE steel at large temperature cycles are attributed to this feature, high mechanical strength having greater influence at the lower temperature cycles (Figure 3). The silicon also imparted a resistance to softening by raising the temperature at which martensite finally decomposed into ferrite and cementite. Molybdenum, which slightly reduced the transformation volume changes, was next added to promote secondary hardening by the precipitation of hard carbides. Copper, which is ferrite soluble, was chosen in preference to nickel because, in addition to providing the same degree of hardenability as nickel, it raised the end temperature of martensite breakdown (see Figure 4); and when present in excess of about 1 per cent, copper contributed to secondary hardening in the temperature range 840-1020 F (450-550 C). The fourth element, vanadium, in this Co-Si-Mo-V steel was added as a strong carbide former to enhance secondary hardening. Figure 5 illustrates the stages in alloy development, the silicon imparting resistance to softening on tempering, and the Mo, Cu, and V contributing to improvement by secondary hardening.

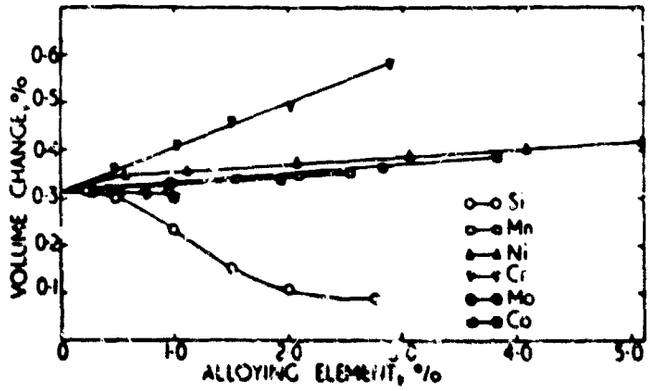

FIGURE 2. EFFECT OF ALLOYING ELEMENTS ON TRANSFORMATION VOLUME CHANGE

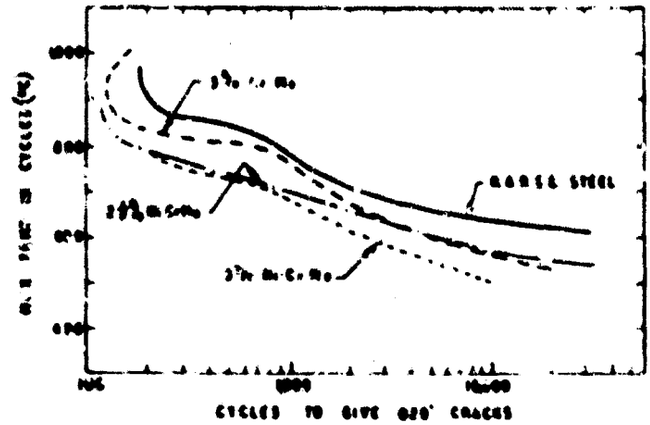

FIGURE 3. THERMAL FATIGUE PROPERTIES

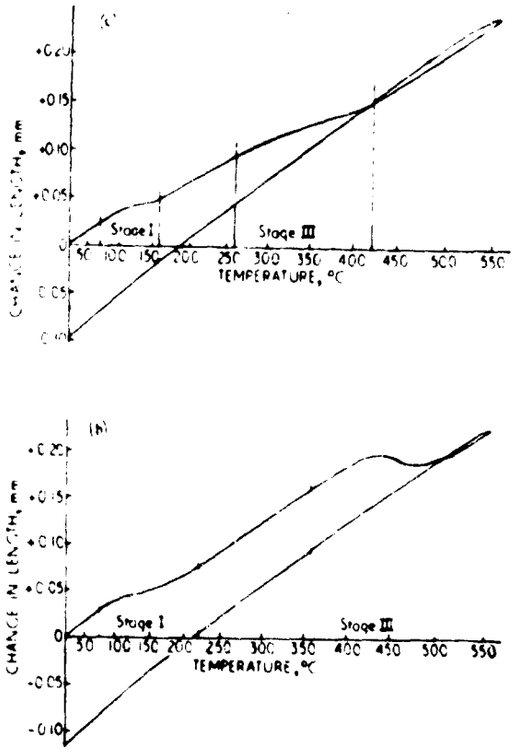

FIGURE 4. EFFECT OF Si ON MARTENSITE BREAKDOWN IN (a) Ni-Cr-Mo AND (b) Si-Mo STEELS

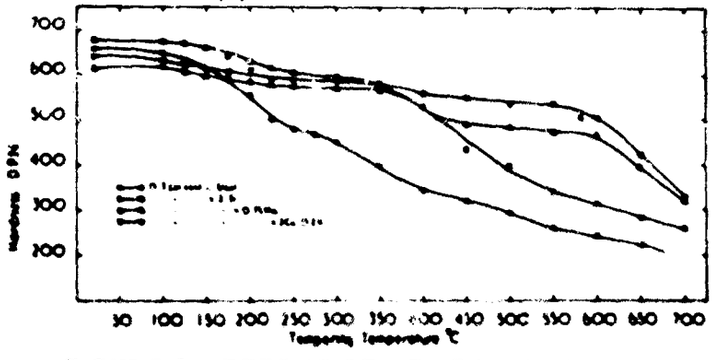

FIGURE 5. EFFECT OF TEMPERING ON HARDNESS

The 5 per cent chromium- nolvbdenum steel originally designed for hot die applications has yielded an important medium alloy series with excellent properties. The chromium, molybdenum, and manganese, produce very deep martensitic hardening in air, and during tempering secondary hardening results from the precip tation of fine carbides of the Mo_2C and VC type.[3] A further development of this steel by slightly increasing carbon and adding tungsten has yielded Vasco MA, which is one of the strongest steels yet produced.

Another major development has resulted from more recent studies of the tough 9 per cent nickel alloy steels by Pascover and Matas.[4] Nickel was selected because it increased toughness, but with this high nickel content, additions of up to 4 per cent cobalt were required to reduce the amount of retained austenite. Silicon in amounts greater than 0.25 per cent was regarded as being undesirable because of its deleterious effect on toughness as measured by the nominal notch strength to yield stress ratio. Carbon also lowered toughness, but to achieve the required strength level amounts of carbon approaching 0.45 per cent were essential. At a strength level of 250 ksi, this alloy HP 9-4-45 in the tempered martensitic condition had V-notch Charpy values in the 20-25 ft.lb range at room temperature. A remarkable improvement was found possible by a controlled transformation of the metastable austenitic structure at 480 F into bainite; this doubled the Charpy values.

From the information available, it appears some secondary hardering may take place in HP 9-4-45, but it is not known whether consideration has been given to building into the alloy some precipitation hardening mechanism not involving carbides, as this might improve strength or produce the same strength with lower carbon content.

On reviewing these developments it will be seen that very high strength depends largely upon the hardness of martensite, but by careful choice of alloying elements control may be exercised over the temperature and mode of martensite breakdown, and additional strengthening may be achieved by secondary hardening. Thus it has been possible to design steels in which very high strength is combined with high reduction of area and elongation values, good notch strength and resistance to impact, and excellent resistance to fatigue.

SUMMARY OF PROPERTIES

Wrought High-Strength Steels

These steels can be grouped conveniently as follows:

(1) Low alloy steels, which include the Ni-Cr-Mo-V (sometimes with Si additions), Cu-Si-Mo-V, Ni-Si-Mo-V, and low Cr-Mo-V [see Table I(a)]

(2) Modified die steels, which are based on the 5Cr-Mo-V composition [see Table I(b)]

(3) High alloy steels, at present confined to the Republic Steel Corporation's HP 9-4-X alloys [see Table I(c)].

In providing a summary of the properties, it is not possible to portray the full characteristics of each steel. Hence, in Table I, properties are given only for typical tempering temperatures, most of the data being taken from the Aerospace Structural Metals Handbook, Volume 1.[5] It will be seen that some of the steels have poor resistance to impact and low elongation values. For designs where these may be tolerated, 0.2 per

TABLE 1. COMPOSITION AND PROPERTIES OF SOME VERY HIGH-STRENGTH STEELS (QUENCHED AND TEMPERED)

	C	Ni	Cr	Mo	V	Si	Co	Other Elements	Tempering Temperature, F	Ftu ksi	Fty ksi	e, per cent	R.A., per cent	Charpy V-ft. lb.
(a) Low Alloy Steels														
4330V	.3	1.8	.8	.4	.07	-	-	-	400	245	200	10	18	15
4340	.4	1.8	.8	.25	-	-	-	-	400	260	217	10	45	10
HY-TUF	.25	1.8	-	.4	-	1.5	-	Mn-1.3	600	230	194	14	52	29 (Izod)
300M	.43	1.8	.8	.4	.05	1.6	-	-	500	296	242	8	23	18
Tricent RX539	.35	1.8	.1	.34	.21	1.55	-	-	660	260	215	10	35	-
NCMV	.45	1.7	1.45	1.0	.24	.20	-	-	575	292	255	8	35	18 (Izod)
USS STRUX	.43	.75	.9	.5	.06 max	-	-	B	500	280	230	10	30	14
D-6-A	.46	.55	1.0	1.0	-	-	-	-	600	282	255	9	35	12
X-200	.43	-	2	.5	.05	1.6	-	-	700	270	230	5	-	15
RARDE	.37	-	-	.75	.25	2	-	Cu 2	1100	245	220	17	42	12
RARDE	.37	-	-	.75	.25	2	-	Cu 2	400	312	255	15	47	20
(b) Hot Work Die Steel														
5Cr (H11)	.4	-	5	1.3	.4	-	-	-	1000	280	230	5	28	10
Vasco MA	.5	-	•	•	•	-	-	W•	1050	344	278	7	33	12
(c) High Alloy and Nickel Maraging Steel														
9Ni-4Co	.4	9	-	5	-	-	4	C .45	600	250	230	9	40	23
9Ni-4Co	.4	9	-	-	-	-	4	C .45	480 1. bainite	270	230	-	-	R.T. 45 -80° 30
18Ni Maraging (300CVM)	-	18	-	5	-	-	8.5	Ti & Al	900	300	293	4	52	20

F_{tu} = ultimate tensile strength
F_{ty} = 0.2 per cent proof stress
e = elongation (measured on 2 in. for American values, 4 A for U.K.)
R.A. = reduction of area
• Denotes alloying elements present - values not yet declared

cent proof stress values greater than 250 ksi and ultimate tensile strength values in excess of 300 ksi can be achieved. On the other hand, there is a preference for higher tempering temperatures, to achieve some improvement in ductility and a reduction in internal stresses, but which necessitates acceptance of slightly lower tensile properties.

Figures 6(a), (b), (c), and (d) show the effect of tempering temperature on ultimate tensile strength, 0.2 per cent proof stress, elongation, reduction of area and Charpy impact values of four quenched and tempered steels, with some comparative values for 18 per cent nickel maraging steels.

With low tempering temperatures, ultimate tensile strengths in the region of 330 ksi are combined with 0.2 per cent proof stress values between 240 and 280 ksi. As the tempering temperature is increased, the tensile strength falls, while the 0.2 per cent proof stress initially increases before decreasing. Thus with the higher tempering temperatures, the ratio of proof stress to ultimate tensile strength is high, approaching .9. Very high ratios are also encountered in the 18 per cent nickel maraging steels. This is a feature which requires attention in view of the effect on design concepts and manufacturing techniques. Increase in tempering temperature results in a general increase in reduction of area and elongation values, while the impact values may pass through a shallow trough before showing a marked increase as softening sets in.

The value of the Charpy V-notch test is often criticised and other notch tests are receiving much attention. However, the low temperature impact properties are very significant when considering metals subjected to high rates of strain, since high rates of strain have the effect of raising the ductile-to-brittle transition temperature. Many of the quenched and tempered steels do not have very high impact properties particularly at yield strength levels above 230 ksi. The nickel-chromium and chromium alloy steels show a more pronounced transition than the Cu-Si-Mo-V steel, the impact properties of which fall steadily with temperature. However, for high impact properties the HP 9-4-45 alloy in the bainitic condition is outstanding, values in excess of 30 ft. lb. (Charpy) being obtained at -100 F with an ultimate tensile strength level of 250 ksi.

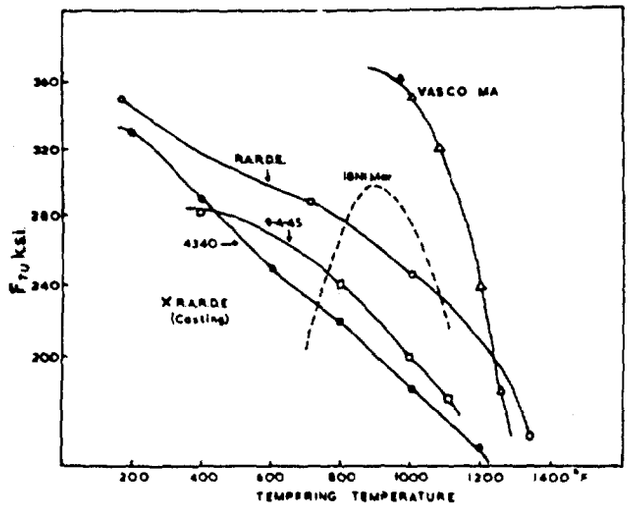

FIGURE 6(a). THE EFFECT OF TEMPERING TEMPERATURE ON ULTIMATE TENSILE STRENGTH

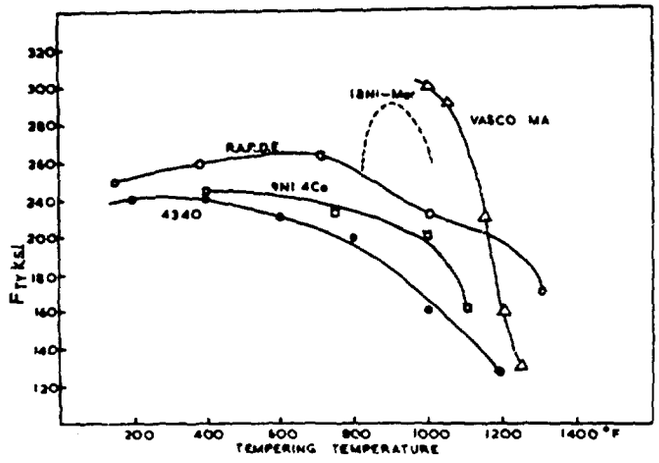

FIGURE 6(b). THE EFFECT OF TEMPERING TEMPERATURE ON 0.2% PROOF STRESS

Fatigue properties are normally related to ultimate tensile strengths, and for very high-strength steels there are significant features by which they differ from those of the medium-strength steels. The S-N curves for some of these steels do not show a fatigue limit which is as clearly defined, and there is still a small drop in fatigue strength between 10^6 and 10^7 cycles. Also, endurance ratios (fatigue limit/ultimate tensile strength) are lower than .5. In Table 2, typical data are given for direct stress fatigue tests on several very high-strength steels; the endurance ratios being calculated on a basis of fatigue strength of 10^6 cycles. Very few results are available for fatigue properties on 9Ni-4Co, but its endurance ratio appears to be slightly lower than those of the other high-strength steels. RARDE steel possesses fatigue properties similar to those of the other low alloy steels, with endurance ratios of the order of .43 at the 280 ksi strength level, but so far only a few results have been obtained under directly comparable conditions.

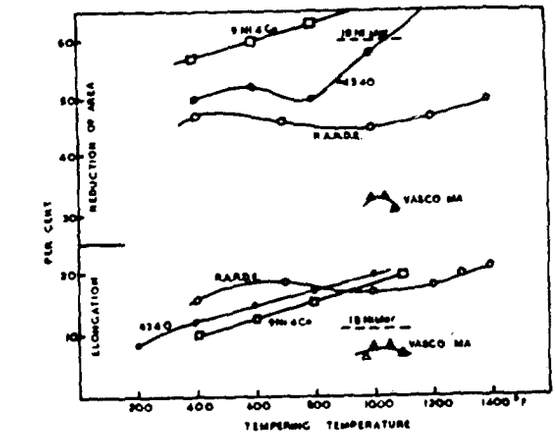

FIGURE 6(c). THE EFFECT OF TEMPERING TEMPERATURE ON REDUCTION OF AREA AND ELONGATION

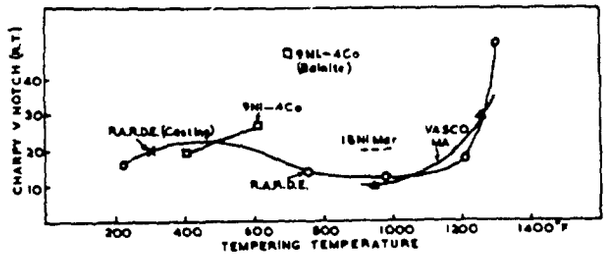

FIGURE 6(d). THE EFFECT OF TEMPERING TEMPERATURE ON CHARPY V NOTCH (ROOM TEMPERATURE VALUES)

TABLE 2. FATIGUE PROPERTIES OF SOME QUENCHED AND TEMPERED HIGH-STRENGTH STEELS

Axial Loading On Longitudinal Test Pieces

Alloy	Stress Ratio A	Stress Ratio R	Stress Concentration	Fatigue Strength ksi/cycles 10^5	10^6	10^7	Fatigue Ratio	Nominal Strength Level
4340	"	-1	Smooth K = 1	130	120	-	.41	290
300M	"	-1	Smooth K = 1	150	120	-	.41	290
Vasco MA	-	-	-	185	158	115	.43	350/360
9Ni-4Co	1	"	Smooth K = 1	120	86	-	.30	290
18Ni - Maraging	"	-1	Smooth K = 1	146	130	122	.45	280

Although it is not proposed to list creep and elevated temperature properties, it will be appreciated that the temperature at which these steels can be used is limited by the resistance to softening during tempering and should be well below the usual tempering temperature. Some of these steels have been known to possess good strength after tempering at 1100 F, and these could be used at temperatures up to, say, 950 F according to the magnitude of the stress and the duration of the heating cycle.

High-Strength Steel Castings

The properties so far discussed relate to wrought products, and it will be appreciated that both sand and investment castings in steels at these high-strength levels would find extensive application. On behalf of RARDE, the British Steel Castings Research Association investigated the influence of alloying elements on microporosity in the Cu-Si-Mo-V steel, and studied the founding properties of alloys possessing the most suitable compositions. Tables 3a and 3b show the composition and properties of a series of casts with various carbon contents. Using vacuum-melting procedures, sand castings can be made with ultimate tensile strengths in the 220-250 ksi range, elongation values between 8 and 12 per cent, and room temperature Charpy V notch impact tests about 20 ft.lb. In addition to casting in block moulds and shell moulds, investment castings were made, and again very good properties were obtained, see Table 4. As with RARDE steel in the wrought form, Charpy impact values for investment cast ings were acceptable even at low temperatures. At room temperatures the values were between 18 and 22 ft.lb., which showed a steady fall with temperature to values between 12 and 15 ft.lb. at -40 F.

The only unfavourable aspect was the low fatigue values, which had a fatigue limit of the order of 45 ksi compared with about 100 ksi for the wrought product. It is not known whether such low values are usual for investment castings, but the subject is being investigated.

TABLE 3a. COMPOSITIONS OF VACUUM-MELTED CHILL-CAST RARDE STEEL SPECIMENS

WQ at 1000 C and T at 300 C

Cast No.	C	Si	Mn	S	P	Cu	Mo	V
	per cent							
V 61	0.10	0.95	0.77	0.012	0.002	0.82	0.63	0.31
V 62	0.14	0.86	0.79	0.011	0.002	0.82	0.65	0.31
V 32	0.21	0.95	0.62	0.005	0.009	2.00	0.85	0.29
V 58	0.27	1.85	0.61	0.012	0.002	1.71	0.71	0.33
V 102	0.36	1.23	0.76	0.012	0.004	2.13	0.86	0.25
V 111	0.44	1.17	0.75	0.011	0.004	1.87	0.73	0.25

TABLE 3b. MECHANICAL PROPERTIES OF VACUUM-MELTED CHILL-CAST RARDE STEEL SPECIMENS

WQ at 1000 C and T at 300 C

Cast No.	U.T.S. ksi	e per cent	R.A. per cent	Charpy Impact V Notch ft.lb.	V.P.N. 30 Kg.
V 61	167	10.7	28	10.5	373
V 62	189	15.6	52	32	425
V 32	205	13.6	39.5	27.2	455
V 58	230	11.9	38.5	19.7	509
V 102	267	5.0	10.5	-	-
V 111	291	6.0	10.0	-	-

TABLE 4. MECHANICAL PROPERTIES OF INVESTMENT CASTINGS

Code Letter	0.2% P.S. ksi	U.T.S. ksi	P.S./U.T.S.	e per cent	R.A. per cent
A 13	208	220	95	6.0	15.2
A 14	217	224	96	5.0	13.8
A 15	199	222	90	5.0	15.2
B 14	210	217	97	4.0	12.3
B 15	206	221	93	6.0	15.2
C 26	216	222	97	7.0	21.0
C 27	212	224	95	7.0	23.8
C 28	210	215	98	8.0	27.9

PROBLEMS AFFECTING THE USE OF QUENCHED-AND-TEMPERED STEELS

This statement of properties does little to portray the problems encountered by manufacturers in obtaining the combination of properties required for particular applications, and, what is more difficult, achieving them, in the actual forging, casting, or fabricated component. In addition there are special problems of protection, stress corrosion, and machining.

All the steels in this class can be made by conventional steelmaking processes, a wide experience being gained in producing economically high-quality high-strength aircraft steels during and since World War II. However, with further increase in strength requirements, problems were encountered in achieving adequate ductility and freedom from possible failure by a rapidly propagating crack.

The main problem affecting the use of quenched and tempered steels may be summarized as follows:

(1) Low level and scatter of transverse properties of aircraft forgings, particularly transverse reduction of area (only 8 to 6 per cent in steels with 260 t 280-ksi UTS) and fatigue resistance.

(2) Poor impact properties, particularly transverse impact properties at low temperatures.

(3) Notch sensitivity, or poor fracture toughness, as experienced in certain forgings, and in the brittle failure of of rocket-motor cases.

(4) Difficulties in machining hardened steels.

(5) Hydrogen embrittlement during protective treatment and stress corrosion.

Improved Properties by Purification

With reference to transverse properties the shape of the component often limits the amount to which transverse properties can be developed by working, and large length to diameter ratios create marked directionality. Thus all other factors influencing ductility are of major importance, especially the embrittling effects of residual elements

and inclusions, and any microstructural variation such as segregation and "banding".

Recent work by Baron at RARDE has shown the deleterious effect phosphorus and tin on the low-temperature impact properties of Ni-Cr-Mo-V gun steels hardened and tempered to 258 ksi ultimate tensile strength. There was evidence that interaction between phosphorus, antimony, arsenic, and tin, when all present, could exaggerate their total effect. The greatest reduction of impact properties (room-temperature Charpy V notch) was produced when 0.1 per cent aluminum was added to a steel melted under nitrogen, thus confirming the need to avoid formation of aluminum nitrides.

In research on materials for rocket-motor cases, Cottrell[6] has shown that sulphur and phosphorus have a detrimental effect on impact strength, fatigue life, ductility, and weldability; also that low levels of residual hydrogen could cause a serious loss of ductility which may lead to brittle fracture.

Thus steelmakers have been faced with the need to reduce residual elements, produce cleaner steels, and virtually eliminate hydrogen. Although much can be done by appropriate selection of materials used in the initial charge and care in slagging and deoxidising operations, the desired properties could not be achieved without the use of vacuum melting. All leading steelmakers are now equipped for vacuum melting, and their experience confirms that by improving purity and cleanness, they can achieve marked improvement in transverse ductility, impact resistance, fatigue strength, and weldability. For example, Hamaker and Yates[7] have shown that transverse reduction of area of about 12 per cent in a 9-inch section of air-melted Vascojet 1000 steel, is increased to more than 30 per cent by consumable-arc melting. In other work[3] on 5 per cent chromium steels, Hamaker reports that vacuum melting resulted in improvements in ductility and toughness, surpassing variations in both carbon content and heat treated strength level, in effectiveness. In the U.K., Child and Oldfield[8] have shown that a high-duty bearing steel having extensive inclusions greater than 0.020 in. in size, after vacuum-arc remelting had only three inclusions in the size range 0.004-0.010 in., and none greater. For higher quality, vacuum-arc melting of an electrode made by vacuum-induction melting is recommended, but commenting on future trends Childs suggests that electron-beam melting may offer advantages, it being possible to hold molten metal at controlled degrees of superheat for any desired time in the absence of refractories. On the other hand, refining can be carried out during vacuum-arc melting, as for example, by remelting through a flux blanket, and the Republic Steel Corporation's carbon deoxidation process recently described by Mates.[9] The advantage of the latter method, which can be applied during vacuum-arc remelting, or during vacuum-ladle degassing, is that the product of deoxidation is a gas, instead of a solid-reaction product.

Hence by achieving high purity many of the factors contributing to low ductility and poor impact resistance may be overcome. Steps can be taken to reduce segregation, and heat treatment can be given to improved uniformity of microstructure. There still remains the possibility of a small defect, a minute crack, or a sharp notch which can initiate a crack under static or fluctuating loads. The extent to which a high-strength steel can resist the formation and propagation of a crack is a most important factor which will largely determine the extent to which the steel will be used.

Notch Sensitivity and Fracture Toughness

The properties of notched specimens may be determined in a variety of ways, but whether they are measured by notched tensile tests, Charpy impact, or calculated as a fracture-toughness parameter, the properties decrease with increase in ultimate tensile strength. Figure 7 is a graph prepared by Klier for N.R.L. Report 6012[10], which shows how rapidly the notch strength of 4340 falls with ultimate tensile strengths above 200 ksi. The actual values obtained are influenced by the test temperature, strain rate, specimen size, and geometry of the notch. While this may be typical of a number of low alloy steels, other quenched-and-tempered steels are less notch sensitive at high-strength levels.

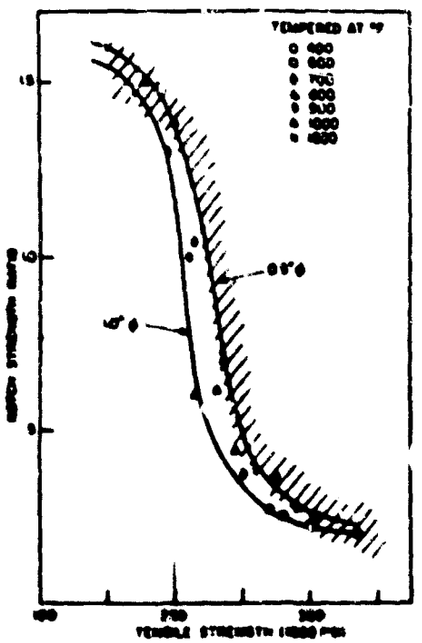

FIGURE 7. THE NOTCH-STRENGTH RATIO VERSUS TENSILE STRENGTH FOR 4340 STEEL TEMPERED AS INDICATED

In general, for sheet at yield strengths of about 200 ksi, there is not a great deal of difference in the notched tensile strengths of all the high-strength steels. As the yield strength increases, the 18Ni-Co-Mo maraged steels retain high notch strength even up to 300 ksi. At yield strengths about 260 ksi, the notch strength of the HP 9-4-X alloys appears to fall to just below 180 ksi, and the remainder of the quenched and tempered steels give notch strengths just above or below 100 ksi. Inadequate data are available for bar and forgings, but it appears the same trend holds, though to a much lesser degree.[13]

The possibility of being able to improve the notch properties of the low alloy steels is worth considering. Isothermal transformation to a lower bainitic structure as used for the HP 9-4-X alloys, might produce improved toughness in the low alloy steels, but so far, this appears to have received little attention. It is thought necessary to avoid a mixed structure, and in particular the presence of upper bainite, since this would reduce toughness and raise the impact transition temperature of steels like 4340.

Another approach might be to limit the tempering to the end of the first stage of martensite breakdown. For example, Kenneford and Williams[11] have observed that the energy absorbed in fracturing unnotched specimens of a 1Ni-1Cr-Mo steel under impact tensile conditions was remarkably high when tempered to the end of the first stage. As shown in Figure 8, the steel tempered at 320 F gave impact tensile values of 81 ft.lb. A marked increase in elongation also occurred at that stage.

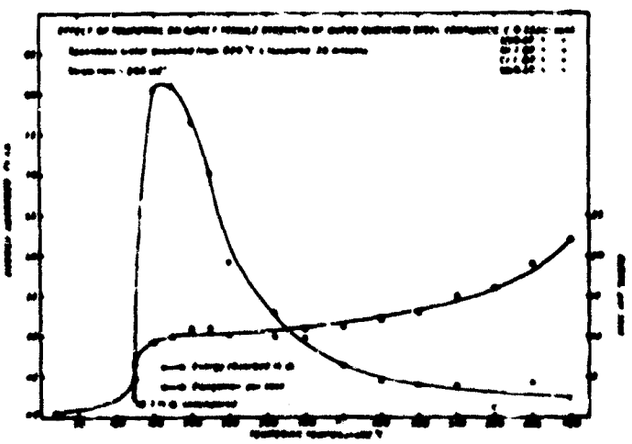

FIGURE 8. EFFECT OF TEMPERING ON IMPACT TENSILE STRENGTH OF W/ TER QUENCHED STEEL CONTAINING 0.55C, 0.67Mn, 1.07Ni, 1.07Cr, and 0.27Mo.

Specimens water quenched from 820 C and tempered 30 minutes.

Strain Rate = 209 sec^{-1}

Of the various fracture toughness criteria, plane-strain fracture toughness, K_{IC}, has been proposed as a parameter which might be used by designers[12], or as a basis for selection of materials. Pascover and Matas[4] have plotted the variation of plane-strain fracture toughness with yield strengths for a number of high-strength steels (see Figure 9). Tentative values for RARDE steels and a value for 18Ni maraging steel have been added.

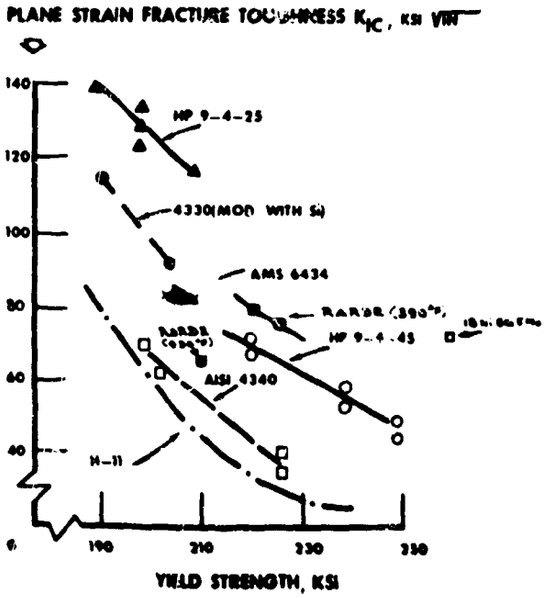

FIGURE 9. THE VARIATION OF PLANE-STRAIN FRACTURE TOUGHNESS WITH YIELD STRENGTH FOR SEVERAL HIGH-STRENGTH STEELS

After Pascover and Matas

The lower value for RARDE steel was obtained on specimens tempered at 930 F (500 C) which usually produces the lowest impact properties.

When considering the failure of a pressure vessel it has been suggested that factors which influence failure are (a) the initial flaw size, (b) fracture toughness of the material, and (c) the operating stress level. Therefore, it is appropriate to include some information about the size of initial flaw. While it is not possible to predict the smallest crack which inspectors would have to detect, it is possible to compare the materials on the basis of relative flaw size. Figure 10 has been prepared partly from data published by Pascover and Matas[14], the relative flaw size being calculated in accordance with the equation

$$\text{Relative flaw size } \left(\frac{a_{cr}}{Q}\right) = \frac{K_{IC}^2}{1.2\sigma_y^2}$$

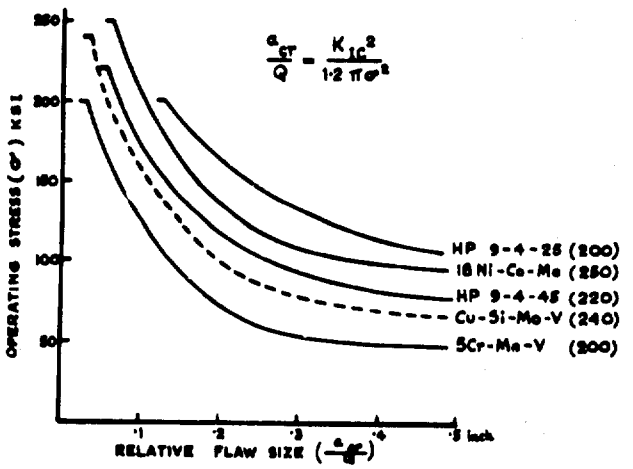

FIGURE 10. THE RELATIVE FLAW SIZE WHICH CAN BE TOLERATED AT VARIOUS OPERATING STRESS LEVELS

where a_{cr} denotes crack length, K_{IC} the fracture toughness, σ the applied stress, and Q denotes the dependency of the stress state induced by a flaw on the geometry of that flaw. Q is actually expressed by $Q = \Phi^2 - .212(\sigma/\sigma ys)^2$, where Φ is the elliptical integral, σ the applied stress, and σys is the 0.2 per cent proof strength.

It will be observed that for operating stresses up to 200 ksi the lower carbon HP 9-4-X alloy shows greatest tolerance with respect to flaw size, but at the highest strength levels the 18Ni-Co-Mo maraged steel is better than existing quenched and tempered steels.

Embrittlement During Electroplating and From Stress Corrosion

Two other embrittling factors are (1) hydrogen embrittlement during electroplating and (2) the effects of corrosion on high-strength steel under high-working or internal stresses.

There are many theories concerning the mechanism of delayed failure by hydrogen, but the most widely accepted theory was that attributed to Troiano and his co-workers[15], who suggested a crack would initiate when a critical combination of hydrogen concentration and triaxial stress state occurred locally, e.g., in the vicinity of a notch. At present there is still insufficient information about the relative merits of the various high-strength steels, but it is suggested that a steel with low diffusion rates would not pick up so much hydrogen during plating. The other property required is the ability to resist crack propagation. It is claimed that the high nickel steels are not so susceptible to hydrogen embrittlement as the low alloy steels, but, as shown, acceptable fracture toughness can be achieved in low alloy steels and where silicon is present in amounts of the order of 1.5 the diffusion rates are low. Steels with a high silicon content have been shown by Cotton to be less susceptible to hydrogen embrittlement than normal steels, and this was supported by Klier, et al., who also suggested that embrittlement is minimised by a low carbon content.

In view of the severity of the problem, a large effort has been devoted to establishing techniques which will minimise embrittlement during cleaning and electroplating, particularly with respect to cadmium and chromium. It is outside the scope of this paper to list the recommended pretreatment, modified plating processes, and post plating heat treatment which have been found satisfactory. It is of interest to note some observations by Dougherty[18] on the effects of post plating heat treatment. He found that relief treatment for 4340 type steel heat treated to 260 ksi electroplated with cadmium or chromium was 580 F (287 C) which is in the range which would cause blue brittleness in that steel.

Providing a solution to the hydrogen embrittlement problem also reduces the possibility of stress corrosion failures, but often extensive service experience is needed to make the correct choice of protective schemes and to ensure reliability in joints and bearings, where plating and painting are not possible. Surface peening is beneficial, but of more importance is the contribution which can be made by the designer in his selection of materials, by avoiding stress raisers, and by minimising galvanic effects from dissimilar metals.

Due to the wide range of stress-corrosion tests in use it is not possible to give a reliable statement of the related properties of the various steels. The absence of hydrogen should be verified by means of a notched tensile test. For example, with 4340 steel hardened to 260-280 ksi ultimate tensile strength a cylindrical specimen of 0.357 in. diameter and a 50 per cent 60 degree notch with a radius of 0.025 in., should not rupture within 200 hours when stressed at 75 per cent of the notch strength of unplated specimens.

HEAT TREATMENT

It is not possible to discuss quenched and tempered steels without some reference to heat treatment, for it is by heat treatment conditions that the combination of properties may be controlled. Within this class, there is a wide range of conditions; from steels such as 4340 which requires water quenching to achieve through hardening in bars over 3 inches diameter, to the 5 per cent chromium-molybdenum-vanadium series which air harden fully in sections up to 10 inches square. A RARDE steel with a 0.35 per cent carbon content can be hardened to 95 per cent martensite in an 8 in. section on water quenching. The Jominy end-quench test results follow this pattern, and for most high-strength steels there is very little fall in hardness along the length of the quenched specimen.

Normal heat treatment procedures and controls are used. In general decarburisation if not removed by machining should be avoided by the use of low humidity inert atmospheres. The usual care is required to avoid distortion and to reduce the risk of quench cracking.

The application of isothermal heat treatment, as required in the HP 9-4-X alloy would require quenching a component in a salt bath in the range 475-485 F. Massive components can produce a marked temperature rise and variation in section tends to produce mixed structures; however, from a knowledge of the isothermal diagram for the steel and the results of some practical trials, it should be possible to programme suitable conditions, adjusting initial bath temperatures or by preliminary cooling at temperatures in the bay of the T-T-T curve.

In the 5 per cent chromium steels, double or triple tempering is recommended to complete the removal of retained austenite and achieve full secondary hardening. No problems occur but additional processes increase costs.

The work by Cottrell on the heat treatment of rocket-motor cases in chromium-molybdenum steel is interesting. He has employed heat treatment conditions which give a controlled decarburisation, to provide a surface layer with improved ductility which contributes to higher bursting strengths.

MACHINING QUENCHED AND TEMPERED STEELS

In the manufacture of armaments for the three services, a great variety of component designs are encountered and each major component presents its special problems. Thus it is not easy to provide a summary statement on machining difficulties. The subject is a vital one, for by establishing rapid and economical methods for machining the quenched and tempered steels, the engineer can avoid the selection of the costly high nickel maraging steels on the basis of machineability.

It is reported that the American aircraft industry has established good techniques using conventional methods for steels in the 280-300 ksi range. The success appears to be due to a sustained effort in developing a satisfactory technique and then rigid control of its use during production.

Generally a preliminary heat treatment is recommended, either a full anneal, isothermal anneal, or normalise and temper, to soften the steel and minimise subsequent distortion. As much metal as possible is removed before hardening and tempering; while on some components a final machining allowance of only 0.050 in. can be recommended, other components such as gun barrels require a generous machining allowance.

For all machining operations maximum rigidity in machine tools, jigs, and fixtures is essential. After grinding operations, inspection for cracks and surface etching to check for damage is recommended. Stress relief treatment should be employed after grinding whenever possible. For some components the final operation consists of shot peening to remove further compressive stresses and give improved resistance to fatigue.

Very hard tool steels such as Vasco "Hypercut" have been introduced and some noteworthy claims have been made for ceramic tool tips. In the U.K., the normal metal removal rate on a gun steel hardened to 160 ksi would be of the order of 7 cu. in./min., but at 220 ksi the rate is down to 2 cu. in./min. Fine cuts on fully hardened steel are difficult, and tapping is particularly troublesome. Plugging a tapped hole finished before hardening is not a reliable solution due to distortion during heat treatment. Improvements have been made in cemented carbide tool materials of the tungsten-cobalt type, and these have been used successfully. There is keen interest in developments in the electrolytic machining techniques which have lead to higher metal removal rates, and which offer a solution to the problem of machining ausformed steels. In addition, suitable chemical contouring techniques have been developed.

It appears, therefore, that machining can be accomplished satisfactorily, but there is a pressing need for further research into tapping, and perhaps milling, of steels which have been hardened to give strengths up to 300 ksi.

POTENTIAL APPLICATIONS

The quenched and tempered steels available at present permit the use of designs based on 0.2 per cent proof stress values up to 300 ksi. At the 300 ksi level, the steel would probably be of the Vasco MA type, possessing deep air-hardening properties and weldable, but allowance would have to be made for the lower ductility to be expected at that strength level. Between 220 and 280 ksi (0.2 per cent proof stress), a wide variety of steels can be considered, ranging from the very tough HP 9-4-X alloys to the slightly stronger and less tough Cu-Si-Mo-V, modified Ni-Cr-Mo-V, and Cr-Mo-V steels. The high-nickel-high-cobalt content of HP 9-4-X might make the alloy more expensive, but economic factors must be considered with respect to safety, ease of production, and other aspects of its application.

In the aircraft industry some 5 to 10 years experience has been gained in the problems and controls necessary for the successful use of quenched and tempered steels in the 250-280 ksi tensile-strength range. Landing-gear components, engine mountings, wing-root fittings, bolts, and tail members have all been made in the low alloy or 5 per cent chromium-type steels. The extent to which weight has been saved can be appreciated

from a comparison made by the Douglas Aircraft Company. The main landing gear of the DC 8 was made primarily in the 4340 C.M. steel heat treated to 260 ksi ultimate tensile strength. If a 180 ksi steel had been used the weight would have been approximately 4500 lbs, a weight increase of 44 per cent. Similar examples of 40 per cent weight saving can be quoted for the use of N.C.M.V. steel at 250 ksi ultimate tensile strength by the Fairey Aviation Company in the main inner tubes for undercarriages in their Delta 2, Gannet Mk. III, and Rotodyne.

It is considered that development of designs for aircraft components at strength levels about 300 ksi is possible with existing quenched and tempered steels, but to improve the position, research is required into the metallurgical factors which influence fracture toughness. Higher strengths would necessitate the use of hot-cold worked high-nickel steels or ausformed low-alloy steels.

Rocket-motor bodies, also, have been manufactured satisfactorily in several high-strength quenched and tempered steels. The problem of microcracks in welds and the metallurgical conditions which influence the bursting strength and nature of the failure have been investigated extensively. In some designs of small rockets, full advantage cannot be taken of the available strength of these steels because reduction in wall thickness would result in a decrease in rigidity or structural stiffness and a corresponding loss of accuracy in flight. On the other hand, for rockets fabricated from strip, either wide strip edge welded or narrow strip resin bonded, further development could make use of quenched and tempered steels improved by ausforming.

The knowledge gained in the use of high-strength steels in aircraft and missiles could be applied effectively to improve power to weight ratio, and give greater mobility in a wide range of military equipment. Quenched and tempered steels can provide the desired combination of properties, which include high strength combined with good ductility over the service temperature range, the ability to withstand high rates of strain, and conditions which impose thermal and/or mechanical fatigue.

Breech rings for large guns are massive and their shape is convenient for upset forging techniques to produce properties uniform in the longitudinal and transverse directions. In gun tubes there is the problem of erosion and temperature effects; and at high-strength levels the presence of notches in the form of rifling and crase cracks may present great difficulty.

The advent of RARDE casting alloy in this strength range opens up new possibilities and the manufacture of a number of components in shapes difficult to forge is under study.

There is a variety of requirements for armour and many ideas of how to provide protection against a range of ammunition. For some applications, high strength combined with high values for low temperature Charpy impact would be an advantage. In view of the good properties obtained for welded HP 9-4-X, it would be interesting to assess the alloy in plate form against various types of attack. Some of the low alloy steels are also weldable and with small improvement of low temperature impact properties might be preferred from consideration of cost and use of alloying elements more readily available.

In tanks and carriages, space is often at a premium, and the use of low alloy high-strength steels would save both weight and space. Springs, both suspension springs and in the form of torsion bars, and valve springs for piston engines, are further examples for future application of quenched and tempered very high-strength steels.

FUTURE TRENDS

The future will still hold a demand for stronger steels and improved ductility and fracture toughness will be required at all strengths above 300 ksi. The initial approach has been made, chiefly by working the metastable austenite of existing quenched and tempered steels. Strengthening without a corresponding loss in ductility has been achieved, and at this stage it appears that main factors are the reduced austenite grain size and the improved dispersion of finer carbides, and the consequential refinement of martensite plate size.

Alloy development should proceed along three main lines:

(1) Development of alloys in compositions which facilitate ausforming

(2) Strengthening by precipitation of compounds other than carbides

(3) Study of isothermal transformation to lower bainite in various alloys and its effect on toughness.

At the same time, further study of the factors affecting fracture toughness is desirable. Among a vast array of problems, it would be interesting to know the effect of the fineness and nature of precipitated carbides on crack propagation, bearing in mind that the carbides themselves are hard and rather brittle.

Machining research is very important, and unless good economic methods can be established, the extent of application of the quenched and tempered steels will be limited and the emphasis will be towards steels of the maraging type.

CONCLUSIONS

It is concluded that many quenched and tempered very high-strength steels are available which possess high strength, combined with good ductility, adequate fracture toughness, good fatigue properties, and satisfactory low-temperature properties. The specific needs of particular designs can be met by appropriate choice of composition, hardening, and tempering temperatures, or isothermal heat treatment.

To satisfy stringent requirements for transverse ductility, toughness, and reliable fatigue properties at these strength levels, it is important to achieve high purity and a high degree of cleanness, with the result that improved steelmaking and refining techniques, and vacuum melting, are used extensively.

Techniques for machining these steels and finishing them in the hardened condition have been worked out, but research to solve problems with certain operations is required. With progress to higher strengths, machining difficulties may limit the extent to which these steels can be used.

The precautions to be taken and the processes to be used for the protection of these steels are understood.

A great deal of practical experience has been gained in the aircraft and missile industries in the reliable use of quenched and tempered steels in the 250-280 ks. ultimate tensile-strength range. The success achieved confirms the need to consider extending the use of this class of steel in other fields of engineering, particularly ordnance, fighting vehicles and other military equipment.

A casting alloy with ultimate tensile strengths in excess of 225 ksi has been developed and will extend the range of applications.

The need for greater fracture toughness has lead to the development of promising 9Ni-4Co steels which can be isothermally transformed to a bainitic structure with excellent properties.

With improved knowledge of factors affecting fracture toughness, further improvements can be made in all high-strength steels. Some quenched and tempered steels can be used for ultimate tensile-strength levels above 300 ksi, and for strengths above 350 ksi their properties could be enhanced by thermal-mechanical working.

Note: RARDE steels are covered by British Patent No. 931,395, U.S. Patent No. 3,070,438, and other overseas patents; while further British and overseas patents are pending.

REFERENCES

(1) Moore, H., The Metallurgist, 1 (2) (March, 1960).

(2) Kenneford, A. S., BISRA Special Report 76, 74-76, 1962, High-Strength Steels Conference.

(3) Hamaker, J. C., Jr., and Vater, E. J., ASTM, 60 (1960)

(4) Pascover, J. S., and Matas, S. J., AIME Symposium, 1963 National Metals Conference (Project 12018, TR 12018-54).

(5) Aerospace Structural Metals Handbook, 1, ASD-TDR-63-741.

(6) Wilkinson, F. J., and Cottrell, C.L.M., Aircraft Production (August and September, 1960).

(7) Yates, D. H., Johnson, A. R., and Hamaker, J. C., Jr., Soc. Aerospace Material and Process Engineers, 6th National Symposium, 1 (November, 1963).

(8) Child, H. C., and Oldfield, G. E., I & S Inst. Special Report No. 77 (1963).

(9) Matas, S. J., ASM Golden Gate Metals Conference (1964).

(10) Klier, E. P., NRL Report 6012 (December, 1963).

(11) Kenneford, A. S., and Williams, T., Unpublished RARDE Report.

(12) Hanna, G. L., and Steigerwald, E. A., Tapco Report ER. 5426 to Bureau of Naval Weapons.

(13) Matas, S. J., Hill, M., and Munger, H. P., Metals Engineering Quarterly, 3 (3) (August, 1963).

(14) Pascover, J. S., and Matas, S. J., Fourth Maraging Steel Project Review (June, 1964) (Project 12018 TR 12018-57)

(15) Johnson, H. H., Sneider, E. J., and Troiano, A. R., WADC Tech. Rept. 57-340 PB. 131654-075 (December, 1957).

(16) Cotton, B. L., Boeing Airplane Company, Report Test T2-1547 (June, 1958).

(17) Klier, E. P., Murdi, B. B., and Sachs, G., Wright Air Development Center Tech. Rept. 56-395-Part III (March, 1957).

(18) Dougherty, E. E., Plating, 415-422 (May, 1964)

THERMOMECHANICAL TREATMENT OF STEEL

by

J. J. Harwood and R. Clark*

INTRODUCTION

Thermomechanical treatment (TMT) has become an accepted descriptive nomenclature for the processing of steels involving a combined cycle of mechanical working and heat treatment to achieve desired mechanical properties. It has assumed particular significance for the development of ultrahigh-strength steels which exhibit useful ductility and toughness characteristics. Such processing combinations are not novel and have had a history of industrial usage, as for example, patenting, strain aging, zero rolling and related processes. Indeed it is somewhat surprising that more concentrated attention to the use of TMT to achieve superior properties did not arise earlier, in view of the prior industrial art which existed. One contributing factor to the recent emergence of interest along these lines has been the increasing requirements for higher strength materials in military and space systems, but as will be noted later, important technological advances can also be achieved for more conventional industrial applications.

CLASSIFICATION OF TMT

A variety of alloys and combinations of deformation and thermal treatments have been investigated during the past several years and a number of recent reports have reviewed the progress in this field quite comprehensively.[1-5]** Radcliffe and Kula[2] have attempted to introduce some degree of systematization in consideration of TMT by classifying the treatments into three principal groups:

I – deformation of austenite prior to transformation
II – deformation of austenite during transformation
III – deformation after transformation of austenite

The Type II treatment includes the well established methods for processing austenitic stainless steels and the semi-austenitic precipitation hardenable stainless steels, involving the transformation of austenite to martensite. In these steels the final structure consists of varying amounts of austenite and martensite and the strengthening occurs as a consequence of strain hardening of both the austenite and the strain-induced martensite. More limited work has been done on deformation during bainite formation in low alloy steels.[6]

The Type III treatments include the deformation and aging of martensites or such isothermal reaction products as bainite. Deformation at room temperature generally is involved, with rapid increases in strength for low deformations; the amount of strengthening increasing, with increasing carbon content. Extremely high strengths (up to 500,000 psi) may be achieved with cold worked (and aged) martensites, but these are usually associated with limited ductility and toughness.[2,7] Related properties have been reported for deformed bainites.[8,9]

Although interesting properties can be achieved by these two types of treatments, most of the recent work and interest has been centered on TMT involving the deformation of austenite prior to quenching to martensite. In view of the more advanced technological development of martensitic steels involving the prior deformation of austenite, discussion in this paper will be confined to this type (Type I) of TMT.

AUSTENITE DEFORMATION TMT

The essential features of this process are the plastic deformation of austenite in a time-temperature range, (such that little or no decomposition to isothermal transformation products occurs) immediately followed by quenching to martensite and subsequent tempering. In principle, the temperature of deformation can be either in the stable or metastable austenitic range, see Figure 1. The former corresponds to the normal hot-working processes for steel and has been designated in the Soviet literature[10] as "High Temperature Thermo Mechanical Treatment" (HTMT). Grange[11] has shown that control of the hot working technique can result in significant reduction in grain size and improved mechanical properties of the final product. By heating and deforming at lower temperatures than in conventional hot working practice, hot working can be utilized, not only to provide an economical method for changing shape, but to provide strength improvements through thermomechanical treatment.

The bulk of activity, however, has been centered on the deformation of metastable austenite, so as to avoid or minimize recrystallization (correspondingly designated as low temperature thermomechanical treatment (LTMT) by the Soviets). The technologically important alloys for achieving optimum strengthening effects by this

* J. J. Harwood, Manager, Metallurgy Department, Scientific Laboratory, and R. Clark, Manager, Metallurgical Engineering Department, Applied Research Office, Ford Motor Company.

** References are given on pages 212 and 213.

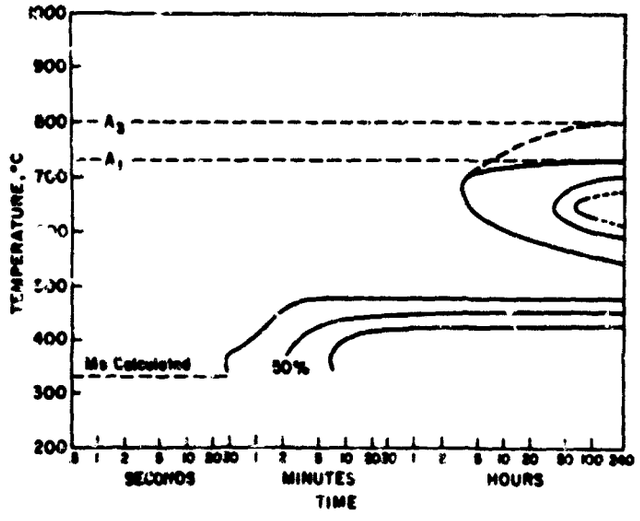

FIGURE 1. TIME-TEMPERATURE-TRANSFORMATION DIAGRAM FOR A 3Mo-3Ni-0.2C STEEL

process are those which exhibit a suppressed pearlite nose and a deep "bay" in the isothermal transformation diagram. These characteristics provide a wide latitude of temperature and time conditions for the deformation of the metastable austenite, without decomposition to isothermal transformation products during the deformation step.

Ausforming[3] has become an accepted term for describing the process of deforming of metastable austenite within the temperature region that exists in the "bay" between the transformation zones of pearlite and bainite, quenching of the strain hardened austenite to martensite, followed by tempering of the martensite so formed. More recently, the term hot-cold working has been gaining recognition[1,5] to cover a broader range of deformation temperatures within the metastable austenitic range.

The significant feature of the process is that martensite formed from deformed austenite has substantially greater strength, with similar or greater ductility and toughness, than that obtained in conventionally quenched and tempered martensitic steels. Depending upon alloy composition and processing variables, a strength increase of over 100,000 psi can be achieved. For example with a Vasco MA steel (Figure 2), ausforming provides:

Tensile strength	450,000 psi
Yield strength	400,000 psi
Elongation	7%
Reduction in area	35%

Typical properties (Figure 3) of ausformed H-11, a leaner alloy steel, are:

Tensile strength	400,000 psi
Yield strength	340,000 psi
Elongation	8%
Reduction in area	40%

It may be noted from Figures 2 and 3 that the strength properties of the ausformed steels at 1000 F are equivalent to the room temperature properties of the conventionally treated alloys.

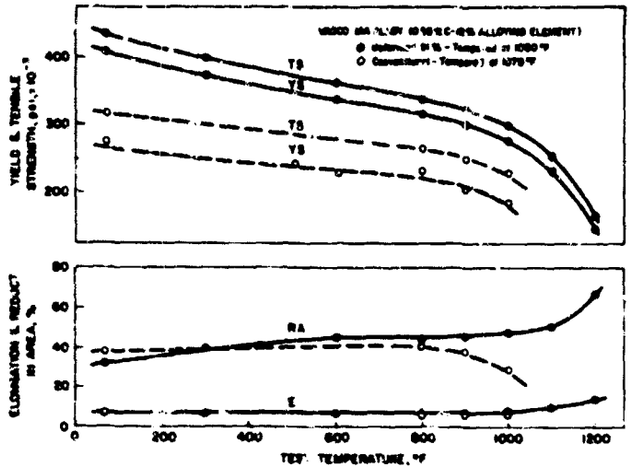

FIGURE 2. EFFECT OF TEMPERATURE ON TENSILE PROPERTIES OF AUSFORMED AND CONVENTIONAL VASCO MA STEEL

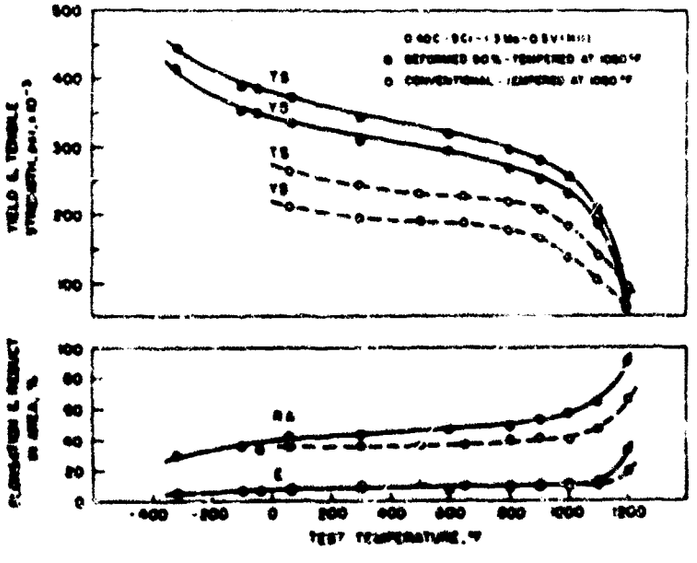

FIGURE 3. EFFECT OF TEMPERATURE ON TENSILE PROPERTIES OF AUSFORMED AND CONVENTIONAL H-11 STEEL

The DMIC report by Marschall[1] is a thorough survey of available information on the hot-cold working response of over 60 different alloy steels

and the influence of such variables as alloy composition, austenitizing temperature, deformation temperature, degree of deformation, tempering treatment, etc., on the final properties. A repetition of such information is not necessary here in the light of existing familiarity with this process in the technical community interested in high-strength steels. Intensive activity during the past few years in our laboratories and elsewhere has led to a clear rationale of the strengthening mechanisms underlying the ausform process, and we thought that it might be more appropriate for the purposes of this conference to present a picture of the important features underlying the strengthening process. It is our belief that this picture is not only useful in rationalizing much of the available data in the literature on the properties of ausformed and not-cold worked martensitic steels, but provides an important guide for the efficient design of alloy composition and working schedules so as to achieve optimum properties, depending upon specific application requirements. In addition we will also discuss some of the application feasibility studies of ausformed steels which are underway at the Ford Motor Company.

MECHANISM OF STRENGTHENING BY AUSFORMING

Numerous mechanisms have been discussed in the literature[1,12,13,14] as contributing to the strengthening of steels by ausforming, involving such features as austenite strain hardening, dispersion hardening, fibering and preferred orientation, fine martensite plate size, interstitial solid solution strengthening by carbon, residual stresses, twinning, carbon-dislocation locking, etc. Consideration of the previously established effects[3,12] of alloy composition, carbon content, and amount and temperature of deformation on the properties of ausformed martensitic steels led to the recognition that the microstructural alterations occurring in the austenite during deformation were exerting a major influence upon the properties of the final martensitic state. It became clear that more information was needed about the deformation response of metastable austenite and the mechanism by which the strain hardened austenitic condition influenced the strength of the subsequently formed martensite.

Macroscopic Behavior of Metastable Austenite

Work,[12] using a steel with an M_s below room temperature (0.33C, 12Cr, 8.5Ni), had shown that the yield strength of austenite increased with increasing amounts of deformation and decreasing temperature of deformation (as would be expected) and that the increases could be correlated with the strength increases for the martensite formed from the strain-hardened austenite over the same deformation conditions. Whereas, all of the results in carbon-containing alloys indicated that the strength properties of the ausformed steels were in direct proportion to the degree of prior deformation of the austenite, Tamura[15] had reported that the hardness of martensite formed from either annealed or strain-hardened austenite was about the same in a low carbon (0.006% C) Fe-30% Ni alloy. This finding was confirmed and extended by Justusson[16] who showed, in fact, that the hardness and yield strength in low-carbon (0.01) Fe-Ni alloys were similar for austenite deformed 90%, martensite formed from such deformed austenite, or martensite formed from annealed austenite. The importance of carbon as an essential feature of the ausform process was obvious and attention was focused on the role of carbon in contributing to precipitation of the austenite, its interrelationship with alloy solutes, its interaction with dislocation structure and its effects on the final martensitic state.

Gerberich and coworkers[17] therefore investigated the macroscopic yield behavior of metastable austenite at 1000 F in a series of steels containing different carbon contents and differing amounts of Cr, Mo, V, and Ni as major alloying elements. Multiple yielding, i.e., serrated stress-strain curves, was exhibited by those steels containing alloy carbide forming elements, whereas when such elements were absent, no such effects were observed. These observations were confirmed by McEvily, et al[14], and an example of serrated stress-strain behavior is shown in Figure 4. The degree of serrations increased with increasing concentration of alloy carbide formers and decreased with decreasing temperature. Such multiple yielding behavior, known as the Portevin-LeChatelier effect, is usually associated with a strong interaction between dislocations and strain-induced precipitates formed during deformation.

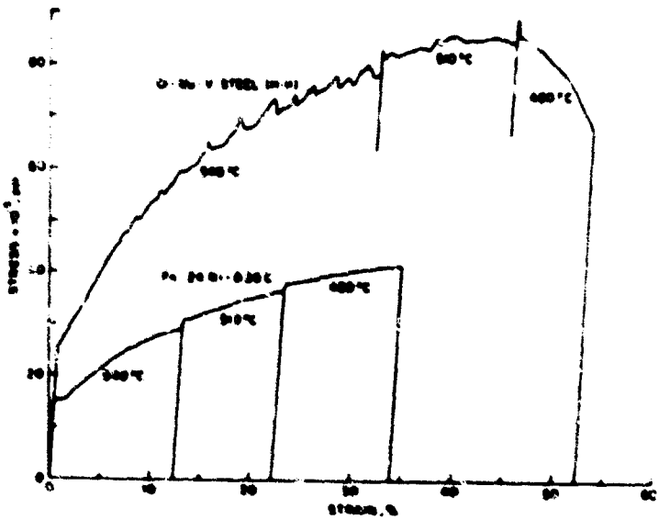

FIGURE 4. STRESS-STRAIN RELATIONSHIPS OF AUSTENITE OF TWO DIFFERENT COMPOSITIONS. TEST TEMPERATURES NOTED ON GRAPH[14]

These preliminary observations led to a more systematic and detailed investigation, by Thomas, Schmatz, and Gerberich,[18] of the strain hardening behavior of metastable austenite. A base composition of Fe-25Ni-0.3C was utilized, with varying amounts of Mo, Cr and V. The nickel composition was adjusted so that the alloys had an M_s temperature of about -40 C, which enabled convenient examination of the austenite behavior. The results again showed that only those alloys containing carbide forming solute elements (e.g., Mo, Cr, V) exhibited serrated stress-strain curves. In addition, the highest strengths and highest strain-hardening response of the austenite were observed in those alloys which exhibited such multiple yielding behavior. Figure 5 shows the comparative stress-strain behavior for two alloys, with and without molybdenum. Note that the room temperature properties of both alloys were similar in the absence of prior deformation, indicating little solid solution strengthening of molybdenum in the austenite. Deformation at elevated temperature (755 K) reveals the significant effect of the molybdenum addition upon the strain hardening response of the austenite (bottom two curves). The most striking effect of the carbide forming elements can be seen by the comparison of the properties of the austenite at room temperature, after deformation at 755 K. The molybdenum containing alloy had a 71% increase in room temperature yield strength, as compared to only a 31% increase in the alloy with no carbide forming element. A useful correlation of the effect of alloying elements upon the strength of room temperature austenite can be obtained through the use of the parameter, nk* (derived from true stress-true strain curves). Figure 6 shows that the higher the elevated temperature strain-hardening response of the alloyed austenites, the higher the room-temperature properties. Of the alloys investigated, molybdenum additions produced the maximum strengthening.

Microstructure of Deformed Metastable Austenite

Such macroscopic behavior of deformed metastable austenite obviously must be related to the microstructural changes in the austenite produced by the deformation process. Two factors which would be of most significance are (a) an increase in dislocation density and point defects and/or (b) the nucleation and precipitation of finely dispersed alloy carbides. Since, as shown in Figure 5, the room temperature deformation of the alloyed austenites indicated little influence of solute carbide formers in solution upon strain hardening response and since, as previously discussed, in the absence of carbon, little effect of prior deformation upon the properties of ausformed alloys had been observed, it appears that increased dislocation density, per se, cannot fully account for the superior room temperature properties of the austenite predeformed at elevated temperatures. The strong effects of carbide forming solutes upon the strain hardening response of the austenite at elevated temperatures and upon the subsequent properties at room temperature are most likely associated with the formation of a fine dispersion of alloy carbides and the interaction of such carbides with deformation induced dislocation substructures. This key role of alloy carbide precipitation in the ausform process had been proposed earlier by McEvily and coworkers[13,14], and their analysis focused attention on this feature of the strengthening process.

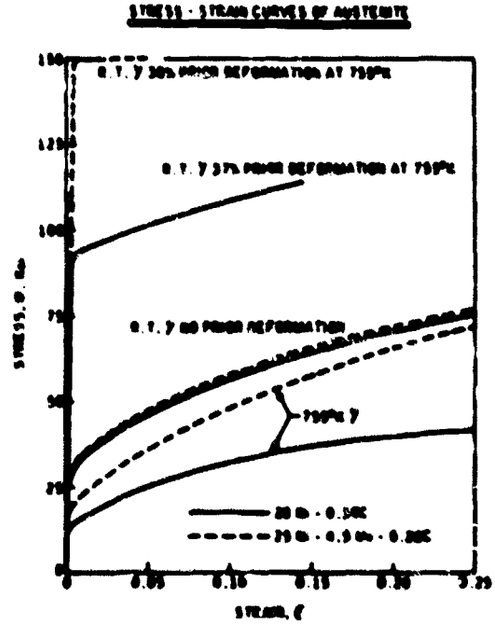

FIGURE 5. STRESS-STRAIN CURVES FOR AUSTENITIC ALLOYS[16]

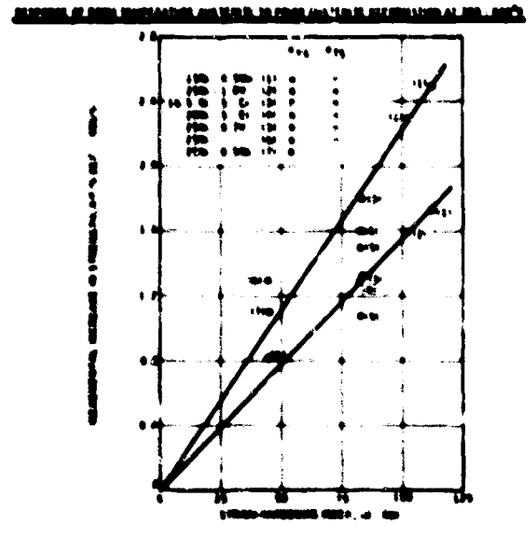

FIGURE 6. USEFULNESS OF nk PARAMETER IN CORRELATING EFFECTS OF ELEVATED TEMPERATURE DEFORMATION OF AUSTENITE UPON ROOM-TEMPERATURE PROPERTIES[18]

*n and k are the stress hardening exponent, and strength coefficient, as defined in $\sigma = k\varepsilon^n$

Strong evidence for the occurrence of such precipitation was obtained by Thomas, et al[18], in the above described study. Using carbon extraction replica techniques, small amounts of alloy carbides were extracted directly from austenite which had been deformed at 510 C, from only those steels containing alloy carbide forming elements. Positive identification of Mo_2C, $Cr_{23}C_6$ and VC (depending upon the alloy) was made. Further direct evidence of alloy carbide formation was observed in thin foil electron transmission microscopy examination. Figure 7 illustrates the presence of carbides in the deformed austenite, associated with complex tangles of dislocations. Yield-strength calculations, based upon measured particle size and effective spacing (using the Orowan model) were in reasonable agreement with the observed strength values.

The increased dislocation density in the deformed austenite introduces nucleation sites for alloy carbide precipitation. In addition, the precipitation of carbides are promoted by the production of vacancies during plastic deformation which enhances the rate of diffusion of alloy carbide forming elements. Calculations of diffusion rates and distances[14, 18] are consistent with such a nucleation and precipitation process. The fine dispersion of alloy carbides not only provides strong barriers to dislocation motion but further increases the rate of work hardening by increasing the rate of dislocation multiplication. Since local depletion of alloying elements would occur as a consequence of precipitation localized increase in stacking fault energies and enhanced cross slip and dislocation tangling would be expected. Indeed prior to precipitation Thomas, et al[18], observed that the deformation structure exhibited dislocation arrangements confined to slip planes, whereas after precipitation complex dislocation tangles appeared.

Thus the recent accumulation of evidence appears to support strongly the earlier proposal of McEvily and coworkers[13, 14] that carbide precipitation during the austenite deformation stage was a major factor in achieving ultrahigh-strength steels by the ausform process. It must be noted that even steels containing small amounts or none of the alloy carbide formers exhibit increased strength after ausforming as compared to conventional quenching and tempering treatments (Figure 8). Such strength increases may be due to the precipitation of iron carbides and the strain hardened response of the austenite. The much higher strength values associated with ausformed steels containing Mo, Cr, V and/or other alloy carbide formers is a consequence of the interaction of strain-induced alloy carbide precipitates and dislocation substructure.

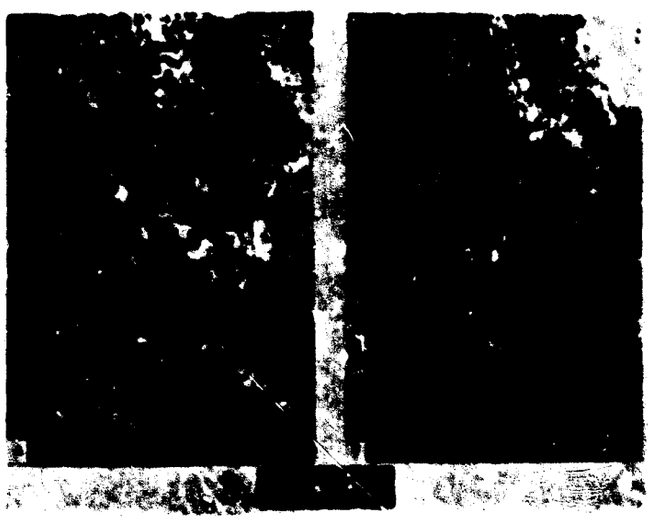

FIGURE 7. TRANSMISSION ELECTRON MICROGRAPHS OF AUSTENITIC SUBSTRUCTURE OF Fe-25Ni-4.5Mo-0.28C ALLOY AFTER 30 PER CENT DEFORMATION AT 510 C[18]

(a) Bright field image; (b) same area using reflection B (matrix and Mo_2C spots). Not. precipitates revealed in dark field image. Photograph was reduced about 25 per cent in printing.

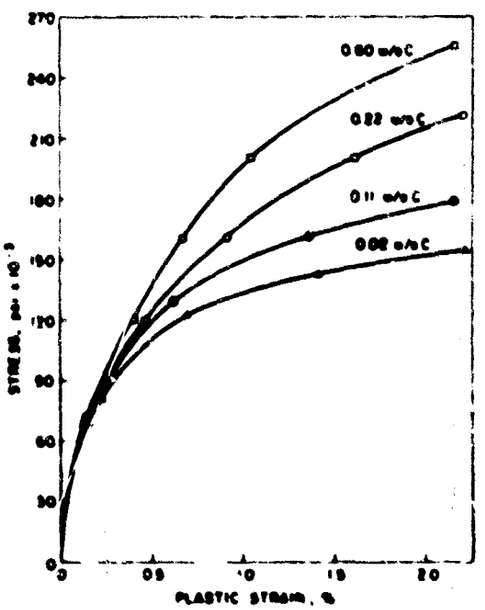

FIGURE 8. STRESS-STRAIN BEHAVIOR OF AS-QUENCHED MARTENSITES AT LIQUID NITROGEN TEMPERATURE[20]

Behavior of Martensite

With this background of information about the deformation induced microstructural changes in the austenite we can consider more specifically the nature of the strengthening mechanism that endows the martensite produced from deformed austenite with its extremely high strength. The work of Schaller and Schmatz[19] showed that direct inheritance by the martensite of defects generated during the deformation of austenite does indeed occur. The inheritance of dislocation substructure and fine alloy carbides is probably the rule rather than the exception. An additional key piece of information came from the studies of McEvily, et al[20], of the sources of strength of conventionally formed acicular martensite. They measured the stress-microstrain behavior of a series of iron nickel carbon martensites whose compositions were chosen so as to obtain a common M_s of about -35 C. They observed that at liquid nitrogen temperatures the flow stress at macroscopic strains increased with increasing carbon content [confirming the earlier observations of Winchell and Cohen[21]], but that permanent plastic strains were obtained at the very low stress of about 10,000 psi, Figure 8. Most strikingly, the initial portions of the microstrain curves were independent of carbon content. These findings led them to conclude that structure of the as-quenched martensite in this system is characterized by a high density of dislocations generated by the volume change that accompanies the austenite-martensite transformation (the volume change is about 4%, and is not too sensitive to carbon content). At liquid nitrogen temperatures, carbon atoms cannot diffuse to dislocations and the carbon distribution in the martensite reflects substantially that which pre-existed in the austenite. The high density of unpinned dislocations permits plastic strains in martensite at very low stresses, whose magnitude is independent of carbon content. At larger strains, the rate of hardening does reflect the carbon level, for as the dislocations move they will eventually interact with the carbon atoms in the matrix. The effectiveness of the carbon-dislocation locking interaction increases with increasing carbon content, saturating out at about 0.5% C. A similar response can be obtained by aging at room temperature, which allows the carbon atoms to diffuse to the dislocations and produce locking.

Thus the macroflow stress of the martensite is essentially that necessary to overcome the short-range resistance of the interstitial atoms (i.e., to unpin the locking points) and in this sense martensite is strengthened by carbon in solution. However, it is much more effective for the dispersion of locking points to be in the form of fine, strong precipitates (such as alloy carbides), for in this situation, the dislocations must bow between the precipitate particles, leaving dislocation loops or tangles around each particle. If the inter-precipitate particle distances are small, <100 Å, significant increases in strength can be achieved. In this connection, it is important to note that the microstrain limit for ausformed alloyed martensites is about 160,000 psi as compared to 10,000 psi for the conventional martensite of Figure 8. The more rapid accumulation of dislocations assures a subsequent high strain hardening rate which is responsible for the observed macroscopic strength levels of 400,000 psi and greater. In correspondence to the mechanical behavior of the austenite, the strength of martensite increases much more significantly with prior deformation of the austenite in those alloys containing alloy carbide formers and therefore, a high strain hardening response of the austenite.

Martensite produced from ausformed alloy austenite, as compared to conventional martensite, is usually finer, more zig-zagged, has a higher dislocation density, contains a fine dispersion of carbide precipitates and much less evidence for twinning - all of which would be expected as a consequence of the precipitation of alloy carbides in the austenite.

Process Variables

To summarize briefly the above picture of the strengthening mechanism of ausformed steels, the principal feature is dispersion hardening resulting from the precipitation of alloy carbides during the deformation of metastable austenite. Those alloys which, as a consequence of carbide precipitation, exhibit the greatest strain harding response of the austenite, produce the strongest martensites. The ausformed martensitic structures contain the deformation produced precipitate and high dislocation densities. The dislocations are both inherited from the austenite and are produced by the lattice shear and dilation associated with the austenite-martensite transformation. As a consequence of the strong interaction between the fine dispersion of alloy carbide precipitates and the dislocation substructure, the martensite also exhibits a higher strength than conventional martensites. It is our belief that this picture leads to a clear understanding of the variables which influence the ausform process and to useful concepts for design of optimum alloy compositions to meet desired strength and associated properties. The interactions of carbon content, alloy composition, amount and temperature of deformation are the controlling factors.

(a) Carbon Content

Carbon is obviously essential. In the absence of carbon there is little or no improvement in properties of alloy martensites by ausforming. It has been observed[12,22] within a limited range of carbon content for the same alloy steel, that the incremental increases in yield strength of the final martensite is independent of carbon content. However, this does not necessarily hold when comparing different alloy steels.

(b) Alloy Composition

One primary function of alloy additions is to increase the stability of metastable austenite by suppressing the pearlite nose and increase the height and depth of the bay between the pearlite and bainite bands. This, of course, provides a greater latitude and flexibility in processing so as to avoid the formation of isothermal transformation products, which result in undesirable mechanical properties. The highest strengths are achieved in alloys which contain alloy carbide forming elements (e.g., Mo, Cr, V) as solutes. Fortunately, these same elements also serve to increase the extent of the metastable austenitic bay. The nucleation of the carbides during the deformation stage is promoted by vacancy enhanced diffusion and elements such as molybdenum more readily form small, finely dispersed carbides and exhibit the greatest effect. The alloy carbide formers must be in solid solution in the austenite to be effective. This is particularly important for vanadium and niobium, whose effectiveness may be less than expected if present in the form of carbides during austenitizing prior to the ausform process. Alloy compositions which exhibit the greatest strain hardening response of the austenite produce the strongest martensite.

Amount and Temperature of Deformation

The greater the amount of deformation, the greater is the strain hardening response of the austenite and the higher the likelihood of nucleating carbide precipitates in a finely dispersed form. Significant increases in strengths are achieved by deformations exceeding about 50%. If the final working temperatures are too high, recovery, recrystallization and grain growth may occur which diminish the overall effectiveness of the process. If the temperatures are too low, the rate of diffusivity of the alloy elements may not be sufficient to nucleate alloy carbides. Finishing temperatures in the vicinity of the "bay" temperatures, about 850-1100 F are the most effective. For steels containing alloy carbide formers, the highest strengths are obtained when the deformation temperature corresponds to that at which secondary hardness peaks are observed in conventionally quenched and tempered steels.

Total Processing Time

For steels with a deep metastable bay, time involved in processing is not a critical factor. Little or no evidence of isothermal transformation products has been observed. Some of the alloys have been held at temperature for many hours, after deformation, with no deleterious effect upon final properties, indicating the high stability of the dislocation-carbide precipitate interaction. With leaner alloys, the TTT diagram is a useful guide, remembering that deformation results in earlier formation of isothermal transformation products.

Tempering Response

Balanced alloy steels (i.e., those in which the carbon and carbide forming elements are in stoichiometric balance) exhibit the best retentivity of strength upon tempering at elevated tempering temperatures. An excess of carbon or carbide forming element leads to rapid softening at elevated temperatures. Tempering of properly alloyed ausformed steels below the temperature of austenite deformation has little effect upon the strength properties of the martensite. The tempering response, Figure 9, of ausformed steels again indicates the role of a stable dispersion of alloy carbide precipitates in maintaining strength. The elevated temperature strength properties of ausformed steels exhibit similar behavior patterns as the tempering curves in Figure 9

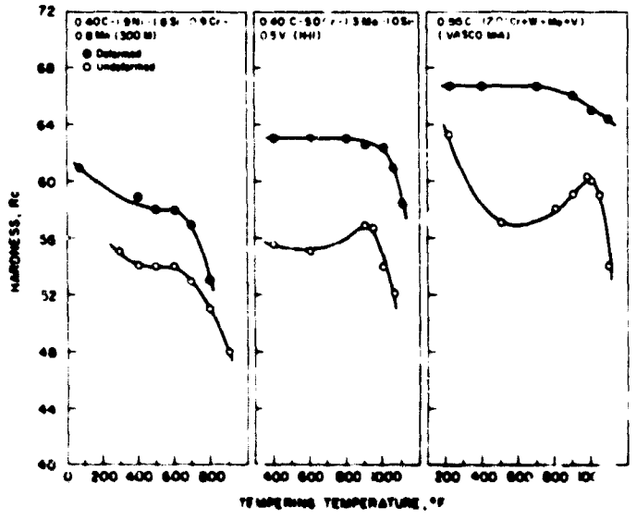

FIGURE 9. TEMPERING RESPONSE COMPARISON OF AUSFORMED AND CONVENTIONAL STEELS

APPLICATION STUDIES OF AUSFORMED STEELS

The technologically interesting combination of properties of high strength, toughness and fatigue resistance have led, naturally, to application studies for the exploitation of ausformed steels. Perhaps the most frequent queries regarding the use of ausformed steels are, "What can be done with steel bars after ausforming?"; "Can other than laboratory size samples be produced?"; "Is there a limitation on methods of working?", "Is the cost of the high alloy steels required for ausforming prohibitive?", "Can the steels be machined?"; "Can they be welded?", etc. The ausforming process is not simple and requires close control of both temperature and deformation and obviously is not the solution to all high strength problems, however, sufficient results are in hand to indicate that, when used intelligently, the process can produce useful components and tools resulting in both improved technical and/or economic performance.

High-Strength, High-Toughness Applications

At the same strength levels, ausformed steels possess greater toughness than conventional quenched and tempered steels (Figure 10) and this advantage has led to consideration of their use for rocket-motor casings, armor and related applications. Large missile cases have been fabricated by shear-spinning techniques and successful attachment of hardware to missile cases by electron beam welding has been demonstrated. Because of the interest in this area the fracture toughness behavior of ausformed steels has received considerable attention. It has been shown[22,23] that the optimum combination of strength, ductility, and fracture toughness results from a maximum of ausform deformation, compatible with a minimum amount of carbon to produce a desired strength level (Figure 11). Indeed properly constituted alloy steels, containing an optimum carbon level, result in a material with excellent fracture toughness. The fracture toughness superiority of ausformed steels, in comparison with competitive materials, can be seen in Figures 12-14 incl. Particularly noteworthy is the excellent behavior of the experimental alloy steel, X2, which is a low-carbon modified H-11 composition.

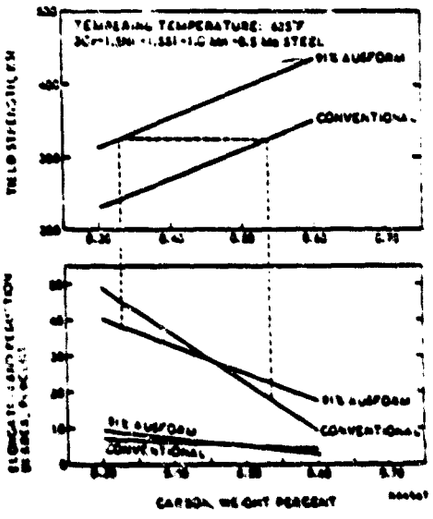

FIGURE 10. STRENGTH AND DUCTILITY PROPERTIES OF AUSFORMED AND CONVENTIONAL STEEL AS FUNCTION OF C CONTENT[22]

At same strength level, ausformed steel has higher ductility.

Automotive Applications

Ausformed steels tend to retain the 50% ratio of endurance limit to tensile strength at higher strength levels than conventional quenched and tempered steels. The excellent fatigue properties of ausformed steels make them especially attractive for cyclically stressed components of an automobile. In such applications, cost factors are important and high alloy steels such as H-11 cannot be used. The alloy steels typically used in automotive applications are in the 8¢ to 12¢/lb. cost range. Of the low alloys suited for ausforming, Ladish D6A alloy (0.5% C, 1% Cr, 1% Mo, 0.5% Ni) at a cost of about 13¢ - 15¢/lb. has shown the most promise, and has been evaluated in several studies, particularly for heavy duty leaf springs.

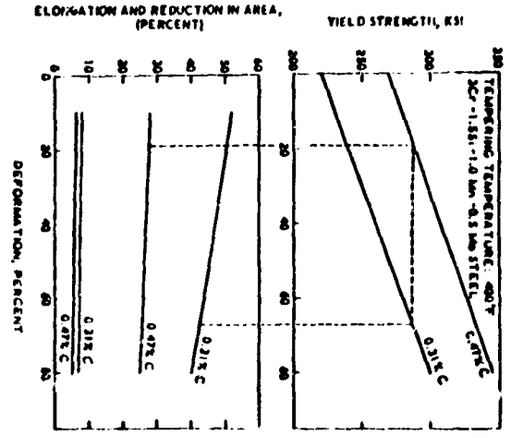

FIGURE 11. STRENGTH AND DUCTILITY PROPERTIES OF AUSFORMED STEEL, AT TWO DIFFERENT CARBON LEVELS, AS A FUNCTION OF AMOUNT OF DEFORMATION[22]

For same strength level, carbon content and higher ausform deformation results in greater ductility.

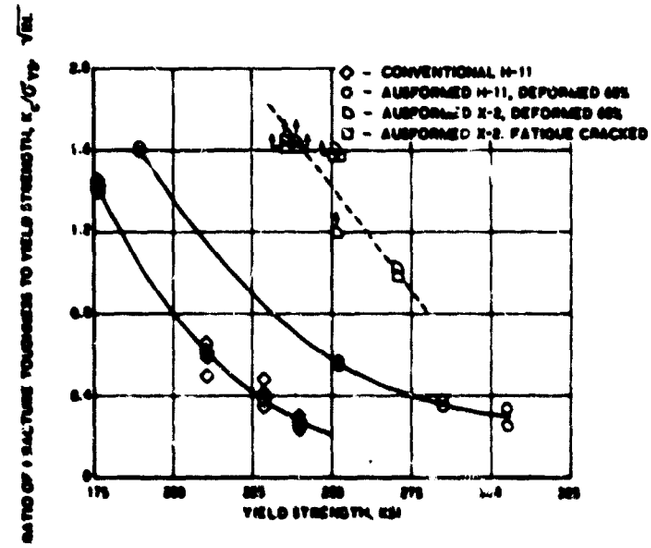

FIGURE 12. FRACTURE-TOUGHNESS-YIELD STRENGTH COMPARISON FOR AUSFORMED AND CONVENTIONAL STEELS[23]

Figure 15 shows the fatigue behavior of SAE 5160 conventional springs and D6A ausformed samples of 1/4" thickness x 2-1/4" wide. These samples were prepared on our laboratory

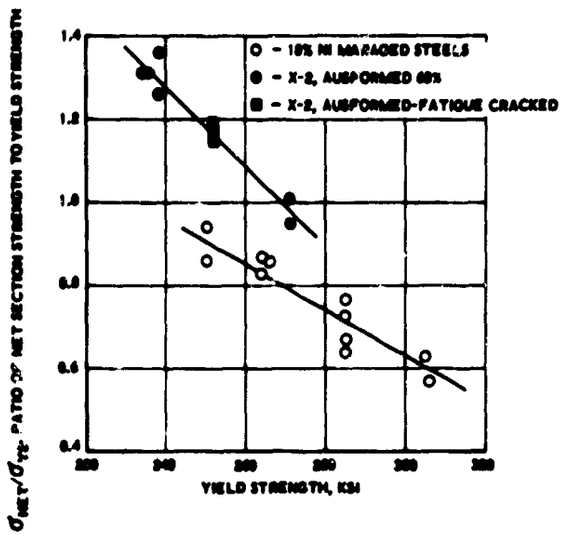

FIGURE 13. FRACTURE TOUGHNESS-YIELD STRENGTH COMPARISON OF AUSFORMED AND MARAGED STEEL[23]

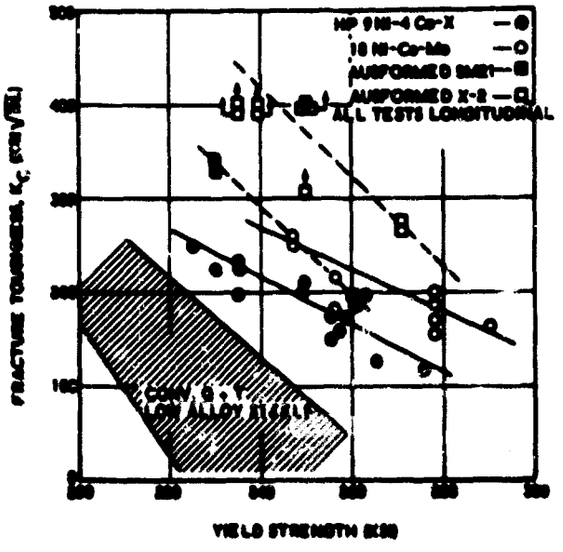

FIGURE 14. FRACTURE TOUGHNESS COMPARISON OF AUSFORMED 5H21 AND X2 STEELS WITH OTHER COMPETITIVE MATERIALS[23]

mill with a maximum separating force of about 62 tons. Based on the properties obtained with these samples, a full scale design was made for a heavy truck spring. The design showed a possibility of a 30% reduction in weight from 196 to 136 lbs., with 8 leaves instead of 17. While some scale-up problems in the form of reduced fatigue lives, have been encountered with 5/8" thick ausformed leaves, it is expected that the six complete springs will be assembled for test by the end of the year. The design was based on the use of leaves, 5/8" thick x 3" wide; which have been produced on a commercial mill, with up to 50% reduction in thickness in one pass. The mill separating force

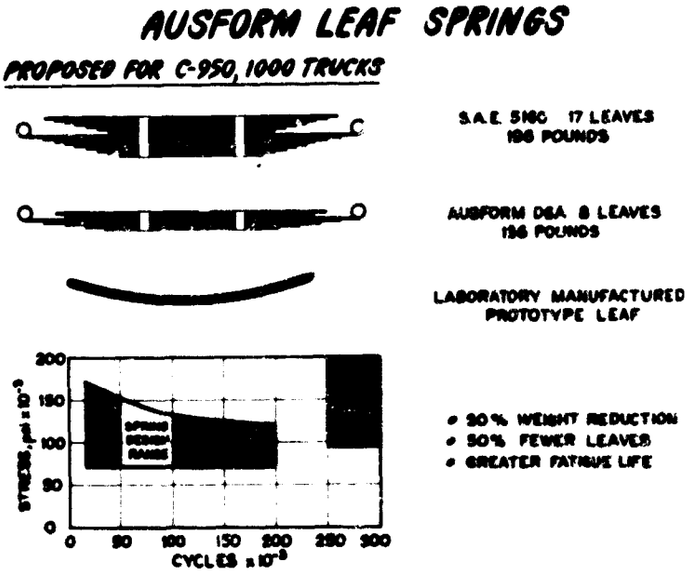

FIGURE 15. ADVANTAGES OF AUSFORMED STEELS FOR LEAF SPRING APPLICATIONS

was about 600 tons in this case and 350 hp were used. Incidentally, plate up to 18" wide and 1/2" thick has now been successfully ausformed on a commercial mill.

In addition to leaf springs, torsion bars are also being considered. Figure 16 shows the torsional properties of ausformed H-11 for several different treatments. The usefulness of strain aging to improve shear fatigue strength is quite remarkable. In addition to H-11, D6A also has excellent torsional fatigue resistance and both straight torsion bars and 'U' shaped flat plates are being considered. The straight bar, while much shorter than a conventional torsion bar (24" vs. 60") has presented end fixture problems which are not easily resolved. The flat 'U' shape is much simpler to fabricate and has added advantages in the vehicle.

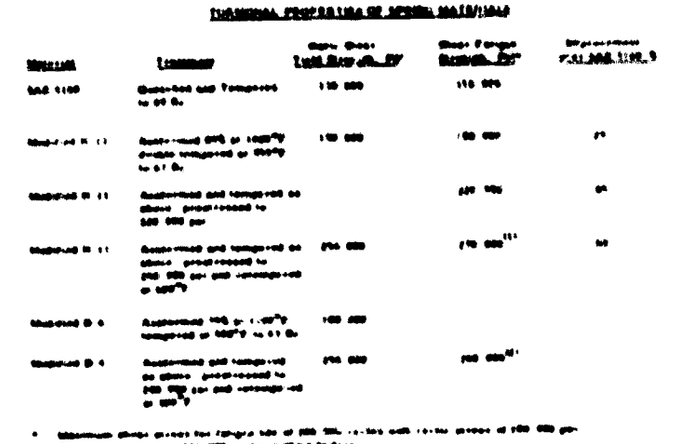

FIGURE 16. TORSIONAL PROPERTIES OF AUSFORMED SPRING MATERIALS

Tooling Applications

Because of the high strength, hot hardness, toughness and fatigue strength of ausformed steels, an obvious area of interest was in tooling applications. At the Ford Motor Company we have investigated the behavior of ausformed H-11 and Vasco MA in cold work and H-13 in hot work applications with notable success.

Figure 17 shows two cold heading punches which were used in our Indianapolis Plant. The conventional tool steel used in these punches was T5, an 18% W, 4% Cr, 1% V, 8% Co alloy. The larger tool was made from ausformed H-11 and produced an average of 100,000 pieces compared to 30,000 for the T5 material. The smaller punch was made from ausformed Vasco MA steel and showed a life increase of 300%; 160,000 pieces compared to 50,000.

FIGURE 17. AUSFORMED COLD HEADING PUNCHES

A small rivet upsetter showed a similar life improvement of 300%; 600,000 pieces produced compared to 200,000.

Figure 18 shows a combined piercing and extrusion punch and illustrates the longitudinal grinding used to improve fatigue life. The conventional tool material in this case was M2 type high-speed steel and the tool failure occurred by fatigue. At an average life of 77,000 pieces, the piercing tip had broken off. Ausformed H-11 tools showed a higher life of 120,000 pieces and the failure was by wear on the extrusion shoulder; the piercing tips did not break off.

FIGURE 18. AUSFORMED PIERCING AND EXTRUSION PUNCH

Another investigation was that of a rivet punch; this was a severe impact and wear application, for which conventional S5 steel was used. The life in this case was measured in useful time and averaged 42 hours for S5 at Rc61, 64 hours for ausformed H-11 at Rc62, and 72 hours for ausformed Vasco MA at Rc66.

Perhaps one of the more interesting trials of ausformed steels has been the use of H-13 as a hot shearing punch in our Canton Forge Plant. The punch is shown in Figure 19 and was used to make a 1" dia. hole in a hot forged blank for a differential side gear. The piercing operation was done on a vertical press at the same time as the outside diameter of the forging was trimmed. The conventional tool material was H-12 steel and the average life of the punch was about 14,000 pieces. The usual mode of failure was by heat checking and washing of the thermal fatigue cracks which when severe enough, gave ragged holes and caused the forging to stick on the piercing punch.

Ausformed H-13 punches which were produced by vertical extrusion on a 400-ton MaxiPress showed an average life of 25,800 pieces and the mode of failure was generally wear. This can be seen in Figure 20. The punch tip wore away and the punches were finally removed from service because of undersize holes. A variety of hardness levels were investigated and it is interesting to note that an ausformed punch tempered at 950 F (Rc 60.5) pierced 39,470 pieces. Subsequently, 20 punch blanks have been produced on a 7" upsetter in H-12 material and tempered to Rc60; these are yet to be tested, and it is believed that they will outlast the H-13 punches because of the 1.4% tungsten content of H-12 included for hot wear resistance.

In discussing the technical importance of using ausformed steels in tooling applications economic factors must also be considered. A quick look at the cost of the material used in the cold heading applications (H-11) indicates a substantial reduction in cost. T5 alloy currently sells for about $3.50/lb. while H-11 costs 60¢ - 75¢ lb.

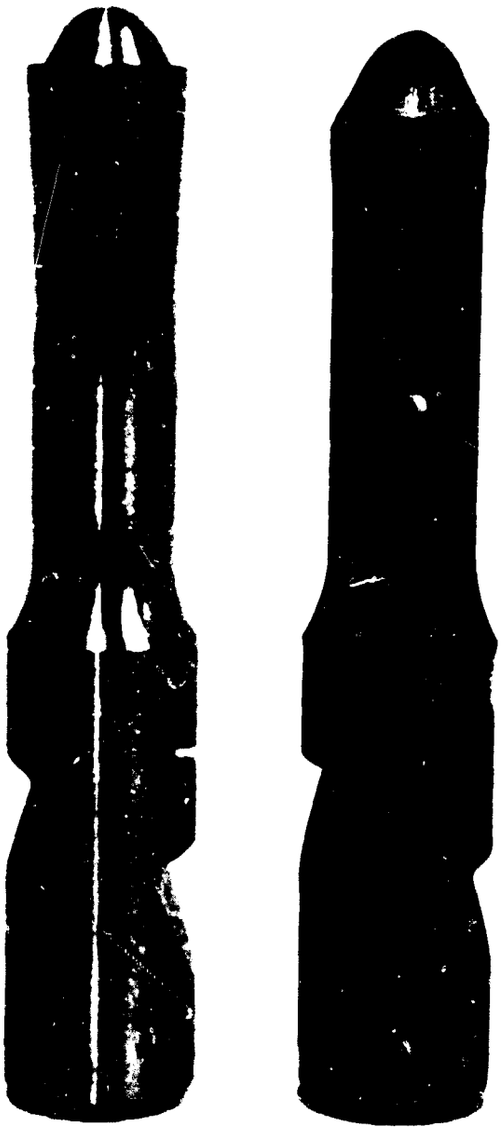

FIGURE 19. AUSFORMED HOT SHEARING PUNCH

Note wear of punch tip after an average life of about 26,000 pieces, as compared to thermal fatigue failures of conventional punches after only 14,000 pieces.

With the exception of the hot piercing punch all of the tools used were ground from rolled bar stock which proved to be quite expensive. The piercing punch was formed by extrusion and as little as 0.020" finish stock was left for final grinding. In this case the material cost was the same for ausformed or conventional tools, but because of the trade off on heat treatment and rough machining cost against ausforming operations, the final tool costs would, on a production basis, be comparable and show real savings to the manufacturing operation in both improved tool life and reduced down time.

FIGURE 20. AUSFORMED PISTON PIN FABRICATED BY BACKWARD EXTRUSION

The use of ausformed steels for tooling has shown exceptional potential and further studies of production techniques are being planned. Extrusion close to final size seems to be a requisite to reduce the finishing costs after ausforming. Three parameters control the amount of stock to be left for finishing: (a) decarburization, which can be controlled by proper billet preparation and furnace atmosphere control, (b) surface transformation because of die chilling which can be almost eliminated by the use of heated dies, and (c) surface finish, which is dependent on proper lubrication of the die during extrusion. Of the three, the problem of lubrication to decrease die loads, improve surface finish and increase die life, is the least controllable. At the moment, no completely satisfactory lubricant has been developed, but graphite-oil mixtures have given reasonable service. The newer tungsten sulphide lubricant is being studied, and shows some promise. In any event, finish grinding and electrochemical or electrical discharge machining, can be used with an ausformed tool blank as readily as on a conventional rough machined and heat treated tool.

Thus far we have only discussed applications involving simple shapes that could be readily rolled or extruded. However, our studies have not been limited to these and Figure 20 shows an example of a backward extrusion of a D6A alloy piston pin. In this case, the slug was placed in a die and hit with two punches simultaneously to produce a hollow cylinder with a central web. The fatigue characteristics of these pins compared with conventional cold extruded and carburized piston pins were similar and such ausformed piston pins met all the engineering requirements for the size produced and tested.

The yield strength of the austenite of H-11 and D6A alloys at the 1000 F deformation temperature has been shown to be in the 15,000 to 20,000 psi range. Consequently, it is possible to form complex shapes although the strain hardening rate is high and the loads required for completion of deformation rise rapidly. Nevertheless, to illustrate feasibility a small gear shape was produced by ausform techniques in the D6A alloy composition. It was possible to produce the solid gear shape by one blow from a right circular cylinder on a 400-ton MaxiPress. When the lower center hole was predrilled, and the upper one was formed by a moving punch, a 95% die cavity fill was reached. The ausformed hardness increase was found at the tooth root where it would be most beneficial for improved fatigue life. This suggests that it would be possible to start the ausforming operation with a hot forged preform to reduce the ausform forging loads but still achieve the ausforming benefits at the tooth root to reduce fatigue failures.

SUMMARY

Thermomechanical treatment of alloy steels, involving the deformation of austenite prior to quenching to martensite, is a highly effective means for achieving ultra high hardness, fatigue strength, fracture toughness and wear resistance. The best properties are obtained in alloys containing balanced compositions of carbon content and alloy carbide forming elements such as Mo, Cr, V, etc. Dispersion hardening of the martensite, as a consequence of strain-induced alloy carbide precipitation during the deformation of the austenite, appears to be a key feature of the Ausform process. A clear understanding of the process variables which influence the ausform process and a basis for design of optimum alloy compositions to meet desired properties are now in hand. Numerous application studies, some of which are approaching a full production state, have indicated that both improved technical performance and economic advantages can be derived from the appropriate utilization of ausformed steels.

ACKNOWLEDGEMENTS

The authors wish to express their gratitude to A. J. McEvily, D. J. Schmatz, T. L. Johnston of the Ford Research Laboratory for providing background information and helpful discussion and to W. W. Gerberich, C. F. Martin, and L. Raymond of the Philco Corporation and G. Thomas of the University of California for making available copies of papers prior to publication.

REFERENCES

(1) Marschall, C. W., "Hot-Cold Working of Steels to Improve Strength", DMIC Report 192, Battelle Memorial Institute, Columbus, Ohio (October 11, 1963).

(2) Radcliffe, S. V., and Kula, E. B., "Deformation, Transformation and Strength", Proceedings of the Conference on Fundamentals of Deformation Processing, Sagamore, New York (August, 1962).

(3) Zackay, V. F., and Justusson, W. M., "The Properties of Martensitic Steels Formed From Strain Hardened Austenite", Special Report 76 "High Strength Steels", The Iron and Steel Inst., London, 14 (1962).

(4) Hopkins, A. D., and Ray, M. J., "A Literature Review on Thermo Mechanical Treatments", Metal Treatment and Drop Forging, 3 (January, 1963).

(5) Matas, S. J., Hill, M., and Munger, H. P., "Ausforming and Hot-Cold Working - Methods and Properties", Mechanical Working of Steel I", edited by P. H. Smith, Met. Soc. Conf., Gordon and Breach, 21, 143 (1963).

(6) Radcliffe, S. V., et al, "The Flow Tempering of High Strength Steel", Man Labs, Inc., Watertown Arsenal Labs. Tech. Dept. No. 320.4/3.1 (April, 1962).

(7) Breyer, N. N., and Polakowski, N. H., "Cold Drawing of Martensitic Steels to 400,000 psi", Trans. ASM, 55, 667 (September, 1962).

(8) Kalish, D., Kuhn, S. A., and Cohen, M., "Thermomechanical Treatments Applied to Ultra High Strength Bainites", to be published by ASTM Symposium on Steels with Yield Strengths over 200,000 psi.

(9) Kalish, D., Kuhn, S. A., and Cohen, M., "Thermomechanical Treatments Applied to H-11 Steel with Special Reference to Bainite Structure", to be published in J. of Mets.

(10) Ivanova, V. S., and Gordiyenko, L. K., "On the Nature of the Strengthening of Metals During Thermomechanical Treatment", Russian Metallurgy and Mining No. 1, 66 (1964).

(11) Grange, R. A., "Microstructural Alterations in Iron and Steel During Hot Working", Proceedings of the Conference on Fundamentals of Deformation Processing, Sagamore, New York (August, 1962).

(12) Schmatz, D. J., Schaller, F. W., and Zackay, V. F., "Structural Aspects and Properties of Martensite of High Strength", Proceedings of Conference on the Relation between Structure and Strength in Metals and Alloys, NPL, England (January, 1963).

(13) McEvily, A. J., and Bush, R. H., "An Investigation of the Notch-Impact Strength of an Ausformed Steel", Trans. ASM, 55, 654 (1962).

(14) McEvily, A. J., Bush, R. H., Schaller, F. W., and Schmatz, D. J., "On the Formation of Alloy Carbides During Ausforming", Trans. ASM, 56, 753 (September, 1963).

(15) Tamura, I., et al, "Hardness and Structure of Ausformed Fe-Ni, and Fe-Ni-C Alloys", Trans. Japan Inst. of Metals, to be published.

(16) Justusson, W. M., and Schmatz, D. J., "Some Observations on the Strength of Martensite Formed from Cold-Worked Austenite", Trans. ASM, 55, 640 (September, 1962).

(17) Gerberich, W. W., Martin, C. F., and Zackay, V. F., "Multiple Yielding of Metastable Austenite in Ausform Steels", Trans. ASM, to be published.

(18) Thomas, G., Schamtz, D. J., and Gerberich, W. W., "Structure and Strength of Some Ausformed Steels, Proc. of 2nd Int'l Symposium on High Strength Materials, Berkeley, California (1964), to be published.

(19) Schaller, F. W., and Schmatz, D. J., "The Inheritance of Defects by Martensite", Acta Met., 11 (10), 1193 (1964).

(20) McEvily, A. J., Ku, R. C., and Johnston, T. L., "Micro Yielding of Martensite", to be published.

(21) Winchell, P. G., and Cohen, M., "Electron Microscopy and Strength of Crystals", edited by G. Thomas and J. Washburn; Interscience, New York, 995 (1963).

(22) Raymond, L., Gerberich, W. W., Martin, C. F., "Effect of Carbon on the Strength, Ductility and Fracture Toughness of Ausformed Steels", Trans. ASM, to be published.

(23) Gerberich, W. W., et al, "Ausform Fabrication and Properties of High Strength Alloy Steel", written communication.

ADDITIVE STRENGTHENING MECHANISMS AND THE STRUCTURE OF STEEL

by

Professor J. Nutting*

The basic mechanisms by which the strength of metals may be raised are now very well understood. The mechanisms which are of practical importance are all derived from the argument that the strength of a metal will be increased if obstacles to dislocation movement through the lattice are incorporated within the structure. Although it is possible to conceive of strengthening mechanisms which would rely upon reducing the number of dislocations, such materials would be structurally unstable, and therefore, unlikely to be of practical use. Consequently, no further attention will be paid here to strengthening mechanisms of this type.

The obstacles to dislocation movement may be solute atoms in the lattice, other dislocations, dispersed phases and grain boundaries, and well established methods have been devised for introducing these various dislocation obstacles. In order to investigate the basic hardening mechanisms for each type of obstacles, research has followed the classical lines of identifying the variables and then attempting to vary one whilst keeping the others constant. As a result, we know much about each of these mechanisms. In the case of steels, all these mechanisms have been briefly reviewed by Kelly and Nutting[1]**, whilst there are numerous reviews dealing with individual hardening mechanisms as applied to a variety of alloy systems, e.g., Kelly and Nicholson[2] on dispersion hardening, and Fleischer and Hibbard[3] on solid-solution hardening.

In recent years, there has been a growing awareness that in order to obtain very high strengths in metals, no single hardening mechanism would be sufficiently effective, but combinations would be required. But what combinations are to be used? As is still the case with most metallurgical developments, it is the empirical and almost intuitive approach of metallurgists that has been successful in achieving suitable combinations. The cold drawing of patented steel wire, and more recently the ausforming operation, have all been developed as a means of producing high strengths, whilst the arguments for the underlying causes are still exercising the more academic metallurgists. However, what is certain is that there is more than one conventional hardening mechanism playing a significant role in each of these cases.

The four basic hardening mechanisms associated with dislocation-dislocation, dislocation-solute, dislocation-dispersed phase, and dislocation-grain boundary interactions, may be combined in six different ways taking two mechanisms at a time, and in four different ways with three mechanisms operating, whilst there is the possibility of making all four operate simultaneously. Thus, eleven cases of additive hardening could be considered.

A brief discussion will be given of these various cases in relation to iron and steel. The structure of high-strength steels produced by cold drawing, by quenching to give martensite, by tempering secondary hardening steels, and by ausforming will then be discussed in relation to the additive effects of the various operative hardening mechanisms.

I. The Interaction of Two Hardening Mechanisms

(a) Solid-Solution and Grain-Boundary Hardening

Petch[4] and co-workers have shown that the lower yield point in α-iron is related to the grain size by an expression of the type:

$$\sigma_{LYP} = \sigma_o + k\left(\frac{1}{D}\right)^{1/2} \qquad (1)$$

σ_{LYP} = lower yield stress

σ_o = frictional stress, i.e., the stress required to make a dislocation move through the lattice

k = constant

D = grain diameter.

If alloying elements are added to α-iron equation (1) is still obeyed, but the value of the frictional stress is raised [see Section I(c)]. The value of k is usually raised for substitutional elements, unless there is an interaction between substitutional and interstitial elements, when k may be lowered. An example of this[5] is the effect of manganese which interacts with nitrogen, so lowering k.

In general, the changes of σ_o and k are more marked with solutes which form interstitial solid solution than with those which form substitutional solid solutions. As an example of this, Codd and Petch[6] showed that the value for k was increased by a factor of 1.5 when boron additions were made to α-iron. However, with the limited solubility of boron in iron, this element would not appear to provide a very suitable means of achieving high strengths in fine-grained iron.

(b) Work Hardening and Grain Boundary Hardening

The flow stress of α-iron is related to the dislocation density[7,8] by an expression of the type:

*Department of Metallurgy, The Houldsworth School of Applied Science, The University, Leeds, England.

**References are given on page 220.

$$\sigma_F = \sigma_o' + k' \ell^{1/2} \quad (2)$$

where σ_F = flow stress

σ_o' = frictional stress

k' = constant

ℓ = average dislocation density.

If the grain size of the iron can be varied, independently of changes in the dislocation density, then it should be possible to add equations (1) and (2) to give the expression:

$$\sigma_F = \sigma_o + \sigma_o' + k\left(\frac{1}{D}\right)^{1/2} + k' \ell^{1/2} \quad (3)$$

Armstrong, Codd, Douthwaite and Petch[9] have attempted to verify this equation. They prepared irons of differing grain sizes by slight variation in the cooling from the austenitic range. They then deformed the specimens by constant amounts, and re-determined the grain-size dependence of the flow stress. If it is assumed that the dislocation density is a function only of the cold work, and not of the initial grain size, then their results showed that for differing amounts of cold work in excess of the yield strain, the value of k in equation (3) remained constant. Their results are shown in Figure 1.

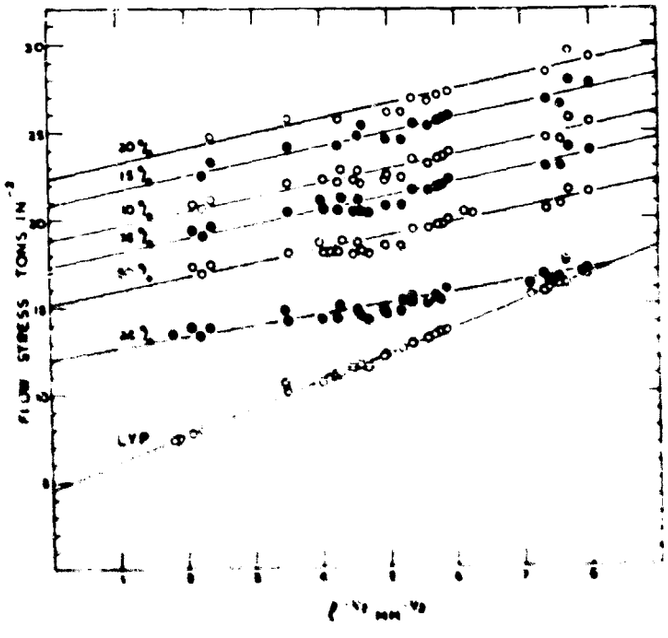

FIGURE 1. DEPENDENCE OF THE FLOW STRESS OF IRON UPON THE GRAIN SIZE AFTER DIFFERENT AMOUNTS OF PLASTIC DEFORMATION

It can be argued that there are limits to the applicability of equation (3). Under normal conditions, dislocation densities greater than $\sim 10^{11}$ are difficult to obtain as are grain sizes of 1_μ or less, thus we might expect equation (3) to hold up these limits. However, the dislocation density produced by cold work is limited by the formation of dislocation tangles outlining subgrains of $\sim 1_\mu$ in diameter. Therefore, if the grain size is reduced below this dislocation tangle subgrain size, we might expect a differing hardening regime to take over. The change in dislocation density and distribution as a function of strain in very fine-grained materials has yet to be determined, but if subgrains are hindered from forming and the dislocations simply pass from one boundary to the other, the hardening would be controlled by the stress required to activate the dislocations. As there would be no work hardening, the flow stress would vary inversely as the length of the dislocation sources (approximately the grain diameter). As a result, the hardness would vary inversely as the grain diameter.

(c) Solid Solution and Work Hardening

Pure iron single crystals have a yield stress of 0.006×10^6 psi, and by solid-solution hardening this yield stress may be raised to 0.1×10^6 psi, that is the strength may be raised from $\sim G/2000$ to $\sim G/100$. In the case of fcc metals, it is known that elements which go into solid solution and lower the stacking fault energy give rise to alloys which work harden more strongly than the pure metals. This effect is very marked with richly alloyed austenitic steels, where the hardening increment is associated not only with the effects of the solutes on the frictional stress, but also on the effects of the changes in stacking fault energy upon the types of dislocation distribution established as the dislocation density is increased by cold work.

With bcc iron, stacking faults of the type found in fcc metals do not exist, but experiments have shown that the addition of suitable solutes may bring about changes in dislocation distribution on cold working which are the equivalent of those found in fcc metals when the stacking fault energy is lowered. But little detailed work has been carried out on the hardening increments to be expected from different solute additions to deformed α-iron.

The effect of interstitial alloy additions to α-iron is very marked. Both carbon and nitrogen greatly raise the flow stress. In annealed iron of low dislocation density, the flow stress is raised by 4.5 psi for each 0.01 atom per cent increase in nickel,[10,11] whereas for carbon or nitrogen, the increase in flow stress is 1200-1500 psi for each 0.01 atom per cent increase.[12,13] If carbon or nitrogen solid solutions of α-iron are cold worked, then the evidence available suggests that a high and uniform dislocation density is obtained without the formation of subgrains. These changes should be associated with a high work-hardening exponent.

(d) Dispersion and Grain-Boundary Hardening

There have been no serious attempts to determine the effects of changes in grain size upon the maximum hardness that could be achieved in a dispersion-hardened system. It seems unlikely that there will be a simple additive effect as in equation (3) because grain boundaries will influence

locally the formation of precipitates. Thus, if soft, precipitate-free regions are produced adjacent to the boundaries, the total volume of such regions will become greater as the grain size becomes smaller. It could be argued, therefore, that in practice, it might be better to keep the grain size large where dispersion hardening--brought about by the decomposition of a supersaturated solution--is the major hardening mechanism. There is some evidence to support this view from the work of Smith and Nutting[14] on the morphological and property changes occurring during the tempering of secondary hardening steels.

There are, however, other possibilities worthy of consideration. Dispersed phases may be present at grain boundaries, in which case they frequently tend to interfere with grain growth. It also seems likely that they will raise the value of k in equation (1). But this has still to be determined by experiment.

(e) Precipitation and Solid-Solution Hardening

Under the action of a stress, dislocations will pass through small coherent precipitates. The effect of the precipitates in raising the yield stress may be looked upon, therefore, simply as an extra frictional stress upon the dislocations. If solute elements are also present, they will also exert a frictional force on the dislocations. Consequently, we may expect simple additive effects from the addition of further solutes to alloys containing coherent precipitates. There are, however, usually practical limitations to the extent to which the solute content can be increased without greatly modifying the nature of the precipitated phases.

When dispersed phases lose coherency, the dislocations may no longer be able to pass through them. Plastic strain is now accommodated in the alloy by the dislocations overcoming the obstacles by a bowing mechanism of the Orowan type. The stress required to bring about bowing depends chiefly upon the inter-particle spacing, consequently changes in the frictional stress, by solute additions, would be expected to have little effect on the overall hardness.

There are other possibilities to be considered. It may be that in some cases, the precipitate barriers to dislocation movement are overcome by cross slip. In this case, alloying to produce an equivalent to a lowering of the stacking fault energy, would prevent cross slip from occurring readily and thus raise the flow stress.

It is to be expected, therefore, that the hardening increments will be more marked in rich alloys at elevated temperatures than at low temperatures.

(f) Work Hardening and Precipitation Hardening

The work hardening of precipitation-hardened alloys has been extensively discussed by Kelly and Nicholson.[2] They point out that where dispersed phases are coherent, then the work-hardening characteristics are very similar to those of pure metals. However, when the dispersed phases are incoherent, the rate of work hardening is usually very much greater than with pure metals.

This rapid rate of work hardening is partly accounted for by the dislocation distribution being modified by the precipitates, in such a way that high and uniform dislocation distributions are found at very low strains. In an Al-4%Cu alloy aged to give the θ' phase, the dislocation density increases from 10^3 to 10^{10} as the strain is increased to 1 per cent. The precipitates may also act as dislocation sources, thus the nature of the interface between the dispersed phase and the matrix will influence the response of the alloy to cold work.

The above considerations apply to alloys deformed plastically up to 10 per cent. Other interesting effects can occur when much larger strains are introduced. Although little is known about the detailed mechanism of high-strain deformation, metallographic examination shows that the parameters of a dispersion can be changed by working. Thus, spherical particles may be elongated and the spacing between particles may be changed. It is possible for a coarse dispersion to be changed into a sufficiently fine one for appreciable hardening to be introduced. If this deformation is carried out at low temperatures, then there may be a further increment of hardening from the increased density of dislocations.

A further possibility is that plastic deformation may induce precipitation, since dislocations are very favourable sites for precipitate nucleation. In these instances, the dislocations may not only be locked by the precipitates forming on them, but the precipitates will also act as further barriers to subsequent dislocation movement.

II. The Interaction of Three Hardening Mechanisms

(a) Solid-Solution, Grain-Boundary and Work Hardening

An experimental approach to this problem has been attempted by Armstrong, et al.[9] Using the technique outlined in I(b), they investigated the effect of different solutes upon the grain size dependence of the flow stress after differing amounts of cold work. In the case of iron, they found that the effect of carbon was to raise the values of σ_0 and k. It was also found that the values of σ_0 and k were raised by the addition of Zn to Cu to give a 70/30 brass, and in both cases the value of k did not vary as the prior strain was increased. It would appear that k will be raised rapidly by solutes which lower the stacking fault energy, and as the dislocation density will also build up rapidly with the alloys of low stacking fault energy, it follows that high strengths could be achieved in cold-worked, fine-grained, low-stacking-fault energy alloys.

(b) Solid-Solution, Dispersed-Phase, and Grain-Boundary Hardening

As pointed out in Section I(d), there would seem to be little advantage to be gained from the point of view of increasing the yield strength by keeping the grain size small of a dispersed-phase hardened alloy. But a further hardening increment is to be expected from the addition of solid-solution forming solutes. Special cases arise, however, when the addition of other solutes may influence the width of a precipitate-free zone at grain boundaries. For example, the addition of silver on an aluminum-magnesium-zinc alloy decreases the width of the precipitate-free zone and increases the strength.

(c) Dispersed-Phase, Grain-Boundary, and Work Hardening

As pointed out in Section I(f), large increases in strength can be achieved by cold working suitable dispersed-phase alloys, and there would seem to be little further advantage to be gained by keeping the grain size small. The strongest dislocation barriers are the precipitate particles, whilst the precipitates, through the nature of their interface with the matrix, govern the dislocation distribution. The grain boundaries would seem to exert little influence on the flow stress under these conditions.

(d) Solid-Solution, Dispersed-Phase and Work Hardening

The addition of alloying elements which go into solid solution in the matrix would appear to be an effective method of increasing still further the strength of work-hardened dispersed-phase alloys. Although the precipitates to some extent govern the type of dislocation distribution established after cold work, further control may be exerted by solutes which lower the stacking fault energy. For example, age-hardened copper-beryllium alloys with a low stacking-fault energy matrix work harden more than precipitation-hardened aluminum alloys, where the stacking fault energy of the matrix is high.

III. The Interaction of Four Hardening Mechanisms

The most effective combination of three hardening mechanisms are probably solid-solution, dispersed-phase, and work hardening. It would appear that changes in the grain size would have little effect on the strength of an alloy hardened by these mechanisms. However, from a practical point of view, a high strength is seldom the only requirement. A high strength must be coupled with adequate ductility. The evidence that is available suggests that with strengthened polycrystalline alloys, the ductility increases as the grain size is decreased; therefore, there would seem to be an advantage in keeping the grain size small. If in keeping the grain size small, the formation of precipitate-free regions adjacent to the boundary can be avoided, then a small increment in hardness is to be expected together with the improved ductility.

From these considerations, it is possible to specify the structural requirement of a very strong alloy as follows. It should have a grain size less than 10μ. It should have a dispersed phase that is semi-coherent or about to become noncoherent. The volume fraction of the dispersed phase should be large. The dispersed phase should be uniformly distributed through the grains with no precipitate-free regions adjacent to the boundary. The spacing of the particles should be between 100-400 A. The matrix should be rich in solute elements, particularly those which would have the effect, or its equivalent, of lowering the stacking-fault energy. The dislocation density should be high (10^{10} - 10^{11} cm^{-2}), and the dislocations should be uniformly distributed and not in subgrain tangles.

IV. Some Examples of Additive Hardening in Steel

(a) Hard-Drawn Steel Wire

The flow stress of patented steel wire may be increased to 0.4×10^6 psi (G/30) by a suitable drawing operation. Electron metallographic examination of thin foils from such specimens shows that the effect of drawing is to reduce the spacing of the pearlite from about 500 A to 100 A (see Figure 2). With such a small spacing dispersion hardening becomes an important hardening mechanism. But the hardening may be enhanced further by the fact that the aspect ratio of the cementite is increased by the drawing so that the structure may almost be looked upon as that of a fiber-reinforced material. Coupled with the changes in the dispersion parameters, the effect of cold drawing is to increase the dislocation density. Some evidence of short lengths of dislocations between the cementite particles can be seen in Figure 2. It appears that this material corresponds to Case I(f) outlined above. There are some elements in solid solution in the steel which might give a slight hardening increment and make the material conform to Case II(d). But it should be possible to add still other solute elements so to raise the strength of the steel still further.

(b) High-Carbon Steel Martensites

There has been much discussion as to the reasons for the high strengths of the fine internally twinned high-carbon steel martensites. Most authors now accept the view that more than one hardening mechanism must be operating, and the factors that have to be considered are:

(1) solid-solution hardening from the interstitial carbon,

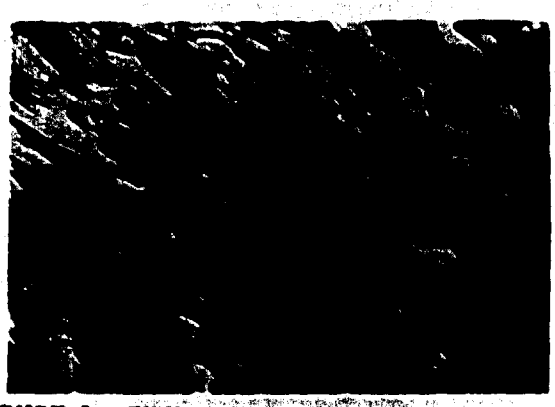

FIGURE 2. TWIN-FOIL TRANSMISSION ELECTRON MICROGRAPH FROM HARD-DRAWN PATENTED STEEL WIRE SHOWING FINE LAMELLAR STRUCTURE
X60,000, Reduced approximately 21 percent in printing.

(2) The substructure of the martensite. Internal twins may act as dislocation barriers in the same way as grain boundaries.

(3) work hardening usually from the high dislocation density generated during the shear transformation.

Winchell and Cohen[15] have obtained much evidence to show the importance of solid-solution hardening. Their results for a range of iron and iron-nickel martensites are given in Figure 3.

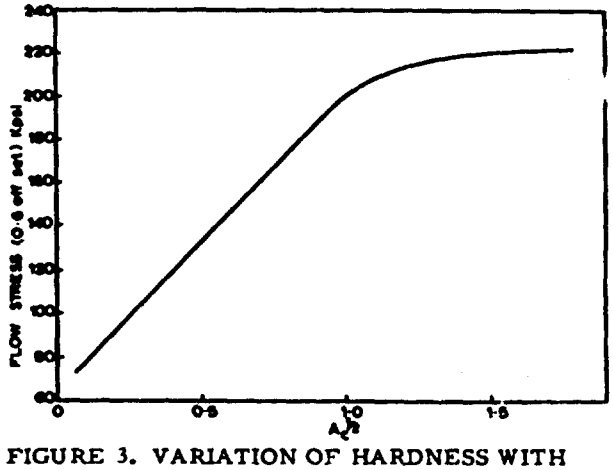

FIGURE 3. VARIATION OF HARDNESS WITH CARBON CONTENT FOR A RANGE OF MARTENSITES IN IRON AND IRON-NICKEL ALLOYS SHOWING NEEDLE LIKE AND TWINNED STRUCTURE

The unsatisfactory aspect of ascribing the whole of the hardening to solid-solution effects, are the marked changes in the rate of hardening with solute concentration.

This has led Kelly and Nutting[16] to stress the importance of the twin interfaces acting in almost the same way as grain boundaries to give dislocation barriers. Winchell and Cohen[17] have adopted a somewhat different approach to the effects of substructure and they have assumed that the effect of the twin interfaces is to limit the length of dislocations. They have shown that it is possible to relate the flow stress of martensite to the solute content, the twin interface spacing, and the dislocation density by the expression:

$$\sigma_F = \sigma_o + 2.4 \times 10^2 h^{-\frac{1}{2}} X_c^{1/3} \qquad (1)$$

where σ_F = flow stress

σ_o = frictional stress. The value observed corresponds to a dislocation density of $\sim 10^{12}$ which is not unreasonable from metallographic observations.

h = twin interface spacing

X_c = wt. % of carbon in solid solution.

More recent research by Kelly[18] on a variety of plain carbon and alloy steel martensites, has shown that internally twinned structures with high interstitial contents are relatively soft after quenching. But if the martensite is aged at room temperature, the hardness rapidly increases. However, the acicular non-internally twinned martensites are not so susceptible to aging treatments. As both the acicular and twinned martensites are known to have high dislocation densities, and as no precipitates can be observed in the twinned and aged martensites, it could be concluded that the aging reaction is not associated with conventional dislocation locking or precipitation hardening mechanisms. One remaining possibility is the strengthening of the twin interfaces as a result of carbon segregation to make them take on the characteristics of grain boundaries. If this were the case, it would appear that the structure of twinned martensite is very similar to that of hard-drawn steel wire. In both cases, they have a ladder-like structure with the twin interfaces or cementite-ferrite interfaces forming the uprights whilst dislocations form the rungs.

A better understanding of the underlying reasons for the hardness of martensite is likely to come from a thorough study of the mechanical properties and microstructures of iron-nitrogen alloys. A start has been made on the electron metallographic study of iron-nitrogen martensites by Gould.[19] He has found that the two types of martensite reported by Kelly and Nutting[16] are also found with iron-nitrogen alloys. An example of the duplex structure obtained at intermediate nitrogen contents is shown in Figure 4.

(c) Secondary Hardening of Vanadium Steels

High strengths may be achieved in steels by tempering martensites containing strong carbide-forming elements. Many authors have pointed out the similarity between the secondary hardening response of vanadium-containing steels and

the age-hardening reactions found in aluminum alloys, and there have been numerous electron metallographic studies using extraction replica techniques which have tended to support these views. However, more recent examination of the secondary hardening phenomenon by Kelly[18] using thin-foil techniques has shown that the chief cause of hardening is not associated with Widmanstatten types of carbide precipitation, but is a result of carbides forming preferentially on dislocations. An example of dislocation nucleated V_4C_3 is shown in Figure 5. In these alloys, the dislocation density is very high as a result of forming acicular martensite during quenching, there are, therefore, many favourable sites for precipitate nucleation. It would follow from this that factors which tended to increase still further the dislocation density after the quench would enhance the hardening response.

(d) Ausforming

In a recent investigation of the metallography of ausformed steels, Thomas, Schmarz, and Gerberich[20] have found that during deformation in the austenite range, precipitation of alloy carbides occurs. These precipitates influence the subsequent generation of dislocations during the working operation, and as pointed out by Schaller and Schmatz,[21] these dislocations may be inherited during the subsequent martensite transformation. The dislocation density may be increased still further as a result of the strains developed during the martensitic transformations. As pointed out by Thomas, et al.,[20] because much of the carbon will be removed from the austenite by precipitation during the ausforming operation, the subsequent martensitic transformation is likely to give rise to the acicular martensite rather than twinned martensite. If sufficient unprecipitated alloying elements are still present, then a further increase in strength may be obtained by tempering to give precipitation on the newly formed transformation dislocations.

The high strength of ausformed steels is seen, therefore, to be a consequence of the additive effects of four hardening mechanisms--a fine grain size from the martensite, a dispersion of alloy carbides produced during ausforming and tempering, the distribution of which is controlled by the dislocation distribution, a high dislocation density generated by working and by the shear transformation, and a small component from the solute elements in substitutional solid solution. It is probable that the interstitial carbon will have been precipitated as carbides, and it may be that if nitrogen could be added without affecting the mode of shear transformation, the strength of ausformed steels could be increased still further.

Acknowledgments

The author would like to thank Dr. P. M. Kelly and Dr. I. Codd of the Metallurgy Department, Leeds University, for many stimulating discussions and providing results of their work prior to publication. He would also like to thank Dr. I. S. Brammar of Aeon Laboratories for providing the micrographs of the hard-drawn steel wire.

FIGURE 4. THIN-FOIL TRANSMISSION ELECTRON MICROGRAPH FROM AN IRON-0.2% NITROGEN MARTENSITE SHOWING AN INTERNALLY TWINNED MARTENSITE PLATE ADJACENT TO NEEDLE MARTENSITE

X120,000 Reduced approximately 21 percent in printing.

FIGURE 5. THIN-FOIL TRANSMISSION ELECTRON MICROGRAPH SHOWING PRECIPITATION OF V_4C_3 ON DISLOCATIONS AFTER TEMPERING A QUENCHED 0.1% C, 1.5% V STEEL FOR 1 HOUR AT 700 C

X120,000, Reduced approximately 21 percent in printing.

References

(1) Kelly, P. M., and Nutting, J., Iron & Steel Institute Special Report No. 76, p 7 (1962).

(2) Kelly, A., and Nicholson, R. B., Prog. Mat. Sci., 10, 149 (1963).

(3) Fleischer, R. L., and Hibbard, W. R., "Relation Between Structure and Mechanical Properties of Metals", N.P.L. Symposium No. 15, Vol. 1, H. M. Stationary Office (1963).

(4) Cracknell, A., and Petch, N. J., Acta Met, 3, 186 (1955).

(5) Heslop, J., and Petch, N. J., Phil. Mag., 2, 649 (1957).

(6) Codd, I., and Petch, N. J., Phil. Mag., 5, 30 (1960).

(7) Keh, A. S., and Weissmann, S., Electron Microscopy and the Strength of Crystals, Edit. G. Thomas & J. Washburn, Interscience, New York (1963).

(8) Hull, D., McIvor, I. D., and Owen, W. S., "Relation Between Structure and Mechanical Properties of Metals", N.P.L. Symposium No. 15, Vol. 2, H. M. Stationary Office (1963).

(9) Armstrong, R., Codd, I., Douthwaite, R. M., and Petch, N. J., Phil. Mag., 73, 45 (1962).

(10) Lacy, C. E., and Gensamer, M., Trans. ASM, 32, 88 (1944).

(11) Rees, W. P., Hopkins, B. E., and Tiplen, H. R., J. Iron & Steel Institute, 177, 93 (1954).

(12) Wert, C., Trans. AIME, 188, 1242 (1950).

(13) Stephenson, E. T., Trans. ASM, 55, 625 (1962).

(14) Smith, E., and Nutting, J., J. Iron & Steel Institute, 187, 314 (1957).

(15) Wichell, P. G., and Cohen, M., Trans. ASM, 55, 347 (1962).

(16) Kelly, P. M., and Nutting, J., Proc. Roy. Soc., A259, 45 (1960).

(17) Winchell, P. G., and Cohen, M., Electron Microscopy and the Strength of Crystals, Edit. G. Thomas and J. Washburn, Interscience, New York, 995 (1963).

(18) Kelly, P. M., Private Communication, The Leeds University.

(19) Codd, I., Private Communication, The Leeds University.

(20) Thomas, G., Schmatz, D., and Gerberich, W., Second International Materials Symposium, University of California, In Press (1964).

(21) Schaller, F., and Schmatz, D., Acta Met., 11, 1193 (1963).

APPENDIX A

PROGRAM FOR TRIPARTITE TECHNICAL COOPERATION PROGRAM

Symposium on Problems in the Load-Carrying Application of High-Strength Steels

October 26, 27, and 28, 1964

General Services Administration Auditorium
18th and F Streets, Washington, D. C.

Registration: 8:30-9:30 a.m., Monday, October 26, 1964

SESSION I Monday, October 26, 1964, 9:30 a.m. to 12:30 p.m.
Chairman: G. C. Deutsch, National Aeronautics and Space Administration, Washington, D. C.
Manager: H. Markus, Frankford Arsenal, Philadelphia, Pennsylvania

This session consists of papers on the broad subject of high-strength steels, to reflect the present state of the art, and on potential applications for these steels, including the design-material interplay.

9:30 Welcome and Introductory Remarks - S. L. Gertsman, Department of Mines and Technical Survey, Ottawa, Canada
9:30 Welcome and Explanatory Remarks on TTCP - R. M. Murray, U. S. Washington Deputy for TTCP
9:30 Philosophy and Operation of Conference - N. E. Promisel, Department of the Navy, Bureau of Naval Weapons, Washington, D. C.
9:50 High-Strength Steel Perspectives - A. M Hall, Battelle Memorial Institute, Columbus, Ohio
10:45 Intermission
11:15 Military Applications and Property Requirements - P. L. Hendricks, H. W. Zoeller, and I. Perlmutter, USAF, Air Force Materials Laboratory, Wright-Patterson Air Force Base, Ohio; J. I. Bluhm, Army Materials Research Agency, Watertown, Massachusetts; Yoder, G. M., Bureau of Naval Weapons, Materials Branch, Washington, D. C.
12:00 Design Parameters in Materials Selection - G. Gerard, ARA Division, Allied Research Associates, Inc., Concord, Massachusetts
12:30 Adjournment

SESSION II Monday, October 26, 1964, 2:00 p.m. to 5:00 p.m.
Chairman: D. K. Hanink, General Motors Corporation, Indianapolis, Indiana
Manager: P. L. Hendricks, USAF, Air Force Materials Laboratory, Wright-Patterson Air Force Base, Ohio

This session deals with production and fabrication, with emphasis on the effects on, and the subsequent properties of, the resulting fabricated products. It includes, therefore, primary and secondary fabrication.

2:00 Effect of Primary Processing on Ultrahigh-Strength Steels - J. C. Hamaker, Vanadium-Alloys Steel Company, Latrobe, Pennsylvania
2:40 Joining of High-Strength Steels - W. F. Savage, Rensselaer Polytechnic Institute, Troy, New York
3:25 Intermission
3:45 Secondary Forming Processes and Their Effects on Resulting Products - W. W. Wood, Vought Aeronautics Division, Ling-Temco-Vought, Inc., Dallas, Texas
4:30 The Surface Integrity of Machined-and-Ground High-Strength Steels - M. Field and J. F. Kahles, Metcut Research Associates, Inc., Cincinnati, Ohio
5:00 Adjournment
6:00-8:00 Social Gathering

SESSION III Tuesday, October 27, 1964, 00 a.m. to 12:00
Chairman: P. Brittain, Hawker-Siddeley Aircraft, Ltd., United Kingdom
Manager: L. Wortley, Department of Materials Research, London, England

This session deals with the very critical topic of corrosion sensitivity of high-strength steels, protection against corrosion, and the effects of protection techniques on the steel behavior.

9:00 Corrosion Protection of High-Strength Steels - S. Goldberg, Bureau of Naval Weapons, Department of the Navy, Washington, D. C.
9:45 Stress-Corrosion Cracking and Corrosion Fatigue of High-Strength Steels - B. F. Brown, U. S. Naval Research Laboratory, Washington, D. C.
10:30 Intermission
11:00 Protection Against Corrosion, Hydrogen Embrittlement - H. G. Cole, Ministry of Aviation, London, England
12:00 Adjournment

SESSION IV Tuesday, October 27, 1964, 2:00 to 5:00 p.m.
Chairman: A. W. Bethune, De Havilland Aircraft of Canada, Ltd., Downsview, Ontario, Canada
Manager: C. Cottee, Army Equipment Engineering Establishment, Ottawa, Canada

This session is devoted to mechanical behavior characteristics of design significance.

2:00 The Notch Toughness of Ultrahigh-Strength Steels in Relation to Design Considerations - R.C.A. Thurston, Department of Mines and Technical Surveys, Ottawa, Canada
2:30 Factors Affecting the Fracture of High-Strength Steels - C.L.M. Cottrell, Bristol Aerojet, Limited, Banwell, Weston-Super-Mare, Somerset, England
3:00 Discussion on Previous Topics
3:45 Intermission
4:15 A Survey of the Fatigue Aspects in the Application of Ultrahigh-Strength Steels - S. R. Swanson, The De Havilland Aircraft of Canada Limited, Malton, Ontario, Canada
5:00 Adjournment

SESSION V Wednesday, October 28, 1964, 9:00 a.m. to 12:00
Chairman: D. J. McPherson, IIT Research Institute, Chicago, Illinois
Manager: M. Achter, U. S. Naval Research Laboratory, Washington, D. C.

This session deals with high-strength steels by technical types so as to obtain an integrated picture of their behavior, properties and processing techniques; and discusses strengthening mechanisms per se.

9:00 The Physical Metallurgy and Properties of Maraging Steels - G. E. Pellissier, United States Steel Corporation, Applied Research Laboratory, Monroeville, Pennsylvania
9:40 The Potentials of Quenched-and-Tempered High-Strength Steels - S. W. Hollingum, Ministry of Defence, Royal Armament Research and Development Establishment, Fort Halstead, Sevenoaks, Kent, England
10:20 Intermission
10:45 Thermomechanical Treatment of Steel - J. J. Harwood and R. Clark, Ford Motor Company, Dearborn, Michigan
11:25 Additive Strengthening Mechanisms and the Structure of Steel - J. Nutting, Department of Metallurgy, The Houldsworth School of Applied Science, The University, Leeds, England
12:00 Summarization of Highlights of Symposium - By Group as follows:
Chairman - N. Mason, Ministry of Aviation, London, England
H. P. Tardif, Canadian Armament Research and Development Establishment, Quebec City, Canada
I. Berman, U.S. Army Materials Research Agency, Watertown Arsenal, Watertown, Massachusetts
P. Hendricks, USAF, Air Force Materials Laboratory, Wright-Patterson Air Force Base, Ohio
J. Fielding, Hawker-Siddeley Aviation, Ltd., Manchester, England
R. J. Runck, DMIC, Battelle Memorial Institute, Columbus, Ohio
12:30 Adjournment of Symposium

APPENDIX B

Temperature Conversions

The general arrangement of this table was devised by Sauveur and Boylston more than 40 years ago. The middle column of figures (in bold-faced type) contains the reading (°F or °C) to be converted. If converting from degrees Fahrenheit to degrees Centigrade, read the Centigrade equivalent in the column headed "C". If converting from Centigrade to Fahrenheit, read the Fahrenheit equivalent in the column headed "F".

F		C	F		C	F		C	F		C	F		C
.....	-458	-272.22	.....	-308	-188.89	-252.4	-158	-105.56	+17.6	-8	-22.22	287.6	142	61.11
.....	-456	-271.11	.....	-306	-187.78	-248.8	-156	-104.44	+21.2	-6	-21.11	291.2	144	62.22
.....	-454	-270.00	.....	-304	-186.67	-245.2	-154	-103.33	+24.8	-4	-20.00	294.8	146	63.33
.....	-452	-268.89	.....	-302	-185.56	-241.6	-152	-102.22	+28.4	-2	-18.89	298.4	148	64.44
.....	-450	-267.78	.....	-300	-184.44	-238.0	-150	-101.11	+32.0	±0	-17.78	302.0	150	65.56
.....	-448	-266.67	.....	-298	-183.33	-234.4	-148	-100.00	+35.6	+2	-16.67	305.6	152	66.67
.....	-446	-265.56	.....	-296	-182.22	-230.8	-146	-98.89	+39.2	+4	-15.56	309.2	154	67.78
.....	-444	-264.44	.....	-294	-181.11	-227.2	-144	-97.78	+42.8	+6	-14.44	312.8	156	68.89
.....	-442	-263.33	.....	-292	-180.00	-223.6	-142	-96.67	+46.4	+8	-13.33	316.4	158	70.00
.....	-440	-262.22	.....	-290	-178.89	-220.0	-140	-95.56	+50.0	+10	-12.22	320.0	160	71.11
.....	-438	-261.11	.....	-288	-177.78	-216.4	-138	-94.44	+53.6	+12	-11.11	323.6	162	72.22
.....	-436	-260.00	.....	-286	-176.67	-212.8	-136	-93.33	+57.2	+14	-10.00	327.2	164	73.33
.....	-434	-258.89	.....	-284	-175.56	-209.2	-134	-92.22	+60.8	+16	-8.89	330.8	166	74.44
.....	-432	-257.78	.....	-282	-174.44	-205.6	-132	-91.11	+64.4	+18	-7.78	334.4	168	75.56
.....	-430	-256.67	.....	-280	-173.33	-202.0	-130	-90.00	+68.0	+20	-6.67	338.0	170	76.67
.....	-428	-255.56	.....	-278	-172.22	-198.4	-128	-89.89	+71.6	+22	-5.56	341.6	172	77.78
.....	-426	-254.44	.....	-276	-171.11	-194.8	-126	-87.78	+75.2	+24	-4.44	345.2	174	78.89
.....	-424	-253.33	.....	-274	-170.00	-191.2	-124	-86.67	+78.8	+26	-3.33	348.8	176	80.00
.....	-422	-252.22	-457.6	-272	-168.89	-187.6	-122	-85.56	+82.4	+28	-2.22	352.4	178	81.11
.....	-420	-251.11	-454.0	-270	-167.78	-184.0	-120	-84.44	+86.0	+30	-1.11	356.0	180	82.22
.....	-418	-250.00	-450.4	-268	-166.67	-180.4	-118	-83.33	+89.6	+32	±0.00	359.6	182	83.33
.....	-416	-248.89	-446.8	-266	-165.56	-176.8	-116	-82.22	+93.2	+34	+1.11	363.2	184	84.44
.....	-414	-247.78	-443.2	-264	-164.44	-173.2	-114	-81.11	+96.8	+36	+2.22	366.8	186	85.56
.....	-412	-246.67	-439.6	-262	-163.33	-169.6	-112	-80.00	+100.4	+38	+3.33	370.4	188	86.67
.....	-410	-245.56	-436.0	-260	-162.22	-166.0	-110	-78.89	+104.0	+40	+4.44	374.0	190	87.78
.....	-408	-244.44	-432.4	-258	-161.11	-162.4	-108	-77.78	107.6	42	5.56	377.6	192	88.89
.....	-406	-243.33	-428.8	-256	-160.00	-158.8	-106	-76.67	111.2	44	6.67	381.2	194	90.00
.....	-404	-242.22	-425.2	-254	-158.89	-155.2	-104	-75.56	114.8	46	7.78	384.8	196	91.11
.....	-402	-241.11	-421.6	-252	-157.78	-151.6	-102	-74.44	118.4	48	8.89	388.4	198	92.22
.....	-400	-240.00	-418.0	-250	-156.67	-148.0	-100	-73.33	122.0	50	10.00	392.0	200	93.33
.....	-398	-238.89	-414.4	-248	-155.56	-144.4	-98	-72.22	125.6	52	11.11	395.6	202	94.44
.....	-396	-237.78	-410.8	-246	-154.44	-140.8	-96	-71.11	129.2	54	12.12	399.2	204	95.56
.....	-394	-236.67	-407.2	-244	-153.33	-137.2	-94	-70.00	132.8	56	13.33	402.8	206	96.67
.....	-392	-235.56	-403.6	-242	-152.22	-133.6	-92	-68.89	136.4	58	14.44	406.4	208	97.78
.....	-390	-234.44	-400.0	-240	-151.11	-130.0	-90	-67.78	140.0	60	15.56	410.0	210	98.89
.....	-388	-233.33	-396.4	-238	-150.00	-126.4	-88	-66.67	143.6	62	16.67	413.6	212	100.00
.....	-386	-232.22	-392.8	-236	-148.89	-122.8	-86	-65.56	147.2	64	17.78	417.2	214	101.11
.....	-384	-231.11	-389.2	-234	-147.78	-119.2	-84	-64.44	150.8	66	18.89	420.8	216	102.22
.....	-382	-230.00	-385.6	-232	-146.67	-115.6	-82	-63.33	154.4	68	20.00	424.4	218	103.33
.....	-380	-228.89	-382.0	-230	-145.56	-112.0	-80	-62.22	158.0	70	21.11	428.0	220	104.44
.....	-378	-227.78	-378.4	-228	-144.44	-108.4	-78	-61.11	161.6	72	22.22	431.6	222	105.56
.....	-376	-226.67	-374.8	-226	-143.33	-104.8	-76	-60.00	165.2	74	23.33	435.2	224	106.67
.....	-374	-225.56	-371.2	-224	-142.22	-101.2	-74	-58.89	168.8	76	24.44	438.8	226	107.78
.....	-372	-224.44	-367.6	-222	-141.11	-97.6	-72	-57.78	172.4	78	25.56	442.4	228	108.89
.....	-370	-223.33	-364.0	-220	-140.00	-94.0	-70	-56.67	176.0	80	26.67	446.0	230	110.00
.....	-368	-222.22	-360.4	-218	-138.89	-90.4	-68	-55.56	179.6	82	27.78	449.6	232	111.11
.....	-366	-221.11	-356.8	-216	-137.78	-86.8	-66	-54.44	183.2	84	28.89	453.2	234	112.22
.....	-364	-220.00	-353.2	-214	-136.67	-83.2	-64	-53.33	186.8	86	30.00	456.8	236	113.33
.....	-362	-218.89	-349.6	-212	-135.56	-79.6	-62	-52.22	190.4	88	31.11	460.4	238	114.44
.....	-360	-217.78	-346.0	-210	-134.44	-76.0	-60	-51.11	194.0	90	32.22	464.0	240	115.56
.....	-358	-216.67	-342.4	-208	-133.33	-72.4	-58	-50.00	197.6	92	33.33	467.6	242	116.67
.....	-356	-215.56	-338.8	-206	-132.22	-68.8	-56	-48.89	201.2	94	34.44	471.2	244	117.78
.....	-354	-214.44	-335.2	-204	-131.11	-65.2	-54	-47.78	204.8	96	35.56	474.8	246	118.89
.....	-352	-213.33	-331.6	-202	-130.00	-61.6	-52	-46.67	208.4	98	36.67	478.4	248	120.00
.....	-350	-212.22	-328.0	-200	-128.89	-58.0	-50	-45.56	212.0	100	37.78	482.0	250	121.11
.....	-348	-211.11	-324.4	-198	-127.78	-54.4	-48	-44.44	215.6	102	38.89	485.6	252	122.22
.....	-346	-210.00	-320.8	-196	-126.67	-50.8	-46	-43.33	219.2	104	40.00	489.2	254	123.33
.....	-344	-208.89	-317.2	-194	-125.56	-47.2	-44	-42.22	222.8	106	41.11	492.8	256	124.44
.....	-342	-207.78	-313.6	-192	-124.44	-43.6	-42	-41.11	226.4	108	42.22	496.4	258	125.56
.....	-340	-206.67	-310.0	-190	-123.33	-40.0	-40	-40.00	230.0	110	43.33	500.0	260	126.67
.....	-338	-205.56	-306.4	-188	-122.22	-36.4	-38	-38.89	233.6	112	44.44	503.6	262	127.78
.....	-336	-204.44	-302.8	-186	-121.11	-32.8	-36	-37.78	237.2	114	45.56	507.2	264	128.89
.....	-334	-203.33	-299.2	-184	-120.00	-29.2	-34	-36.67	240.8	116	46.67	510.8	266	130.00
.....	-332	-202.22	-295.6	-182	-118.89	-25.6	-32	-35.56	244.4	118	47.78	514.4	268	131.11
.....	-330	-201.11	-292.0	-180	-117.78	-22.0	-30	-34.44	248.0	120	48.89	518.0	270	132.22
.....	-328	-200.00	-288.4	-178	-116.67	-18.4	-28	-33.33	251.6	122	50.00	521.6	272	133.33
.....	-326	-198.89	-284.8	-176	-115.56	-14.8	-26	-32.22	255.2	124	51.11	525.2	274	134.44
.....	-324	-197.78	-281.2	-174	-114.44	-11.2	-24	-31.11	258.8	126	52.22	528.8	276	135.56
.....	-322	-196.67	-277.6	-172	-113.33	-7.6	-22	-30.00	262.4	128	53.33	532.4	278	136.67
.....	-320	-195.56	-274.0	-170	-112.22	-4.0	-20	-28.89	266.0	130	54.44	536.0	280	137.78
.....	-318	-194.44	-270.4	-168	-111.11	-0.4	-18	-27.78	269.6	132	55.56	539.6	282	138.89
.....	-316	-193.33	-266.8	-166	-110.00	+3.2	-16	-26.67	273.2	134	56.67	543.2	284	140.00
.....	-314	-192.22	-263.2	-164	-108.89	+6.8	-14	-25.56	276.8	136	57.78	546.8	286	141.11
.....	-312	-191.11	-259.6	-162	-107.78	+10.4	-12	-24.44	280.4	138	58.89	550.4	288	142.22
.....	-310	-190.00	-256.0	-160	-106.67	+14.0	-10	-23.33	284.0	140	60.00	554.0	290	143.33

Temperature Conversions

F		C	F		C	F		C	F		C	F		C
557.6	292	144.44	870.8	466	241.11	1832.0	1000	537.78	3398.0	1870	1021.1	4964.0	2740	1504.4
561.2	294	145.56	874.4	468	242.22	1850.0	1010	543.33	3416.0	1880	1026.7	4982.0	2750	1510.0
564.8	296	146.67	878.0	470	243.33	1868.0	1020	548.89	3434.0	1890	1032.2	5000.0	2760	1515.6
568.4	298	147.78	881.6	472	244.44	1886.0	1030	554.44	3452.0	1900	1037.8	5018.0	2770	1521.1
572.0	300	148.89	885.2	474	245.56	1904.0	1040	560.00	3470.0	1910	1043.3	5036.0	2780	1526.7
575.6	302	150.00	888.8	476	246.67	1922.0	1050	565.56	3488.0	1920	1048.9	5054.0	2790	1532.2
579.2	304	151.11	892.4	478	247.78	1940.0	1060	571.11	3506.0	1930	1054.4	5072.0	2800	1537.8
582.8	306	152.22	896.0	480	248.89	1958.0	1070	576.67	3524.0	1940	1060.0	5090.0	2810	1543.3
586.4	308	153.33	899.6	482	250.00	1976.0	1080	582.22	3542.0	1950	1065.6	5108.0	2820	1548.9
590.0	310	154.44	903.2	484	251.11	1994.0	1090	587.78	3560.0	1960	1071.1	5126.0	2830	1554.4
593.6	312	155.56	906.8	486	252.22	2012.0	1100	593.33	3578.0	1970	1076.7	5144.0	2840	1560.0
597.2	314	156.67	910.4	488	253.33	2030.0	1110	598.89	3596.0	1980	1082.2	5162.0	2850	1565.6
600.8	316	157.78	914.0	490	254.44	2048.0	1120	604.44	3614.0	1990	1087.8	5180.0	2860	1571.1
604.4	318	158.89	917.6	492	255.56	2066.0	1130	610.00	3632.0	2000	1093.3	5198.0	2870	1576.7
608.0	320	160.00	921.2	494	256.67	2084.0	1140	615.56	3650.0	2010	1098.9	5216.0	2880	1582.2
611.6	322	161.11	924.8	496	257.78	2102.0	1150	621.11	3668.0	2020	1104.4	5234.0	2890	1587.8
615.2	324	162.22	928.4	498	258.89	2120.0	1160	626.67	3686.0	2030	1110.0	5252.0	2900	1593.3
618.8	326	163.33	932.0	500	260.00	2138.0	1170	632.22	3704.0	2040	1115.6	5270.0	2910	1598.9
622.4	328	164.44	935.6	502	261.11	2156.0	1180	637.78	3722.0	2050	1121.1	5288.0	2920	1604.4
626.0	330	165.56	939.2	504	262.22	2174.0	1190	643.33	3740.0	2060	1126.7	5306.0	2930	1610.0
629.6	332	166.67	942.8	506	263.33	2192.0	1200	648.89	3758.0	2070	1132.2	5324.0	2940	1615.6
633.2	334	167.78	946.4	508	264.44	2210.0	1210	654.44	3776.0	2080	1137.8	5342.0	2950	1621.1
636.8	336	168.89	950.0	510	265.56	2228.0	1220	660.00	3794.0	2090	1143.3	5360.0	2960	1626.7
640.4	338	170.00	953.6	512	266.67	2246.0	1230	665.56	3712.0	2100	1148.9	5378.0	2970	1632.2
644.0	340	171.11	957.2	514	267.78	2264.0	1240	671.11	3830.0	2110	1154.4	5396.0	2980	1637.8
647.6	342	172.22	960.8	516	268.89	2282.0	1250	676.67	3848.0	2120	1160.0	5414.0	2990	1643.3
651.2	344	173.33	964.4	518	270.00	2300.0	1260	682.22	3866.0	2130	1165.6	5432.0	3000	1648.9
654.8	346	174.44	968.0	520	271.11	2318.0	1270	687.78	3884.0	2140	1171.1	5450.0	3010	1654.4
658.4	348	175.56	971.6	522	272.22	2336.0	1280	693.33	3902.0	2150	1176.7	5468.0	3020	1660.0
662.0	350	176.67	975.2	524	273.33	2354.0	1290	698.89	3920.0	2160	1182.2	5486.0	3030	1665.6
665.6	352	177.78	978.8	526	274.44	2372.0	1300	704.44	3938.0	2170	1187.8	5504.0	3040	1671.1
669.2	354	178.89	982.4	528	275.56	2390.0	1310	710.00	3956.0	2180	1193.3	5522.0	3050	1676.7
672.8	356	180.00	986.0	530	276.67	2408.0	1320	715.56	3974.0	2190	1198.9	5540.0	3060	1682.2
676.4	358	181.11	989.6	532	277.78	2426.0	1330	721.11	3992.0	2200	1204.4	5558.0	3070	1687.8
680.0	360	182.22	993.2	534	278.89	2440.0	1340	726.67	4010.0	2210	1210.0	5576.0	3080	1693.3
683.6	362	183.33	996.8	536	280.00	2462.0	1350	732.22	4028.0	2220	1215.6	5594.0	3090	1698.9
687.2	364	184.44	1000.4	538	281.11	2480.0	1360	737.78	4046.0	2230	1221.1	5612.0	3100	1704.4
690.8	366	185.56	1004.0	540	282.22	2498.0	1370	743.33	4064.0	2240	1226.7	5702.0	3150	1732.2
694.4	368	186.67	1007.6	542	283.33	2516.0	1380	748.89	4082.0	2250	1232.2	5792.0	3200	1760.0
698.0	370	187.78	1011.2	544	284.44	2534.0	1390	754.44	4100.0	2260	1237.8	5882.0	3250	1787.7
701.6	372	188.89	1014.8	546	285.56	2552.0	1400	760.00	4118.0	2270	1243.3	5972.0	3300	1815.5
705.2	374	190.00	1018.4	548	286.67	2570.0	1410	765.56	4136.0	2280	1248.9	6062.0	3350	1843.3
708.8	376	191.11	1022.0	550	287.78	2588.0	1420	771.11	4154.0	2290	1254.4	6152.0	3400	1871.1
712.4	378	192.22	1040.0	560	293.33	2606.0	1430	776.67	4172.0	2300	1260.0	6242.0	3450	1898.8
716.0	380	193.33	1058.0	570	298.89	2624.0	1440	782.22	4190.0	2310	1265.6	6332.0	3500	1926.6
719.6	382	194.44	1076.0	580	304.44	2642.0	1450	787.78	4208.0	2320	1271.1	6422.0	3550	1954.4
723.2	384	195.56	1094.0	590	310.00	2660.0	1460	793.33	4226.0	2330	1276.7	6512.0	3600	1982.2
726.8	386	196.67	1112.0	600	315.56	2678.0	1470	798.89	4244.0	2340	1282.2	6602.0	3650	2010.0
730.4	388	197.78	1130.0	610	321.11	2696.0	1480	804.44	4262.0	2350	1287.8	6692.0	3700	2037.7
734.0	390	198.89	1148.0	620	326.67	2714.0	1490	810.00	4280.0	2360	1293.3	6782.0	3750	2065.5
737.6	392	200.00	1166.0	630	332.22	2732.0	1500	815.56	4298.0	2370	1298.9	6872.0	3800	2093.3
741.2	394	201.11	1184.0	640	337.78	2750.0	1510	821.11	4316.0	2380	1304.4	6962.0	3850	2121.1
744.8	396	202.22	1202.0	650	343.33	2768.0	1520	826.67	4334.0	2390	1310.0	7052.0	3900	2148.8
748.4	398	203.33	1220.0	660	348.89	2786.0	1530	832.22	4352.0	2400	1315.6	7142.0	3950	2176.6
752.0	400	204.44	1238.0	670	354.44	2804.0	1540	837.78	4370.0	2410	1321.1	7232.0	4000	2204.4
755.6	402	205.56	1256.0	680	360.00	2822.0	1550	843.33	4388.0	2420	1326.7	7322.0	4050	2232.2
759.2	404	206.67	1274.0	690	365.56	2840.0	1560	848.89	4406.0	2430	1332.2	7412.0	4100	2260.0
762.8	406	207.78	1292.0	700	371.11	2858.0	1570	854.44	4424.0	2440	1337.8	7502.0	4150	2287.7
766.4	408	208.89	1310.0	710	376.67	2876.0	1580	860.00	4442.0	2450	1343.3	7592.0	4200	2315.5
770.0	410	210.00	1328.0	720	382.22	2894.0	1590	865.56	4460.0	2460	1348.9	7682.0	4250	2343.3
773.6	412	211.11	1346.0	730	387.78	2912.0	1600	871.11	4478.0	2470	1354.4	7772.0	4300	2371.1
777.2	414	212.22	1364.0	740	393.33	2930.0	1610	876.67	4496.0	2480	1360.0	7862.0	4350	2398.8
780.8	416	213.33	1382.0	750	398.89	2948.0	1620	882.22	4514.0	2490	1365.6	7952.0	4400	2426.6
784.4	418	214.44	1400.0	760	404.44	2966.0	1630	887.78	4532.0	2500	1371.1	8042.0	4450	2454.4
788.0	420	215.56	1418.0	770	410.00	2984.0	1640	893.33	4550.0	2510	1376.7	8132.0	4500	2482.2
791.6	422	216.67	1436.0	780	415.56	3002.0	1650	898.89	4568.0	2520	1382.2	8222.0	4550	2510.0
795.2	424	217.78	1454.0	790	421.11	3020.0	1660	904.44	4586.0	2530	1387.8	8312.0	4600	2537.7
798.8	426	218.89	1472.0	800	426.67	3038.0	1670	910.00	4604.0	2540	1393.3	8402.0	4650	2565.5
802.4	428	220.00	1490.0	810	432.22	3056.0	1680	915.56	4622.0	2550	1398.9	8492.0	4700	2593.3
806.0	430	221.11	1508.0	820	437.78	3074.0	1690	921.11	4640.0	2560	1404.4	8582.0	4750	2621.1
809.6	432	222.22	1526.0	830	443.33	3092.0	1700	926.67	4658.0	2570	1410.0	8672.0	4800	2648.8
813.2	434	223.33	1544.0	840	448.89	3110.0	1710	932.22	4676.0	2580	1415.6	8762.0	4850	2676.6
816.8	436	224.44	1562.0	850	454.44	3128.0	1720	937.78	4694.0	2590	1421.1	8852.0	4900	2704.4
820.4	438	225.56	1580.0	860	460.00	3146.0	1730	943.33	4712.0	2600	1426.7	8942.0	4950	2732.2
824.0	440	226.67	1598.0	870	465.56	3164.0	1740	948.89	4730.0	2610	1432.2	9032.0	5000	2760.0
827.6	442	227.78	1616.0	880	471.11	3182.0	1750	954.44	4748.0	2620	1437.8	9122.0	5050	2787.7
831.2	444	228.89	1634.0	890	476.67	3200.0	1760	960.00	4766.0	2630	1443.3	9212.0	5100	2815.5
834.8	446	230.00	1652.0	900	482.22	3218.0	1770	965.56	4784.0	2640	1448.9	9302.0	5150	2843.3
838.4	448	231.11	1670.0	910	487.78	3236.0	1780	971.11	4802.0	2650	1454.4	9392.0	5200	2871.1
842.0	450	232.22	1688.0	920	493.33	3254.0	1790	976.67	4820.0	2660	1460.0	9482.0	5250	2898.8
845.6	452	233.33	1706.0	930	498.89	3272.0	1800	982.22	4838.0	2670	1465.6	9572.0	5300	2926.6
849.2	454	234.44	1724.0	940	504.44	3290.0	1810	987.78	4856.0	2680	1471.1	9662.0	5350	2954.4
852.8	456	235.56	1742.0	950	510.00	3308.0	1820	993.33	4874.0	2690	1476.7	9752.0	5400	2982.2
856.4	458	236.67	1760.0	960	515.56	3326.0	1830	998.89	4892.0	2700	1482.2	9842.0	5450	3010.0
860.0	460	237.78	1778.0	970	521.11	3344.0	1840	1004.4	4910.0	2710	1487.8	9932.0	5500	3037.7
863.6	462	238.89	1796.0	980	526.67	3362.0	1850	1010.0	4928.0	2720	1493.3	10022.0	5550	3065.5
867.2	464	240.00	1814.0	990	532.22	3380.0	1860	1015.6	4946.0	2730	1498.9	10112.0	5600	3093.3

LIST OF DMIC TECHNICAL REPORTS ISSUED

DEFENSE METALS INFORMATION CENTER
Battelle Memorial Institute
Columbus, Ohio 43201

Copies of the technical reports listed below may be obtained from DMIC at no cost by U. S. Government agencies, U. S. Government contractors, subcontractors, and/or their suppliers. Others may purchase copies of these reports from Clearinghouse for Federal Scientific and Technical Information, U. S. Department of Commerce, Springfield, Virginia 22151. The CFSTI reference numbers (PB or AD prefix numbers) and prices are shown in parentheses. HC refers to Hard Copy price; Mf refers to Microfiche price. Orders to CFSTI should refer to the reference numbers and be prepaid.

Number	Title
*150	A Review of Bending Methods for Stainless Steel Tubing, March 2, 1961 (PB 151109, $1.50)
151	Environmental and Metallurgical Factors of Stress-Corrosion Cracking in High-Strength Steels, April 14, 1961 (PB 151110, $0.75)
152	Binary and Ternary Phase Diagrams of Columbium, Molybdenum, Tantalum, and Tungsten, April 28, 1961 (AD 257739, $3.50)
*153	Physical Metallurgy of Nickel-Base Superalloys, May 5, 1961 (AD 258041, $1.25)
154	Evolution of Ultrahigh-Strength, Hardenable Steels for Solid-Propellant Rocket-Motor Cases, May 25, 1961 (AD 257976, $1.25)
155	Oxidation of Tungsten, July 17, 1961 (AD 263598, $3.00)
156	Design Information an AM-350 Stainless Steel for Aircraft and Missiles, July 28, 1961 (AD 262407, $1.50)
157	A Summary of the Theory of Fracture in Metals, August 7, 1961 (PB 181081, $1.75)
*158	Stress-Corrosion Cracking of High-Strength Stainless Steels in Atmospheric Environments, September 15, 1961 (AD 266005, $1.25)
159	Gas-Pressure Bonding, September 25, 1961 (AD 265133, $1.25)
160	Introduction to Metals for Elevated-Temperature Use, October 27, 1961 (AD 268647, $2.50)
161	Status Report No. 1 on Department of Defense Refractory Metals Sheet-Rolling Program, November 2, 1961 (AD 267077, $1.00)
162	Coatings for the Protection of Refractory Metals from Oxidation, November 24, 1961 (AD 271384, $3.50)
163	Control of Dimensions in High-Strength Heat-Treated Steel Parts, November 29, 1961 (AD 270045, $1.00)
164	Semiaustenitic Precipitation-Hardenable Stainless Steels, December 6, 1961 (AD 274805, $2.75)
165	Methods of Evaluating Welded Joints, December 28, 1961 (AD 272088, $2.25)
166	The Effect of Nuclear Radiation on Structural Metals, September 15, 1961 (AD 265839, $2.50)
*167	Summary of the Fifth Meeting of the Refractory Composites Working Group, March 12, 1962 (AD 274804, $2.00)
168	Beryllium for Structural Applications, 1958-1960, May 18, 1962 (AD 278723, $3.50)
169	The Effect of Molten Alkali Metals on Containment Metals and Alloys at High Temperatures, May 18, 1962 (AD 278654, $1.50)
170	Chemical Vapor Deposition, June 4, 1962 (AD 281887, $2.25)
171	The Physical Metallurgy of Cobalt-Base Superalloys, July 6, 1962 (AD 283356, $2.25)
172	Background for the Development of Materials to be Used in High-Strength-Steel Structural Weldments, July 31, 1962 (AD 284265, $3.00)
173	New Developments in Welded Fabrication of Large Solid-Fuel Rocket-Motor Cases, August 6, 1962 (AD 284829, $1.00)
174	Electron-Beam Processes, September 15, 1962 (AD 287433, $1.75)
175	Summary of the Sixth Meeting of the Refractory Composites Working Group, September 24, 1962 (AD 287029, $1.75)
176	Status Report No. 2 on Department of Defense Refractory Metals Sheet-Rolling Program, October 15, 1962 (AD 288127, $1.25)
177	Thermal Radiative Properties of Selected Materials, November 15, 1962, Volume I (AD 294345, $3.00), Volume II (AD 294346, $4.00)
178	Steels for Large Solid-Propellant Rocket-Motor Cases, November 20, 1962 (AD 292258, $1.00)
179	A Guide to the Literature on High-Velocity Metalworking, December 3, 1962 (AD 403495, $3.50)
180	Design Considerations in Selecting Materials for Large Solid-Propellant Rocket-Motor Cases, December 10, 1962 (AD 294695, $2.00)
181	Joining of Nickel-Base Alloys, December 20, 1962 (AD 296174, $2.00)
182	Structural Considerations in Developing Refractory Metal Alloys, January 31, 1963 (AD 419383, $1.00)
183	Binary and Ternary Phase Diagrams of Columbium, Molybdenum, Tantalum, and Tungsten (Supplement to DMIC Report 152), February 7, 1963 (AD 407907, $2.75)
184	Summary of the Seventh Meeting of the Refractory Composites Working Group, May 30, 1963 (AD 413567, $1.75)
185	The Status and Properties of Titanium Alloys for Thick Plate, June 14, 1963 (AD 421029, $1.50)
186	The Effect of Fabrication History and Microstructure on the Mechanical Properties of Refractory Metals and Alloys, July 10, 1963 (AD 423952, $1.75)
187	The Application of Ultrasonic Energy in the Deformation of Metals, August 16, 1963 (AD 423962, $2.25)
188	The Engineering Properties of Columbium and Columbium Alloys, September 6, 1963 (AD 426255, $3.50)
189	The Engineering Properties of Tantalum and Tantalum Alloys, September 13, 1963 (AD 426344, $2.50)
190	The Engineering Properties of Molybdenum and Molybdenum Alloys, September 20, 1963 (AD 426264, $4.00)

* DMIC supply exhausted; copies may be ordered from CFSTI.

Number	Title
191	The Engineering Properties of Tungsten and Tungsten Alloys, September 27, 1963 (AD 425547, $2.75)
192	Hot-Cold Working of Steel to Improve Strength, October 11, 1963 (AD 425948, $2.00)
193	Tungsten Research and Development Review, October 23, 1963 (AD 425474, $1.50)
194	A Discussion of the Physical Metallurgy of the 18 Per Cent Nickel Maraging Steels, November 15, 1963 (AD 430082, $0.75)
195	Properties of Coated Refractory Metals, January 10, 1964 (AD 435782, $2.25)
196	Hydrogen-Induced, Delayed, Brittle Failures of High-Strength Steels, January 20, 1964 (AD 601116, $3.00)
197	Cracking in High-Strength Steel Weldments - A Critical Review, February 7, 1964 (AD 438432, $4.00)
198	The Mechanical Properties of the 18 Per Cent Nickel Maraging Steels, February 24, 1964 (AD 600427, $2.75)
199	The Application of High Pressure in Metal-Deformation Processing - Report of an Informal Symposium of the Metalworking Process and Equipment Program, March 2, 1964 (AD 437328, $2.00)
200	Vacuum Degassing in the Production of Premium-Quality Steels, March 11, 1964 (AD 601823, $4.00)
201	U. S. Government Metalworking Processes and Equipment Program, March 18, 1964 (AD 600088, $2.25)
202	The Effects of High-Pressure, High-Temperature Hydrogen on Steel, March 26, 1964 (AD 601389, $2.00)
203	Explosive Forming of Metals, May 8, 1964
204	The Welding and Brazing of Alloy 718, June 1, 1964
205	The Effects of Heat-Treating and Testing Environments on the Properties of Refractory Metals, August 20, 1964
206	An Introduction to Magnesium Alloys, August 26, 1964
207	Current Methods of Fracture-Toughness Testing of High-Strength Alloys With Emphasis on Plane Strain, August 31, 1964
208	Metal Deformation Processing, Volume 1, A Survey Conducted as Part of the Metalworking Process and Equipment Program (MPEP), August 14, 1964
209	Second Status Report of the U. S. Government Metalworking Processes and Equipment Program, November 23, 1964

Unclassified
Security Classification

DOCUMENT CONTROL DATA - R&D

(Security classification of title, body of abstract and indexing annotation must be entered when the overall report is classified)

1 ORIGINATING ACTIVITY (Corporate author)
Battelle Memorial Institute
Defense Metals Information Center
505 King Avenue, Columbus, Ohio 43201

2a REPORT SECURITY CLASSIFICATION
Unclassified

2b GROUP
--

3 REPORT TITLE Problems in the Load-Carrying Application of High-Strength Steels - A Symposium Sponsored by the Tripartite Technical Cooperation Program (TTCP) Subgroup P on Materials, Working Panel on Metals

4 DESCRIPTIVE NOTES (Type of report and inclusive dates)
DMIC Report, October 26-28, 1964

5 AUTHOR(S) (Last name, first name, initial)
Please see author index in Table of Contents

6 REPORT DATE	7a TOTAL NO OF PAGES	7b NO OF REFS
October 26-28, 1964	233	241

8a CONTRACT OR GRANT NO	9a ORIGINATOR'S REPORT NUMBER(S)
AF 33(615)-1121	DMIC Report 210
b PROJECT NO 8975	
c	9b OTHER REPORT NO(S) (Any other numbers that may be assigned this report)
d	

10 AVAILABILITY/LIMITATION NOTICES Copies may be obtained from DMIC at no cost by Government contractors, subcontractors, and their suppliers. Others may purchase copies from: Clearinghouse for Federal Scientific and Technical Information U. S. Department of Commerce, Springfield, Virginia 22151.

11 SUPPLEMENTARY NOTES	12 SPONSORING MILITARY ACTIVITY
	United States Air Force, Research and Technology Division, Wright-Patterson Air Force Base, Ohio 45433

13 ABSTRACT

This report represents the compilation of papers on the problems in the load-carrying application of high-strength steels. The papers were presented in five sessions at a symposium sponsored by the Tripartite Technical Cooperation Program on October 26-28, 1964, in Washington, D. C. Session I consists of papers on the broad subject of high-strength steels, to reflect the present state of the art, and on potential applications for these steels, including the design-material interplay. Session II papers deal with production and fabrication, with emphasis on the effects on, and the subsequent properties of, the resulting fabricated products. Session III papers deal with the very critical topic of corrosion sensitivity of high-strength steels, protection against corrosion, and the effects of protection techniques on steel behavior. The papers in Session IV are devoted to mechanical behavior characteristics of design significance. The papers of the last session deal with high-strength steels by technical types so as to obtain an integrated picture of their behavior, properties and processing techniques; the papers also discuss strengthening mechanisms per se.

DD FORM 1473

Unclassified
Security Classification

14 KEY WORDS		LINK A		LINK B		LINK C	
		ROLE	WT	ROLE	WT	ROLE	WT
High-strength steel	Analysis						
Production	Military application						
Application	Primary processing						
Machining	Surface integrity						
Forming	Corrosion						
Joining	Design						
Physical metallurgy	Heat treatment						
Physical properties	Economics						
Mechanical properties	Inspection						

INSTRUCTIONS

1. ORIGINATING ACTIVITY: Enter the name and address of the contractor, subcontractor, grantee, Department of Defense activity or other organization *(corporate author)* issuing the report.

2a. REPORT SECURITY CLASSIFICATION: Enter the overall security classification of the report. Indicate whether "Restricted Data" is included. Marking is to be in accordance with appropriate security regulations.

2b. GROUP: Automatic downgrading is specified in DoD Directive 5200.10 and Armed Forces Industrial Manual. Enter the group number. Also, when applicable, show that optional markings have been used for Group 3 and Group 4 as authorized.

3. REPORT TITLE: Enter the complete report title in all capital letters. Titles in all cases should be unclassified. If a meaningful title cannot be selected without classification, show title classification in all capitals in parenthesis immediately following the title.

4. DESCRIPTIVE NOTES: If appropriate, enter the type of report, e.g., interim, progress, summary, annual, or final. Give the inclusive dates when a specific reporting period is covered.

5. AUTHOR(S): Enter the name(s) of author(s) as shown on or in the report. Enter last name, first name, middle initial. If military, show rank and branch of service. The name of the principal author is an absolute minimum requirement.

6. REPORT DATE: Enter the date of the report as day, month, year; or month, year. If more than one date appears on the report, use date of publication.

7a. TOTAL NUMBER OF PAGES: The total page count should follow normal pagination procedures, i.e., enter the number of pages containing information.

7b. NUMBER OF REFERENCES: Enter the total number of references cited in the report.

8a. CONTRACT OR GRANT NUMBER: If appropriate, enter the applicable number of the contract or grant under which the report was written.

8b, 8c, & 8d. PROJECT NUMBER: Enter the appropriate military department identification, such as project number, subproject number, system numbers, task number, etc.

9a. ORIGINATOR'S REPORT NUMBER(S): Enter the official report number by which the document will be identified and controlled by the originating activity. This number must be unique to this report.

9b. OTHER REPORT NUMBER(S): If the report has been assigned any other report numbers *(either by the originator or by the sponsor)*, also enter this number(s).

10. AVAILABILITY/LIMITATION NOTICES: Enter any limitations on further dissemination of the report, other than those imposed by security classification, using standard statements such as:

(1) "Qualified requesters may obtain copies of this report from DDC."

(2) "Foreign announcement and dissemination of this report by DDC is not authorized."

(3) "U. S. Government agencies may obtain copies of this report directly from DDC. Other qualified DDC users shall request through _____."

(4) "U. S. military agencies may obtain copies of this report directly from DDC. Other qualified users shall request through _____."

(5) "All distribution of this report is controlled. Qualified DDC users shall request through _____."

If the report has been furnished to the Office of Technical Services, Department of Commerce, for sale to the public, indicate this fact and enter the price, if known.

11. SUPPLEMENTARY NOTES: Use for additional explanatory notes.

12. SPONSORING MILITARY ACTIVITY: Enter the name of the departmental project office or laboratory sponsoring *(paying for)* the research and development. Include address.

13. ABSTRACT: Enter an abstract giving a brief and factual summary of the document indicative of the report, even though it may also appear elsewhere in the body of the technical report. If additional space is required, a continuation sheet shall be attached.

It is highly desirable that the abstract of classified reports be unclassified. Each paragraph of the abstract shall end with an indication of the military security classification of the information in the paragraph, represented as (TS), (S), (C), or (U).

There is no limitation on the length of the abstract. However, the suggested length is from 150 to 225 words.

14. KEY WORDS: Key words are technically meaningful terms or short phrases that characterize a report and may be used as index entries for cataloging the report. Key words must be selected so that no security classification is required. Identifiers, such as equipment model designation, trade name, military project code name, geographic location, may be used as key words but will be followed by an indication of technical context. The assignment of links, rules, and weights is optional.